SYNTHESIS OF ORGANOBORON COMPOUNDS BY DIFUNCTIONALIZATION OF ALKENES

YAN MENG

A dissertation
submitted to the Faculty of
the department of Chemistry
in partial fulfillment
of the requirements for the degree of
Doctor of Philosophy

Boston College
Morrissey College of Arts and Sciences
Graduate School

October 2020

Synthesis of organoboron compounds by difunctionalization of alkenes

Yan Meng

Advisor: Professor James P. Morken, Ph.D.

Abstract: This dissertation details two different alkene difunctionalization strategies that are utilized in the synthesis of three types of organoboron species in racemic and enantioenriched fashion. Chapter one will introduce the carbohydrate and DBU co-catalyzed transition-metal-free enantioselective diboration reactions of unactivated alkenes. Mechanistic insights guided reaction condition design will be discussed. In chapter two, a nickel-catalyzed conjunctive cross-coupling of 9-BBN borane and carboxylic acid derivatives is presented. Its development and detailed mechanistic studies, along with the efforts in asymmetric induction will be covered. Finally, the first enantio- and diastereoselective synthesis of 1,2-*anti*-silylboronates enabled by palladium-catalyzed conjunctive cross-coupling will be described. The optimization of chemo-, enantio- and diastereoselectivity in the reactions and their following transformations (e.g. oxidation and amination) is demonstrated.

ACKNOWLEDGEMENTS

First and foremost, I want to give my highest appreciation and gratitude to my nice and kind advisor, Dr. James P. Morken. As I always tell people who asked about my advisor, Joining his group is the only thing that I have never regret in grad school. I have learned a lot from him, not only chemistry-related things but also his philosophy of life, excitement to chemistry, and commitment to work, which shaped my thoughts and will continue inspiring me for the rest of my life.

Secondly, I want to thank all the Morken group members and alumni who have helped and supported me along the way. I want to thank my dear mentor, Dr. Jason Shields. It would not be possible to finish my Ph.D. without help and guidance from him. He shed light on the darkest time of my graduate time. Every chapter below is coming from the collaboration with others, and I would like to thank everyone who has worked with me (in chapter order)---Dr. Lu Yan, Dr. Chunyin Law, Ziyin Kong, and Dr. Jesse Myhill. It was enjoyable and exciting to work with them. I want to thank several Morken group colleagues who didn't work directly on the same project with me. But still, meaningful discussions with them pushed me forward to be a better scientist, namely Dr. Xun Liu, Dr. Gabriel Lovinger, Dr. Adam Szymaniak, Dr. Matteo Chierchia, Dr. Emma Edelstein, Dr. Sheila Namirembe Dr. Byran

Ingollia and Peilin Xu. I am very thankful to Chenlong Zhang and Yucheng Mu for their scholarship and friendship, who made my graduate school life less painful but more delightful. I want to thank Chenlong Zhang, Byran Ingollia, and Yucheng Mu for sharing their suggestions on this dissertation. Besides, I would like to thank my wonderful friend, Jingjing Xie, for bearing with me and comforting me along this challenging process. Thank you for accepting me and standing by my side as who I am.

Lastly, I am incredibly grateful to my parents for their unconditional love and care for 27 years. I never thank you enough for being there for me without a doubt. Thank you for being proud of me, and I hope I can make you proud all the time.

To my dear and loving parents.

TABLE OF CONTENT

List of Abbreviations

Å: angstrom

Ac: acetyl

acac: acetylacetonyl

9-BBN: 9-borabicyclo(3.3.1)nonane

BINAP: 2,2'-bis(diphenylphosphino)-1,1'-binaphthyl

$B_2(cat)_2$: bis(catecholato)diboron

$B_2(eg)_2$: bis(ethyleneglycolato)diboron

$B_2(neo)_2$: bis(neopentylglycolato)diboron

$B_2(pin)_2$: bis(pinacolato)diboron

$B_2(pro)_2$: Propanediol diboron

Bn: benzyl

Bz: benzoyl

cat: catechol

cod: 1,5-cyclooctadiene

conv: conversion

Cy: cyclohexyl

DART: direct analysis in real time

dba: dibenzylideneacetone

DCM: dichloromethane

DCE: 1,2-dichloroethane

DFT: density functional theory

DHR: (2S,3R,4S)-2-methyltetrahydro-2H-pyran-3,4-diol

DHQ: dihydroquinine

DMAP: 4-dimethylaminopyridine

DME: dimethoxyethane

DMF: N,N-dimethylformamide

DMSO: dimethyl sulfoxide

d.r.: diastereomeric ratio

e.e.: enantiomeric excess

equiv.: equivalent(s)

e.r.: enantiomeric ratio

ESI: electrospray ionization

EtOAc: ethyl acetate

GC: gas chromatography

h: hour(s)

HRMS: high-resolution mass Spectrometry

IPA: isopropanol

IR: infrared spectroscopy

M: molar

MALDI: matrix-assisted laser desorption/ionization

MeCN: acetonitrile

min: minutes

MS: molecular sieves

NBS: N-bromosuccinimide

NMR: nuclear magnetic resonance

neo: neopentylglycol

N.R: no reaction

N.D.: none determined

NHC: N-heterocyclic carbene

pin: pinacol

ppm: parts per million

Pd(OAc) 2 : palladium (II) acetate

pmb: p-methoxybenzyl

PyBox: pyridine bis(oxazoline)

Quinap: 1-(2-diphenylphosphino-1-naphthyl)isoquinoline

rac: racemic

RCM: ring-closing metathesis

rt: room temperature

Ruphos: 2-dicyclohexylphosphino-2′,6′-diisopropoxybiphenyl

SFC: supercritical fluid chromatography

TADDOL: 2,2-dimethyl-α,α,α’,α’-tetraaryl-1,3-dioxolane-4,5-dimethanol

TBAF: tetrabutylammonium fluoride

TBDPS: t-butyldiphenylsilyl

TBS: t-butyldimethylsilyl

TBS-DHG: (2R,3S,4R)-2-(((tert-butyldimethylsilyl)oxy)methyl)tetrah

ydro-2H-pyran-3,4-diol

TCD: trans-cyclohexanediol

TES: triethylsilyl

Tf: trifluoromethanesulfonyl

THF: tetrahydrofuran

TLC: thin layer chromatography

TMS: trimethylsilyl

tol: toluene

TS: transition state

UV: ultraviolet

xylyl: dimethylphenyl

Chapter 1

Carbohydrate/DBU Cocatalyzed Alkene Diboration: Mechanistic Insight Provides Enhanced Catalytic Efficiency and Substrate Scope

1.1 Introduction

Organoboron compounds are valuable and versatile reagents in modern organic synthesis. Besides the well-known Suzuki cross-coupling for C-C bond formation[1], an array of methods have been developed to convert C-B bonds to other C-C bonds or C-heteroatom bonds (Scheme 1.1).[2]

Scheme 1. 1 versatility of organoboron compounds

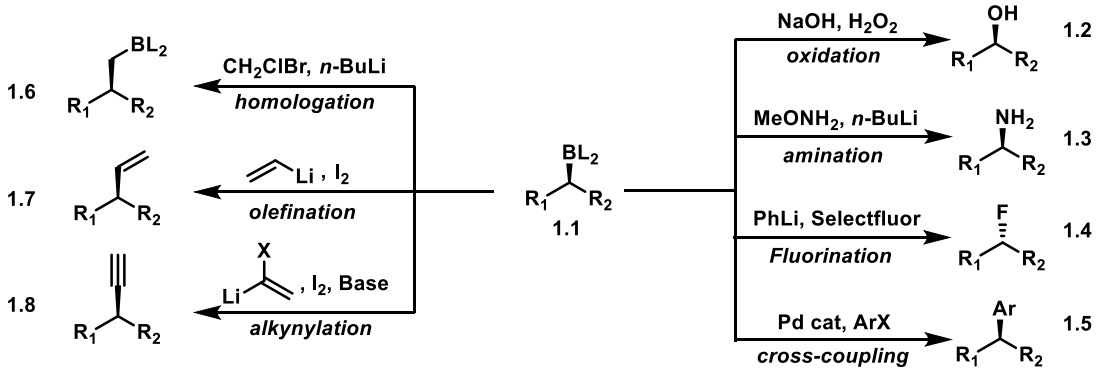

[1] D. Imao, B. W. Glasspoole, V. S. Laberge, C. M. Crudden, *J. Am. Chem. Soc.* **2009**, *131*, 5024

[2] a) C. Snyder, B.C. S. Rao, G. Zweiful, H. C. Brown, *Tetrahedron*. **1986**, *42*, 5505; b) S. N. Mlynarski, A. S. Karns, J. P. Morken, *J. Am. Chem. Soc.* **2012**, *134*, 16449; c) C. Sandford, R. Rasappan, V. K. Aggarwal, *J. Am. Chem. Soc.* **2015**, *137*, 10100; d) K. M. Sadhu, D.S. Matteson, *J. Am. Chem. Soc.* **1983**, *105*, 2077; e) N. L. Polston, C. C. Whitney, G. Zweiful, *J. Am. Chem. Soc.* **1968**, *90*, 6243; f) Y. Wang, A. Noble, E. L. Myers, V. K. Aggarwal, *Angew. Chem. Int. Ed*. **2016**, *55*, 4270

Our group is particularly interested in the 1,2-diboronate because of its unique reactivity. Since the first example of alkene diboration was reported in 1995[3], significant amount of effort has been contributed to the synthesis of 1,2-diboronates. Many transition metals (e.g., Pd, Ni, Pt, Rh)[4], when combined with appropriate ligands, have been found to catalyze the diboration reaction in either a racemic or an enantioselective manner. However, the cost of metals and ligands limits the broad application of these methods in industry and academia.

Inspired by a racemic transition metal-free diboration reported by Fernandez[5], an enantioselective carbohydrate/DBU co-catalyzed diboration reaction was developed in 2016.[6] Unlike transition metal catalysis, carbohydrate catalysts are relatively inexpensive and are easily accessible from commercially available compounds. Moreover, the reaction is easy to conduct and does not require rigorous exclusion of air and moisture. Terminal alkenes were converted to products with high yield and enantioselectivity, while *trans* alkenes suffered from poor reactivity. High temperature and extended reaction

[3] R. T. Baker, P. Nguyen, T. B. Marder, S. A. Westcott, *Angew. Chem. Int. Ed.* **1995**, *34*, 1336
[4] J. P. Morken in Comprehensive Organic Synthesis**,** 2nd Edition (Ed: P. Knochel, G. A. Molander), Elsevier, Waltham, MA, **2014**, vol. 4, pp. 939
[5] A. Bonet, C. Pubill-Ulldemolins, C. Bo, H. Cluyas, E. Fernanadez, *Angew. Chem. Int. Ed.* **2011**, *50*, 7158
[6] L. Fang, L. Yan, F. Haeffner, J. P. Morken, *J. Am. Chem. Soc*. **2016**, *138*, 2508

time were necessary to ensure a moderate yield with these more encumbered substrates and this resulted in lower selectivity. While some understanding of mechanism was obtained from computational studies, a detailed experimental mechanistic investigation was still needed.

Herein, an enhanced version of an enantioselective transition-metal free diboration reaction is presented. Mechanistic studies were performed to facilitate the development of a more efficient reaction system with an expanded substrate scope, and this new process applied to terminal alkenes as well as *trans* alkenes.

1.2 Background

1.2.1 The utility of 1,2-diboron compounds

While two vicinal boron atoms can be simultaneously converted into the same functional group, they can also undergo selective transformation into different functional groups, delivering otherwise hard-to-access valuable compounds.

For instance, as shown in Scheme 1.2, chiral 1,2-diboronates could be

converted into diols or diamines with retention of stereochemistry[7]. On the other hand, the primary organoboronate could undergo selective homologation [8] or cross-coupling [9] to produce more complex motifs. Additionally, our group developed a selective oxidation protocol where the secondary C-B bond reacts without affecting the primary organoboron; the remaining C-B unit could later undergo amination or cross-coupling.[10] With the utility of enantioenriched 1,2-diboronates illustrated by these powerful transformations, the synthesis of these species became an attractive direction to pursue.

Scheme 1. 2 Transformations of 1,2-bisboronates

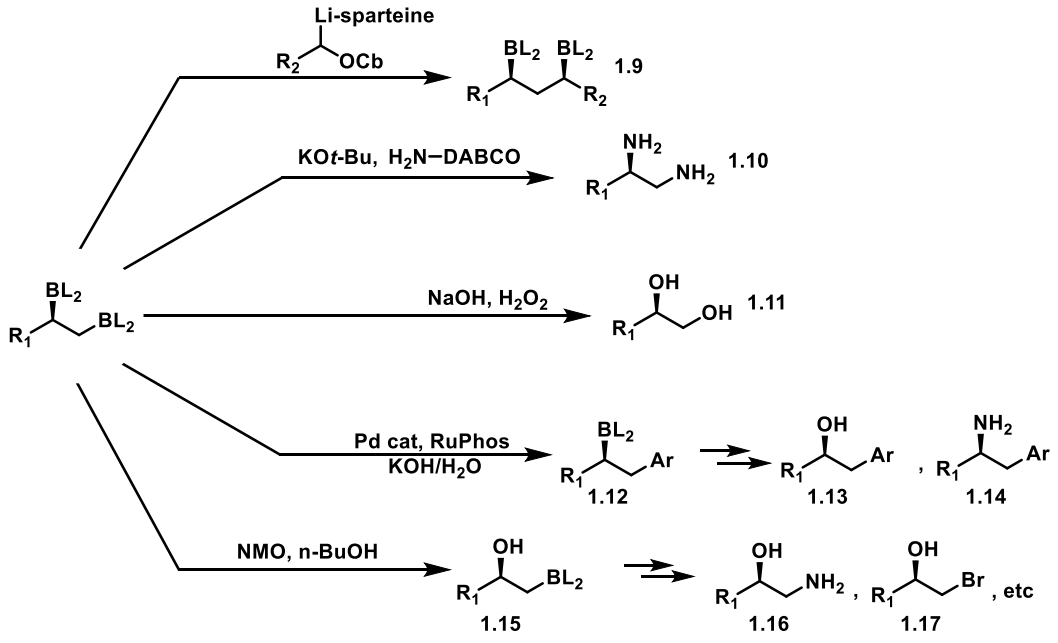

[7] X. Liu, Q. Zhu, D. Chen, L. Wang, L. Jin, C. Liu, *Angew. Chem. Int. Ed*. **2020**, *59*, 2745
[8] A. Fawcett, D. Nitsch, M. Ali, J. M. Bateman, E. L. Myers, V. K. Aggarwal, *Angew. Chem. Int. Ed*. **2016**, *55*, 14663
[9] S. N. Mlynarski, C. H. Schuster, J. P. Morken, *Nature.* **2014**, *505*, 386
[10] L. Yan, J. P. Morken, *Org. lett.* **2019**, *21*, 3760

1.2.2 Synthesis of 1,2-diboronates

The alkene diboration reaction represents one of the most important and straightforward approaches toward the synthesis of 1,2-diboronates. Herein, various methods of alkene diboration are summarized and discussed.

1.2.2.1 Transition metal-catalyzed diboration

The most common alkene diboration reactions are catalyzed by a transition-metal complex following the general mechanism shown in Scheme 1.3. The transition metal complex undergoes oxidative addition with the diboron compound to form **(1.19)**. Upon association of the alkene substrate, migratory insertion forges one C-B bond and one C-M bond; eventually, the remaining C-B bond is formed through reductive elimination.

Scheme 1. 3 General catalytic cycle of transition metal-catalyzed diboration

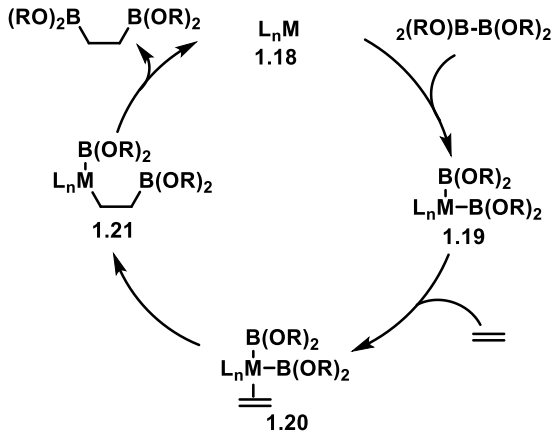

1.2.2.1.1 Synthesis of racemic 1,2-diboronates

The first example of transition metal-catalyzed alkene diboration was reported by Baker and Marder in 1995.[3] In this reaction, B_2cat_2 was added across a styrene-type substrate with a catalytic amount of Au and diphosphine ligand (Scheme 1.4).

Scheme 1. 4 First catalytic diboration reaction catalyzed by gold complex

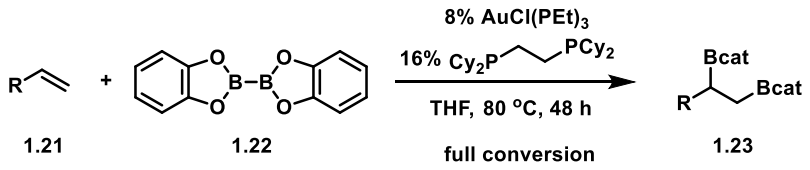

Two years later, Miyaura[11] and Smith[12], independently discovered that platinum also promoted the diboration reaction of alkenes with either B_2pin_2 or B_2cat_2 as diboron reagents. High yields were delivered with terminal alkenes and activated internal alkenes as substrates (Scheme 1.5).

Scheme 1. 5 Platinum catalyzed diboration reactions

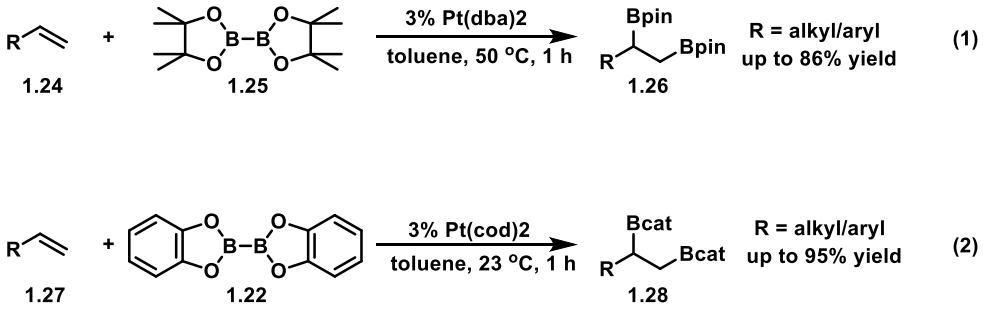

[11] T. Ishiyama, M. Yamamoto, N. Miyaura, *Chem. Commun.* **1997**, 689.
[12] C N. Iverson, M. R. Smith III, *Organometalllics.* **1997**, *16*, 2757

Shortly afterward, Marder reported that rhodium was also catalytically active in the diboration reaction.[13] Both terminal and disubstituted aromatic alkene substrates reacted with excellent efficiency (Scheme 1.6). For synthetic purposes, the development of enantioselective methods was needed.

Scheme 1. 6 Rhodium catalyzed diboration reactions

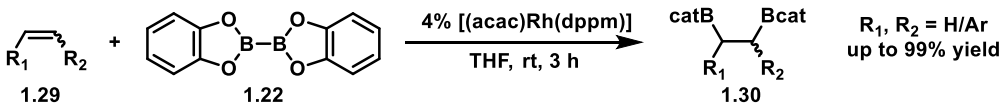

1.2.2.1.2 Synthesis of enantioenriched 1,2-diboronates

The first attempt at an enantioselective synthesis of 1,2-diboronates was made in 1998 by Marder.[14] As shown in Scheme 1.7, although a moderate level of selectivity was obtained with menthol-derived chiral diboron species, the method proved the concept that chirality of boronate's ligand could induce enantioselectivity, which sheds light on the further exploration of asymmetric catalytic reactions.

Scheme 1. 7 Chiral diboron induced enantioselective diboration reaction

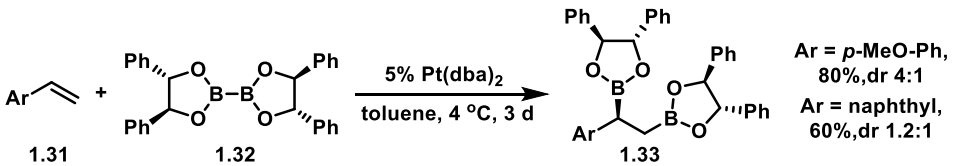

[13] C. Dai, E. G. Robins, A. J. Scott, W. Clegg, D. S. Yufit, J. A. K. Howard, T. B. Marder, *Chem. Commun.* **1998**, 1983

[14] T. B. Marder, N. C. Norman, C. R. Rice, *Tetrahedron Letters.***1998**, *39*, 155

In 2003, our group reported the first case of catalytic synthesis of highly enantioenriched 1,2-diboronates.[15] A catalyst composed of Rh and Quinap along with B_2cat_2 as diboron reagent was employed to induce high enantioselectivity (Scheme 1.8). The method is effective for various disubstituted *E* alkenes (**1.36, 1.37**) as well as terminal alkenes with an adjacent quaternary carbon center (**1.38, 1.39**). However, other terminal alkenes and internal *Z*-alkenes suffered from low enantioselectivity, although the efficiency was still high.

Scheme 1. 8 Chiral rhodium complex catalyzed diboration reactions

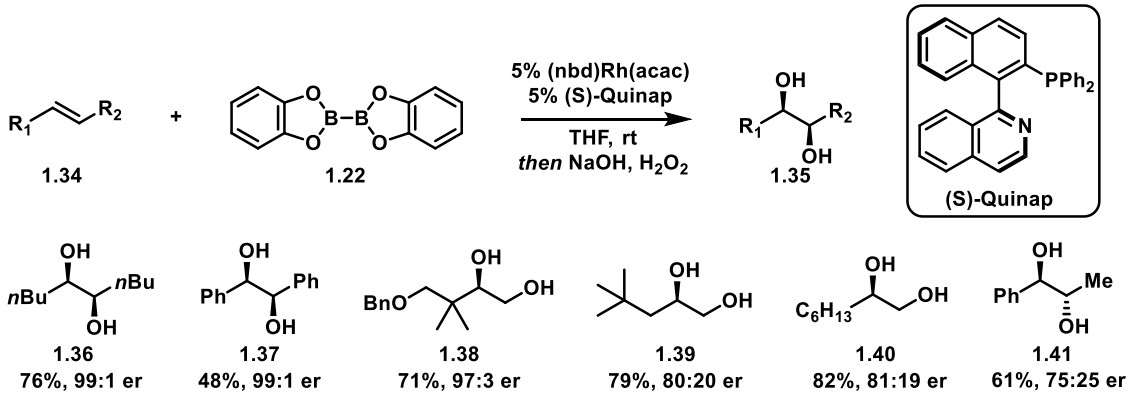

The challenge posed by the asymmetric synthesis of diboronates from terminal alkenes was solved in 2009 by the introduction of a catalyst composed of platinum and a TADDOL-derived phosphonite ligand.[16] One of

[15] a) J. B. Morgan, S. P. Miller, J. P. Morken, *J. Am. Chem. Soc.* **2003**, *125*, 8702; b) S. Trudeau, J. B. Morgan, M. Shrestha, J. P. Morken, *J. Org. Chem.* **2005**, *70*, 9538

[16] a) L. T. Kliman, S. N. Mlynarski, J. P. Morken, *J. Am. Chem. Soc.* **2009**, *131*, 13210; b) J. R. Coombs, F. Haeffner, L. T. Kliman, J. P. Morken, *J. Am. Chem. Soc.* **2013**, *135*, 11222

the advantages of this design is the utilization of the air-stable diboron reagent B_2pin_2 instead of B_2cat_2 which is air and moisture sensitive (Scheme 1.9). Later in 2013, Nishiyama reported another enantioselective diboration of terminal alkenes that employed a rhodium/Phebox complex as the catalyst (Scheme 1.10).[17] Although both methods apply to terminal alkenes and are complementary to the diboration of internal *E* alkenes by rhodium/Quinap system, the enantioselective diboration of internal *Z* alkenes is still considered as an undeveloped process.

Scheme 1. 9 Platium and TADDOL ligand catalyzed diboration of terminal alkenes

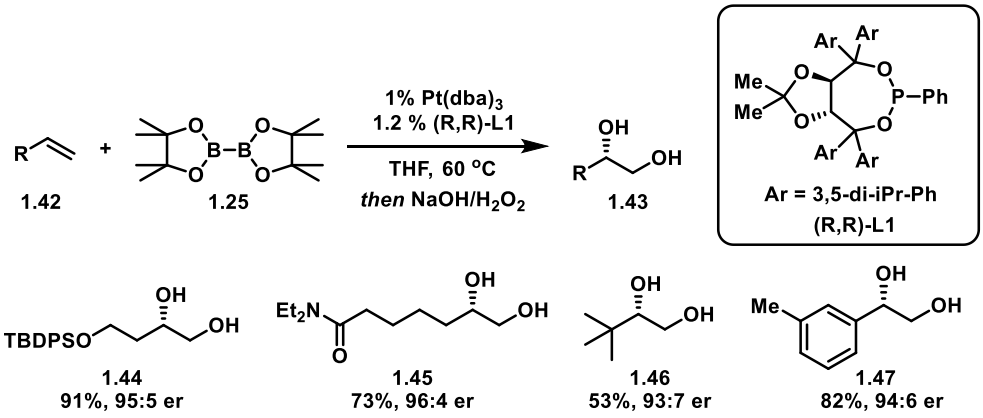

Scheme 1. 10 Rh/PheBox complex catalyzed diboration reactions of terminal alkenes

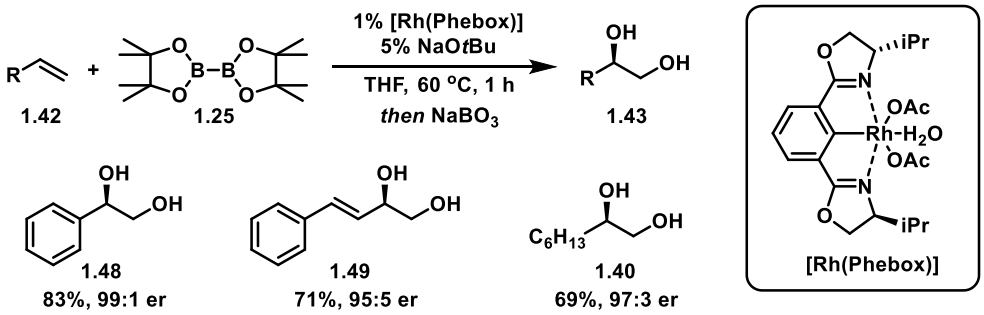

[17] K. Toribatake, H. Nishiyama, *Angew. Chem. Int. Ed.* **2013**, *52,* 11011

1.2.2.1.3 Copper-catalyzed synthesis of 1,2-diboronates

Hoveyda reported an alternative method for the synthesis of enantioenriched 1,2-diboronates through Cu-catalyzed double protoboration of alkynes (Scheme 1.11).[18] The reaction involves a Cu(I)-boron intermediate that is generated from transmetallation between a copper alkoxide and of B_2pin_2. This Cu(I)-boryl intermediate then is added across the alkyne and the formed alkenyl cooper intermediate (**1.52)** is protonated by methanol to produce the *E* alkenyl boronate intermediate (**1.53)** and regenerate the Cu(I)-alkoxide catalyst. Alkene (**1.53)** undergoes a similar protoboration catalytic cycle and ultimately furnishes the chiral 1,2-diboronate. The electronic property of the organoboron intermediate (**1.53)** dictates the regioselectivity of the second borylcupration process so that the 1,2-bis-boronate was produced as the major product.

Scheme 1. 11 Synthesis of enantioenriched 1,2-diboronates by double protoboration of alkynes

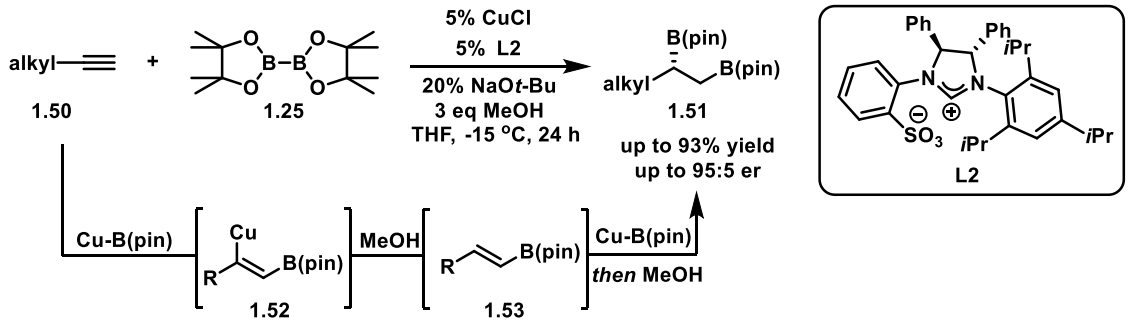

[18] Y. Lee, H. Jang, A. H. Hoveyda, *J. Am. Chem. Soc.* **2009**, *131*, 18234

1.2.2.1.4 Other transition metal-catalyzed diboration reactions

Besides the diboration of simple mono-alkenes, several other alkene-containing compounds have also been studied as substrates in enantioselective diboration reactions (Scheme 1.12). For example, palladium with a TADDOL -derived phosphoramidite ligand could catalyze asymmetric diboration of mono-substituted allenes to deliver products with one chiral allylic boron moiety and one alkenyl boronate.[19] Moreover, our group also developed chemo- and enantio-selective 1,4-diboration of 1,3-dienes by Pt/TADDOL derived complex.[20] Enantioselective 1,2-diboration of 1,3-dienes has also been demonstrated to produce 1,4-diboronates.[21]

Scheme 1. 12 Transition metal-catalyzed diboration reactions of orther alkene-cotaining substrates

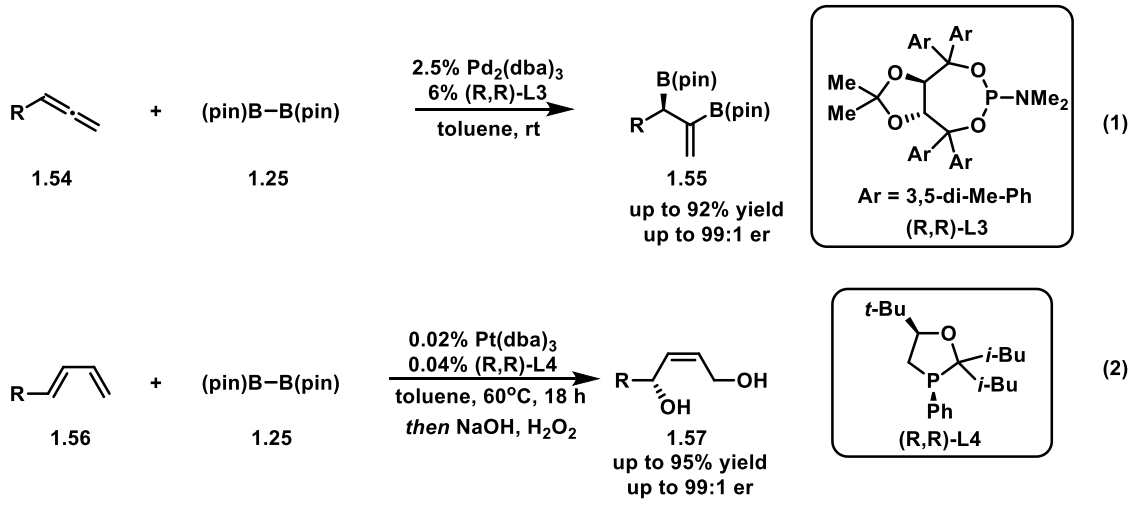

[19] a) N. F. Pelz, A. R. Woodward, H. E. Burks, J. D. Sieber, J. P. Morken. *J. Am. Chem. Soc*. **2004**, *126*, 16328; b) H. E. Burks, S. Liu and J. P. Morken *J. Am. Chem. Soc*. **2007**, *129*, 8766

[20] C. H. Schuster and J. P. Morken *Angew. Chem. Int. Ed*. **2011**, *50*, 7906

[21] L. T. Kliman, S. N. Mlynarski, G. E. Ferris and J. P. Morken *Angew. Chem. Int. Ed*. **2012**, *51*, 521

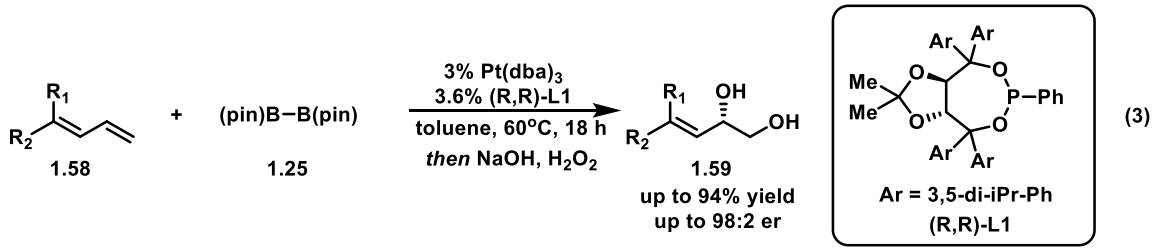

(3)

1.2.2.2 Transition-metal free diboration of alkenes

1.2.2.2.1 Synthesis of racemic 1,2-diboronates

A remarkable transition-metal free diboration was reported by Fernandez in 2010.[5] As shown in Scheme 1.13, vicinal diboronate products were afforded with good yield in the presence of a catalytic amount of cesium carbonate and five equivalents of methanol. Based on computational analysis, the mechanism of the reaction was proposed as follows: alkoxide activation of the diboron compound polarizes the B-B bond, which enables the trivalent boron to be nucleophile and electrophile at the same time. This carbene-like property of this complex allows intermediate (**1.62)** to react with an alkene to generate a three-membered ring intermediate (**1.64)** with associated trivalent boron. The cyclic species (**1.64)** quickly collapses with the tetra-coordinated boron attacking the boric ester to release the final product. Although rare, the

anionic borocycle intermediate (**1.64)** is precedented, as reported by Eisch[22], Schuster[23], and Denmark.[24]

Scheme 1. 13 Transition metal free diboration of alkenes

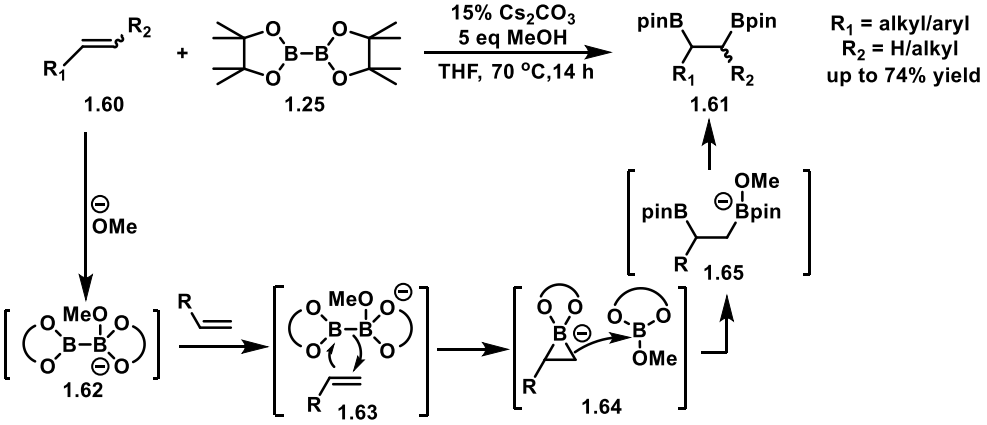

1.2.2.2.2 Synthesis of enantioenriched 1,2-diboronates

A modestly enantioselective version of the transition-metal free alkene diboration was reported by Fernandez group one year after their first racemic method.[25] However, although various chiral alcohols were employed in super-stoichiometric amounts, the enantioselectivity was not satisfying for any of the substrates (Scheme 1.14).

[22] J. J. Eisch, K. Tamao, R. J. Wilcsek, *J. Am. Chem. Soc.* **1975**, *97*, 895
[23] a) M. A. Kropp, K. Bhamidapaty, G. B. Schuster, *J. Am Chem. Soc.* **1988**, *110*, 6252; b) M. A. Kropp, M. Ballargeon,K. M. Park, K. Bhamidapaty, G. B. Schuster, *J. Am. Chem. Soc.* **1991**, *113*, 2155
[24] S. E. Denmark, K. Nishide, A. Faucher, *J. Am. Chem. Soc.* **1991**, *113*, 6675
[25] A. Bonet, C. Sole, H. Gulyas, E. Fernandez, *Org. Biomol. Chem.* **2012**, *10*, 6621

Scheme 1. 14 Chiral base promoted enantioselective diboration of alkenes

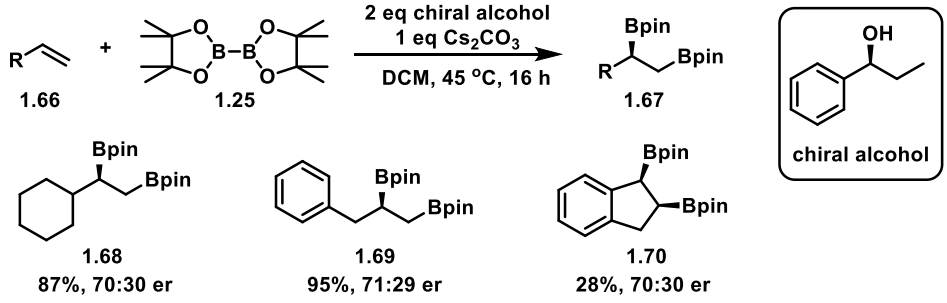

A breakthrough in the enantioselective catalytic diboration was achieved by our group in 2016.[5] Inspired by Brown's work that organoboronic esters could undergo transesterification with vicinal 1,2-diols[26], a catalytic amount of chiral 1,2-diol was employed with the expectation that transesterification could yield chiral diboron reagents that induce the enantioselectivity. After surveying various chiral diols, the commercially available sugar-derived *anti* diols, TBS-DHG and DHR, were found to be effective with high efficiency and produce both *R* and *S* enantiomers, respectively.

Using this process, variety of unactivated terminal alkenes were transformed into chiral diol products after diboration/oxidation. Good yield and selectivity were obtained, even when only 10 mol% of the catalyst was

[26] C. D. Roy, H. C. Brown, *J. Organomet. Chem.* **2007**, *692*, 784.

employed (Scheme 1.15). However, the reactivity suffered when certain types of alkenes were used as substrates (e.g., **1.76** and **1.78**). Although the yield was improved when a stronger base and elevated temperature were used, the enantioselectivity decreased due to the competing uncatalyzed background reaction (**1.77**). A more efficient and selective catalytic system was needed.

Scheme 1. 15 Carbohydrate derivative catalyzed enantioselective synthesis of 1,2-diboronates

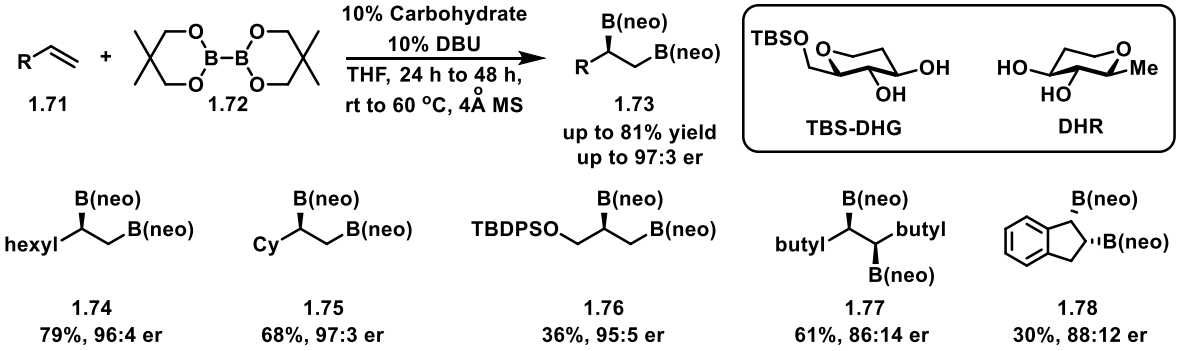

The tentative mechanism was proposed according to the DFT calculation (M06-2X/6-31+G*; PCM solvation model: THF) done by Fredrik Haeffner.[6] Based on the ligand exchange studies done by Brown[26] and the mass spectroscopy data of exchanged chiral boronic esters[5], the doubly exchanged chiral diboron compounds are proposed to be formed by reactions of B_2neo_2 with TBS-DHG. Instead of traditional 1,1-bonded diboron, ring strain in the 1,1-bonding mode (**1.79**) causes the chiral diboron species to adapt a 1,2-bonding mode (**1.80**) and is supported by DFT calculations

(Scheme 1.16).[5] The simplified catalyst, chiral *anti*-1,2-cyclohexane diol, adopts 1,2-bonded structure with an advantage of 8.9 kcal/mol energy, whereas a typical diboron compound, B_2neo_2 favors 1,1-bonding mode (**1.72)** by 12 kcal/mol.

Scheme 1. 16 Energy difference between 1,1-bonding mode and 1,2-bonding mode

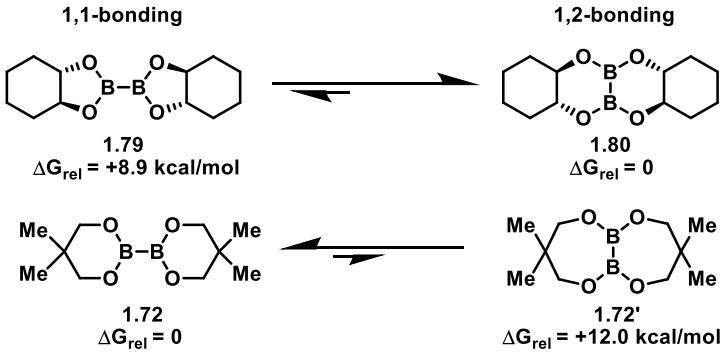

Once the chiral diboron species (**1.80)** are formed, the rest of the catalytic cycle is similar to that proposed by Fernandez (Scheme 1.17). The 1,2-bonded chiral diboron intermediate is activated by Lewis base to furnish (**1.80-OMe)** followed by the formation of the anionic boracycle (**1.81)**, which attacks the appended boron to deliver the diboron product. Based on the DFT calculation, the transition state TS-1 is considered as a lower barrier pathway, compared to the possible transition state TS-1A, an transition state for 1,1-bonded catalyst. We believe that the preference of TS-1 over TS-1A originates from the electron-electron repulsion (Scheme 1.17b). In 1,2-bonding mode,

all lone pairs on oxygens are pointed away from the breaking B-B bond, while two lone pairs of electrons on oxygens bisects the B-B bond in 1,1-bonded mode. Lastly, the neopentyl glycols exchange with the catalyst to release the final product and close the catalytic cycle. Although plausible, more experimental mechanistic studies were needed to support this proposal.

Scheme 1. 17 DFT calculation supported proposed mechanism for carbohydrate-catalyzed diboration (M06-2X/6-31+G*; PCM solvation model: THF)

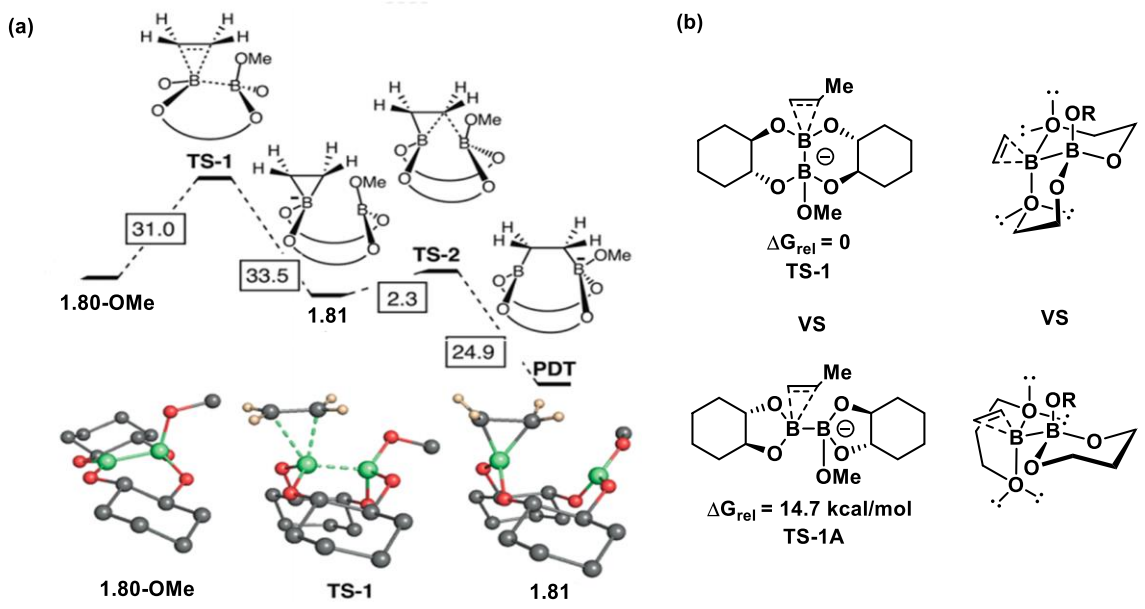

In summary, diboronate compounds produced from the diboration of alkenes are versatile building blocks. Even though transition-metal catalyzed diboration reactions were well-developed, transition-metal free methods represent more attractive strategies and necessitate further investigation and optimization.

1.3 Reaction development

1.3.1 Preliminary kinetic studies

As mentioned in the last section, although the first highly enantioselective transition-metal free diboration had been developed in 2016[5], there were still gaps that needed to be filled in terms of reactivity and selectivity. Therefore, to guide the optimization of carbohydrate-derivative catalyzed diboration reactions, my colleague, Dr. Lu Yan, conducted preliminary kinetic studies. Reaction calorimetry was used to collect kinetic data during experiments with varying concentrations of either catalyst, alkene, or diboron starting material. The rate law was revealed as first-order in diboron, zero-order in alkene, and first-order in the catalyst (Scheme 1.18). This intriguing result suggests that the alkene is not involved in the turnover-limiting step and only one molecule of the catalyst present in the turnover-limiting step. Hence, the turnover limiting step is not likely the diboration step, but a ligand exchange step. Considering a result from mass spectrometry that no mono-exchanged chiral diboron species (**1.83** & **1.84)** are present, the first ligand replacement (**1.82-1.83**) was proposed as the turnover limiting step; the second equivalent of catalyst is installed so fast that intermediate (**1.83** & **1.84)** is not detectable. More details are explained in Dr. Lu Yan's thesis.

Scheme 1. 18 Preliminary kinetic studies revealed the turnover limiting step

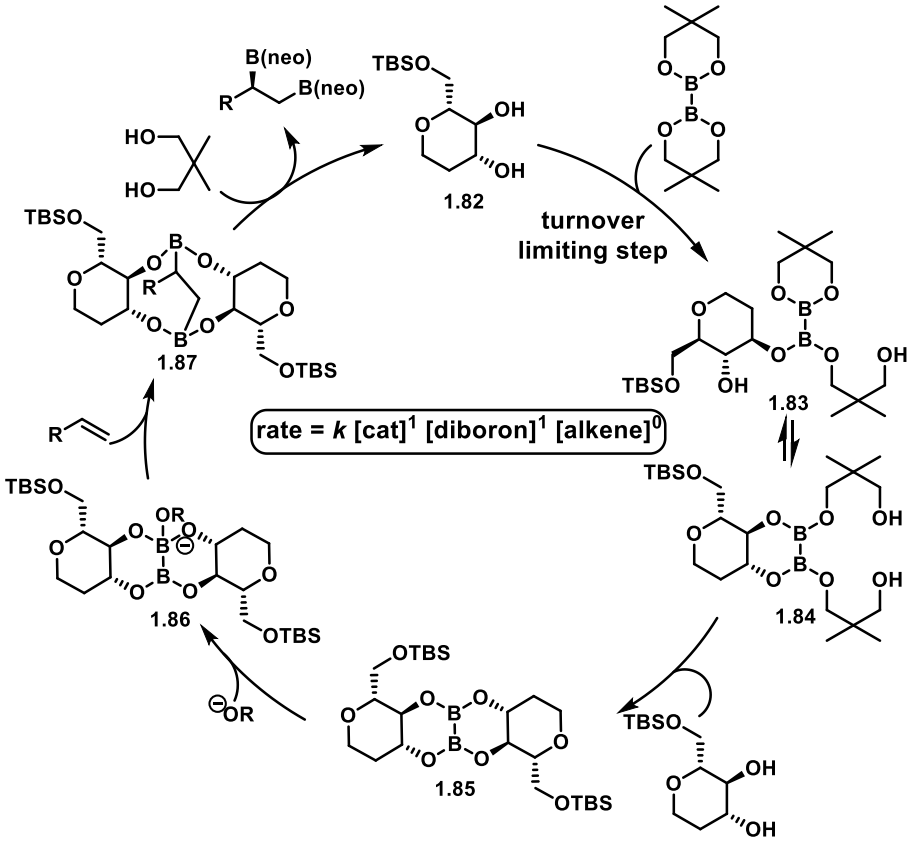

1.3.2 Reaction optimizations

Both the efficiency and selectivity were problematic in the first generation of the carbohydrate-catalyzed diboration reaction. The strategy was to solve both issues by developing a more efficient reaction that operates at a lower temperature. In preliminary experiments, higher enantioselectivity was obtained when the reaction was operated at a cooler temperature, likely due to minimized uncatalyzed background reactions. Thus, the reactivity at

low temperature became the main problem to be addressed. In light of the rate-limiting step being the first exchange step of the catalyst and diboron reagent, it was considered that the reactivity might be boosted by facilitating the rate-limiting step through either catalyst design or diboronate ligand design.

1.3.2.1 Reaction optimization by catalyst design

We envisioned that developing ligands that exchange faster could increase the reaction rate. Thus, the design of C_2-symmetric chiral cyclic *anti* diols was considered. Unlike the working ligand, TBS-DHG, which only has one chiral substituent adjacent to the *anti* diol component, the C_2-symmetric design offers two chiral substituents which might also provide a more enantioselective reaction. After extensive literature search and experimental exploration[27], the synthetic route shown in Scheme 1.19 was developed. Inexpensive and commercially available 1,4-benzoquinone (**1.88**) was first dibrominated and then reduced to 1,4-diol (**1.89**) by $NaBH_4$. The diacetate **(1.90)** resulting from acylation of diol was resolved into enantiopure

[27] G. Vogel, H. Altenbach, O. Plettenburg, *J. Med. Chem*. **1999**, *42*, 1262

Scheme 1. 19 Designed synthetic route for the synthesis of C_2-symmetric chiral cyclic anti-diols

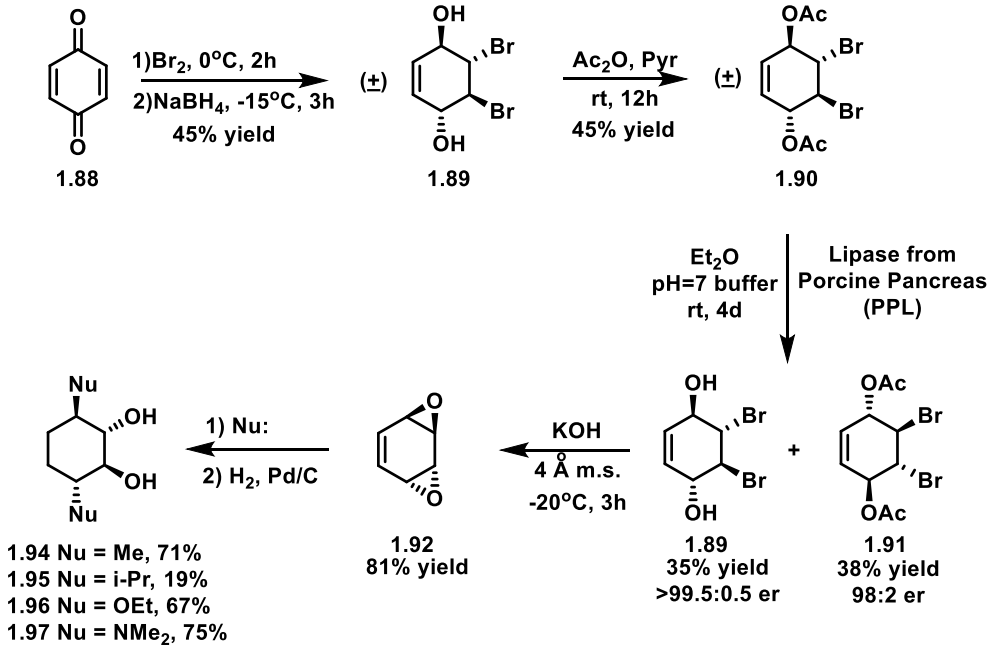

enantiomers by lipase from porcine pancreas (PPL). Then, a base-promoted substitution of the chiral dibromide produced chiral diepoxide (**1.92**), a very reactive electrophile. Subsequent to nucleophilic opening and hydrogenation, the diepoxide is converted to C_2-symmetric chiral cyclic *anti* diol. Because of the late-stage derivatization feature of the synthetic route, a library of chiral cyclic *anti* diols was synthesized and examined (Scheme 1.20).

Unfortunately, none of these catalysts exceeded the yield and enantioselectivity that TBS-DHG delivered in catalytic diboration reactions, although diol (**1.94**) showed similar enantioselectivity as TBS-DHG. Bigger substituents (**1.95**) led to lower enantioselectivity. The results above

Scheme 1. 20 C_2-symmetric cyclic anti-diols catalyzed enantioselective diboration reactions

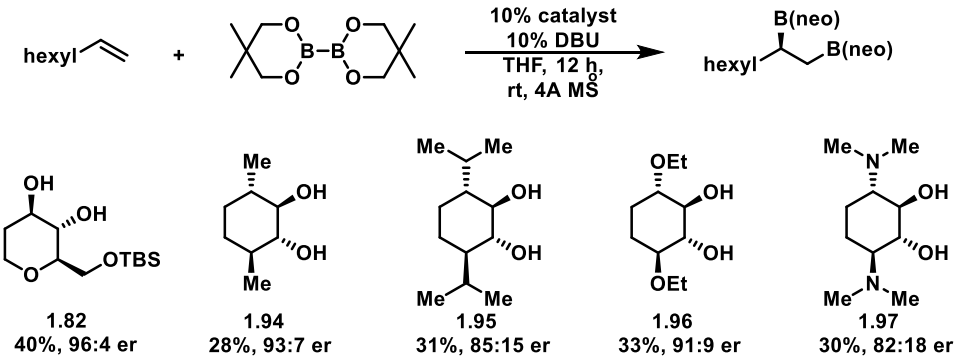

suggested that the size of the substituent next to the diol component is important with methyl group as an optimal one. However, the C_2-symmetric design did not promote reactivity nor selectivity. Presumably, the cumbersome sterics of two adjacent substituents in these ligands impedes their exchanges with achiral diboron reagents.

Similarly, different protecting groups on DHG (**1.98-1.100**) also failed to provide improved reaction outcomes (Scheme 1.21). Considering the cost of the C_2-symmetric catalyst and the availability of carbohydrate derivatives, TBS-DHG was still considered as a more reasonable choice.

Scheme 1. 21 The influence of protecting groups in DHG catalysts

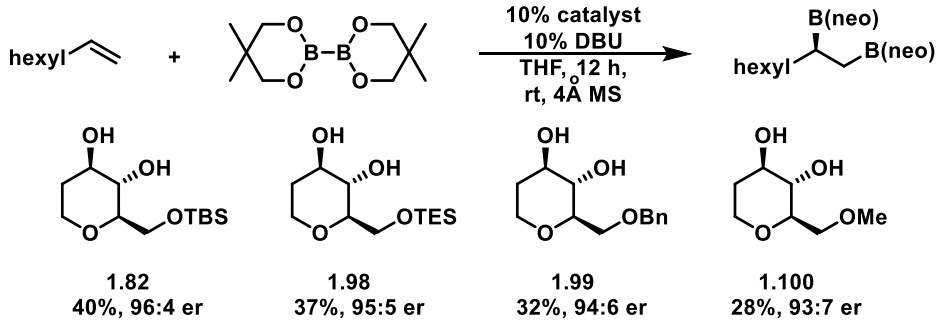

1.3.2.2 Reaction optimization of ligand on boron

Instead of catalyst design, a more reactive diboron reagent with a labile diol ligand was envisioned as a means to enhance the reactivity at low temperature. Various diboron reagents bearing different diol ligands were synthesized and examined at room temperature with 10% of TBS-DHG as the catalyst (Scheme 1.22). The original condition with B_2neo_2 only produced a 40% yield of the product. Presumably, the Thorpe-Ingold effect from the geminal dimethyl substituents makes the neopentyl glycol group a relatively stable ligand for boron. Indeed, more hindered B_2pin_2 and $B_2(dmp)_2$ (dimethylpentyl) suffered from even lower reactivity. Hence, $B_2(eg)_2$, a less hindered diol and one where ring-strain is incorporated in the diboron reagent, was proposed and synthesized. Although a substantial enhancement in reactivity was realized with $B_2(eg)_2$ (ethylene glycol), the product enantiomeric ratio decreased to 91:9, as a result of uncatalyzed background reaction. The competing background reaction dominated when B_2cat_2 was used as a diboron reagent due to the high reactivity of B_2cat_2. $B_2(OH)_4$ failed to turn over the catalytic cycle which led to a low yield. A "Goldilocks" ligand that balances the reactivity and selectivity was found in $B_2(pro)_2$ (propanediol), which delivered a noticeable enhancement in reactivity without sacrificing the

enantioselectivity. Further improvement was obtained by employing two equivalents of $B_2(pro)_2$ and 4 Å molecular sieves which raised the yield to 95% with 95:5 er.

Scheme 1. 22 Optimization of diboration reaction by designing diboron reagents

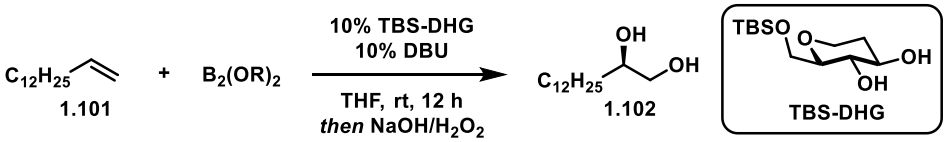

entry	diboron	yield	er
1	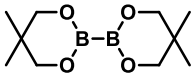	40%	96:4
2	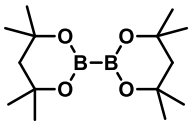	15%	81:19
3	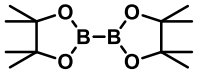	10%	69:31
4	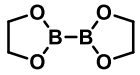	75%	91:9
5	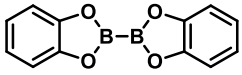	98%	51:49
6	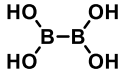	10%	67:33
7	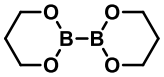	56%	95:5
8	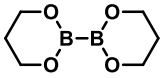 (2 eq) + 4Å MS	95%	95:5

1.3.3 Substrate scope exploration

1.3.3.1 Scope of terminal alkenes

With the reaction conditions optimized for diboration at room temperature, a range of unactivated terminal alkenes were examined with both TBS-DHG and DHR to afford both enantiomers of the products. As shown in Scheme 1.23, simple alkenes bearing hydrocarbon chains (**1.106-1.109**) were converted to chiral diols in excellent yield and selectivity after diboration and oxidation sequence. Aromatic and hetero-aromatic alkenes (e.g., furan, thiophene, pyridine, Boc-indole) starting materials could also be transformed. Of note, the second generation carbohydrate-catalyzed enantioselective diboration was much more efficient than the first generation as highlighted in products (**1.106)**, (**1.108)** and (**1.116)**. Because of the mild reaction conditions, many functional groups were tolerated, including protected hydroxyl group (**1.44**), ketone (**1.118**), ester (**1.117**), and bromide (**1.119**). High diastereo-selectivity observed in products (**1.120**) and (**1.121**) suggested that the selectivity is primarily controlled by the catalyst with a minimum amount of

Scheme 1. 23 Substrate scope of carbohydrate-catalyzed diboration of terminal alkenes

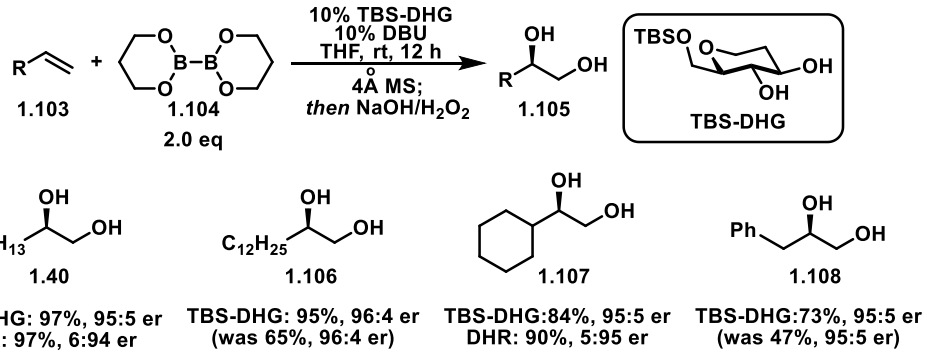

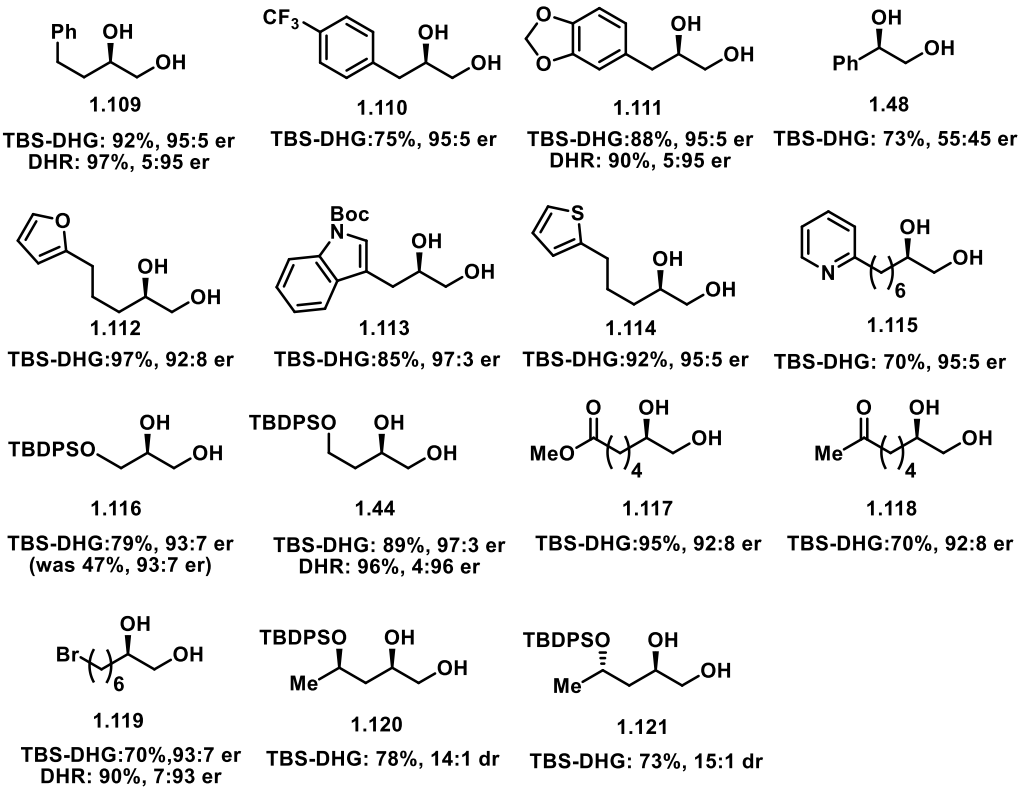

matched and mismatched interactions. Unfortunately, albeit very reactive, styrene-type starting materials like (**1.48**) reacted with low enantioselectivity as the electronic property of styrene might alter the mechanism, which could lead to an aryl ring stabilized anionic intermediate.

1.3.4 Scope of internal alkenes

Another exciting advance provided by the second generation transition-metal free diboration is the reactivity of internal alkenes. Slightly harsher conditions were employed: three equivalents of B_2pro_2 in ethyl acetate solvent

Scheme 1. 24 Substrate scope of carbohydrate catalyzed diboration of internal alkenes

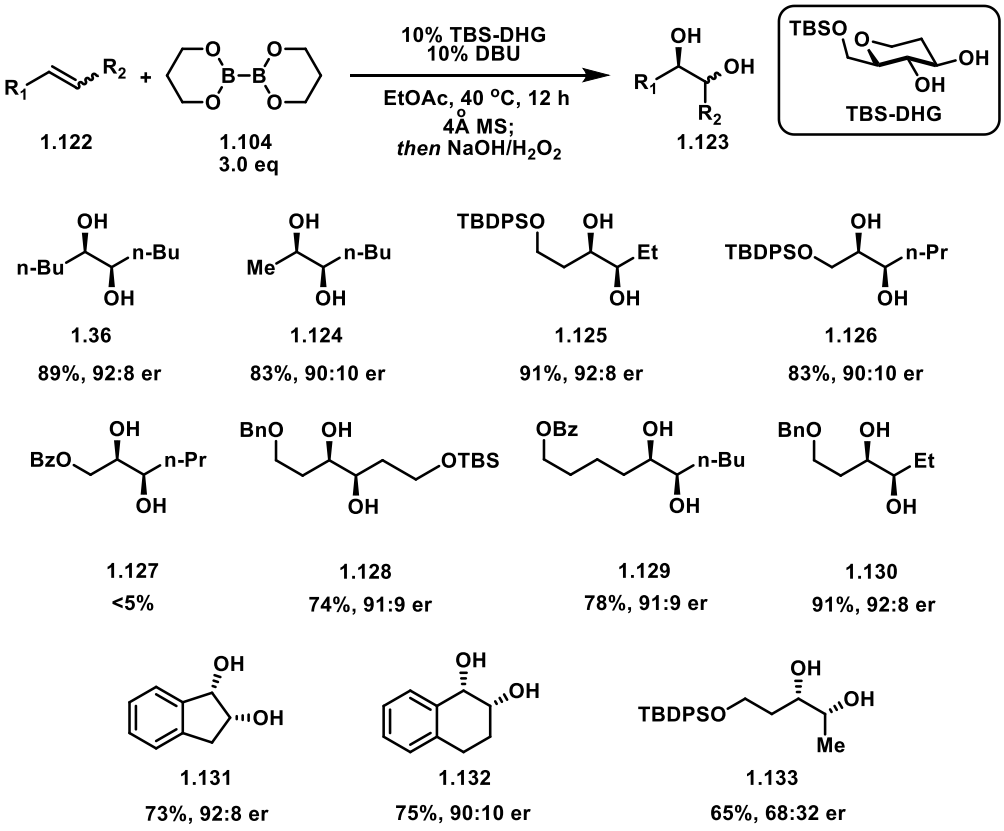

at 40 °C. Compared to the previous method, higher yield and enantioselectivity were obtained at lower reaction temperature and with shorter reaction time. As depicted in Scheme 1.24, not only acyclic enantioenriched *syn* diols (**1.124-1.130**), but cyclic products (**1.131)** and (**1.132)** derived from cyclic alkenes could be obtained with this method. Nevertheless, the enantioselective diboration of *cis* alkenes was still a challenging reaction, likely because the two prochiral faces of a *cis* alkene are similarly encumbered. Using similar conditions as for diboration of *trans*

alkenes only produced 68:32 er when *cis* alkenes were employed. Although multiple attempts were made to enhance the selectivity, there was no significant improvement in this reaction. This synthetic difficulty has not been resolved until the palladium-catalyzed cross-coupling of vicinal silylboronates was developed in 2020 (see Chapter 3).

1.3.4 Origin of enantioselectivity

The activated chiral diboron species studied earlier[6] was examined in more detail by DFT calculations done by Fredrik Haeffner. Similar to the proposal in the previous studies, the anionic boracycle appears to be formed and then transformed through intramolecular attack by a trivalent borate in a stereoretentive fashion. According to previous calculations, the stereochemistry-determining step is the formation of the boracycle. The origin of enantioselectivity could therefore be rationalized by calculation as well, as depicted in Scheme 1.25. Four possible transition states were calculated based on how the alkene substrate approaches to the chiral diboron catalyst. It is not surprising that the transition states M and N suffer a high energetic penalty due to the steric clash between the methyl group on the alkene and the alkoxide. The preference of TS-major over the minor one could be attributed

Scheme 1. 25 Possible transition states proposed by DFT calculation (M06-2X/6-31+G*; PCM solvation model: THF)

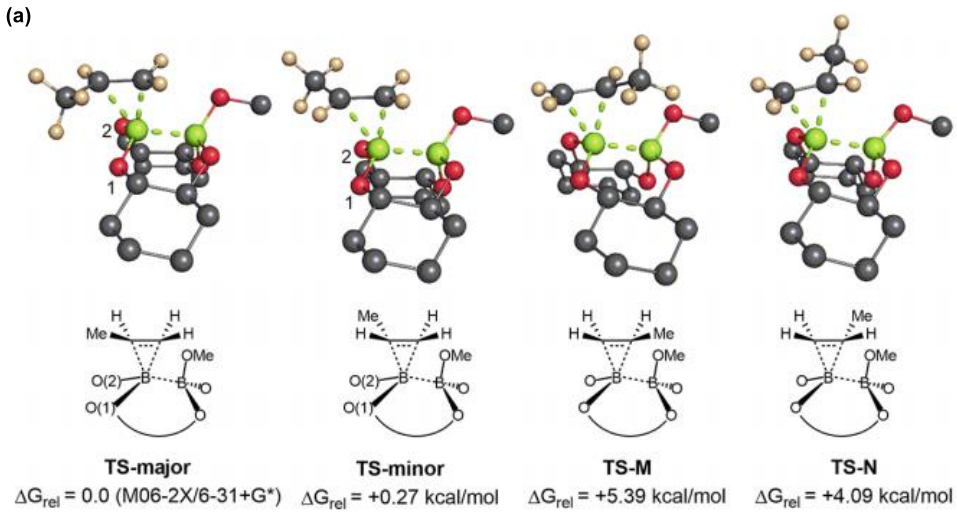

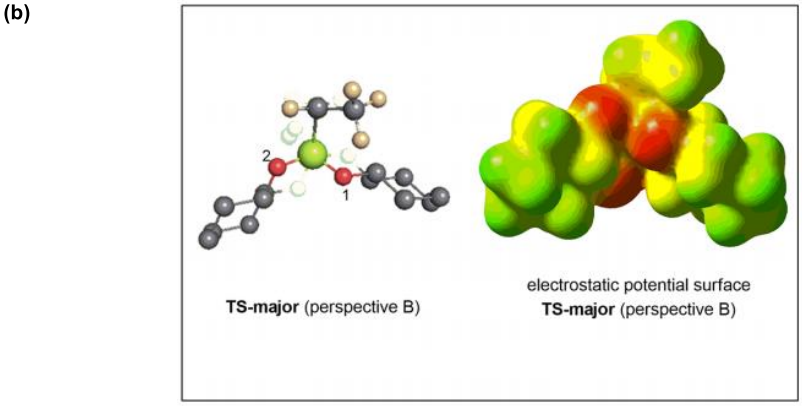

to the repulsion between nonbonding and bonding orbitals. As shown in TS-major (perspective B), the pair of nonbonding electrons in oxygen 2 that sits in the pseudo-axial position is directly pointed toward the alkene C-H bond, whereas the lone pairs on oxygen 1 are directed away from the alkene substituent. On the other hand, in the TS-minor, the pseudo-axial lone pair of oxygen 2 would have stronger interactions with the alkene substituent, which

renders it unfavored. The simplicity introduced for easy DFT calculation (1-propene as the substrate, cyclohexanediol as the catalyst, and methoxide as the base) might account for the small energy difference between TS-major and TS-minor that is not representative of the enantioselectivity achieved in the reaction.

1.3.5 Practical features

1.3.5.1 Preparation of TBS-DHG

The carbohydrate derived catalysts, TBS-DHG and DHR, were initially prepared through a four-step sequence from commercial available *D*-glucal triacetate (Scheme 1.26). Intermediate (**1.143**), containing an unprotected primary alcohol, was produced via heterogeneous hydrogenation, followed by an enzymatic selective deacylation. Finally, silyl protection of the alcohol and

Scheme 1. 26 Previous methods for the synthesis of TBS-DHG catalyst

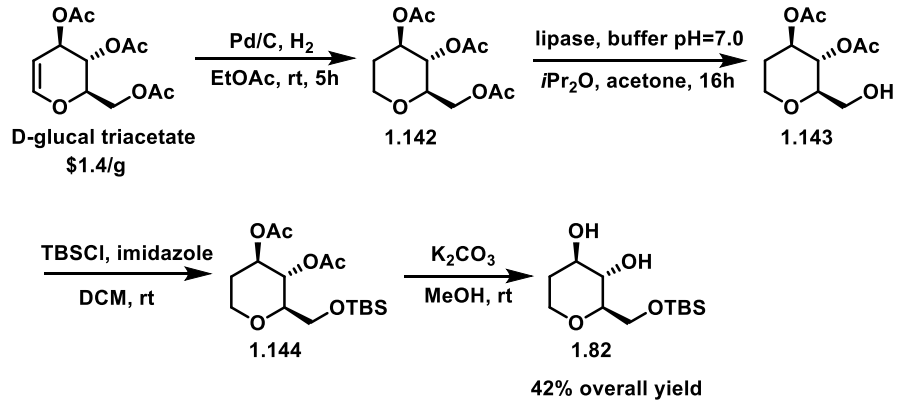

deacylation delivered the TBS-DHG. Although efficient, the enzymatic deacylation is time-consuming and hard to work-up and purify.

Therefore, a revised synthetic route was developed that employed the same hydrogenation as the first step. Instead of selective deacylation, a global deacylation was conducted, followed by selective protection of the primary hydroxyl group by careful control of the reaction conditions. This process produces the catalyst in three steps. Using a similar approach, the DHR catalyst was prepared from commercially available *L*-rhamnal diacetate through hydrogenation and deacylation reactions (Scheme 1.27).

Scheme 1. 27 Current methods for the synthesis of TBS-DHG and DHR catalysts

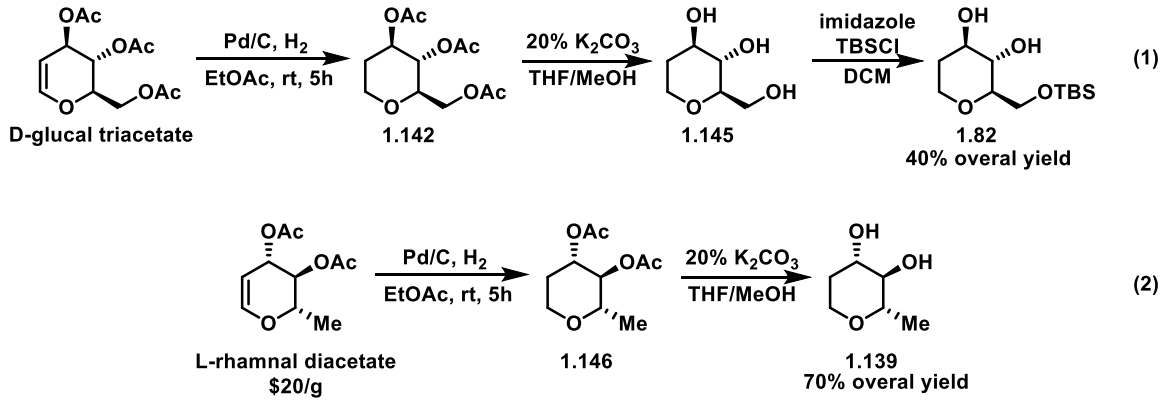

1.3.5.2 Preparative scale diboration reaction

Compared to the previous method, the use of 1,3-propanediol-derived diboron reagents not only enhanced the reactivity but also eased the work-up

and purification steps. Since 1,3-propanediols are much more polar and soluble in water than neopentyl glycols, a simple aqueous wash during oxidative work-up removes most of the diols. The obtained crude product is pure enough that silica gel chromatography is often unnecessary. To further demonstrate the robustness and simplicity of the reaction, a 20 mmol scale reaction was conducted with 1-octene as substrate. As shown in Scheme 1.28, only 1.5 equivalents of freshly prepared B_2pro_2 derived from $B_2(OH)_4$ was required to produce 2.73 g of the chiral diol product within four hours at room temperature.

Scheme 1. 28 gram-scale synthsis of enantioenriched chiral diols

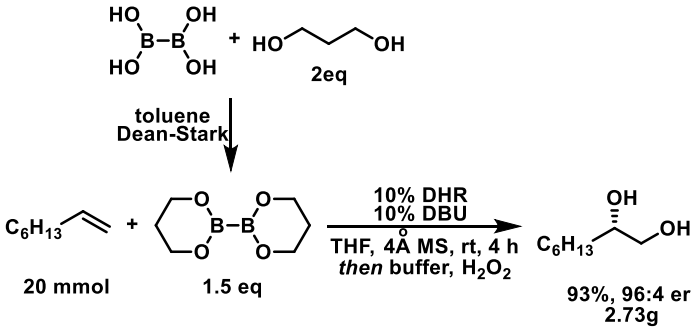

1.3.5.3 One-pot transformation

To demonstrate the utility of the products, a one-pot reaction sequence was designed for the substrate (**1.147)**. After the diboration of (**1.147)**, the

crude material was treated with acid to deprotect the primary hydroxyl group, which later served as a directing group in the palladium-catalyzed cross-coupling reaction with bromobenzene. The complexity of the molecule was built up quickly from simple starting materials with good yield and enantio- and diastereo-selectivities (Scheme 1.29).

Scheme 1. 29 One-pot diboration/directed cross-coupling reaction of trans alkenes

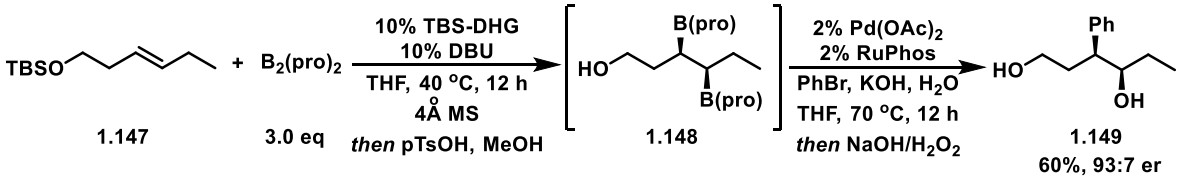

1.4 Conclusion

A carbohydrate-catalyzed enantioselective diboration reaction was refined and optimized to convert unactivated alkenes into vicinal chiral dimetallics in a more efficient manner than the previous process. The mechanism was further investigated computationally and experimentally. The use of B_2pro_2 enabled a fast and relatively "greener" preparation of chiral diols with a minimum amount of toxic waste streams. Although excellent results were achieved with terminal alkenes and *trans* alkenes, other approaches are needed to access the diboration products of *cis* alkenes.

1.5 Experimental data

1.51 General Information

^{1}H NMR spectra were recorded on Varian Gemini-500 (500 MHz), Varian Gemini-600 (600 MHz) or Varian Gemini 400 (400 MHz) spectrometer. Chemical shifts are reported in ppm with the solvent resonance as the internal standard ($CDCl_3$: 7.26 ppm). Data are reported as follows: integration, chemical shift, multiplicity (s = singlet, d = doublet, t = triplet, q = quartet, p = pentet, m = multiplet, br = broad, app = apparent), and coupling constants (Hz). ^{13}C NMR spectra were recorded on either a Varian Gemini-500 (125 MHz) or a Varian Gemini-600 (150 MHz) spectrometer with complete proton decoupling. Chemical shifts are reported in ppm with the solvent resonance as the internal standard ($CDCl_3$: 77.16 ppm). ^{11}B NMR spectra were recorded on a Varian Gemini-500 (160 MHz). Chemical shifts are reported in ppm with an external standard ($BF_3 \cdot Et_2O$: 0 ppm). Infrared (IR) spectra were recorded on a Bruker alpha-P Spectrometer. Frequencies are reported in wavenumbers (cm^{-1}) as follows: strong (s), broad (br), medium (m), and weak (w). Optical rotations were measured on a Rudolph Analytical Research Autopol IV Polarimeter. High-resolution mass spectrometry (DART) was performed at the Mass Spectrometry Facility, Boston College, Chestnut

Hill, MA. Liquid chromatography was performed using forced flow (flash chromatography) on silica gel (SiO2, 230 x 450 Mesh) purchased from Silicycle. Thin layer chromatography (TLC) was performed on 25 μm silica gel glass backed plates from Silicycle. Visualization was performed using ultraviolet light (254 nm), ceric ammonium molybdate (CAM) in ethanol, or potassium permanganate.

Analytical chiral supercritical fluid chromatography (SFC) was performed on a TharSFC Method Station II equipped with Waters 2998 Photodiode Array Detector with isopropanol or methanol as the modifier. Analytical chiral gas-liquid chromatography (GLC) was performed on an Agilent Technologies 6850 Series chromatography with a flame ionization detector, and a Supelco β -Dex 120 column with helium as the carrier gas.

All reactions were conducted in the oven- or flame-dried glassware under an inert atmosphere of nitrogen or argon. Tetrahydrofuran (THF), diethyl ether (Et_2O), dichloromethane (CH_2Cl_2), and toluene were purified using Pure Solv MD-4 solvent purification system, from Innovative Technology, Inc., by passing the solvent through two activated alumina columns after purging with argon. Tetrahydroxydiboron was purchased from Frontier Scientific. It was recrystallized by water before use. Bis(neopentyl

glycolato)diboron was purchased from Oakwood Chemicals. D-glucal triacetate was purchased from Alfa Aesar. (1S, 2S)-trans-1,2-cyclohexanediol and (1R, 2R)-trans-1,2-cyclohexanediol were purchased from Acros Organics. Phosphate buffer solution (PH = 7.0) was purchased from Fisher Scientific. Tris(dibenzylideneacetone)dipalladium(0) and Ruphos were purchased from Strem Chemicals. Activated 4A Molecular Sieves was bought from Sigma-Aldrich. All other reagents were purchased either from Aldrich, Alfa Aesar, Acros, Oakwood Chemicals, Combi Blocks, or TCI and were used without further purification.

1.5.2 Catalysts Preparation

1.5.2.1 Synthesis of TBS-DHG catalyst.

A flame-dried round-bottomed flask equipped with a stir bar was charged with D-glucal triacetate (4.36 g, 16.0 mmol), palladium on carbon (5%, 0.85 g, 0.80 mmol) and ethyl acetate (30 mL). The vessel was purged with hydrogen gas and the reaction mixture was allowed to stir at room temperature under balloon pressure of hydrogen for 5 hours. The mixture was then filtered through a pad of silica gel. The filtrate was concentrated by

rotary evaporation to afford crude oil (**1.142)**. The crude product was used for next step without further purification.

A round-bottomed flask was equipped with a stir bar and a solution of the crude product **1.142** (1.00 g, 3.65 mmol) in tetrahydrofuran (10 mL), and methanol (10 mL) was added to the flask. To the reaction mixture was then added potassium carbonate (0.13 g, 0.91 mmol). The reaction was allowed to stir at room temperature for 16 h. Silica gel (2.6 g) was then added to the reaction. Solvents were removed by rotary evaporation. The crude material was purified through a silica gel column (hexane: acetone: methanol=10:10:2) to afford the product **1.145** as white solid. (0.50 g, 92% yield). Spectral data and physical data are in accordance with the literature report[28]. ^{1}H NMR (600 MHz, Methanol-d4) δ 3.95 (ddd, J = 11.7, 4.9, 1.6 Hz, 1H), 3.87 (dd, J = 11.8, 2.3 Hz, 1H), 3.66 (dd, J = 11.7, 5.7 Hz, 1H), 3.58 – 3.50 (m, 1H), 3.47 (td, J = 12.2, 2.1 Hz, 1H), 3.22 – 3.12 (m, 2H), 2.04 – 1.81 (m, 1H), 1.63 (tdd, J = 12.9, 11.4, 5.0 Hz, 1H). ^{13}C NMR (151 MHz, Methanol-d4) δ 83.7, 75.3, 74.9, 67.8, 64.5, 36.4. HRMS-(DART+) for $C_6H_{13}O_4$ $[M+H]^+$: calculated: 149.0814. found: 149.0806.

[28] Kikuo, I.; Tsunetoshi, H. *J. Org. Chem.* **1970**, *35*, 606.

A flame-dried round-bottomed flask equipped with a stir bar was charged with imidazole (0.34 g, 5.06 mmol) and product **1.145** (0.50 g, 3.37 mmol). The flask was sealed with a septum, and flushed with nitrogen gas for 5 minutes. To the round-bottomed flask was then added *tert*-butyldimethylsilyl chloride (0.61 g, 4.05 mmol) dissolved in dichloromethane (6 mL). The reaction mixture was allowed to stir at room temperature under nitrogen for 6 h. The reaction mixture was then treated with water (10 mL). The layers were separated and the aqueous layer was extracted three times with dichloromethane. The combined organic layers were dried over Na_2SO_4, filtered, and concentrated by rotary evaporation to afford crude product. The crude product was purified through a silica gel column (50% ethyl acetate in hexane) to afford the TBS-DHG catalyst as a white solid (0.64 g, 71% yield). Spectral data were in accordance with the literature report[6].

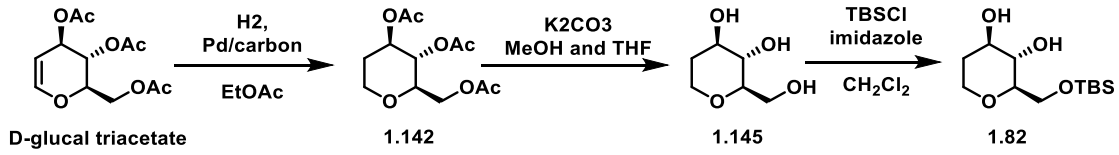

1.5.2.2 Synthesis of DHR catalyst.

A round-bottomed flask equipped with a stir bar was charged with L-rhamnal diacetate (2.14 g, 10.0 mmol), palladium on carbon (5%, 0.53 g, 0.50

mmol), and ethyl acetate (20 mL). The vessel was purged with hydrogen gas and the reaction mixture was allowed to stir at room temperature under balloon pressure of hydrogen for 5 hours. The mixture was then filtered through a pad of silica gel. The filtrate was concentrated by rotary evaporation to afford crude oil **1.146**. The crude product was used for the next step without further purification.

A round-bottomed flask was equipped with a stir bar and a solution of the crude product **1.146** (1.08 g, 5 mmol) in tetrahydrofuran (10 mL) and methanol (10 mL). The reaction mixture was then added potassium carbonate (0.13 g, 1.25 mmol). The reaction was allowed to stir at room temperature for 16 h and was then added 2.6g silica gel. The reaction was concentrated by rotary evaporation. The crude was purified through a silica gel column (70% ethyl acetate in hexane) to afford the product **DHR catalyst 1.139** as white solid. (463 mg, 70% yield). Spectral data were in accordance with literature report[6].

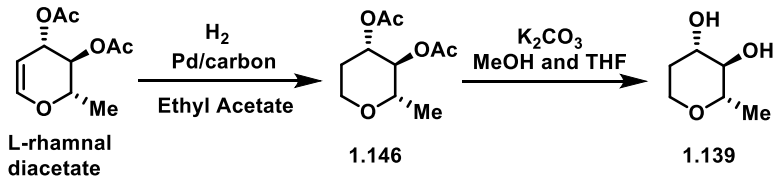

1.5.3 Preparation of B_2pro_2

To a round-bottomed flask equipped with a magnetic stir bar was added tetrahydoxydiboron (1.91 g, 21.27 mmol), 1,3-propanediol (3.04 ml, 41.91 mmol), and toluene (25 ml). Then a Dean-Stark distillation head was installed. The reaction was refluxed at 160 °C for 6 h. Toluene was then removed by rotary evaporation to afford crude product. The crude product was recrystallized by hexane and dichloromethane to afford the propanediol diboron as white solid (2.50 g, 70% yield). Spectral data were in accordance with the literature report[6]. HRMS-(DART+) for $C_6H_{13}B_2O_4$ $[M+H]^+$: calculated: 171.1, found:171.1008.

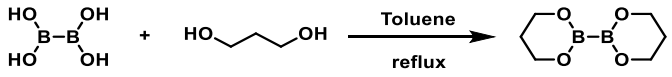

1.5.4 Preparation of Alkenes

1.5.4.1 General Procedure for silyl protection of alkenes

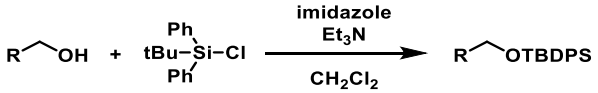

To a flame-dried round-bottomed flask equipped with a stir bar was added imidazole (1.02 g, 15 mmol). The flask was purged with nitrogen for 5

min. Dichloromethane (20 ml), alcohol substrate (10 mmol), Et_3N (2.09 ml, 15 mmol) was then added. tert-Butyl (chloro)diphenylsilane (2.57 ml, 10 mmol) was added to the reaction mixture in drop. The reaction was allowed to stir at room temperature for 16 h. Water (20 ml) was then added to the reaction. The layers were separated. The aqueous layer was extracted by dichloromethane twice. The organic layers were combined, dried over sodium sulfate, filtered, and condensed under vacuum to afford the crude product.

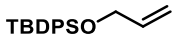

(allyloxy)(tert-butyl)diphenylsilane. The title compound was prepared by the representative procedure without modification. The crude product was purified by silica gel column with hexane to afford the product as a colorless oil (2.61 g, 88% yield). Spectral data was in accordance with the literature report[29]. HRMS-(DART+) for $C_{19}H_{24}OSi$ $[M+H]^+$: calculated: 297.1675, found:297.1662.

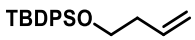

[29] Kliman, L. K. ; Mlynarski, S. N.; Morken, J. P. *J. Am. Chem. Soc.* **2009**, *131*, 13210.

(but-3-en-1-yloxy)(tert-butyl)diphenylsilane. The title compound was prepared by the representative procedure without modification. The crude product was purified by a silica gel column with hexane to afford the product as a colorless oil (2.95 g, 95% yield). Spectral data were in accordance with the literature report.[11] HRMS-(DART+) for $C_{20}H_{26}OSi$ $[M+H]^+$: calculated: 311.1831, found: 311.1815.

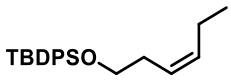

(Z)-tert-butyl(hex-3-en-1-yloxy)diphenylsilane. The title compound was prepared by the representative procedure without modification. The crude product was purified by silica gel column with hexane to afford the product as colorless oil (3.12 g, 92% yield). ^{1}H NMR (500 MHz, $CDCl_3$) δ 7.78 – 7.60 (m, 4H), 7.50 – 7.31 (m, 6H), 5.48 – 5.39 (m, 1H), 5.38 – 5.29 (m, 1H), 3.65 (t, J = 7.0 Hz, 2H), 2.31 (q, J = 7.1 Hz, 2H), 2.06 – 1.91 (m, 2H), 1.05 (dd, J = 2.1, 0.7 Hz, 9H), 0.92 (t, J = 7.4 Hz, 3H). ^{13}C NMR (126 MHz, $CDCl_3$) δ 135.6, 134.0, 133.5, 129.5, 127.6, 124.9, 76.7, 63.8, 30.7, 26.8, 20.6, 19.2, 14.3. HRMS-(DART+) for $C_{22}H_{30}OSi$ $[M+H]^+$: calculated:339.2144, found: 339.2160. IR(neat): 3071.27(w), 3050.30(w), 3010.25(w), 2960.51(m),

2931.33(m), 2892.88(m), 2858.24(m), 1462.68(m), 1188.08(s), 1091.21(s), 700.85(s), 504.80(m), cm^{-1} .

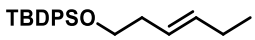

(E)-tert-butyl(hex-3-en-1-yloxy)diphenylsilane. The title compound was prepared by the representative procedure without modification. The crude product was purified by a silica gel column with hexane to afford the product as a colorless oil (3.01 g, 88% yield). Spectral data were in accordance with the literature. [30] HRMS-(DART+) for $C_{22}H_{30}OSi$ $[M+H]^+$: calculated: 339.2144, found: 339.2152.

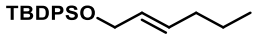

(E)-tert-butyl(hex-2-en-1-yloxy)diphenylsilane. The title compound was prepared by the representative procedure without modification. The crude product was purified by silica gel column with hexane to afford the product as colorless oil (3.20 g, 95% yield). ^1H NMR (600 MHz, $CDCl_3$) δ 7.82 – 7.56 (m, 4H), 7.55 – 7.30 (m, 6H), 5.65 (dtt, *J* = 14.9, 6.6, 1.5 Hz, 1H), 5.55 (dtt, *J*

[30] Nishioka, Y.; Uchida, T.; Katsuki, T. *Angew. Chem. Int. Ed.* **2013**, *52*, 1739.

= 15.3, 5.2, 1.4 Hz, 1H), 4.17 (dd, *J* = 5.1, 1.4 Hz, 2H), 2.28 – 1.79 (m, 2H), 1.39 (h, *J* = 7.4 Hz, 2H), 1.06 (s, 9H), 0.90 (t, *J* = 7.4 Hz, 3H). ^{13}C NMR (151 MHz, $CDCl_3$) δ 138.2, 136.6, 133.9, 132.2, 131.5, 130.2, 67.4, 37.0, 29.5, 25.0, 21.9, 16.3. HRMS-(DART+) for $C_{22}H_{30}OSi$ $[M+H]^+$: calculated:337.1988, found: 337.1987. IR(neat): 2957.87(m), 2929.83(m), 2857.54(m), 1462.35(m), 1427.69(m), 1110.55(s), 700.97(s), 504.60(s), cm^{-1}.

1.5.4.2 Preparation of oct-7-en-2-one.

The title compound was prepared by a literature procedure. The spectral data were in accordance with the literature reference[31].

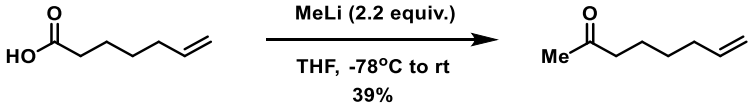

1.5.4.3 Preparation of methyl hept-6-enoate.

The title compound was prepared by literature procedure. The spectral data was in accordance with the literature reference.[13]

[31] Rosillo, M.; Arnáiz, E.; Abdi, D.; Blanco-Urgoiti, J.; Domínguez, G.; and Pérez-Castells, J. *Eur. J. Org. Chem.* **2008**, *23*, 3917.

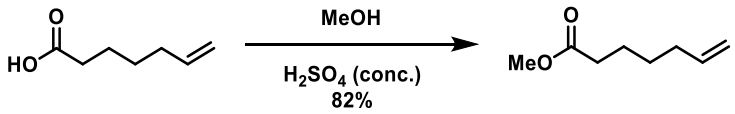

1.5.4.4 Preparation of (R)-tert-butyl(pent-4-en-2-yloxy)diphenylsilane and (S)-tert-butyl(pent-4-en-2-yloxy)diphenylsilane.

To a flame-dried round-bottomed flask equipped with a stir bar was added CuI (381 mg, 2 mmol) in the glovebox. The flask was sealed by rubber septa and removed from the glovebox. The flask was charged with tetrahydrofuran (30 ml) under nitrogen. The reaction was cooled down to -78 ^{o}C by dry ice/ acetone bath. Vinyl magnesium bromide (1M in THF, 20 ml, 20 mmol) was then added dropwise. The reaction was allowed to stir at -78 ^{o}C for another 15 min, and then the propylene oxide (0.70 ml, 10 mmol) was added in one shot. The reaction was then allowed to stir at -78^{o}C for one hour and room temperature for another one hour. Upon the completion of the reaction, water and ammonium chloride were added to the reaction mixture. Layers were separated. The aqueous layer was extracted by diethyl ether twice. The organic layers were combined, dried over sodium sulfate, filtered. Diethyl ether was removed by atmospheric distillation. The residue was taken to next step without further purification.

To a flame-dried round-bottomed flask equipped with stir bar was added imidazole (1.02 g, 15 mmol). The flask was then purged with nitrogen for 10 min. Crude product dissolved in dichloromethane (15 ml) and trimethylamine (2.09 ml, 15 mmol) was then added. To the reaction mixture above was added tert-butyl(chloro)diphenylsilane (2.60 ml, 10 mmol) in drop. The reaction was allowed to stir at room temperature for 12 h. Water was then added to the reaction and layers were separated. The aqueous layer was extracted by dichloromethane twice. The organic layers were combined, dried over sodium sulfate, filtered and condense to crude.

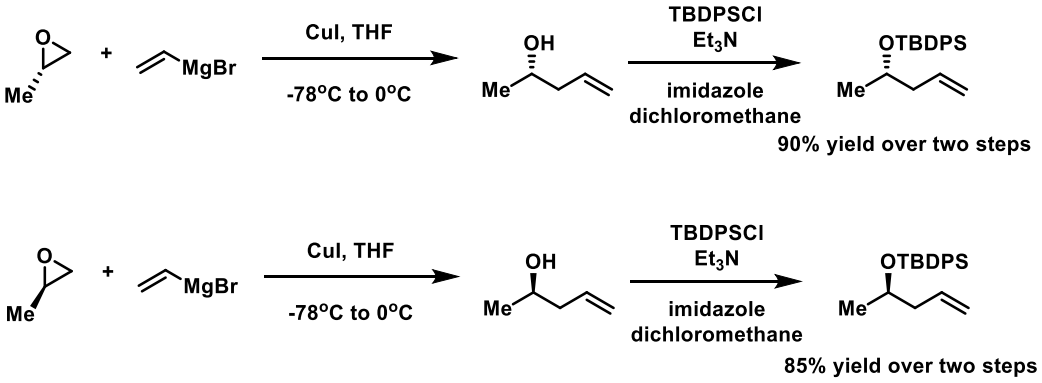

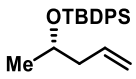

(R)-tert-butyl(pent-4-en-2-yloxy)diphenylsilane. The crude was purified through a silica gel column (pure hexane) to afford the product as a yellow oil

(2.93 g, 90% yield over 2 steps). Spectra data were in accordance with the literature report[32].

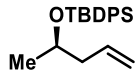

(S)-tert-butyl(pent-4-en-2-yloxy)diphenylsilane. The crude was purified through a silica gel column (pure hexane) to afford the product as a yellow oil (2.76 g, 85% yield over 2 steps). Spectra data were in accordance with the literature report[33].

1.5.4.5 Preparation of heteroaryl substituted terminal alkenes.

The following alkenes were prepared according to the literature procedure.[34]

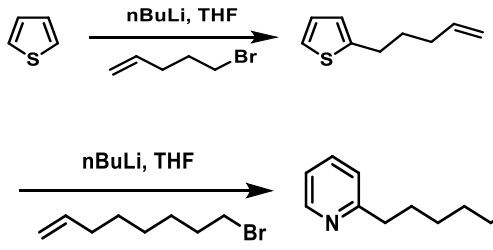

[32] Bujaranipalli, S.; Das, S.; *Tetrahedron Letters,* **2015**, *56*, 3747.
[33] Fuwa, H.; Sasaki, M. *Org. Lett.* **2008**, *10*, 2549.
[34] Kalaitzakis, D.; Antonatou, E.; Vassilikogiannakis, G. *Chem. Commun.* **2014**, *50*, 400.

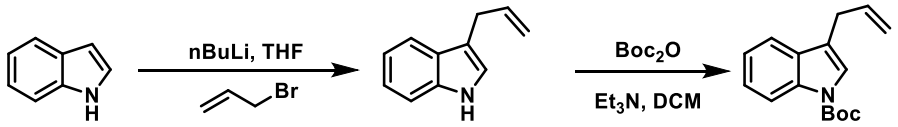

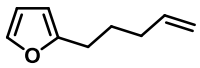

2-(pent-4-en-1-yl)furan. Spectral data is in accordance with literature report.[16] HRMS-(DART+) for $C_9H_{13}O$ $[M+H]^+$: calculated: 137.0966, found: 137.0972. IR(neat): 3074.91(w), 2931.49(m), 1640.38(m), 1438.92(m), 990.79(m), 910.58(s), 850.40(s), 688.71(s), cm^{-1}.

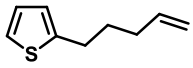

2-(pent-4-en-1-yl)thiophene. ^1H NMR (500 MHz, $CDCl_3$) δ 7.11 (d, 1H), 6.92 (dd, *J* = 5.2, 3.1 Hz, 1H), 6.79 (d, *J* = 3.4 Hz, 1H), 5.83 (ddt, *J* = 18.8, 10.2, 5.7 Hz, 1H), 5.04 (d, *J* = 17.1 Hz, 1H), 4.99 (d, *J* = 12.0 Hz, 1H),2.85 (t, *J* = 7.6 Hz, 2H), 2.13 (q, *J* = 7.0 Hz, 2H), 1.79 (p, *J* = 7.5, 2H).. ^{13}C NMR (151 MHz, $CDCl_3$) δ 148.0, 140.9, 129.3, 126.8, 125.5, 117.7, 35.7, 33.5, 31.9. HRMS-(DART+) for $C_9H_{13}S$ $[M+H]^+$: calculated: 153.0738, found: 153.0742.

IR(neat): 3074.90(w), 2976.43(w), 2931.72(m), 2855.96(w), 1640.42(m), 1438.99(m), 1239.25(m), 910.51(s), 688.57(s), cm^{-1}.

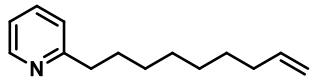

2-(non-8-en-1-yl)pyridine. ^{1}H NMR (600 MHz, $CDCl_3$) δ 8.52 (d, *J* = 4.9 Hz, 1H), 7.57 (td, *J* = 7.7, 1.9 Hz, 1H), 7.13 (d, *J* = 7.8 Hz, 1H), 7.08 (dd, *J* = 7.3, 5.1 Hz, 1H), 5.80 (ddt, *J* = 17.0, 10.2, 6.7 Hz, 1H), 4.98 (dd, *J* = 17.1, 1.9 Hz, 1H), 4.92 (dt, *J* = 10.2, 1.6 Hz, 1H), 2.77 (t, *J* = 7.9 Hz, 2H), 2.07 – 1.98 (m, 2H), 1.81 – 1.65 (m, 3H), 1.49 – 1.16 (m, 9H). ^{13}C NMR (151 MHz, $CDCl_3$) δ 165.2, 151.9, 141.8, 138.8, 125.3, 123.5, 116.8, 41.1, 36.4, 32.6, 31.99, 31.97, 31.8, 31.5. . HRMS-(DART+) for $C_{14}H_{22}N$ $[M+H]^+$: calculated: 204.1752, found: 204.175. IR(neat): 3075.46(w), 3006.84(w), 2924.45(s), 2853.67(s), 1589.37(m), 1473.65(m), 1433.62(m), 908.13(s), 747.12(s), cm^{-1}.

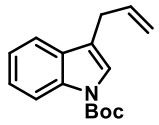

***tert*-butyl 2-allyl-1H-indole-1-carboxylate** ^{1}H NMR (600 MHz, $CDCl_3$) δ 8.15 (s, 1H), 7.53 (d, *J* = 7.8 Hz, 1H), 7.39 (s, 1H), 7.32 (d, *J* = 7.4 Hz, 1H),

7.24 (d, J = 7.4 Hz, 1H), 6.05 (ddt, J = 16.7, 10.0, 6.4 Hz, 1H), 5.19 (dd, J = 17.0, 1.6 Hz, 1H), 5.13 (dd, J = 9.9, 1.2 Hz, 1H), 3.46 (dd, J = 6.4, 1.2 Hz, 2H), 1.68 (s, 9H). ^{13}C NMR (151 MHz, $CDCl_3$) δ 152.5, 138.5, 133.2, 127.0, 125.5, 125.0, 121.9, 121.7, 118.8, 117.9, 86.0, 32.2, 31.0, 30.8. HRMS-(DART+) for $C_{16}H_{20}NO_2$ $[M]^+$: calculated: 258.1494, found: 258.1489. IR(neat): 2978.63(w), 1730.85(s), 1452.63(s), 1367.49(s), 1254.90(s), 1158.46(s), 1075.68(s), 744.59(m), cm^{-1}.

1.5.4.6. General Procedure for Benzyl protection of alkenes.

To a flame-dried round-bottomed flask equipped with a stir bar was added sodium hydride (144 mg, 6 mmol) in the glove box. The flask was sealed with rubber septa and then removed from the box. A nitrogen inlet was then applied. THF (20 ml) was added under nitrogen. The reaction flask was cooled down to 0^{o}C by an ice bath. Alcohol substrate (5 mmol) was then added dropwise. The reaction mixture was allowed to stir at room temperature for 30 minutes. Benzyl bromide (0.714 ml, 5 mmol) was then added to the reaction. The reaction mixture was allowed to stir at room temperature for 12 h. The reaction was then cooled down to 0 ^{o}C by ice bath. 10ml of water was added to the reaction. The mixture was then transferred to a supranational

funnel. Layers were then separated. The aqueous layer was extracted by dichloromethane (2*15 ml). The organic layers were combined, dried over sodium sulfate, filtered, and condense to crude.

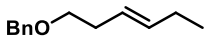

(E)-((hex-3-en-1-yloxy)methyl)benzene. The title compound was prepared according to the standard procedure. The crude was purified through a silica gel column (3% ethyl acetate in hexane) to afford the product as a clear oil (818 mg, 86% yield). Spectral data are in accordance with the literature report[35].

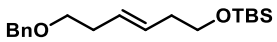

(E)-((6-(benzyloxy)hex-3-en-1-yl)oxy)(tert-butyl)dimethylsilane. The title compound was prepared according to the standard procedure. The starting material was synthesized according to the literature procedure[11]. The crude was purified through silica gel column (2% ethyl acetate in hexane) to afford the product as clear oil (1.36 g, 85% yield). ^{1}H NMR (400 MHz, $CDCl_3$) δ

[35] Movassaghi, M.; Ahmad, K. O. *Angew. Chem. Int. Ed.* **2008**, *47*, 8909 –8912.

7.32 (d, J = 4.6 Hz, 4H), 7.30 – 7.25 (m, 1H), 5.52 – 5.45 (m, 2H), 4.50 (s, 2H), 3.60 (t, J = 7.0 Hz, 2H), 3.47 (d, J = 7.0 Hz, 2H), 2.31 (dtd, J = 8.6, 4.9, 2.3 Hz, 2H), 2.21 (tdd, J = 6.4, 4.4, 1.4 Hz, 2H), 0.87 (s, 9H), 0.03 (s, 6H). ^{13}C NMR (126 MHz, $CDCl_3$) δ 138.8, 128.9, 128.7, 128.6, 127.9, 127.7, 73.1, 70.4, 63.4, 36.6, 33.4, 26.2, 18.6, -5.0. HRMS-(DART+) for $C_{19}H_{36}O_2SiN[M+NH_4]^+$: calculated: 338.2515, found: 338.2528.

1.5.4.7 General Procedure for Benzoyl Protection.

To a flame dried round-bottomed flask with a stir bar was added DMAP (61.09 mg, 0.5 mmol). The flask was then purged with nitrogen. DCM (20 ml), trans-5-decen-1-ol (0.594 ml, 5 mmol), trimethylamine (1.39 ml, 10 mmol) and benzoyl chloride (1.16 ml, 10 mmol) was then added. The reaction was allowed to stir at room temperature for 14 h.

The reaction was then quenched by water (10 ml). The reaction mixture was transferred to a sep funnel. The layers were separated. The aqueous layer was extracted by dichloromethane 3 times (20 ml per time). Organic layers were combined and dry over sodium sulfate, filtered, and condense to crude.

The crude mixture was purified on a silica gel column by 5% ethyl acetate in hexane to afford the product as yellow oil (1.30 g, 86% yield).

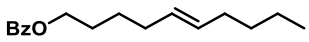

(E)-dec-5-en-1-yl benzoate. ^{1}H NMR (600 MHz, $CDCl_3$) δ 8.04 (d, J = 7.1 Hz, 2H), 7.55 (d, J = 7.4 Hz, 1H), 7.44 (t, J = 7.8 Hz, 2H), 5.54 – 5.19 (m, 2H), 4.32 (t, J = 6.6 Hz, 2H), 2.30 – 1.85 (m, 4H), 1.77 (dt, J = 15.2, 6.8 Hz, 2H), 1.63 – 1.39 (m, 2H), 1.39 – 1.26 (m, 3H), 0.89 (t, J = 7.0 Hz, 3H). ^{13}C NMR (151 MHz, $CDCl_3$) δ 166.8, 132.9, 131.3, 129.7, 129.7, 128.5, 65.1, 32.4, 32.3, 31.9, 28.3, 26.2, 22.4, 14.1. HRMS-(DART+) for C17H25O6 [M+H]+: calculated: 261.1855, found: 261.186.

1.5.5 Experimental Procedure for Alkene Diboration/Oxidation and Product Characterization.

1.5.5.1 General Procedure for terminal alkenes with TBS-DHG catalyst.

In the glove box, an oven-dried 2-dram vial equipped with a magnetic stir bar was charged with TBS-DHG catalyst (5.25 mg, 0.02 mmol, 0.1 equiv), propanediol diboron (67.91 mg, 0.40 mmol, 2.0 equiv), 4A molecular sieves

(20 mg), the alkene substrate (0.20 mmol, 1.0 equiv) and THF (0.20 mL). DBU (3.00 µl, 0.02 mmol, 0.1 equiv) was then added to the solution. The vial was sealed with a Teflon septum, removed from the glove box. The reaction mixture was stirred at room temperature for 12 hours. The reaction was cooled to 0 °C (ice/water) and charged with 3 M sodium hydroxide (0.6 mL), followed by dropwise addition of 30% hydrogen peroxide (0.3 mL). The reaction was gradually warmed to room temperature and stirred for another 4 hours at room temperature. The reaction was then cooled to 0 °C (ice/water) and saturated aqueous sodium thiosulfate (4 mL) was added dropwise over 5 minutes. The reaction mixture was diluted with ethyl acetate. Aqueous and organic layers were separated. The aqueous layer was further extracted with ethyl acetate (3 x 15 mL). The combined organics were dried over sodium sulfate, filtered, and concentrated by rotary evaporation to afford crude reaction mixture.

1.5.5.2 General Procedure for terminal alkenes with DHR catalyst.

In the glove box, an oven-dried 2-dram vial equipped with a magnetic stir bar was charged with DHR catalyst (2.6 mg, 0.02 mmol, 0.1 equiv), propanediol diboron (67.91 mg, 0.40 mmol, 2.0 equiv), 4A molecular sieves

(20 mg), the alkene substrate (0.20 mmol, 1.0 equiv) and THF (0.20 mL). DBU (0.003 ml, 0.02 mmol, 0.1 equiv) was then added to the solution. The vial was sealed with a Teflon septum, removed from the glove box. The reaction mixture was stirred at room temperature for 12 hours. The reaction was cooled to 0 °C (ice/water) and charged with 3 M sodium hydroxide (0.6 mL), followed by dropwise addition of 30% hydrogen peroxide (0.3 mL). The reaction was gradually warmed to room temperature and stirred for another 4 hours at room temperature. The reaction was then cooled to 0 °C (ice/water) and saturated aqueous sodium thiosulfate (4 mL) was added dropwise over 5 minutes. The reaction mixture was diluted with ethyl acetate. Aqueous and organic layers were separated. The aqueous layer was further extracted with ethyl acetate (3 x 15 mL). The combined organics were dried over sodium sulfate, filtered, and concentrated by rotary evaporation to afford crude reaction mixture.

1.5.5.3 General Procedure for internal alkenes with TBS-DHG catalyst.

In the glove box, an oven-dried 2-dram vial equipped with a magnetic stir bar was charged with TBS-DHG catalyst (7.87 mg, 0.03 mmol, 0.15 equiv), propanediol diboron (101.89 mg, 0.60 mmol, 2.0 equiv), 4 Å

molecular sieves (30 mg), the alkene substrate (0.20 mmol, 1.0 equiv) and ethyl acetate (0.20 mL). DBU (4.50 µl, 0.03 mmol, 0.15 equiv) was then added to the solution. The vial was sealed with a Teflon septum, removed from the glove box. The reaction mixture was allowed to stir at 40°C for 12 hours. The reaction was then cooled to 0 °C (ice/water) and charged with THF (0.2 ml), 3 M sodium hydroxide (0.6 mL), followed by dropwise addition of 30% hydrogen peroxide (0.3 mL). The reaction was gradually warmed to room temperature and stirred for another 4 hours at room temperature. The reaction was then cooled to 0 °C (ice/water) and saturated aqueous sodium thiosulfate (4 mL) was added dropwise over 5 minutes. The reaction mixture was diluted with ethyl acetate. Aqueous and organic layers were separated. The aqueous layer was further extracted with ethyl acetate (3 x 15 mL). The combined organics were dried over Na_2SO_4, filtered, and concentrated by rotary evaporation to afford crude reaction mixture.

1.5.5.4 General Procedure for terminal alkenes with TBS-DHG catalyst.

In the glove box, an oven-dried 2-dram vial equipped with a magnetic stir bar was charged with TBS-DHG catalyst (5.25 mg, 0.02 mmol, 0.1 equiv), Bis(neopentyl glycolato)diboron (90.35 mg, 0.40 mmol, 2.0 equiv), 4 Å

molecular sieves (20 mg), the alkene substrate (0.20 mmol, 1.0 equiv) and THF (0.20 mL). DBU (3.00 ml, 0.02 mmol, 0.1 equiv) was then added to the solution. The vial was sealed with a Teflon septum, removed from the glove box. The reaction mixture was stirred at room temperature for 12 hours. The reaction was cooled to 0 °C (ice/water) and charged with 3 M sodium hydroxide (0.6 mL), followed by dropwise addition of 30% hydrogen peroxide (0.3 mL). The reaction was gradually warmed to room temperature and stirred for another 4 hours at room temperature. The reaction was then cooled to 0 °C (ice/water) and saturated aqueous sodium thiosulfate (4 mL) was added dropwise over 5 minutes. The reaction mixture was diluted with ethyl acetate. Aqueous and organic layers were separated. The aqueous layer was further extracted with ethyl acetate (3 x 15 mL). The combined organics were dried over sodium sulfate, filtered, and concentrated by rotary evaporation to afford crude reaction mixture.

1.5.5.5 Full Characterizations and Proof of Stereochemistry (with TBS-DHG catalyst)

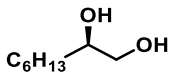

(R)-octane-1,2-diol (1.40). The diboration was performed according to the general procedure A with 1-octene (22.44 mg, 0.20 mmol, 32.4 μL). To remove the catalyst, the crude reaction mixture was treated with TBAF (1.0 M in THF, 0.20 mL) at room temperature and stirred for 0.5h. The reaction mixture was then concentrated by rotary evaporation, and the resulting crude product was purified on silica gel (50% ethyl acetate in hexanes) to afford the product as white solid (28.30 mg, 97% yield). Spectral data and optical rotation are in accordance with the literature report.[36] HRMS-(DART+) for C8H22NO2 $[M+NH_4]^+$: calculated: 164.1651, found: 164.1655.

Analysis of Stereochemistry:

The 1,2-diol was treated with 2,2-dimethoxypropane and catalytic toluenesulfonic acid. The resulting ketal was compared to the racemic ketal of octane-1,2-diol prepared from dihydroxylation of 1-octene with ruthenium trichloride and sodium periodiate.[37] The absolute stereochemistry was assigned by analogy.

Chiral GLC (β-dex, Supelco, 100 °C 30min, 20 psi)- analysis of the acetonide of octane-1,2-diol.

[36] Toribatake, K.; Nishiyama, H; *Angew. Chem. Int. Ed.* **2013**, *52*, 11011.
[37] Shing, T. K. M.; Tam, E. K. W.; Tai, V. W.-F.; Chung, I. H. F.; Jiang, Q. *Chem. Eur. J.* **1996**, *2*, 50.

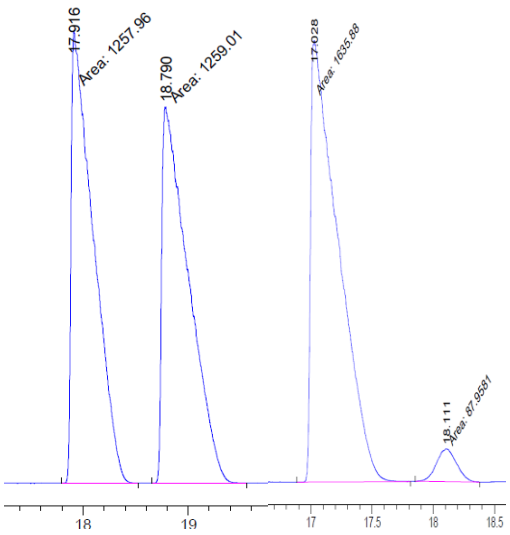

racemic product diboration product

Peak #	RetTime [min]	Type	Width [min]	Area [pA*s]	Height [pA]	Area %
1	17.028	MM	0.2614	1635.88281	104.29852	94.89755
2	18.111	MM	0.1889	87.95814	7.76046	5.10245

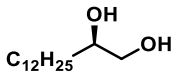

(R)-tetradecane-1,2-diol (1.106). The diboration was performed according to the general procedure A with 1-tetradecene substrate (94%, 41.78 mg, 0.20 mmol, 54 μL). The crude reaction mixture was purified on silica gel (40% ethyl acetate in hexanes) to afford the product as white solid (43.7 mg, 95% yield). Spectral data and optical rotation are in accordance with the literature

report. [38] HRMS-(DART+) for C14H34NO2 $[M+NH4]^+$: calculated: 248.2590, found: 248.2583.

Analysis of Stereochemistry:

The 1,2-diol was treated with 2,2-dimethoxypropane and catalytic toluenesulfonic acid. The resulting ketal was compared to the racemic ketal of tetradecane-1,2-diol prepared from dihydroxylation of 1-tetradecene with ruthenium trichloride and sodium periodiate.[19] The absolute stereochemistry was assigned by analogy. The authentic (*R*)-isomer was prepared from the Sharpless asymmetric dihydroxylation of 1-tetradecene utilizing AD-mix-β[39].

Chiral GLC (β-dex, Supelco, 120 °C 15min, then 0.5°C /min to 180°C, 20 psi)-analysis of the acetonide of tetradecane-1,2-diol.

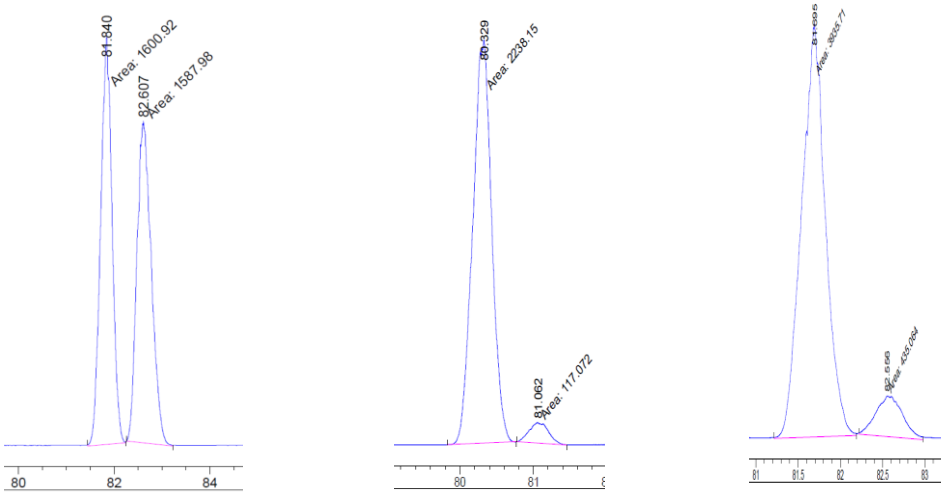

[38] Stallforth, P.; Adibekian, A.; Seeberger, H. P. *Org. Lett.,* **2008,** *10,* 1573.

[39] Sharpless, K. B.; Amberg, W.; Bennani, Y. L.; Crispino, G. A.; Hartung, J.; Jeong, K.-S.; Kwong, H.-L.; Morikawa, K.; Wang, Z.-M.; Xu, D.; Zhang, X.-L. *J. Org. Chem*. **1992**, *57*, 2768.

racemic product diboration product authentic product

Peak #	RetTime [min]	Type	Width [min]	Area [pA*s]	Height [pA]	Area %
1	80.329	MM	0.2978	2238.15308	125.27486	95.02927
2	81.062	MM	0.3038	117.07190	6.42210	4.97073

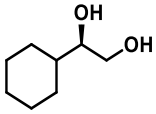

(R)-1-cyclohexylethane-1,2-diol (1.107). The diboration was performed according to the general procedure A with vinyl cyclohexane (22.04 mg, 0.20 mmol, 27.4 μL). To remove the catalyst, the crude reaction mixture was treated with TBAF (1.0 M in THF, 0.20 mL) at room temperature and stirred for 0.5h. The reaction mixture was then concentrated by rotary evaporation, and the resulting crude product was purified on silica gel (50% ethyl acetate in hexanes) to afford the product as white solid (24.2 mg, 84% yield). Spectral data and optical rotation are in accordance with the literature report.[40] HRMS-(DART+) for $C_8H_{15}O$ $[M+H-H_2O]^+$: calculated:127.1123, found:127.1117.

Analysis of Stereochemistry:

[40] Gally, C.; Nestl, B. M.; Hauer, B. *Angew. Chem. Int. Ed.* **2015,** *54,* 12952.

The 1,2-diol was treated with 2,2-dimethoxypropane and catalytic toluenesulfonic acid. The resulting ketal was compared to the racemic ketal of 1-cyclohexylethane-1,2-diol prepared from dihydroxylation of vinyl cyclohexane with ruthenium trichloride and sodium periodiate.[19] The absolute stereochemistry was assigned by analogy

Chiral GLC (β-dex, Supelco, 130 °C 20 min)- analysis of the acetonide of 1-cyclohexylethane-1,2-diol

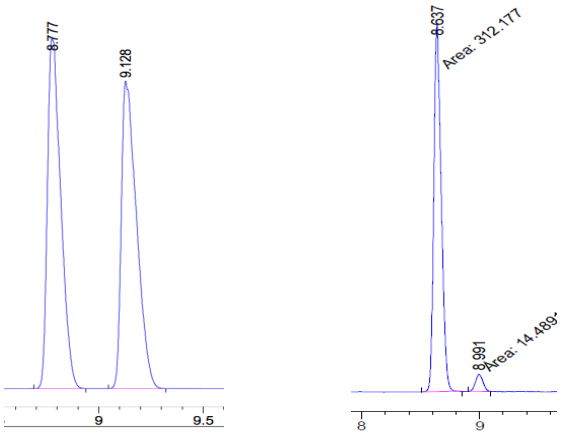

racemic product diboration product

Peak #	RetTime [min]	Type	Width [min]	Area [pA*s]	Height [pA]	Area %
1	8.637	MM	0.0728	312.17676	71.49557	95.56456
2	8.991	MM	0.0726	14.48905	3.32531	4.43544

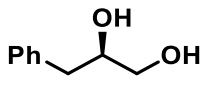

(R)-3-phenylpropane-1,2-diol (1.108). The diboration was performed according to the general procedure A with allyl benzene (23.64 mg, 0.50

mmol, 26.56 μL). The crude reaction mixture was purified on silica gel (50% ethyl acetate in hexanes) to afford the product as white solid (28.2 mg, 73% yield). Spectral data and optical rotation are in accordance with the literature report.[41] HRMS-(DART+) for $C_9H_{11}O$ $[M-H_2O+H]^+$: calculated: 135.081, found: 135.0804.

Analysis of Stereochemistry:

The 1,2-diol was compared to the racemic 3-phenylpropane-1,2-diol prepared from dihydroxylation of allyl benzene with ruthenium trichloride and sodium periodiate.[19] The absolute stereochemistry was assigned by analogy.

Chiral SFC (Chiracel OJ-H, 4% isopropanol, 3 mL/min, 100 bar, 35 °C, 210-270 nm) – analysis of 3-phenylpropane-1,2-diol.

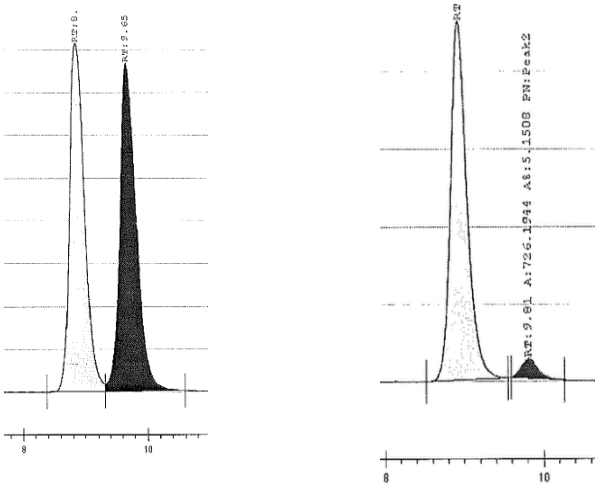

[41] Toribatake, K.; Nishiyama, H.; *Angew. Chem. Int. Ed.* **2013**, *52*, 11011.

racemic product diboration product

Peak Info					
Peak No	% Area	Area	RT (min)	Height (mV)	K'
1	94.8492	13372.3692	8.93	927.252	0.0068
2	5.1508	726.1944	9.81	50.3872	0.0074
Total:	100	14098.5636			

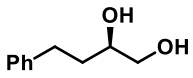

(R)-4-phenylbutane-1,2-diol (1.109). The diboration was performed according to the general procedure A with 4-phenyl-1-butene (26.44 mg, 0.20 mmol, 30.04 μL). The crude reaction mixture was purified on silica gel (50% ethyl acetate in hexanes) to afford the product as clear oil (29.9 mg, 92% yield). Spectral data and optical rotation are in accordance with the literature report.[23] HRMS-(DART+) for C10H15O2 $[M+H]^+$: calculated: 167.1072, found: 167.108.

Analysis of Stereochemistry:

The 1,2-diol was treated with 2,2-dimethoxypropane and catalytic toluenesulfonic acid. The resulting ketal was compared to the racemic ketal of 4-phenylbutane-1,2-diol prepared from dihydroxylation of 4-phenyl-1-butene with ruthenium trichloride and sodium periodiate.[19] The absolute stereochemistry was assigned by analogy.

Chiral GLC (β-dex, Supelco, 120 °C 5min, then 0.5°C /min to 140°C, 20 psi)-analysis of the acetonide of 4-phenylbutane-1,2-diol.

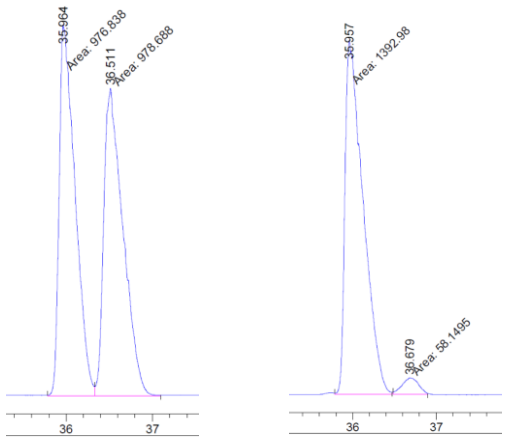

racemic product diboration product

Peak #	RetTime [min]	Type	Width [min]	Area [pA*s]	Height [pA]	Area %
1	35.228	MM	0.2604	2155.20508	137.93863	96.27333
2	35.995	MM	0.2186	83.42645	6.36162	3.72667

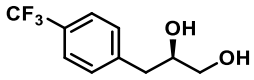

(R)-3-(4-(trifluoromethyl)phenyl)propane-1,2-diol (1.110). The diboration was performed according to the general procedure A with 1-allyl-4-(trifluoromethyl)benzene (37.24 mg, 0.20 mmol, 33.48 µL). The crude

reaction mixture was purified on silica gel (50% ethyl acetate in hexanes) to afford the product as white solid (33.03 mg, 75% yield). ^{1}H NMR (600 MHz, $CDCl_3$) δ 7.57 (d, *J* = 7.9 Hz, 2H), 7.35 (d, *J* = 8.0 Hz, 2H), 4.02 – 3.90 (m, 1H), 3.71 (d, *J* = 11.3 Hz, 1H), 3.52 (dd, *J* = 10.8, 7.1 Hz, 1H), 2.95 – 2.74 (m, 2H), 2.17 (s, 1H), 1.96 (s, 1H). ^{13}C NMR (151 MHz, $CDCl_3$) δ 144.7, 132.3, 128.2, 128.1, 128.1, 128.1, 75.3, 68.6, 42.1. HRMS-(DART+) for $C_{10}H_{10}F_3O$ $[M\text{-}H_2O+H]^+$: calculated: 203.0684, found: 203.0691. IR (neat): 3353.92 (w), 2927.94(w), 1325.19(s), 1161.95(m), 1110.74(s), 1066.81(s), 1019.48(m). $[\alpha]_D^{20}$= +13.045 (c=1.0725, $CHCl_3$, l=50 mm).

Analysis of Stereochemistry:

The 1,2-diol was compared to the racemic 3-(4-(trifluoromethyl)phenyl)propane-1,2-diol prepared from dihydroxylation of 1-allyl-4-(trifluoromethyl)benzene with ruthenium trichloride and sodium periodiate.[19] The absolute stereochemistry was assigned by analogy.

Chiral SFC (Chiracel AS-H, 8% isopropanol, 3 mL/min, 100 bar, 35 °C, 210-270 nm) – analysis of 3-(4-(trifluoromethyl)phenyl)propane-1,2-diol.

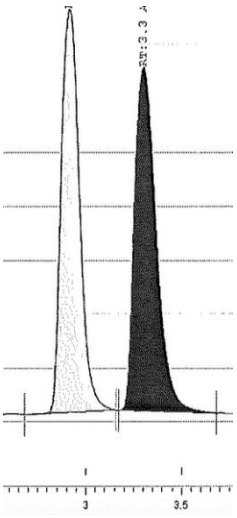

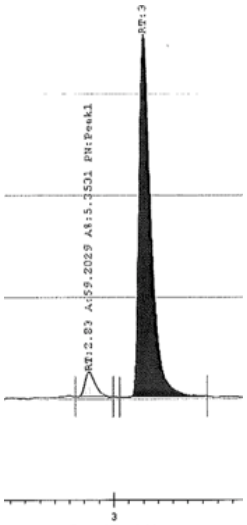

racemic product diboration product

Peak Info

Peak No	% Area	Area	RT (min)	Height (mV)	K'
1	5.3531	59.2029	2.83	12.2273	0.0027
2	94.6469	1046.7511	3.2	178.6614	0.003
Total:	100	1105.954			

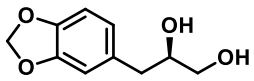

(R)-3-(benzo[d][1,3]dioxol-5-yl)propane-1,2-diol (1.111). The diboration was performed according to the general procedure A with safrole (32.44 mg, 0.20 mmol, 29.60 μL). The crude reaction mixture was purified on silica gel (50% ethyl acetate in hexanes) to afford the product as white solid (34.53 mg, 88% yield). Spectral data and optical rotation are in accordance with the

literature report.[42] HRMS-(DART+) for $C_{10}H_{11}O_3$ $[M-H_2O+H]^+$: calculated: 179.0708, found: 179.0715.

Analysis of Stereochemistry:

The 1,2-diol was compared to the racemic 3-(benzo[d][1,3]dioxol-5-yl)propane-1,2-diol prepared from dihydroxylation of safrole with ruthenium trichloride and sodium periodiate.[19] The absolute stereochemistry was assigned by analogy.

Chiral SFC (Chiracel ODR-H, 8% isopropanol, 3 mL/min, 100 bar, 35 °C, 210-270 nm) – analysis of 3-(benzo[d][1,3]dioxol-5-yl)propane-1,2-diol.

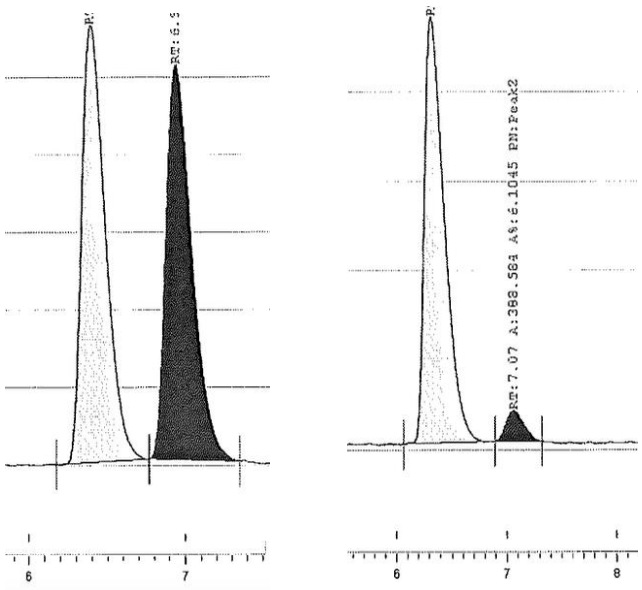

[42] Sawant, R. T.; Waghmode, S. B. *Synthetic Communications.* **2010**, *40*, 2269.

racemic product diboration product

Peak Info					
Peak No	% Area	Area	RT (min)	Height (mV)	K'
1	93.8955	5976.94	6.31	475.5711	0.0084
2	6.1045	388.584	7.07	33.6678	0.0094
Total:	100	6365.524			

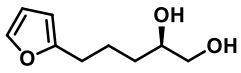

(R)-5-(furan-2-yl)pentane-1,2-diol (1.112). The diboration was performed according to the general procedure A with 2-(pent-4-en-1-yl)furan (27.22 mg, 0.20 mmol). To remove the catalyst, the crude reaction mixture was treated with TBAF (1.0 M in THF, 0.20 mL) at room temperature and stirred for 0.5h. The reaction mixture was then concentrated by rotary evaporation, and the resulting crude product was purified on silica gel (50% ethyl acetate in hexanes) to afford the product as a clear oil (32.98 mg, 97% yield). Spectral data is in accordance with the literature report.[16] HRMS-(DART+) for C9H15O3 $[M+H]^+$: calculated: 171.1021, found: 171.1016. IR(neat): 3388.02(m), 2936.59(m), 2871.32(m), 1146.36(s), 1089.11(s), 1046.01(s), 600.19(w). $[\alpha]_D^{20}$= -11.958 (c=1.02, $CHCl_3$, l=50 mm).

Analysis of Stereochemistry:

The 1,2-diol was compared to the racemic 5-(furan-2-yl)pentane-1,2-diol prepared from dihydroxylation of 2-(pent-4-en-1-yl)furan with ruthenium trichloride and sodium periodiate.[19] The absolute stereochemistry was assigned by analogy.

Chiral SFC (Chiracel ODR-H, 5% isopropanol, 3 mL/min, 100 bar, 35 °C, 210-270 nm) – analysis of 5-(furan-2-yl)pentane-1,2-diol.

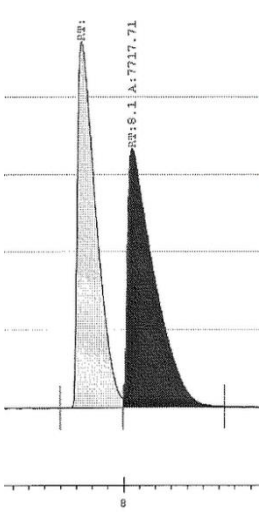

racemic product

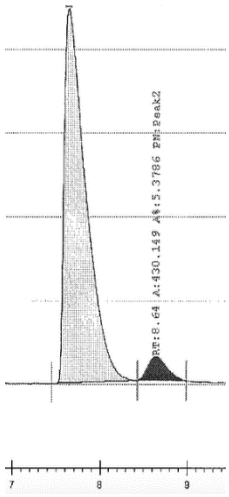

diboration product

Peak Info					
Peak No	% Area	Area	RT (min)	Height (mV)	K'
1	94.6214	7567.2424	7.64	446.8813	0.0087
2	5.3786	430.149	8.64	28.7569	0.0098
Total:	100	7997.3914			

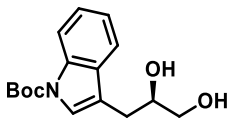

***tert*-butyl (R)-3-(2,3-dihydroxypropyl)-1H-indole-1-carboxylate (1.113).**

The diboration was performed according to the general procedure A with tert-

butyl 3-allyl-1H-indole-1-carboxylate (51.47 mg, 0.20 mmol). The crude reaction mixture was purified on silica gel (50% ethyl acetate in hexanes) to afford the product as white solid (49.50 mg, 85% yield). ^{1}H NMR (600 MHz, $CDCl_3$) δ 8.14 (s, 1H), 7.55 (d, *J* = 7.7 Hz, 1H), 7.52 – 7.45 (m, 1H), 7.33 (t, *J* = 7.8 Hz, 1H), 7.25 (d, *J* =7.7 Hz, 1H), 4.18 – 3.99 (m, 1H), 3.77 (ddd, *J* = 11.1, 6.4, 3.3 Hz, 1H), 3.59 (ddd, *J* = 11.1, 6.8, 5.4 Hz, 1H), 2.92 (ddd, *J* = 14.6, 5.3, 1.1 Hz, 1H), 2.87 (ddd, *J* = 14.6, 7.9, 0.9 Hz, 1H), 2.11 (s, 1H), 1.87 (s, 1H), 1.67 (s, 9H). ^{13}C NMR (151 MHz, $CDCl_3$) δ 152.3, 138.3, 133.1, 127.2, 126.7, 125.2, 121.6, 119.0, 118.0, 86.3, 74.1, 68.9, 31.7, 30.9. HRMS-(DART+) for $C16H22NO_4$ $[M+H]^+$: calculated: 292.1549, found: 292.1541. IR (neat): 3349.53(br), 2977.24(w), 2930.89(w), 1726.44(s), 1451.24(s), 1308.41(s), 1225.24(s), 1024.74(s), 856.53(s), 766.87(s), 745.67(s). $[\square]_D^{20}$= +3.498 (c=1.086, $CHCl_3$, l=50 mm).

Analysis of Stereochemistry:

The 1,2-diol was compared to the racemic tert-butyl-3-(2,3-dihydroxypropyl)-1H-indole-1-carboxylate prepared from dihydroxylation of tert-butyl 3-allyl-1H-indole-1-carboxylate with ruthenium trichloride and sodium periodiate.[19] The absolute stereochemistry was assigned by analogy.

Chiral SFC (Chiracel ODR-H, 5% isopropanol, 3 mL/min, 100 bar, 35 °C, 210-270 nm) – analysis of tert-butyl-3-(2,3-dihydroxypropyl)-1H-indole-1-carboxylate.

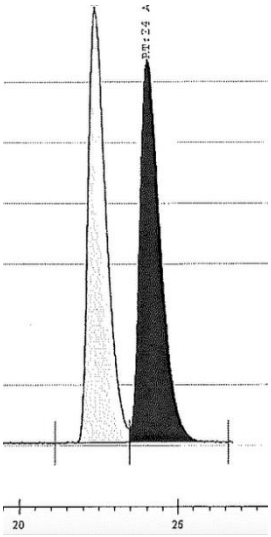

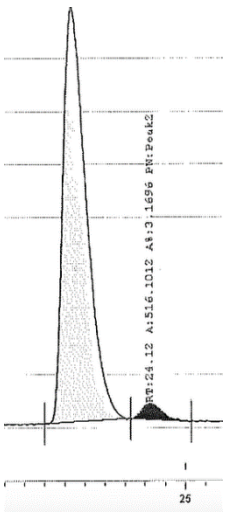

racemic product diboration product

Peak Info

Peak No	% Area	Area	RT (min)	Height (mV)	K'
1	96.8304	15766.7729	22.16	396.0168	0.0212
2	3.1696	516.1012	24.12	15.3297	0.0231
Total:	100	16282.8741			

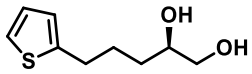

(R)-5-(thiophen-2-yl)pentane-1,2-diol (1.114). The diboration was performed according to the general procedure A with 2-(pent-4-en-1-yl)thiophene (30.45 mg, 0.20 mmol). To remove the catalyst, the crude

reaction mixture was treated with TBAF (1.0 M in THF, 0.20 mL) at room temperature and stirred for 0.5h. The reaction mixture was then concentrated by rotary evaporation, and the resulting crude product was purified on silica gel (50% ethyl acetate in hexanes) to afford the product as clear oil (34.27 mg, 92% yield). ^{1}H NMR (400 MHz, $CDCl_3$) δ 7.11 (dd, J = 5.1, 1.2 Hz, 1H), 6.91 (dd, J = 5.1, 3.3 Hz, 1H), 6.79 (dt, J = 3.4, 1.0 Hz, 1H), 3.74 (dtd, J = 9.8, 6.5, 3.0 Hz, 1H), 3.65 (dd, J = 11.0, 3.1 Hz, 1H), 3.44 (dd, J = 11.0, 7.6 Hz, 1H), 2.87 (t, J = 7.5 Hz, 2H), 2.27 – 1.59 (m, 3H), 1.59 – 1.45 (m, 2H). ^{13}C NMR (101 MHz, $CDCl_3$) δ 144.9, 126.7, 124.2, 123.0, 72.0, 66.8, 32.4, 29.8, 27.7. HRMS-(DART+) for $C_9H_{13}OS$ $[M\text{-}H_2O+H]^+$: calculated: 169.0687, found: 169.0693. IR (neat): 3346.03(br), 2934.55(m), 2861.76(w), 1428.62(w), 1050.73(s), 870.95(w), 849.36(m), 823.85(w). $[\alpha]_D^{20}$= -1.598 (c=0.685, $CHCl_3$, l=50 mm).

Analysis of Stereochemistry:

The 1,2-diol was compared to the racemic 5-(thiophen-2-yl)pentane-1,2-diol prepared from dihydroxylation of 2-(pent-4-en-1-yl)thiophene with ruthenium trichloride and sodium periodiate.[19] The absolute stereochemistry was assigned by analogy.

Chiral SFC (Chiracel OJ-H, 4% isopropanol, 3 mL/min, 100 bar, 35 °C, 210-270 nm) – analysis of 5-(thiophen-2-yl)pentane-1,2-diol.

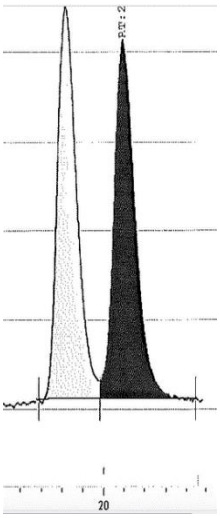

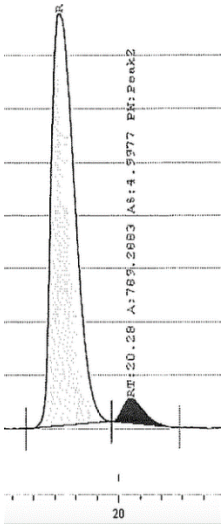

racemic product diboration product

Peak Info					
Peak No	% Area	Area	RT (min)	Height (mV)	K'
1	95.0023	15003.6324	18.6	386.6355	0.0262
2	4.9977	789.2883	20.28	23.4958	0.0286
Total:	100	15792.9207			

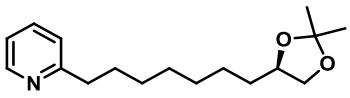

(R)-2-(7-(2,2-dimethyl-1,3-dioxolan-4-yl)heptyl)pyridine (1.115). The diboration was performed according to the general procedure A with 2-(non-8-en-1-yl)pyridine (40.67 mg, 0.20 mmol). The crude reaction mixture was dissolved in ethyl acetate (5 mL) and filtered through a short pad of silica gel

with ethyl acetate (10 ml). Solvent was then removed by rotatory evaporation. Because the product diol co-eluted with 1,3-propanediol, the resulting residue was treated with 2,2-dimethoxypropane (0.50 mL) and catalytic toluenesulfonic acid, then stirred at 60 °C for 30 min. Reaction mixture was filtered through a short pad of silica gel with 30% ethyl acetate in hexane. Solvents were removed by rotatory evaporation to afford the crude acetal product. The crude acetal product was purified on silica gel (10% ethyl acetate in hexanes) to afford the product as colorless oil (38.84 mg, 70% yield). ^{1}H NMR (400 MHz, $CDCl_3$) δ 8.50 (ddd, *J* = 4.9, 1.9, 1.0 Hz, 1H), 7.56 (td, *J* = 7.6, 1.9 Hz, 1H), 7.11 (dt, *J* = 7.8, 1.1 Hz, 1H), 7.07 (ddd, *J* = 7.5, 4.9, 1.2 Hz, 1H), 4.14 – 3.93 (m, 2H), 3.50 – 3.43 (m, 1H), 2.81 – 2.70 (m, 2H), 1.77 – 1.55 (m, 4H), 1.38 (s, 3H), 1.37 – 1.26 (m, 13H). ^{13}C NMR (151 MHz, $CDCl_3$) δ 165.1, 151.8, 138.8, 125.3, 123.5, 111.2, 78.8, 72.2, 41.1, 36.2, 32.5, 32.2, 32.0, 31.9, 29.6, 28.41, 28.37. HRMS-(DART+) for $C_{14}H_{22}NO$ $[M\text{-}H_2O+H]^+$: calculated: 220.1701, found: 220.1705. IR (neat): 2984.46(w), 2928.68(s), 2855.59(m), 1589.88(m), 1568.79(w), 1473.87(m), 1434.04(m), 1377.75(m), 1368.34(m), 1213.79(m), 1058.04(s). $[\alpha]_D^{20}$= -10.870 (c=1.02, $CHCl_3$, l=50 mm).

Analysis of Stereochemistry:

The acetal was compared to the racemic 2-(7-(2,2-dimethyl-1,3-dioxolan-4-yl)heptyl)pyridine prepared from dihydroxylation of 2-(non-8-en-1-yl)pyridine with ruthenium trichloride and sodium periodiate.[19] The absolute stereochemistry was assigned by analogy.

Chiral SFC (Chiracel AD-H, 3% isopropanol, 3 mL/min, 100 bar, 35 °C, 210-270 nm) – analysis of 2-(7-(2,2-dimethyl-1,3-dioxolan-4-yl)heptyl)pyridine.

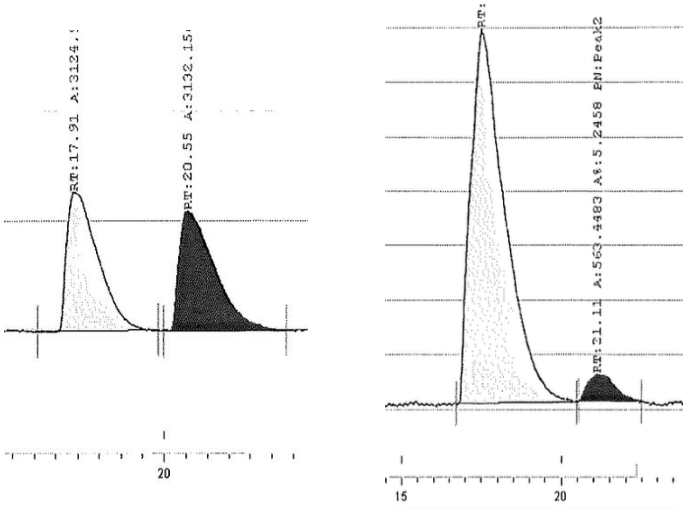

racemic product diboration product

Peak Info

Peak No	% Area	Area	RT (min)	Height (mV)	K'
1	94.7542	10177.4096	17.48	137.4022	0.0185
2	5.2458	563.4483	21.11	9.7609	0.0223
Total:	100	10740.8579			

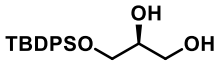

(S)-3-((tert-butyldiphenylsilyl)oxy)propane-1,2-diol (1.116). The diboration was performed according to the general procedure A with

(allyloxy)(tert-butyl)diphenylsilane (59.30 mg, 0.20 mmol). The crude reaction mixture was purified on silica gel (30% ethyl acetate in hexanes) to afford the product as white solid (52.22 mg, 79% yield). ^{1}H NMR (600 MHz, $CDCl_3$) δ 7.69 – 7.62 (m, 4H), 7.47 – 7.42 (m, 2H), 7.42 – 7.38 (m, 4H), 3.87 – 3.58 (m, 5H), 2.55 (d, J = 5.3 Hz, 1H), 1.93 (t, J = 6.1 Hz, 1H), 1.07 (s, 9H). ^{13}C NMR (151 MHz, $CDCl_3$) δ 135.5, 135.5, 132.9, 132.8, 129.9, 129.9, 127.9, 127.8, 71.9, 71.8, 65.2, 63.8, 26.9, 26.9, 26.8, 19.2. HRMS-(DART+) for $C_{19}H_{27}O_3Si$ $[M+H]^+$: calculated: 331.1730, found: 331.1731. IR (neat):3392.72(br), 3071.05(w), 3048.48(w), 2999.17(m), 2930.34(m), 2857.66(m), 1427.57(m), 1112.13(s), 823.82(m), 740.33(m), 701.55(s), 613.59(m). $[\alpha]_D^{20}$= -4.650 (c=1.213, $CHCl_3$, l=50 mm).

Analysis of Stereochemistry:

The 1,2-diol was compared to the racemic 3-((tert-butyldiphenylsilyl)oxy)propane-1,2-diol prepared from dihydroxylation of (allyloxy)(tert-butyl)diphenylsilane with ruthenium trichloride and sodium periodiate.[19] The absolute stereochemistry was assigned by analogy.

Chiral SFC (Chiracel OD-H, 8% isopropanol, 3 mL/min, 100 bar, 35 °C, 210-270 nm) – analysis of 3-((tert-butyldiphenylsilyl)oxy)propane-1,2-diol.

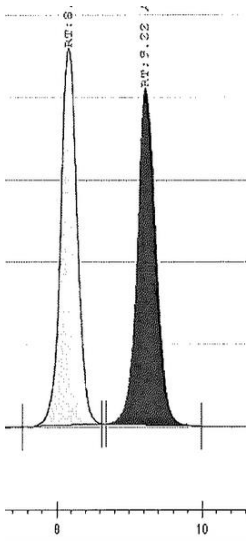

racemic product

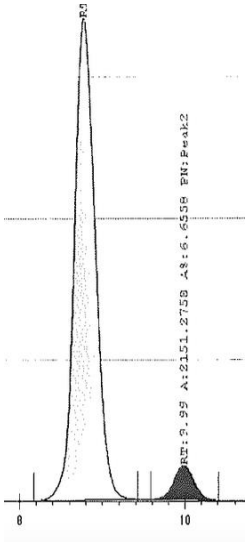

diboration product

Peak Info

Peak No	% Area	Area	RT (min)	Height (mV)	K'
1	49.7193	14564.0959	8.16	914.0679	0.0136
2	50.2807	14728.5662	9.22	815.9865	0.0154
Total:	100	29292.6621			

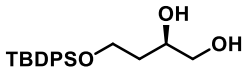

(R)-4-((tert-butyldiphenylsilyl)oxy)butane-1,2-diol (1.44). The diboration was performed according to the general procedure A with (but-3-en-1-yloxy)(tert-butyl)diphenylsilane (62.10 mg, 0.20 mmol). The crude reaction mixture was purified on silica gel (30% ethyl acetate in hexanes) to afford the product as white solid (61.33 mg, 89% yield). Spectral data and optical rotation are in accordance with literature report.[23] HRMS-(DART+) for $C_{20}H_{29}O_3Si$ $[M+H]^+$: calculated: 345.1886, found: 345.1895. IR (neat):

3392.72(br), 3071.05(w), 3048.48(w), 2999.17(m), 2930.34(m), 2857.66(m), 1471.82(m), 1112.13(s), 823.82(m), 740.33(m), 701.55(s), 613.59(m), 505.32(m), 489.90(m).

Analysis of Stereochemistry:

The 1,2-diol was compared to the 4-((tert-butyldiphenylsilyl)oxy)butane-1,2-diol prepared from dihydroxylation of (but-3-en-1-yloxy)(tert-butyl)diphenylsilane with ruthenium trichloride and sodium periodiate.[13] The absolute stereochemistry was assigned by analogy.

Chiral SFC (Chiracel ODR-H, 5% isopropanol, 3 mL/min, 100 bar, 35 °C, 210-270 nm) – analysis of 4-((tert-butyldiphenylsilyl)oxy)butane-1,2-diol.

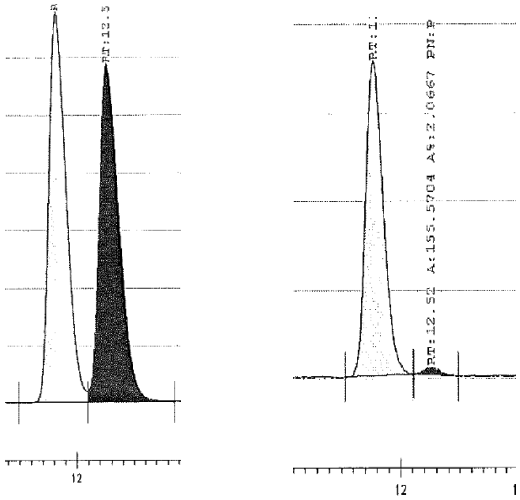

racemic product diboration product

Peak Info					
Peak No	% Area	Area	RT (min)	Height (mV)	K'
1	97.9333	7371.9665	11.54	353.533	0.0092
2	2.0667	155.5704	12.52	8.819	0.01
Total:	100	7527.5369			

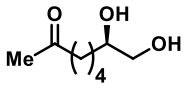

(R)-7,8-dihydroxyoctan-2-one (1.118). The diboration was performed according to the general procedure A with oct-7-en-2-one (25.24 mg, 0.20 mmol). The crude reaction mixture was purified on silica gel (80% ethyl acetate in hexanes) to afford the product as clear oil (22.43 mg, 70% yield). ^{1}H NMR (500 MHz, $CDCl_3$) δ 3.76 – 3.68 (m, 1H), 3.64 (dd, J = 11.1, 3.1 Hz, 1H), 3.43 (dd, J = 11.0, 7.6 Hz, 1H), 2.45 (t, J = 7.2 Hz, 2H), 2.13 (s, 3H), 1.68 – 1.50 (m, 2H), 1.51 – 1.28 (m, 4H). ^{13}C NMR (126 MHz, $CDCl_3$) δ 209.1, 76.7, 71.9, 66.8, 43.5, 32.8, 29.9, 25.0, 23.5. HRMS-(DART+) for $C_8H_{15}O_3$ $[M+H]^+$: calculated: 159.1021, found: 159.1017. IR (neat): 3398.9 (br s), 2926.2 (s), 2858.8 (m), 1706.4 (s), 1459.5 (w), 1408.9 (w), 1363.0 (m), 1163.4 (w), 1054.2 (m), 599.8 (w). $[\alpha]_D^{20}$= -3.587 (c=1.150, $CHCl_3$, l=50 mm).

Analysis of Stereochemistry:

The 1,2-diol was treated with 2,2-dimethoxypropane and catalytic toluenesulfonic acid. The resulting ketal was compared to the racemic ketal of 7,8-dihydroxyoctan-2-one prepared from dihydroxylation of oct-7-en-2-one with ruthenium trichloride and sodium periodiate.[19] The absolute stereochemistry was assigned by analogy.

Chiral GLC (β-dex, Supelco, 70 °C 5min, 2°C/min to 180°C, 20 psi)- analysis of the acetonide of 7,8-dihydroxyoctan-2-one.

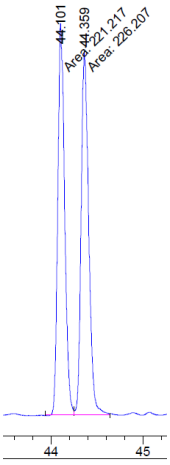

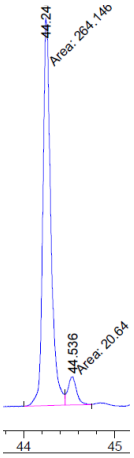

racemic product diboration product

Peak #	RetTime [min]	Type	Width [min]	Area [pA*s]	Height [pA]	Area %
1	44.240	MF	0.1013	264.14587	43.46013	92.75245
2	44.536	FM	0.1091	20.64001	3.15330	7.24755

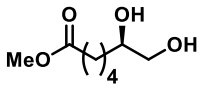

methyl (R)-6,7-dihydroxyheptanoate (1.117). The diboration was performed according to the general procedure A with methyl hept-6-enoate (28.44 mg, 0.20 mmol). The crude reaction mixture was purified on silica gel (ethyl acetate) to afford the product as clear oil (33.48 mg, 95% yield).

Spectral data and optical rotation are in accordance with literature report.[43] HRMS-(DART+) for $C_8H_{17}O_4$ $[M+H]^+$: calculated: 177.1127, found: 177.1129. IR (neat): 3376.11(br), 2936.54(m), 2864.97(m), 1734.23(s), 1437.01(m), 1200.46(s), 1174.54(s), 1104.72(s), 1052.86(s), 1016.51(s).

Analysis of Stereochemistry:

The 1,2-diol was treated with 2,2-dimethoxypropane and catalytic toluenesulfonic acid. The resulting ketal was compared to the racemic ketal of 6,7-dihydroxyheptanoate prepared from dihydroxylation of methyl hept-6-enoate with ruthenium trichloride and sodium periodiate.[19] The absolute stereochemistry was assigned by analogy.

Chiral GLC (β-dex, Supelco, 70 °C 5min, 2°C/min to 180°C, 20 psi)- analysis of the acetonide of 6,7-dihydroxyheptanoate.

racemic product diboration product

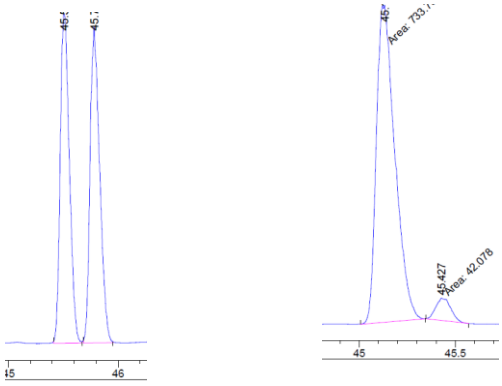

[43] Fang, L.; Yan, L.; Haeffner, F.; Morken, J. P. *J. Am. Chem. Soc.* **2016**, *138*, 2508.

Peak #	RetTime [min]	Type	Width [min]	Area [pA*s]	Height [pA]	Area %
1	45.132	MM	0.1115	733.78345	109.71555	94.57661
2	45.427	MM	0.0911	42.07802	7.70144	5.42339

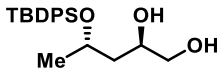

(2R,4R)-4-((tert-butyldiphenylsilyl)oxy)pentane-1,2-diol (1.121). The diboration was performed according to the general procedure A with (R)-tert-butyl(pent-4-en-2-yloxy)diphenylsilane (64.91 mg, 0.20 mmol). The crude reaction mixture was purified on silica gel (30% ethyl acetate in hexane) to afford the product as clear oil (52.35 mg, 73% yield). ^{1}H NMR (600 MHz, $CDCl_3$) δ 7.74 – 7.66 (m, 4H), 7.48 – 7.35 (m, 6H), 4.28 – 4.17 (m, 1H), 4.12 – 4.03 (m, 1H), 3.57 (dd, *J* = 11.2, 3.4 Hz, 1H), 3.41 (dd, *J* = 11.1, 6.6 Hz, 1H), 1.77 (ddd, *J* = 14.4, 10.4, 4.0 Hz, 1H), 1.44 (dddd, *J* = 14.4, 5.3, 2.5, 1.1 Hz, 1H), 1.14 (d, *J* = 6.3 Hz, 3H), 1.07 (s, 9H). ^{13}C NMR (151 MHz, $CDCl_3$) δ 138.6, 138.53, 138.49, 138.45, 136.43, 135.9, 132.6, 132.5, 130.43, 130.42, 130.3, 130.2, 71.6, 71.2, 70.0, 43.0, 29.71, 29.65, 29.62, 25.3, 21.8. HRMS-(DART+) for $C_{21}H_{31}O_3Si$ $[M+H]^+$: calculated: 359.2042, found: 359.205. IR (neat): 3364.08(br), 3070.82(w), 3049.21(w), 2960.86(m), 2930.57(m),

2857.04(m), 1427.21(m), 1108.09(s), 1065.27(m), 1037.05(m), 1006.08(m), 821.74(s), 701.38(m), 611.06(s). $[\alpha]_D^{20}$= -1.406 (c=0.972, $CHCl_3$, l=50 mm).

Proof of stereochemistry: The relative configuration was assigned by comparison of the ^{13}C NMR and ^{1}H NMR spectrum with that reported in the literature.[44]

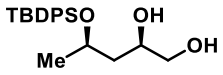

(2R,4S)-4-((tert-butyldiphenylsilyl)oxy)pentane-1,2-diol (1.120). The diboration was performed according to the general procedure A with (S)-tert-butyl(pent-4-en-2-yloxy)diphenylsilane (64.91 mg, 0.20 mmol). The crude reaction mixture was purified on silica gel (30% ethyl acetate in hexane) to afford the product as clear oil (55.94 mg, 73% yield). ^{1}H NMR (600 MHz, $CDCl_3$) δ 7.78 – 7.65 (m, 4H), 7.54 – 7.32 (m, 6H), 4.19 – 4.09 (m, 1H), 3.93 (ddt, *J* = 8.9, 6.8, 3.5 Hz, 1H), 3.57 (dd, *J* = 11.1, 3.5 Hz, 1H), 3.41 (dd, *J* = 11.1, 6.5 Hz, 1H), 1.74 (ddd, *J* = 14.3, 8.9, 8.1 Hz, 1H), 1.55 (ddd, *J* = 14.3, 4.5, 3.5 Hz, 1H), 1.05 (s, 9H), 1.03 (d, *J* = 6.1 Hz, 3H). ^{13}C NMR (151 MHz, $CDCl_3$) δ 138.6, 138.50, 138.48, 138.44, 136.9, 136.1, 132.5, 132.3, 130.43,

[44] Kumar, P.; Gupta, P.; Vasudeva Naida, S.; *Chem. Eur. J.* **2006**, *12*, 1397.

130.42, 130.3, 130.2, 73.5, 72.5, 69.5, 44.8, 29.6, 29.1, 26.6, 21.8. HRMS-(DART+) for $C_{21}H_{31}O_3Si$ $[M+H]^+$: calculated: 359.2042, found: 359.2043. IR (neat): 3364.08(br), 3070.82(w), 3049.21(w), 2960.86(m), 2930.57(m), 2857.04(m), 1427.21(m), 1108.09(s), 1065.27(m), 1037.05(m), 1006.08(m), 821.74(s), 701.38(m), 611.06(s). $[\alpha]_D^{20}$= -16.026 (c=0.967, $CHCl_3$, l=50 mm).

Proof of stereochemistry:

The relative configuration was assigned by comparison of the ^{13}C NMR and ^1H NMR spectrum with that reported in the literature[26].

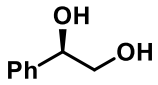

(R)-1-phenylethane-1,2-diol (1.48). The diboration was performed according to the general procedure A with styrene (20.83 mg, 0.20 mmol). To remove the catalyst, the crude reaction mixture was treated with TBAF (1.0 M in THF, 0.20 mL) at room temperature and stirred for 0.5 h. The reaction mixture was then concentrated by rotary evaporation, and the resulting crude product was purified on silica gel (50% ethyl acetate in hexanes) to afford the product as white solid (16.58 mg, 60% yield). Spectral data is in accordance

with literature report.[18] HRMS-(DART+) for C_8H_9O $[M-H_2O+H]^+$: calculated: 121.0653, found: 121.0659.

Analysis of Stereochemistry:

The 1,2-diol was treated with 2,2-dimethoxypropane and catalytic toluenesulfonic acid. The resulting ketal was compared to the racemic ketal of 1-phenylethane-1,2-diol prepared from dihydroxylation of styrene with ruthenium trichloride and sodium periodiate.[19] The absolute stereochemistry was assigned by analogy. The authentic (*R*)-isomer was prepared from the Sharpless asymmetric dihydroxylation of 1-tetradecene utilizing AD-mix-β.[21]

Chiral GLC (β-dex, Supelco, 140 °C 15min, 20 psi)- analysis of the acetonide of 1-phenylethane-1,2-diol

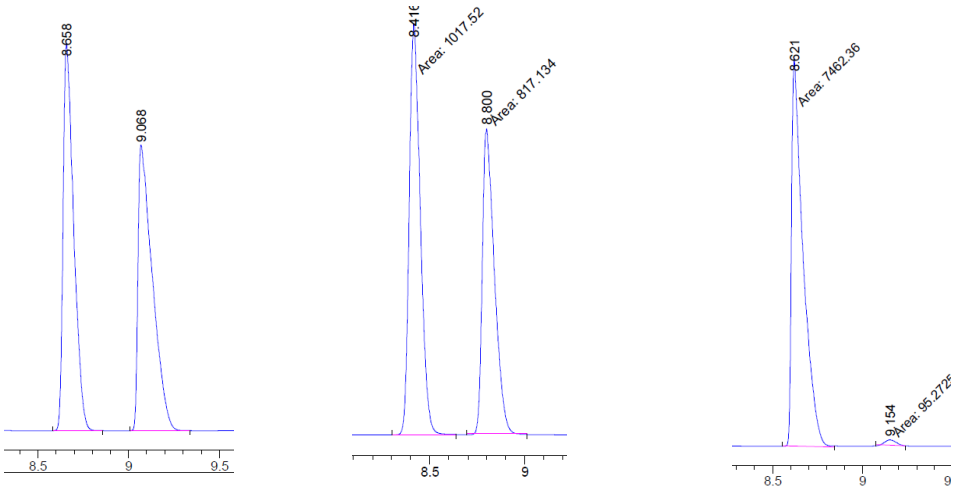

racemic product diboration product Sharpless dihydroxylation product

Peak #	RetTime [min]	Type	Width [min]	Area [pA*s]	Height [pA]	Area %
1	8.416	MM	0.0673	1017.51855	251.94304	55.46110
2	8.800	MM	0.0729	817.13422	186.89059	44.53890

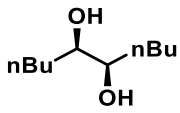

(5R,6R)-decane-5,6-diol (1.36). The diboration was performed according to the general procedure C with (E)-dec-5-ene (28.05 mg, 0.20 mmol). The crude reaction mixture was purified on silica gel (25% ethyl acetate in hexanes) to afford the product as white solid (31.0 mg, 89% yield). Spectral data is in accordance with literature report.[45] HRMS-(DART+) for $C_{10}H_{21}O$ [M-H_2O+H]$^+$: calculated: 157.1592, found: 157.1589. IR (neat): 3347.86(br), 2955.18(s), 2929.84(s), 2858.41(s), 14.63.88(m), 1144.86(m), 1117.08(m), 1069.11(m), 1048.42(s), 1001.50(m). [□]$_D^{20}$= +24.662 (c=1.195, $CHCl_3$, l=50 mm).

Analysis of Stereochemistry:

[45] Dobler, C.; Mehltretter, G. M.; Sundermeier, U.; Beller, M. *J. Am. Chem. Soc.* **2000**, *122*, 10289.

The 1,2-diol was treated with 2,2-dimethoxypropane and catalytic toluenesulfonic acid. The resulting ketal was compared to the racemic ketal of decane-5,6-diol prepared from dihydroxylation of (E)-dec-5-ene with ruthenium trichloride and sodium periodiate.[19] The absolute stereochemistry was assigned by analogy. The authentic (*R*)-isomer was prepared from the Sharpless asymmetric dihydroxylation of (E)-dec-5-ene utilizing AD-mix-β.[21]

Chiral GLC (β-dex, Supelco, 70 °C 15min, 0.25°C/min to 90 °C 20 psi)-analysis of the acetonide of decane-5,6-diol.

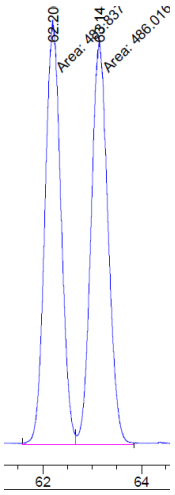

racemic product

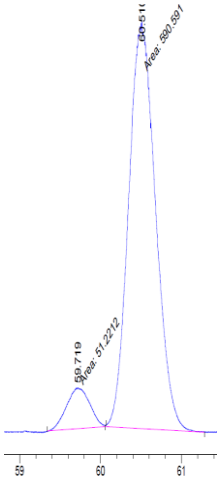

diboration product

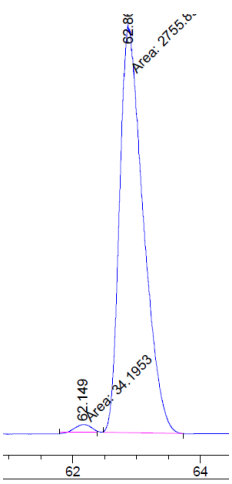

Sharpless dihydroxylation product

Peak #	RetTime [min]	Type	Width [min]	Area [pA*s]	Height [pA]	Area %
1	59.719	MM	0.3277	51.22122	2.60471	7.98071
2	60.510	MM	0.3821	590.59149	25.76274	92.01929

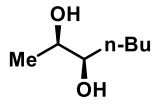

(2R,3R)-octane-2,3-diol (1.124). The diboration was performed according to the general procedure C with (E)-oct-2-ene (22.4 mg, 0.20 mmol). The crude reaction mixture was purified on silica gel (30% ethyl acetate in hexanes) to afford the product as clear oil (24.2 mg, 83% yield). ^{1}H NMR (600 MHz, $CDCl_3$) δ 3.58 (p, J = 6.3 Hz, 1H), 3.37 – 3.29 (m, 1H), 2.11 (s, 2H), 1.56 – 1.44 (m, 2H), 1.44 – 1.22 (m, 6H), 1.18 (d, J = 6.3 Hz, 3H), 0.89 (t, J = 6.8 Hz, 3H). ^{13}C NMR (151 MHz, $CDCl_3$) δ 76.5, 71.1, 33.6, 32.1, 25.5, 22.8, 19.7, 14.2. HRMS-(DART+) for $C_8H_{19}O_2$ $[M+H]^+$: calculated: 147.1385, found: 147.1379. IR (neat): 3356.13(br), 2955.49(s), 2928.07(s), 2858.13(s), 1458.61(m), 1375.80(m), 1057.67(s). $[\alpha]_D^{20}$= +14.579 (c=1.135, $CHCl_3$, l=50 mm).

Analysis of Stereochemistry:

The 1,2-diol was treated with 2,2-dimethoxypropane and catalytic toluenesulfonic acid. The resulting ketal was compared to the racemic ketal of octane-2,3-diol prepared from dihydroxylation of (E)-oct-2-ene with ruthenium trichloride and sodium periodiate.[19] The absolute stereochemistry was assigned by analogy.

Chiral GLC (β-dex, Supelco, 70 °C 15min, 0.25°C/min to 90 °C 20 psi)-analysis of the acetonide of (2R,3R)-octane-2,3-diol.

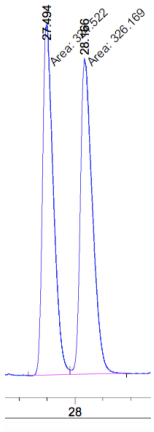

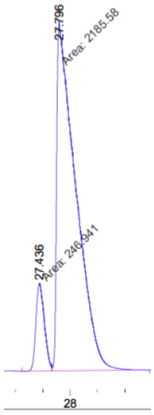

Racemic product diboration product

Peak #	RetTime [min]	Type	Width [min]	Area [pA*s]	Height [pA]	Area %
1	27.436	MF	0.1790	246.94102	22.99488	10.15166
2	27.796	FM	0.3999	2185.57837	91.07913	89.84834

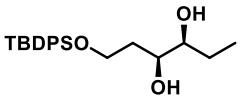

(3S,4S)-1-((tert-butyldiphenylsilyl)oxy)hexane-3,4-diol (1.125). The diboration was performed according to the general procedure C with (E)-tert-butyl(hex-3-en-1-yloxy)diphenylsilane (67.71 mg, 0.20 mmol). The crude reaction mixture was purified on silica gel (25% ethyl acetate in hexanes) to afford the product as clear oil (52.91 mg, 71% yield). ^{1}H NMR (600 MHz, $CDCl_3$) δ 7.71 – 7.64 (m, 4H), 7.52 – 7.35 (m, 6H), 3.89 (d, J = 6.2 Hz, 2H),

3.77 (ddd, J = 9.0, 4.8, 2.9 Hz, 1H), 3.38 (dt, J = 8.8, 4.5 Hz, 1H), 1.83 (ddt, J = 15.3, 9.1, 6.3 Hz, 1H), 1.69 (dtd, J = 14.4, 4.7, 2.9 Hz, 1H), 1.65 – 1.40 (m, 2H), 1.06 (s, 9H), 1.00 (t, J = 7.4 Hz, 3H). ^{13}C NMR (151 MHz, $CDCl_3$) δ 138.20, 138.17, 135.6, 135.5, 132.6, 132.54, 130.48, 78.4, 76.2, 65.5, 37.8, 29.5, 29.0, 21.7, 12.8. HRMS-(DART+) for $C_{22}H_{33}O_3Si$ $[M+H]^+$: calculated: 373.2199, found: 373.2202. IR (neat): 3380.43(br), 3070.65(w), 3049.63(w), 2930.36(m), 2857.15(m), 1471.68(w), 1427.52(m), 1390.03(w), 1361.20(w), 1110.38(s), 701.43(s), 504.73(s). $[\alpha]_D^{20}$= -5.074 (c=1.0, $CHCl_3$, l=50 mm).

Analysis of Stereochemistry:

The 1,2-diol was compared to the racemic 1-((tert-butyldiphenylsilyl)oxy)hexane-3,4-diol prepared from dihydroxylation of (E)-tert-butyl(hex-3-en-1-yloxy)diphenylsilane with ruthenium trichloride and sodium periodiate.[19] The absolute stereochemistry was assigned by analogy.

Chiral SFC (Chiracel ODR-H, 5% isopropanol, 3 mL/min, 100 bar, 35 °C, 210-270 nm) – analysis of 1-((tert-butyldiphenylsilyl)oxy)hexane-3,4-diol.

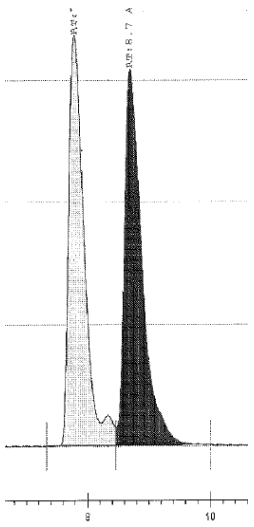

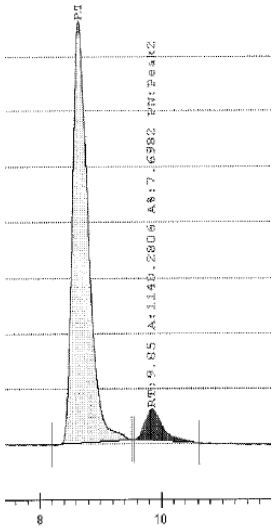

racemic product diboration product

Peak Info					
Peak No	% Area	Area	RT (min)	Height (mV)	K'
1	92.3018	13672.0097	8.64	759.236	0.007
2	7.6982	1140.2806	9.85	56.7644	0.008
Total:	100	14812.2903			

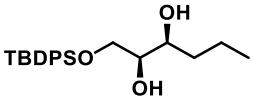

(2S,3S)-1-((tert-butyldiphenylsilyl)oxy)hexane-2,3-diol (1.126). The diboration was performed according to the general procedure C with (E)-tert-butyl(hex-2-en-1-yloxy)diphenylsilane (67.71 mg, 0.20 mmol). The crude reaction mixture was purified on silica gel (25% ethyl acetate in hexanes) to afford the product as clear oil (37.26 mg, 50% yield). ^{1}H NMR (500 MHz, $CDCl_3$) δ 7.71 – 7.64 (m, 4H), 7.50 – 7.36 (m, 6H), 3.79 (dd, *J* = 10.5, 4.0 Hz, 1H), 3.73 (dd, *J* = 10.5, 5.5 Hz, 1H), 3.69 – 3.63 (m, 1H), 3.56 – 3.48 (m, 1H),

2.69 (d, J = 6.0 Hz, 1H), 2.59 (d, J = 4.3 Hz, 1H), 1.58 – 1.28 (m, 4H), 1.08 (s, 9H), 0.91 (t, J = 7.0 Hz, 3H). ^{13}C NMR (151 MHz, $CDCl_3$) δ135.6, 135.5, 132.7, 130.0, 127.9, 73.4, 71.7, 66.3, 35.6, 26.9, 19.2, 18.7,14.0. HRMS-(DART+) for $C_{22}H_{33}O_3Si$ $[M+H]^+$: calculated: 373.2199, found: 373.2178. IR (neat): 3395.09(br), 3070.93(w), 2957.15(s), 2930.68(s), 2858.00(s), 1471.90(w), 1427.90(s), 1113.87(s), 708.13(s). $[\square]_D^{20}$= +1.2890 (c=1.26, $CHCl_3$, l=50 mm).

Analysis of Stereochemistry:

The 1,2-diol was compared to the racemic1-((tert-butyldiphenylsilyl)oxy)hexane-2,3-diol prepared from dihydroxylation of (E)-tert-butyl(hex-2-en-1-yloxy)diphenylsilane with ruthenium trichloride and sodium periodiate.[19] The absolute stereochemistry was assigned by analogy.

Chiral SFC (Chiracel OJ-H, 3% isopropanol, 3 mL/min, 100 bar, 35 °C, 210-270 nm) – analysis of 1-((tert-butyldiphenylsilyl)oxy)hexane-2,3-diol.

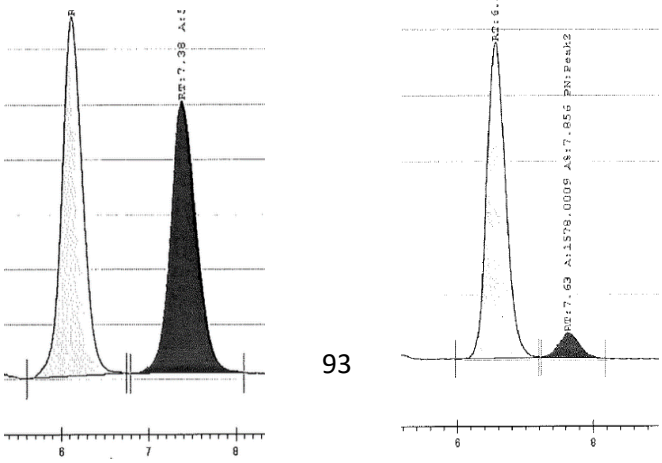

racemic product diboration product

Peak Info

Peak No	% Area	Area	RT (min)	Height (mV)	K'
1	92.144	18508.5084	6.57	954.7038	0.0095
2	7.856	1578.0009	7.63	75.3119	0.0111
Total:	100	20086.5093			

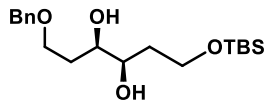

(3R,4R)-1-(benzyloxy)-6-((tert-butyldimethylsilyl)oxy)hexane-3,4-diol (1.128). The diboration was performed according to the general procedure C with (E)-((6-(benzyloxy)hex-3-en-1-yl)oxy)(tert-butyl)dimethylsilane (64.11 mg, 0.20 mmol). The crude reaction mixture was purified on silica gel (30% ethyl acetate in hexanes) to afford the product as clear oil (52.4 mg, 74% yield). ^{1}H NMR (400 MHz, $CDCl_3$) δ 4.51 (s, 2H), 3.91 – 3.77 (m, 2H), 3.76 – 3.60 (m, 4H), 3.45 (s, 1H), 3.09 (s, 1H), 1.96 – 1.61 (m, 4H), 0.88 (s, 9H), 0.06 (s, 6H). ^{13}C NMR (126 MHz, $CDCl_3$) δ 138.3, 128.6, 127.9, 73.8, 73.5, 73.0, 68.4, 61.9, 35.4, 33.3, 26.0, 18.3, -5.3, -5.3. HRMS-(DART+) for $C_{19}H_{35}O_4Si$ $[M+H]^+$: calculated: 355.2305, found: 355.2318. IR (neat): 3424.04(br), 2952.80(m), 2927.46(m), 2856.16(m), 1253.92(m), 1090.05(s), 834.88(s), 811.67(s). $[\alpha]_D^{20}$= -1.002 (c=1.000, $CHCl_3$, l=50 mm)

Analysis of Stereochemistry:

The 1,2-diol was compared to the racemic (3R,4R)-1-(benzyloxy)-6-((tert-butyldimethylsilyl)oxy)hexane-3,4-diol prepared from dihydroxylation of (E)-((6-(benzyloxy)hex-3-en-1-yl)oxy)(tert-butyl)dimethylsilane with ruthenium trichloride and sodium periodiate.[19] The absolute stereochemistry was assigned by analogy.

Chiral SFC (Chiracel OJ-H, 2% isopropanol, 3 mL/min, 100 bar, 35 °C, 210-270 nm) – analysis of (3R,4R)-1-(benzyloxy)hexane-3,4-diol.

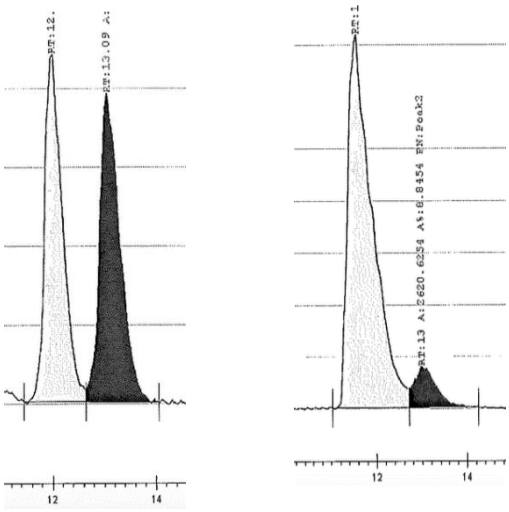

Racemic product diboration product

Peak Info					
Peak No	% Area	Area	RT (min)	Height (mV)	K'
1	91.1546	27006.4746	11.61	716.8822	0.0121
2	8.8454	2620.6254	13	77.8071	0.0136
Total:	100	29627.1			

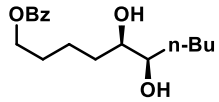

(5R,6R)-5,6-dihydroxydecyl benzoate (1.129). The diboration was performed according to the general procedure C with (E)-dec-5-en-1-yl benzoate (52.76 mg, 0.20 mmol). The crude reaction mixture was purified on silica gel (30% ethyl acetate in hexanes) to afford the product as clear oil (45.9 mg, 78% yield). ^{1}H NMR (500 MHz, $CDCl_3$) δ 8.04 (d, J = 7.2 Hz, 2H), 7.56 (d, J = 7.4 Hz, 1H), 7.44 (d, J = 7.5 Hz, 2H), 4.35 (t, J = 6.6 Hz, 2H), 3.58 – 3.30 (m, 2H), 2.06 (d, J = 4.1 Hz, 1H), 1.93 (s, 1H), 1.82 (tdd, J = 12.8, 7.4, 5.6 Hz, 2H), 1.74 – 1.27 (m, 10H), 0.91 (t, J = 7.2 Hz, 3H). ^{13}C NMR (126 MHz, $CDCl_3$) δ 166.9, 133.1, 130.6, 129.7, 128.5, 74.7, 74.5, 65.1, 33.5, 33.4, 29.0, 28.0, 22.9, 22.5, 14.2. HRMS-(DART+) for $C_{17}H_{27}O_4$ $[M+H]^+$: calculated: 295.1909, found: 295.1905. IR (neat): 3356.13(br), 2928.07(s), 2858.13(s), 1458.61(m), 1375.80(m), 1057.67(s). $[\square]_D^{20}$= +14.676 (c=1.09, $CHCl_3$, l=50 mm)

Analysis of Stereochemistry:

The 1,2-diol was compared to the racemic (5R,6R)-5,6-dihydroxydecyl benzoate prepared from dihydroxylation of (E)-dec-5-en-1-yl benzoate with

ruthenium trichloride and sodium periodiate.[19] The absolute stereochemistry was assigned by analogy.

Chiral SFC (Chiracel ODR-H, 7% isopropanol, 3 mL/min, 100 bar, 35 °C, 210-270 nm) – analysis of (5R,6R)-5,6-dihydroxydecyl benzoate.

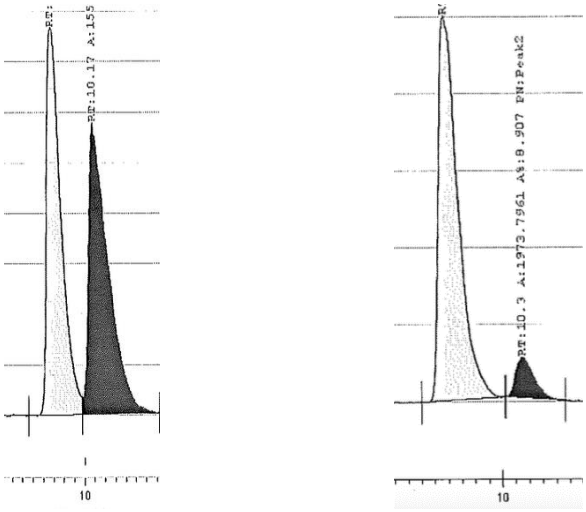

Racemic product diboration product

Peak Info

Peak No	% Area	Area	RT (min)	Height (mV)	K'
1	91.093	20186.277	9.15	997.1616	0.0101
2	8.907	1973.7961	10.3	104.7765	0.0114
Total:	100	22160.0731			

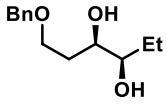

(3R,4R)-1-(benzyloxy)hexane-3,4-diol (1.130). The diboration was performed according to the general procedure C with (E)-((hex-3-en-1-

yloxy)methyl)benzene (38.06 mg, 0.20 mmol). The crude reaction mixture was purified on silica gel (30% ethyl acetate in hexanes) to afford the product as clear oil (41.3 mg, 92% yield). ^{1}H NMR (400 MHz, $CDCl_3$) δ 7.43 – 7.26 (m, 4H), 4.52 (s, 1H), 3.90 – 3.55 (m, 3H), 3.48 – 3.23 (m, 1H), 3.13 (s, 1H), 2.47 (s, 1H), 2.05 – 1.69 (m, 2H), 1.66 – 1.36 (m, 2H), 0.97 (d, J = 7.4 Hz, 3H). ^{13}C NMR (151 MHz, $CDCl_3$) δ 140.4, 131.1, 130.5, 130.4, 78.4, 76.03, 76.01, 71.1, 35.9, 29.0, 12.8. HRMS-(DART+) for $C_{13}H_{21}O_3$ $[M+H]^+$: calculated: 225.1491, found: 225.1501. IR (neat): 3424.04(br), 2952.79(s), 2927.45(s), 2856.16(m), 1253.94(m), 1090.08(s), 834.88(s), 811.68(s). $[\alpha]_D^{20}$= +1.086 (c=1.105, $CHCl_3$, l=50 mm)

Analysis of Stereochemistry:

The 1,2-diol was compared to the racemic (3R,4R)-1-(benzyloxy)hexane-3,4-diol prepared from dihydroxylation of (E)-((hex-3-en-1-yloxy)methyl)benzene with ruthenium trichloride and sodium periodiate.[13] The absolute stereochemistry was assigned by analogy.

Chiral SFC (Chiracel ODR-H, 5% isopropanol, 3 mL/min, 100 bar, 35 °C, 210-270 nm) – analysis of (3R,4R)-1-(benzyloxy)hexane-3,4-diol.

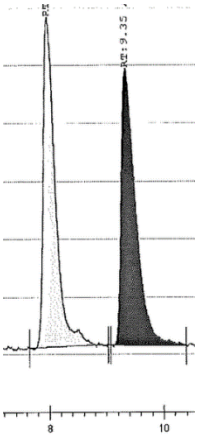

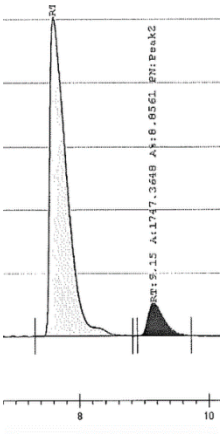

Racemic product diboration product

Peak Info

Peak No	% Area	Area	RT (min)	Height (mV)	K'
1	91.1439	17983.244	7.61	1002.8404	0.0074
2	8.8561	1747.3648	9.15	101.161	0.0089
Total:	100	19730.6088			

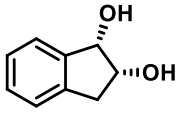

(1S,2R)-2,3-dihydro-1H-indene-1,2-diol (1.131). The diboration was performed according to the general procedure C with indene (23.23 mg, 0.20 mmol). To remove the catalyst, the crude reaction mixture was treated with TBAF (1.0 M in THF, 0.20 mL) at room temperature and stirred for 0.5h. The reaction mixture was then concentrated by rotary evaporation, and the resulting crude product was purified on silica gel (50% ethyl acetate in hexanes) to afford the product as white solid (15.02 mg, 50% yield). ^{1}H NMR

(500 MHz, $CDCl_3$) δ 7.43 (dt, *J* = 5.7, 3.2 Hz, 1H), 7.35 – 7.20 (m, 3H), 5.00 (d, *J* = 5.0 Hz, 1H), 4.51 (s, 1H), 3.13 (ddd, *J* = 16.3, 5.9, 3.7 Hz, 1H), 2.96 (dt, *J* = 16.4, 3.6 Hz, 1H), 2.51 (s, 1H), 2.43 (s, 1H). ^{13}C NMR (126 MHz, $CDCl_3$) δ 128.9, 127.2, 125.4, 125.0, 76.0, 73.5, 38.7. HRMS-(DART+) for C_9H_9O $[M\text{-}H_2O+H]^+$: calculated: 133.0653, found: 133.0659. IR (neat): 3314.86(br), 3070.24(w), 3046.34(w), 3023.68(w), 2950.25(w), 2927.07(w), 1404.80(w), 1260.64(m), 1154.55(m), 1110.66(s), 1069.97(s), 1045.31(m), 734.37(s). $[\alpha]_D^{20}$= -35.252 (c=1.115, $CHCl_3$, l=50 mm).

Analysis of Stereochemistry:

The 1,2-diol was compared to the racemic 2,3-dihydro-1H-indene-1,2-diol prepared from dihydroxylation of indene with ruthenium trichloride and sodium periodiate.[19] The absolute stereochemistry was assigned by analogy. The authentic (*1R, 2S*)-isomer was prepared from the Sharpless asymmetric dihydroxylation of indene utilizing AD-mix-β.[21]

Chiral SFC (Chiracel OJ-H, 5% isopropanol, 3 mL/min, 100 bar, 35 °C, 210-270 nm) – analysis of 2,3-dihydro-1H-indene-1,2-diol.

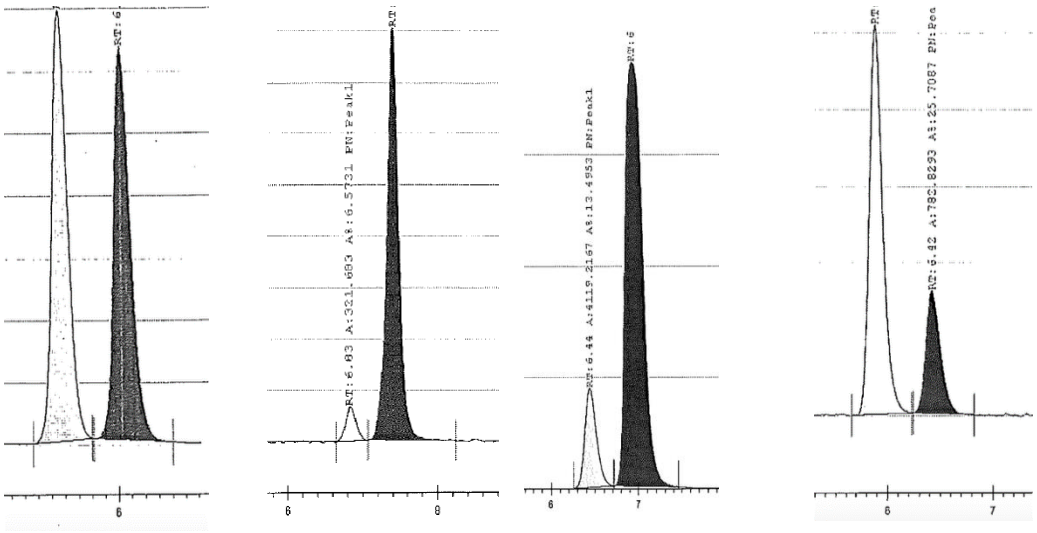

Racemic product diboration product coinjection Sharpless dihydroxylation

Peak Info					
Peak No	% Area	Area	RT (min)	Height (mV)	K'
1	6.5731	321.683	6.83	33.3762	0.0058
2	93.4269	4572.2383	7.4	401.4721	0.0063
Total:	100	4893.9213			

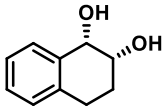

(1S,2R)-1,2,3,4-tetrahydronaphthalene-1,2-diol (1.132). The diboration was performed according to the general procedure C with 1,2-dihydronaphthalene (26.04 mg, 0.20 mmol). To remove the catalyst, the crude reaction mixture was treated with TBAF (1.0 M in THF, 0.20 mL) at room temperature and stirred for 0.5h. The reaction mixture was then concentrated by rotary evaporation, and the resulting crude product was purified on silica gel (50% ethyl acetate in hexanes) to afford the product as white solid (18.06

mg, 55% yield). Spectral data and optical rotation are in accordance with literature report.[46] HRMS-(DART+) for $C_{10}H_{11}O$ $[M\text{-}H_2O+H]^+$: calculated: 147.081, found: 147.0811.

Analysis of Stereochemistry:

The 1,2-diol was compared to the racemic 1,2,3,4-tetrahydronaphthalene-1,2-diol prepared from dihydroxylation of 1,2-dihydronaphthalene with ruthenium trichloride and sodium periodiate.[19] The absolute stereochemistry was assigned by analogy.

Chiral SFC (Chiracel OJ-H, 5% isopropanol, 3 mL/min, 100 bar, 35 °C, 210-270 nm) – analysis of 1,2,3,4-tetrahydronaphthalene-1,2-diol

racemic product

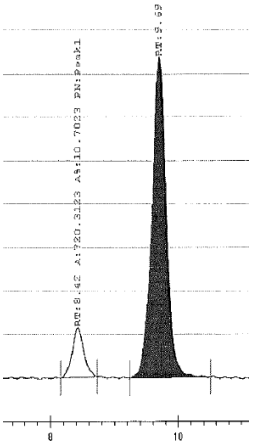

diboration product

[46] Zang, C.; Liu, Y.; Xu, Z.; Tse, C.; Guan, X.; Wei, J.; Huang, J.; Che, C. *Angew. Chem. Int. Ed.* **2016**, *55*, 10253.

Peak Info

Peak No	% Area	Area	RT (min)	Height (mV)	K'
1	10.7023	720.3123	8.42	56.6425	0.0075
2	89.2977	6010.142	9.69	368.5802	0.0087
Total:	100	6730.4543			

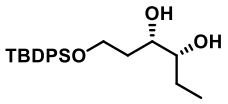

(3R,4S)-1-((tert-butyldiphenylsilyl)oxy)hexane-3,4-diol (1.133). The diboration was performed according to the general procedure C with (Z)-tert-butyl(hex-3-en-1-yloxy)diphenylsilane (67.71 mg, 0.20 mmol). The crude reaction mixture was purified on silica gel (25% ethyl acetate in hexanes) to afford the product as clear oil (43.22 mg, 58% yield). ^{1}H NMR (600 MHz, $CDCl_3$) δ 7.73 – 7.62 (m, 4H), 7.56 – 7.31 (m, 6H), 4.06 – 3.77 (m, 3H), 3.71 – 3.42 (m, 2H), 2.30 (d, *J* = 4.2 Hz, 1H), 1.92 – 1.77 (m, 1H), 1.65 (dddd, *J* = 14.6, 4.9, 3.4, 2.4 Hz, 1H), 1.55 – 1.42 (m, 2H), 1.06 (s, 9H), 1.00 (t, *J* = 7.4 Hz, 3H). ^{13}C NMR (151 MHz, $CDCl_3$) δ 138.2, 135.5, 135.4, 132.57, 132.55, 130.5, 79.3, 78.4, 77.0, 66.1, 34.7, 29.4, 27.7, 21.7, 13.0. HRMS-(DART+) for $C_{22}H_{33}O_3Si$ $[M+H]^+$: calculated: 373.2199, found: 373.221. IR (neat): 3384.76(br), 2958.53(m), 2930.28(m), 2856.85(m), 1471.75(w), 1427.68(m), 1390.09(w), 1361.33(w), 1112.05(s), 1079.47(s), 704.14(s).

Analysis of Stereochemistry:

The 1,2-diol was compared to the racemic 1-((tert-butyldiphenylsilyl)oxy)hexane-3,4-diol prepared from dihydroxylation of (Z)-tert-butyl(hex-3-en-1-yloxy)diphenylsilane with ruthenium trichloride and sodium periodiate.[19] The absolute stereochemistry was assigned by analogy.

Chiral SFC (Chiracel OJ-H, 3% isopropanol, 3 mL/min, 100 bar, 35 °C, 210-270 nm) – analysis of 1-((tert-butyldiphenylsilyl)oxy)hexane-3,4-diol.

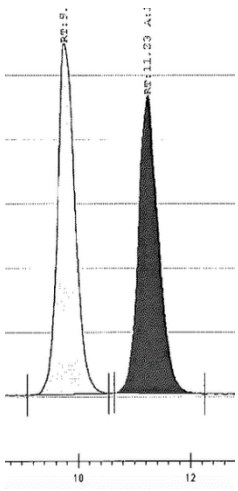

racemic product

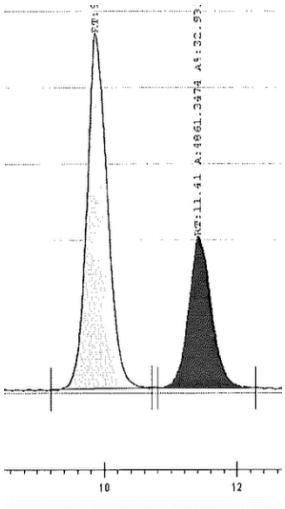

diboration product

Peak Info

Peak No	% Area	Area	RT (min)	Height (mV)	K'
1	67.0682	9900.5327	9.85	465.3841	0.0101
2	32.9318	4861.3474	11.41	198.0105	0.0117
Total:	100	14761.8801			

1.5.5.6 Full Characterizations and Proof of Stereochemistry (with DHR catalyst)

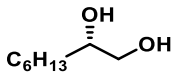

(S)-octane-1,2-diol (1.40). The diboration was performed according to the general procedure B with 1-octene (22.44 mg, 0.20 mmol, 32.4 μL). The crude product was purified on silica gel (50% ethyl acetate in hexanes) to afford the product as white solid (28.30 mg, 97% yield). Spectral data and optical rotation are in accordance with the literature report.[18] HRMS-(DART+) for C8H22NO2 $[M+NH_4]^+$: calculated: 164.1651, found: 164.1655.

Analysis of Stereochemistry:

The 1,2-diol was treated with 2,2-dimethoxypropane and catalytic toluenesulfonic acid. The resulting ketal was compared to the racemic ketal of octane-1,2-diol prepared from dihydroxylation of 1-octene with ruthenium trichloride and sodium periodiate.[19] The absolute stereochemistry was assigned by analogy.

Chiral GLC (β-dex, Supelco, 100 °C 30min, 20 psi)- analysis of the acetonide of octane-1,2-diol.

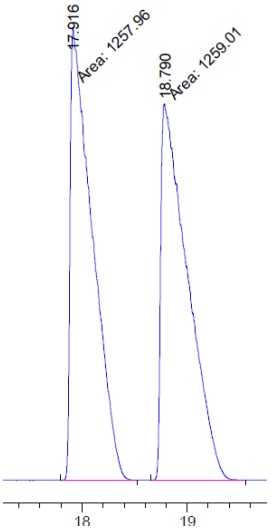

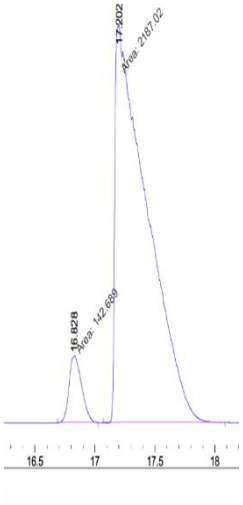

racemic product diboration product

Peak #	RetTime [min]	Type	Width [min]	Area [pA*s]	Height [pA]	Area %
1	16.828	MM	0.1204	142.68919	19.75522	6.12477
2	17.202	MM	0.3076	2187.01807	118.51307	93.87523
Totals :				2329.70726	138.26829	

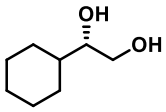

(S)-1-cyclohexylethane-1,2-diol (1.107). The diboration was performed according to the general procedure B with vinyl cyclohexane (22.04 mg, 0.20 mmol, 27.4 µL). The crude product was purified on silica gel (50% ethyl

acetate in hexanes) to afford the product as white solid (23.9 mg, 83% yield). Spectral data and optical rotation are in accordance with the literature report.[22] HRMS-(DART+) for $C_8H_{15}O$ $[M+H-H_2O]^+$: calculated:127.1123, found:127.1117.

Analysis of Stereochemistry:

The 1,2-diol was treated with 2,2-dimethoxypropane and catalytic toluenesulfonic acid. The resulting ketal was compared to the racemic ketal of 1-cyclohexylethane-1,2-diol prepared from dihydroxylation of vinyl cyclohexane with ruthenium trichloride and sodium periodiate.[19] The absolute stereochemistry was assigned by analogy

Chiral GLC (β-dex, Supelco, 130 °C 20 min)- analysis of the acetonide of 1-cyclohexylethane-1,2-diol

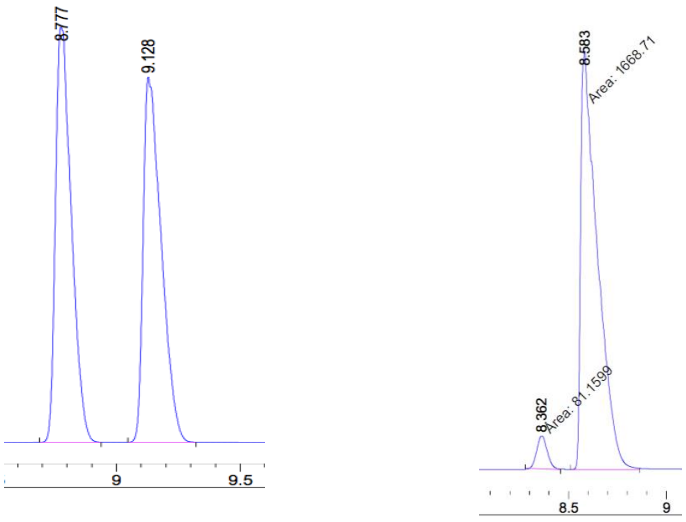

racemic product diboration product

Peak #	RetTime [min]	Type	Width [min]	Area [pA*s]	Height [pA]	Area %
1	8.362	MM	0.0616	81.15990	21.95622	4.63806
2	8.583	MM	0.0996	1668.70691	279.33691	95.36194

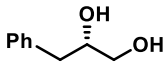

(S)-4-phenylbutane-1,2-diol (1.109). The diboration was performed according to the general procedure B with 4-phenyl-1-butene (26.44 mg, 0.20 mmol, 30.04 μL). The crude reaction mixture was purified on silica gel (50% ethyl acetate in hexanes) to afford the product as clear oil (31.54 mg, 97% yield). Spectral data and optical rotation are in accordance with the literature report.[23] HRMS-(DART+) for C10H15O2 $[M+H]^+$: calculated: 167.1072, found: 167.108.

Analysis of Stereochemistry:

The 1,2-diol was treated with 2,2-dimethoxypropane and catalytic toluenesulfonic acid. The resulting ketal was compared to the racemic ketal

of 4-phenylbutane-1,2-diol prepared from dihydroxylation of 4-phenyl-1-butene with ruthenium trichloride and sodium periodiate.[19] The absolute stereochemistry was assigned by analogy.

Chiral GLC (β-dex, Supelco, 120 °C 5min, then 0.5°C /min to 140°C, 20 psi)-analysis of the acetonide of 4-phenylbutane-1,2-diol.

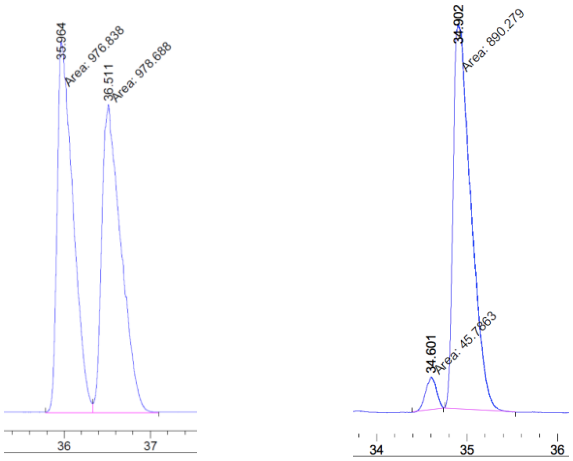

racemic product diboration product

Peak #	RetTime [min]	Type	Width [min]	Area [pA*s]	Height [pA]	Area %
1	34.601	MM	0.1379	45.78631	5.53192	4.89136
2	34.902	MM	0.2266	890.27930	65.47097	95.10864

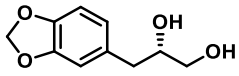

(S)-3-(benzo[d][1,3]dioxol-5-yl)propane-1,2-diol (1.111). The diboration was performed according to the general procedure B with safrole (32.44 mg,

0.20 mmol, 29.60 μL). The crude reaction mixture was purified on silica gel (50% ethyl acetate in hexanes) to afford the product as white solid (38.8 mg, 99% yield). Spectral data and optical rotation are in accordance with the literature report.[24] HRMS-(DART+) for C10H11O3 $[M-H_2O+H]^+$: calculated: 179.0708, found: 179.0715.

Analysis of Stereochemistry:

The 1,2-diol was compared to the racemic 3-(benzo[d][1,3]dioxol-5-yl)propane-1,2-diol prepared from dihydroxylation of safrole with ruthenium trichloride and sodium periodiate.[19] The absolute stereochemistry was assigned by analogy.

Chiral SFC (Chiracel ODR-H, 8% isopropanol, 3 mL/min, 100 bar, 35 °C, 210-270 nm) – analysis of 3-(benzo[d][1,3]dioxol-5-yl)propane-1,2-diol.

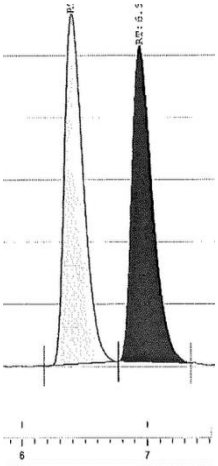

racemic product

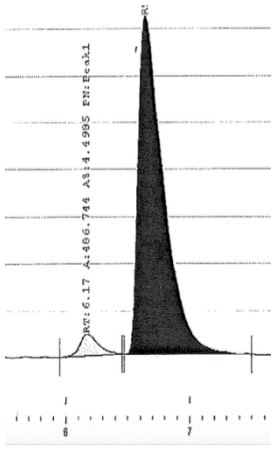

diboration product

Peak Info

Peak No	% Area	Area	RT (min)	Height (mV)	K'
1	4.4985	486.744	6.17	46.8535	0.0054
2	95.5015	10333.3923	6.64	719.9659	0.0058
Total:	100	10820.1363			

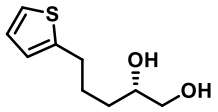

(S)-5-(thiophen-2-yl)pentane-1,2-diol (1.114). The diboration was performed according to the general procedure A with 2-(pent-4-en-1-yl)thiophene (30.45 mg, 0.20 mmol). The crude product was purified on silica gel (50% ethyl acetate in hexanes) to afford the product as clear oil (29.8 mg, 80% yield). ^{1}H NMR (400 MHz, $CDCl_3$) δ 7.11 (dd, J = 5.1, 1.2 Hz, 1H), 6.91 (dd, J = 5.1, 3.3 Hz, 1H), 6.79 (dt, J = 3.4, 1.0 Hz, 1H), 3.74 (dtd, J = 9.8, 6.5, 3.0 Hz, 1H), 3.65 (dd, J = 11.0, 3.1 Hz, 1H), 3.44 (dd, J = 11.0, 7.6 Hz, 1H), 2.87 (t, J = 7.5 Hz, 2H), 2.27 – 1.59 (m, 3H), 1.59 – 1.45 (m, 2H). ^{13}C NMR (101 MHz, $CDCl_3$) δ 144.9, 126.7, 124.2, 123.0, 72.0, 66.8, 32.4, 29.8, 27.7. HRMS-(DART+) for $C_9H_{13}OS$ $[M\text{-}H_2O+H]^+$: calculated: 169.0687, found: 169.0693. IR (neat): 3346.03(br), 2934.55(m), 2861.76(w), 1428.62(w), 1050.73(s), 870.95(w), 849.36(m), 823.85(w). $[\alpha]_D^{20}$= -1.598 (c=0.685, $CHCl_3$, l=50 mm).

Analysis of Stereochemistry:

The 1,2-diol was compared to the racemic 5-(thiophen-2-yl)pentane-1,2-diol prepared from dihydroxylation of 2-(pent-4-en-1-yl)thiophene with ruthenium trichloride and sodium periodiate.[19] The absolute stereochemistry was assigned by analogy.

Chiral SFC (Chiracel OJ-H, 4% isopropanol, 3 mL/min, 100 bar, 35 °C, 210-270 nm) – analysis of 5-(thiophen-2-yl)pentane-1,2-diol.

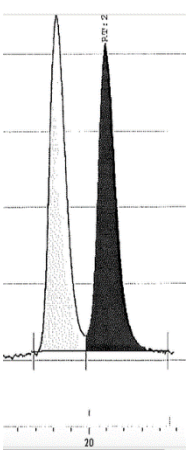

racemic product

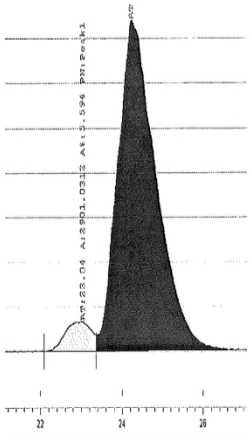

diboration product

Peak Info

Peak No	% Area	Area	RT (min)	Height (mV)	K'
1	5.594	2901.0312	23.04	64.7142	0.0179
2	94.406	48958.6678	24.23	738.6956	0.0189
Total:	100	51859.699			

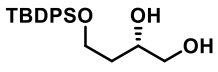

(S)-4-((tert-butyldiphenylsilyl)oxy)butane-1,2-diol (1.44). The diboration was performed according to the general procedure B with (but-3-en-1-

yloxy)(tert-butyl)diphenylsilane (62.10 mg, 0.20 mmol). The crude reaction mixture was purified on silica gel (30% ethyl acetate in hexanes) to afford the product as white solid (66.14 mg, 96% yield). Spectral data and optical rotation are in accordance with literature report.[23] HRMS-(DART+) for $C_{20}H_{29}O_3Si$ $[M+H]^+$: calculated: 345.1886, found: 345.1895. IR (neat): 3392.72(br), 3071.05(w), 3048.48(w), 2999.17(m), 2930.34(m), 2857.66(m), 1471.82(m), 1112.13(s), 823.82(m), 740.33(m), 701.55(s), 613.59(m), 505.32(m), 489.90(m).

Analysis of Stereochemistry:

The 1,2-diol was compared to the 4-((tert-butyldiphenylsilyl)oxy)butane-1,2-diol prepared from dihydroxylation of (but-3-en-1-yloxy)(tert-butyl)diphenylsilane with ruthenium trichloride and sodium periodiate.[19] The absolute stereochemistry was assigned by analogy.

Chiral SFC (Chiracel ODR-H, 5% isopropanol, 3 mL/min, 100 bar, 35 °C, 210-270 nm) – analysis of 4-((tert-butyldiphenylsilyl)oxy)butane-1,2-diol.

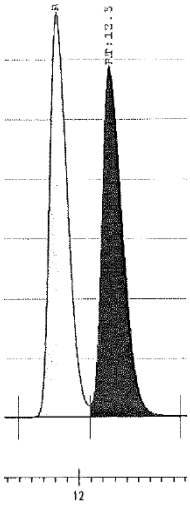

racemic product

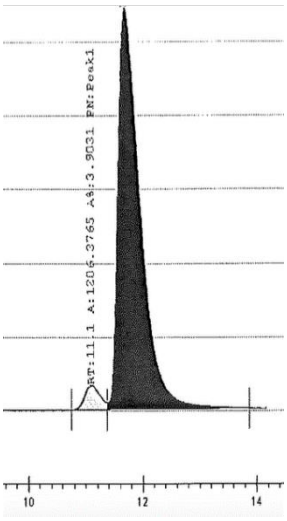

diboration product

Peak Info

Peak No	% Area	Area	RT (min)	Height (mV)	K'
1	3.9031	1206.3765	11.1	65.307	0.0117
2	96.0969	29701.8286	11.68	1085.8772	0.0123
Total:	100	30908.2051			

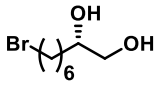

(S)-8-bromooctane-1,2-diol (1.119). The diboration was performed according to the general procedure A with 8-bromooct-1-ene (38.02 mg, 0.20 mmol). The crude reaction mixture was purified on silica gel (30% ethyl acetate in hexane) to afford the product as clear oil (40.52 mg, 90% yield). ^{1}H NMR (600 MHz, $CDCl_3$) δ 3.73 – 3.67 (m, 1H), 3.65 (dd, J = 11.0, 3.1 Hz, 1H), 3.47 – 3.35 (m, 3H), 1.85 (dd, J = 1059.8, 7.4 Hz, 2H), 1.52 – 1.39 (m, 5H), 1.39 – 1.28 (m, 3H). ^{13}C NMR (151 MHz, $CDCl_3$) δ 74.9, 69.4, 36.6,

35.7, 35.3, 31.4, 30.7, 28.0. HRMS-(DART+) for $C_8H_{18}BrO_2$ $[M+H]^+$: calculated: 225.049, found: 225.0484. IR (neat): 3347.12(br), 2930.22 (s), 2856.22 (m), 1462.14(m), 1429.61(m), 1255.16(m), 1140.02(m), 1054.50(s), 868.96 (m). $[\alpha]_D^{20}$= -2.066 (c=1.215, $CHCl_3$, l=50 mm).

Analysis of Stereochemistry:

The 1,2-diol was treated with 2,2-dimethoxypropane and catalytic toluenesulfonic acid. The resulting ketal was compared to the racemic ketal of 8-bromooctane-1,2-diol prepared from dihydroxylation of 8-bromooct-1-ene with ruthenium trichloride and sodium periodiate.[19] The absolute stereochemistry was assigned by analogy.

Chiral GLC (β-dex, Supelco, 120 °C 10min, 0.5°C/min to 180°C, 20 psi)-analysis of the acetonide of 8-bromooctane-1,2-diol.

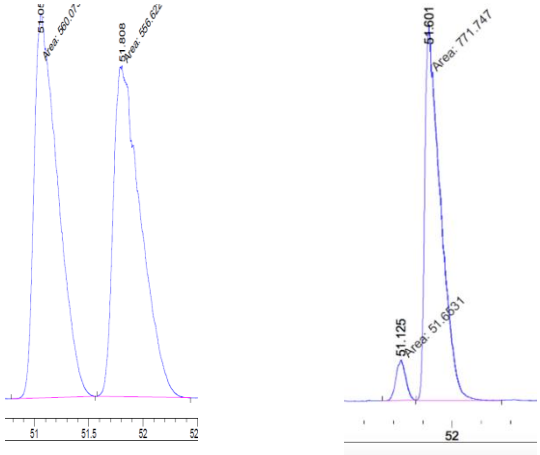

racemic product diboration product

Peak #	RetTime [min]	Type	Width [min]	Area [pA*s]	Height [pA]	Area %
1	51.125	MM	0.1915	51.65312	4.49532	6.27315
2	51.601	MM	0.3092	771.74683	41.59966	93.72685

1.5.5.7 Proof of Stereochemistry (with Bis(neopentyl glycolato)diboron)

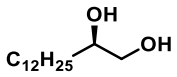

(R)-tetradecane-1,2-diol (1.106). The diboration was performed according to the general procedure D with 1-tetradecene substrate (94%, 41.78 mg, 0.20 mmol, 54 μL). The crude reaction mixture was purified on silica gel (40% ethyl acetate in hexanes) to afford the product as white solid (30.0 mg, 65% yield).

Analysis of Stereochemistry:

The 1,2-diol was treated with 2,2-dimethoxypropane and catalytic toluenesulfonic acid. The resulting ketal was compared to the racemic ketal of tetradecane-1,2-diol prepared from dihydroxylation of 1-tetradecene with ruthenium trichloride and sodium periodiate.[19]

Chiral GLC (β-dex, Supelco, 120 °C 15min, then 0.5°C /min to 180°C, 20 psi)-analysis of the acetonide of tetradecane-1,2-diol

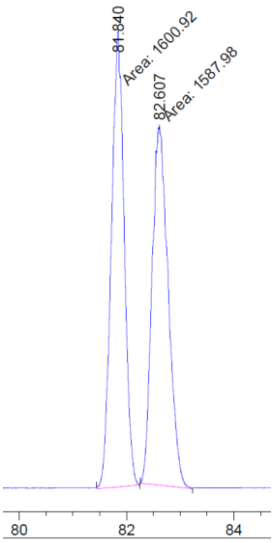

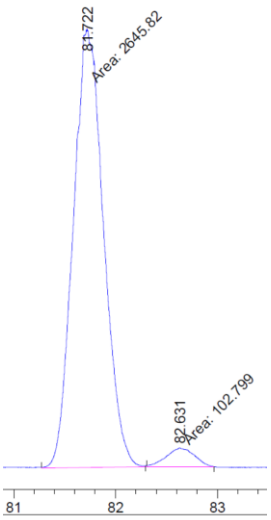

racemic product diboration product

Peak #	RetTime [min]	Type	Width [min]	Area [pA*s]	Height [pA]	Area %
1	81.722	MM	0.3444	2645.81689	128.05505	96.25999
2	82.631	MM	0.3142	102.79861	5.45218	3.74001

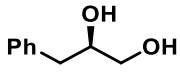

(R)-3-phenylpropane-1,2-diol (1.108). The diboration was performed according to the general procedure D with allyl benzene (23.64 mg, 0.50 mmol, 26.56 µL). The crude reaction mixture was purified on silica gel (50%

ethyl acetate in hexanes) to afford the product as white solid (14.4 mg, 47% yield).

Analysis of Stereochemistry:

The 1,2-diol was compared to the racemic 3-phenylpropane-1,2-diol prepared from dihydroxylation of allyl benzene with ruthenium trichloride and sodium periodiate.[13] The absolute stereochemistry was assigned by analogy.

Chiral SFC (Chiracel OJ-H, 4% isopropanol, 3 mL/min, 100 bar, 35 °C, 210-270 nm) – analysis of 3-phenylpropane-1,2-diol.

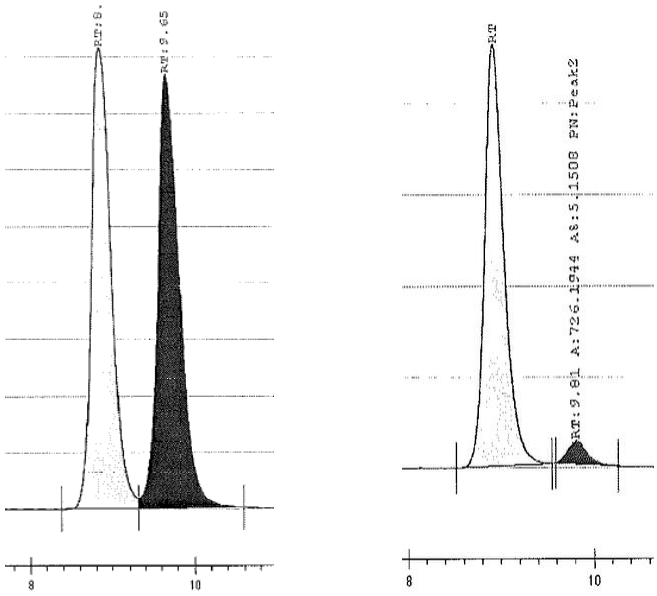

racemic product diboration product

Peak Info					
Peak No	% Area	Area	RT (min)	Height (mV)	K'
1	95.3829	25442.9155	8.91	1088.8435	0.0074
2	4.6171	1231.6012	9.77	48.5118	0.0081
Total:	100	26674.5167			

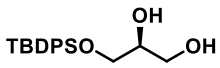

(S)-3-((tert-butyldiphenylsilyl)oxy)propane-1,2-diol (1.116). The diboration was performed according to the general procedure D with (allyloxy)(tert-butyl)diphenylsilane (59.30 mg, 0.20 mmol). The crude reaction mixture was purified on silica gel (30% ethyl acetate in hexanes) to afford the product as white solid (24.0 mg, 36% yield).

Analysis of Stereochemistry:

The 1,2-diol was compared to the racemic 3-((tert-butyldiphenylsilyl)oxy)propane-1,2-diol prepared from dihydroxylation of (allyloxy)(tert-butyl)diphenylsilane with ruthenium trichloride and sodium periodiate.[19] The absolute stereochemistry was assigned by analogy.

Chiral SFC (Chiracel OD-H, 8% isopropanol, 3 mL/min, 100 bar, 35 °C, 210-270 nm) – analysis of 3-((tert-butyldiphenylsilyl)oxy)propane-1,2-diol.

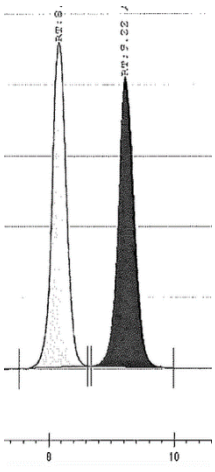

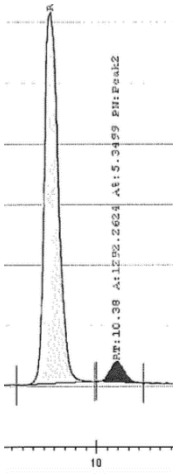

racemic product diboration product

1.5.6 Experimental procedure for large scale reaction.

A round-bottomed flask equipped with a magnetic stir bar was added tetrahydoxydiboron (2.76g, 30.8 mmol), 1,3-propanediol (4.45 ml, 61.6 mmol), and toluene (70 ml). A Dean-Stark distillation head was then equipped. The reaction was refluxing at 160°C for 6h. Toluene was then removed by rotary evaporation to afford the crude product as white solid. The crude product was used directly in the diboration reaction without further purification.

To the 250 ml round-bottomed flask with crude propanediol diboron and stir bar was added DHR catalyst (264.31 mg, 2 mmol), 4A molecular sieves

(1.0 g), anhydrous ethyl acetate (20 ml) 1-octene (3.23 ml, 20 mmol) and DBU (304.48 mg, 2 mmol). The flask was sealed with rubber septa and was then removed from the glove box. The reaction was allowed to stir at room temperature for 12h. The reaction was cooled to 0 °C (ice/water) and charged with pH=7 buffer solution (40 mL), followed by slow addition of 30% hydrogen peroxide (20 mL). The reaction was gradually warmed to room temperature and stirred for another 4 hours at room temperature. The reaction was then cooled to 0 °C (ice/water) and saturated aqueous sodium thiosulfate (40 mL) was added slowly over 5 minutes. The reaction mixture was diluted with ethyl acetate. Aqueous and organic layers were separated. The aqueous layer was further extracted with ethyl acetate (3 x 50 mL). The combined organics were dried over sodium sulfate, filtered, and concentrated by rotary evaporation to afford crude reaction mixture. The crude product was purified on silica gel (50% ethyl acetate in hexanes) to afford the product as white solid (2.73, 93% yield).

Analysis of Stereochemistry:

The 1,2-diol was treated with 2,2-dimethoxypropane and catalytic toluenesulfonic acid. The resulting ketal was compared to the racemic ketal

of octane-1,2-diol prepared from dihydroxylation of 1-octene with ruthenium trichloride and sodium periodiate.[13] The absolute stereochemistry was assigned by analogy.

Chiral GLC (β-dex, Supelco, 100 °C 30 min, 20 psi)- analysis of the acetonide of octane-1,2-diol.

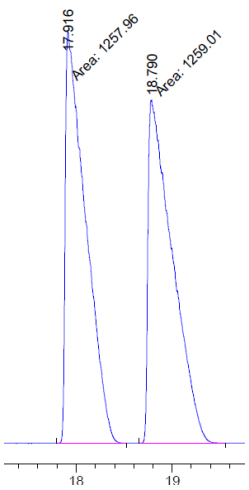

racemic product

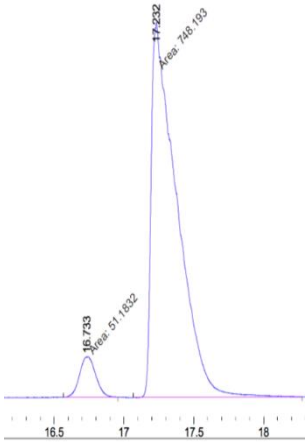

diboration product

Peak #	RetTime [min]	Type	Width [min]	Area [pA*s]	Height [pA]	Area %
1	16.733	MM	0.1345	51.18321	6.34325	6.40289
2	17.232	MM	0.2117	748.19299	58.91286	93.59711

^{1}H NMR, CD_3OD, 600M

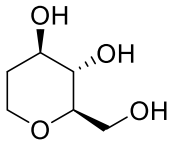

1.145

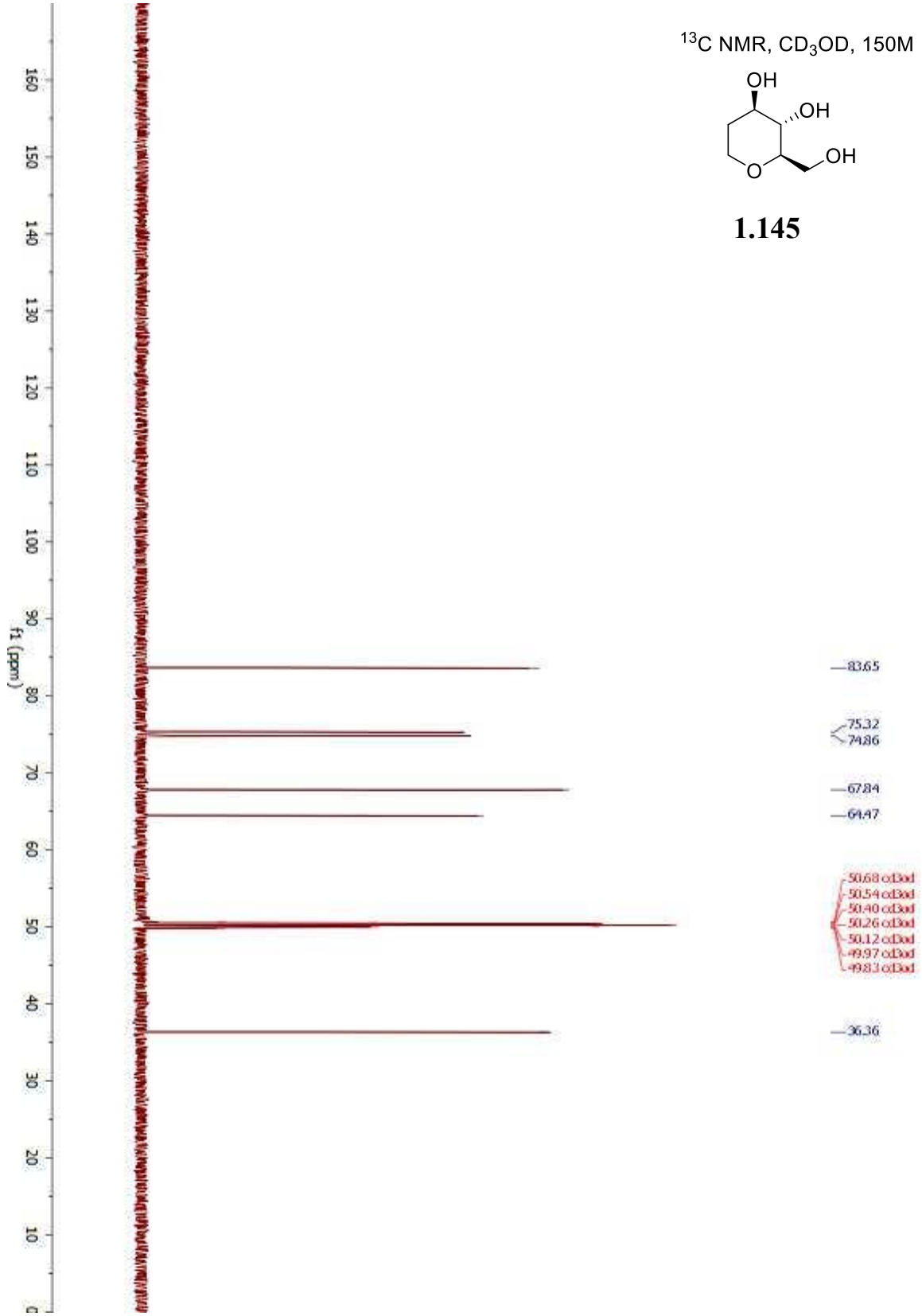
^{13}C NMR, CD_3OD, 150M
OH
OH
OH
O
1.145
f1 (ppm)
160
150
140
130
120
110
100
90
80
70
60
50
40
30
20
10
0
83.65
75.32
74.86
67.84
64.47
50.68 cd3od
50.54 cd3od
50.40 cd3od
50.26 cd3od
50.12 cd3od
49.97 cd3od
49.83 cd3od
36.36

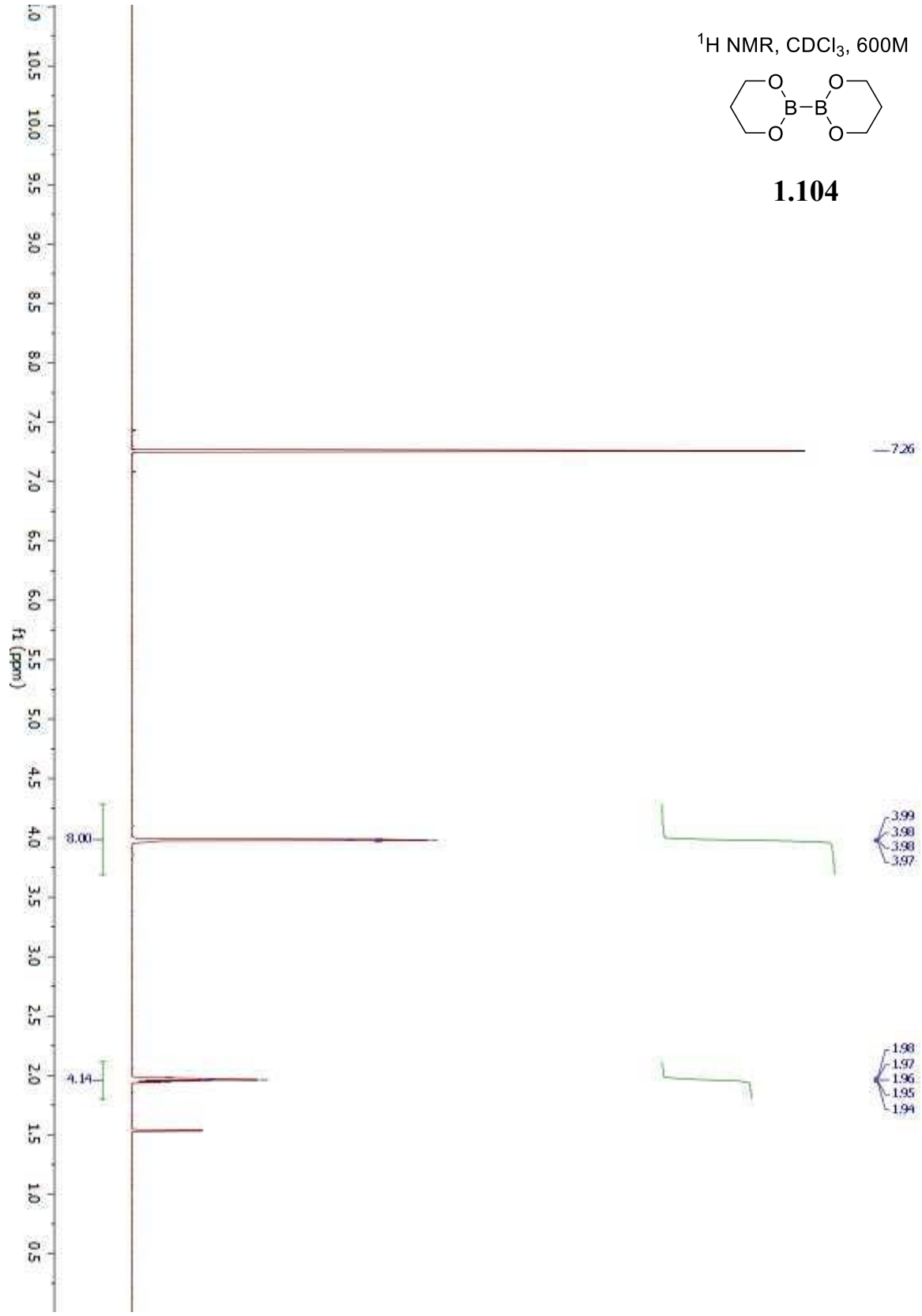
^{1}H NMR, $CDCl_3$, 600M
1.104
7.26
8.00
4.14
3.99
3.98
3.98
3.97
1.98
1.97
1.96
1.95
1.94
f1 (ppm)

^{13}C NMR, $CDCl_3$, 150M

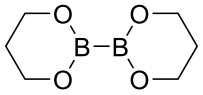

1.104

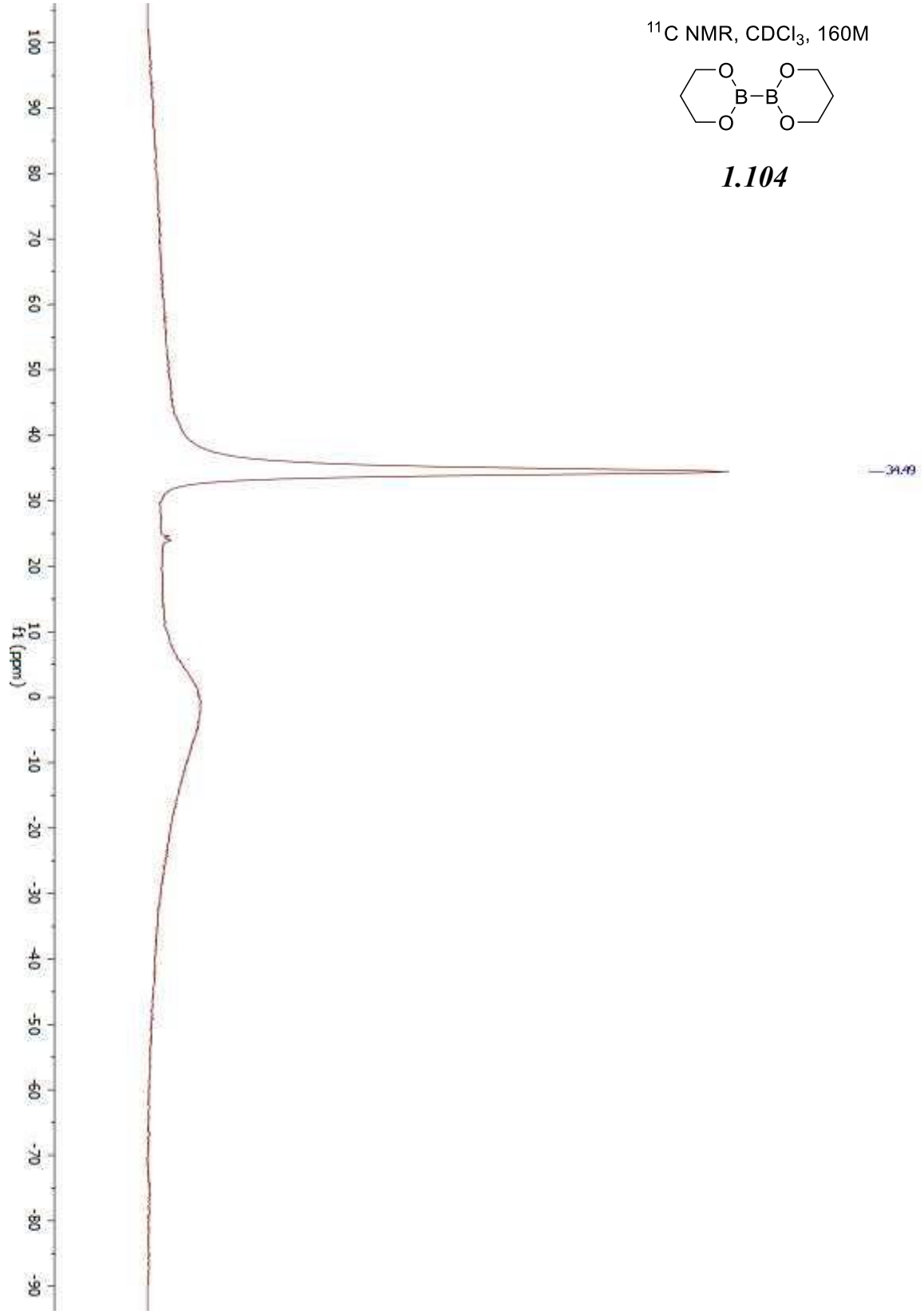

^{11}C NMR, $CDCl_3$, 160M

1.104

^{1}H NMR, $CDCl_3$, 500M

TBDPSO

S1

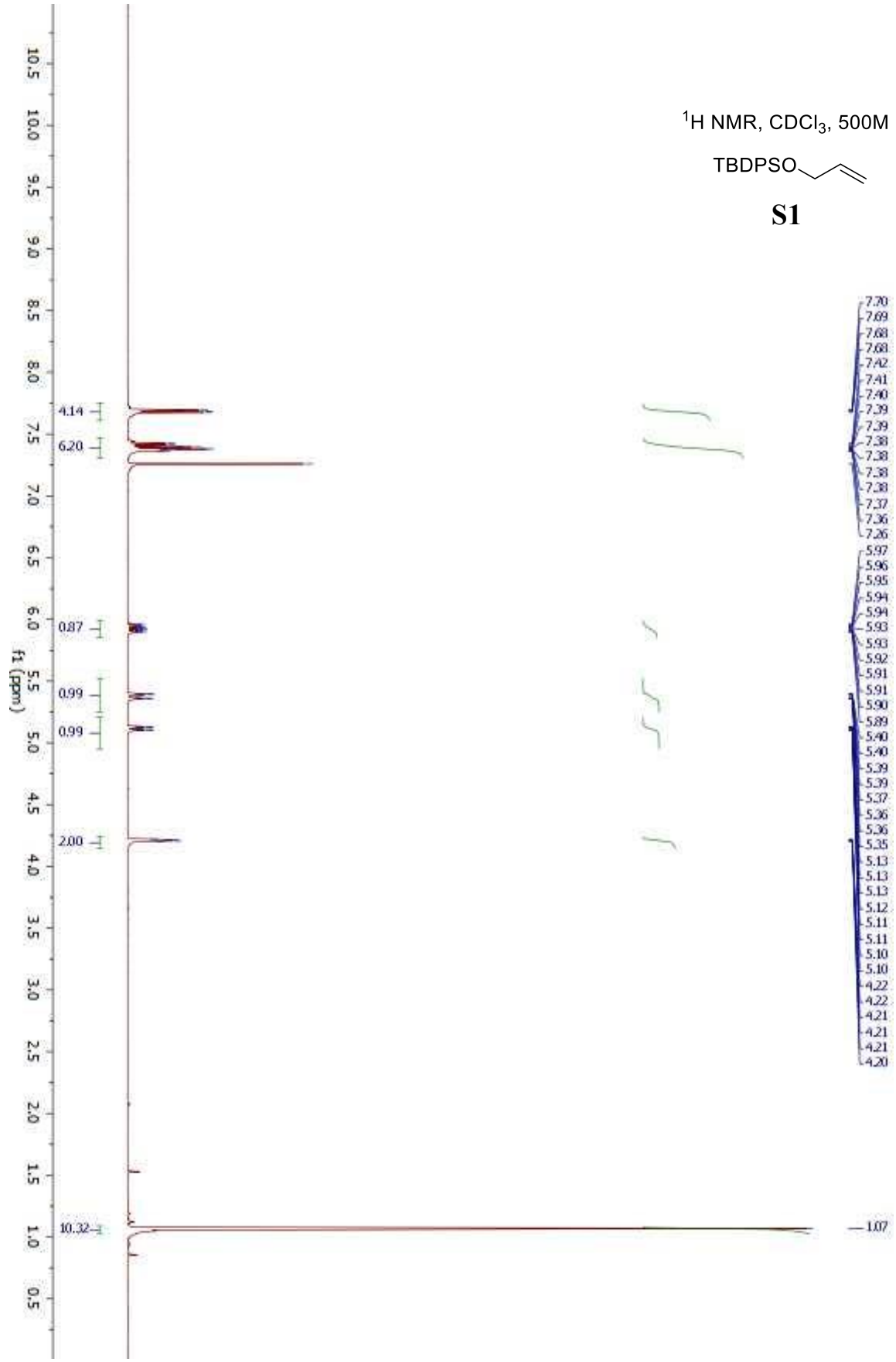

^{1}H NMR, $CDCl_3$, 600M

TBDPSO

S2

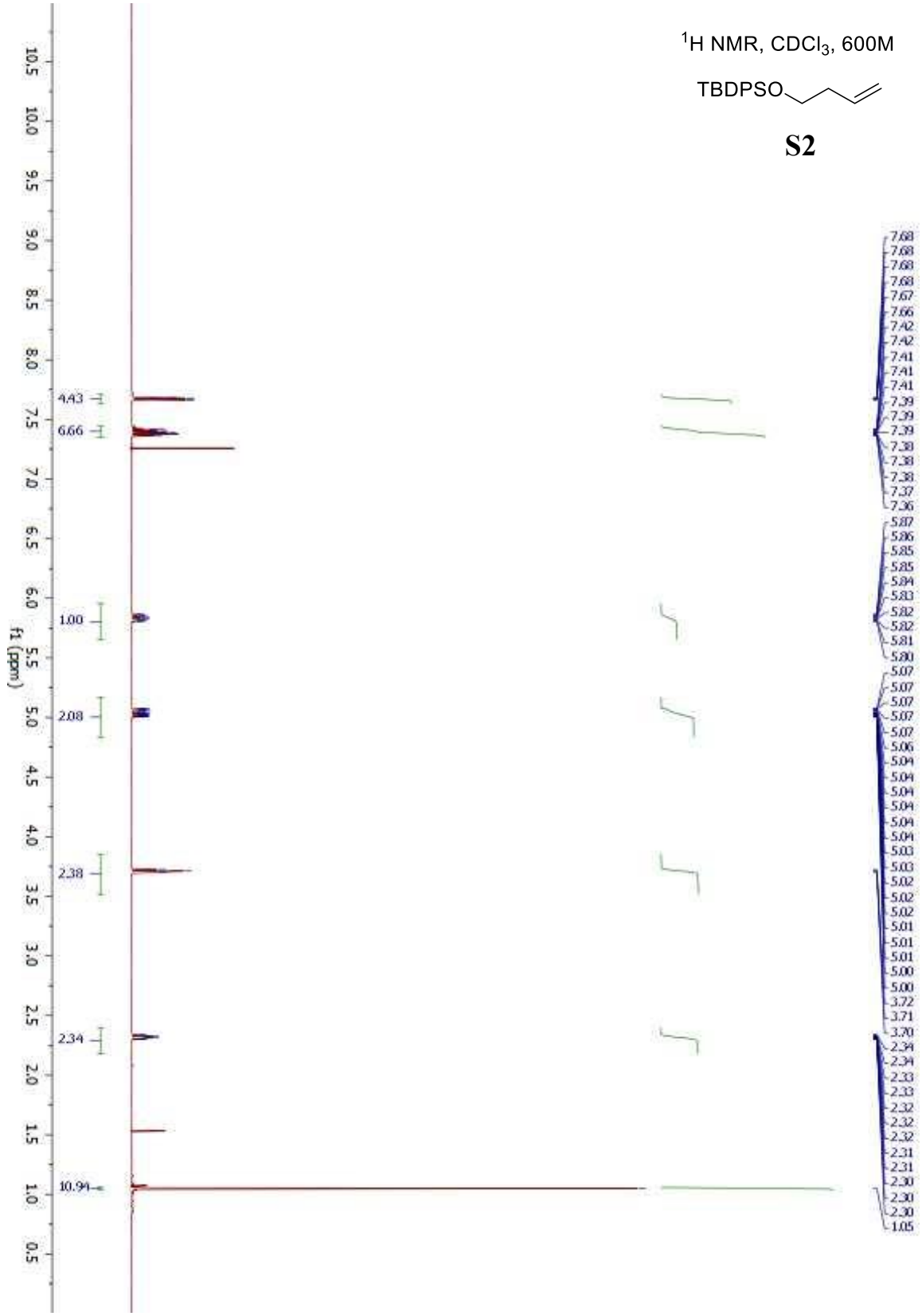

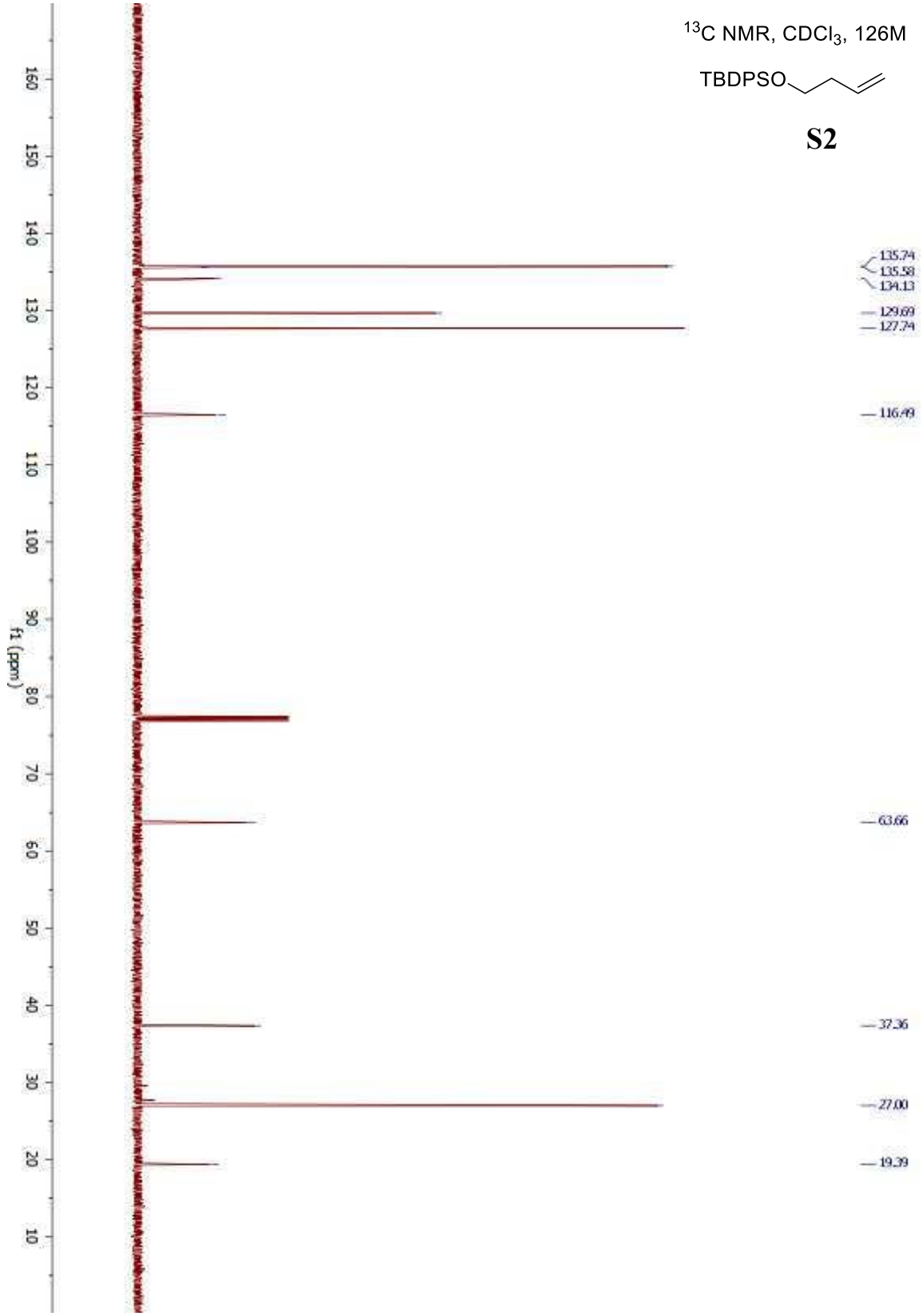
^{13}C NMR, $CDCl_3$, 126M
TBDPSO
S2
135.74
135.58
134.13
129.69
127.74
116.49
63.66
37.36
27.00
19.39
f1 (ppm)

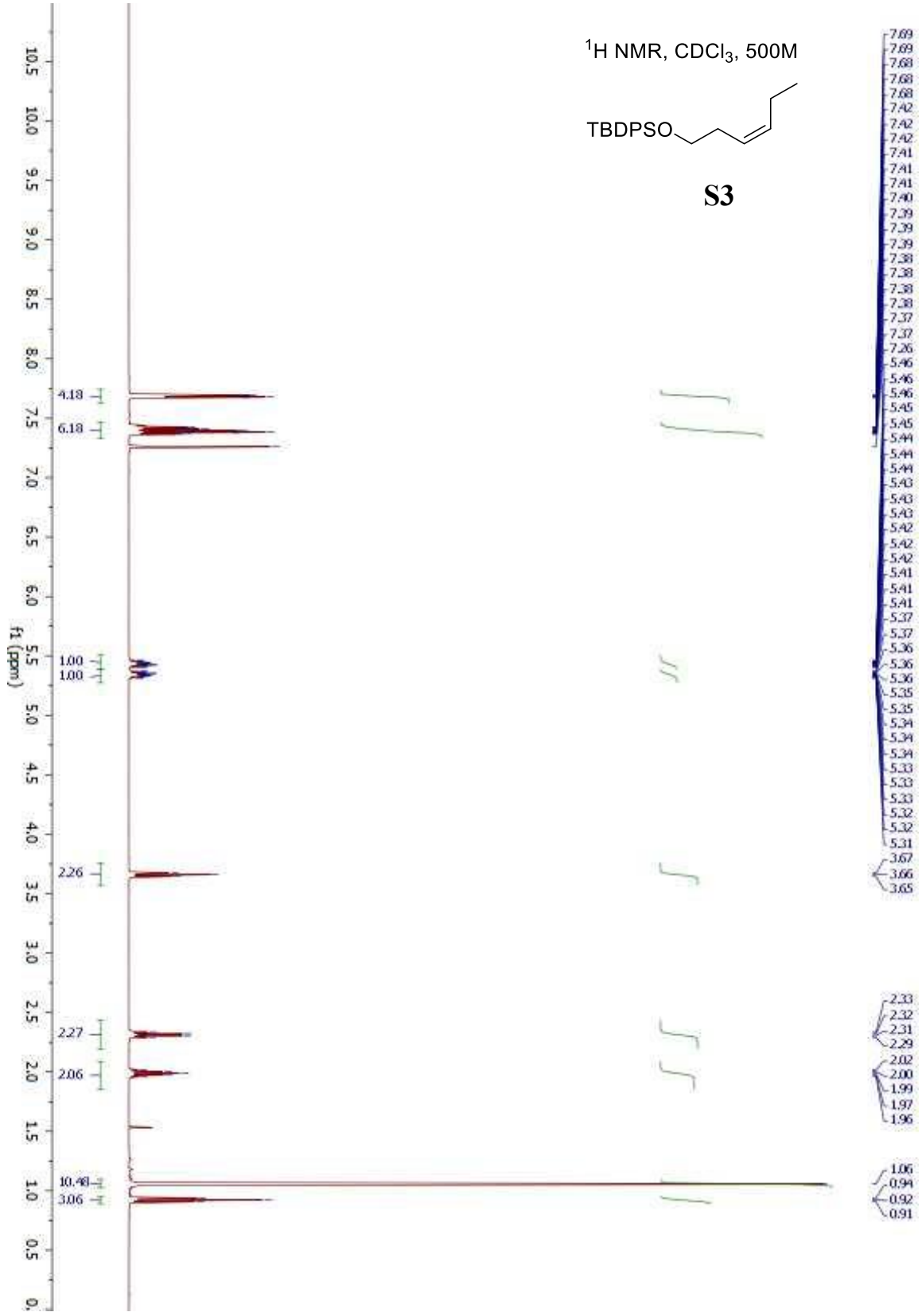
^{1}H NMR, $CDCl_3$, 500M
TBDPSO
S3
f1 (ppm)
4.18
6.18
1.00
1.00
2.26
2.27
2.06
10.48
3.06

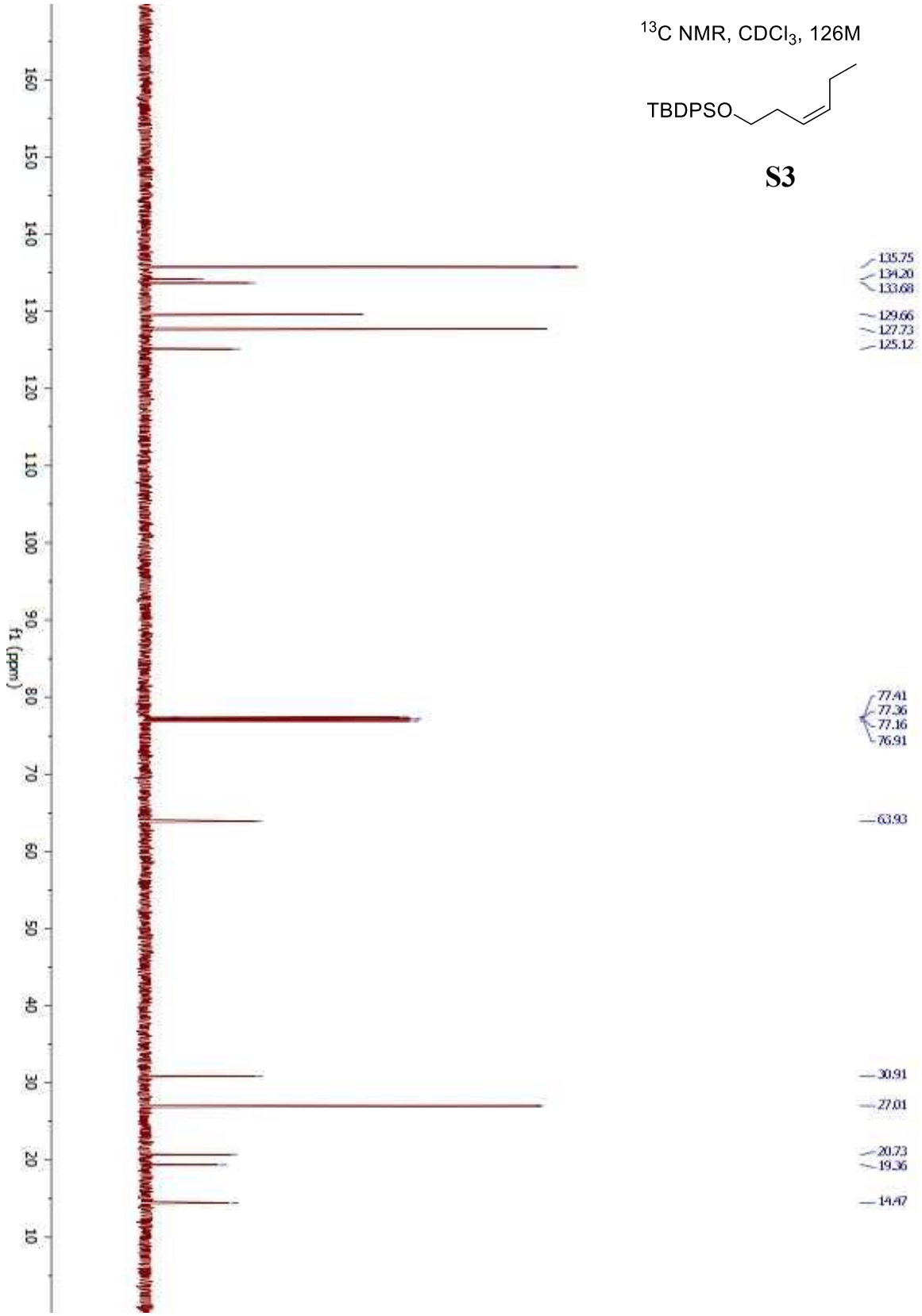
^{13}C NMR, $CDCl_3$, 126M
TBDPSO
S3
135.75
134.20
133.68
129.66
127.73
125.12
77.41
77.36
77.16
76.91
63.93
30.91
27.01
20.73
19.36
14.47
f1 (ppm)

^{1}H NMR, $CDCl_3$, 500M

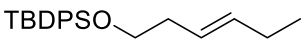

S4

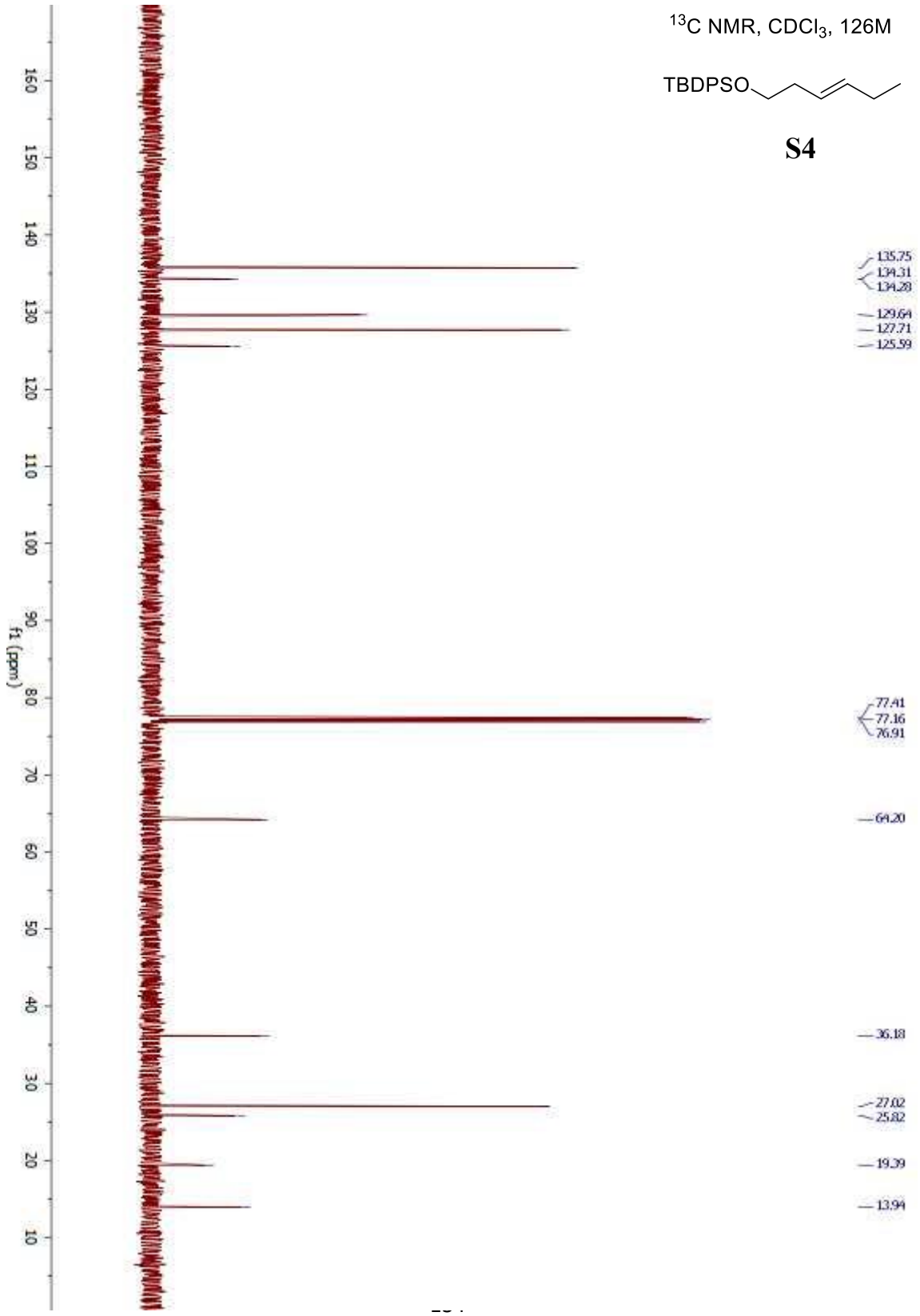
^{13}C NMR, $CDCl_3$, 126M
TBDPSO
S4
135.75
134.31
134.28
129.64
127.71
125.59
77.41
77.16
76.91
64.20
36.18
27.02
25.82
19.39
13.94
f1 (ppm)

^{1}H NMR, $CDCl_3$, 600M

TBDPSO

S5

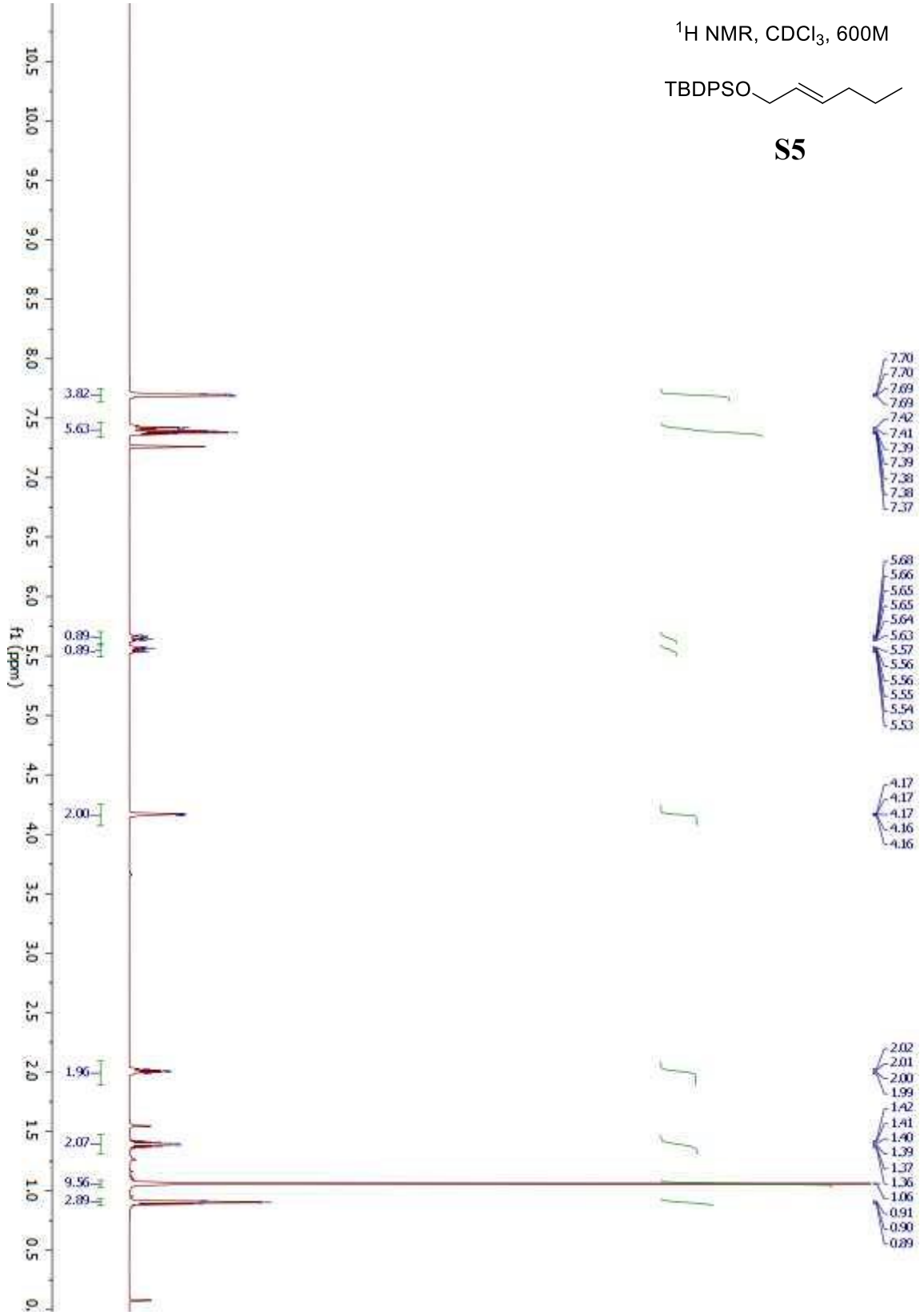

^{13}C NMR, $CDCl_3$, 150M

TBDPSO

S5

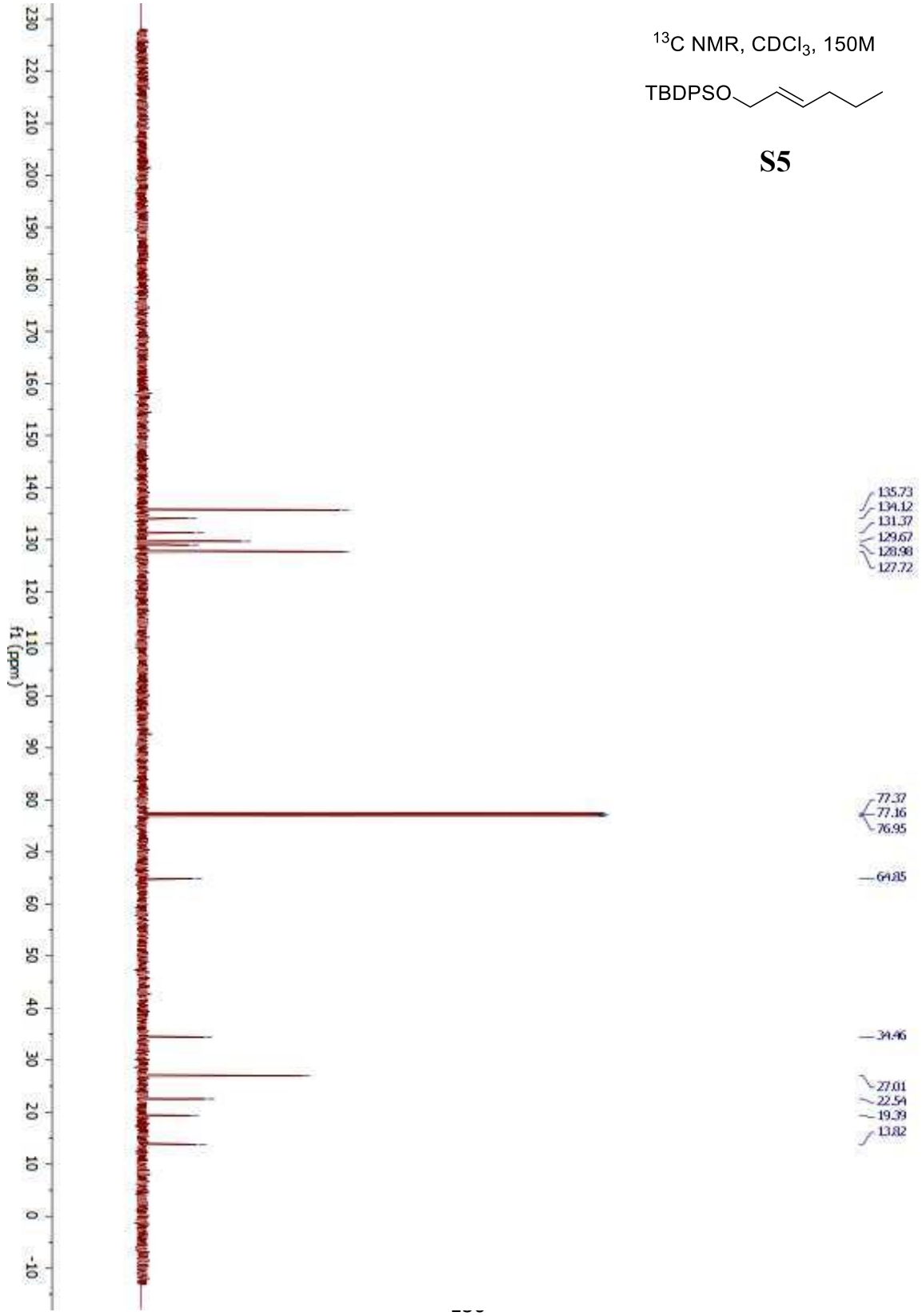

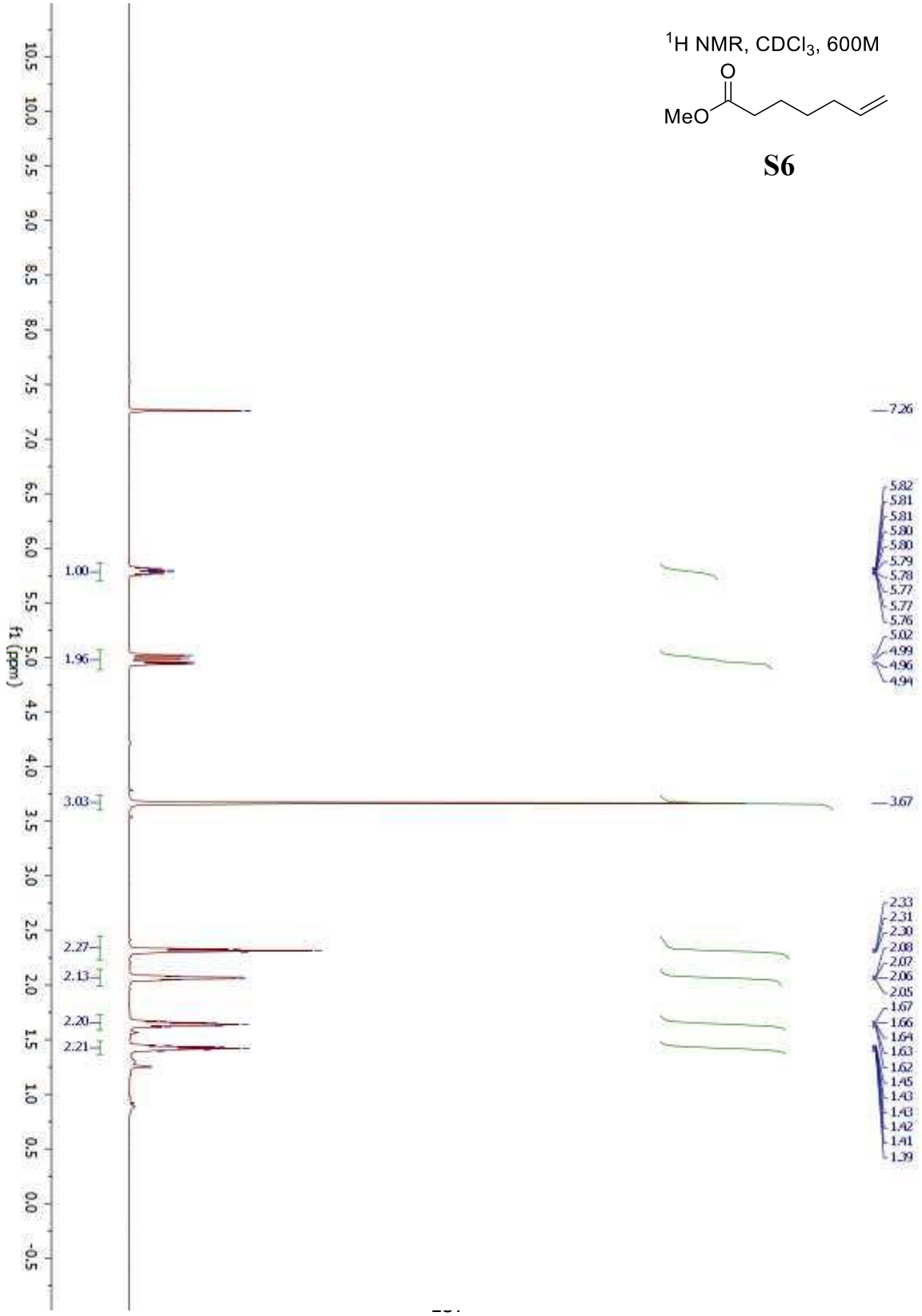
^{1}H NMR, $CDCl_3$, 600M
O
MeO
S6
f1 (ppm)
7.26
5.82
5.81
5.81
5.80
5.80
5.79
5.78
5.77
5.77
5.76
5.02
4.99
4.96
4.94
3.67
2.33
2.31
2.30
2.08
2.07
2.06
2.05
1.67
1.66
1.64
1.63
1.62
1.45
1.43
1.43
1.42
1.41
1.39
1.00
1.96
3.03
2.27
2.13
2.20
2.21

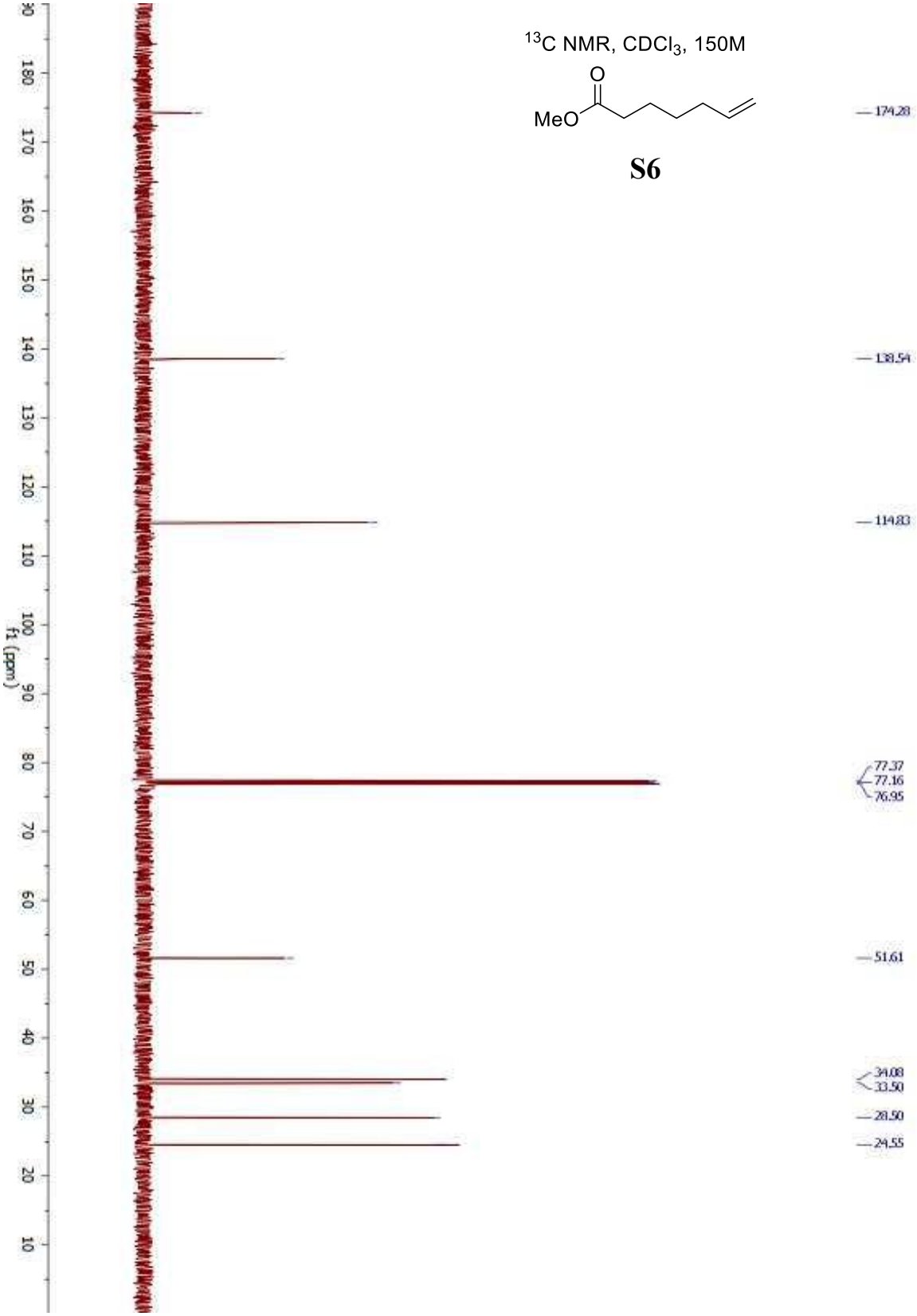
^{13}C NMR, $CDCl_3$, 150M
MeO
S6
f1 (ppm)
174.28
138.54
114.83
77.37
77.16
76.95
51.61
34.08
33.50
28.50
24.55

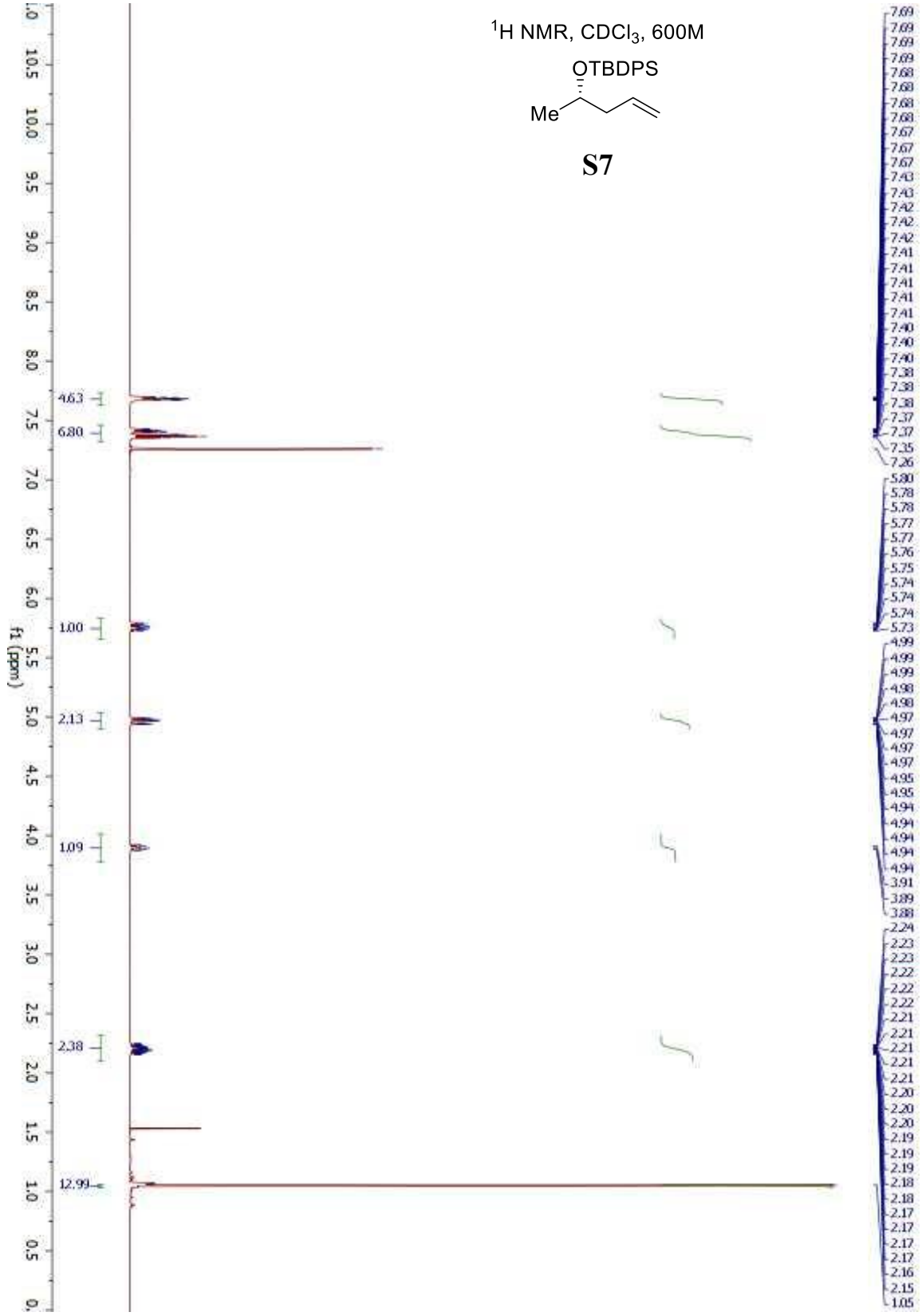
^{1}H NMR, $CDCl_3$, 600M
OTBDPS
Me
S7
f1 (ppm)
4.63
6.80
1.00
2.13
1.09
2.38
12.99

^{13}C NMR, $CDCl_3$, 126M

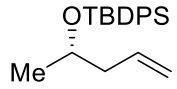

S7

^{1}H NMR, $CDCl_3$, 500M

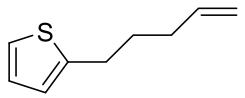

S8

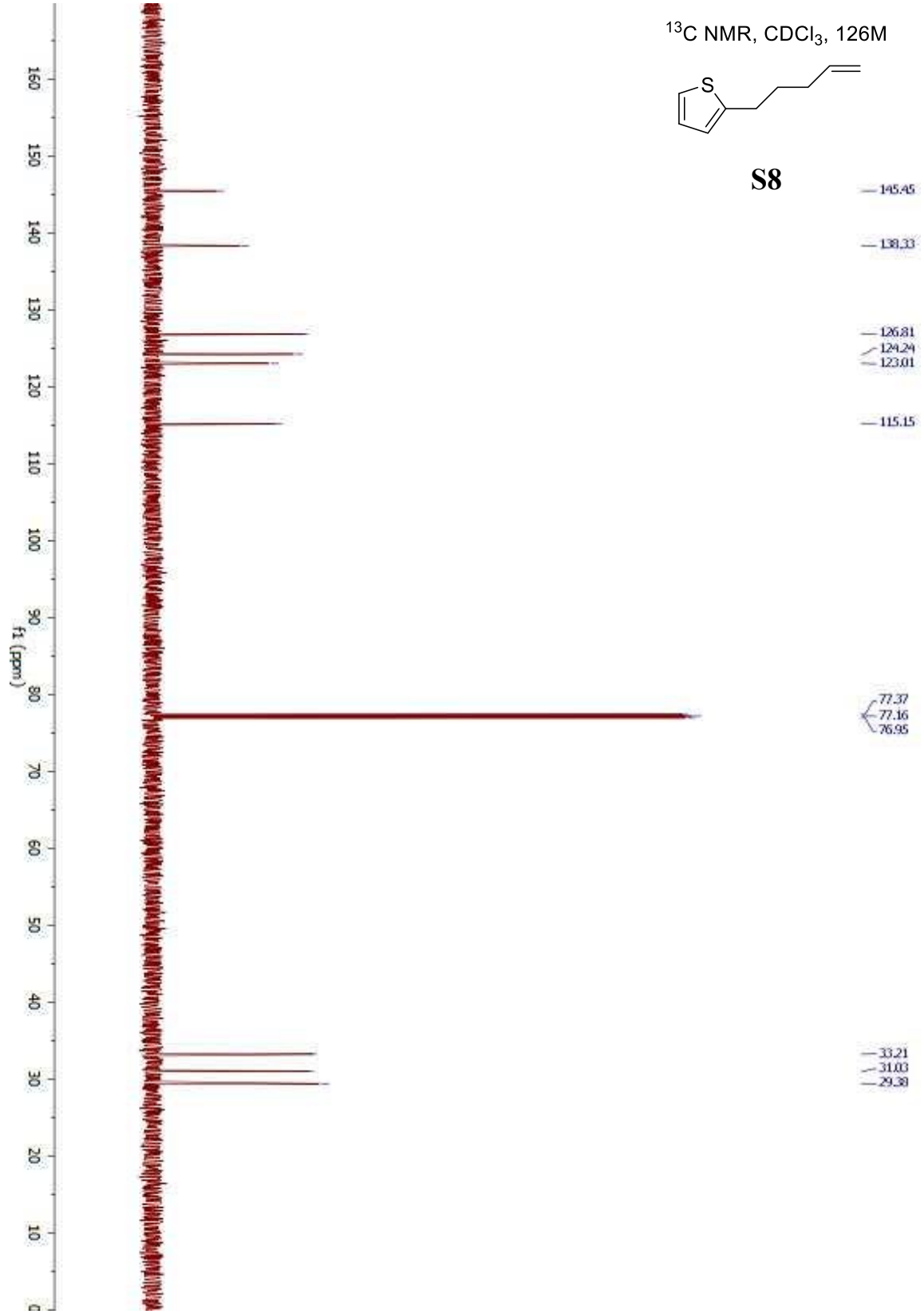
^{13}C NMR, $CDCl_3$, 126M
S
S8
145.45
138.33
126.81
124.24
123.01
115.15
77.37
77.16
76.95
33.21
31.03
29.38
f1 (ppm)

^{1}H NMR, $CDCl_3$, 500M

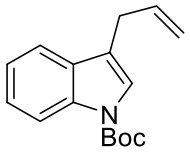

S9

^{13}C NMR, $CDCl_3$, 126M

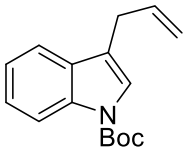

S9

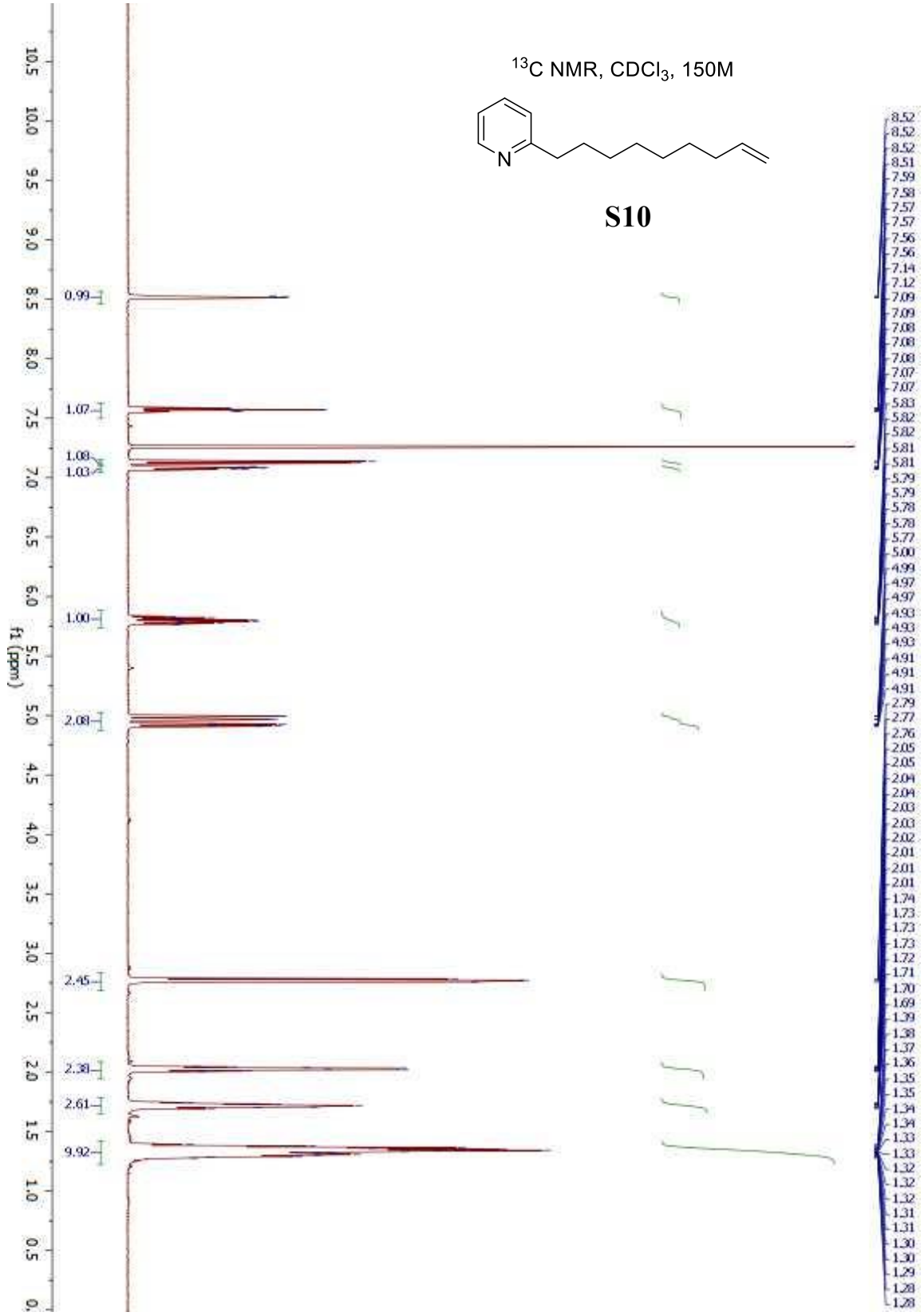
^{13}C NMR, $CDCl_3$, 150M
N
S10
f1 (ppm)
0.99
1.07
1.08
1.03
1.00
2.08
2.45
2.38
2.61
9.92

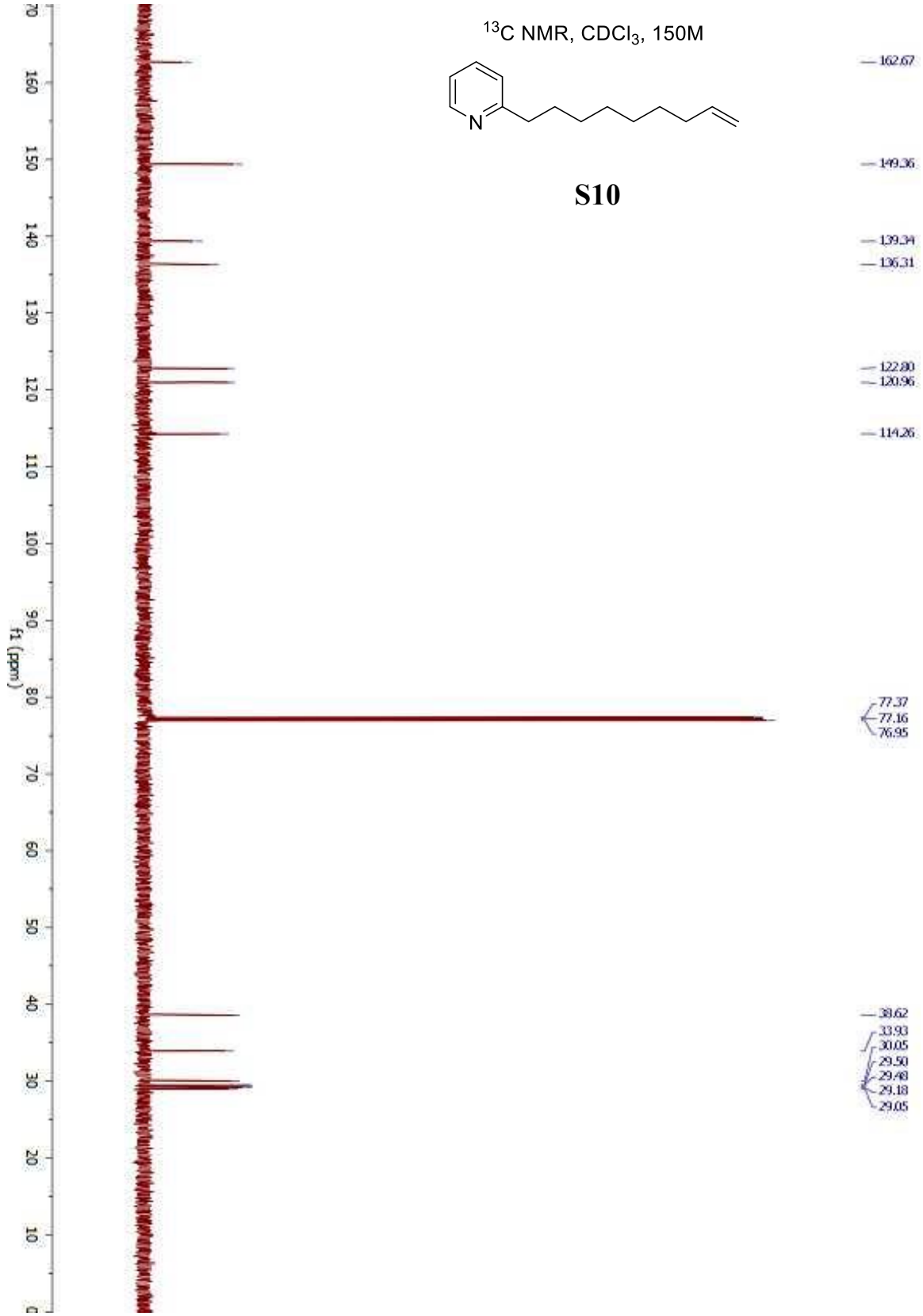
^{13}C NMR, $CDCl_3$, 150M
N
S10
f1 (ppm)
162.67
149.36
139.34
136.31
122.80
120.96
114.26
77.37
77.16
76.95
38.62
33.93
30.05
29.50
29.48
29.18
29.05

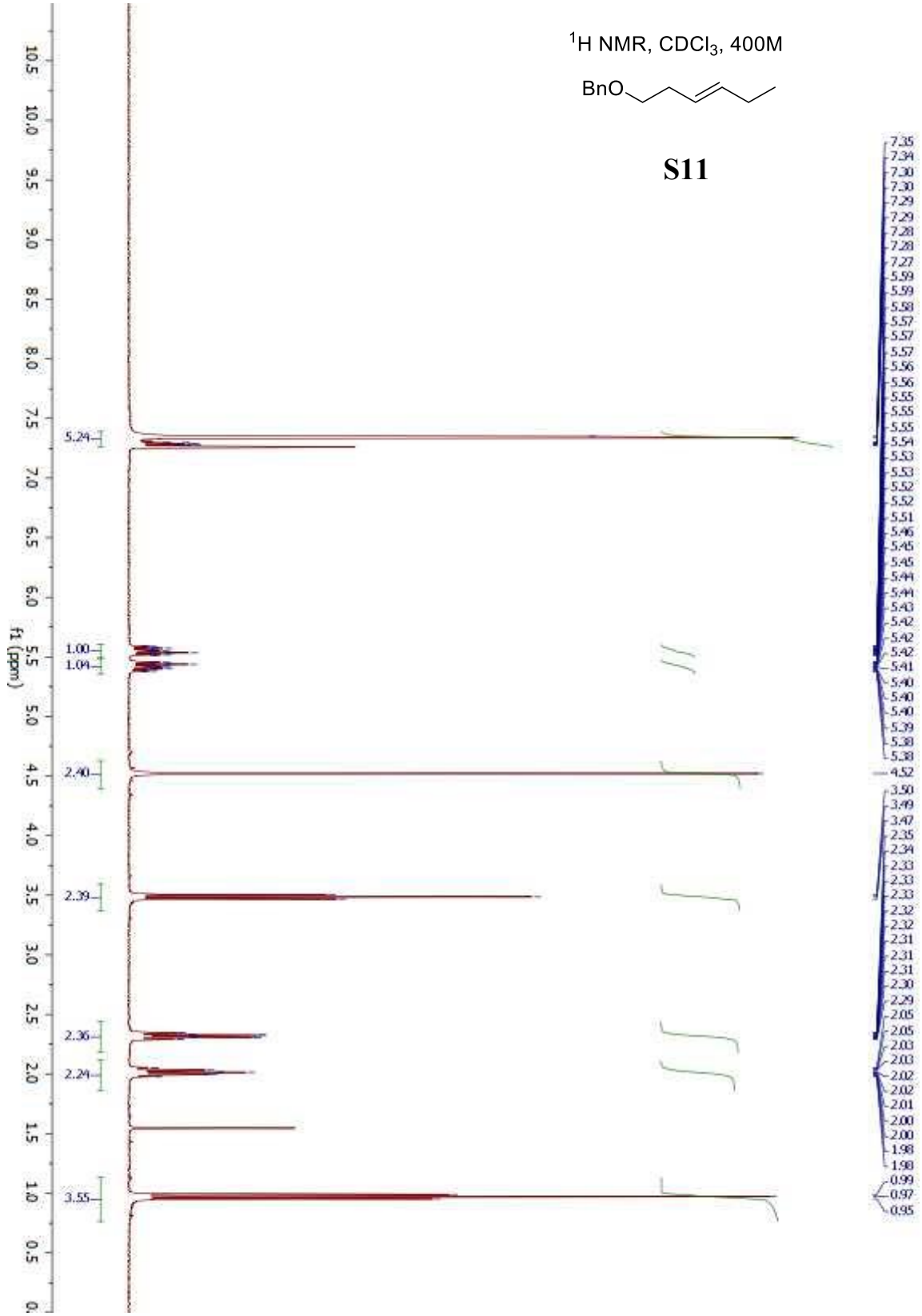
^{1}H NMR, $CDCl_3$, 400M
BnO
S11
f1 (ppm)
5.24
1.00
1.04
2.40
2.39
2.36
2.24
3.55

^{13}C NMR, $CDCl_3$, 150M

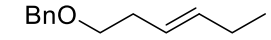

S11

^{1}H NMR, $CDCl_3$, 400M

BnO OTBS

S12

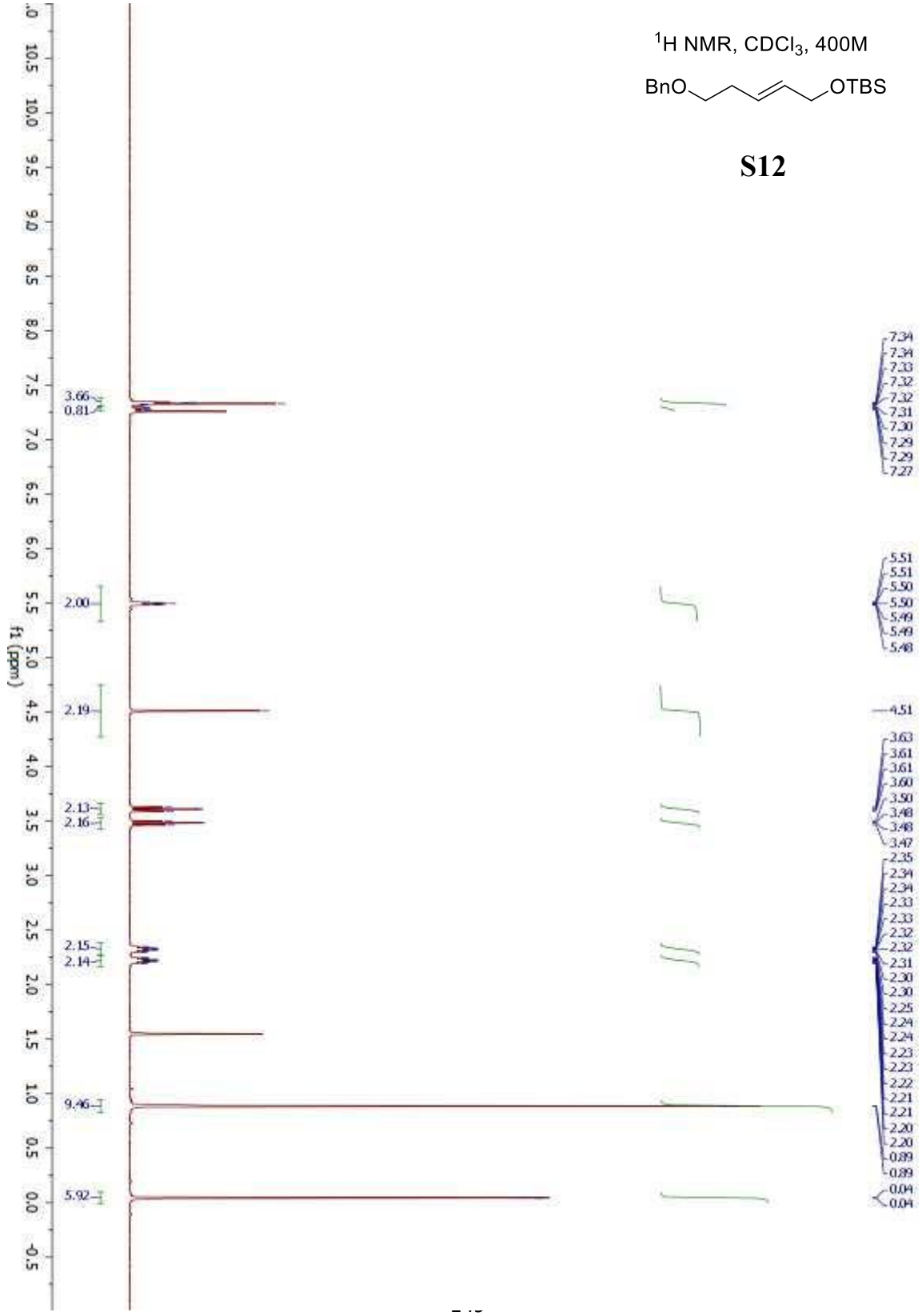

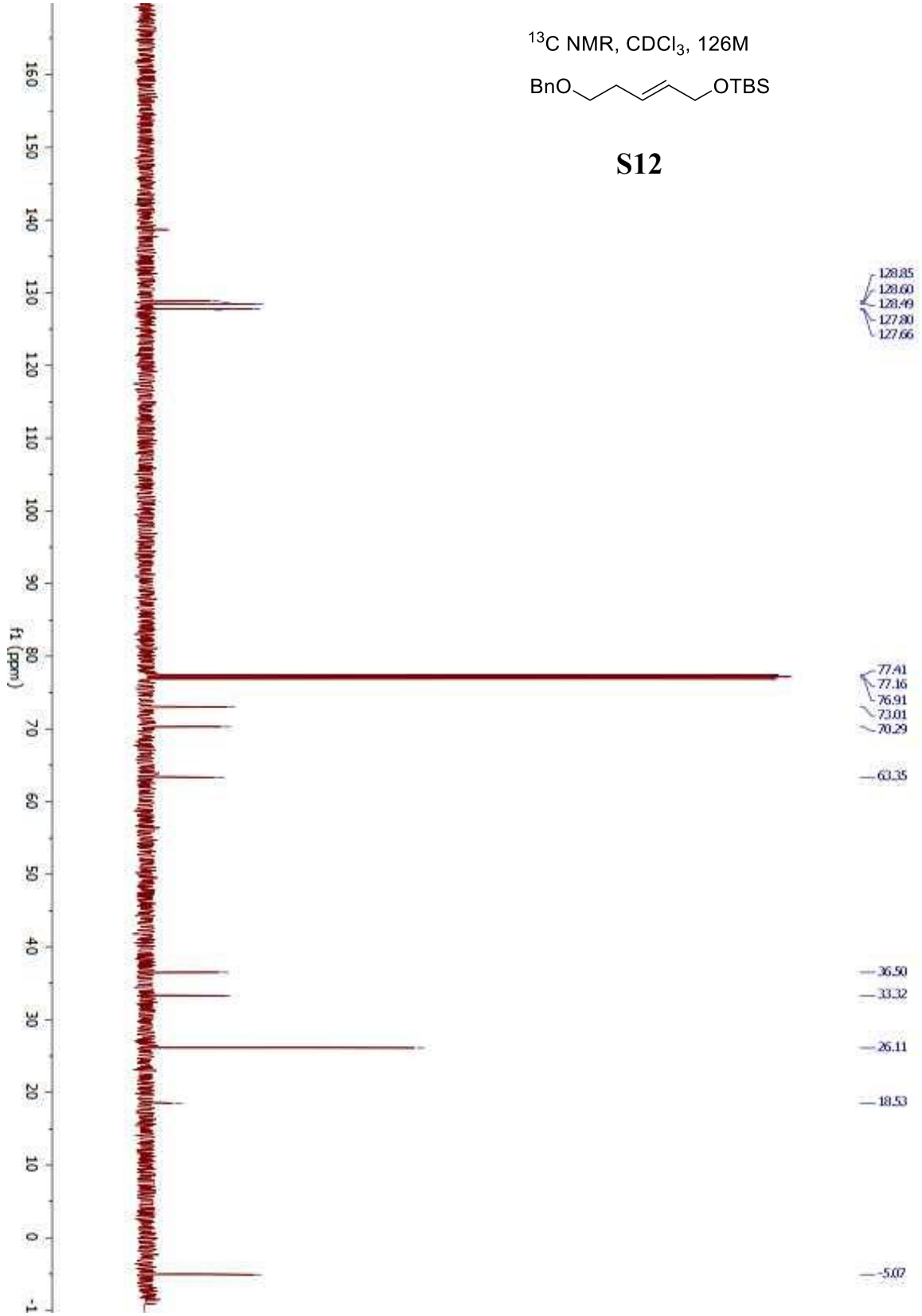
^{13}C NMR, $CDCl_3$, 126M
BnO
OTBS
S12
128.85
128.60
128.49
127.80
127.66
77.41
77.16
76.91
73.01
70.29
63.35
36.50
33.32
26.11
18.53
-5.07
f1 (ppm)

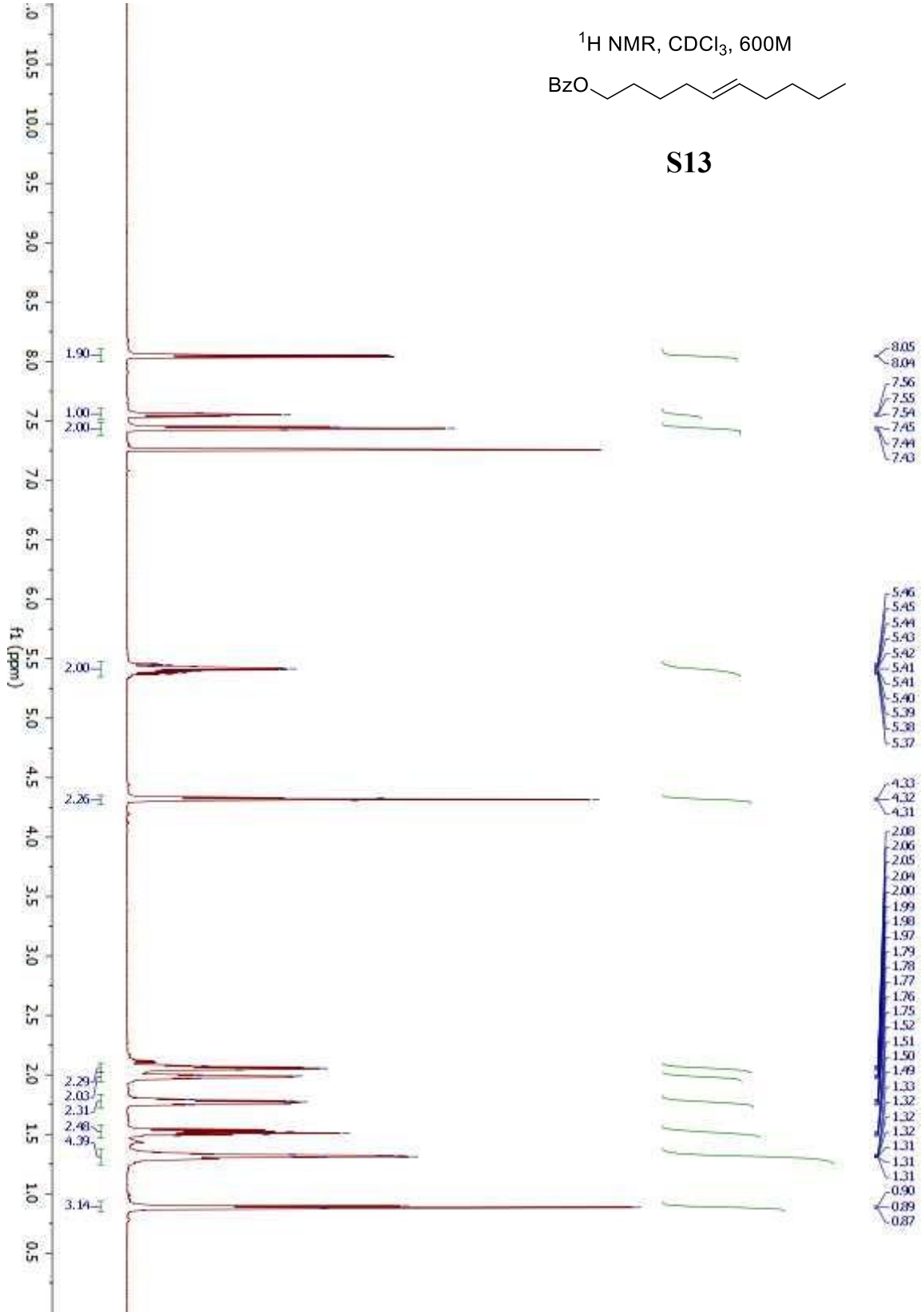
^{1}H NMR, $CDCl_3$, 600M
BzO
S13
f1 (ppm)

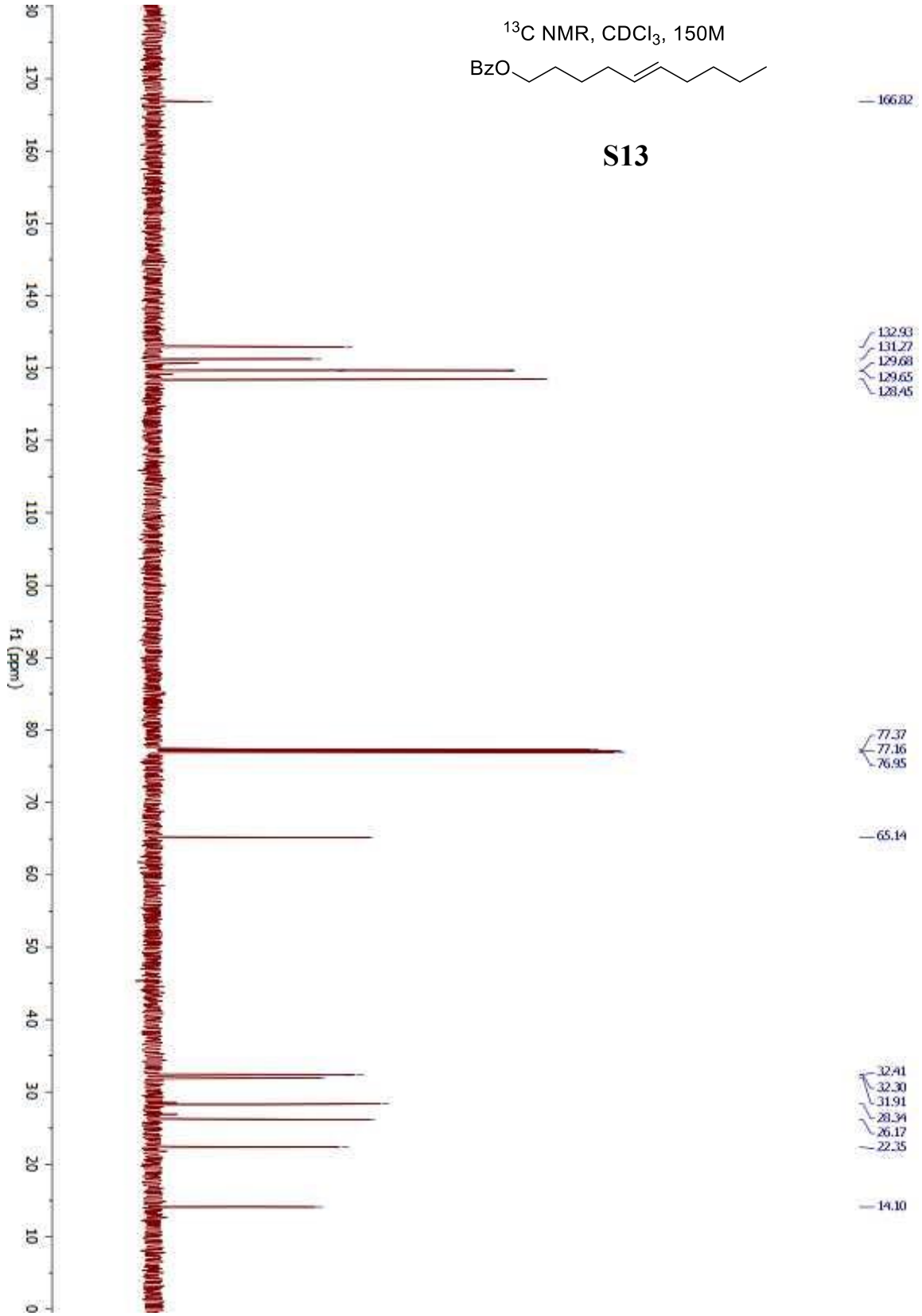
^{13}C NMR, $CDCl_3$, 150M
BzO
S13
166.82
132.93
131.27
129.68
129.65
128.45
77.37
77.16
76.95
65.14
32.41
32.30
31.91
28.34
26.17
22.35
14.10
f1 (ppm)

^{1}H NMR, $CDCl_3$, 500M

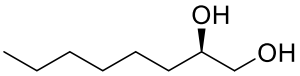

1.106

^{13}C NMR, $CDCl_3$, 150M

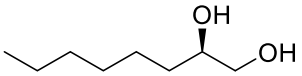

1.106

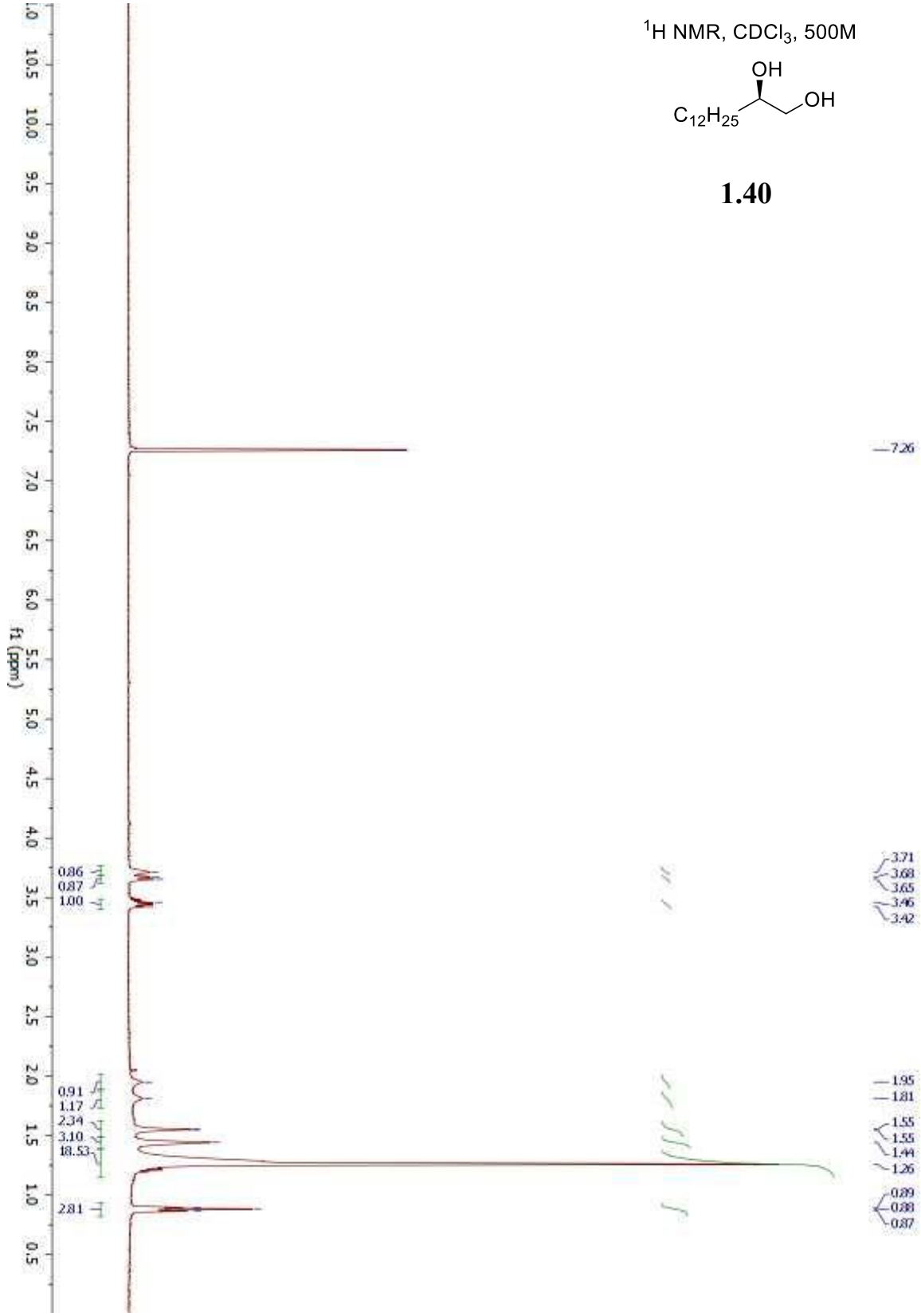
^{1}H NMR, $CDCl_3$, 500M
OH
OH
$C_{12}H_{25}$
1.40
f1 (ppm)
7.26
3.71
3.68
3.65
3.46
3.42
1.95
1.81
1.55
1.55
1.44
1.26
0.89
0.88
0.87
0.86
0.87
1.00
0.91
1.17
2.34
3.10
18.53
2.81

^{13}C NMR, $CDCl_3$, 150M

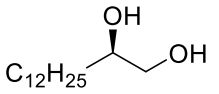

1.40

^{1}H NMR, $CDCl_3$, 600M

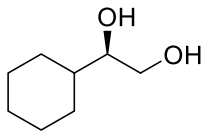

1.107

^{13}C NMR, $CDCl_3$, 150M

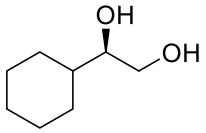

1.107

^{1}H NMR, $CDCl_3$, 600M

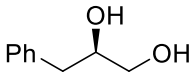

1.108

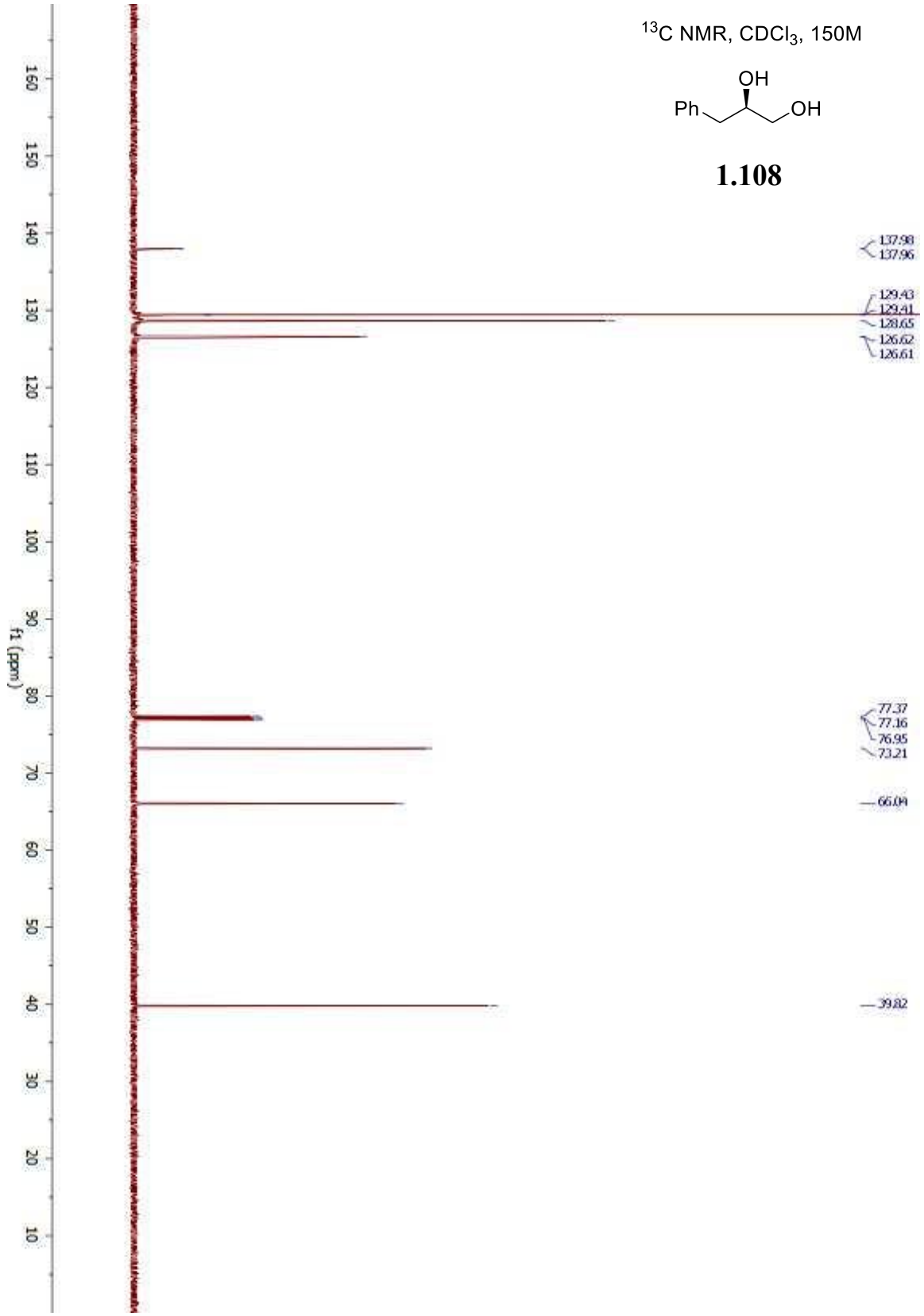
^{13}C NMR, $CDCl_3$, 150M
OH
Ph
OH
1.108
137.98
137.96
129.43
129.41
128.65
126.62
126.61
77.37
77.16
76.95
73.21
66.09
39.82
f1 (ppm)

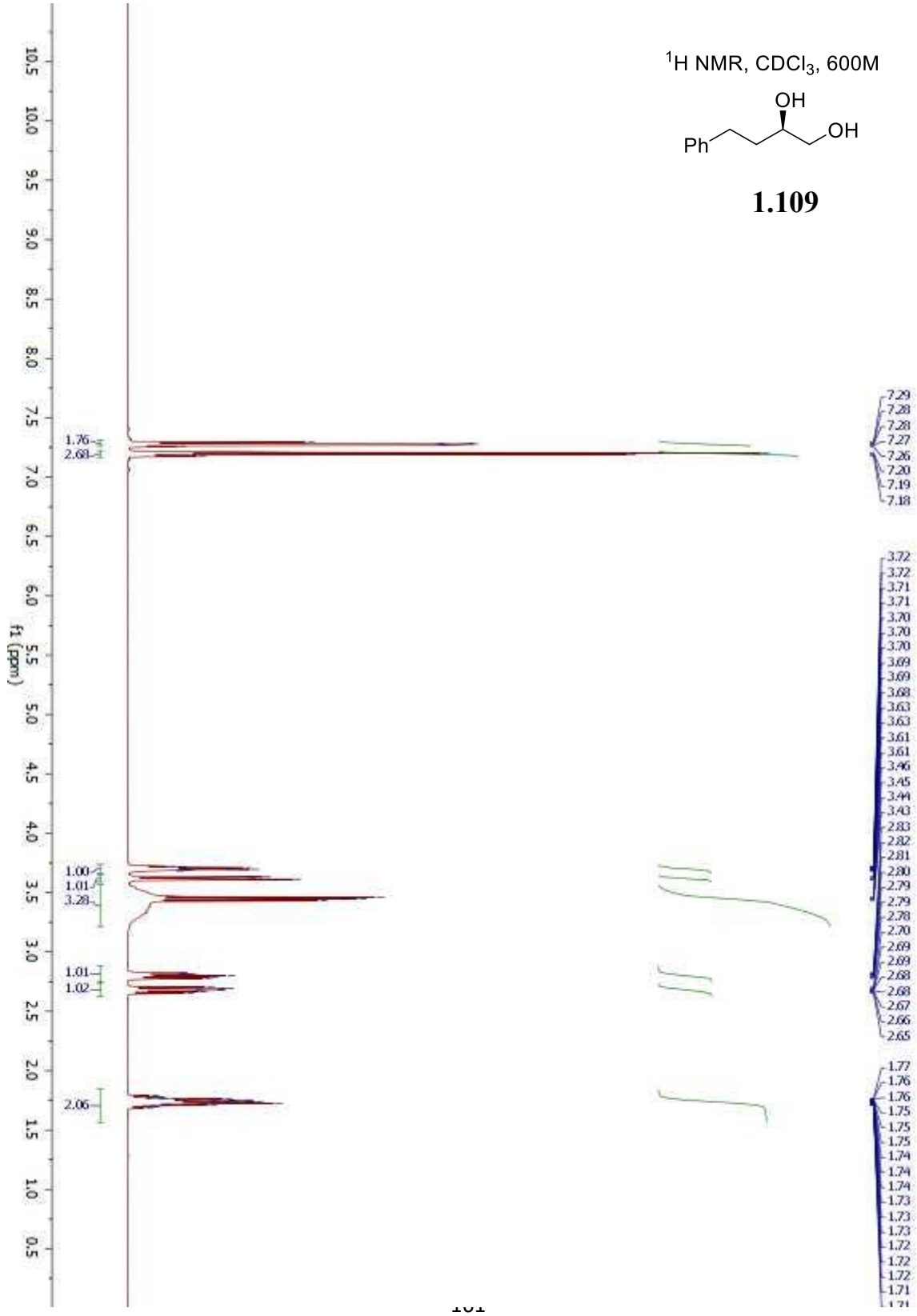
^{1}H NMR, $CDCl_3$, 600M
OH
OH
Ph
1.109
f1 (ppm)
1.76
2.68
1.00
1.01
3.28
1.01
1.02
2.06

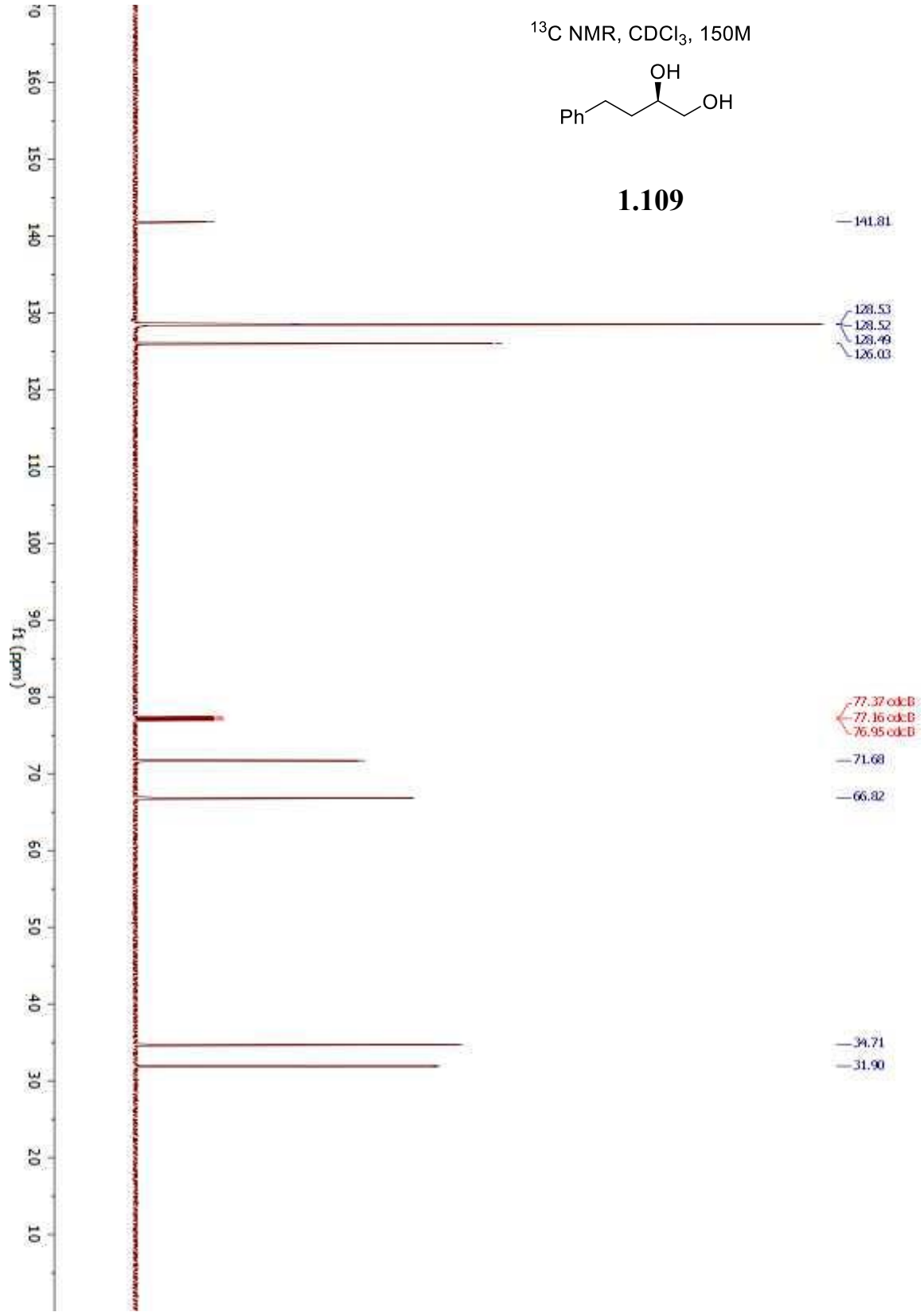
^{13}C NMR, $CDCl_3$, 150M
OH
Ph
OH
1.109
141.81
128.53
128.52
128.49
126.03
77.37 cdcl3
77.16 cdcl3
76.95 cdcl3
71.68
66.82
34.71
31.90
f1 (ppm)

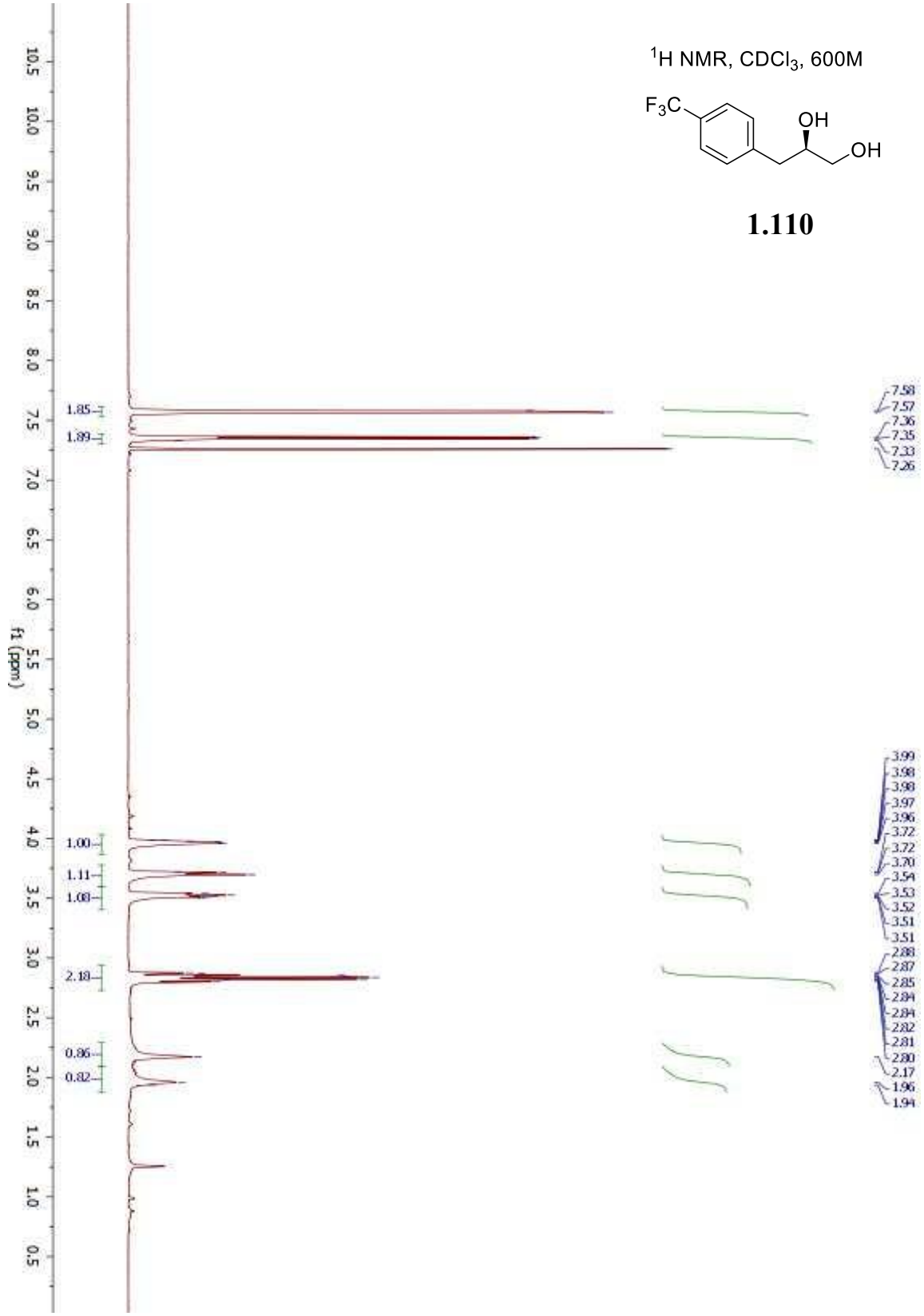
^{1}H NMR, $CDCl_3$, 600M
F_3C
OH
OH
1.110
f1 (ppm)
1.85
1.89
1.00
1.11
1.08
2.18
0.86
0.82
7.58
7.57
7.36
7.35
7.33
7.26
3.99
3.98
3.98
3.97
3.96
3.72
3.72
3.70
3.54
3.53
3.52
3.51
3.51
2.88
2.87
2.85
2.84
2.84
2.82
2.81
2.80
2.17
1.96
1.94

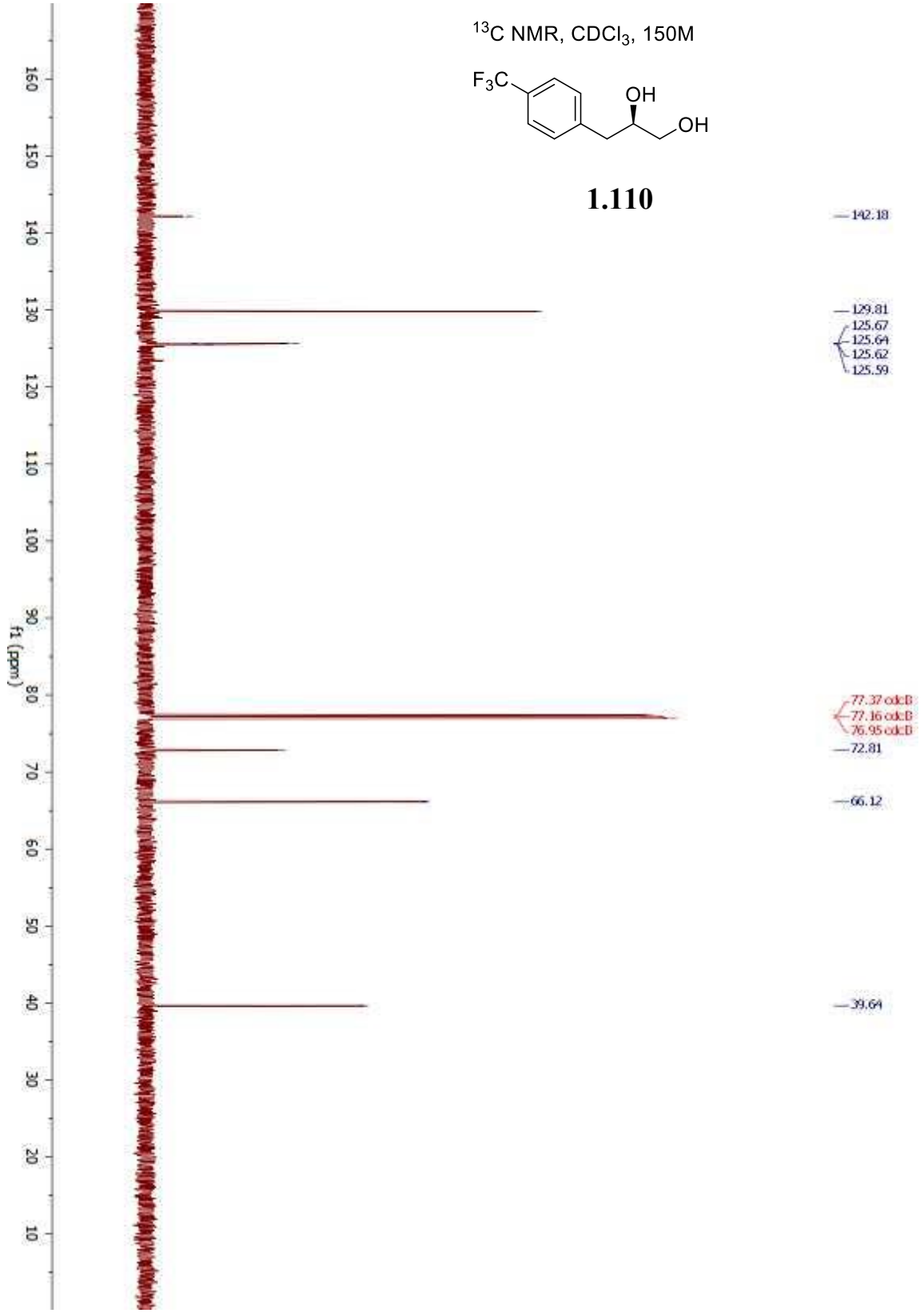
^{13}C NMR, $CDCl_3$, 150M
F_3C
OH
OH
1.110
142.18
129.81
125.67
125.64
125.62
125.59
77.37 odcb
77.16 odcb
76.95 odcb
72.81
66.12
39.64
f1 (ppm)

^{1}H NMR, $CDCl_3$, 600M

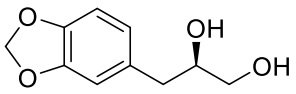

1.111

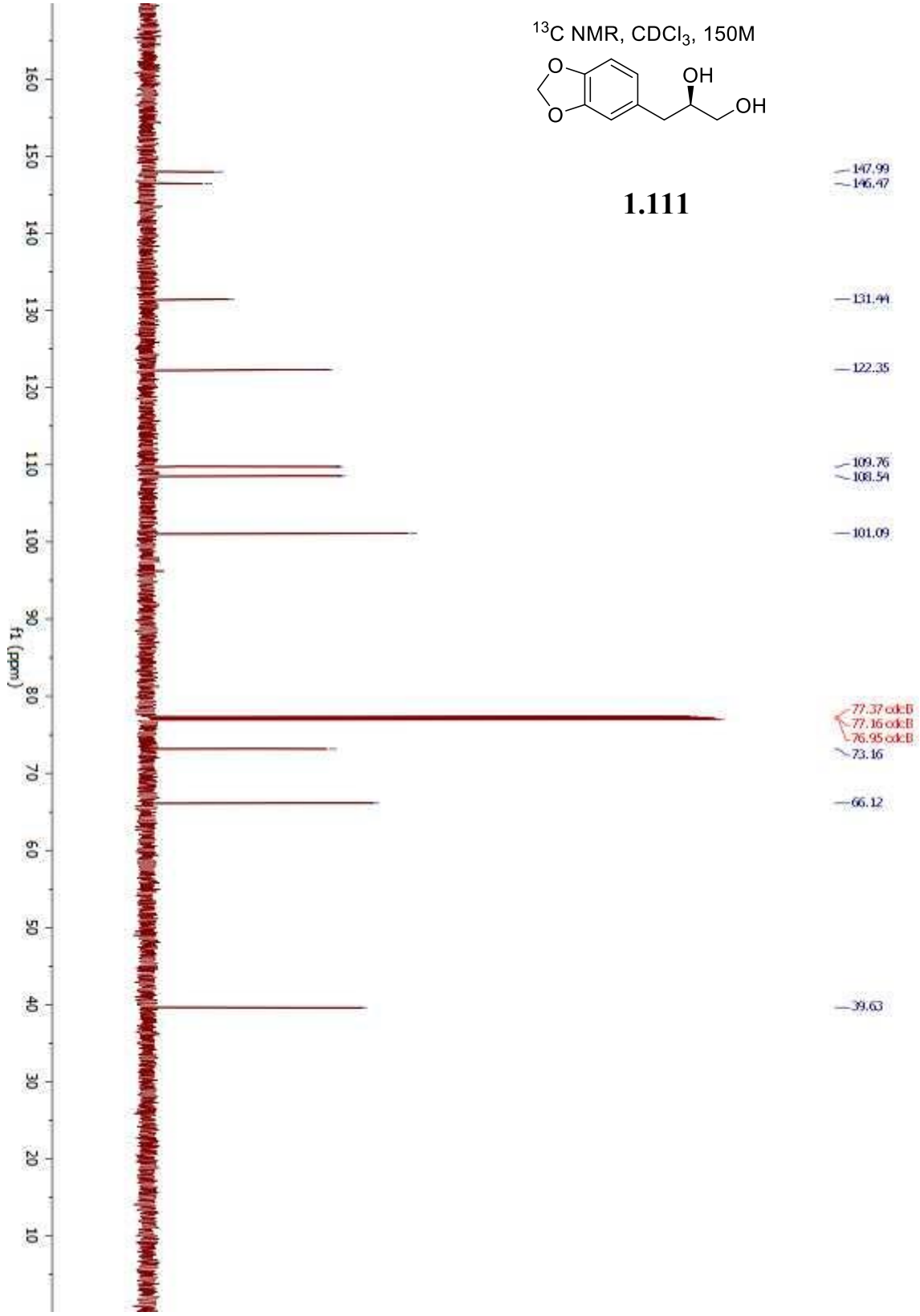
^{13}C NMR, CDCl$_3$, 150M
OH
OH
1.111
147.99
146.47
131.44
122.35
109.76
108.59
101.09
77.37 cdcl3
77.16 cdcl3
76.95 cdcl3
73.16
66.12
39.63
f1 (ppm)

^{1}H NMR, $CDCl_3$, 400M

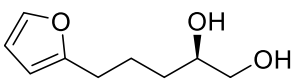

1.112

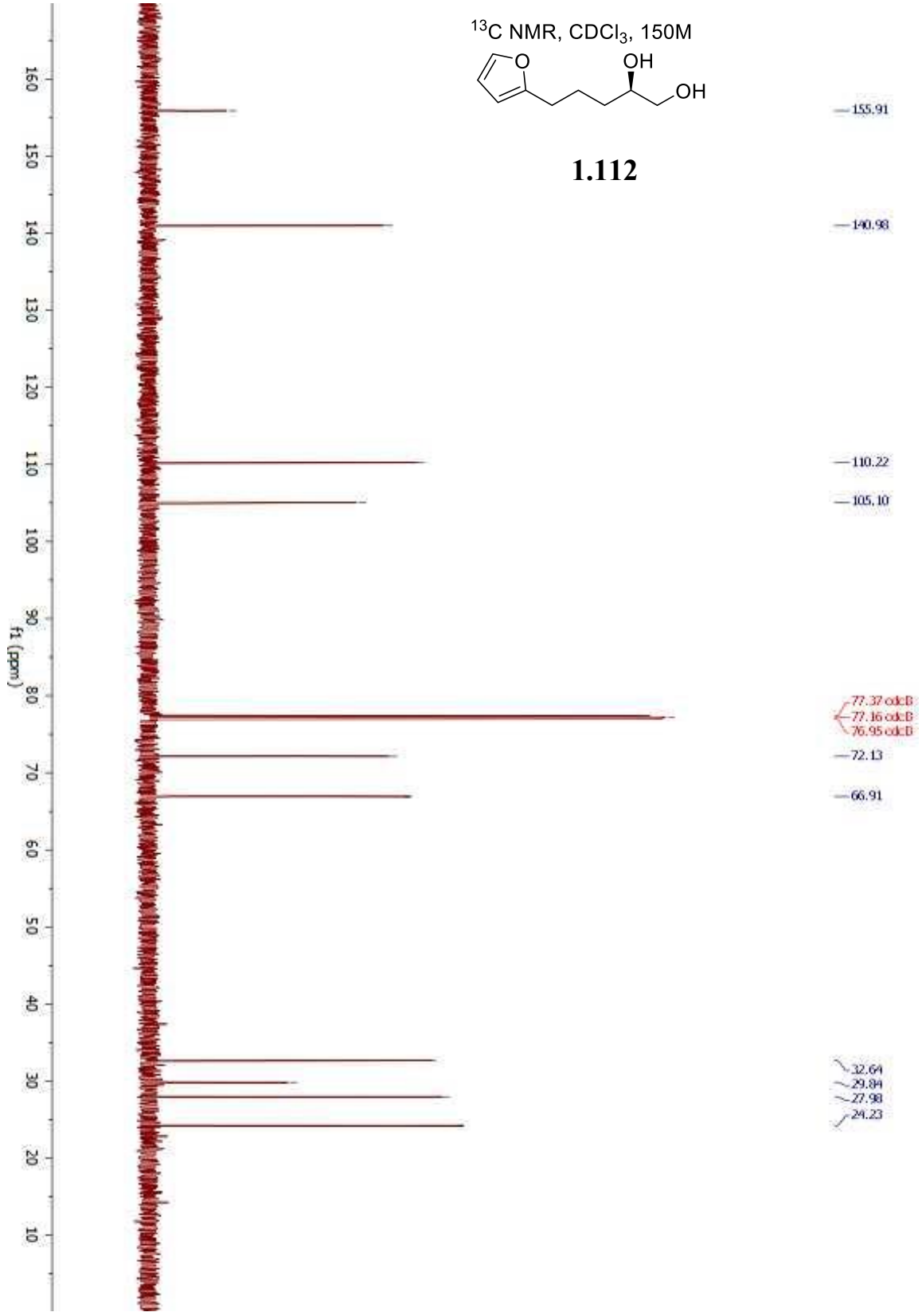
^{13}C NMR, $CDCl_3$, 150M
O
OH
OH
1.112
155.91
140.98
110.22
105.10
77.37 cdcl3
77.16 cdcl3
76.95 cdcl3
72.13
66.91
32.64
29.84
27.98
24.23
f1 (ppm)

^{1}H NMR, $CDCl_3$, 600M

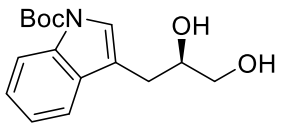

1.113

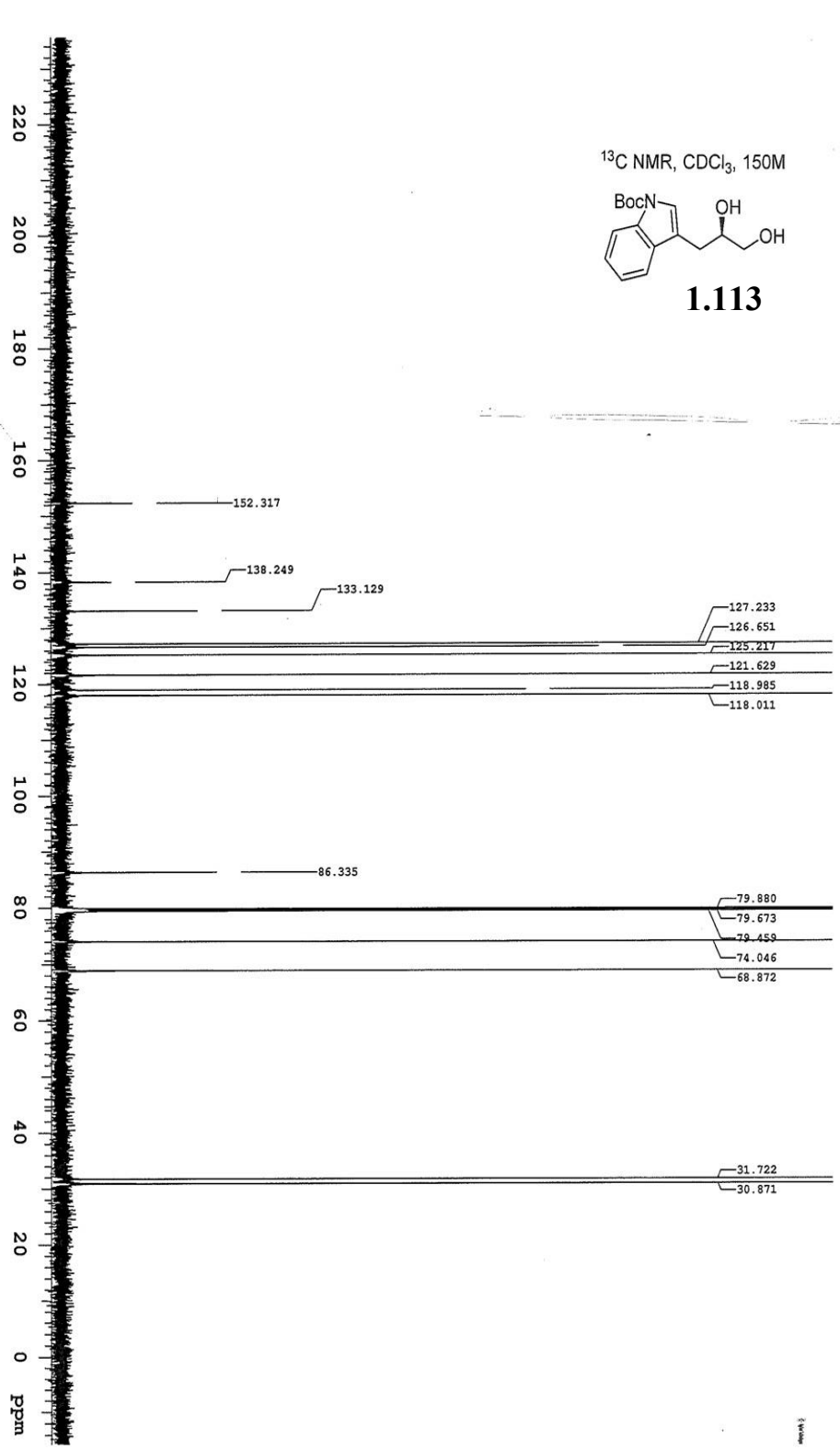
^{13}C NMR, $CDCl_3$, 150M
BocN
OH
OH
1.113
152.317
138.249
133.129
127.233
126.651
125.217
121.629
118.985
118.011
86.335
79.880
79.673
79.459
74.046
68.872
31.722
30.871
220
200
180
160
140
120
100
80
60
40
20
0
ppm

^{1}H NMR, $CDCl_3$, 400M

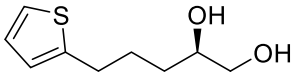

1.114

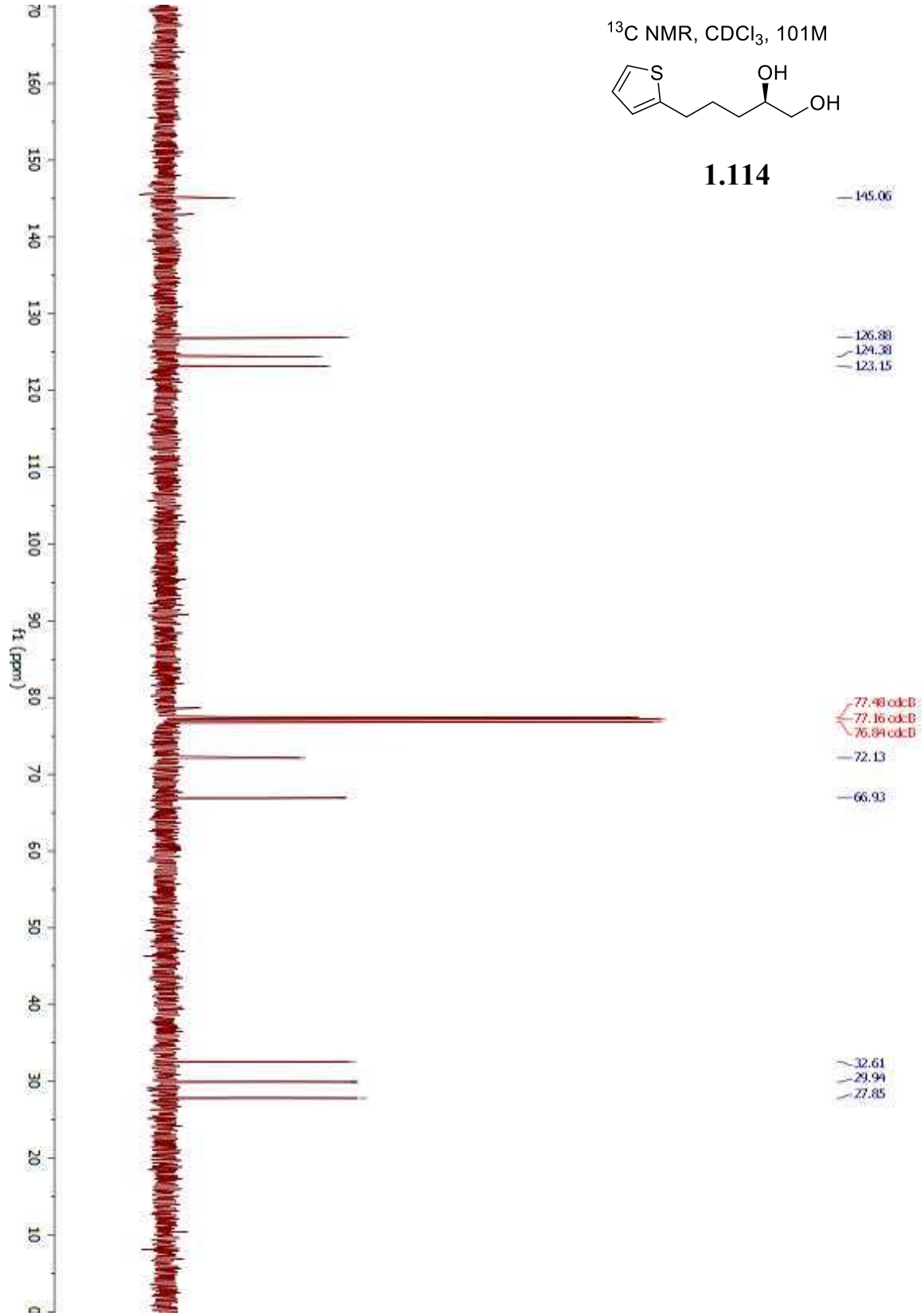
^{13}C NMR, $CDCl_3$, 101M
S
OH
OH
1.114
145.06
126.88
124.38
123.15
77.48 cdcl3
77.16 cdcl3
76.84 cdcl3
72.13
66.93
32.61
29.94
27.85
f1 (ppm)

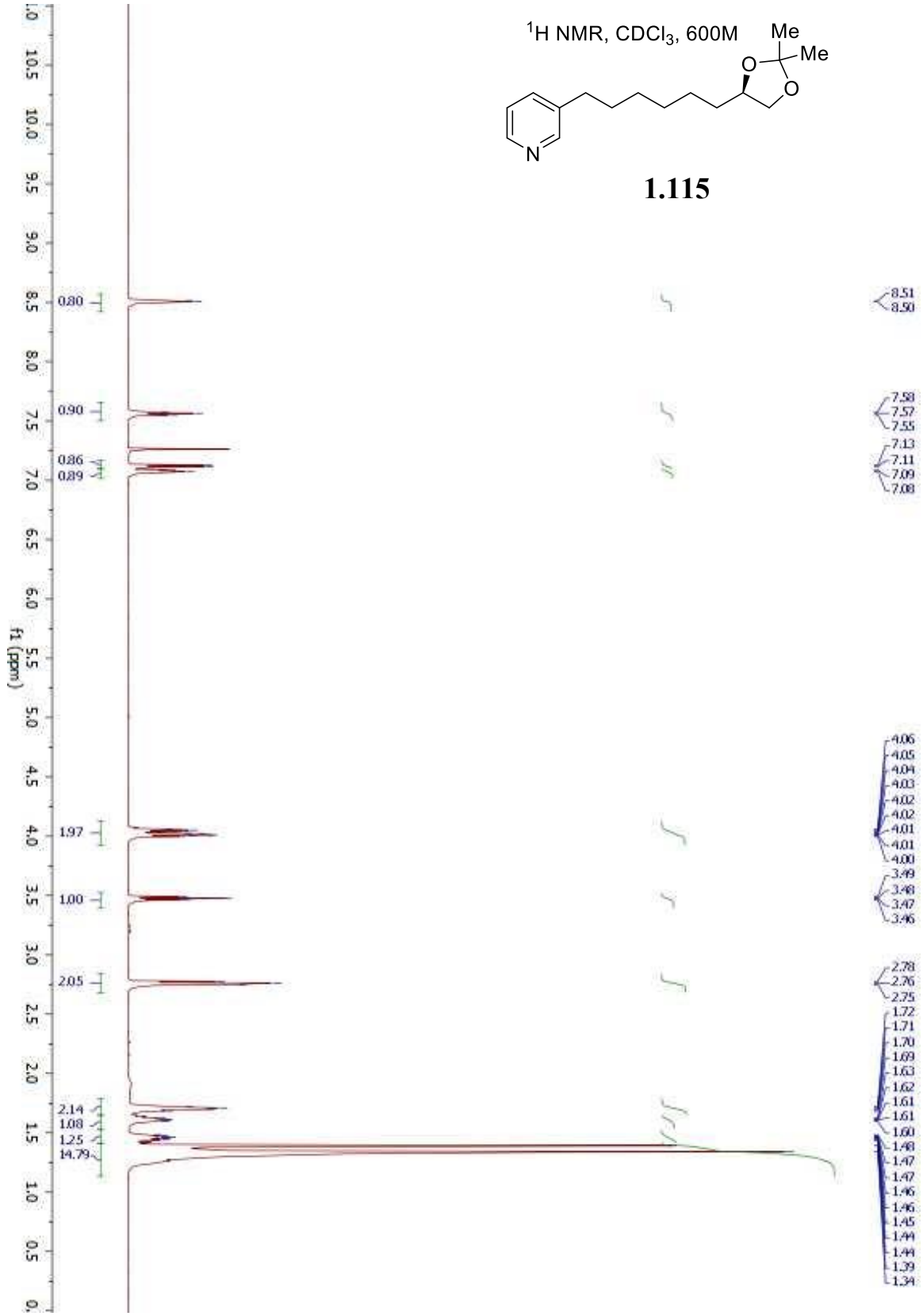
1H NMR, CDCl3, 600M
Me
Me
O
O
N
1.115
f1 (ppm)
0.80
0.90
0.86
0.89
1.97
1.00
2.05
2.14
1.08
1.25
14.79
8.51
8.50
7.58
7.57
7.55
7.13
7.11
7.09
7.08
4.06
4.05
4.04
4.03
4.02
4.02
4.01
4.01
4.00
3.49
3.48
3.47
3.46
2.78
2.76
2.75
1.72
1.71
1.70
1.69
1.63
1.62
1.61
1.61
1.60
1.48
1.47
1.47
1.46
1.46
1.45
1.44
1.44
1.39
1.34

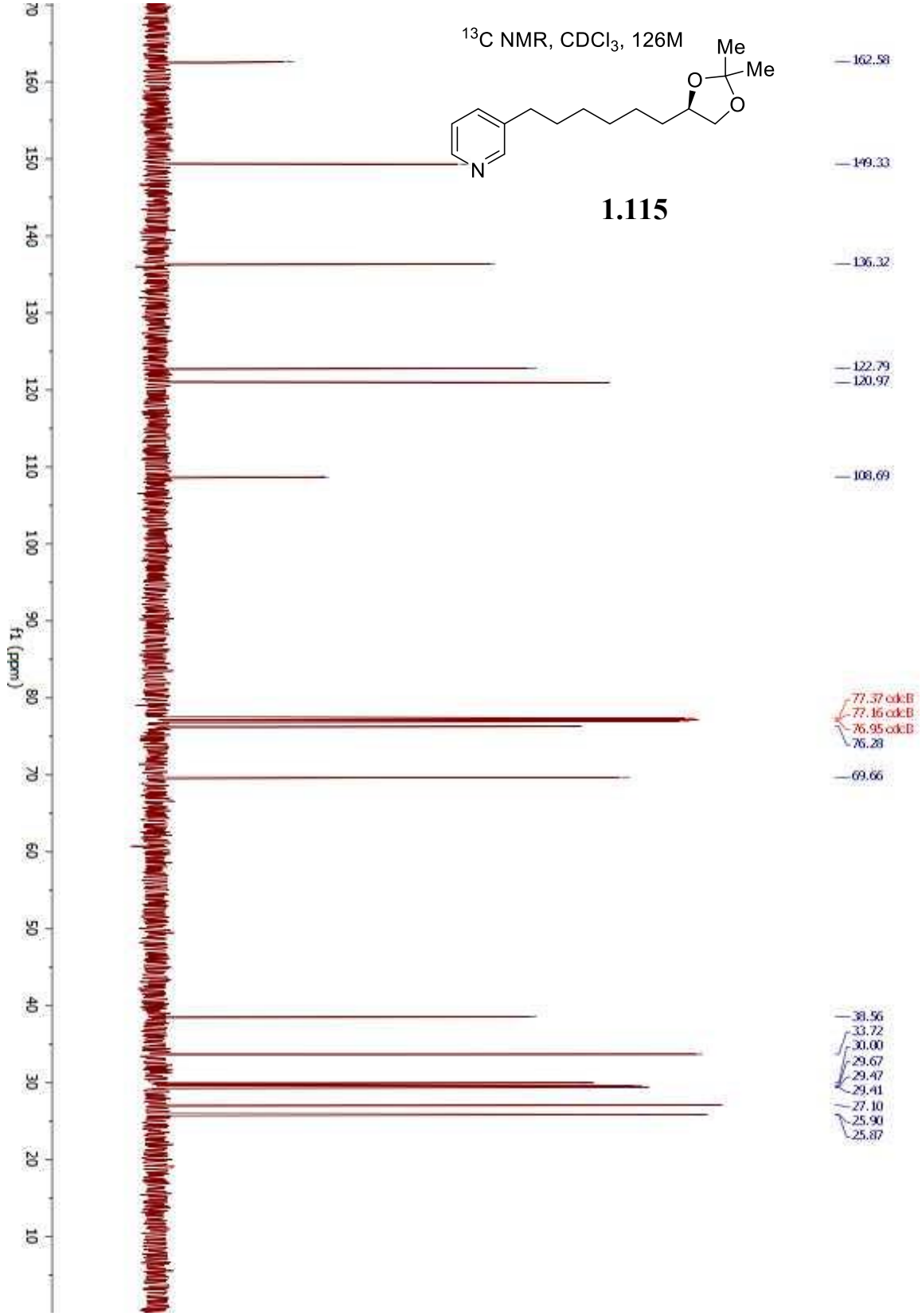
^{13}C NMR, $CDCl_3$, 126M
Me
Me
O
O
N
1.115
162.58
149.33
136.32
122.79
120.97
108.69
77.37 cdcl3
77.16 cdcl3
76.95 cdcl3
76.28
69.66
38.56
33.72
30.00
29.67
29.47
29.41
27.10
25.90
25.87
f1 (ppm)

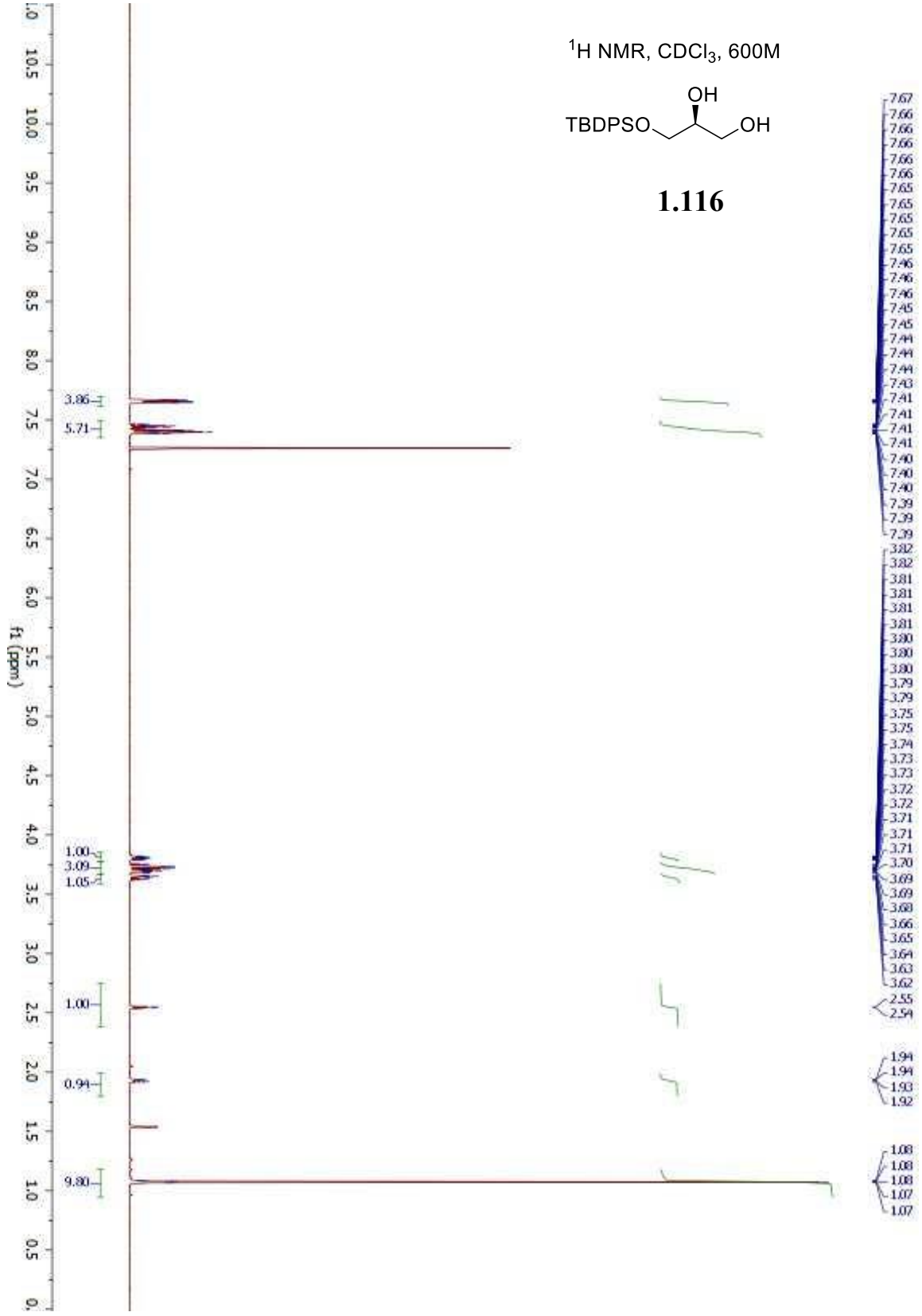
^{1}H NMR, $CDCl_3$, 600M
OH
TBDPSO
OH
1.116
f1 (ppm)
3.86
5.71
1.00
3.09
1.05
1.00
0.94
9.80

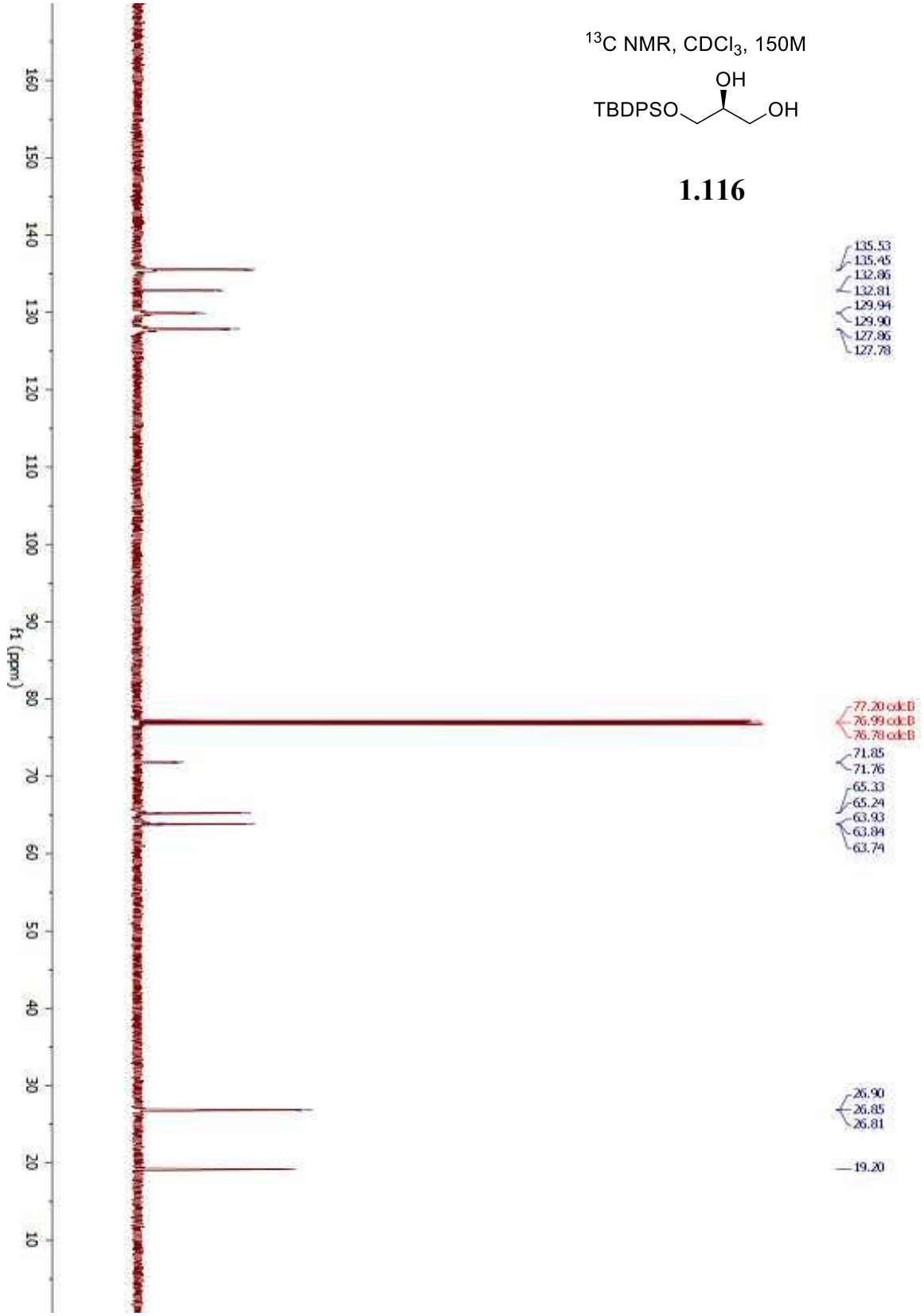
^{13}C NMR, $CDCl_3$, 150M
OH
TBDPSO
OH
1.116
135.53
135.45
132.86
132.81
129.94
129.90
127.86
127.78
77.20 cdcl3
76.99 cdcl3
76.78 cdcl3
71.85
71.76
65.33
65.24
63.93
63.84
63.74
26.90
26.85
26.81
19.20
f1 (ppm)

^{1}H NMR, $CDCl_3$, 600M

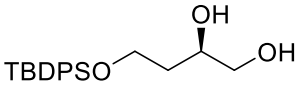

1.44

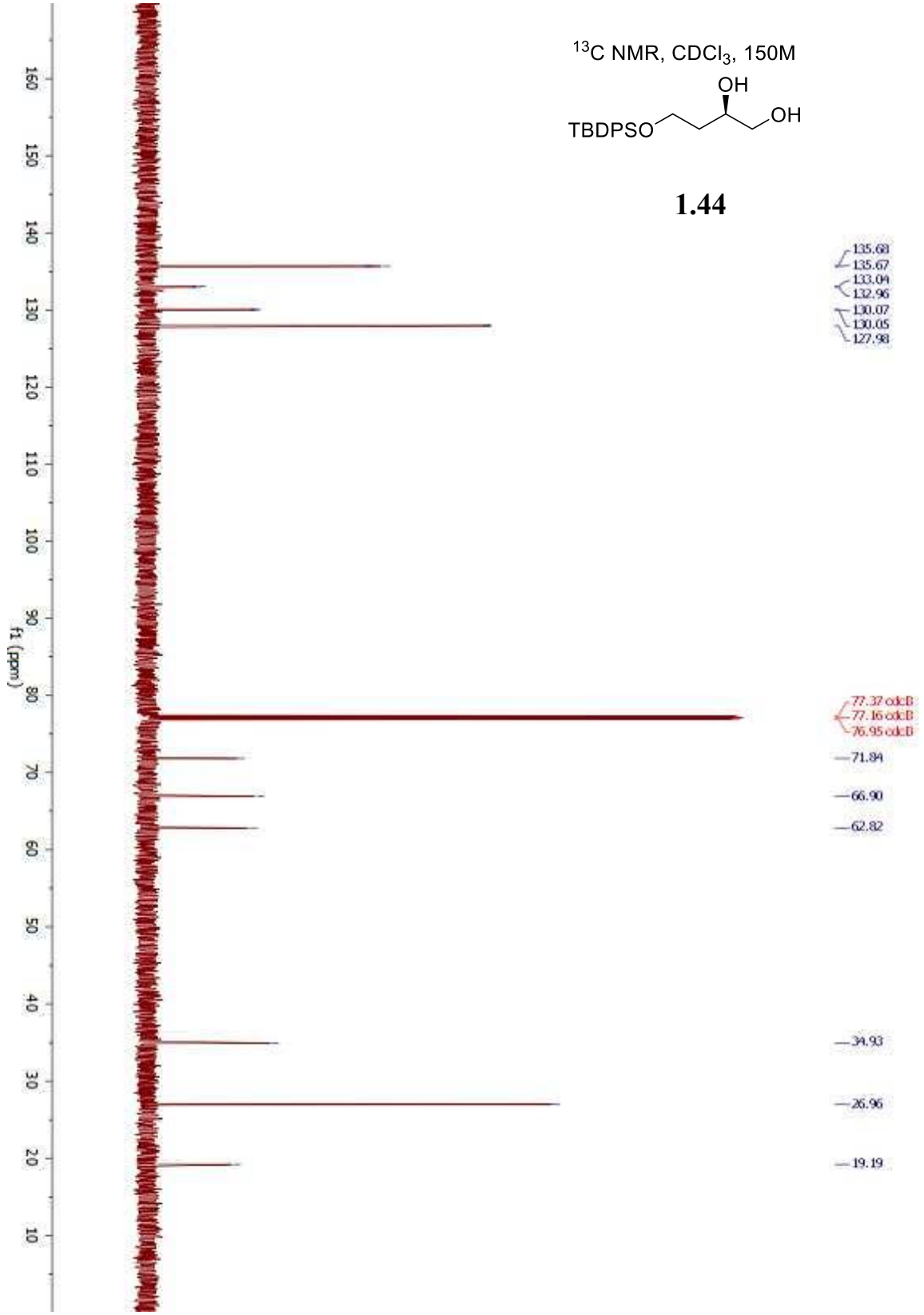
^{13}C NMR, $CDCl_3$, 150M
OH
TBDPSO
OH
1.44
135.68
135.67
133.04
132.96
130.07
130.05
127.98
77.37 odcb
77.16 odcb
76.95 odcb
71.84
66.90
62.82
34.93
26.96
19.19
f1 (ppm)

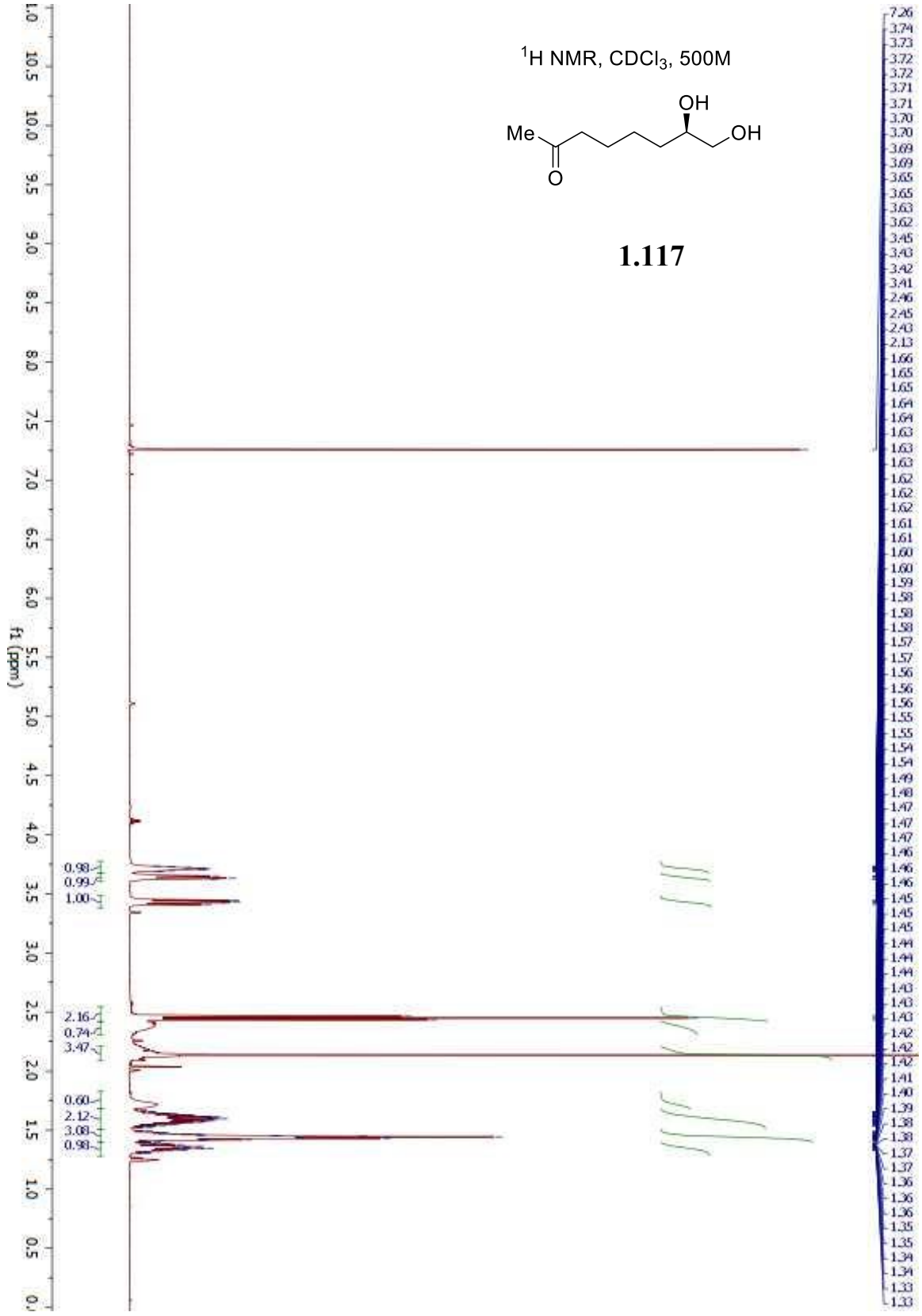
^{1}H NMR, $CDCl_3$, 500M
OH
Me
OH
O
1.117
f1 (ppm)
0.98
0.99
1.00
2.16
0.74
3.47
0.60
2.12
3.08
0.98

^{13}C NMR, $CDCl_3$, 126M

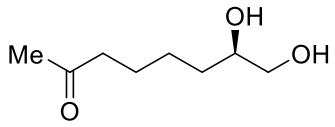

1.117

^{1}H NMR, $CDCl_3$, 600M

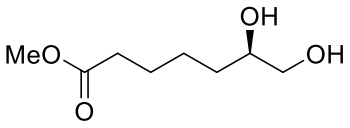

1.118

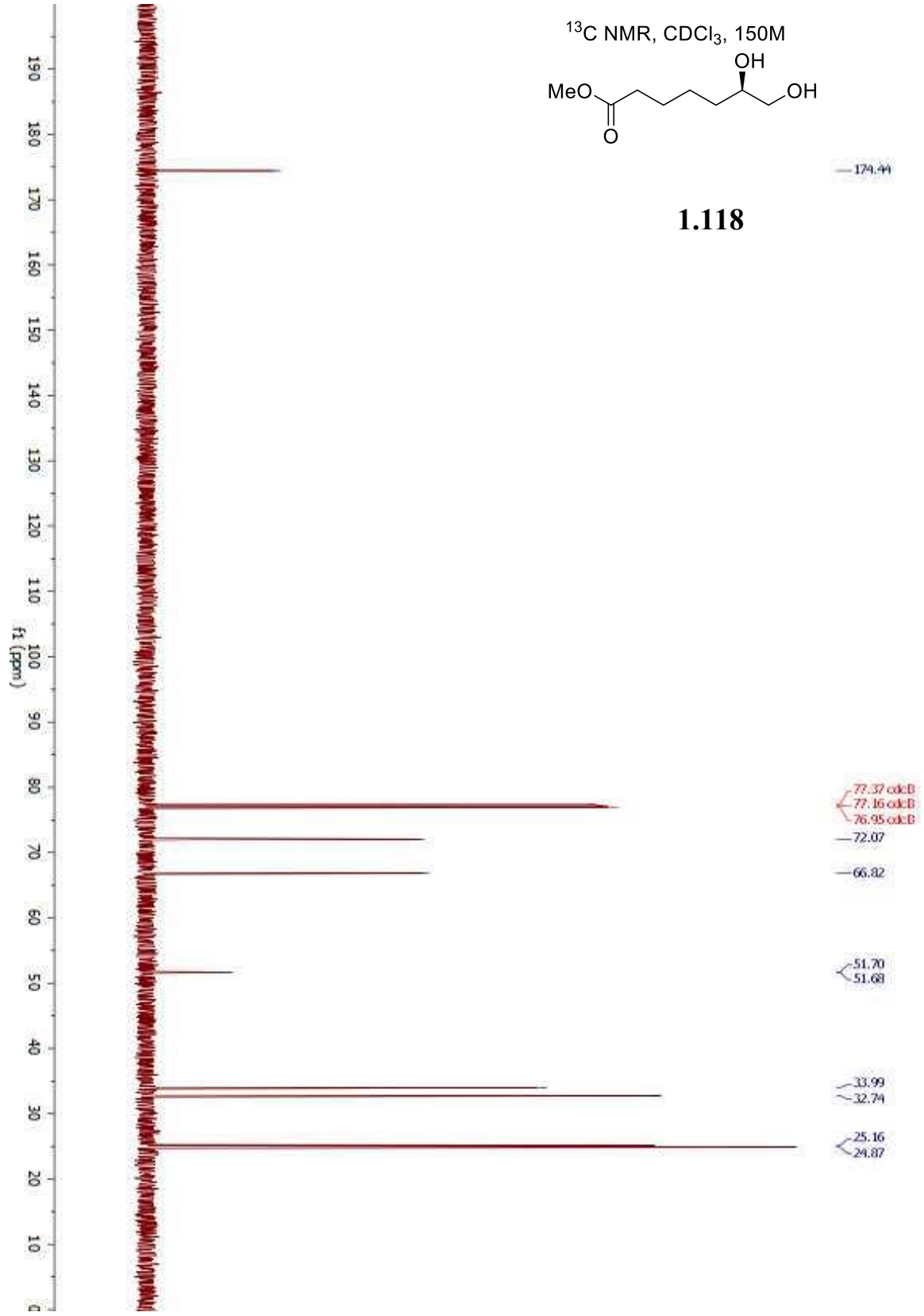
^{13}C NMR, $CDCl_3$, 150M
OH
MeO
OH
O
174.44
77.37 cdcl3
77.16 cdcl3
76.95 cdcl3
72.07
66.82
51.70
51.68
33.99
32.74
25.16
24.87
f1 (ppm)

1.118

^{1}H NMR, $CDCl_3$, 500M

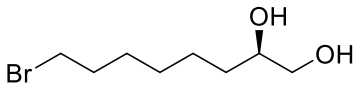

1.119

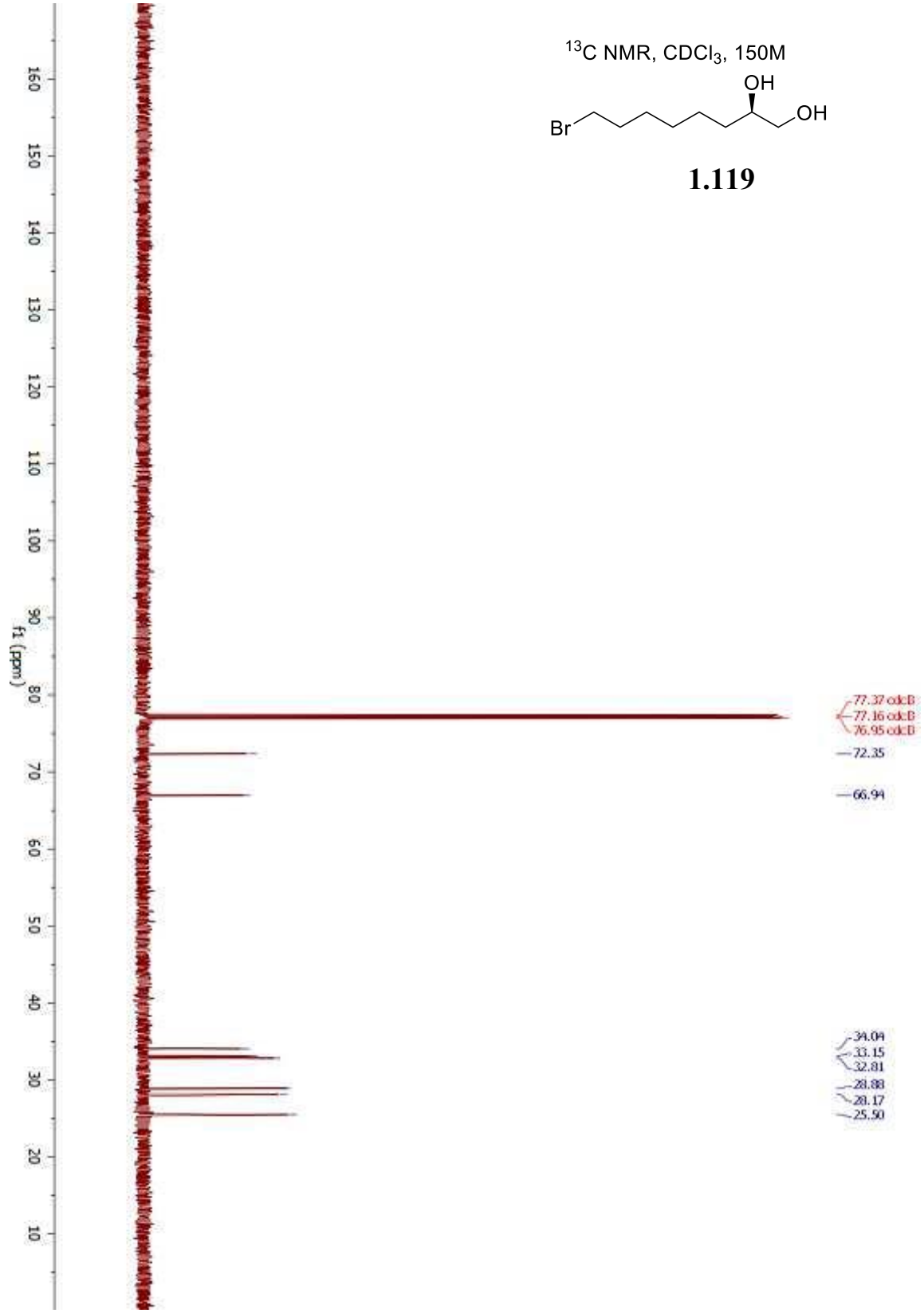
^{13}C NMR, $CDCl_3$, 150M
OH
Br
OH
1.119
f1 (ppm)
160
150
140
130
120
110
100
90
80
70
60
50
40
30
20
10
77.37 cdcl3
77.16 cdcl3
76.95 cdcl3
72.35
66.94
34.09
33.15
32.81
28.88
28.17
25.50

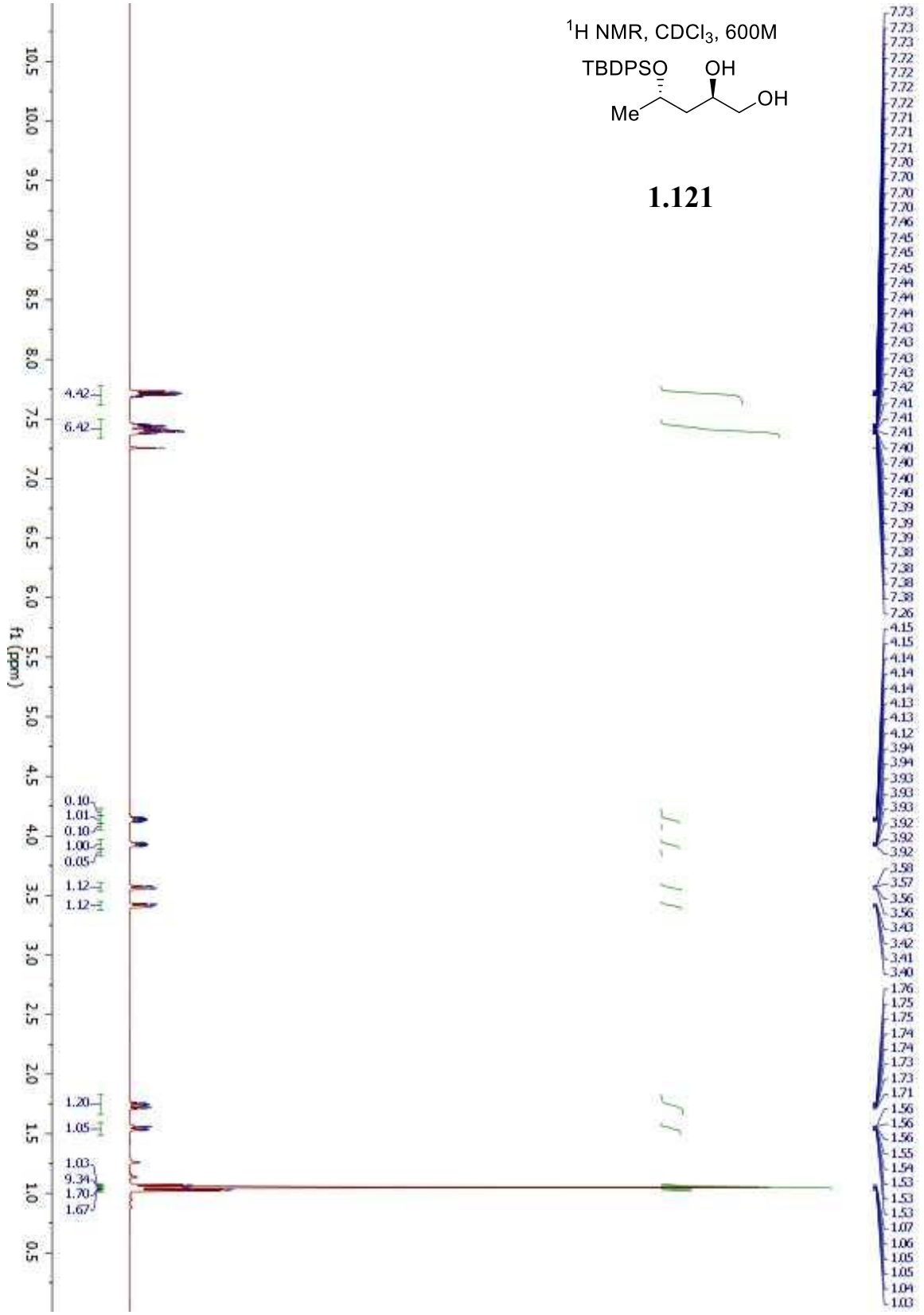
^{1}H NMR, $CDCl_3$, 600M
TBDPSO
OH
OH
Me
1.121
f1 (ppm)

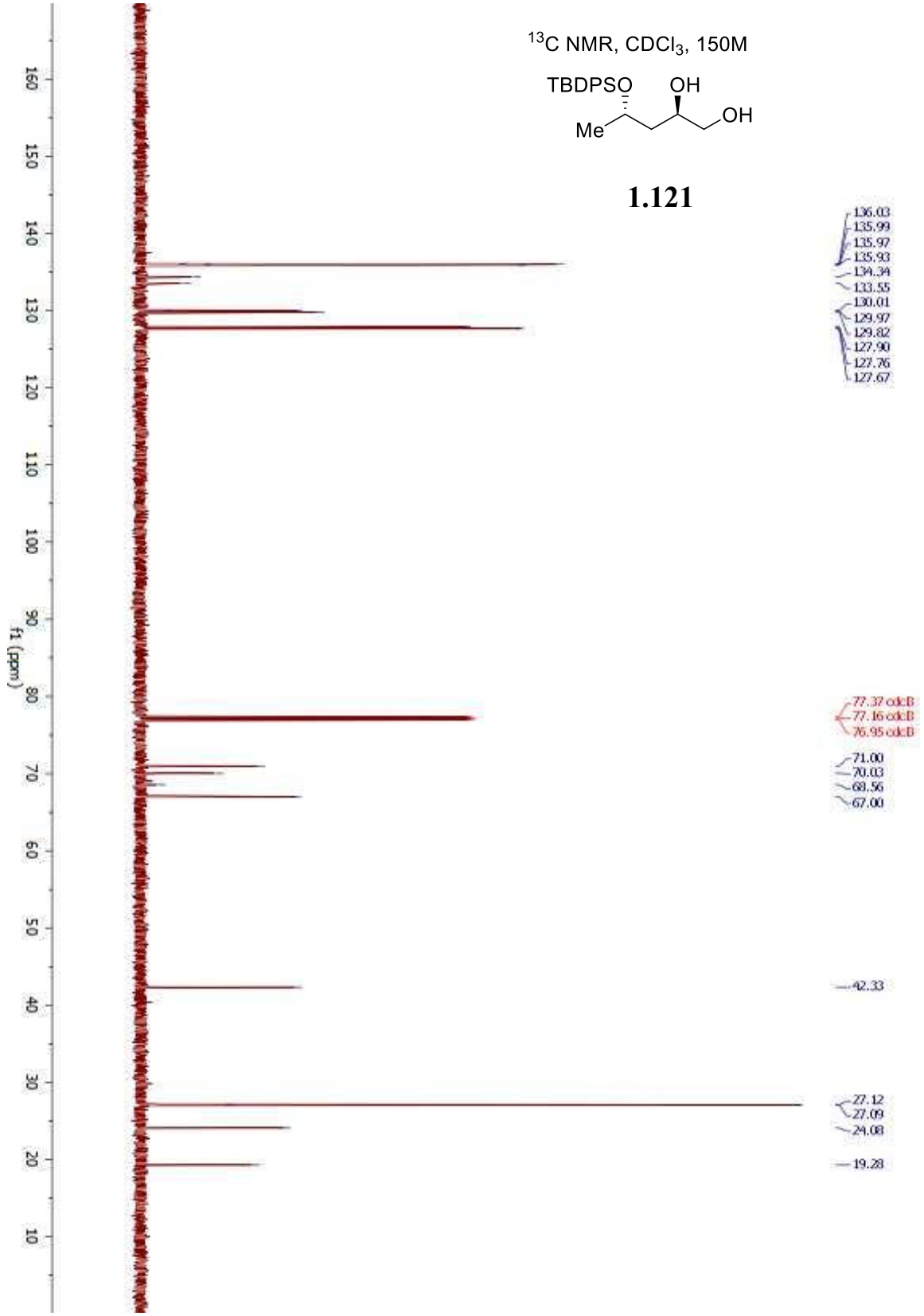
^{13}C NMR, $CDCl_3$, 150M
TBDPSO
OH
OH
Me
1.121
f1 (ppm)
136.03
135.99
135.97
135.93
134.34
133.55
130.01
129.97
129.82
127.90
127.76
127.67
77.37 cdcl3
77.16 cdcl3
76.95 cdcl3
71.00
70.03
68.56
67.00
42.33
27.12
27.09
24.08
19.28

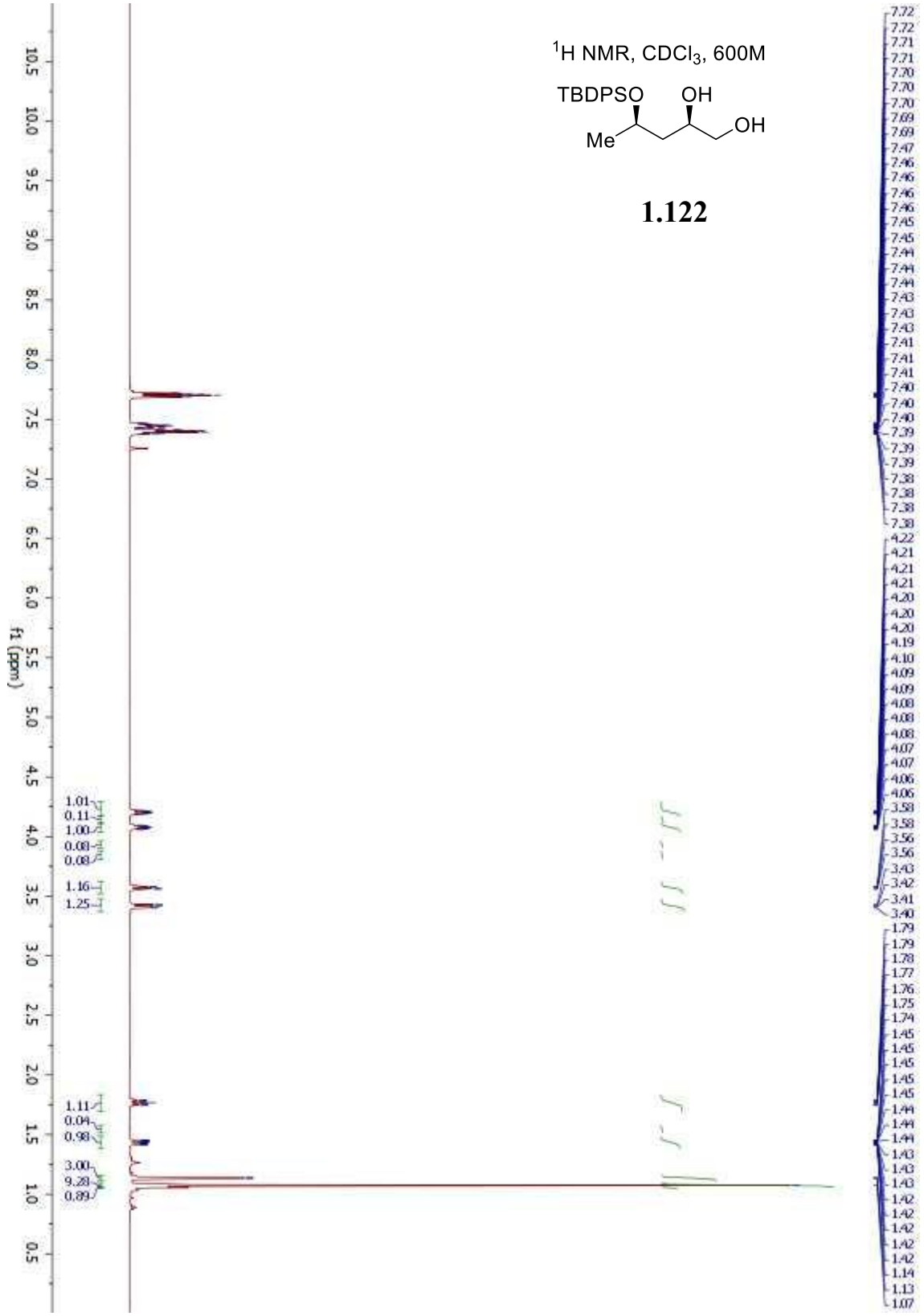
^{1}H NMR, $CDCl_3$, 600M
TBDPSO
OH
OH
Me
1.122
f1 (ppm)

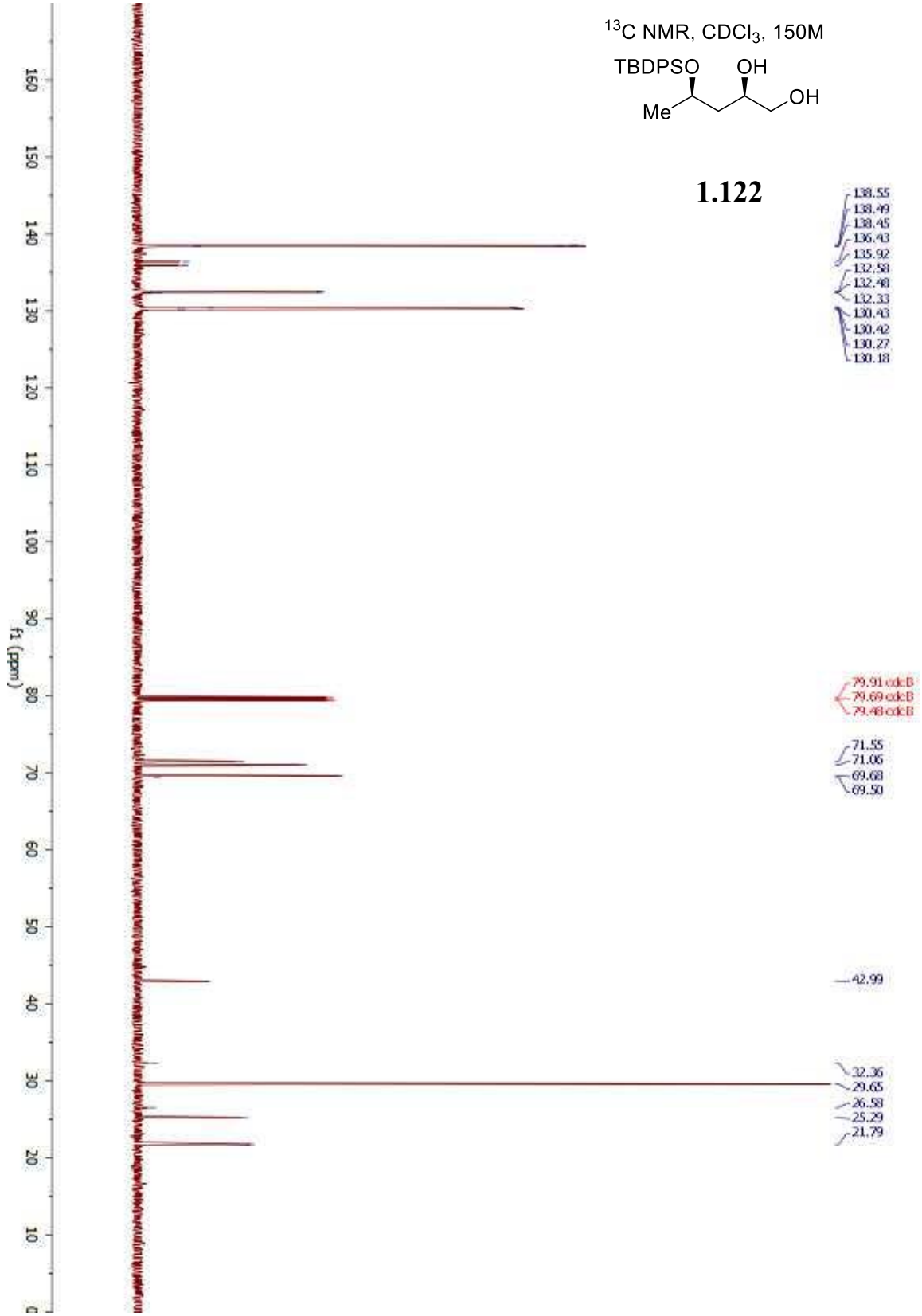
^{13}C NMR, $CDCl_3$, 150M
TBDPSO
OH
OH
Me
1.122
138.55
138.49
138.45
136.43
135.92
132.58
132.48
132.33
130.43
130.42
130.27
130.18
79.91 cdcl3
79.69 cdcl3
79.48 cdcl3
71.55
71.06
69.68
69.50
42.99
32.36
29.65
26.58
25.29
21.79
f1 (ppm)

^{1}H NMR, $CDCl_3$, 600M

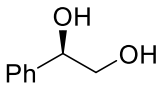

1.48

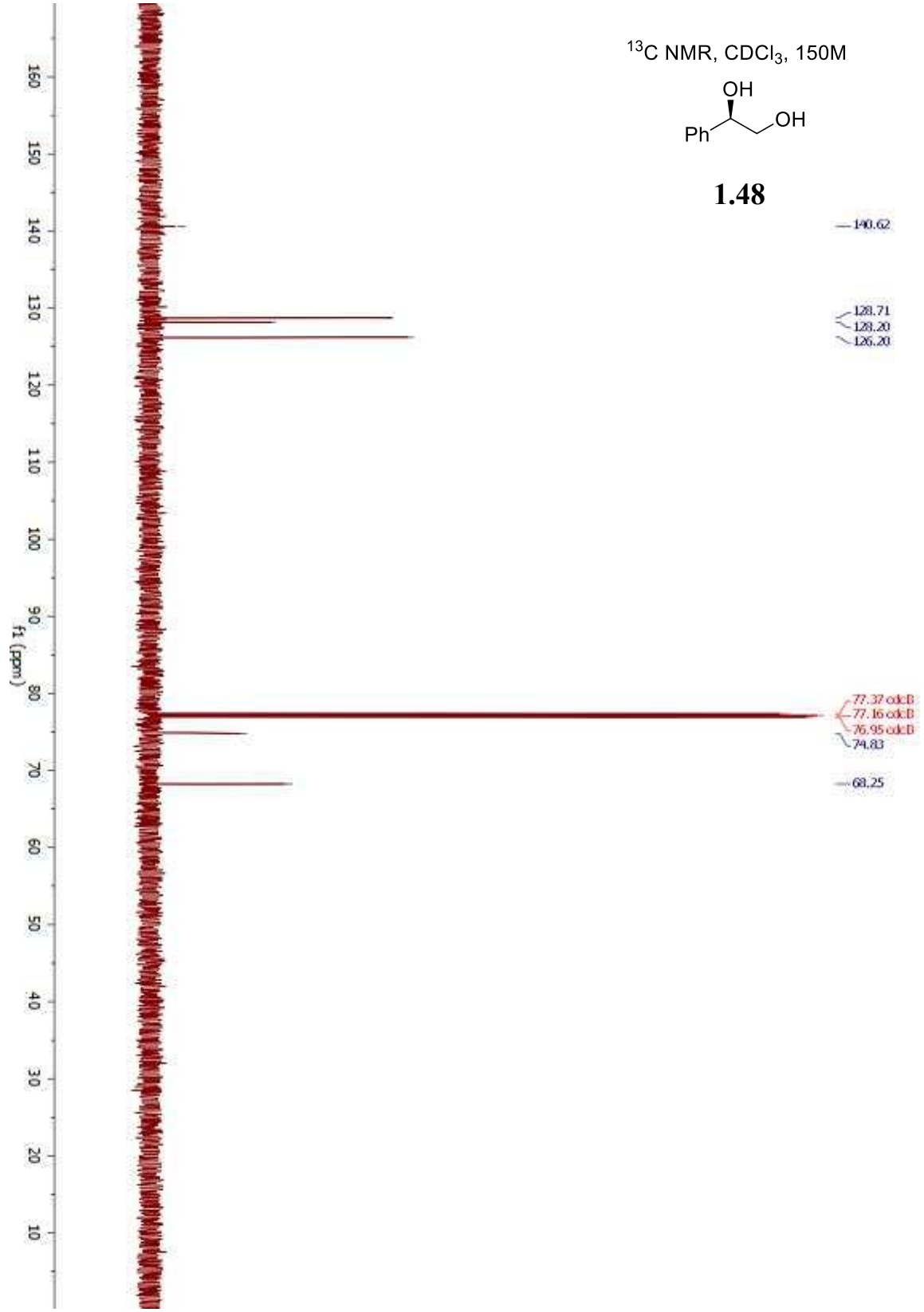
^{13}C NMR, $CDCl_3$, 150M
OH
OH
Ph
1.48
140.62
128.71
128.20
126.20
77.37 odcb
77.16 odcb
76.95 odcb
74.83
68.25
f1 (ppm)

^{1}H NMR, $CDCl_3$, 500M

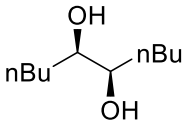

1.36

^{13}C NMR, $CDCl_3$, 126M

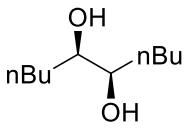

1.36

^{1}H NMR, $CDCl_3$, 600M

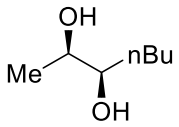

1.124

^{13}C NMR, $CDCl_3$, 150M

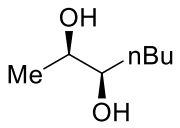

1.124

^{1}H NMR, $CDCl_3$, 600M

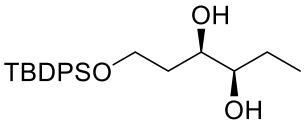

1.125

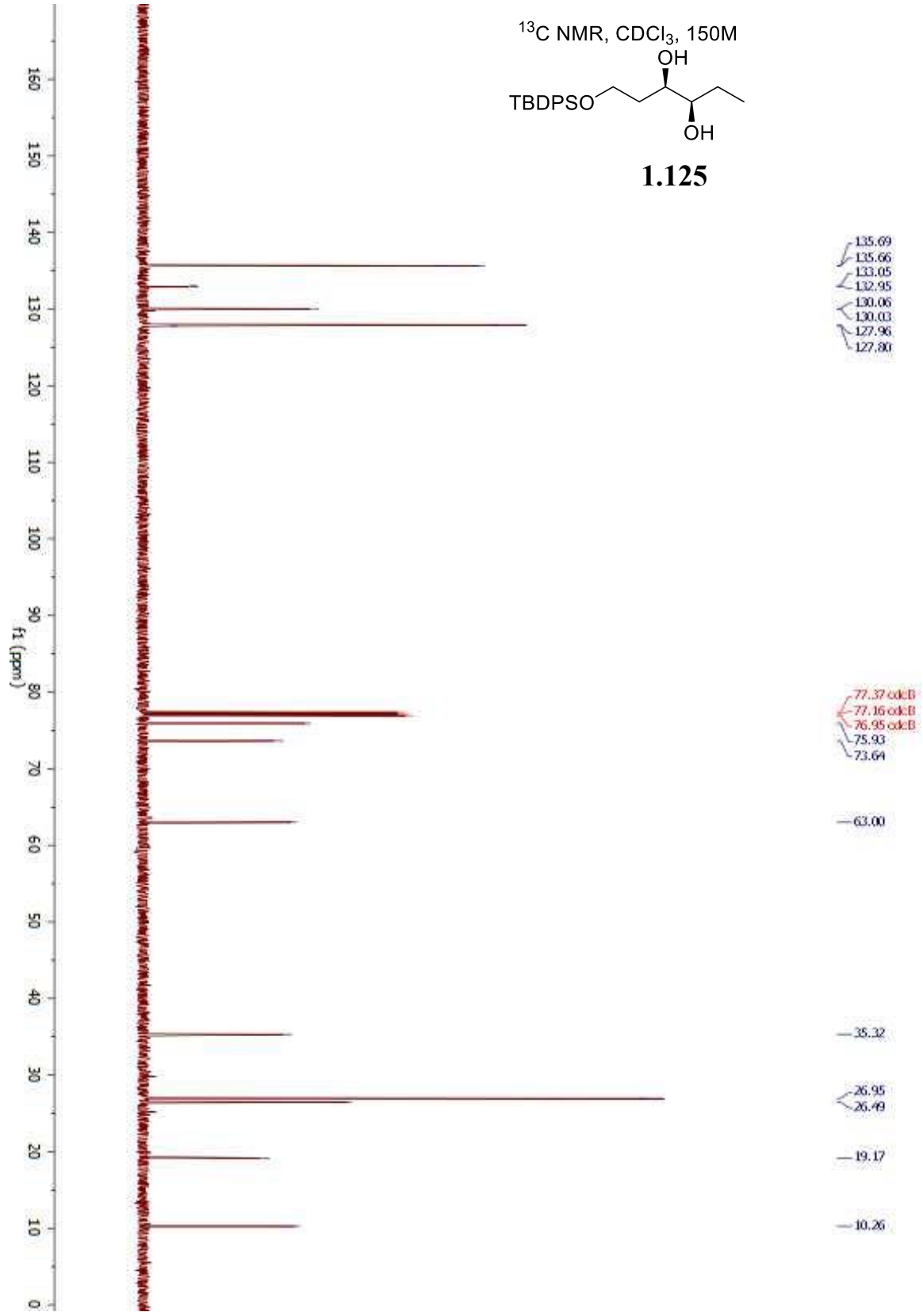
^{13}C NMR, $CDCl_3$, 150M
OH
TBDPSO
OH
1.125
135.69
135.66
133.05
132.95
130.06
130.03
127.96
127.80
77.37 cdcl3
77.16 cdcl3
76.95 cdcl3
75.93
73.64
63.00
35.32
26.95
26.49
19.17
10.26
f1 (ppm)
160
150
140
130
120
110
100
90
80
70
60
50
40
30
20
10
0

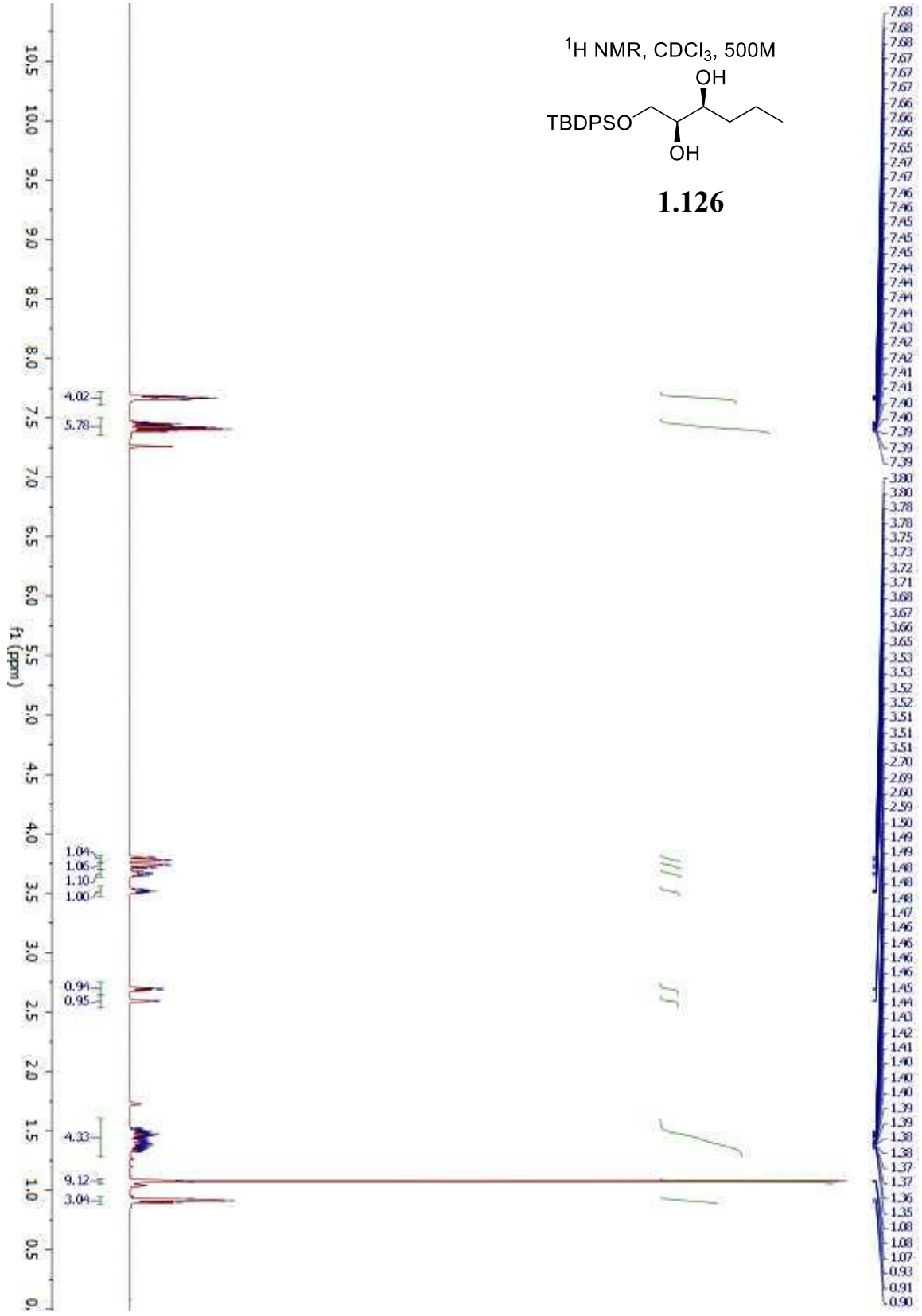
^{1}H NMR, $CDCl_3$, 500M
OH
TBDPSO
OH
1.126
f1 (ppm)
4.02
5.78
1.04
1.06
1.10
1.00
0.94
0.95
4.33
9.12
3.04

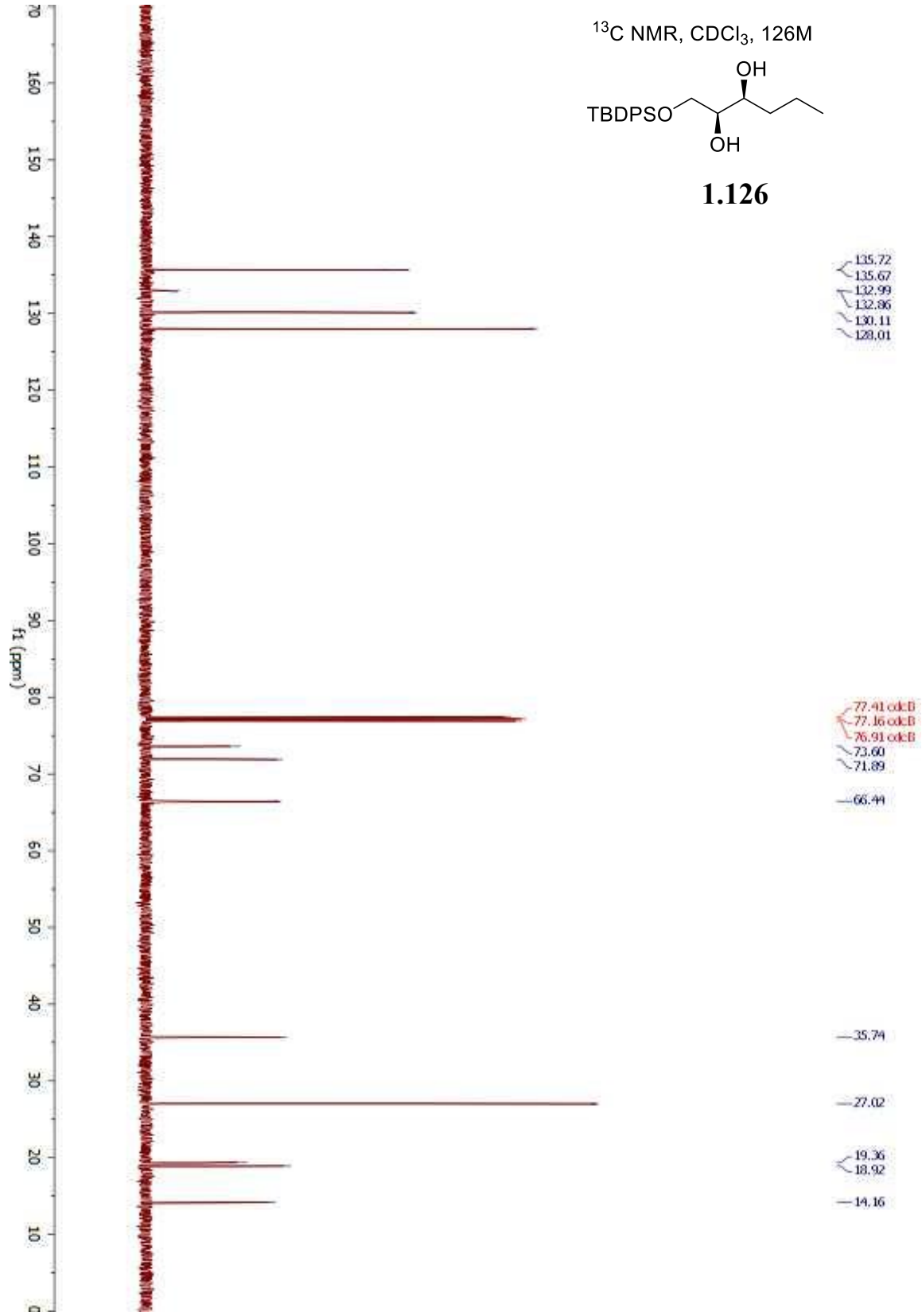
^{13}C NMR, $CDCl_3$, 126M
OH
TBDPSO
OH
1.126
135.72
135.67
132.99
132.86
130.11
128.01
77.41 cdcl3
77.16 cdcl3
76.91 cdcl3
73.60
71.89
66.44
35.74
27.02
19.36
18.92
14.16
f1 (ppm)

^{1}H NMR, $CDCl_3$, 400M

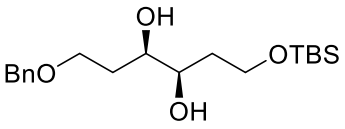

1.128

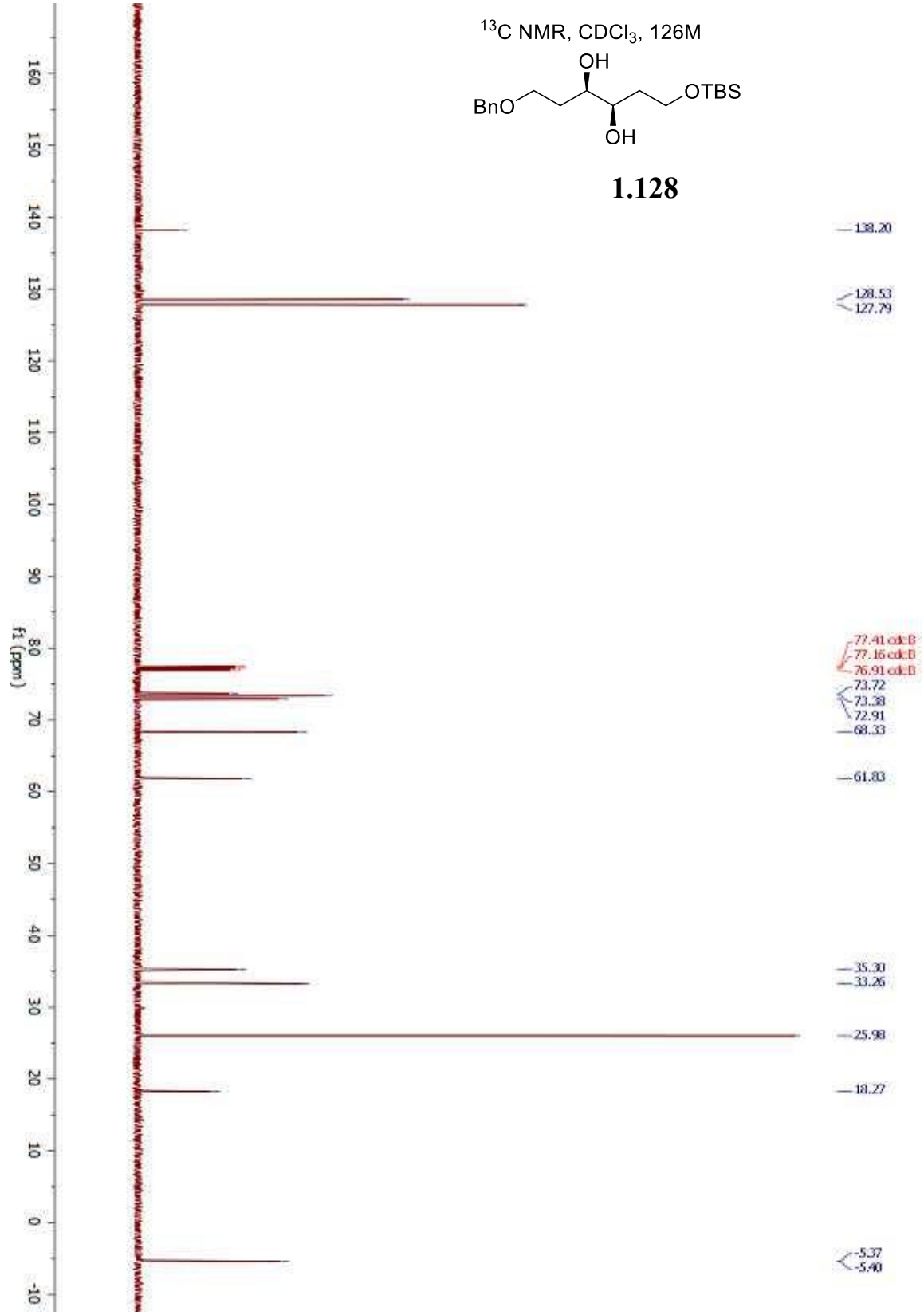
^{13}C NMR, $CDCl_3$, 126M
OH
BnO
OTBS
OH
1.128
138.20
128.53
127.79
77.41 cdcl3
77.16 cdcl3
76.91 cdcl3
73.72
73.38
72.91
68.33
61.83
35.30
33.26
25.98
18.27
-5.37
-5.40
f1 (ppm)

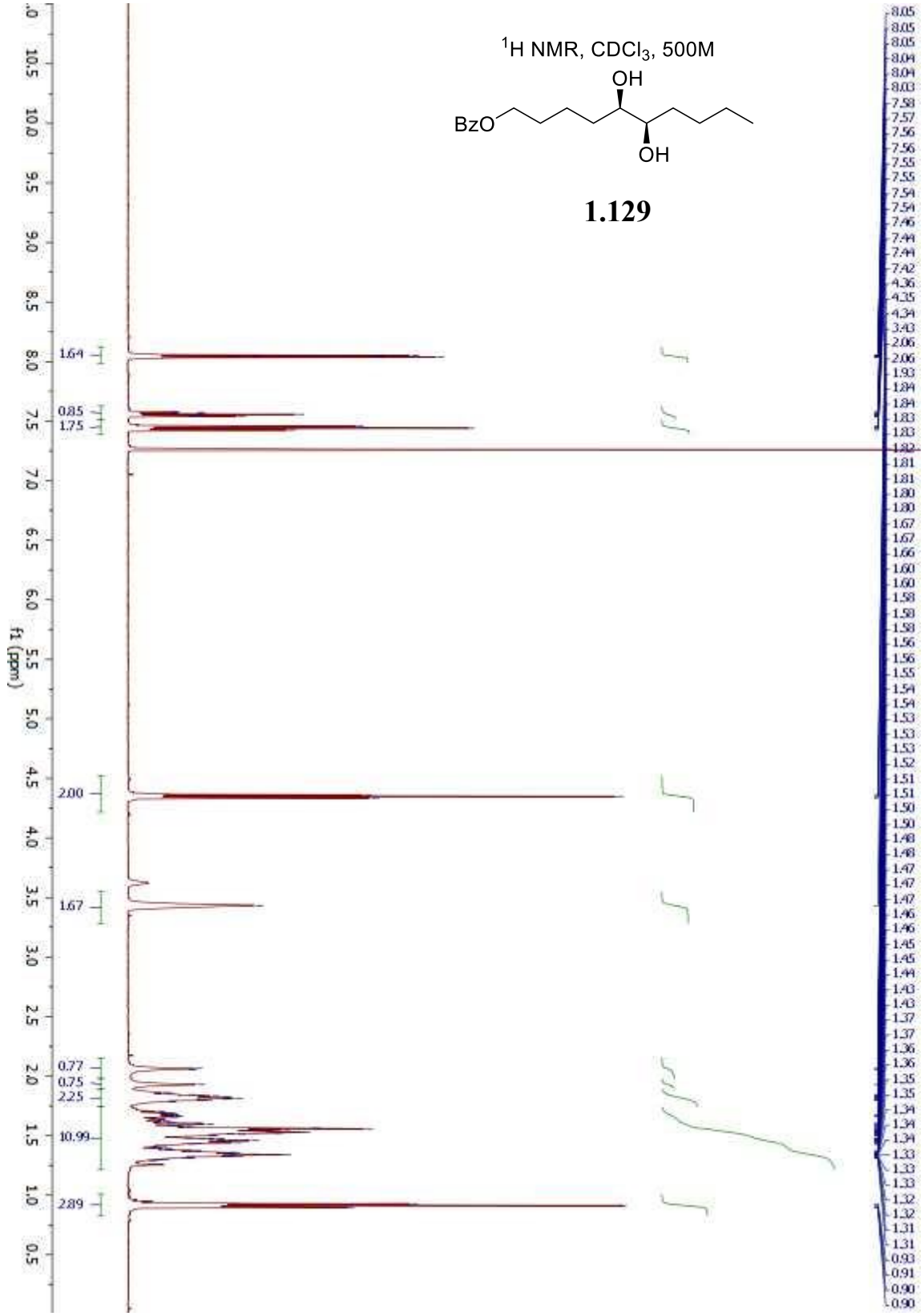
^{1}H NMR, $CDCl_3$, 500M
OH
BzO
OH
1.129
f1 (ppm)
1.64
0.85
1.75
2.00
1.67
0.77
0.75
2.25
10.99
2.89

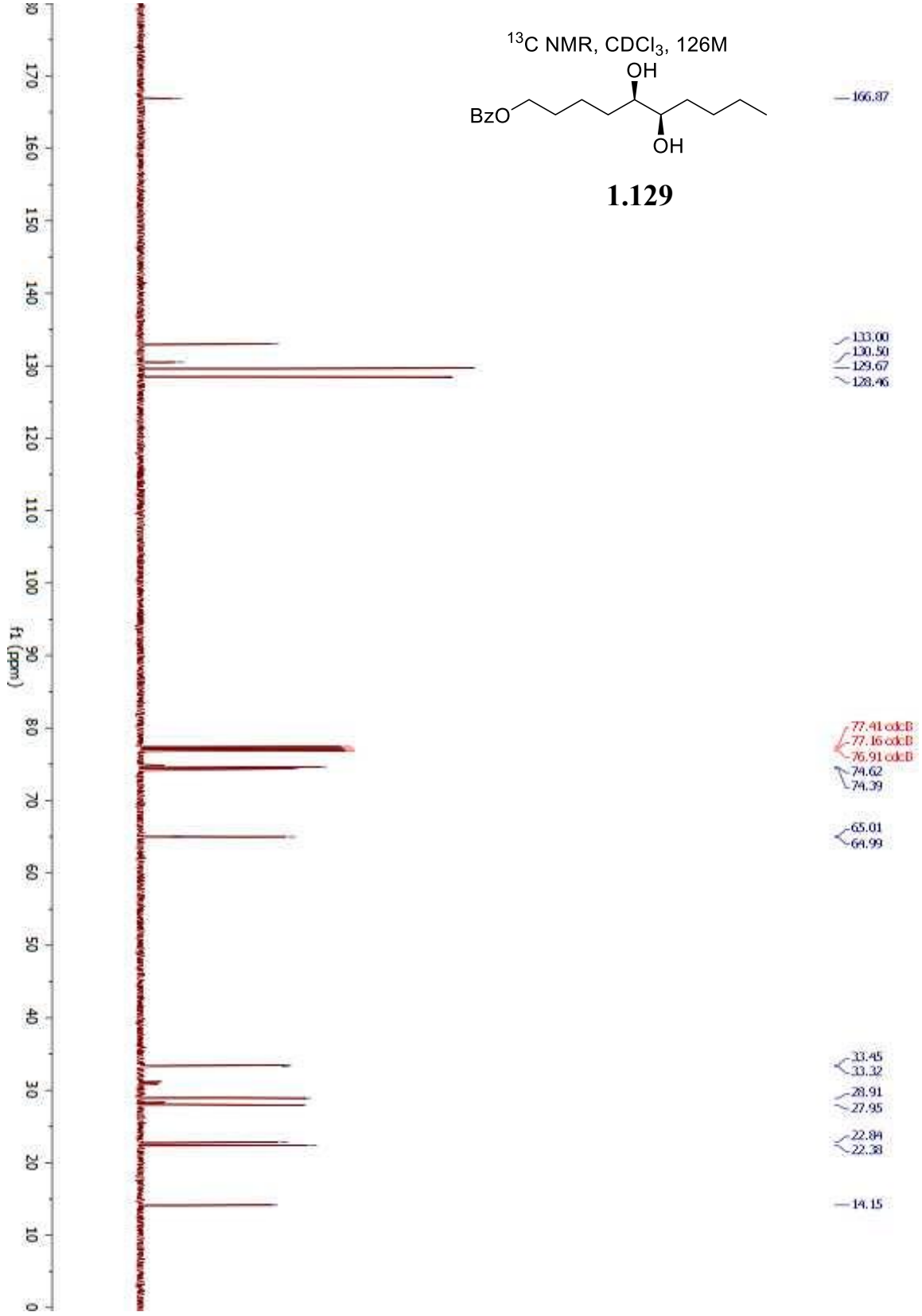
^{13}C NMR, $CDCl_3$, 126M
OH
BzO
OH
1.129
166.87
133.00
130.50
129.67
128.46
77.41 cdcl3
77.16 cdcl3
76.91 cdcl3
74.62
74.39
65.01
64.99
33.45
33.32
28.91
27.95
22.84
22.38
14.15
f1 (ppm)

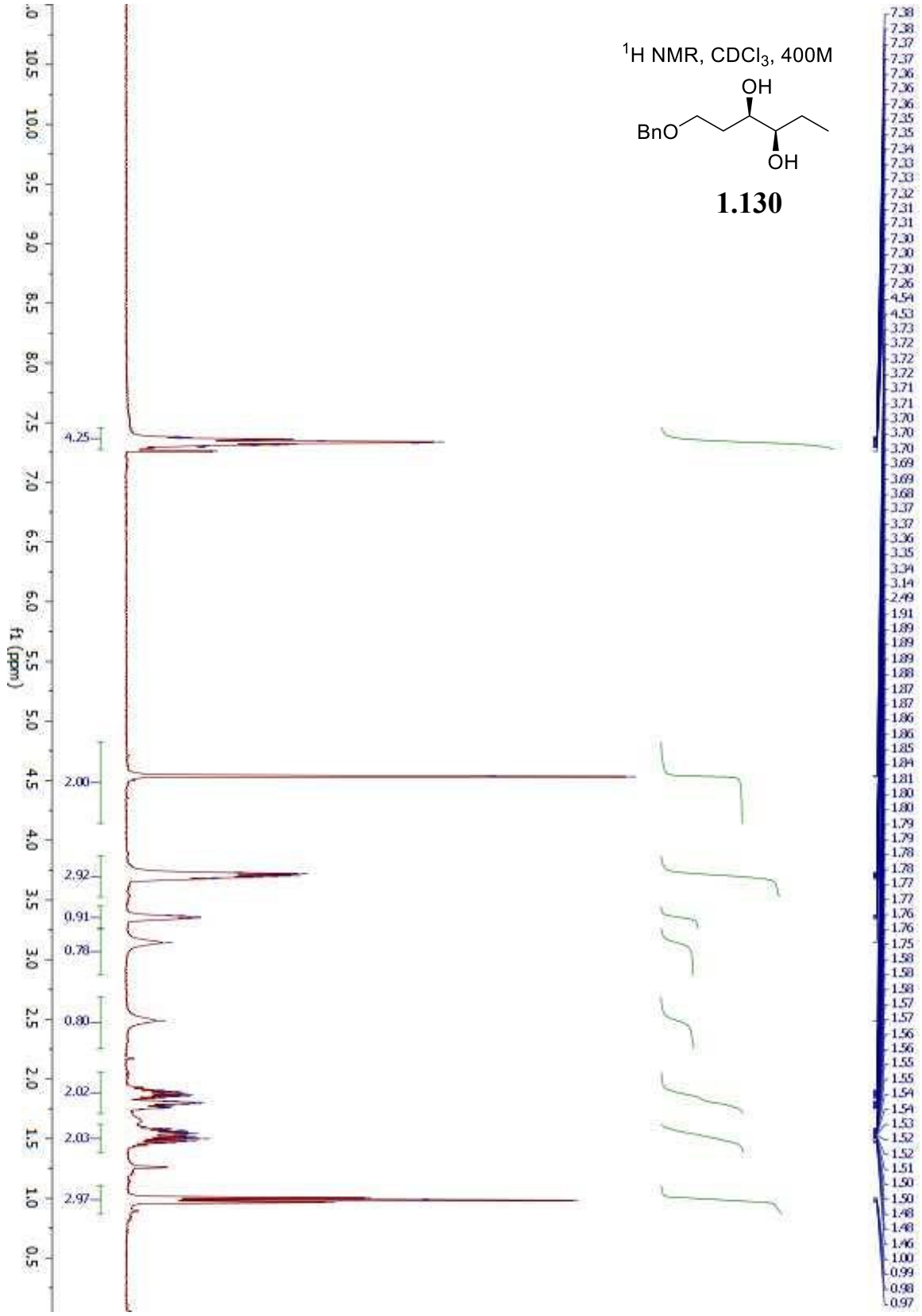
^{1}H NMR, $CDCl_3$, 400M
OH
BnO
OH
1.130
f1 (ppm)
4.25
2.00
2.92
0.91
0.78
0.80
2.02
2.03
2.97

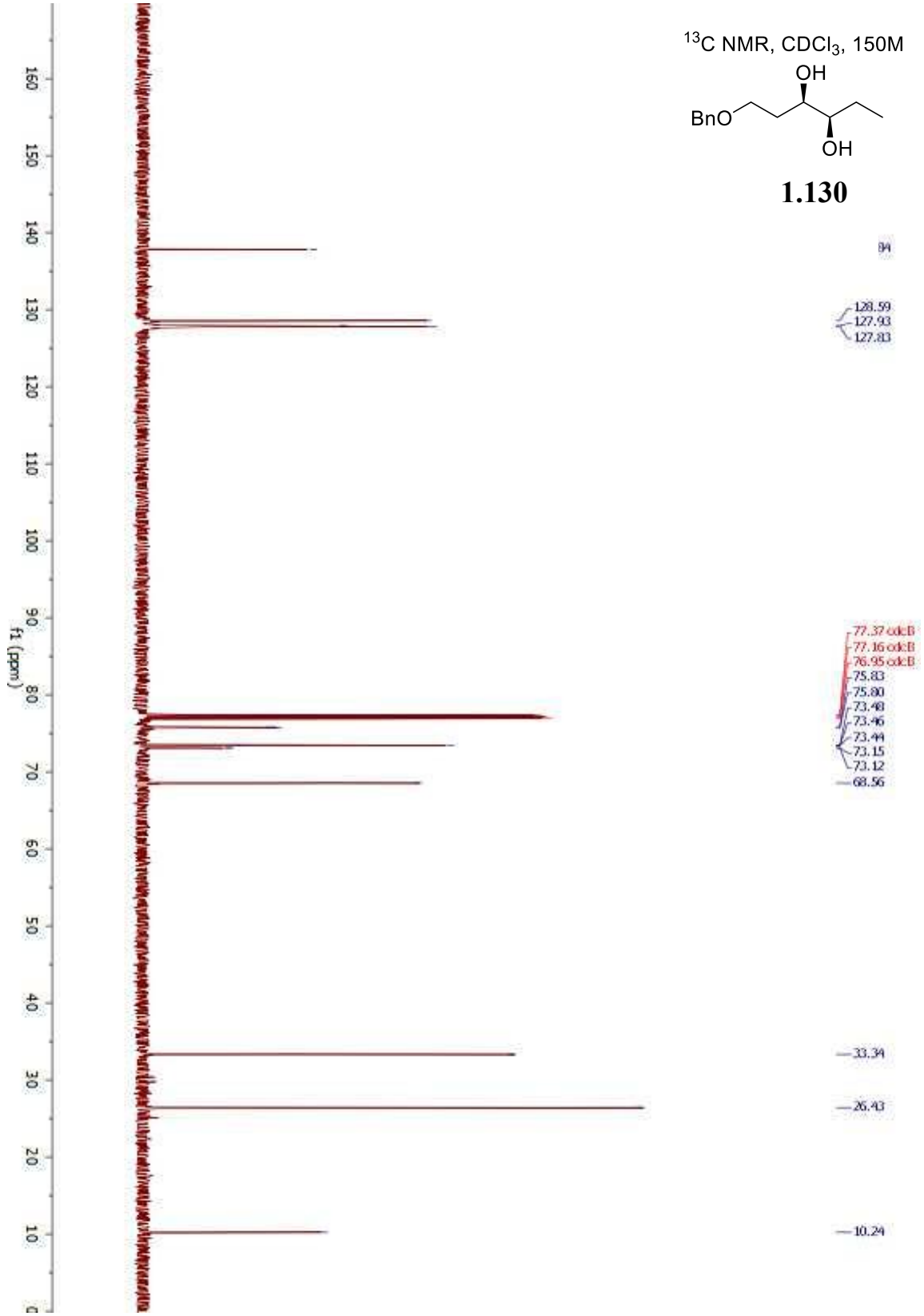
^{13}C NMR, $CDCl_3$, 150M
OH
BnO
OH
1.130
84
128.59
127.93
127.83
77.37 cdcB
77.16 cdcB
76.95 cdcB
75.83
75.80
73.48
73.46
73.44
73.15
73.12
68.56
33.34
26.43
10.24
f1 (ppm)

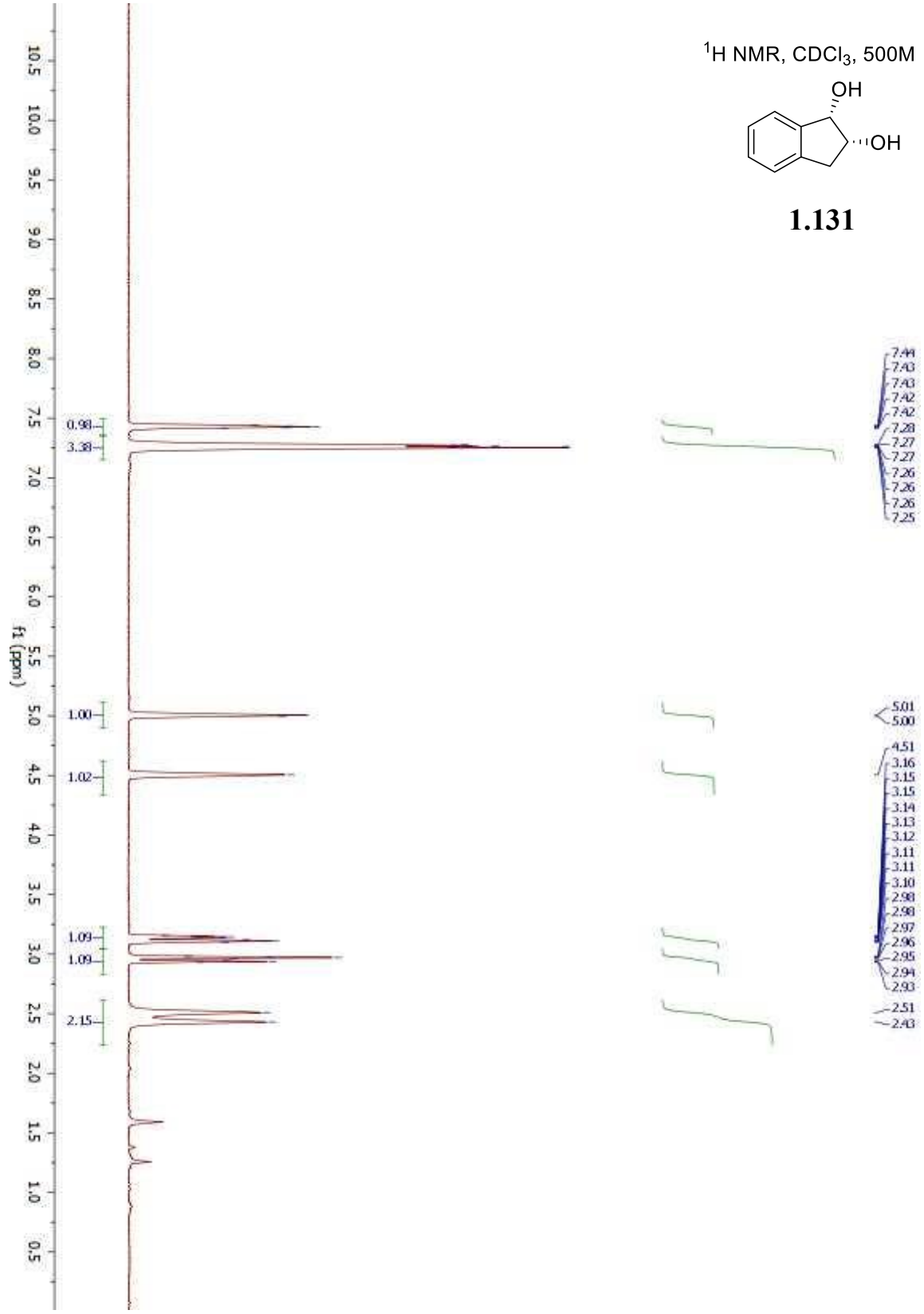
^{1}H NMR, $CDCl_3$, 500M
OH
OH
1.131
f1 (ppm)
0.98
3.38
1.00
1.02
1.09
1.09
2.15
7.44
7.43
7.43
7.42
7.42
7.28
7.27
7.27
7.26
7.26
7.26
7.25
5.01
5.00
4.51
3.16
3.15
3.15
3.14
3.13
3.12
3.11
3.11
3.10
2.98
2.98
2.97
2.96
2.95
2.94
2.93
2.51
2.43

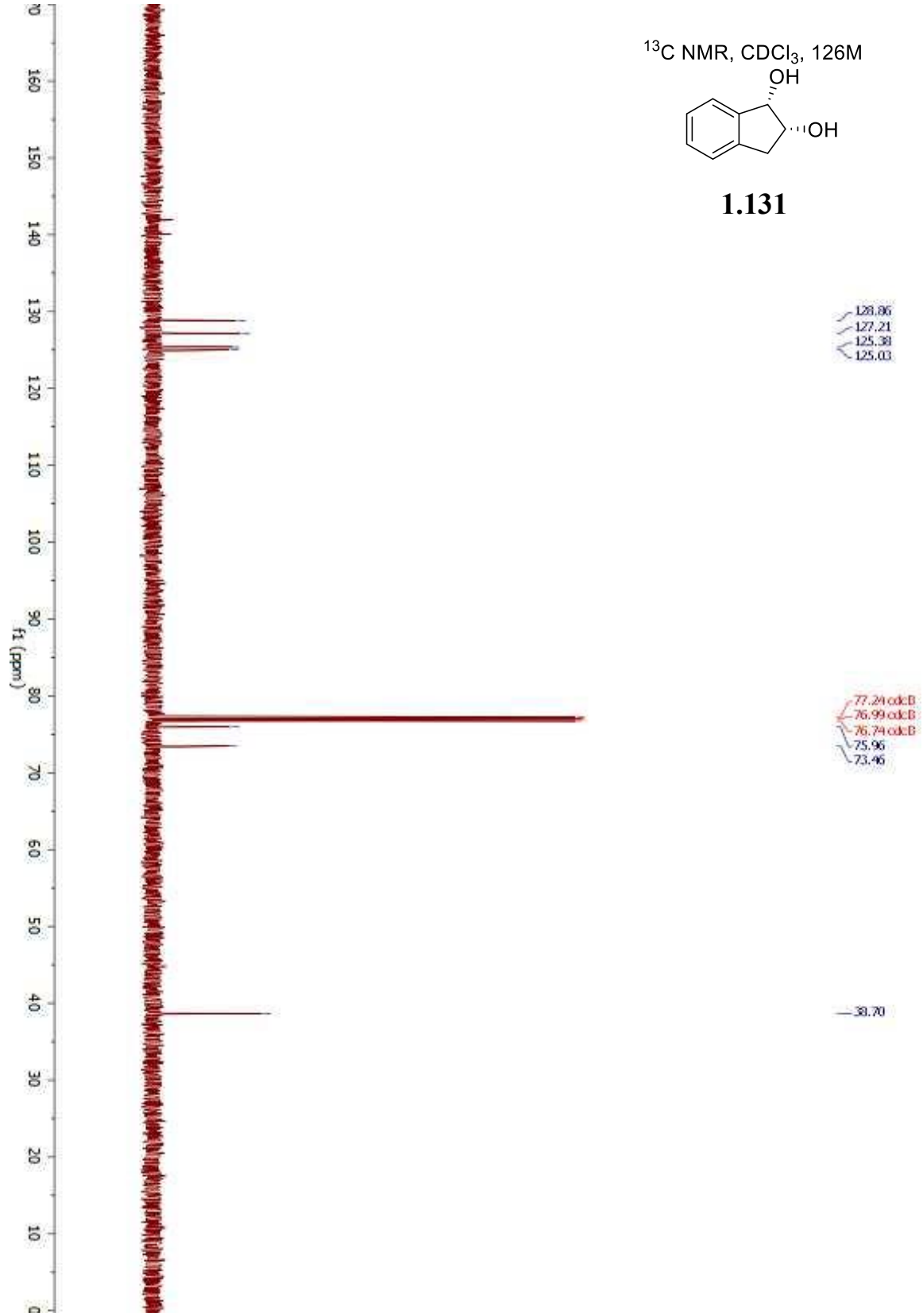
^{13}C NMR, $CDCl_3$, 126M
OH
OH
1.131
128.86
127.21
125.38
125.03
77.24 cdcl3
76.99 cdcl3
76.74 cdcl3
75.96
73.46
38.70
f1 (ppm)

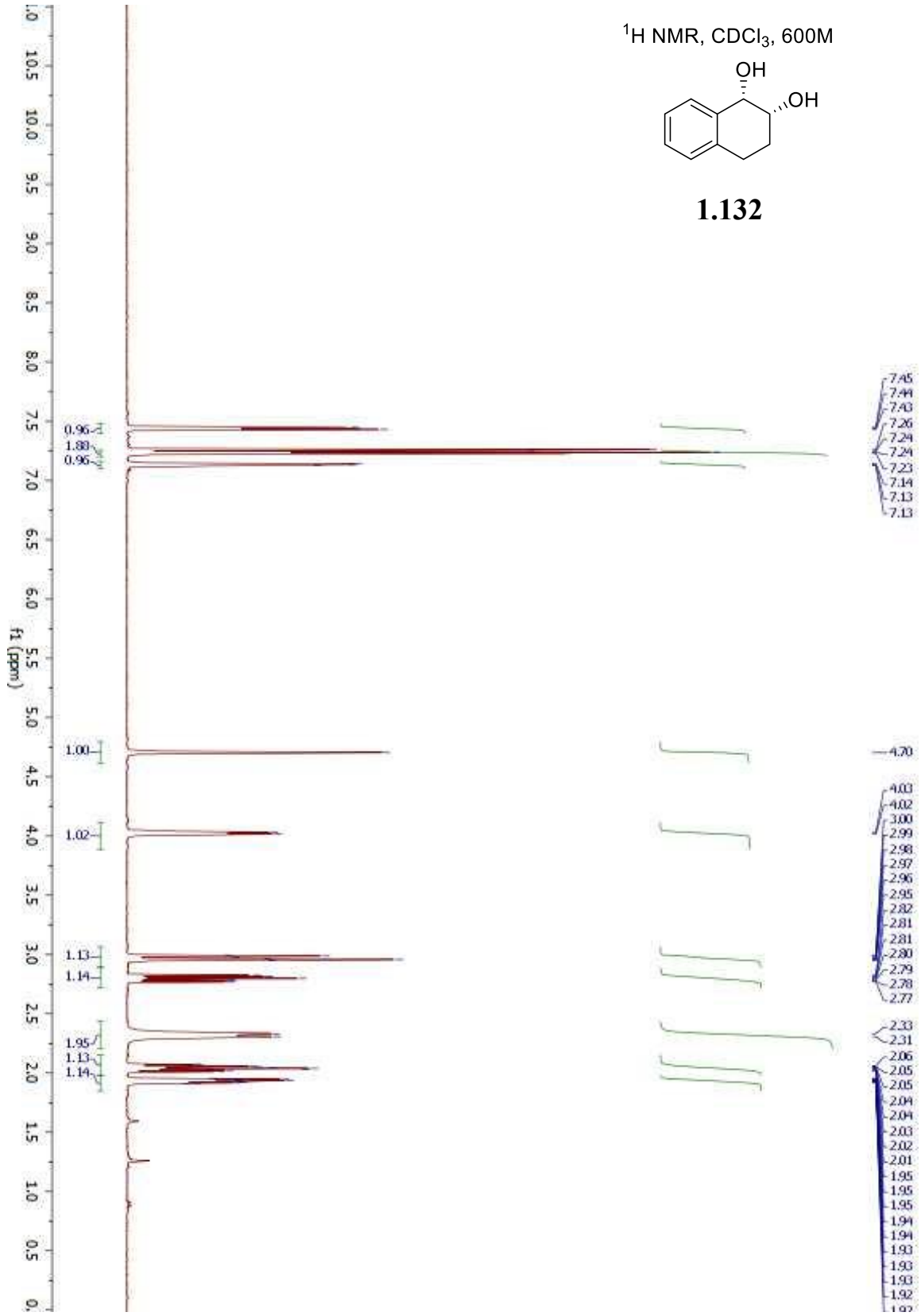
^{1}H NMR, $CDCl_3$, 600M
OH
OH
1.132
f1 (ppm)
0.96
1.88
0.96
1.00
1.02
1.13
1.14
1.95
1.13
1.14
7.45
7.44
7.43
7.26
7.24
7.24
7.23
7.14
7.13
7.13
4.70
4.03
4.02
3.00
2.99
2.98
2.97
2.96
2.95
2.82
2.81
2.81
2.80
2.79
2.78
2.77
2.33
2.31
2.06
2.05
2.05
2.04
2.04
2.03
2.02
2.01
1.95
1.95
1.95
1.94
1.94
1.93
1.93
1.93
1.92

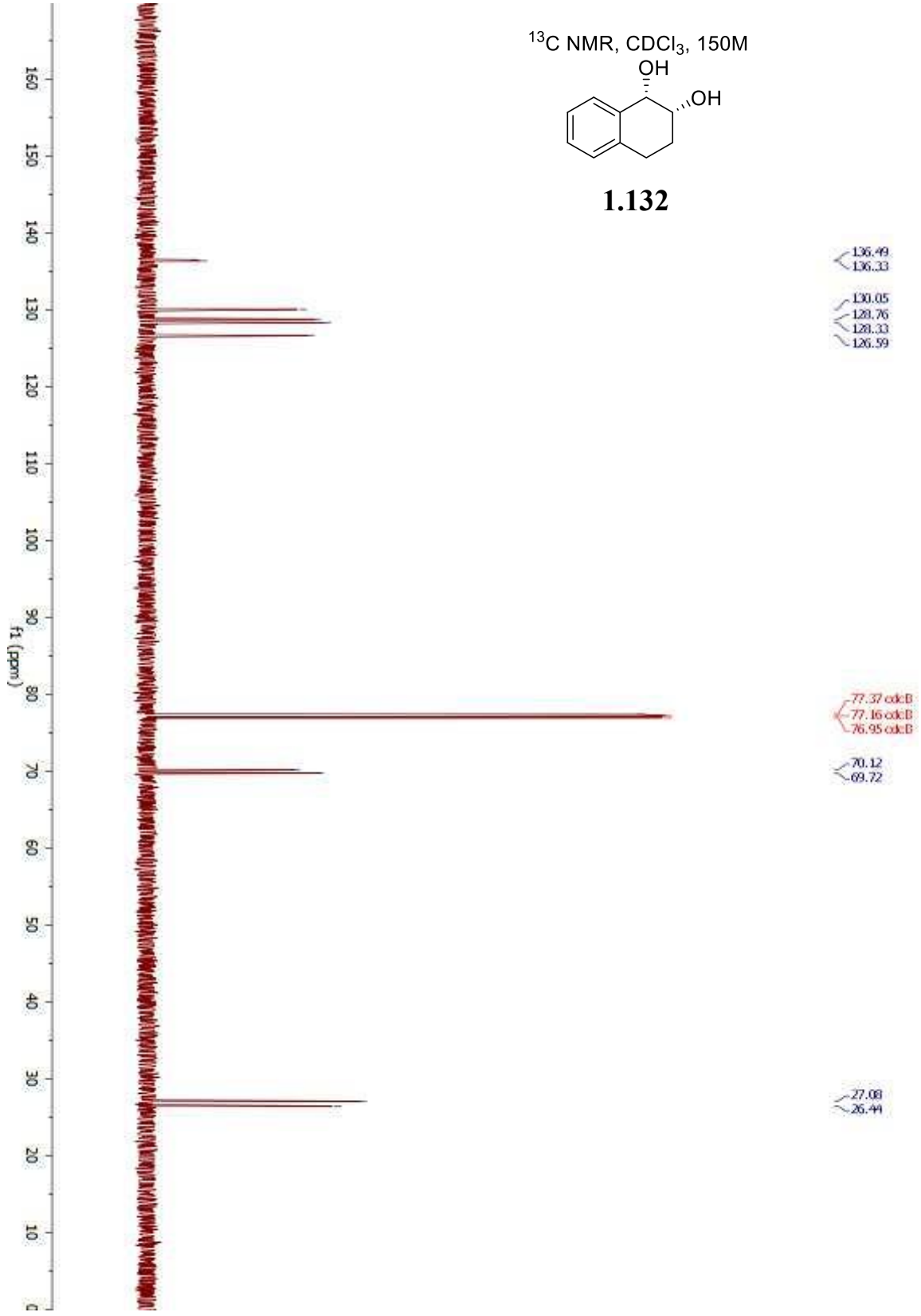
^{13}C NMR, $CDCl_3$, 150M
OH
OH
1.132
136.49
136.33
130.05
128.76
128.33
126.59
77.37 cdcl3
77.16 cdcl3
76.95 cdcl3
70.12
69.72
27.08
26.44
f1 (ppm)

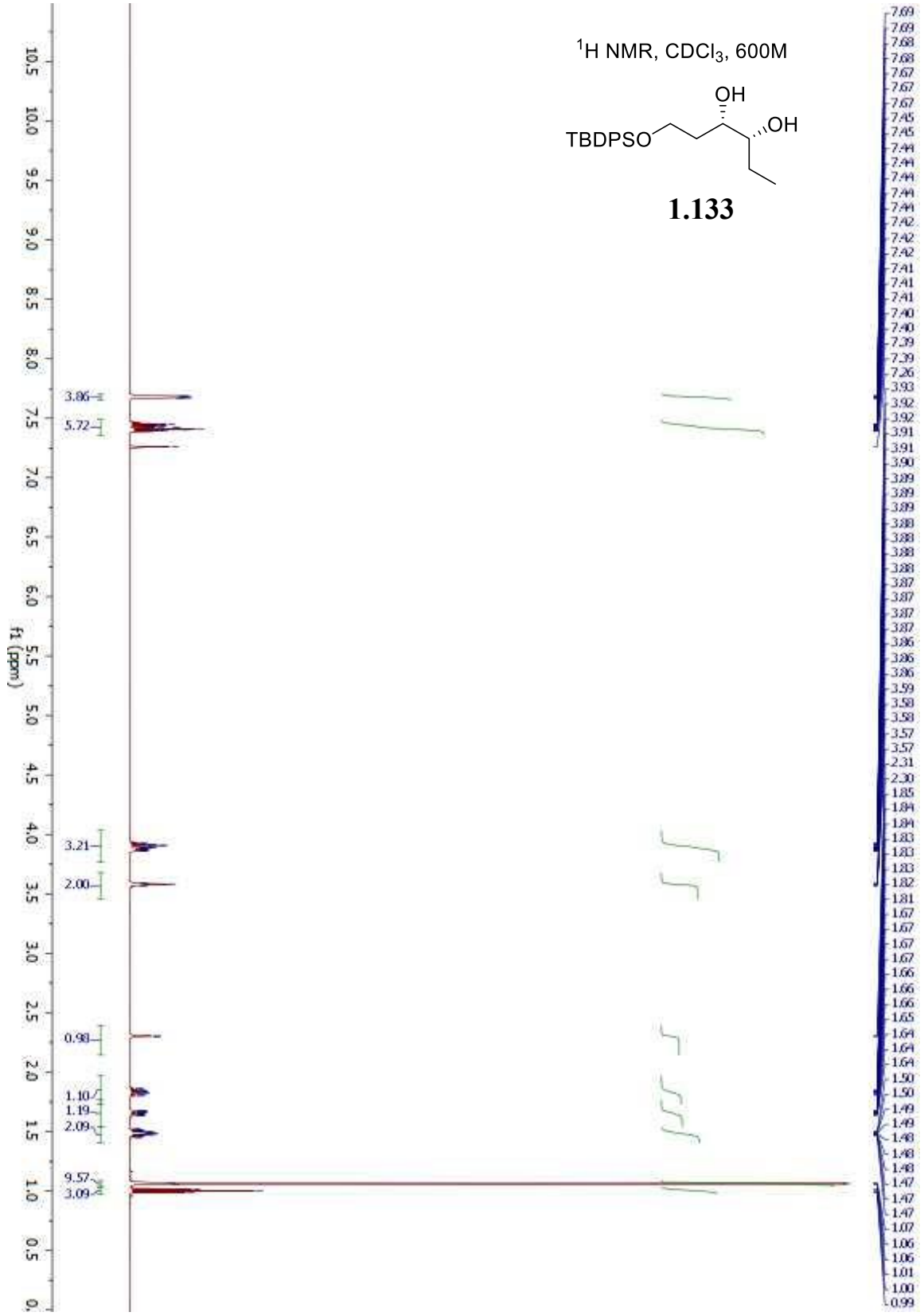
^{1}H NMR, $CDCl_3$, 600M
OH
TBDPSO
OH
1.133
f1 (ppm)
3.86
5.72
3.21
2.00
0.98
1.10
1.19
2.09
9.57
3.09

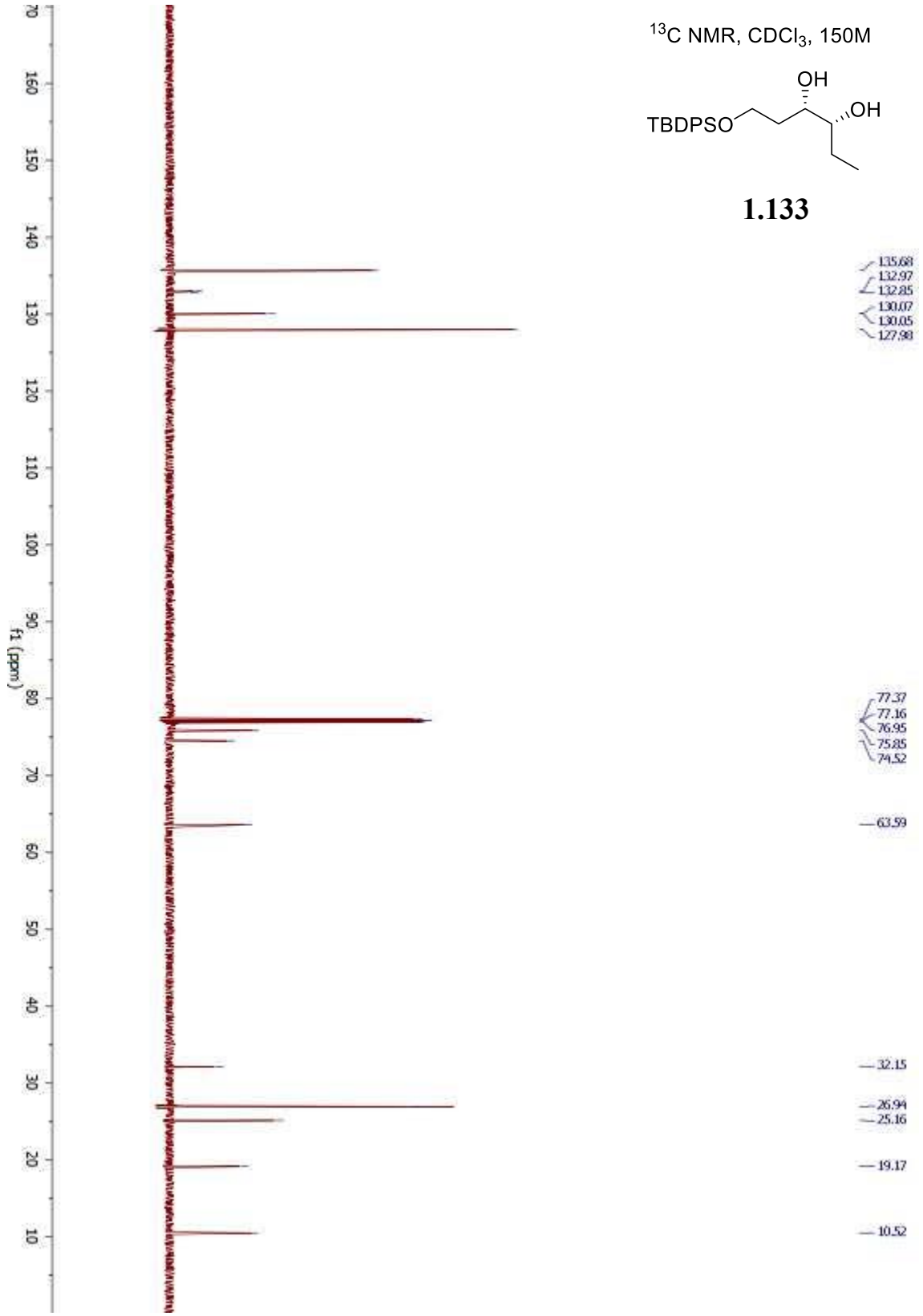
^{13}C NMR, $CDCl_3$, 150M
OH
OH
TBDPSO
1.133
135.68
132.97
132.85
130.07
130.05
127.98
77.37
77.16
76.95
75.85
74.52
63.59
32.15
26.94
25.16
19.17
10.52
f1 (ppm)

Chapter 2

Catalytic Conjunctive Coupling of Carboxylic Acid Derivatives with 9- BBN-Derived Ate Complexes

2.1 Introduction

β-Boryl carbonyls are versatile compounds that can be easily converted to synthetically useful structures including *β*-hydroxy ketones and *β*-amino ketones. Complementary to the C–C bond disconnection strategy in aldol and Mannich reactions, the 1,4-addition of a boryl bond to a conjugated enone, followed by oxidation or amination, provides an alternative way to construct β-hydroxy or β-amino carbonyl species. Many methods for the boronate conjugate addition have been developed and these processes can be accomplished with transition-metal catalysis[1] or small molecule catalysis (Scheme 2.1).[2] Although conjugate borylation exhibits high levels of

[1] a) J. E. Lee, J. Yun*, Angew. Chem., Int. Ed.* **2008**, *47*,145; b) I. H. Chen, L. Yin, W. Itano, M. Kanai, M. Shibasaki*, J. Am. Chem. Soc.* **2009**, *131*, 11664; c) J. M. O'Brien, K. S. Lee, A. H. Hoveyda, *J. Am. Chem. Soc.* **2010***, 132*, 10630

[2] a) H. Wu, S. Radomkit, J. M. O'Brien, A. H. Hoveyda, *J. Am. Chem. Soc.* **2012**, *134*, 8277; b) H. Wu, J. M. Garcia, F. Haeffner, S. Radomkit, A. R. Zhugralin, A. H. Hoveyda, *J. Am. Chem. Soc.* **2015**, *137*, 10585

reactivity and selectivity, the preparation of required stereodefined starting materials could be tedious.

Scheme 2. 1 Synthesis of ß-boryl carbonyls by conjugate addition

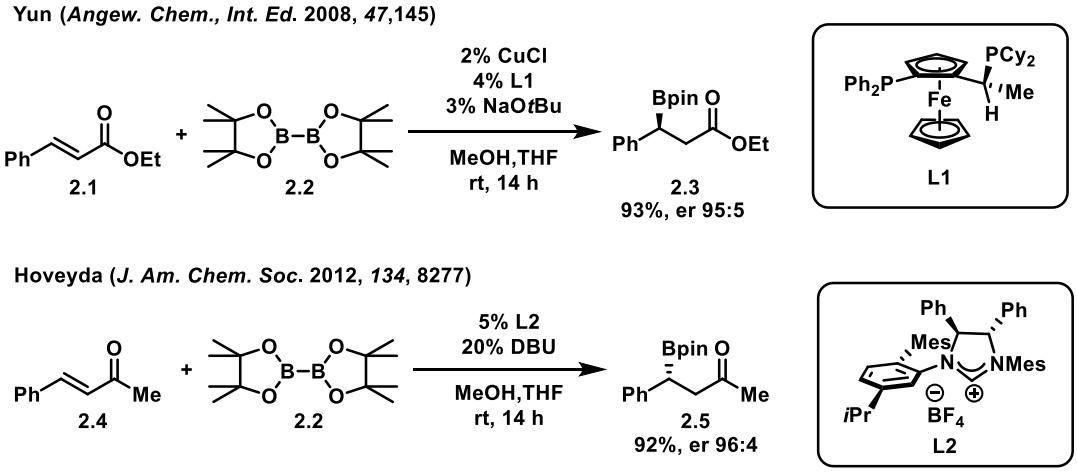

Sparked by the conjunctive cross-coupling reaction of alkenyl boron 'ate' complexes and hydrocarbon electrophiles, a new class of conjunctive cross-coupling employing acyl chlorides or acid anhydrides as electrophiles was proposed (Scheme 2.2). Similar to previously reported conjunctive cross-couplings, this strategy forges two C–C bonds across the alkenyl boron compounds, which allows modular construction of β-boryl carbonyls from three simple starting materials: a nucleophile R_1, an acyl electrophile, and the

Scheme 2. 2 Conjunctive cross-coupling of acyl electrophiles

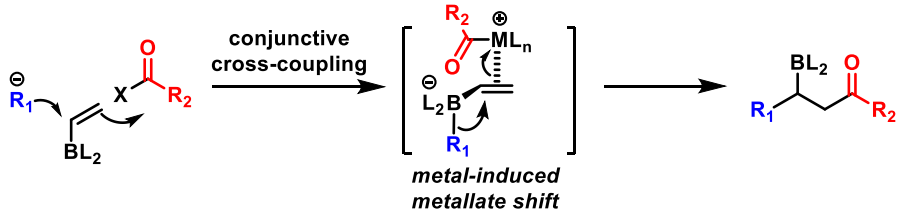

vinyl boron species. Of note, this strategy may employ different substrate pools compared to the conjugate borylation reaction.

Herein, we report a nickel-catalyzed conjunctive cross-coupling reaction of 9-BBN borane-derived 'ate' complexes and carboxylic acid derivatives to prepare *β*-keto boranes, an unprecedented type of borane species. Mechanistic studies, as well as further transformations, were also conducted on this new process.

2.2 Background

2.2.1 1,2-Metallate rearrangement

The first example of a 1,2-metallate shift was reported by Hillman at DuPont in 1962.[3] In his article, one of the alkyl groups in a CO-coordinated borane 'ate' complex underwent 1,2-migration from boron to the carbon atom in CO. Activated by another Lewis acidic borane, the rest of the alkyl groups on boron migrated as well to form the trialkyl boroxine (**2.8)** as a final product. Inspired by this transformation, a variety of new C–C bond formation

[3] M. E. D. Hillman, *J. Am. Chem. Soc*., **1962,** *84,* 4715

methods[4] have been developed such as Zweifel olefination and Matteson homologation, both of which represent a genre of 1,2-metallate shift reactions that will be discussed.

Scheme 2. 3 Conjunctive cross-coupling of acyl electrophiles

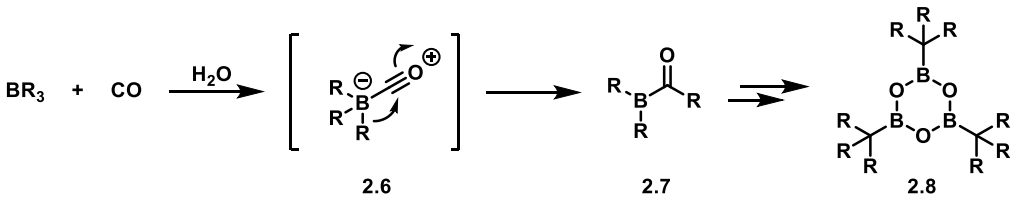

2.2.1.1 Migration to *sp3* carbon

In 1985, Matteson disclosed the first homologation of an organoboronate using dichloromethyllithium as a starting material to generate secondary α-boryl halide (Scheme 2.4). [5] Asymmetric versions of homologation reaction were established with either a stoichiometric chiral auxiliary (Scheme 2.5a)[6] or substoichiometric amounts of chiral Lewis acid (Scheme 2.5b).[7]

[4] C. Sandford, V. K. Aggarwal, *Chem. Commun.,* **2017**, *53*, 5481
[5] a) D. S. Matteson, R. Ray, *J. Am. Chem. Soc*. **1980**, *102*, 7590; b) K. M. Sadhu, D. S. Matteson, *Organometallics* **1985**, *4*, 1687
[6] a) D. S. Matteson, *Tetrahedron*, **1998**, *54*, 10555; b) J. L. Stymiest, G. Dutheuil, A. Mahmood, V. K. Aggarwal, *Angew. Chem*. **2007**, *119*, 7635
[7] P. K. Jadhav, H.-W. Man, *J. Am. Chem. Soc*., **1997**, *119*, 846

Scheme 2. 4 Original Matteson homologation reaction

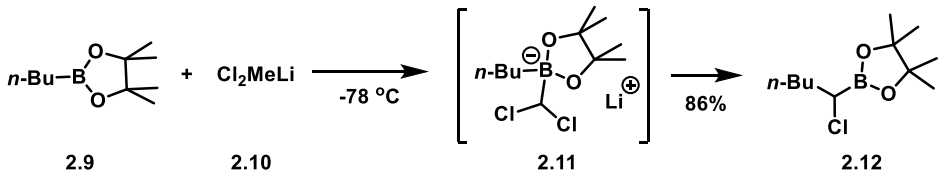

Scheme 2. 5 Asymmetric Matteson homologation reactions

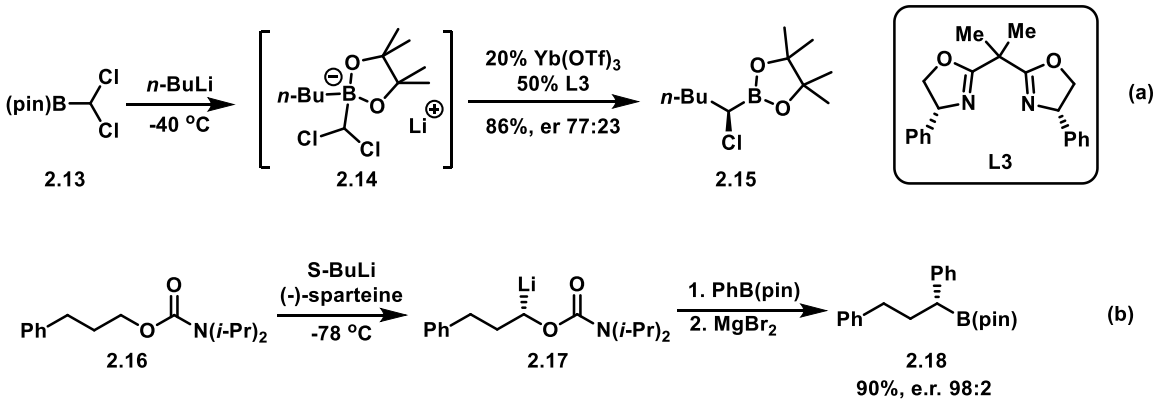

Recently, Aggarwal described a new type of 1,2-metallate rearrangement in which a carbon atom serves as a leaving group *in lieu of* heteroatom.[8] As pictured in Scheme 2.6, a facile 1,2-metallate shift cleaved the C–C bond and form the C–Pd bond simultaneously, which, upon reductive elimination, furnished a substituted cyclobutane with excellent diastereoselectivity. The desired reaction is likely promoted by the release of ring strain in the bicyclo[1.1.0] butane.

[8] A. Fawcett, T. Biberger, V. K. Aggarwal, *Nat. Chem.,* **2019**, *11*, 117

Scheme 2. 6 ring strain release promoted 1,2-migration to sp^3 carbon

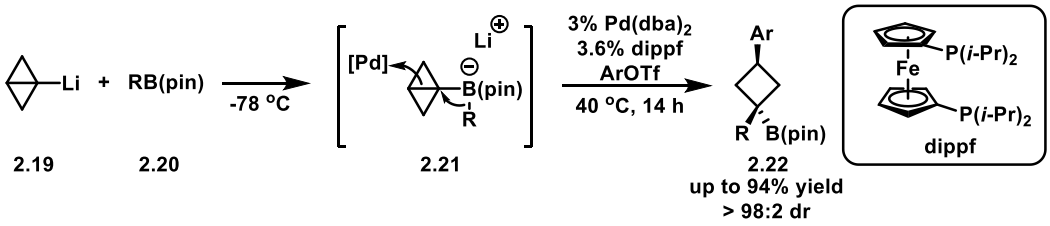

2.2.1.2 Migration to *sp* and sp^2 carbon

2.2.1.2.1 Migration induced by external electrophiles

In 1965, Binger and Koster reported the first case of an external electrophile induced 1,2-metallate shift to an unsaturated hydrocarbon.[9] Upon activation by dialkylchloroborane, the alkynyl borane derived 'ate' complex (**2.23**) underwent 1,2-migration to construct 1,2-diborane (**2.25**) (Scheme 2.7).

Scheme 2.7 Electrophilic borane induced 1,2-migration to sp carbon

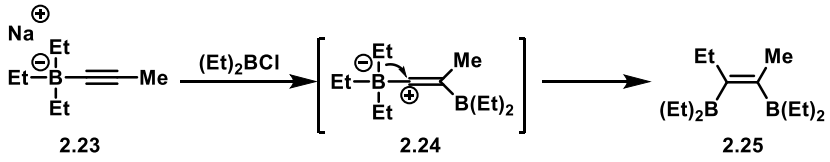

Shortly thereafter, the Zweifel group described the first 1,2-metallate shift to a C(sp^2)-hybridized carbon with iodine as the electrophilic activator.[10]

[9] P. Binger, R. Koster, *Tetrahedron Lett.* **1965**, *6,* 1901
[10] G. Zweifel, H. Arzoumanian, C. C. Whitney, *J. Am. Chem. Soc*. **1967**, *89*, 3652

In this article, alkenyl borane (**2.26**) was converted into a 1,2-disubstituted alkene (**2.29**) after an iodine-induced 1,2-migration and base-promoted *anti*-elimination. The stereochemical outcome in the reaction suggests a stereospecific *antiperiplanar* 1,2-metallate shift mechanism (Scheme 2.8). Evans[11], Matteson[12], and Aggarwal[13] have introduced several modifications to enhance the reactivity and expanded the substrate scope to boronic esters and Grignard reagents. Besides stereodefined substituted alkenes, substituted arenes like furans, pyrroles, and indoles could also be synthesized by Zweifel olefination from corresponding lithiated heteroarenes and organoboron species (Scheme 2.9).[14]

Scheme 2.8 Iodine induced Zweifel olefination

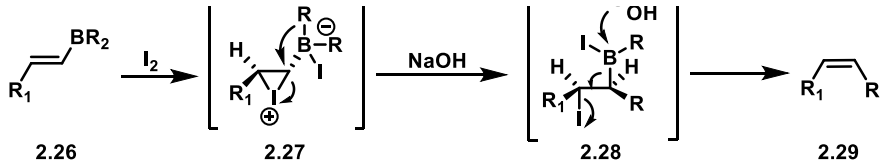

Scheme 2.9 Synthesis of substituted arenes through Zweifel olefination

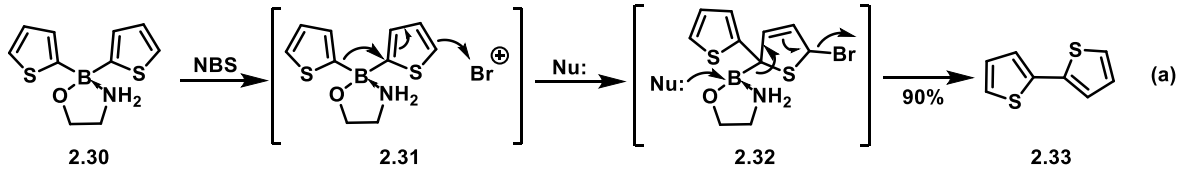

[11] a) D. A. Evans, R. C. Thomas, J. A. Walker, *Tetrahedron Lett*, **1976**, *17*, 1427; b) D. A. Evans, T. C. Crawford, R. C. Thomas, J. A. Walker, *J. Org. Chem.* **1976**, *41*, 3947

[12] D. S. Matteson, P. K. Jesthi, *J. Organomet. Chem.* **1976**, *110*, 25.

[13] R. J. Armstrong, W. Niwetmarin, V. K. Aggarwal, *Org. Lett.* **2017**, *19*, 2762

[14] a) A. B. Levy, *J. Org. Chem*. **1978**, *42*, 4684; b) E. R. Marinelli, A. B. Levy, *Tetrahedron Lett.* **1979**, *25*, 2313; c) I. Akimoto, A. Suzuki, *Synthesis* **1979**, *2*, 146; d) T. Sotoyama, S. Hara, A. Suzuki, *Bull. Chem. Soc. Jpn.* **1979**, *52*, 1865; e) A. Bonet, M. Odachowski, D. Leonori, S. Essafi, V. K. Aggarwal, *Nat. Chem.* **2014**, *6*, 584; f) P. Conti-Ramsden, J. N. Harvey, D. Leonori, V. K. Aggarwal, *J. Am. Chem. Soc*. **2016**, *138*, 9521

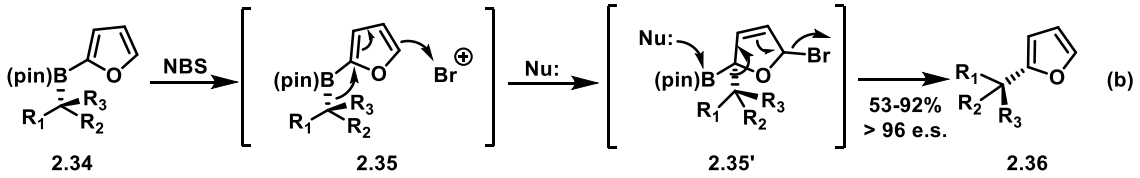

In addition to halide activator, a handful of examples have been reported with carbon electrophiles induced migration, as shown in Scheme 2.10. The Utimoto group demonstrated that aldehydes[15] and epoxides[16] could induce the 1,2-metallate shift to produce 1,3-diols and 1,4-diols after oxidation of the products. *β*-Hydroxy carboxylic acids were also prepared by 1,2-migration and oxidation in the presence of the CO_2 as an activator.[17]

Scheme 2.10 Other electrophiles induced 1,2-migration to sp² carbon

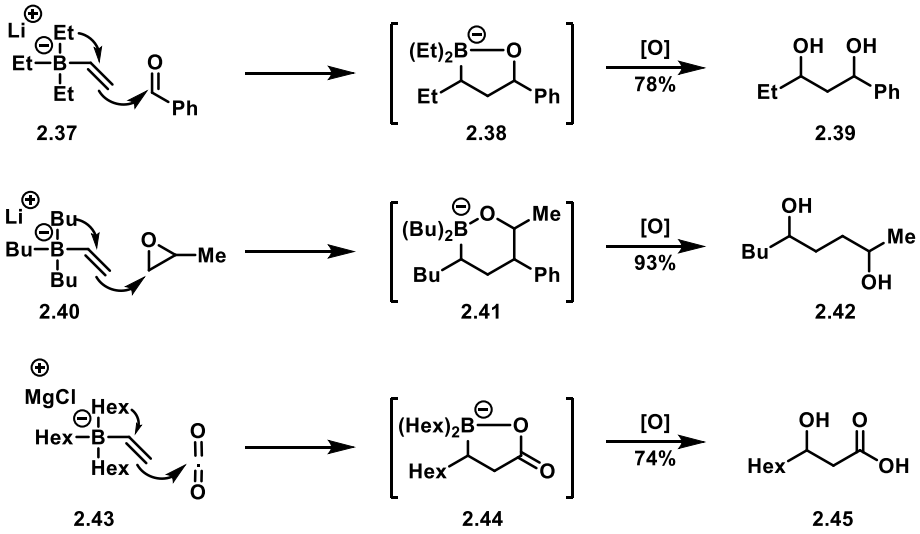

[15] K. Utimoto, K. Uchida, H. Nozaki, *Tetrahedron* **1977**, *33*, 1949
[16] K. Utimoto, K. Uchida, H. Nozaki, *Tetrahedron Lett*. **1973**, *14*, 4527
[17] M. Z. Deng, D. A. Lu, W. H. Xu, *J. Chem. Soc., Chem. Comm.* **1985,** *21*, 1478

2.2.1.2.2 Migration induced by transition-metal complex

Although rare, transition-metals were also demonstrated as valid Lewis acidic activators for 1,2-metallate rearrangement. In Pelter [18] and Wrackmeyer's[19] early studies on transition-metal induced migration, alkynyl borane 'ate' complexes underwent the 1,2-metallate shift when a stoichiometric amount of iron dienyl complex or cationic platinum acetylide complex was employed.

Scheme 2.11 Transition metal-induced 1,2-migration to sp carbon

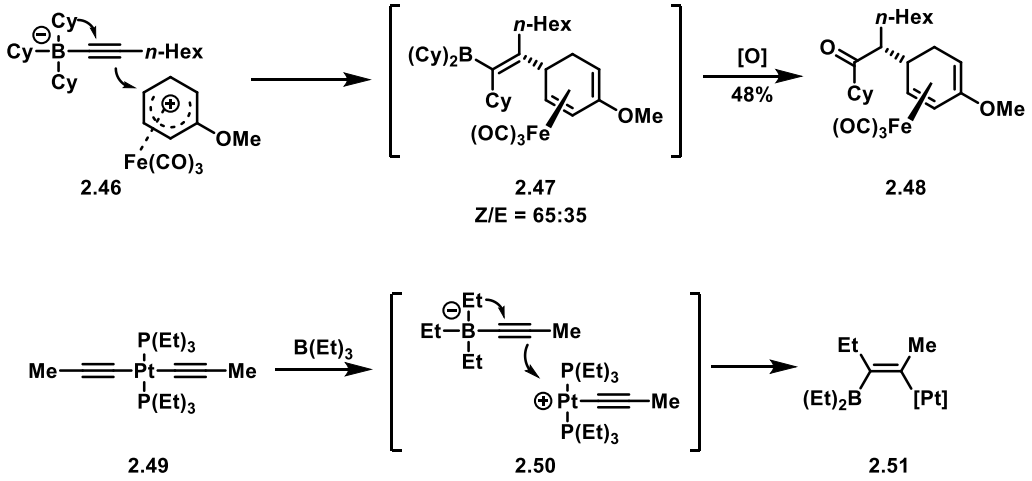

The first catalytic method for the metal-induced 1,2-metallate shift was revealed in 1990 by the Deng group.[20] The migration of alkyl groups in an alkynyl borane derived 'ate' complex was catalyzed by a π-allyl-palladium

[18] A. Pelter, K. J. Gould, *J. Chem. Soc., Chem. Commun.* **1974,** 1029
[19] A. Sebald, B. Wrackmeyer, *J. Chem. Soc., Chem. Commun*. **1983**, 309
[20] Y. Chan, N. S. Li, M. Z. Deng, *Tetrahedron Lett*. **1990**, *31*, 2405

complex through an outer-sphere attack (Scheme 2.12). The Ishikura group[21] also reported a similar π-allyl-palladium complex induced 1,2-metallate shift of an indole-borane derived 'ate' complex (**2.55**) (Scheme 2.13a). Enantio- and diastereoselective 1,2-metallate shift of a similar indole-boronic ester complex (**2.59**) was accomplished by Ready and co-workers with Pd/(*S*)-BINAP complex as a chiral catalyst (Scheme 2.13b).[22]

Scheme 2.12 Transition metal-catalyzed 1,2-migration to sp carbon

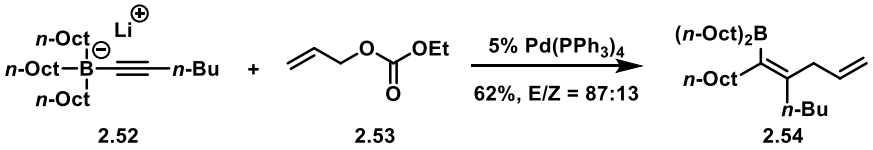

Scheme 2.13 Synthesis of substituted indoles through 1,2-metallate shifts

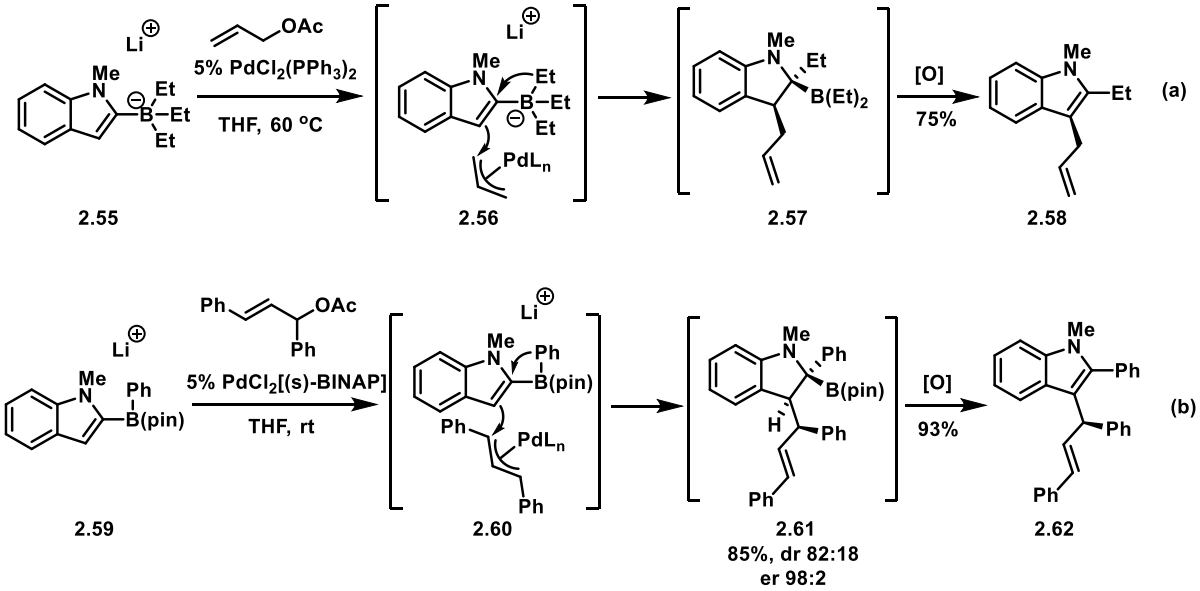

[21] a) M. Ishikura, M. Terashima, *J. Chem. Soc., Chem. Commun*. **1991**, 1219; b) M. Ishikura, H. Kato, *Tetrahedron* **2002**, *58*, 9827; c) M. Ishikura, Y. Matsuzaki, I. Agata, N. Katagiri, *Tetrahedron* **1998**, *54*, 13929

[22] S. Panda, J. M. Ready, *J. Am. Chem. Soc.* **2017,** *139*, 6038

Besides the allyl-palladium complex, the aryl palladium species derived from the oxidative addition of aryl halide were also examined by Murakami, although the author proposed a different mechanism. Instead of 1,2-metallate rearrangement[23], they considered a Heck-type carbopalladation of the alkynyl borane 'ate' complex, followed by a stereoinvertive reductive displacement of Pd to deliver the alkenyl products (Scheme 2.14a). Although the proposal is plausible, they could not rule out the possibility of the mechanism featuring a stereospecific antiperiplanar 1,2-metallate shift (Scheme 2.14b).

Scheme 2.14 Possible mechanisms of Aryl palladium induced 1,2-metallate rearrangement

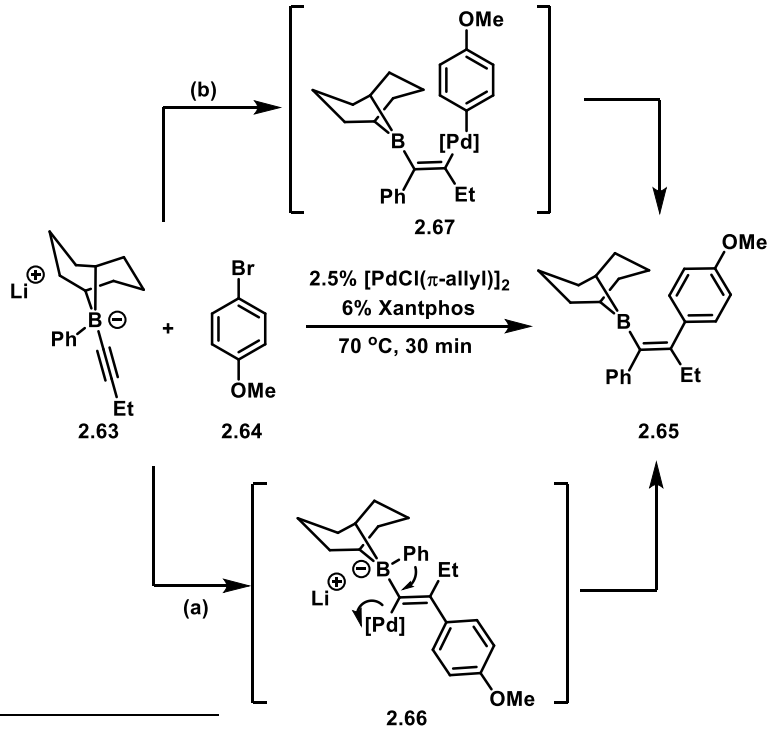

[23] a) N, Ishida, T. Miura, M. Murakami, *Chem. Commun.* **2007**, 4381. b) N. Ishida, M. Narumi, M. Murakami, *Org. Lett.* **2008**, *10*, 1279; c) N. Ishida, Y. Shimamoto, M. Murakami, *Org. Lett*. **2009**, *11*, 5434. d) I. Naoki, S.Tatsuo, S. Shota, M. Tomoya, M. Murakami, *Bull. Chem. Soc. Jpn.,* **2010**, *83*, 1380; e) N. Ishia, W. Ikemoto, M. Narumi, M. Murakami, *Org. Lett*. **2011**, *13*, 3008

Although various transition-metals might be sufficiently electrophilic to induce the 1,2-metallate rearrangement of alkynyl borane 'ate' complex, there were very limited examples[21,22] of corresponding 1,2-metallate shift of alkenyl boron 'ate' complexes and none employing boronic esters as substrates until the development of conjunctive cross-coupling in the Morken lab.

2.2.2 Conjunctive cross-coupling

2.2.2.1 Mechanistic proposal of conjunctive cross-coupling

Inspired by the mechanism of the Zweifel olefination, a 1,2-metallate rearrangement of alkenyl boronate 'ate' complex was proposed but with a transition-metal complex as a catalyst. As shown in the tentative catalytic cycle (Scheme 2.15), the oxidative addition adduct (**2.68)** binds to the *in situ*-generated alkenyl boronate 'ate' complex (**2.69)** and induces the 1,2-metallate shift. The final product is formed upon the reductive elimination of intermediate (**2.71**). Overall, a modular three-component reaction is realized with the addition of one nucleophile and one electrophile across an alkenyl boronate. With proper ligand design, enantioenriched secondary boronates could be produced. However, unproductive pathways (e.g., direct

transmetallation of intermediate (**2.70)** or β-hydride elimination of intermediate **2.71**) are also possible and need to be prevented.

Scheme 2.15 Proposed catalytic cycle for conjunctive cross-coupling

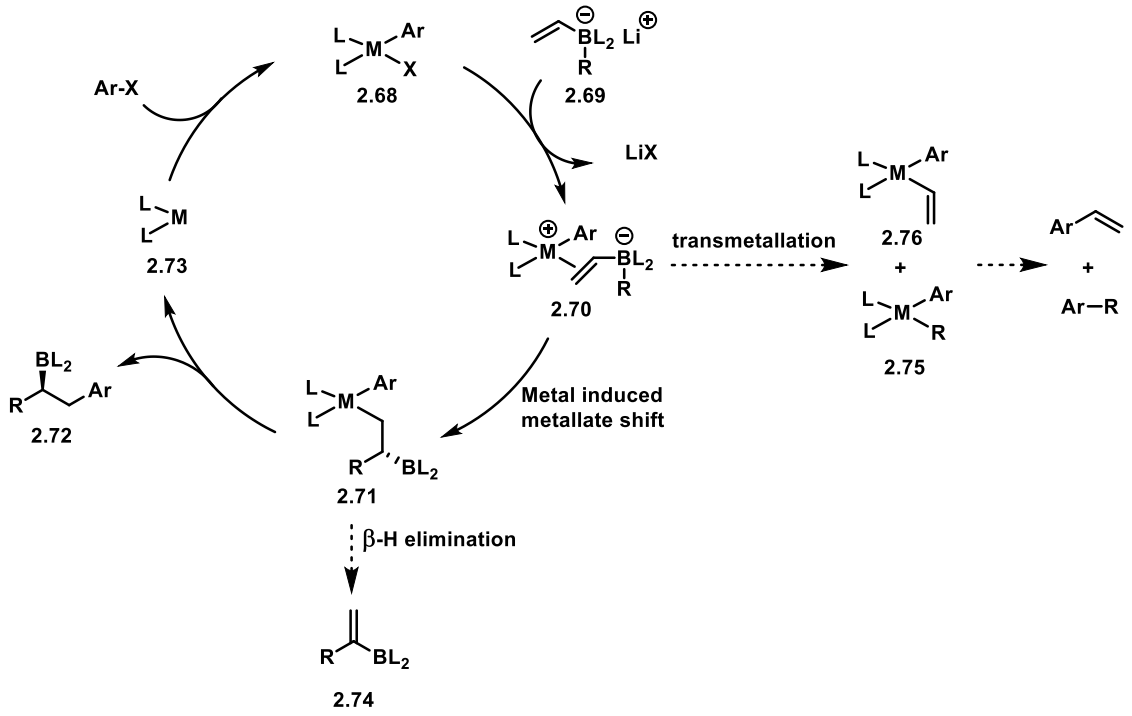

2.2.2.2 Pd-catalyzed conjunctive cross-coupling

The first generation Pd-catalyzed conjunctive cross-coupling was developed in 2016.[24] A Pd/MandyPhos complex was found to be effective in promoting the 1,2-metallate shift of *in situ*-generated vinyl B(neo)-derived

[24] L. Zhang, G. J. Lovinger, E. K. Edelstein, A. A. Szymaniak, M. P. Chierchia, J. P. Morken, *Science*, **2016**, *351*, 70

'ate' complex (**2.78)** with high efficiency and enantioselectivity (Scheme 3.16). The reaction exhibits broad functional group tolerance with both aromatic (**2.79**) and aliphatic organolithium reagents (**2.80**).

Scheme 2.16 First Pd-catalyzed conjunctive cross-coupling

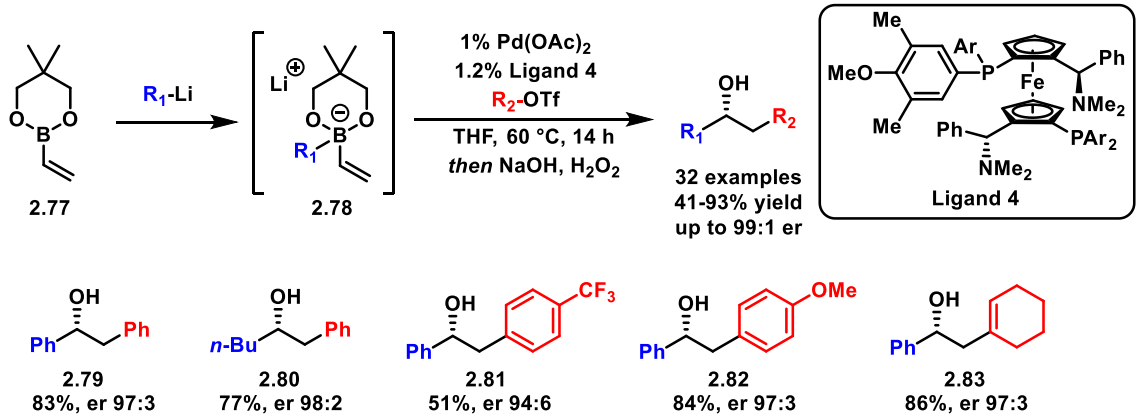

Noteworthy, the pre-assembled 'ate' complex could be produced not only by reacting vinyl B(neo) with an organolithium, but also by mixing vinyllithium with an organoboronate (Scheme 2.17). This feature might find its value when the corresponding organolithium reagent (e.g., cyclohexyllithium) could not be obtained easily.

Scheme 2.17 Alternative way to generate 'ate' complex for conjunctive cross-coupling

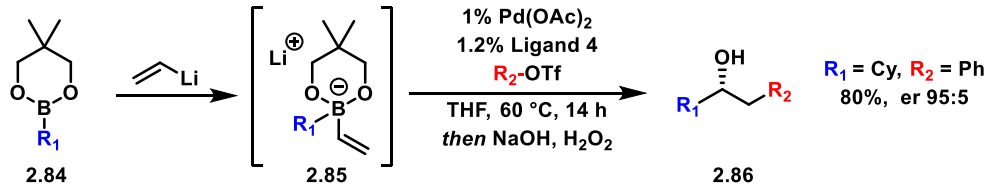

In terms of electrophiles, the reaction tolerated a range of sp^2 hybridized organotriflate electrophiles, including both aryl (**2.81,2.82**) and alkenyl triflates (**2.83**). Unfortunately, halide electrophiles were not compatible with the system due to the inhibition effect of catalysis by the halide. Inhibition occurs when the oxidative adduct involving the aryl halide is formed: the square planar four coordinate complex is fully saturated and does not release halide readily. Thus, binding of the alkenyl boronate 'ate' complex is prevented[25]. On the other hand, the corresponding intermediate of organotriflate adduct readily dissociates and has one open coordination site available.

Deuterium labeling experiments using *trans*-deutero vinyllithium produced the product with high diastereoselectivity. The *anti* relationship between boron and deuterium suggests that the reaction undergoes a stereospecific antiperiplanar 1,2-metallate shift instead of the alternative mechanism involving carbopalladation, transmetallation, and reductive elimination, which leads to *syn* relationship between boron and deuterium. Although Murakami's invertive reductive displacement mechanism would fit

[25] a) A. Jutand, *Appl. Organomet. Chem*. **2004**, *18*, 574; b) F. Ozawa, A. Kubo, T. Hayashi, *J. Am. Chem. Soc.* **1991**, *113*, 1417

the same stereochemical outcome, it is considered very unlikely by density function theory (DFT) calculations[24].

Scheme 2.18 Deuterium labeling experiments of Pd-catalyzed conjunctive cross-couplings

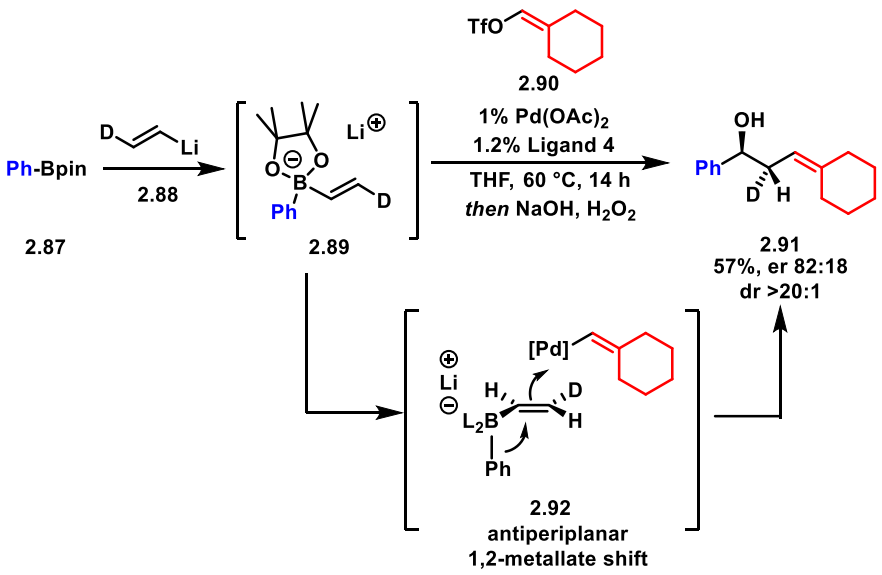

The challenge posed by aryl halide electrophiles was resolved in a second generation of the palladium-catalyzed conjunctive cross-coupling reported in 2017.[26] In this study, aryl halides were enabled as competent coupling partners by employing sodium triflate as a halide scavenger.[27] Halogen anion is abstracted by sodium cation to form NaX as a precipitate. This process provides an open coordination site for the 'ate' complex to bind.

[26] G. J. Lovinger, M. D. Aparece, J. P. Morken, *J. Am. Chem. Soc*. **2017**, *139*, 3153
[27] J. G. P. Delis, J. H. Groen, K. Vrieze, P. W. N. M. van Leeuwen, N. Veldman, A. L. Spek, *Organometallics* **1997**, *16*, 551

Besides halide electrophiles, Grignard reagents, which possess better functional group compatibility and commercial availability, were also found to be active as nucleophiles when NaOTf was employed.

Scheme 2.19 Improved reactivity and substrate scope of Pd-catalyzed conjunctive cross-couplings

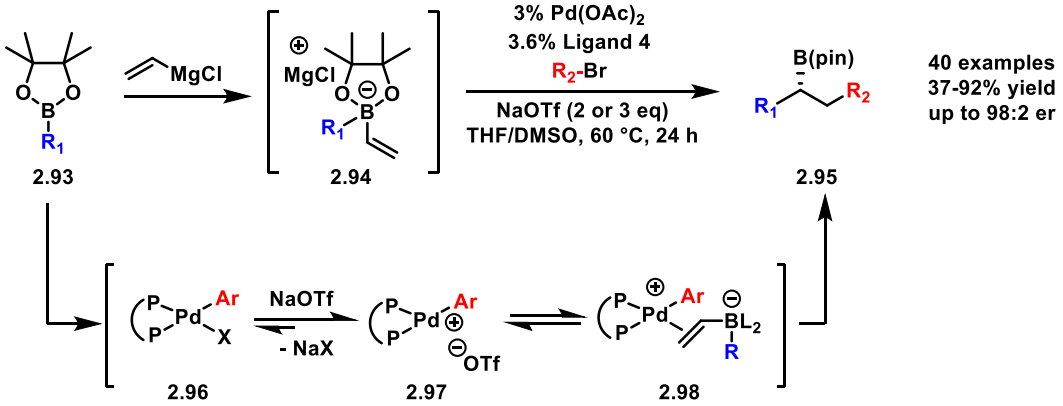

Besides aliphatic and aromatic migrating groups, alkenyl groups were found to be competent migrating groups and this facilitates the synthesis of useful chiral allyl boronates (Scheme 2.20 a).[28] In 2018, α- and β-substituted alkenyl boronate derived 'ate' complexes were introduced in conjunctive cross-coupling with good yield and enantioselectivity (Scheme 2.20 b,c).[29,30] A more detailed discussion of these reactions is provided in Chapter 3.

[28] E. K. Edelstein, S. Namirembe, J. P. Morken, *J. Am. Chem. Soc*. **2017**, *139*, 5027
[29] J.A. Myhill, L. Zhang, G. J. Lovinger, J. P. Morken, *Angew. Chem. Int. Ed*. **2018**, *57*, 12799
[30] J. A. Myhill, C. A. Wilhelmsen, L. Zhang, J. P. Morken, *J. Am. Chem. Soc*. **2018**, *140*, 15181

Scheme 2.20 Other advances in Pd-catalyzed conjunctive cross-couplings

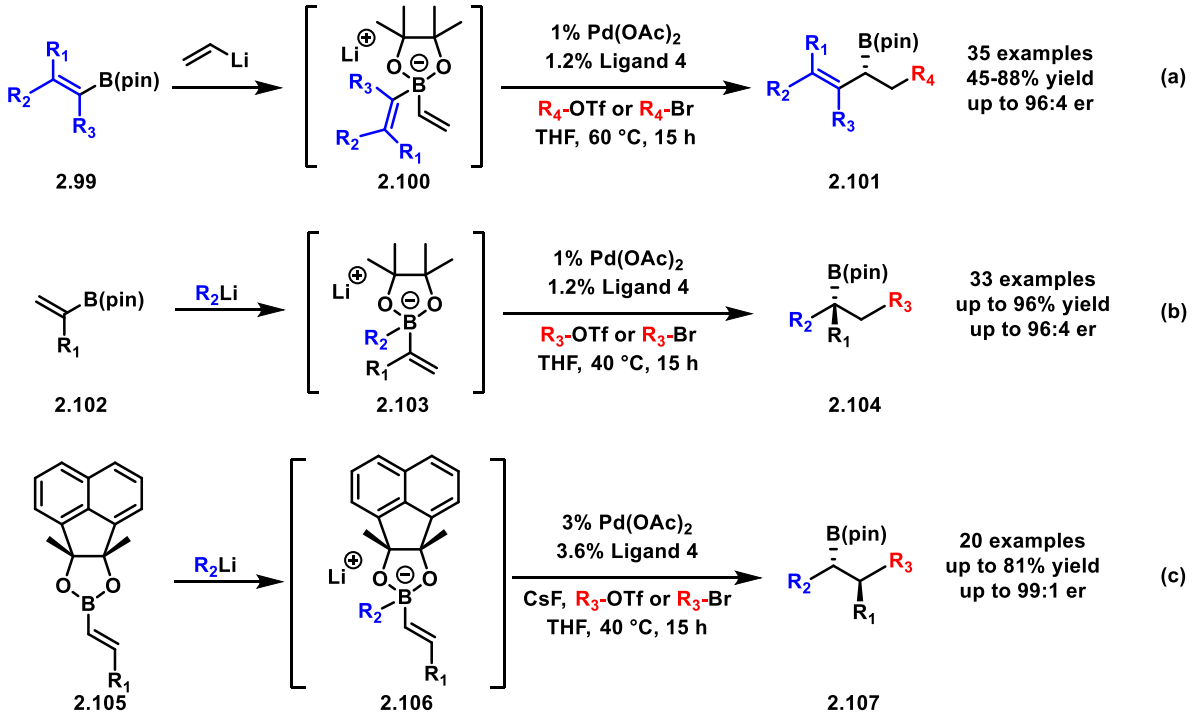

2.2.2.3 Ni-catalyzed conjunctive cross-coupling

A nickel complex was also developed as an effective catalyst in the conjunctive cross-coupling reaction.[31] The reactive alkyl borane-derived 'ate' complex was utilized as the substrate along with a nickel pre-catalyst and a chiral diamine ligand to generate enantioenriched secondary alcohols after oxidative workup (Scheme 2.21). Deuterium labeling experiments and other mechanistic studies suggest that the nickel-catalyzed conjunctive cross-

[31] M. Chierchia, C. Law, J. P. Morken, *Angew. Chem. Int. Ed.* **2017**, 56, 11870

coupling proceeds through a similar catalytic cycle that for Pd-catalysis (Scheme 2.15). Numerous useful transformations (e.g., amination, olefination, cyanomethylation) were conducted to showcase the utility of chiral 9-BBN borane products, which were rarely reported in the literature (Scheme 2.22).

Scheme 2.21 Ni-catalyzed conjunctive cross-coupling of 9-BBN borane derived 'ate' complex

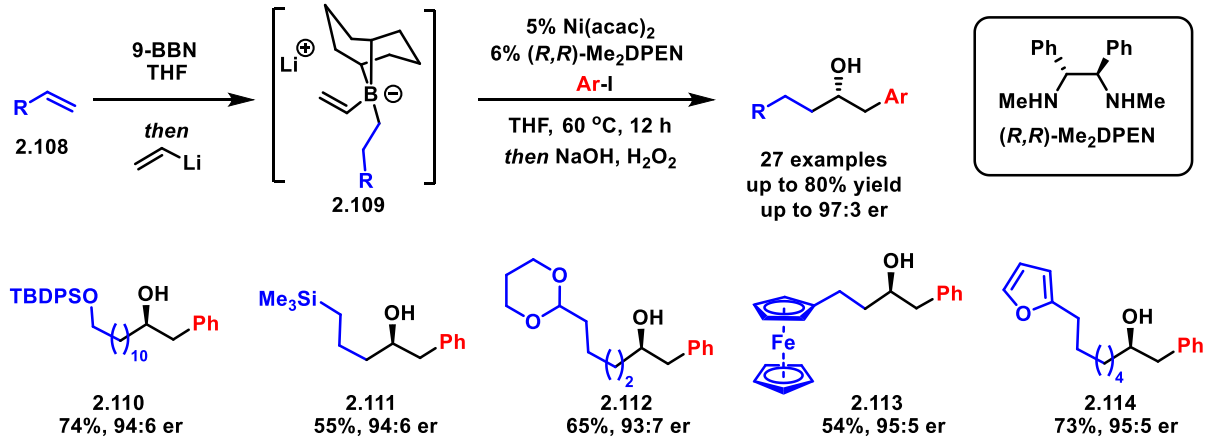

Scheme 2.22 Versatility of chiral secondary alkyl 9-BBN boranes

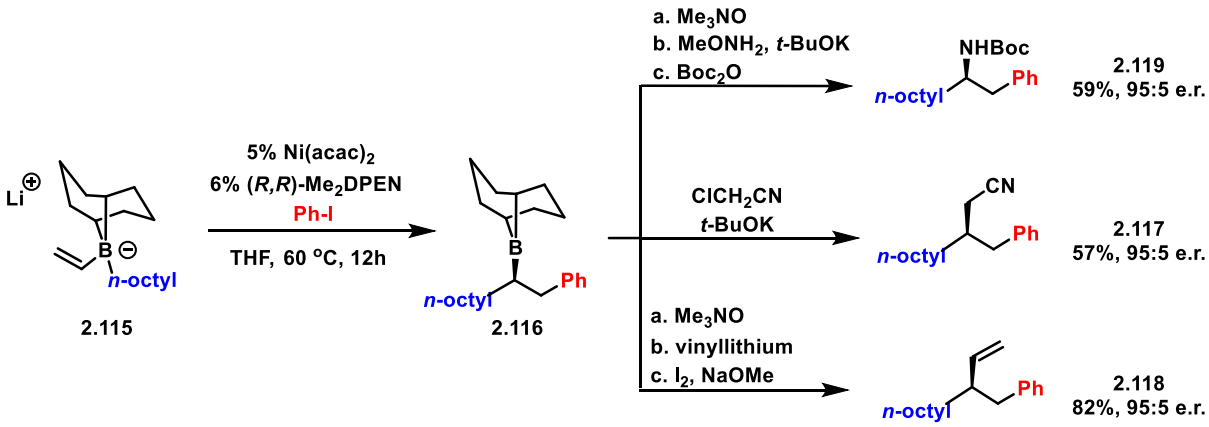

Another advance in Ni-catalyzed conjunctive cross-coupling was also established in 2017.[32] In this study, sp^3 hybridized halide electrophiles were introduced into the reaction with Ni/PyBox complex as a catalyst (Scheme 2.23). Unlike the classic catalytic mechanism applied to the former nickel-catalyzed conjunctive cross-coupling reaction, the mechanistic pathways were determined by the nature of aliphatic halide electrophiles (Scheme 2.24). The oxidation of alkyl halides by nickel complex follows a halogen atom abstraction mechanism to generate alkyl radicals (**2.132**). If the alkyl radicals are stabilized by the adjacent electron-withdrawing substituents (e.g., **2.123-2.126**), they will preferentially attack the electron-rich alkenyl boronate 'ate' complex (**2.134**) instead of recombining with the nickel catalyst (**2.133**). Then, another single electron transfer takes place on the newly formed α-boryl radical (**2.135**) to yield an α-boryl cation (**2.136)**, which delivers the racemic products after 1,2-migration. Similar reactivities had also been reported by Studer[33] and Aggarwal.[34]

Alternatively, if the alkyl radicals are nucleophilic, they will quickly recombine with Ni complex (**2.133)** and undergo the classic conjunctive

[32] G. J. Lovinger, J. P. Morken, *J. Am. Chem. Soc*. **2017**, *139*, 17293
[33] M. Kischkewitz, K. Okamoto, C. Mü ck-Lichtenfeld, A. Studer, *Science* **2017**, *355*, 936
[34] M. Silvi, C. Sandford, V. K. Aggarwal, *J. Am. Chem. Soc.* **2017**, *139*, 5736

cross-coupling mechanism to construct enantioenriched products. A variety of enantioenriched secondary alkyl boronates (**2.127-2.130**), were prepared in this manner with sp^2 hybridized nucleophiles.

Scheme 2.23 Ni-catalyzed conjunctive cross-couplings with alkyl halide electrophiles

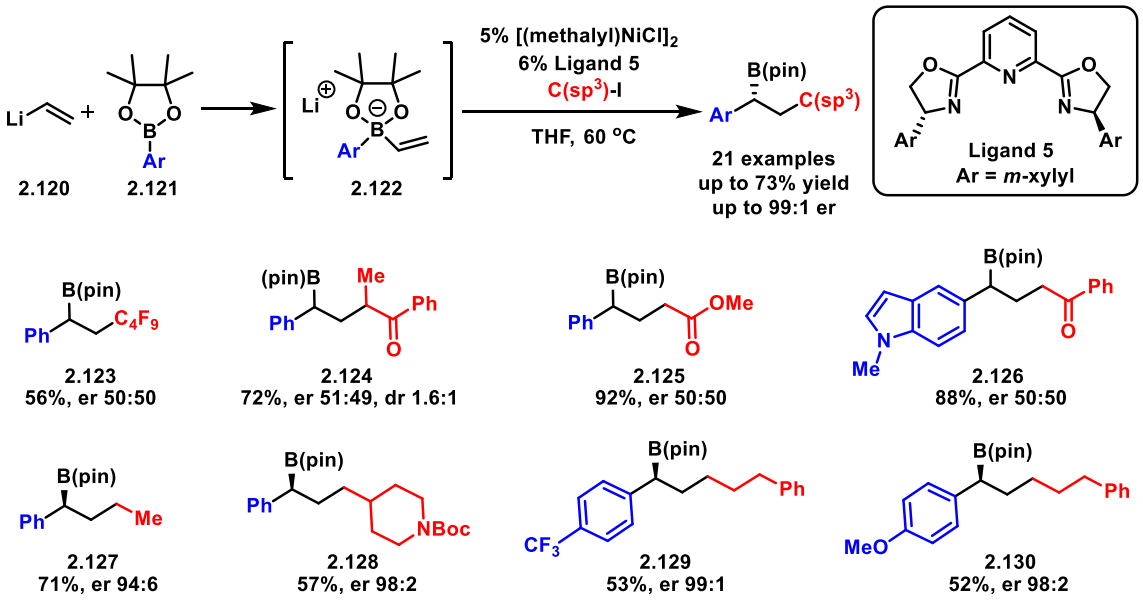

Scheme 2.24 Two operating mechanism for Ni-catalyzed conjunctive cross-coupling of alkyl halides

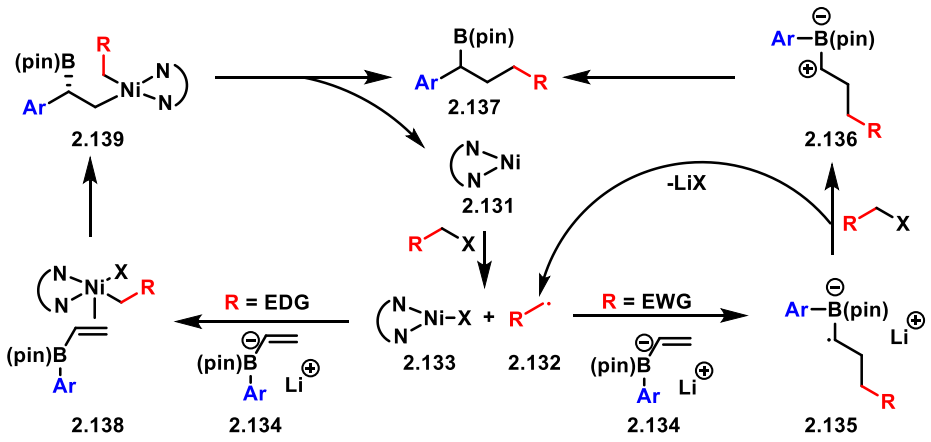

The conjunctive cross-coupling of sp^3 hybridized migrating groups and electrophiles was not demonstrated until early 2020.[35] In this case, a similar nickel/PyBox catalytic system was adopted with a newly designed boronate ligand, methylated acenaphthoquinone (mac), to enable the synthesis of chiral secondary alkyl boronates.

Scheme 2.25 Ni-catalyzed conjunctive cross-coupling of aliphatic migrating groups and electrophiles

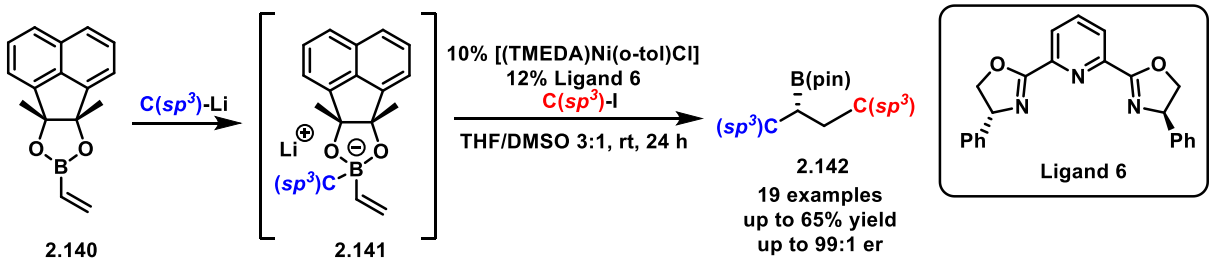

2.2.3 Acyl electrophiles in Ni-catalyzed cross-coupling reactions

Carbonyl electrophiles have been engaged in nickel complex promoted reactions since the studies of oxidative addition of cyclic anhydrides to nickel/bipyridine were disclosed by the Yamamoto group.[36] Compound **(2.146)** generated from the oxidative addition adduct **(2.145)** by decarbonylation was identified and partially characterized after ligand exchange with dpe (Scheme 2.26a). The full characterization of similar

[35] S. M. Koo, A. J. Vendola, S. N. Momm, J. P. Morken, *Org. Lett*. **2020**, *22*, 666
[36] K. Sano, T. Yamamoto, A. Yamamoto, *Chem. Lett*. **1983**, *12*, 115

intermediate (**2.151)** was conducted by Weix[37] and Gong[38] independently in 2014, in which aliphatic acid chlorides were employed as acyl electrophiles (Scheme 2.26b).

Scheme 2.26 Ni/bpy complex in oxidiative addition of acyl eletrophiles

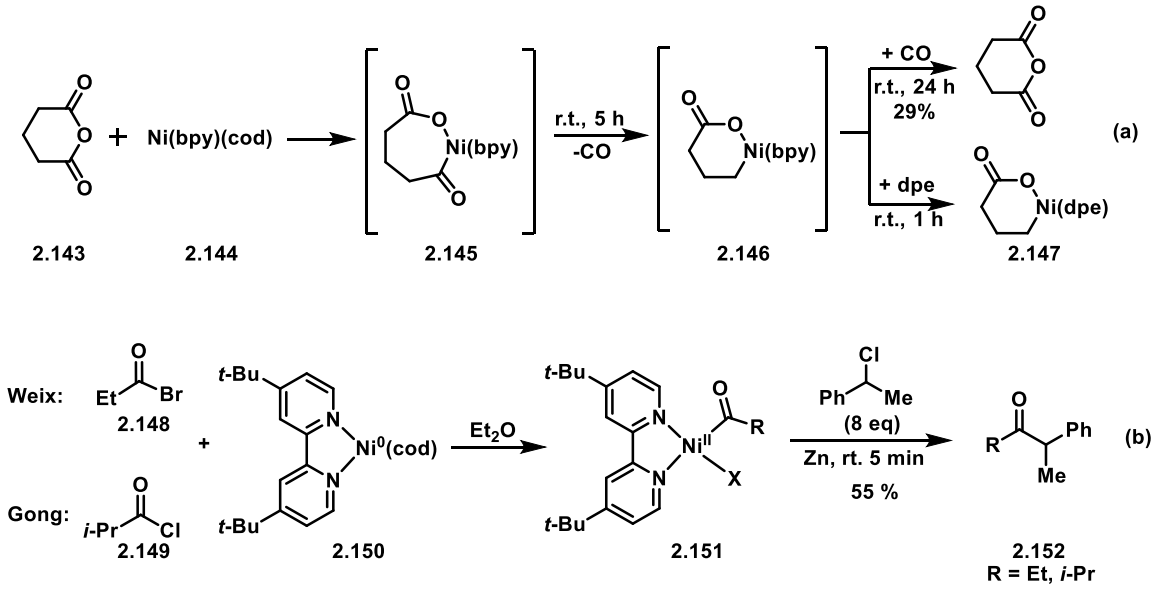

The first catalytic cross-coupling of cyclic anhydrides enabled by nickel/bipyridine complexes was developed by Rovis in 2001.[39] In his mechanistic proposal, oxidative addition adduct **(2.156)** underwent transmetallation with diethylzinc, followed by reductive elimination, to produce the products as zinc salts (Scheme 2.27).

[37] A. C. Wotal, R. D. Ribson, D. J. Weix, *Organometallics* **2014**, *33*, 5874
[38] C. Zhao, X. Jia, X. Wang, H. Gong, *J. Am. Chem. Soc.* **2014**, *136*, 17645
[39] a) E. A. Bercot, T. Rovis, *J. Am. Chem. Soc.* **2001***, 124*, 174; b) Y. Zhang, T. Rovis, *J. Am. Chem. Soc*. **2004**, *126*, 15964

Scheme 2.27 The first Ni/bpy complex catalyzed cross-couplings of acyl electrophiles

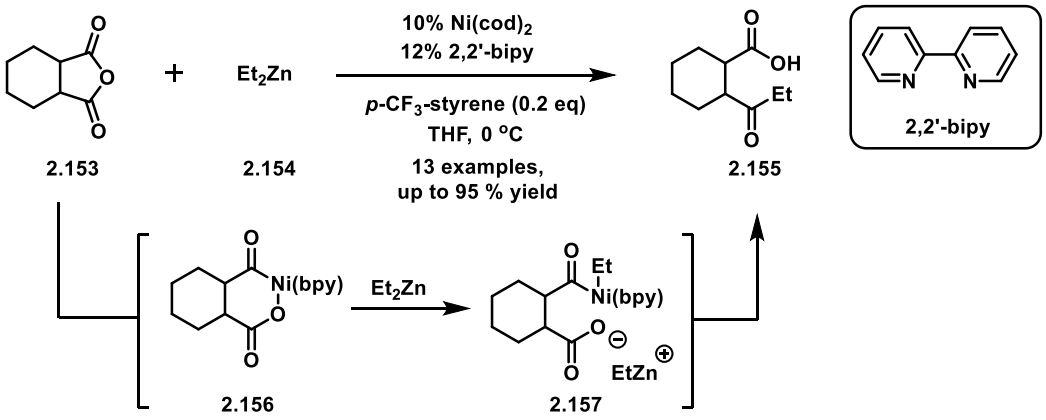

Reductive cross-coupling is another important research area where acyl electrophiles are utilized in nickel catalysis (Scheme 2.28). Weix[40] and Gong[41] have elaborated several methods for the reductive cross electrophiles couplings between acid chlorides and aliphatic halides by nickel/bpy catalytic system. In 2013, Reisman reported an enantioselective variation of nickel-catalyzed cross-electrophile-coupling with PheBox as the chiral ligand on nickel.[42] All the methods mentioned above suggest that the nickel/bpy complex is able to undergo oxidative addition with various carboxylic acid-derivatives and that subsequently, the complex participates in cross-coupling reactions.

[40] A. C. Wotal, D. J. Weix, *Org. Lett*. **2012**, *14*, 1476
[41] a) H. Yin, C. Zhao, H. You, Q. Lin, H. Gong, *Chem. Commun*. **2012**, *48*, 7034; b) F, Wu, W. Lu, Q. Qian, Q. Ren, H. Gong, *Org. Lett*. **2012**, *14*, 3044
[42] A. H. Cherney, N. T. Kadunce, S. E. Reisman, *J. Am. Chem. Soc.* **2013**, *135*, 7442

Scheme 2.28 Ni/bpy complex catalyzed reductive cross-couplings of acyl electrophiles and aliphatic halides

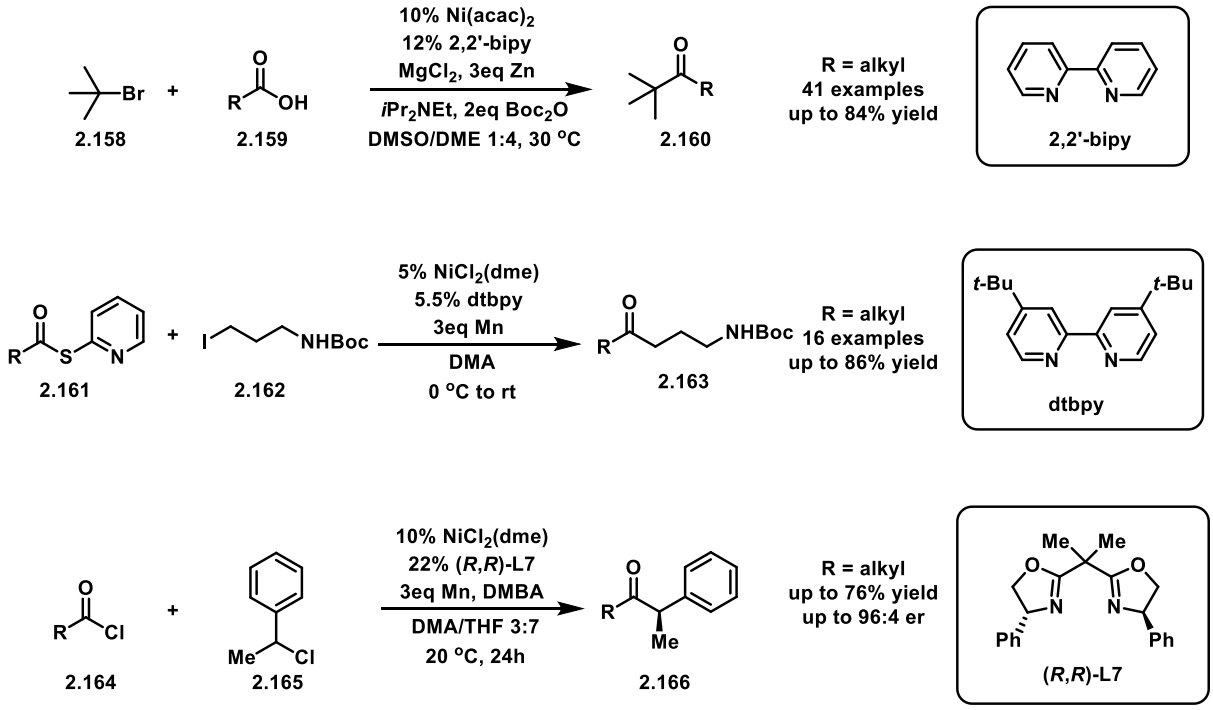

The mechanism of Ni-catalyzed cross-electrophiles-coupling of acyl chlorides and alkyl halides are largely depending on the nature of the electrophiles (Scheme 2.29). When the aliphatic iodide is employed, the catalyst tends to react with alkyl iodide first to form an oxidative addition adduct first, which undergoes bimetallic ligand exchange to generate the bis-alkylated Ni(II)-species. Then, it reacts with acyl electrophile to produce the product and regenerate the oxidative addition adduct. The reductant is employed to rescue the dihalogenated nickel(II) species and there is no

intermediate reduction in the working catalytic cycle.[37,40] (pathway a) When benzyl chlorides are used, the nickel complex prefers oxidative addition with acyl chlorides first, followed by the reduction to generate nickel(I)-complex. The second oxidative addition and subsequent reductive elimination produce the coupling product (pathway b).[38,42] The radical inner sphere oxidative addition allows the generation of enantioenriched ketones from racemic benzyl chlorides.[42]

Scheme 2.29 Possible mechanisms of Ni-catalyzed cross-electrophiles-coupling

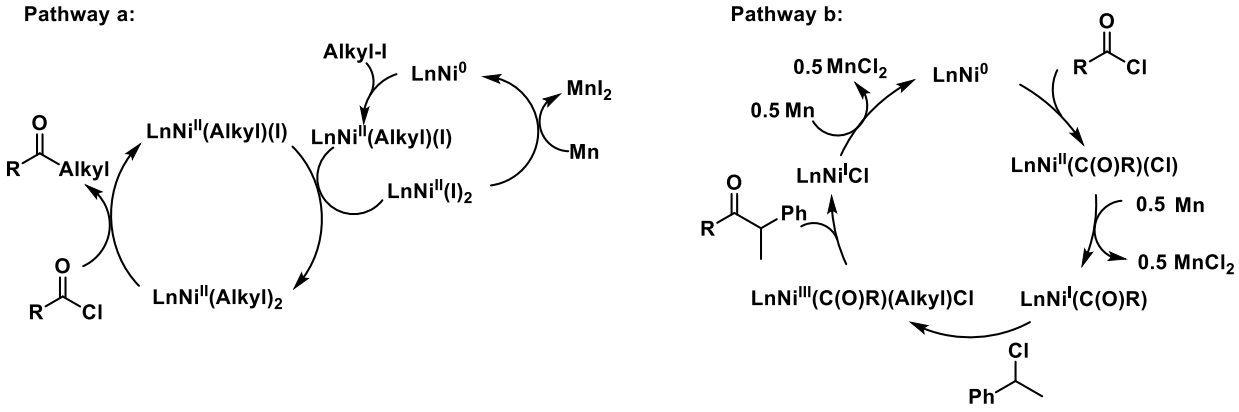

2.3 Experiment design

2.3.1 Reaction design

The scope of conjunctive cross-coupling reactions had been extended to both organoboranes and organoboronates with various migrating groups

(e.g., alkyl, aryl, and alkenyl migrating groups). However, the scope of electrophiles was restricted to halogenated hydrocarbons. Thus, another class of electrophiles, carboxylic acid derivatives, were considered to broaden the scope of the reaction (Scheme 2.30). The products, β-boryl carbonyls, are valuable compounds that are generally prepared from boron-Cu conjugate addition to α,β-unsaturated carbonyl species.[1,2] Whereas the suggested conjunctive cross-coupling with acyl electrophiles could conceivably provide an alternative disconnection strategy for the synthesis of β-boryl ketones.

Scheme 2.30 Conjunctive cross-coupling: a new method for the synthesis of β-boryl carbonyls

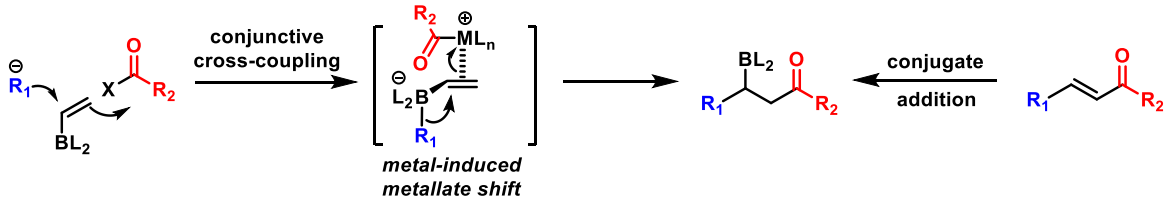

Because of the halide inhibition effect observed in Pd-catalyzed conjunctive cross-coupling[30], the nickel-catalyzed system was adopted. Considering that Ni/bpy complex has been described as an effective catalyst to undergo oxidative addition with acid anhydrides and promote the cross-coupling reactions, initial studies were performed with Ni/bpy complex as the catalyst and 9-BBN borane-derived 'ate' complex as substrates. To our delight,

the simple Ni/bpy catalytic system provided promising results with a 58% yield after oxidative workup.

Scheme 2.31 Initial attempts on Ni-catalyzed conjunctive cross-coupling of anhydrides

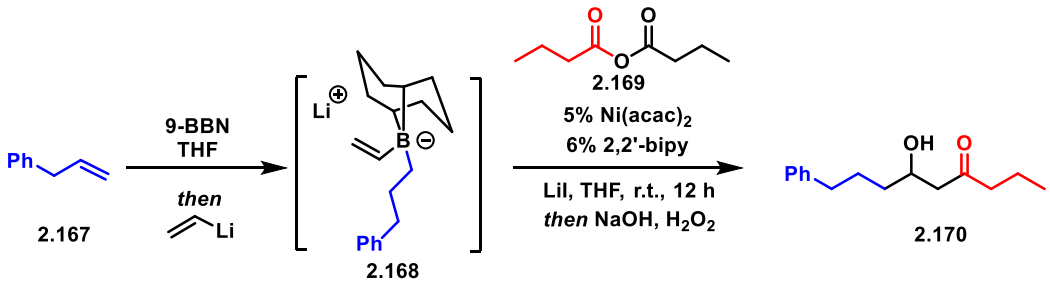

Entry	Variation from the condition above	Yield
1	None	58 %
2	No 2,2'-bipy	0 %
3	No $Ni(acac)_2$	0 %
4	No LiI	0 %

2.3.2 Reaction optimization

2.3.2.1 Functions of halide

An exciting outcome was obtained when additives were investigated. In particular, it was found that LiI provided an efficient reaction (Scheme 2.31, entry 4). Further studies on the effects of LiOTf and other lithium halides suggest that the halide anion is the important component in that LiOTf completely shuts down the reaction (Scheme 2.32, entry 2) while other lithium

halides provided similar levels of reactivity as LiI (Scheme 2.32, entry 3-5). Furthermore, it was also demonstrated that only a catalytic amount of halide is required (entry 6), and the source of halide anion could be the nickel precatalyst, as shown in entry 7. Besides anhydrides, acid chlorides also

Scheme 2.32 Optimization of reaction conditions: functions of additives

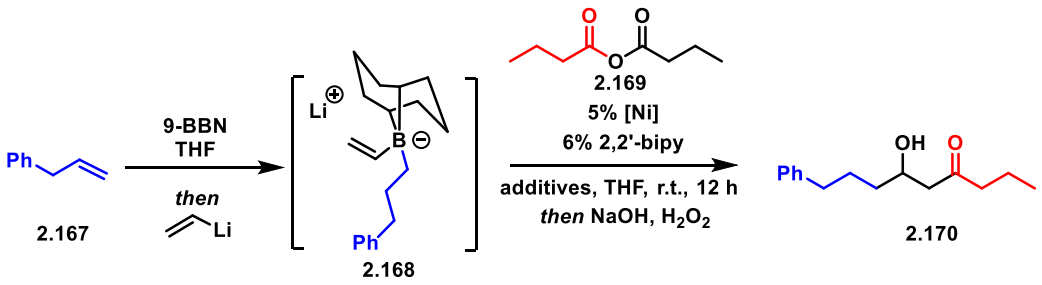

Entry	Ni pre-catalyst	Additive	Yield
1	$Ni(acac)_2$	LiI	58%
2	$Ni(acac)_2$	LiOTf	0%
3	$Ni(acac)_2$	LiF	47%
4	$Ni(acac)_2$	LiCl	61%
5	$Ni(acac)_2$	LiBr	64%
6	$Ni(acac)_2$	LiBr (0.1 eq)	59%
7	$NiBr_2$ glyme	-	63%
8[a]	$NiBr_2$ glyme	-	65%

a. 1.0 eq butyryl chloride is used in replace of butyric anhydride

proved to be effective substrates and therefore were selected as model substrates due to commercial availability (entry 8). The hypothesis for the functions of halides is that halides can rescue the nickel catalyst after oxidative addition by exchanging with carboxylate ligand which potentially could

occupy two coordination sites. After the ligand exchange, the newly available coordination site can bind with boron 'ate' complex to promote the conjunctive cross-coupling (details see **2.3.4.1**).

2.3.2.2 Ligand design

Although the reactivity of aliphatic acid chlorides was high under the condition specified in Scheme 2.33 (entry 1), aromatic substrates were not as reactive (entry 3). Hence, an array of bipyridine ligands with varying substituents were synthesized and examined to enhance the reactivity. While electron-donating substituents led to diminished yields (**L9, L10**), bipyridines with electron-withdrawing groups (**L11, L12**) exhibited high efficiency in

Scheme 2.33 Optimization of the reactivity by ligand design

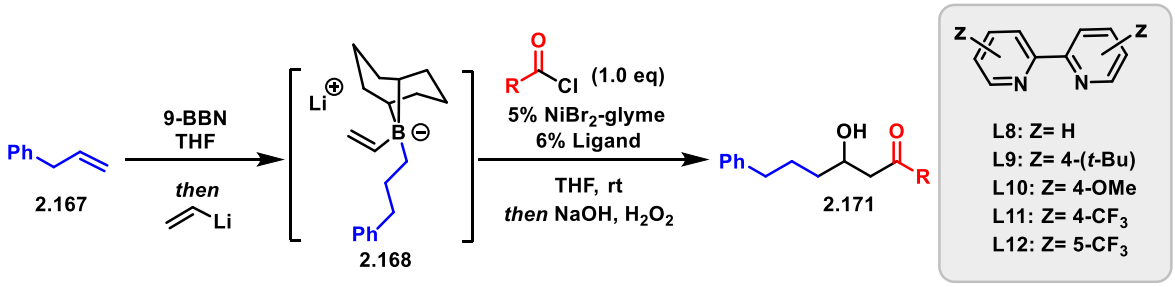

Entry	R	Ligand	Time	Yield
1	propyl	L8	1 h	65%
2	propyl	none	1 h	<5%
3	Ph	L8	1 h	40%
4	propyl	L9	1 h	32%

5	propyl	L10	1 h	42%
6	propyl	L11	1 h	76%
7	propyl	L12	1 h	78%
8	Ph	L12	1 h	75%
9	propyl	L12	2 min	75%

catalyzing the conjunctive cross-coupling reactions. A possible explanation for this result is that the possible turnover limiting step of acyl electrophile conjunctive cross-coupling, reductive elimination step, is accelerated by electron-withdrawing bipyridine ligands. With more electron-poor nickel species, faster reductive elimination could be expected and higher yield could be obtained in 1 hour. **Ligand 12** furnished the highest reactivity toward both aliphatic and aromatic substrates and therefore was chosen as the optimal ligand. It is worth noting that the reaction speed is so fast with **L3** that 75% conversion was achieved within two minutes.

2.3.3 Substrate scope

With the optimized reaction conditions, a range of acid chlorides was investigated (Scheme 2.34). For example, simple aliphatic acid chlorides with long-chains or branched chains (**2.172-2.175**) reacted efficiently, whereas the use of *tert*-butyl substituted acid chloride led to diminished yield presumably

due to steric hindrance. Furthermore, the functional group tolerance of the reaction was showcased with products (**2.177**) and (**2.178**). In terms of aromatic acid chlorides, although acceptable yields were achieved in all substrates, electron-rich substrates were more reactive than their electron-poor counterpart, which potentially could be attributed to the electronic properties

Scheme 2.34 Substrate scope of acid chlorides in conjunctive cross-coupling

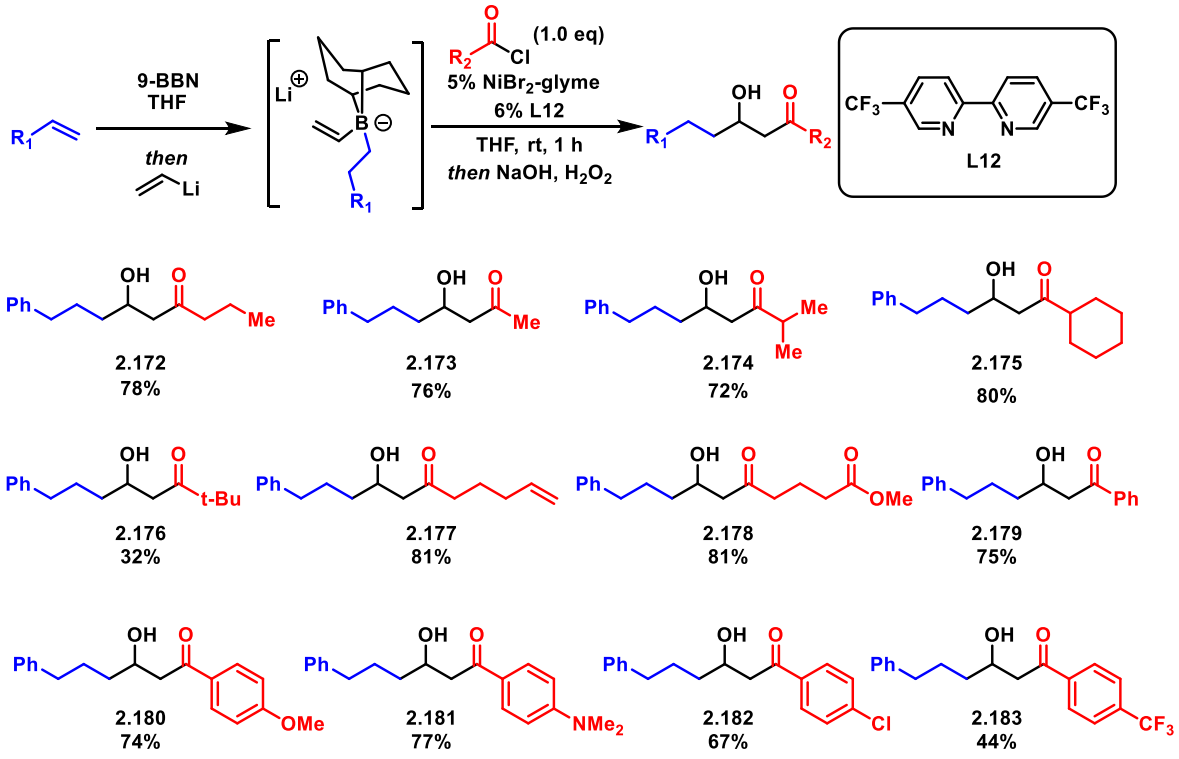

of the oxidative addition adduct. After the oxidative addition of electron-poor aromatic acid chloride like **2.182** and **2.183**, the adduct is also electron-poor and reluctant to share electrons with the alkenyl 'ate' complex through back-bonding, which is crucial for the 1,2-metallate rearrangement.

Furthermore, the method possessed a broad scope of migrating groups. As presented in Scheme 2.35, simple alkyl groups, including α-branched and β-branched hydrocarbons (**2.186** and **2.187**), migrated with high efficiency. Various functional groups, such as an acetal (**2.190**) and polyalkene (**2.191**), were well-tolerated. Not only alkyl groups but also aryl groups (**2.192**) were found to be competent migrating groups.

Scheme 2.35 Substrate scope of migrating groups in conjunctive cross-coupling

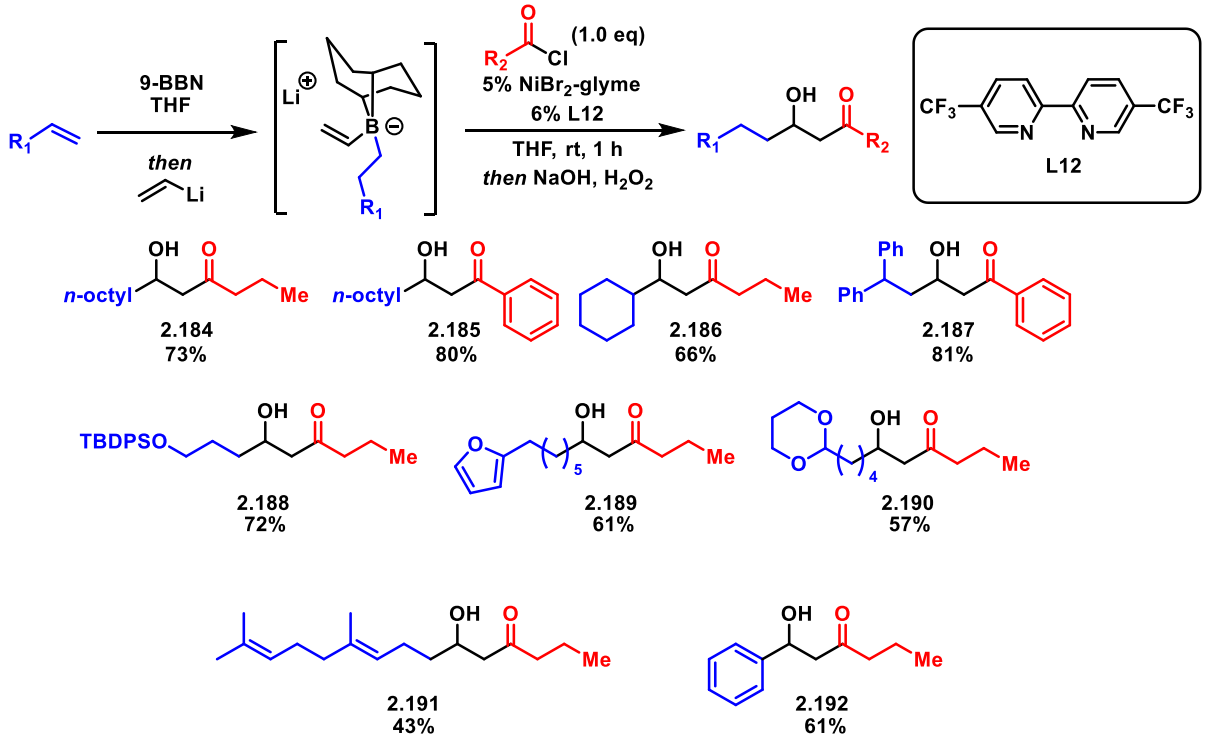

Besides acid chlorides, anhydrides were also showcased as competent substrates in the Ni-catalyzed conjunctive cross-coupling of acyl electrophiles. As depicted in Scheme 2.36, Ni/bpy complex promoted the transformations of various anhydrides (e.g., aliphatic and aromatic anhydrides and mixed anhydride **2.199**) to corresponding hydroxyketones in good yields. In the case of mixed anhydride **2.199**, the sterically less hindered carbonyl group was selectively converted into the product.

Scheme 2.36 Substrate scope of anhydrides in conjunctive cross-coupling

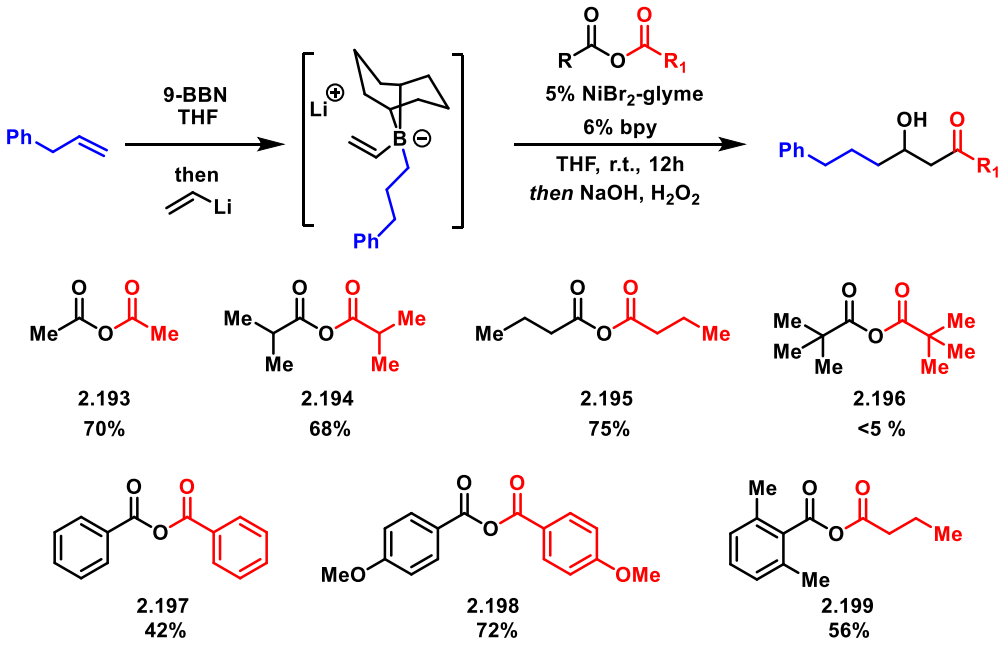

2.3.4 Mechanistic studies

2.3.4.1 Proposed catalytic cycle

It is believed that the Ni-catalyzed conjunctive cross-coupling with acyl electrophiles happens through the catalytic cycle shown in Scheme 2.15, as illustrated in the first generation palladium-catalyzed conjunctive cross-coupling. Oxidative addition of acyl electrophiles to the nickel complex generates intermediate (**2.201)**, which binds to the 'ate' complex and induces 1,2-metallate rearrangement to produce intermediate (**2.203)**. Then, reductive elimination furnishes the final product and regenerates the catalyst (**2.200)** (Scheme 2.37). If the starting material is anhydride, the binding sites of oxidative addition adducts are saturated as acetates serve as bidentate ligands.

Scheme 2.37 Proposed catalytic cycle of Ni-catalyzed conjunctive cross-coupling

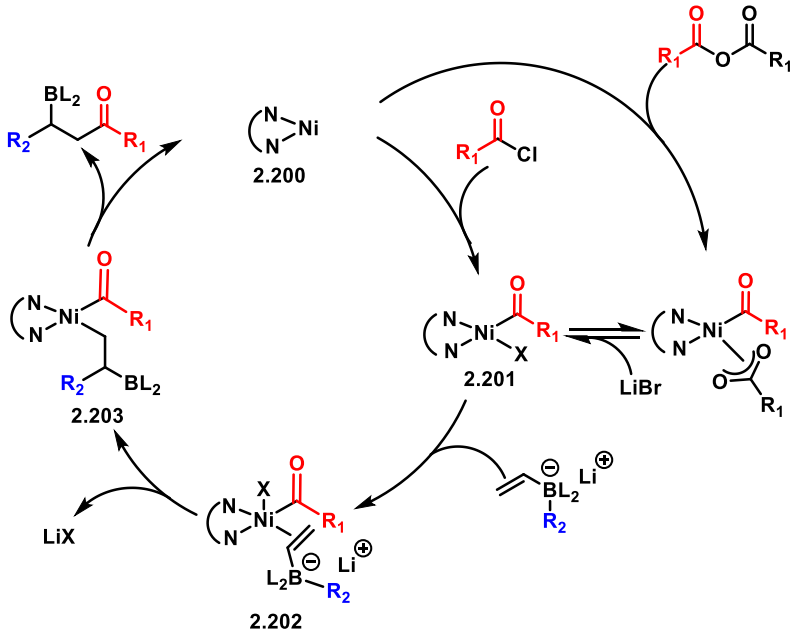

Then, external halide additives are needed to replace the acetate through ligand exchange so that the 'ate' complex can coordinate with the complex and proceed forward. To get a better insight into the mechanism of the reaction, multiple mechanistic experiments were conducted regarding the possible catalytic cycle.

2.3.4.2 Probing a possible radical mechanism

Radical trapping and radical clock experiments (Scheme 2.38) were conducted to probe for a potential radical pathway,[43] as described in previous nickel-catalyzed conjunctive cross-coupling.[29] When two equivalents of 1,4-cyclohexadiene were added as a radical scavenger, the reaction proceeded

Scheme 2.38 Radical clock and radical trapping experiments

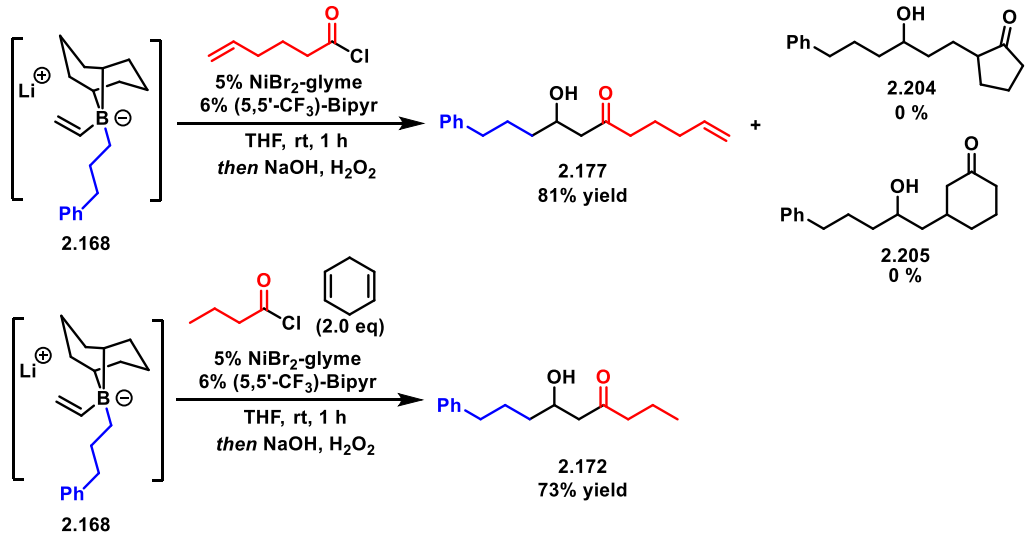

[43] C. Chatgilialoglu, D. Crich, M. Komatsu, I. Ryu, *Chem. Rev*. **1999**, *99*, 1991

with unaltered productivity. Moreover, there was no detectable amount of five- or six-membered cyclization products (**2.204** and **2.205**) observed during the radical clock experiment. Both results suggest that the radical mechanism is not likely to be the dominant pathway in the reaction.

2.3.4.3 Oxidative addition

To further probe our mechanistic proposal, the oxidative addition adduct **2.208** was firstly investigated (Scheme 2.39). The oxidative addition adduct (**2.208)** prepared and characterized according to previous literature[38] was subjected to the 'ate' complex stoichiometrically with butyryl chloride as substrate. The reaction furnished the desired product (**2.174**) with comparable yield as a normal catalytic reaction, which suggests that the oxidative addition adduct is catalytically competent.

Scheme 2.39 Synthesis of oxidative addition adduct and its application in the conjunctive cross-coupling reaction

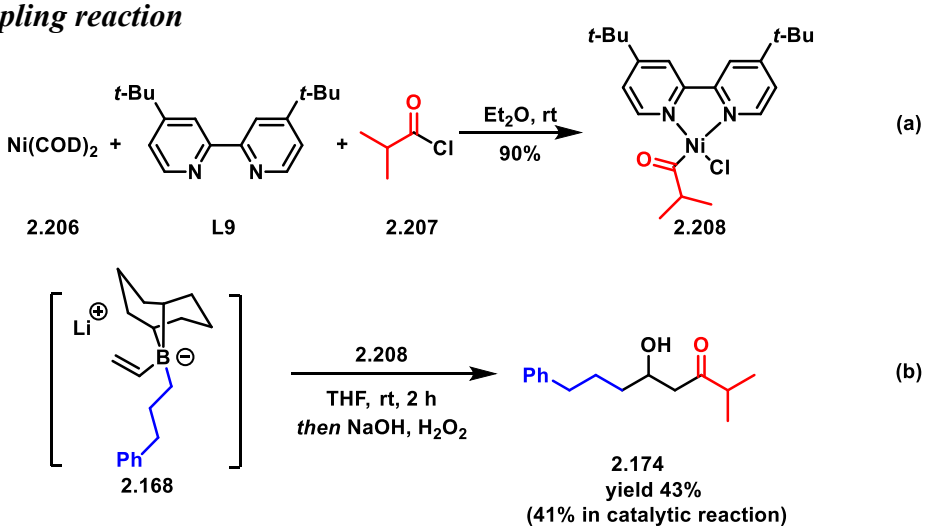

2.3.4.4 1,2-metallate rearrangement

The critical step in the mechanistic proposal is the 1,2-metallate rearrangement step, which was proposed as a nickel-induced stereospecific antiperiplanar migration. To probe this, a deuterium labeling experiment was designed to distinguish between the 1,2-metallate shift mechanism and a carbonickelation/ transmetallation pathway (Scheme 2.40). In this experiment, a *trans* deuterium-labeled 'ate' complex (**2.211)** was subjected to the standard reaction conditions where greater than 20:1 diastereoselectivity was obtained with deuteride and borane in an *anti* relationship. This high level of diastereoselectivity strongly suggests that the reaction proceeds through the

Scheme 2.40 Deuterium labeling experiments suggested stereospecific 1,2-metallate shift

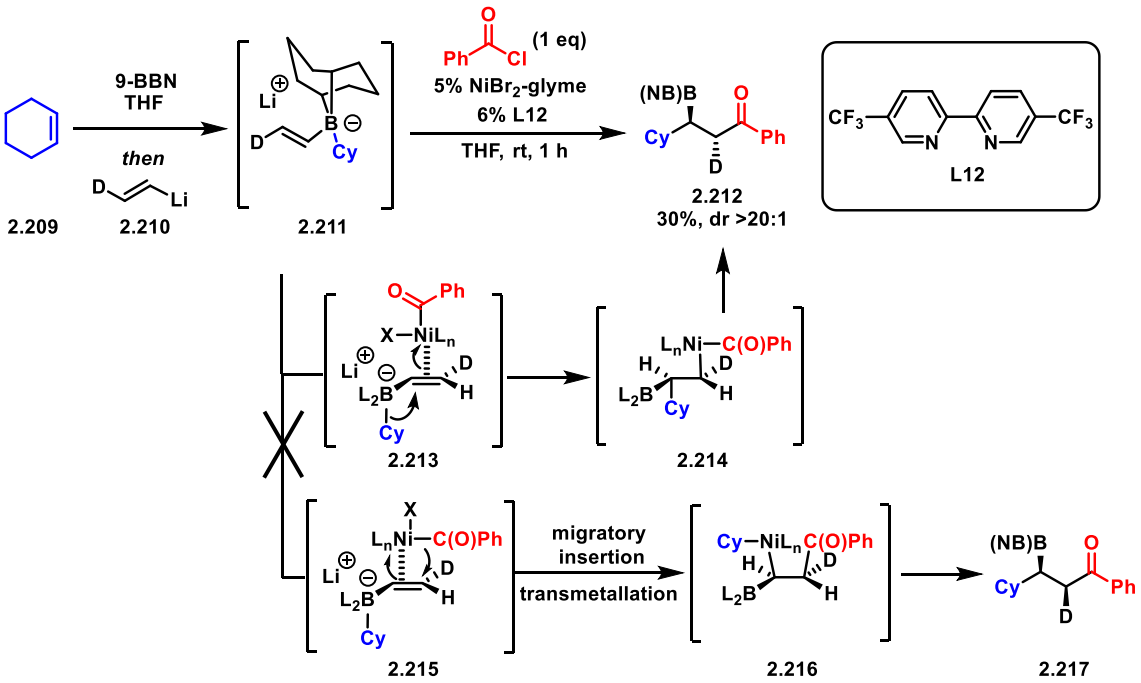

stereospecific 1,2-metallate shift process (**2.213**) instead of the alternative carbometallation/transmetallation sequence (**2.215** and **2.216**) in which *syn* relationship of borane and deuteride is anticipated (**2.217**).

2.3.4.5 Order of oxidative addition and 1,2-metallate shift

Because of the feasible Ni(I)/Ni(III) catalytic cycle, potentially the reaction could occur by a Ni(I)-induced 1,2-metallate shift followed by oxidative addition and reductive elimination to furnish the product. To further evaluate this possibility, experiments with a chiral ligand on nickel were carried out as described in Scheme 2.41. In these experiments, acyl chlorides bearing different substituents were subjected to Ni/Box complex-catalyzed conjunctive cross-coupling reaction. The results revealed that enantioselectivity varied when different acyl electrophiles were employed. This indicates that the acyl electrophiles are attached to the chiral nickel species in the stereochemistry determining step. Since the 1,2-metallate shift is likely the stereochemistry determining step, this observation suggests that oxidative addition is likely to proceed before the 1,2-metallate shift.

Scheme 2.41 Influenece of acyl substituents on enantioselectivity in conjunctive cross-coupling

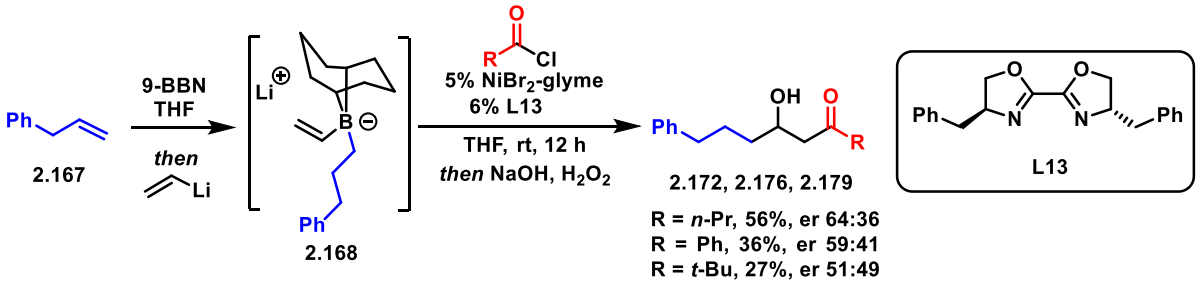

2.3.5 Transformations

Other than oxidative workup to furnish the β-hydroxy ketones, several valuable transformations of β-ketoboranes were examined. Air stable β-boryl ketimines were prepared by treating the conjunctive cross-coupling product with the corresponding amine in MeOH or water (Scheme 2.42). Unlike other 9-BBN borane species, the β-boryl ketimine compounds are stable to air and moisture likely because of the strong coordination of ketimine nitrogen to 9-BBN borane, as revealed by the ^{11}B NMR of the product (δ 1.96 ppm). The X-ray structure of compound (**2.222**) also indicated that the distance between boron and nitrogen is 1.68 Å, which is comparable to the bond length of a formal B–N bond. Although the X-ray structure of corresponding β-boryl ketone was not accessible, its ^{11}B NMR also revealed relatively strong bonding between oxygen and boron with a resonance at 21.5 ppm (Scheme

2.43). However, this strong coordination electronically prevents the external nucleophiles from attacking the organoboron unit in the product, which limits the possible transformations. Additionally, the bulkiness of the 9-BBN backbone made it even harder to be functionalized. Multiple efforts, including amination and homologation, failed to achieve the desired transformations.

Scheme 2.42 Synthesis of β-boryl ketimins from β-ketoboranes

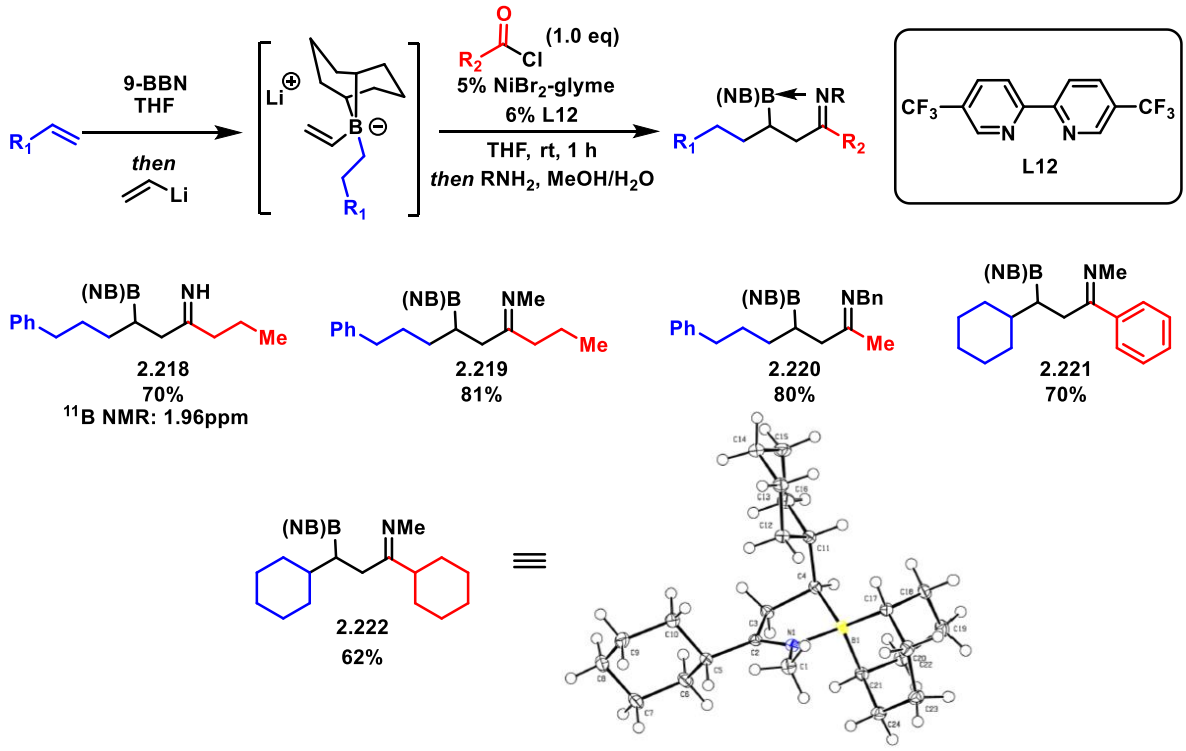

Although the coordination between the carbonyl and the boron prevented it from further functionalization other than oxidation, it activated the carbonyl group and enabled a diastereoselective alkylation reaction. As

shown in Scheme 2.43, the conjunctive cross-coupling product (**2.179**) was firstly deprotonated by methyllithium at -78 °C. The chemoselectivity of deprotonation over nucleophilic addition is driven by the sterics. Deprotonation at methylene carbon is much less steric demanding compared to nucleophilic attack the carbonyl carbon to form a tetrasubstituted carbon. The formed five-membered ring through enolation is rigid enough to control the facial selectivity by sterics when the electrophile approaches. As noted in the scheme, both methyl and allyl groups could be installed with high diastereoselectivity.

Scheme 2.43 Diastereoselective alkylation of conjunctive cross-coupling products

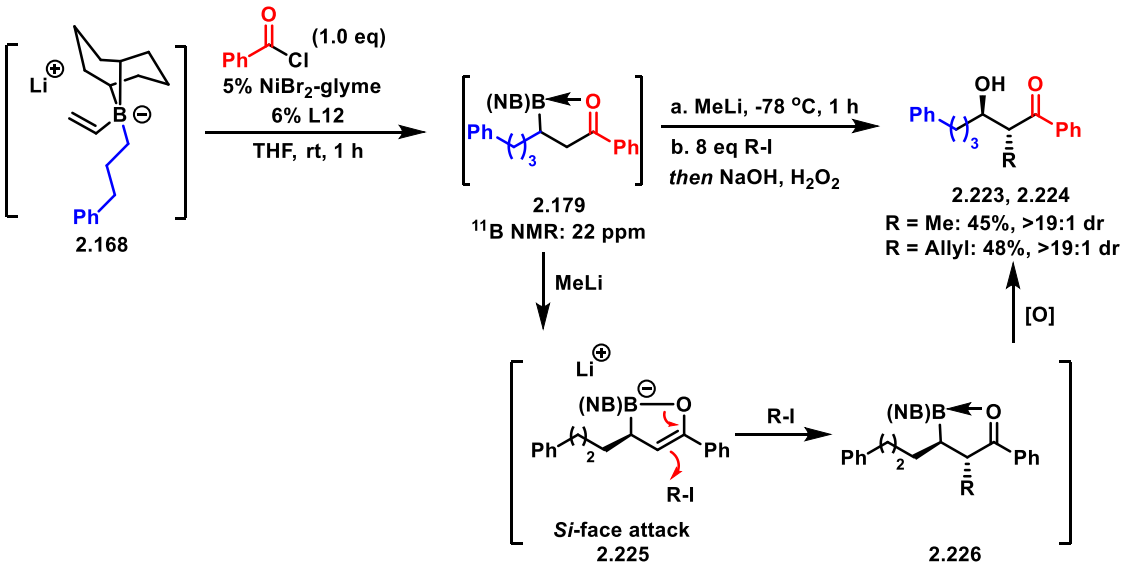

2.3.6 Studies of enantioselective conjunctive cross-coupling of acyl electrophiles

2.3.6.1 Chiral ligands on nickel-induced enantioselectivity

Encouraged by the result shown in 2.3.4.5, a library of chiral no-linker bis-oxazoline ligands with different substitution patterns were synthesized. However, as depicted in Scheme 2.44, despite the varied sizes of the substituents (**L13-L15, L19** and **L22**), there was no clear trend on the enantioselectivity. Not only the disubstituted oxazolines, other designs including *tetra*-substituted (**L18, L20**) and mixed non-C_2-symmetric Box ligand (**L17**) were also proved to be not effective to induce high enantioselectivity. Besides the Box ligands, other backbones that possess similar bite angles as bipyridines were also proposed and evaluated. Unfortunately, none of these ligands (e.g., chiral bipyridines **L24** and **L25**, chiral diimines **L26-L28**) was able to improve the enantioselectivity. The failed chiral ligand design could be attributed to the lack of understanding of the geometry of key intermediates (Scheme 2.45). The coordination site that the alkenyl 'ate' complex is taken in the Ni complex could be different as shown in (**2.227)** and (**2.228)**. Thus, the interactions between substrates and ligands are uncertain. Besides, the pre-migration intermediate could be in

either square planar (**2.229)** or square pyramidal geometry (either **2.227** or **2.228**) depending on the association status of the halide, which affects the geometry and ultimately, the induction of chirality.

Scheme 2.44 Enantioselective conjunctive cross-coupling of 9-BBN boranes and acyl chlorides

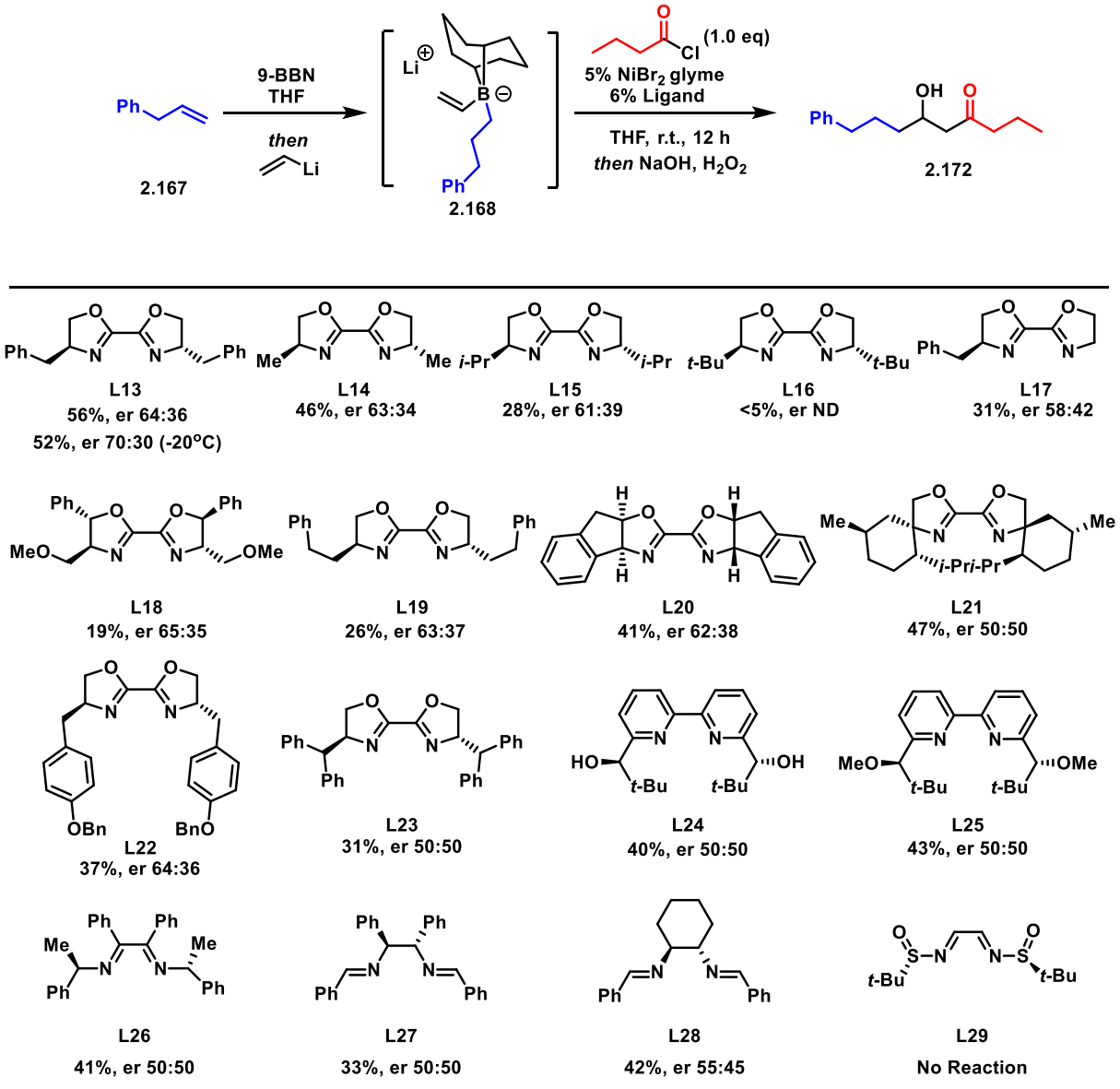

Scheme 2.45 Possible intermediates before stereodetermining 1,2-metallate shift

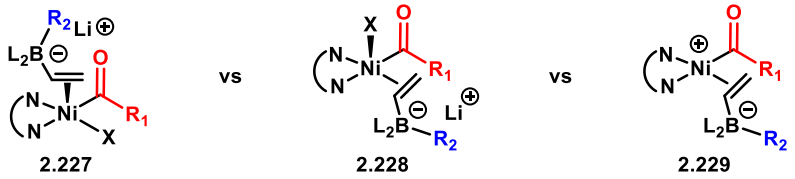

2.3.6.2 Chiral ligands on borane-induced enantioselectivity

An alternative option to obtain an enantiomerically enriched product is to use chiral borane species as substrates. Although the widely used chiral borane, Ipc-borane-derived 'ate' complex failed to produce high diastereoselectivity, TMS-10-BBD, a class of chiral borane developed by Soderquist, [44] was competent to provide products with 85:15 er as a preliminary result. The possible stereochemistry model is proposed (Scheme 2.47). Because of the stereospecific 1,2-antiperiplanar feature of the migration, one of the two possible transition states for Ni complex association was

Scheme 2.46 TMS-10-BBD borane enabled enantioselective conjunctive cross-couplings of acyl eletrophiles

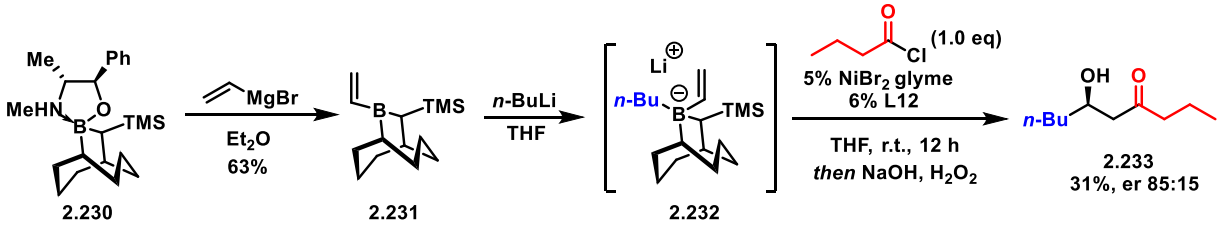

[44] C. H. Burgos, E. Canales, K. Matos, J. A. Soderquist, *J. Am. Chem. Soc.* **2005**, *127*, 8044

unfavored due to the steric clash between the big TMS group and the catalyst. Even though the selectivity of the reaction was far from excellent, it proved the concept that conjunctive cross-coupling of acyl electrophiles could be rendered in an enantioselective fashion. A better understanding of the mechanism and related intermediates would benefit the design of a catalytic enantioselective reaction.

Scheme 2.47 Stereochemical model of TMS-10-BBD borane involved conjunctive cross-coupling reaction

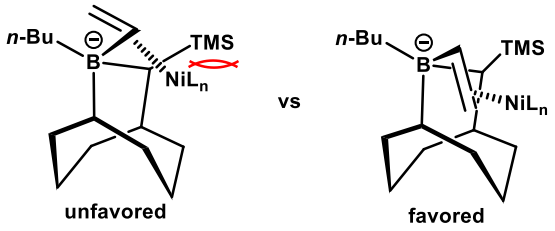

2.4 Conclusion

In summary, the electrophile scope of Ni-catalyzed conjunctive cross-coupling is expanded to carboxylic acid derivatives. An array of β-trialkyl boryl carbonyls were prepared from readily available alkenes in high efficiency. The products exhibit uncommon reactivity, which can be useful in synthetic chemistry. Preliminary results obtained from the development of an

enantioselective version of the reaction shed light on further investigation of the catalytic asymmetric synthesis of *β*-boryl carbonyls.

2.5 Experimental data

2.5.1 General Information

^{1}H NMR spectra were recorded on either a Varian Gemini-500 (500 MHz), Varian Gemini-600 (600 MHz), or Varian Inova-500 (500 MHz) spectrometer. Chemical shifts are reported in ppm with the solvent resonance as the internal standard ($CDCL_3$: 7.24 ppm). Data are reported as follows: chemical shift, integration, multiplicity (s = singlet, d = doublet, t = triplet, q = quartet, p = pentet, m = multiplet), and coupling constants (Hz). ^{13}C NMR spectra were recorded on either a Varian Gemini-500 (125 MHz), Varian Gemini-600 (150 MHz) or a Varian Inova-500 (125 MHz) spectrometer with complete proton decoupling. Chemical shifts are reported in ppm with the solvent resonance as the internal standard ($CDCL_3$: 77.2 ppm). Chemical shifts are reported in ppm using phosphoric acid as the external standard (H_3PO_4: 0.0 ppm). ^{11}B NMR spectra were recorded on a Varian Gemini-500 (128 MHz) spectrometer. ^{19}F NMR spectra were recorded on a Varian Gemini-500 (470 MHz) spectrometer. Infrared (IR) spectra were recorded on

a Bruker alpha-P Spectrometer. Frequencies are reported in wavenumbers (cm^{-1}) as follows: strong (s), broad (br), medium (m), and weak (w). Optical rotations were measured on a Rudolph Analytical Research Autopol IV Polarimeter. High-resolution mass spectrometry (DART+) was performed at the Mass Spectrometry Facility, Boston College, Chestnut Hill, MA. Liquid chromatography was performed using forced flow (flash chromatography) on silica gel (SiO_2, 230 x 450 Mesh) purchased from Silicycle. Thin-layer chromatography (TLC) was performed on 25 μm silica gel glass-backed plates from Silicycle. Visualization was performed using ultraviolet light (254 nm), ceric ammonium molybdate (CAM) in ethanol or phosphomolybdic acid, and cerium(IV) sulfate in ethanol with sulfuric acid (Seebach).

Analytical chiral supercritical fluid chromatography (SFC) was performed on a TharSFC Method Station II equipped with Waters 2998 Photodiode Array Detector with isopropanol as the modifier.

All reactions were conducted in the oven- or flame-dried glassware under an inert atmosphere of nitrogen or argon. Tetrahydrofuran (THF), diethyl ether (Et_2O), dichloromethane (DCM), and toluene were purified using Pure Solv MD-4 solvent purification system, from Innovative Technology, Inc., bypassing the solvent through two activated alumina

columns after purging with argon. Nickel(II) bromide-glyme was purchased from Sigma Aldrich, 9-Borabicyclo[3.3.1]nonane 0.5M solution in THF was purchased from Alfa Aesar (of note, cross-coupling reactions resulted in slightly diminished yields when a BBN solution from Sigma Aldrich was employed, or when borane reagents were prepared from BBN dimer). All other reagents were purchased from Sigma Aldrich, Alfa Aesar, Oakwood Chemicals, Combi-Blocks, or Acros Organics and used without further purification.

2.5.2 Experimental Procedures

2.5.2.1 Procedures for preparation of alkenyl substrates and acyl electrophiles

All alkenyl starting material and acyl electrophiles not mentioned below are commercially available and used as received.

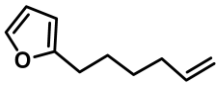 **2-(hex-5-enyl)furan (S-1).** The title compound was prepared according to the procedure reported in the literature.[45] All spectral data were

[45] S. Hobson, R. Marquez, *Org. Biomol. Chem.* **2006**, *4*, 3808.

in accordance with previously published results.

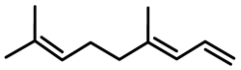 ***(E)*-4,8-dimethylnona-1,3,7-triene (S-2).** The title compound was synthesized in two steps starting with the oxidation of geraniol as reported by Stahl *et al.*[46] followed by Wittig olefination. The spectral data were in accordance with the literature.[47]

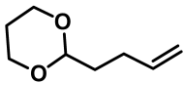 **2-(but-3-en-1-yl)-1,3-dioxane (S-3).** The title compound was synthesized from 4-pentenal according to the procedure reported by Karimi *et al*.[48] The spectral data were in accordance with the literature.

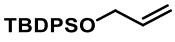 **(allyloxy)(tert-butyl)diphenylsilane (S-4).** The title compound was prepared according to the procedure reported in the literature. All spectral data were in accordance with previously published results.[49]

[46] J. Hoover, S. Stahl, *J. Am. Chem. Soc.* **2011**, *133*, 16901.
[47] H. Davies, Ø Loe, D. Stafford*, Org. Lett.* **2005**, *7*, 5561.
[48] H. Firouzabadi, N, Iranpoor, B. Karimi, *Synlett*. **1999**, 321.
[49] B. Lin, Y, Zhao, Y. Lai, T. Loh, *Angew. Chem. Int. Ed.* **2012**, *51*, 8041.

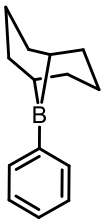

9-phenyl-9-borabicyclo[3.3.1]nonane (S-5). The title compound was prepared according to the procedure reported in the literature. All spectral data were in accordance with the literature.[50]

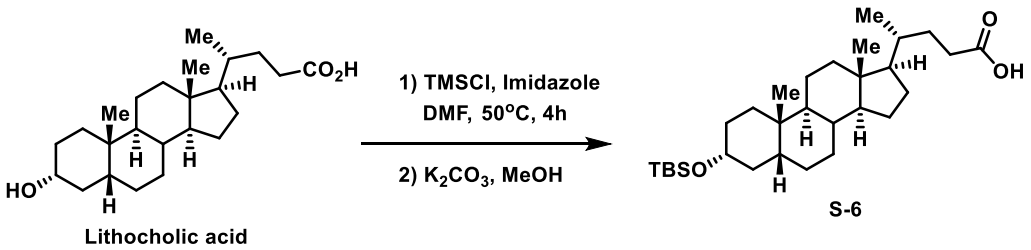

(4R)-4-((3R,5R,9S,10S,13R,14S,17R)-3-((tert-butyldimethylsilyl)oxy)-10,13 dimethylhexa-deca-hydro -1H-cyclopenta[a]phenanthren-17-yl)pentanoic acid (S-6). The title compound was prepared according to the procedure reported in the literature.[51] All spectral data were in accordance with the literature.

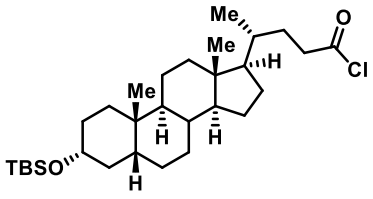

(4R)-4-((3R,5R,9S,10S,13R,14S,17R)-3-((tert-butyl dimethyl-silyl oxy)-10,13dimethylhexadecahydro 1H-

[50] G. Fang, O. Wallner, N. Di Blasio, X. Ginesta, J. Harvey, V. Aggarwal, *J. Am. Chem. Soc*. **2007**, *129*, 14632.
[51] C. Joe, A. Doyle, *Angew. Chem. Int. Ed.* **2016**, *55*, 4040.

cyclopenta[a]phenanthren-17-yl)pentanoyl chloride (S-7). To an oven-dried scintillation vial was added **S-6** (500 mg, 0.98 mmol). The vial was purged with nitrogen for 2 minutes. To it was added THF (1 mL) and Et_2O (1 mL). The reaction mixture was cooled to 0°C at which point oxalyl chloride (137 mg, 1.08 mmol) was added followed by 1 small drop of DMF. The reaction mixture was warmed up to room temperature and stirred overnight. The solvent was evaporated under vacuum to afford the product as a white solid (394 mg, 79%).

^{1}H NMR (400 MHz, CDCL3) δ 3.66-3.49 (m, 1H), 2.96-2.88 (m, 1H), 2.85-2.76 (m, 1H), 1.95-1.02 (m, 26H), 0.92 (s, 3 H), 0.91 (s, 3H), 0.89 (s, 9H), 0.63 (s, 3H), 0.06 (s, 6H). **^{13}C NMR** (150 MHz, CDCL3) δ 174.40, 72.96, 56.53, 55.95, 44.55, 42.93, 42.42, 40.34, 40.26, 37.07, 36.01,35.73, 35.12, 34.74, 31.23, 31.18, 28.33, 27.43, 26.53, 26.13, 24.32, 23.53, 20.94, 18.49, 18.37,12.17, -4.44. **IR** (neat) ν_{max} 2929.9 (s), 2862.9 (s), 1707.5 (s), 1446.9 (m), 1249.0 (m), 1092.5 (m), 869.5 (m), 853.5 (m), 774.4 (m). **HRMS** (DART) for $C_{30}H_{53}O_2Si$ $(M\text{-}Cl)^+$: Calc'd: 473.3815, found: 473.3753.

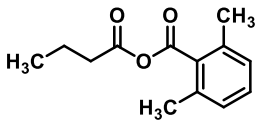

butyric 2,6-dimethylbenzoic anhydride (S-8). The title compound was prepared according to the procedure reported in literature.[7] All spectral data were in accordance with the literature.

2.5.2.2 General Procedure for Conjunctive Cross-Coupling

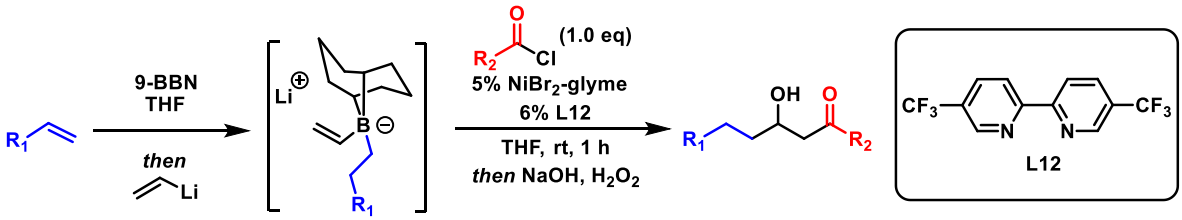

In a glove box, under argon, an oven-dried 2-dram vial equipped with a magnetic stir bar was charged with a solution of 9-BBN in THF (0.52 mL, 0.5 M, 0.26 mmol, 1.30 equiv.). The vial was cooled to 0 °C, and the olefin (0.26 mmol, 1.30 equiv.) was added. The reaction mixture was allowed to warm to room temperature and stir for 3 hours before being cooled back to 0 °C. A solution of vinyllithium (for the synthesis of halide free vinyllithium see ref) in THF (0.16 mL, 1.38 M, 0.22 mmol, 1.10 equiv.) was added to the reaction mixture which was then warmed to room temperature and stirred for

5 minutes. Meanwhile, a solution of $NiBr_2$-glyme (0.010 mmol, 0.050 equiv.) and **L3** (see ref[52] for its synthesis) (0.012 mmol, 0.060 equiv.) in THF (0.4 mL) was allowed to complex for 5 minutes under inert atmosphere. The catalyst solution was added to the boron 'ate' mixture at room temperature followed by addition of acyl chloride (0.20 mmol, 1.00 equiv.) The reaction vial was sealed with a septum cap, taken out of the glovebox and stirred at room temperature for 1h, after which point the reaction mixture was cooled to 0 °C and 30% H_2O_2 (0.5 mL) were added along with 3 M NaOH (0.5 mL). The reaction mixture was allowed to warm up to room temperature and stirred for 3 hours. Aq. saturated $Na_2S_2O_3$ (1 mL) solution was then added to quench the remaining H_2O_2. The aqueous phase was EtOAc (3 x 2 mL). The combined organic layers were dried over $MgSO_4$, filtered, concentrated under reduced pressure, and subsequently purified via silica gel column chromatography to provide the desired products.

Note: In all cases, a stock solution of 9-BBN derivatives could be prepared and stored in a freezer for as long as one month, before the addition of vinyllithium, without any diminishing yield.

[52] Y. Forst, S. Becker, P. Caubere, *Tetrahedron*, **1994**, *50*, 11893.

The procedure for conjunctive cross-coupling reaction utilizing anhydrides as electrophiles is identical to the one reported above except the commercially available 2,2'-bipyridine is used as the ligand.

2.5.3 Characterization of conjunctive cross-coupling products

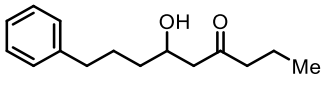

6-hydroxy-9-phenylnonan-4-one (2.172). The reaction was performed according to the general procedure with 9-BBN in THF (0.52 mL, 0.5 M, 0.26 mmol, 1.30 equiv.), allylbenzene (30.7 mg, 0.26 mmol, 1.30 equiv.), halide-free vinyllithium in THF (0.16 mL, 1.38 M, 0.22 mmol, 1.10 equiv.), a solution of $NiBr_2$-glyme (3.09 mg, 0.010 mmol, 0.050 equiv.) and **L3** (3.51 mg, 0.012 mmol, 0.060 equiv.) in THF (0.4 mL), butanoyl chloride (21.3 mg, 0.20 mmol, 1.00 equiv.). The crude mixture was purified by column chromatography (20% EtOAc in hexane, stain in $KMnO_4$) to afford the product as a colorless oil (37 mg, 79% yield).

^{1}H NMR (400 MHz, CDCL3) δ 7.31-7.25 (m, 2H), 7.23-7.14 (m, 3H), 4.11-4.02 (m, 1H), 3.06 (d, *J* = 3.4 Hz, 1H), 2.68-2.54 (m, 3H), 2.48 (dd, *J* = 17.6, 9.1 Hz, 1H), 2.39 (t, *J* = 7.3 Hz, 2H), 1.87-1.74 (m, 1H), 1.73-1.48 (m, 4H),

1.46-1.36 (m, 1H), 0.91 (t, J = 7.4 Hz, 3H).**^{13}C NMR** (150 MHz, CDCL3) δ 212.5, 142.4, 128.5, 128.4, 125.9, 67.6, 49.0, 45.6, 36.1, 35.8, 27.4, 17.2, 13.8. **IR** (neat) ν_{max} 3397.7 (br, s), 2931.6 (s), 1706.5 (s), 1603.4 (w), 1495.9 (w), 1407.5 (m), 1375.4 (m), 1096.3 (m), 750.4 (s), 700.6 (s) cm^{-1}. **HRMS** (DART) for $C_{15}H_{23}O_2$ $[M+H]^+$: Calc'd: 235.1691, found: 235.1693.

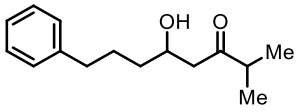

5-hydroxy-2-methyl-8-phenyloctan-3-one (2.174).

The reaction was performed according to the general procedure with 9-BBN in THF (0.52 mL, 0.5 M, 0.26 mmol, 1.30 equiv.), allylbenzene (30.7 mg, 0.26 mmol, 1.30 equiv.), halide-free vinyllithium in THF (0.16 mL, 1.38 M, 0.22 mmol, 1.10 equiv.), a solution of $NiBr_2$-glyme (3.09 mg, 0.010 mmol, 0.050 equiv.) and **L3** (3.51 mg, 0.012 mmol, 0.060 equiv.) in THF (0.4 mL), isobutyryl chloride (21.3 mg, 0.20 mmol, 1.00 equiv.). The crude mixture was purified by column chromatography (20% EtOAc in hexane, stain in $KMnO_4$) to afford the product as a colorless oil (33.7 mg, 72% yield).

^{1}H NMR (500 MHz, CDCL3) δ 7.30-7.25 (m, 2H), 7.20-7.15 (m, 3H), 4.10-3.99 (m, 1H), 3.28-3.01 (br s, 1H). 2.71-2.46 (m, 5H), 1.88-1.73 (m, 1H),

1.72-1.62 (m, 1H), 1.59-1.50 (m, 1H), 1.48-1.38 (m, 1H), 1.10 (d, J = 6.9 Hz, 6H). **^{13}C NMR** (126 MHz, CDCL3) δ 216.4, 142.4, 128.5, 128.4, 125.9, 67.6, 46.6, 41.6, 36.1, 35.9, 27.4, 18.2, 18.1. **IR** (neat) 3479.2 (br, m), 2968.7 (m), 2931.8 (s), 1705.7 (s), 1603.2 (w), 1496.0 (m), 1093.6 (m), 1043.0 (w), 750.64 (m), 700.56 (m) cm^{-1}. **HRMS** (DART) for $C_{15}H_{23}O_2$ $[M+H]^+$: Calc'd: 235.1693, found: 235.1703.

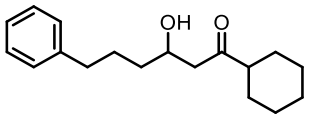

1-cyclohexyl-3-hydroxy-6-phenylhexan-1-one (2.175). The reaction was performed according to the general procedure with 9-BBN in THF (0.52 mL, 0.5 M, 0.26 mmol, 1.30 equiv.), allylbenzene (30.7 mg, 0.26 mmol, 1.30 equiv.), halide-free vinyllithium in THF (0.16 mL, 1.38 M, 0.22 mmol, 1.10 equiv.), a solution of $NiBr_2$-glyme (3.09 mg, 0.010 mmol, 0.050 equiv.) and **L3** (3.51 mg, 0.012 mmol, 0.060 equiv.) in THF (0.4 mL), cyclohexanecarbonyl chloride (29.3 mg, 0.20 mmol, 1.00 equiv.). The crude mixture was purified by column chromatography (20% EtOAc in hexane, stain in $KMnO_4$) to afford the product as a colorless oil (43.9 mg, 80% yield).

^{1}H NMR (500 MHz, CDCL3) δ 7.37-7.33 (m, 2H), 7.28-7.22 (m, 3H), 4.17-

4.04 (m, 1H), 3.26 (d, J = 3.2 Hz, 1H), 2.74-2.66 (m, 3H), 2.57 (dd, J = 17.7, 9.2 Hz, 1H), 2.42-2.34 (m, 1H), 1.96-1.82 (m, 5H), 1.78-1.69 (m, 2H), 1.65-1.57 (m, 1H), 1.55-1.46 (m, 1H), 1.44-1.22 (m, 5H). **^{13}C NMR** (150 MHz, CDCL3) δ 215.8, 142.4, 128.6, 128.3, 125.8, 67.6, 51.5, 46.8, 36.0, 35.8, 28.4, 27.4, 25.9, 25.7. **IR** (neat) ν_{max} 3457.1 (m), 2924.5 (m), 1670.2 (s), 1602.0 (s), 1221.6 (m), 1022.6 (m), 969.3 (m), 827.4 (s), 613.0 (w), 580.1 (w) cm^{-1}. **HRMS** (DART) for $C_{18}H_{27}O_2$ $[M+H]^+$: Calc'd: 275.2006, found: 275.1996.

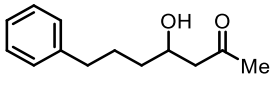

4-hydroxy-7-phenylheptan-2-one (2.173). The reaction was performed according to the general procedure with 9-BBN in THF (0.52 mL, 0.5 M, 0.26 mmol, 1.30 equiv.), allylbenzene (30.7 mg, 0.26 mmol, 1.30 equiv.), halide-free vinyllithium in THF (0.16 mL, 1.38 M, 0.22 mmol, 1.10 equiv.), a solution of $NiBr_2$-glyme (3.09 mg, 0.010 mmol, 0.050 equiv.) and **L3** (3.51 mg, 0.012 mmol, 0.060 equiv.) in THF (0.4 mL), acetyl chloride (15.7 mg, 0.20 mmol, 1.00 equiv.). The crude mixture was purified by column chromatography (20% EtOAc in hexane, stain in $KMnO_4$) to afford the product as a colorless oil (37 mg, 76% yield).

^{1}H NMR (600 MHz, CDCL3) δ 7.28-7.24 (m, 2H), 7.20-7.14 (m, 3H), 4.08-

4.00 (m, 1H), 3.02-2.94 (s, 1H), 2.66-2.57 (m, 3H), 2.51 (dd, J = 17.8, 9.2 Hz, 1H), 2.15 (s, 3H), 1.83-1.74 (m, 1H), 1.70-1.60 (m, 1H), 1.56-1.49 (m, 1H), 1.45-1.38 (m, 1H). **^{13}C NMR** (126 MHz, CDCL3) δ 210.1, 142.3, 129.5, 128.4, 125.9, 67.4, 50.0, 35.9, 35.8, 30.8, 27.3. **IR** (neat) ν_{max} 3456.6 (m), 2923.3 (m), 1667.7 (s), 1596.0 (s), 1459.1 (m), 1261.6 (m), 987.8 (m), 826.3 (m), 746.4 (m), 700.5 (m), 580.1 (s), 552.2 (m). **HRMS** (DART) for $C_{13}H_{19}O_2$ $(M+H)^+$: Calc'd: 207.1380, found: 207.1370.

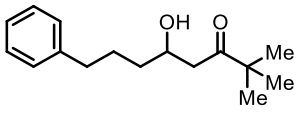

5-hydroxy-2,2-dimethyl-8-phenyloctan-3-one (2.176).

The reaction was performed according to the general procedure with 9-BBN in THF (0.52 mL, 0.5 M, 0.26 mmol, 1.30 equiv.), allylbenzene (30.7 mg, 0.26 mmol, 1.30 equiv.), halide-free vinyllithium in THF (0.16 mL, 1.38 M, 0.22 mmol, 1.10 equiv.), a solution of $NiBr_2$-glyme (2.20 mg, 0.010 mmol, 0.050 equiv.) and **L3** (3.51 mg, 0.012 mmol, 0.060 equiv.) in THF (0.4 mL), pivaloyl chloride (24.1 mg, 0.20 mmol, 1.00 equiv.). The crude mixture was purified by column chromatography (20% EtOAc in hexane, stain in $KMnO_4$) to afford the product as a colorless oil (15.9 mg, 32% yield).

^{1}H NMR (600 MHz, CDCL3) δ 7.28 (m, 2H), 7.18 (m, 3H), 4.02 (m, 1H), 3.27 (d, *J* = 3.1 Hz, 1H), 2.67 (dd, *J* = 17.8, 2.5 Hz, 1H), 2.64 (t, *J* = 7.6 Hz, 2H), 2.53 (dd, *J* = 17.8, 9.2 Hz, 1H), 1.81 (m, 1H), 1.69 (m, 1H), 1.56 (m, 1H), 1.45 (m, 1H), 1.13 (s, 9H). **^{13}C NMR** (151 MHz, CDCL3) δ 217.9, 142.4, 128.5, 128.4, 128.4, 128.4, 125.8, 67.7, 44.5, 43.1, 43.1, 36.0, 35.9, 27.4, 26.4, 26.4, 26.3. **IR** (neat) ν_{max} 3453.9 (br, w), 3026.0 (w), 2929.3 (m), 2860.8 (m), 1698.3 (s), 1603.3 (w), 1496.0 (m), 1477.9 (m), 1453.3 (m), 1394.1 (w), 1365.6 (m), 1066.6 (m), 1030.1 (w), 1007.5 (w), 843.7 (w), 748.4 (s), 698.7 (s), 578.2 (w), 536.9 (w) cm^{-1}. **HRMS** (DART) for $C_{16}H_{25}O_2$ $[M+H]^+$: Calc'd: 249.1849, found: 249.1840.

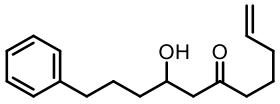

8-hydroxy-11-phenylundec-1-en-6-one (2.177). The reaction was performed according to the general procedure with 9-BBN in THF (0.52 mL, 0.5 M, 0.26 mmol, 1.30 equiv.), allylbenzene (30.7 mg, 0.26 mmol, 1.30 equiv.), halide-free vinyllithium in THF (0.16 mL, 1.38 M, 0.22 mmol, 1.10 equiv.), a solution of $NiBr_2$-glyme (3.09 mg, 0.010 mmol, 0.050 equiv.) and **L3** (3.51 mg, 0.012 mmol, 0.060 equiv.) in THF (0.4 mL), hex-5-enoyl chloride (26.5 mg, 0.20 mmol, 1.00 equiv.). The crude mixture was purified by column chromatography (20% EtOAc in hexane, stain in $KMnO_4$)

to afford the product as a colorless oil (42.2 mg, 81% yield).

^{1}H NMR (500 MHz, CDCL3) δ 7.29-7.24 (m, 2H), 7.19-7.15 (m, 3H), 5.74 (ddt, *J* = 16.9, 10.2, 6.7 Hz, 1H), 5.03-4.95 (m, 2H), 4.11-4.01 (m, 1H), 3.09 (br s, 1H), 2.63 (t, *J* = 7.7,Hz, 2H), 2.55 (dd, *J* = 17.5, 2.8 Hz, 1H), 2.48 (dd, *J* = 17.5, 9.1 Hz, 1H), 2.41 (t, *J* = 7.4 Hz, 2H), 2.04 (q, *J* = 7.1 Hz, 2H), 1.83-1.75 (m, 1H), 1.71-1.62 (m, 3H), 1.57-1.49 (m, 1H), 1.46-1.38 (m, 1H). **^{13}C NMR** (150 MHz, CDCL3) δ 212.2, 142.3, 137.8, 128.4, 128.4, 125.8, 115.4, 67.5, 49.1, 42.8, 36.0, 35.8, 33.0, 27.3, 22.6. **IR** (neat) ν_{max} 3448.8 (br, m), 2933.1 (m), 1705.0 (m), 1640.4 (w), 1407.9 (m), 1275.6 (w), 1097.4 (m), 912.0 (m), 749.7 (s), 699.5 (s) cm^{-1}. **HRMS** (DART) for $C_{17}H_{25}O_2$ $[M+H]^+$: Calc'd: 261.1849, found: 261.1853.

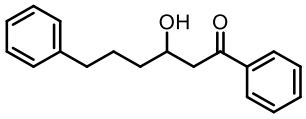

3-hydroxy-1,6-diphenylhexan-1-one (2.179). The reaction was performed according to the general procedure with 9-BBN in THF (0.52 mL, 0.5 M, 0.26 mmol, 1.30 equiv.), allylbenzene (30.7 mg, 0.26 mmol, 1.30 equiv.), halide-free vinyllithium in THF (0.16 mL, 1.38 M, 0.22 mmol, 1.10 equiv.), a solution of $NiBr_2$-glyme (3.09 mg, 0.010 mmol, 0.050

equiv.) and **L3** (3.51 mg, 0.012 mmol, 0.060 equiv.) in THF (0.4 mL), benzoyl chloride (28.1 mg, 0.20 mmol, 1.00 equiv.). The crude mixture was purified by column chromatography (20% EtOAc in hexane, stain in $KMnO_4$) to afford the product as a colorless oil (40.3 mg, 75% yield).

^{1}H NMR (500 MHz, CDCL3) δ 7.95 (d, *J* = 7.4 Hz, 2H), 7.59 (t, *J* = 7.4 Hz, 1H), 7.47 (t, *J* = 7.7 Hz, 2H), 7.29 (t, *J* = 7.4 Hz, 2H), 7.24-7.16 (m, 3H), 4.30-4.19 (m, 1H), 3.28 (d, *J* = 3.3 Hz, 1H), 3.15 (dd, *J* = 17.7, 2.6 Hz, 1H), 3.04 (dd, *J* = 17.9, 9.1 Hz, 1H), 2.68 (t, *J* = 7.6 Hz, 1H), 1.94-1.83 (m, 1H), 1.80-1.71 (m, 1H), 1.71-1.63 (m, 1H), 1.61-1.52 (m, 1H). **^{13}C NMR** (150 MHz, CDCL3) δ 201.0, 142.4, 136.8, 133.6, 128.8, 128.5, 128.4, 128.1, 125.8, 67.7, 45.1, 36.1, 35.9, 27.5. **IR** (neat) ν_{max} 3481.1 (m), 2931.4 (w), 2901.1 (w), 1676.1 (s), 1595.3 (w), 1219.1 (w), 1098.0 (m), 748.7 (m), 698.6 (m), 686.4 (s), 583.2 (m) cm^{-1}. **HRMS** (DART) for $C_{18}H_{21}O_2$ $[M+H]^+$: Calc'd: 269.1536, found: 269.1545.

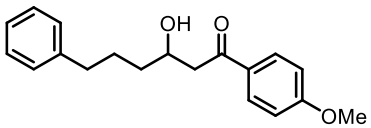

3-hydroxy-1-(4-methoxyphenyl)-6-phenylhexan-1-one (2.180). The reaction was performed according to the general procedure

with 9-BBN in THF (0.52 mL, 0.5 M, 0.26 mmol, 1.30 equiv.), allylbenzene (30.7 mg, 0.26 mmol, 1.30 equiv.), halide-free vinyllithium in THF (0.16 mL, 1.38 M, 0.22 mmol, 1.10 equiv.), a solution of $NiBr_2$-glyme (3.09 mg, 0.010 mmol, 0.050 equiv.) and **L3** (3.51 mg, 0.012 mmol, 0.060 equiv.) in THF (0.4 mL), 4-methoxybenzoyl chloride (34.1 mg, 0.20 mmol, 1.00 equiv.). The crude mixture was purified by column chromatography (20% EtOAc in hexane, stain in $KMnO_4$) to afford the product as a white solid (44.1 mg, 74% yield).

^{1}H NMR (400 MHz, CDCL3) 7.92 (d, *J* = 8.9 Hz, 2H), 7.33-7.24 (m, 2H), 7.21-7.13 (m, 3H), 6.92 (d, *J* = 8.9 Hz, 2H), 4.30-4.10 (m, 1H), 3.86 (s, 3H), 3.41 (br s, 1H), 3.10 (dd, *J* = 17.5, 2.5 Hz, 1H), 2.95 (dd, *J* = 17.5, 9.1 Hz 1H), 2.67 (t, *J* = 7.5 Hz, 2H), 1.93-1.81 (m, 1H), 1.80-1.59 (m, 2H), 1.58-1.46 (m, 1H). **^{13}C NMR** (150 MHz, CDCL3) δ 199.6, 163.9, 142.4, 130.5, 129.9, 128.5, 128.4, 125.8, 113.9, 67.8, 55.6, 44.6, 36.1, 35.9, 27.5. **IR** (neat) ν_{max} 3483.6 (br, s), 2926.0 (s), 1709.6 (s), 1603.0 (w), 1496.0 (w), 1168.3 (m), 1093.8 (m), 751.1 (m), 701.5 cm^{-1}. **HRMS** (DART) for $C_{19}H_{23}O_3$ $[M+H]^+$: Calc'd: 299.1642, found: 299.1649.

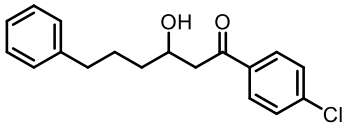

1-(4-chlorophenyl)-3-hydroxy-6-phenylhexan-1-one (2.182). The reaction was performed according to the general procedure with 9-BBN in THF (0.52 mL, 0.5 M, 0.26 mmol, 1.30 equiv.), allylbenzene (30.7 mg, 0.26 mmol, 1.30 equiv.), halide-free vinyllithium in THF (0.16 mL, 1.38 M, 0.22 mmol, 1.10 equiv.), a solution of $NiBr_2$-glyme (3.09 mg, 0.010 mmol, 0.050 equiv.) and **L3** (3.51 mg, 0.012 mmol, 0.060 equiv.) in THF (0.4 mL), 4-chlorobenzoyl chloride (35.0 mg, 0.20 mmol, 1.00 equiv.). The crude mixture was purified by column chromatography (20% EtOAc in hexane, stain in $KMnO_4$) to afford the product as a colorless oil (40.6 mg, 67% yield).

^{1}H NMR (600 MHz, CDCL3) δ 7.87 (d, *J* = 8.3 Hz, 2H), 7.44 (d, *J* = 8.0 Hz, 2H), 7.28 (t, 2H, *J* = 7.5 Hz, 2H), 7.22-7.16 (m, 3H), 4.28-4.19 (m, 1H), 3.17 (d, *J* = 3.4 Hz, 1H), 3.08 (dd, *J* = 17.7, 2.7 Hz, 1H), 3.01 (dd, *J* = 17.7, 9.1 Hz, 1H), 2.67 (t, *J* = 7.6 Hz, 2H), 1.92-1.84 (m, 1H), 1.78-1.70 (m, 1H), 1.68-1.62 (m, 1H), 1.58-1.51 (m, 1H). **^{13}C NMR** (150 MHz, CDCL3) δ 199.6, 142.3, 140.1, 135.1, 129.6, 129.1, 128.5, 128.4, 125.9, 67.6, 45.2, 36.1, 35.8, 27.4. **IR** (neat) ν_{max} 3483.6 (br, s), 2931.8 (w), 2901.4 (w), 1675.4 (s), 1587.7 (w), 1494.0 (m), 1399.8 (m), 1091.8 (s), 1039.2 (m), 986.0 (m), 831.8 (m), 816.9

(s), 733.4 (s), 534.3 (s) cm^{-1}. **HRMS** (DART) for $C_{18}H_{21}O_2Cl$ $[M+H]^+$: Calc'd: 303.1146, found: 303.1143.

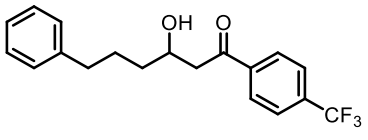

3-hydroxy-6-phenyl-1-(4-(trifluoromethyl)-phenyl) hexan-1-one (2.183). The reaction was performed according to the general procedure with 9-BBN in THF (0.52 mL, 0.5 M, 0.26 mmol, 1.30 equiv.), allylbenzene (30.7 mg, 0.26 mmol, 1.30 equiv.), halide-free vinyllithium in THF (0.16 mL, 1.38 M, 0.22 mmol, 1.10 equiv.), a solution of $NiBr_2$-glyme (3.09 mg, 0.010 mmol, 0.050 equiv.) and **L3** (3.51 mg, 0.012 mmol, 0.060 equiv.) in THF (0.4 mL), 4-(trifluoromethyl)benzoyl chloride (41.7 mg, 0.20 mmol, 1.00 equiv.). The crude mixture was purified by column chromatography (20% EtOAc in hexane, stain in $KMnO_4$) to afford the product as a white solid (30.0 mg, 44% yield).

^{1}H NMR (600 MHz, CDCL3) δ 8.04 (d, *J* = 7.6 Hz, 2H), 7.74 (d, *J* = 8.0 Hz, 2H), 7.29 (t, *J* = 8.0 Hz, 2H), 7.21-7.16 (m, 3H), 4.34-4.22 (m, 1H), 3.14 (dd, *J* = 17.7, 2.9 Hz, 1H), 3.08 (dd, *J* = 17.7, 8.7 Hz, 1H), 3.02 (s, 1H), 2.68 (t, *J* = 7.6 Hz, 2H), 1.93-1.84 (m, 1H), 1.79-1.71 (m, 1H), 1.70-1.63 (m, 1H), 1.60-

1.52 (m, 1H). **^{13}C NMR** (126 MHz, CDCL3) δ 199.8, 142.3, 139.5, 128.5, 128.5, 128.5, 125.9, 125.9, 125.9, 125.8, 67.6, 45.6, 36.1, 35.8, 27.4. **IR** (neat) ν_{max} 3484.8 (s), 2930.9 (w), 2900.1 (w), 1681.9 (s), 1578.8 (w), 1508.7 (m), 1326.7 (s), 1168.7 (m), 891.6 (m), 843.7 (m), 702.5 (w), 605.8 (w) cm^{-1}. **HRMS** (DART) for $C_{19}H_{20}O_2F_3$ $[M+H]^+$: Calc'd: 337.1410, found: 337.1396.

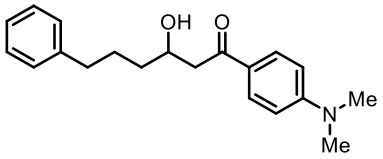

1-(4-(dimethylamino)phenyl)-3-hydroxy-6-phenyl-hexan-1-one (2.181). The reaction was performed according to the general procedure with 9-BBN in THF (0.52 mL, 0.5 M, 0.26 mmol, 1.30 equiv.), allylbenzene (30.7 mg, 0.26 mmol, 1.30 equiv.), halide-free vinyllithium in THF (0.16 mL, 1.38 M, 0.22 mmol, 1.10 equiv.), a solution of $NiBr_2$-glyme (3.09 mg, 0.010 mmol, 0.050 equiv.) and **L3** (3.51 mg, 0.012 mmol, 0.060 equiv.) in THF (0.4 mL), 4-(dimethylamino)benzoyl chloride (36.7 mg, 0.20 mmol, 1.00 equiv.). The crude mixture was purified by column chromatography (20% EtOAc in hexane, stain in $KMnO_4$) to afford the product as a colorless oil (48.0 mg, 77% yield).

^{1}H NMR (500 MHz, CDCL3) δ 7.85 (d, *J* = 9.1 Hz, 2H), 7.34-7.26 (m, 2H),

7.22-7.13 (m, 3H), 6.64 (d, J = 9.1 Hz, 2H), 4.24-4.16 (m, 1H), 3.73 (s, 1H), 3.10 (dd, J = 17.3, 2.4 Hz, 1H), 3.06 (s, 6H), 2.88 (dd, J = 17.3, 9.3 Hz, 1H), 2.67 (t, J = 7.6 Hz, 2H), 1.93-1.83 (m, 1H), 1.79-1.70 (m, 1H), 1.69-1.61 (m, 1H), 1.58-1.50 (m, 1H). **^{13}C NMR** (150 MHz, CDCL3) δ 199.1, 153.0, 142.4, 130.5, 128.6, 128.3, 125.7, 124.8, 110.7, 68.1, 43.8, 40.1, 36.2, 35.9, 27.5. **IR** (neat) ν_{max} 3467.7 (br, w), 2926.1 (w), 1650.0 (w), 1594.59 (s), 1529.7 (w), 1371.4 (m), 1185.7 (m), 1169.2 (m), 818.5 (w), 749.9 (m), 700.1 (w), 578.8 (w). **HRMS** (DART) for $C_{20}H_{26}NO_2$ $[M+H]^+$: Calc'd: 312.1952, found: 312.1958.

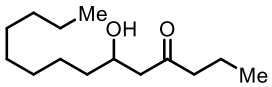

6-hydroxytetradecan-4-one (2.184). The reaction was performed according to the general procedure with 9-BBN in THF (0.52 mL, 0.5 M, 0.26 mmol, 1.30 equiv.), 1-octene (mg, 0.26 mmol, 1.30 equiv.), halide-free vinyllithium in THF (0.16 mL, 1.38 M, 0.22 mmol, 1.10 equiv.), a solution of $NiBr_2$-glyme (3.09 mg, 0.010 mmol, 0.050 equiv.) and **L3** (3.51 mg, 0.012 mmol, 0.060 equiv.) in THF (0.4 mL), butanoyl chloride (21.3 mg, 0.20 mmol, 1.00 equiv.). The crude mixture was purified by column chromatography (20% EtOAc in hexane, stain in $KMnO_4$) to afford the product as a colorless oil (33.3 mg, 73% yield).

^{1}H NMR (500 MHz, CDCL3) δ 4.05-3.97 (m, 1H), 3.06 (br s, 1H), 2.57 (dd, *J* = 17.5, 2.8 Hz, 1H), 2.47 (dd, 1H), 2.39 (t, *J* = 7.3 Hz, 2H), 1.59 (h, *J* = 7.3 Hz, 2H), 1.52-1.17 (m, 14H), 0.90 (t, *J* = 7.4 Hz, 3H), 0.86 (t, *J* = 6.8 Hz, 3H). **^{13}C NMR** (150 MHz, CDCL3) δ 212.5, 67.7, 49.1, 45.7, 36.6, 31.9, 29.6, 29.6, 29.3, 25.6, 22.7, 17.2, 14.2, 13.7. **IR** (neat) ν_{max} 3243.6 (br, m), 2957.26 (m), 2916.29 (s), 2848.0 (m), 1701.1 (s), 1464.7 (m), 1385.7 (m), 1132.3 (m), 1094.1 (m), 1026.7 (m), 889.0 (m), 724.2 (m), 627.5 (m). **HRMS** (DART) for $C_{14}H_{29}O_2$ $[M+H]^+$: Calc'd: 229.2162, found: 229.2172.

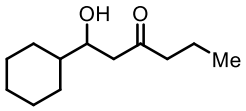

1-cyclohexyl-1-hydroxyhexan-3-one (2.186). The reaction was performed according to the general procedure with 9-BBN in THF (0.52 mL, 0.5 M, 0.26 mmol, 1.30 equiv.), cyclohexene (21.4 mg, 0.26 mmol, 1.30 equiv.), halide-free vinyllithium in THF (0.16 mL, 1.38 M, 0.22 mmol, 1.10 equiv.), a solution of $NiBr_2$-glyme (3.09 mg, 0.010 mmol, 0.050 equiv.) and **L3** (3.51 mg, 0.012 mmol, 0.060 equiv.) in THF (0.4 mL), butanoyl chloride (21.3 mg, 0.20 mmol, 1.00 equiv.). The crude mixture was purified by column chromatography (20% EtOAc in hexane, stain in $KMnO_4$) to afford the

product as a colorless oil (26.2 mg, 66% yield).

^{1}H NMR (600 MHz, CDCL3) δ 3.79 (m, 1H), 2.97 (s, 1H), 2.58 (dd, *J* = 17.3, 2.4 Hz, 1H), 2.49 (dd, *J* = 17.3, 9.6 Hz, 1H), 2.41 (t, *J* = 7.3 Hz, 2H), 1.85-1.80 (m, 1H), 1.77-1.70 (m, 2H), 1.67-1.56 (m, 4H), 1.36-1.30 (m, 1H), 1.26-1.09 (m, 3H), 1.06-0.95 (m, 2H), 0.91 (t, *J* = 7.4 Hz, 3H). **^{13}C NMR** (151 MHz, CDCL3) δ 212.9, 71.8, 46.2, 45.7, 43.1, 28.9, 28.4, 26.5, 26.3, 26.2, 17.2, 13.8. **IR** (neat) ν_{max} 3448.47 (br, w), 2922.89 (s), 2851.52 (s), 1703.34 (s), 1449.53 (m), 1406.80 (m), 1370.87 (m), 1308.33 (m), 1274.22 (m), 1126.81 (m), 1107.68 (m), 1064.88 (m), 1027.24 (m), 988.76 (m), 956.59 (w), 892.38 (w), 531.90 (w) cm^{-1}. **HRMS** (DART) for $C_{12}H_{23}O_2$ $[M+H]^+$: Calc'd: 199.1693, found: 199.1688.

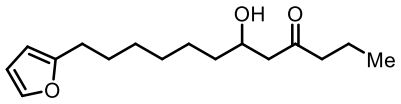

12-(furan-2-yl)-6-hydroxydodecan-4-one (2.189). The reaction was performed according to the general procedure with 9-BBN in THF (0.52 mL, 0.5 M, 0.26 mmol, 1.30 equiv.), **S-1** (39.0 mg, 0.26 mmol, 1.30 equiv.), halide-free vinyllithium in THF (0.16 mL, 1.38 M, 0.22 mmol, 1.10 equiv.), a solution of $NiBr_2$-glyme (3.09 mg, 0.010 mmol, 0.050

equiv.) and **L3** (3.51 mg, 0.012 mmol, 0.060 equiv.) in THF (0.4 mL), butanoyl chloride (21.3 mg, 0.20 mmol, 1.00 equiv.). The crude mixture was purified by column chromatography (20% EtOAc in hexane, stain in $KMnO_4$) to afford the product as a colorless oil (32.5 mg, 61% yield).

^{1}H NMR (500 MHz, CDCL3) δ 7.96 (d, J = 8.0 Hz, 2H), 7.59 (t, J = 7.4 Hz, 1H), 7.47 (t, *J* = 7.8 Hz, 2H), 7.29 (s, 1H), 6.29 – 6.24 (m, 1H), 5.97 (d, *J* = 3.1 Hz, 1H), 4.22 (m, 1H), 3.24 (d, *J* = 3.2 Hz, 1H), 3.17 (dd, *J* = 17.6, 2.6 Hz, 1H), 3.04 (dd, *J* = 17.6, 9.0 Hz, 1H), 2.62 (t, *J* = 7.6 Hz, 2H), 1.69-1.58 (m, 3H), 1.56-1.47 (m, 2H), 1.46-1.31 (m, 5H). **^{13}C NMR** (126 MHz, CDCL3) δ 201.1, 156.6, 140.7, 136.9, 133.6, 128.8, 128.2, 110.1, 104.7, 67.8, 45.1, 36.6, 29.4, 29.2, 28.1, 28.0, 25.6. **IR** (neat) ν_{max} 3454.2 (br, w), 2928.7 (m), 2855.9 (w), 1676.5 (s), 1596.8 (m), 1580.4 (w), 1507.0 (w), 1448.5 (m), 1282.8 (w), 1209.9 (s), 1180.0 (w), 1146.2 (m), 1072.1 (w), 1002.5 (s), 922.2 (w), 884.2 (w), 797.0 (w), 752.4 (s), 727.1 (s), 688.8 (s), 662.1 (w), 599.3 (s), 586.6 (m), 536.1 (w) cm^{-1}. **HRMS** (DART) for $C_{19}H_{25}O_3$ $[M+H]^+$: Calc'd: 301.1798, found: 301.1796.

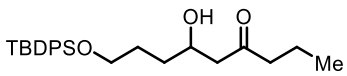

9-((tert-butyldiphenylsilyl)oxy)-6-hydroxynonan-

4-one (2.188). The reaction was performed according to the general procedure with 9-BBN in THF (0.52 mL, 0.5 M, 0.26 mmol, 1.30 equiv.), **S-4** (77.1 mg, 0.26 mmol, 1.30 equiv.), halide-free vinyllithium in THF (0.16 mL, 1.38 M, 0.22 mmol, 1.10 equiv.), a solution of $NiBr_2$-glyme (2.20 mg, 0.010 mmol, 0.050 equiv.) and **L3** (3.51 mg, 0.012 mmol, 0.060 equiv.) in THF (0.4 mL), butanoyl chloride (21.3 mg, 0.20 mmol, 1.00 equiv.). The crude mixture was purified by column chromatography (20% EtOAc in hexane, stain in $KMnO_4$) to afford the product as a colorless oil (59.4 mg, 72% yield).

^{1}H NMR (400 MHz, CDCL3) δ 7.70-7.64 (m, 4H), 7.46-7.34 (m, 6H), 4.11-4.01 (m, 1H), 3.69 (t, *J* = 5.4 Hz, 1H), 3.24 (d, *J* = 3.2 Hz, 1H), 2.60-2.46 (m, 2H), 2.41 (t, *J* = 7.3 Hz, 2H), 1.84-1.51 (m, 6H), 1.05 (s, 9H), 0.92 (t, *J* = 7.4 Hz, 3H). **^{13}CNMR** (126 MHz, CDCL3) δ 212.3, 135.7, 135.7, 129.7, 127.7, 67.6, 64.0, 49.2, 45.7, 33.3, 28.7, 27.0, 19.3, 17.2, 13.8. **IR** (neat) ν_{max} 3398.7 (br, s), 2938.1 (s), 2857.0 (s), 1705.4 (s), 1471.7 (w), 1427.8 (m), 1112.2 (s), 741.2 (m), 704.6 (s), 614.8 (m) cm^{-1}. **HRMS** (DART) for $C_{25}H_{37}O_3Si$ $[M+H]^+$: Calc'd: 413.2507, found: 413.2505.

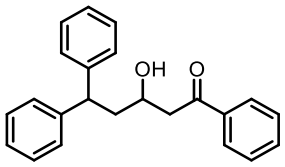

3-hydroxy-1,5,5-triphenylpentan-1-one (2.187). The reaction was performed according to the general procedure with 9-BBN in THF (0.52 mL, 0.5 M, 0.26 mmol, 1.30 equiv.), 1,1-diphenylethylene (46.9 mg, 0.26 mmol, 1.30 equiv.), halide-free vinyllithium in THF (0.16 mL, 1.38 M, 0.22 mmol, 1.10 equiv.), a solution of $NiBr_2$-glyme (3.09 mg, 0.010 mmol, 0.050 equiv.) and **L3** (3.51 mg, 0.012 mmol, 0.060 equiv.) in THF (0.4 mL), benzoyl chloride (28.1 mg, 0.20 mmol, 1.00 equiv.). The crude mixture was purified by column chromatography (20% EtOAc in hexane, stain in $KMnO_4$) to afford the product as a colorless oil (53.5 mg, 66% yield).

^{1}H NMR (500 MHz, CDCL3) δ 7.90 (d, *J* = 7.1 Hz, 2H), 7.58 (t, *J* = 7.2 Hz, 1H), 7.46 (t, *J* = 8.0 Hz, 2H), 7.28-7.33 (m, 7H), 7.22-7.14 (m, 2H), 4.37 (dd, *J* = 10.4, 5.3 Hz, 1H), 4.06-4.13 (m, 1H), 3.29 (d, *J* = 3.0 Hz, 1H), 3.15 (dd, *J* = 17.7, 3.0 Hz, 1H), 3.09 (dd, *J* = 17.9, 8.6 Hz, 1H), 2.37-2.30 (m, 1H), 2.29-2.22 (m, 1H). **^{13}C NMR** (151 MHz, CDCL3) δ 200.7, 145.2, 144.0, 136.8, 133.6, 128.7, 128.7, 128.6, 128.3, 128.1, 127.8, 126.4, 126.2, 65.7, 47.0, 45.4, 42.4. **IR** (neat) ν_{max} 3453.6 (br, w), 3059.46 (w), 3025.76 (w), 2932.68 (w), 1677.08 (m), 1597.17 (m), 1580.33 (w), 1493.16 (m), 1448.68 (m), 1408.9

(w), 1361.21 (w), 1280.47 (w), 1207.21 (m), 1180.85 (w), 1157.8 (w), 1076.32 (w), 1057.11 (w), 1030.94 (m), 1001.18 (w), 985.06 (w), 917.21 (w), 867.75 (w), 782.43 (w), 752.34 (s), 738.94 (m), 697.82 (s), 619.35 (w), 590.07 (w), 550.93 (w) cm^{-1}. **HRMS** (DART) for $C_{23}H_{23}O_2$ $[M+H]^+$: Calc'd: 331.1693, found: 331.1695.

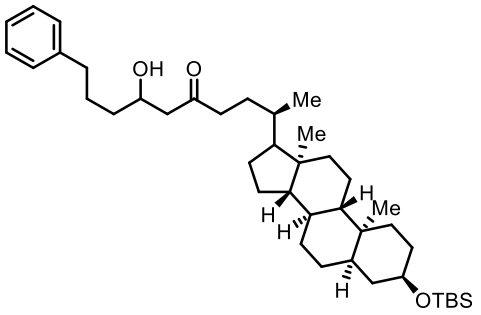

(2R)-2-((3R,5R,8R,9S,10S,13R,14S)-3-((tert-butyldi-methylsilyl)oxy)-10,13-dimethylhexa-decahydro-1H-cyclopenta[a]phenanthren-17-yl)-7-hydroxy-10-phenyldecan-5-one (2.188). The reaction was performed according to the general procedure with 9-BBN in THF (0.52 mL, 0.5 M, 0.26 mmol, 1.30 equiv.), allylbenzene (30.7 mg, 0.26 mmol, 1.30 equiv.), halide-free vinyllithium in THF (0.16 mL, 1.38 M, 0.22 mmol, 1.10 equiv.), a solution of $NiBr_2$-glyme (3.09 mg, 0.010 mmol, 0.050 equiv.) and **L3** (3.51 mg, 0.012 mmol, 0.060 equiv.) in THF (0.4 mL), **S-7** (101.9 mg, 0.20 mmol, 1.00 equiv.). The crude mixture was purified by column chromatography (20% EtOAc in hexane, stain in $KMnO_4$) to afford the product as a colorless oil (63.7 mg, 50% yield).

^{1}H NMR (400 MHz, CDCL3) δ 7.30-7.24 (m, 2H), 7.21-7.15 (m, 3H), 4.10-3.99 (m, 1H), 3.62-3.53 (m, 1H), 3.09 (dd, *J* = 8.1, 3.4 Hz, 1H), 2.64 (t, *J* = 7.6 Hz, 2H), 2.59-2.39 (m, 3H), 2.37-2.27 (m, 1H), 1.96-1.01 (m, 34H), 0.93-0.85 (m, 15H), 0.62 (s, 3H), 0.06 (s, 6H). **^{13}C NMR** (150 MHz, CDCL3) δ 213.1, 142.3, 128.5, 128.4, 125.8, 72.9, 67.6, 67.5, 56.5, 56.0, 49.0, 49.0, 42.8, 42.4, 40.6, 40.3, 40.2, 37.0, 36.0, 36.0, 35.8, 35.7, 35.3, 34.7, 31.1, 29.7, 28.3, 27.4, 27.3, 26.5, 26.1, 24.3, 23.5, 20.9, 18.5, 18.4, 12.1, -4.4. **IR** (neat) ν_{max} 3480.1 (br, m), 2929.1 (s), 2853.5 (m), 1699.0 (s), 1603.1 (w), 1495.8 (w), 1451.0 (m), 749.9 (m), 700.2 (m) cm^{-1}. **HRMS** (DART) for $C_{41}H_{69}O_3Si$ $[M+H]^+$: Calc'd: 637.5016, found: 637.5005.

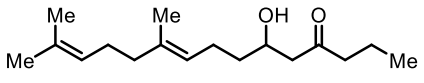

(*E*)-6-hydroxy-10,14-dimethylpentadeca-9,13-dien-4-one (2.191). The reaction was performed according to the general procedure with 9-BBN in THF (0.52 mL, 0.5 M, 0.26 mmol, 1.30 equiv.), **S-2** (39.1 mg, 0.26 mmol, 1.30 equiv.), halide-free vinyllithium in THF (0.16 mL, 1.38 M, 0.22 mmol, 1.10 equiv.), a solution of $NiBr_2$-glyme (3.09 mg, 0.010 mmol, 0.050 equiv.) and **L3** (3.51 mg, 0.012 mmol, 0.060 equiv.) in THF (0.4 mL), butanoyl chloride (21.3 mg, 0.20 mmol, 1.00 equiv.).

The crude mixture was purified by column chromatography (20% EtOAc in hexane, stain in $KMnO_4$) to afford the product as a colorless oil (22.9 mg, 43% yield).

^{1}H NMR (500 MHz, CDCL3) δ 5.14-5.10 (t, *J* = 6.8 Hz, 1H), 5.09-5.06 (t, *J* = 6.6 Hz, 1H), 4.07-4.01 (m, 1H), 3.01 (d, *J* = 3.5 Hz, 1H), 2.59 (dd, *J* = 17.5, 2.8 Hz, 1H), 2.50 (dd, *J* = 17.5, 9.1 Hz, 1H), 2.40 (t, *J* = 7.3 Hz, 2H), 2.17-2.03 (m, 4H), 2.01-1.95 (m, 2H), 1.67 (s, 3H), 1.65-1.52 (m, 9H), 1.45-1.37 (m, 1H), 0.92 (t, *J* = 7.4 Hz, 3H). **^{13}C NMR** (150 MHz, CDCL3) δ 212.4, 135.9, 131.5, 124.3, 123.7, 67.4, 49.1, 45.7, 39.8, 36.5, 26.8, 25.8, 24.0, 17.8, 17.2, 16.1, 13.8. **IR** (neat) ν_{max} 3457.78 (br, m), 2962.6 (s), 2925.23 (s), 1706.5 (s), 1447.7 (m), 1376.3 (m), 1126.6 (w), 1103.0 (m), 1036.7 (w), 834.9 (w) cm^{-1}. **HRMS** (DART) for $C_{16}H_{25}O_3$ $[M+H]^+$: Calc'd: 265.1804, found: 265.1796.

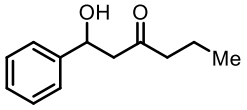

1-hydroxy-1-phenylhexan-3-one (2.192). The reaction was performed according to the general procedure with slight modification. 9-phenyl-9-borabicyclo[3.3.1]nonane (**S-5**) (51.5 mg, 0.26 mmol, 1.30

equiv.) was synthesized independently as mentioned above, diluted with 0.5 mL THF, and to it was added halide-free vinyllithium in THF (0.16 mL, 1.38 M, 0.22 mmol, 1.10 equiv.), a solution of $NiBr_2$-glyme (2.20 mg, 0.010 mmol, 0.050 equiv.) and **L3** (3.51 mg, 0.012 mmol, 0.060 equiv.) in THF (0.4 mL), followed by butanoyl chloride (21.3 mg, 0.20 mmol, 1.00 equiv.). The crude mixture was purified by column chromatography (20% EtOAc in hexane, stain in $KMnO_4$) to afford the product as a colorless oil (23.5 mg, 61% yield).

^{1}H NMR (400 MHz, CDCL3) δ 7.46-7.19 (m, 5H), 5.16 (dd, *J* = 8.7, 3.5 Hz, 1H), 3.38 (s, 1H), 2.85 (dd, *J* = 17.4, 8.8 Hz, 1H), 2.78 (dd, *J* = 17.4, 3.6 Hz, 1H), 2.41 (t, *J* = 7.3 Hz, 2H), 1.62 (h, *J* = 7.3 Hz, 2H), 0.92 (t, *J* = 7.3 Hz, 3H). **^{13}CNMR** (150 MHz, CDCL3) δ 211.6, 142.9, 128.6, 127.7, 125.7, 70.0, 51.1, 45.7, 17.1, 13.7. **IR** (neat) ν_{max} 3400.3 (br, m), 2960.9 (m), 1702.3 (s), 1493.8 (w), 1453.4 (m), 1369.7 (m), 1067.2 (m), 1029.9 (m), 757.2 (m), 701.3 (s) cm^{-1}. **HRMS** (DART) for $C12H20NO_2$ $[M+H]^+$: Calc'd: 210.1489, found: 210.1488.

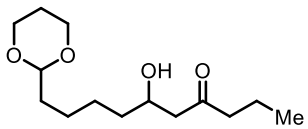

10-(1,3-dioxan-2-yl)-6-hydroxydecan-4-one (2.190).

The reaction was performed according to the general procedure with 9-BBN in THF (0.52 mL, 0.5 M, 0.26 mmol, 1.30 equiv.), **S-3** (37.0 mg, 0.26 mmol, 1.30 equiv.), halide-free vinyllithium in THF (0.16 mL, 1.38 M, 0.22 mmol, 1.10 equiv.), a solution of $NiBr_2$-glyme (3.09 mg, 0.010 mmol, 0.050 equiv.) and **L3** (3.51 mg, 0.012 mmol, 0.060 equiv.) in THF (0.4 mL), butanoyl chloride (21.3 mg, 0.20 mmol, 1.00 equiv.). The crude mixture was purified by column chromatography (20% EtOAc in hexane, stain in $KMnO_4$) to afford the product as a colorless oil (29.5 mg, 57% yield).

^{1}H NMR (500 MHz, CDCL3) δ 7.94 (d, *J* = 7.2 Hz, 2H), 7.57 (t, *J* = 7.5 Hz, 1H), 7.46 (t, *J* = 7.6 Hz, 2H), 4.51 (t, *J* = 5.1 Hz, 1H), 4.21 (m, 1H), 4.08 (dd, *J* = 10.7, 5.0 Hz, 2H), 3.74 (td, *J* = 11.0, 2.0 Hz, 2H). 3.26 (m, 1H), 3.14 (dd, *J* = 17.5, 2.5 Hz, 1H), 3.02 (dd, *J* = 17.6, 9.0 Hz, 1H), 2.11-2.01 (m, 1H), 1.67-1.56 (m, 3H), 1.55-1.47 (m, 2H), 1.46-1.35 (m, 3H), 1.33-1.31 (m, 1H). **^{13}CNMR** (126 MHz, CDCL3) δ 201.0, 136.9, 133.6, 128.7, 128.1, 102.3, 67.7, 67.0, 45.1, 36.5, 35.2, 25.9, 25.5, 24.0. **IR** (neat) ν_{max} 3453.7 (br, w), 2926.6 (w), 2854.7 (w), 1678.1 (m), 1597.0 (w), 1580.2 (w), 1448.7 (w), 1430.8 (w), 1404.3 (w), 1376.8 (w), 1283.1 (w), 1240.1 (m), 1212.8 (m), 1181.3 (w), 1142.2 (s), 1092.3 (m), 992.9 (m), 935.5 (w), 893.9 (w), 864.0

(w), 837.6 (w), 754.4 (m), 690.8 (m), 661.9 (w), 644.1 (w), 586.5 (w), 534.8 (w) cm^{-1}. **HRMS** (DART) for $C_{17}H_{25}O_4$ $[M+H]^+$: Calc'd: 293.1747, found: 293.1751.

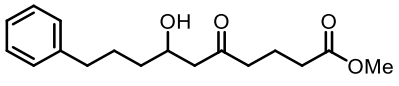

methyl 7-hydroxy-5-oxo-10-phenyldecanoate (2.178). The reaction was performed according to the general procedure with 9-BBN in THF (0.52 mL, 0.5 M, 0.26 mmol, 1.30 equiv.), allylbenzene (30.7 mg, 0.26 mmol, 1.30 equiv.), halide-free vinyllithium in THF (0.16 mL, 1.38 M, 0.22 mmol, 1.10 equiv.), a solution of $NiBr_2$-glyme (3.09 mg, 0.010 mmol, 0.050 equiv.) and **L3** (3.51 mg, 0.012 mmol, 0.060 equiv.) in THF (0.4 mL), methyl 5-chloro-5-oxopentanoate (32.9 mg, 0.20 mmol, 1.00 equiv.). The crude mixture was purified by column chromatography (20% EtOAc in hexane, stain in $KMnO_4$) to afford the product as a colorless oil (47.4 mg, 81% yield).

^{1}H NMR (400 MHz, CDCL3) δ 7.27-7.22 (m, 2H), 7.18-7.13 (m, 3H), 4.07-3.98 (m, 1H), 3.64 (s, 3H), 2.61 (t, *J* = 7.4 Hz, 2H), 2.57-2.43 (m, 4H), 2.31 (t, *J* = 7.4 Hz, 2H), 1.87 (p, *J* = 7.2 Hz, 2H), 1.80-1.71 (m, 1H), 1.70-1.57 (m, 1H), 1.56-1.46 (m, 1H), 1.45-1.34 (m, 1H) .**^{13}C NMR** (126 MHz, CDCL3) δ

211.2, 173.6, 142.3, 128.4, 128.3, 125.8, 77.8, 77.1, 76.8, 67.5, 51.7, 49.2, 42.4, 36.0, 35.7, 33.0, 27.3, 18.7. **IR** (neat) ν_{max} 3406.6 (br, w), 2936.73 (m), 1734.15 (s), 1709.71 (m), 1602.66 (w), 1172.31 (m), 1086.32 (m), 750.20 (m), 700.61 (m) cm^{-1}. **HRMS** (DART) for $C_{17}H_{25}O_4$ $[M+H-H_2O]^+$: Calc'd: 293.1747, found: 203.1737.

2.5.4 Procedures and characterization for boron-enolate alkylation

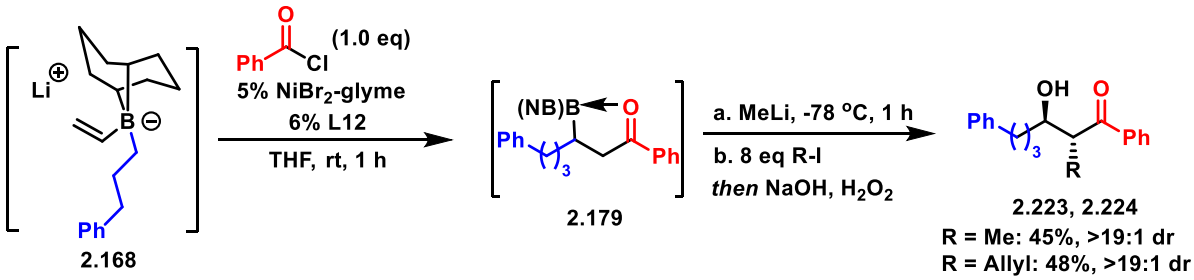

***anti*-3-hydroxy-2-methyl-1,5-diphenylpentan-1-one** (2.223). In a glove box, under argon, an oven-dried 2-dram vial equipped with a magnetic stir bar was charged with a solution of 9-BBN in THF (0.52 mL, 0.5 M, 0.26 mmol, 1.30 equiv.). The vial was cooled to 0 °C, and styrene (27.1 mg, 0.26 mmol, 1.30 equiv.) was added. The reaction mixture was allowed to warm to room temperature and stir for 3 hours before being cooled back to 0°C. A solution of vinyllithium (for the synthesis of halide free vinyllithium see ref[1]) in THF (0.16 mL, 1.38 M, 0.22 mmol, 1.10 equiv.) was added to the reaction mixture

which was then warmed to room temperature and stirred for 5 minutes. Meanwhile a solution of $NiBr_2$-glyme (3.09 mg, 0.010 mmol, 0.050 equiv.) and L3 (see ref[10] for its synthesis) (3.51 mg, 0.012 mmol, 0.060 equiv.) in THF (0.4 mL) was allowed to complex for 5 minutes under inert atmosphere. The catalyst solution was added to the boron 'ate' mixture at room temperature followed by the addition of benzoyl chloride (28.1 mg, 0.20 mmol, 1.00 equiv.). The reaction vial was sealed with a septum cap, taken out of the glovebox and stirred at room temperature for 1h, after which point the reaction mixture was cooled to -78 °C and methyllithium in Et_2O (0.15 mL, 1.6M, 0.24 mmol, 1.2 equiv.) was added dropwise through a syringe under an inert atmosphere. The reaction mixture was allowed to warm up to 0°C and stir for 30 minutes. After cooling the reaction mixture back to -78°C, iodomethane (113 mg, 0.60 mmol, 4.0 equiv.) was added dropwise. The reaction mixture was then warmed up to room temperature and stir for 2 hours. After cooling the reaction mixture to 0°C, 30% H_2O_2 (0.5 mL) was added along with a pH=7 buffer solution (0.5 mL). The reaction mixture was allowed to warm up to room temperature and stir for 3 hours. Aq. saturated $Na_2S_2O_3$ (1 mL) solution was then added to quench the remaining H_2O_2. The aqueous phase was EtOAc (3 x 2 mL). The combined organic layers were dried over

$MgSO_4$, filtered, concentrated under reduced pressure, and the crude mixture was purified by 2 runs of column chromatography (1st: 20% EtOAc in hexane, 2nd: 100% chloroform, stain in $KMnO_4$) to afford the product as a colorless oil (24.2 mg, 45% yield, >19:1 d.r.).

^{1}H NMR (600 MHz, CDCL3) δ 7.94 (d, *J* = 7.0 Hz, 2H), 7.58 (t, *J* = 7.2 Hz, 1H), 7.48 (t, *J* = 7.8 Hz, 2H), 7.29-7.25 (m, 3H), 7.22-7.16 (m, 2H), 3.93-3.85 (m, 1H), 3.59-3.52 (m, 1H), 3.04 (d, *J* = 7.1 Hz, 1H), 2.96-2.88(m, 1H), 2.75-2.69 (m, 1H), 1.91-1.78 (m, 1H), 1.27 (d, *J* = 7.2 Hz, 3H). **^{13}C NMR** (150 MHz, CDCL3) δ 205.9, 142.2, 136.6, 133.6, 128.8, 128.6, 128.5, 128.52, 125.9, 73.5, 45.9, 37.0, 32.3, 29.8, 15.7. **IR** (neat) ν_{max} 3489.3 (br, m), 2926.8 (m), 1677.9 (s), 1596.3 (w), 1495.6 (m), 1453.9 (m), 1375.8 (w), 1209.5 (m), 971.7 (m), 702.0 (s) cm^{-1}. **HRMS** (DART) for $C_{18}H_{21}O_2$ $[M+H]^+$: Calc'd: 269.1542, found: 269.1536.

The relative stereochemistry of the product was determined by comparison of ^{1}H NMR spectrum with the diastereochemically-enriched authentic sample prepared according to the procedure reported by Evans.[53]

[53] D. Evans, J. Tedrow, J. Shaw, C. Downey, *J. Am. Chem. Soc*. **2002**, *124*, 392.

Table S1 Survey of bases for boron-enolate alkylation

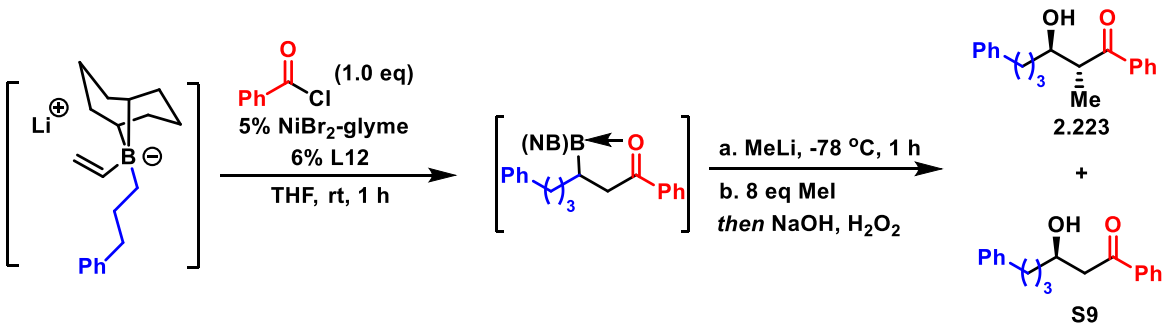

Base	2.223(%)	S9(%)
***i*PrLi (1.7M pentane solution)**	17%	0%
***n*BuLi (2.6M hexane solution)**	39%	0%
MeLi (1.42M Et_2O solution)	45%	0%
LDA	0%	62%
***i*Pr_2NEt**	0%	58%

The formation of **S9** is presumably due to the inefficient deprotonation of **2.223** and its subsequent oxidation.

2.5.5 Synthesis and characterization of 9-BBN-Schiff-base

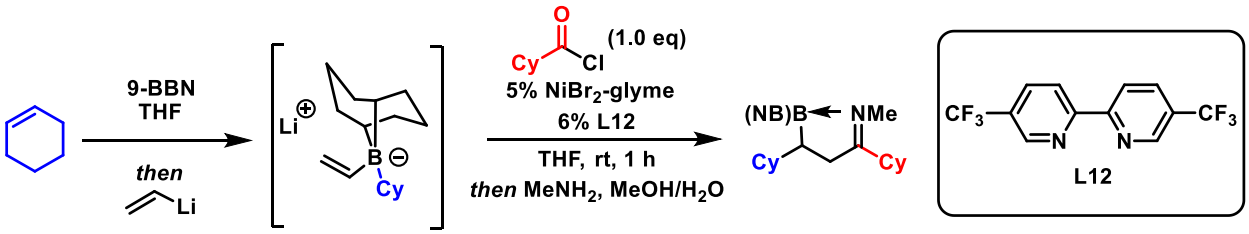

(E)-3-(9-borabicyclo[3.3.1]nonan-9-yl)-1,3-dicyclohexyl-N-methyl-propan-1-imine (2.222). In a glove box, under argon, an oven-dried 2-dram vial equipped with a magnetic stir bar was charged with a solution of 9-BBN in THF (0.52 mL, 0.5 M, 0.26 mmol, 1.30 equiv.). The vial was cooled to 0 °C, and cyclohexene (21.4 mg, 0.26 mmol, 1.30 equiv.) was added. The reaction mixture was allowed to heat up to 60 °C and stir for 3 hours before being cooled back to 0 °C. A solution of vinyllithium (for the synthesis of halide free vinyllithium see ref[1]) in THF (0.16 mL, 1.38 M, 0.22 mmol, 1.10 equiv.) was added to the reaction mixture which was then warmed to room temperature and stirred for 5 minutes. Meanwhile a solution of $NiBr_2$-glyme (3.09 mg, 0.010 mmol, 0.050 equiv.) and L3 (see ref[10] for its synthesis) (0.012 mmol, 0.060 equiv.) in THF (0.4 mL) was allowed to complex for 5 minutes under an inert atmosphere. The catalyst solution was added to the boron 'ate' mixture at room temperature followed by the addition of cyclohexanecarbonyl chloride (29.3 mg, 0.20 mmol, 1.00 equiv.). The reaction vial was sealed with a septum cap, taken out of the glovebox, and stirred at room temperature for 1h, after which point the reaction mixture was cooled to 0 °C and 40% methylamine aqueous solution (1mL) was added. The reaction mixture was allowed to warm up to room temperature and stirred for 1h. The aqueous phase

was EtOAc (3 x 2 mL). The combined organic layers were dried over $MgSO_4$, filtered, concentrated under reduced pressure, and subsequently purified via silica gel column chromatography (20% CH_2Cl_2 in hexane, stain in $KMnO_4$) to provide 31 as a white solid (55.4 mg, 78%).

^{1}H NMR (400 MHz, CDCL3) δ 3.28 (s, 3H), 2.61-2.51 (m, 1H), 2.50-2.37 (m, 2H), 2.30-2.18 (m, 1H), 2.10-1.94 (m, 1H), 1.93-0.98 (m, 31H), 0.94 (s, 1H), 0.39 (qd, *J* = 12.3, 3.6 Hz, 1H), 0.31 (s, 1H) .**^{13}C NMR** (126 MHz, CDCL3) δ 189.0, 40.4, 37.7, 36.9, 35.7, 35.1, 34.3, 33.2, 31.9, 30.7, 30.6, 29.4, 29.4, 27.3, 27.3, 27.1, 25.9, 25.9, 25.8, 25.2, 24.2. **IR** (neat) ν_{max} 2916.9 (s), 2839.6 (s), 1637.0 (m), 1446.7 (m), 1332.1 (w), 1028.6 (m), 904.8 (s), 733.6 (s) cm^{-1}**. HRMS** (DART) for $C_{24}H_{43}BN$ $[M+H]^+$: Calc'd: 356.3483, found: 356.3489.

The structure was characterized by X-ray crystallography. Crystals were grown by slow evaporation with Et_2O in a 1-dram vial at room temperature.

2.5.6 Mechanistic studies

2.5.6.1 Deuterium-labeling experiments

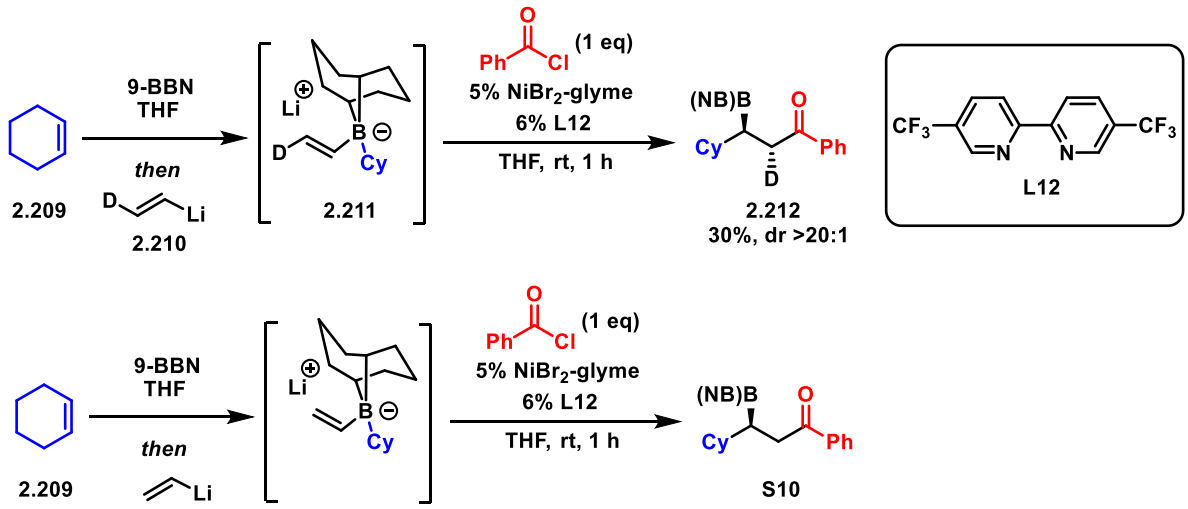

The trans-deuterium labeled vinyl lithium was prepared as described in previous reports.[54]

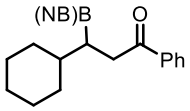

3-(9-borabicyclo[3.3.1]nonan-9-yl)-3-cyclohexyl-1-phenylpropan-1-one (S10). In a glove box, under argon, an oven-dried 2-dram vial equipped with a magnetic stir bar was charged with a solution of 9-BBN in THF (0.52 mL, 0.5 M, 0.26 mmol, 1.30 equiv.). The vial was cooled to 0°C, and cyclohexene (21.4 mg, 0.26 mmol, 1.30 equiv.) was added via syringe. The reaction mixture was heated to 60 °C and stir for 3 hours before being cooled back to 0 °C. A solution of vinyllithium (for the synthesis of

[54] L. Zhang, G. Lovinger, E. Edelstein, A. Szymaniak, M. Chierchia, J. Morken, *Science* **2015**, *351*, 70.

halide free vinyllithium see ref[1]) in THF (0.16 mL, 1.38 M, 0.22 mmol, 1.10 equiv.) was added to the reaction mixture which was then warmed to room temperature and stirred for 5 minutes. Meanwhile, a solution of $NiBr_2$-glyme (0.010 mmol, 0.050 equiv.) and **L3** (see ref[10] for its synthesis) (3.51 mg, 0.012 mmol, 0.060 equiv.) in THF (0.4 mL) was allowed to complex for 5 minutes under an inert atmosphere. The catalyst solution was added to the boron 'ate' mixture at room temperature followed by the addition of benzoyl chloride (28.1 mg, 0.20 mmol, 1.00 equiv.). The reaction vial was sealed with a septum cap, taken out of the glovebox and stirred at room temperature for 1h. The crude mixture was concentrated in vacuo and purified by silica gel column chromatography (20% CH_2Cl_2 in hexane, stain in $KMnO_4$) to afford the product as a yellow oil (37.0 mg, 55% yield).

^{1}H NMR (500 MHz, CDCL3) δ 8.13 (d, *J* = 8.1 Hz, 2H), 7,74 (t, *J* = 7.5 Hz, 1H), 7.56 (t, *J* = 8.1 Hz, 2H), 3.48 (d, *J* = 19.4 Hz, 1H), 3.15 (dd, *J* = 19.4, 8.3 Hz, 1H), 2.06-1.87 (m, 4H), 1.80-1.12 (m, 18H), 1.02-0.92 (m, 1H), 0.89-0.77 (m, 2H), 0.37 (dq, *J* = 12.2, 3.5 Hz, 1H). **^{13}C NMR** (150 MHz, CDCL3) δ 212.9, 136.4, 131.2, 130.8, 129.3, 40.0, 38.2, 33.4, 33.2, 32.6, 30.1, 27.2, 26.8, 26.7, 25.1. **^{11}B NMR** (150 MHz, CDCL3) δ 21.5. **IR** (neat) ν_{max} 2916.9 (s),

2839.6 (s), 1637.0 (m), 1446.7 (m), 1332.1 (w), 1028.6 (m), 904.8 (s), 733.6 (s) cm^{-1}. **HRMS** (DART) for $C_{23}H_{34}BO$ $[M+H]^+$: Calc'd: 337.2697, found: 337.2700.

The resonances of the two diastereotopic protons adjacent to the carbonyl group in ^1H NMR are identified by a series of COESY NMR and 1D NOESY NMR analysis presented below.

From COESY NMR spectrum, it is seen that the proton with resonance at 3.15 ppm couples with H_c with a resonance at 1.28 ppm, whereas the resonance at 3.48 ppm shows no appreciable coupling with H_c. Therefore, it is determined that the 3.15 ppm resonance corresponds to H_b while the 3.48 ppm resonance corresponds to H_a.

COESY NMR of S-10

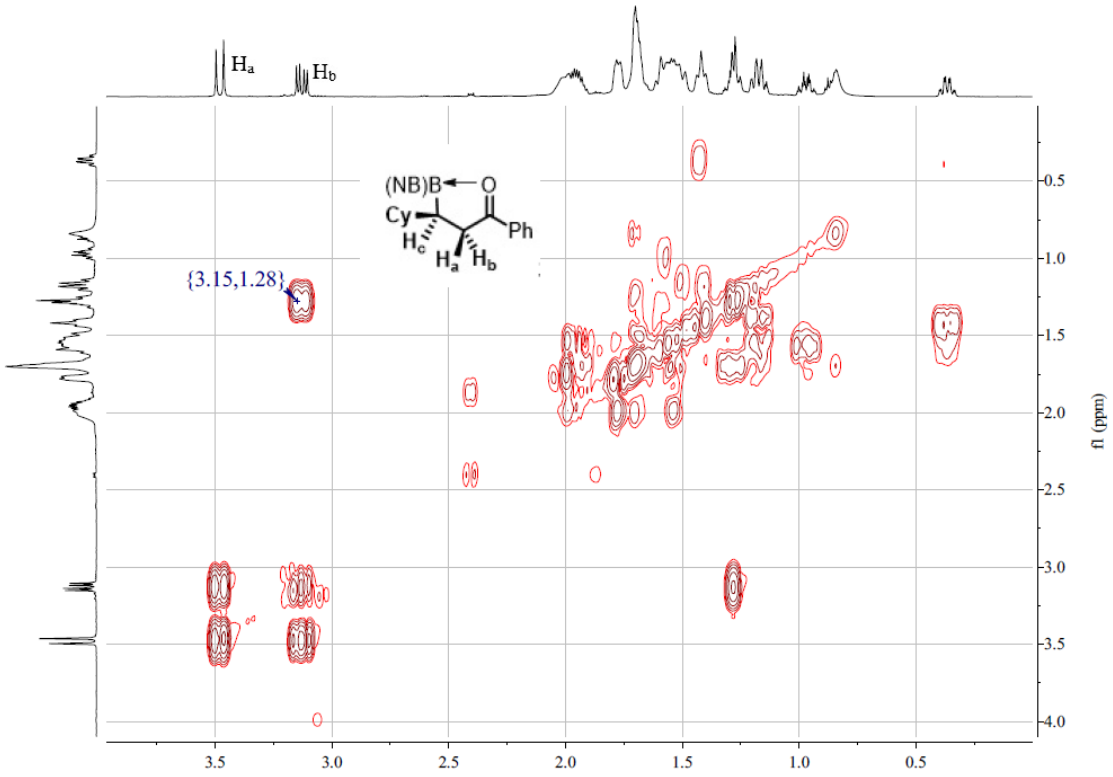

NOESY NMR was also carried out to support the findings about the resonances of the two diasterotopic protons. Selective irradiation of the resonance at 3.15 ppm led to NOE of H_c with resonance at 1.28ppm, whereas selective irradiation of the resonance at 3.48 ppm led to no observable NOE of H_c.

1D-NOESY NMR of S-10 (selective irradiation at 3.15 ppm)

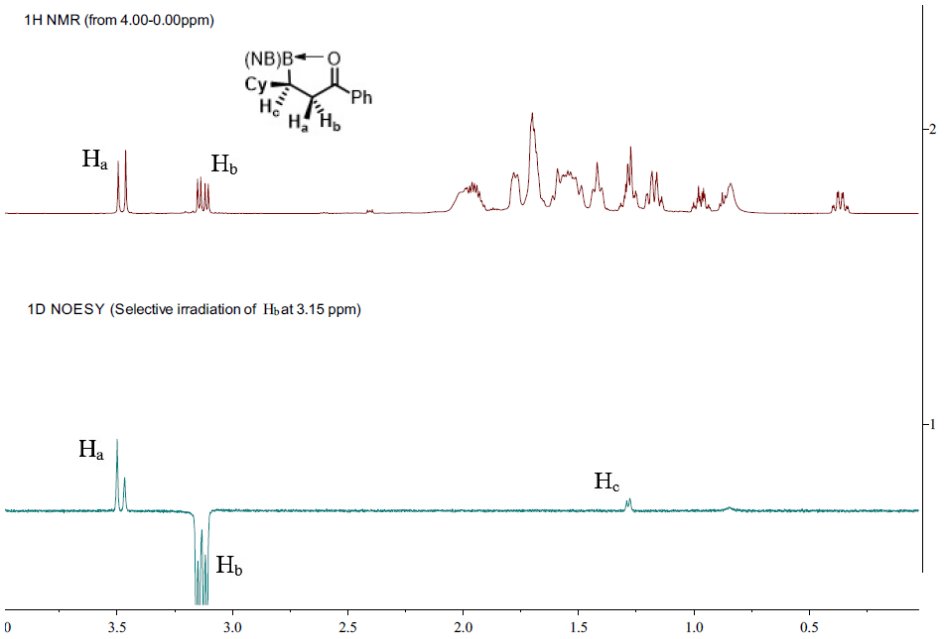

1D-NOESY NMR of S-10 (selective irradiation at 3.48 ppm)

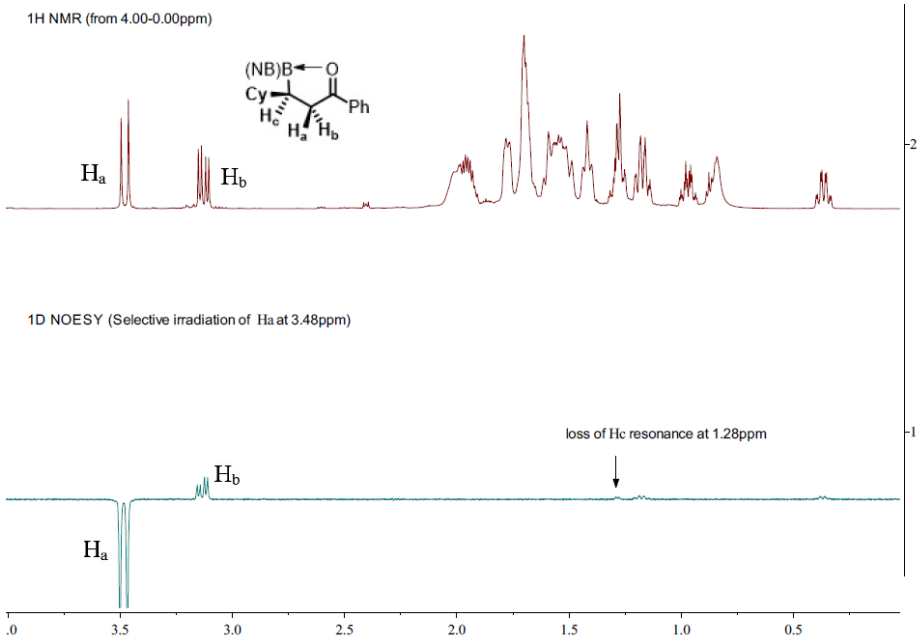

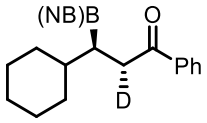

***anti*-3-(9-borabicyclo[3.3.1]nonan-9-yl)-3-cyclohexyl-1-phenylpro-pan-1-one-2-d (2.212).** The reaction was performed according to the procedure for synthesis of **S-7** with 9-BBN in THF (0.52 mL, 0.5 M, 0.26 mmol, 1.30 equiv.), cyclohexene (21.4 mg, 0.26 mmol, 1.30 equiv.), deuterium labeled vinyl lithium in THF (0.27 mL, 0.82 M, 0.22 mmol, 1.10 equiv.), a solution of $NiBr_2$-glyme (3.09 mg, 0.010 mmol, 0.050 equiv.) and **L3** (3.51 mg, 0.012 mmol, 0.060 equiv.) in THF (0.4 mL), benzoyl chloride (28.1 mg, 0.20 mmol, 1.00 equiv.). The crude mixture was purified by column chromatography (20% CH_2Cl_2 in hexane, stain in $KMnO_4$) to afford the product as a yellow oil (21.1 mg, 30% yield).

^{1}H NMR (500 MHz, CDCL3) δ 7.57 (d, *J* = 7.8 Hz, 2H), 7,75 (t, *J* = 7.5 Hz, 1H), 7.57 (t, *J* = 7.8 Hz, 2H), 3.48 (s, 1H), 2.13-1.88 (m, 3H), 1.81-1.40 (m, 3H), 1.36-1.11 (m, 5H), 1.04-0.94 (m, 1H), 0.91-0.71 (m, 2H), 0.37 (dq, *J* = 12.2, 3.4 Hz, 1H).**^{13}C NMR** (126 MHz, CDCL3) δ 213.0, 136.4, 131.2, 130.9, 129.3, 38.0, 33.5, 33.4, 32.5, 30.1, 30.1, 27.2, 26.8, 26.7, 25.1. **^{11}B NMR** (150 MHz, CDCL3) δ 21.5. **IR** (neat) ν_{max} 2922.2 (s), 2851.6 (m), 1679.1 (m),

1597.5 (w), 1447.4 (s), 1272.3 (m), 1206.3 (m), 746.4 (s), 689.0 (s), 651.4 (w) cm^{-1}.

The relative stereochemistry was determined by a comparison of its ^{1}H NMR spectrum with its non-deuterium labeled counterpart (**S-10**).

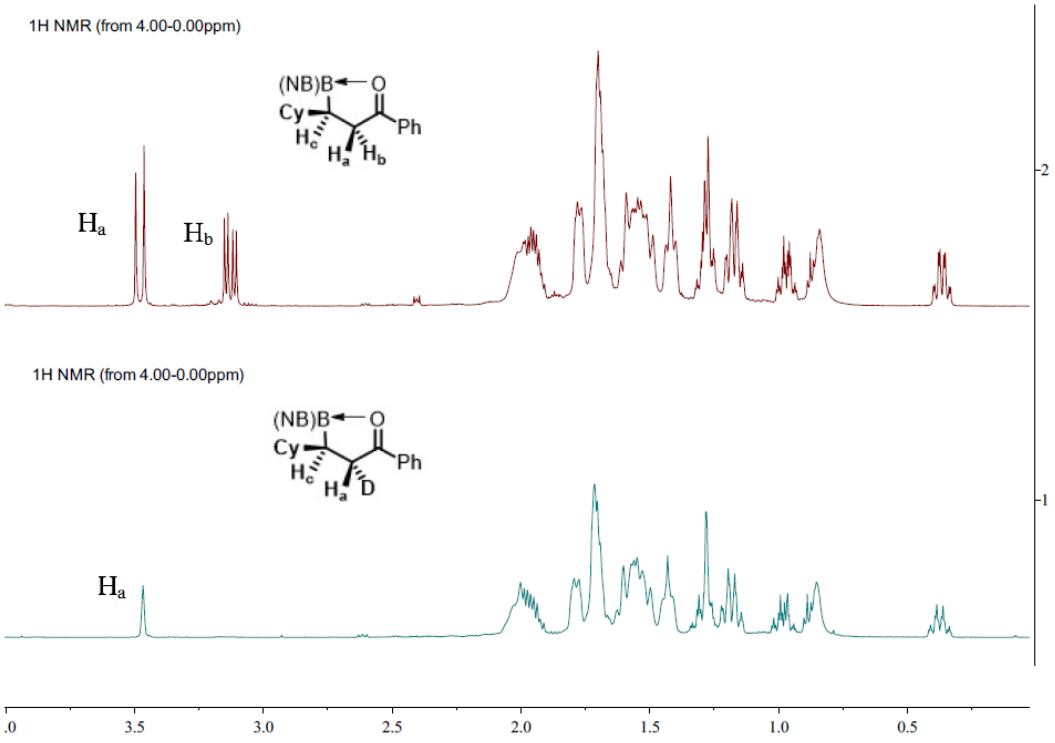

2.5.6.2 Stoichiometric experiments

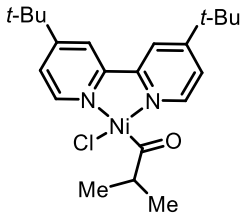

2.208

Ni(II) oxidative addition complex (2.208). The title compound was prepared according to the procedure reported by Gong with slight modifications.[55] In an argon-filled glove box, to an oven-dried scintillation vial was added $Ni(COD)_2$ (248 mg, 0.90 mmol, 1.0 equiv.) and Et_2O (4 mL). The reaction mixture was allowed to stir for 0.5h at room temperature at which point 4,4'-di-tert-butyl-2,2'-bipyridine (341 mg, 0.90 mmol, 1.0 equiv.) in Et_2O (4 mL) was added dropwise. The resulting mixture was allowed to stir at room temperature, at which point, a solution of *iso*-butyryl chloride (96.0 mg, 0.90 mmol, 1.0 equiv.) in Et_2O (1 mL) was added via a syringe. The mixture was allowed to stir for 1h. The suspension was then allowed to settle down and the supernatant was removed via syringe leaving behind red solid which was triturated with Et_2O (2 mL x 4). The red solid was then dried under vacuum, affording 27 (351 mg, 90%). All spectral data was in accordance with the literature.[11]

[55] C. Zhao, J. Xiao, X. Wang, H. Gong, *J. Am. Chem. Soc.* **2014**, *136*, 17645.

^{1}H NMR (500 MHz, DMF-d_7) δ 8.99 (br s, 1H), 8.72 (br s, 2H), 8.21 (br s, 1H), 7.88 (d, J = 40.3 Hz, 2H), 3.49 (s, 1H), 1.58 (s, 18H), 1.47 (s, 6H). ^{13}CNMR (150 MHz, DMF-d_7) δ 260.0, 164.2, 163.3, 155.3, 152.2, 150.6, 148.0, 124.2, 123.2, 119.9, 118.7, 45.2, 35.6, 18.5.

Stoichiometric Conjunctive Cross-Coupling Reaction

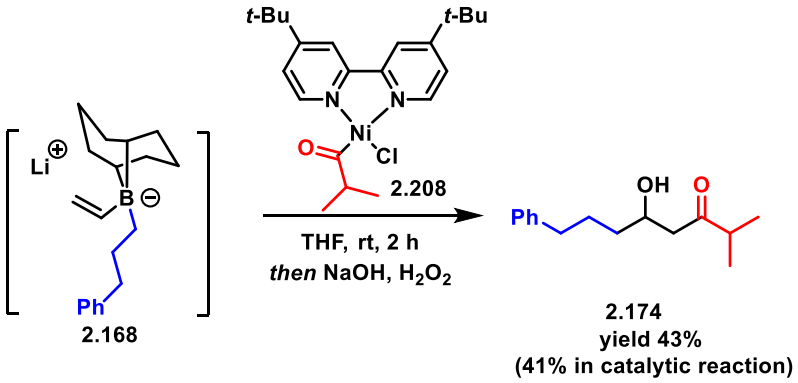

In a glovebox, under argon, an oven-dried 2-dram vial equipped with a magnetic stir bar was charged with a solution of 9-BBN in THF (0.40 mL, 0.5 M, 0.20 mmol, 1.00 equiv.). The vial was cooled to 0°C, and allylbenzene (23.6 mg, 0.20 mmol, 1.00 equiv.) was added. The reaction mixture was allowed to warm to room temperature and stir for 3 hours before being cooled back to 0°C. A solution of vinyllithium (for the synthesis of halide free vinyllithium see ref[1]) in THF (0.15 mL, 1.38 M, 0.22 mmol, 1.00 equiv.) was

added to the reaction mixture which was then warmed to room temperature and stirred for 5 minutes. To the vial was added 27 (86.7 mg, 0.20 mmol, 1.0 equiv.) in one portion at room temperature. The reaction vial was sealed with a septum cap, taken out of the glovebox and stirred at room temperature for 1h, after which point the reaction mixture was cooled to 0°C and 30% H_2O_2 (0.5 mL) were added along with 3 M NaOH (0.5 mL). The reaction mixture was allowed to warm up to room temperature and stirred for 3 hours. Aq. saturated $Na_2S_2O_3$ (1 mL) solution was then added to quench the reaction. The aqueous phase was EtOAc (3 x 2 mL). The combined organic layers were dried over $MgSO_4$, filtered, concentrated under reduced pressure, and subsequently purified via silica gel column chromatography to provide 4 as a colorless oil (20.2 mg, 43%).

2.5.6.3 Experiments with chiral bis(oxazoline) ligands

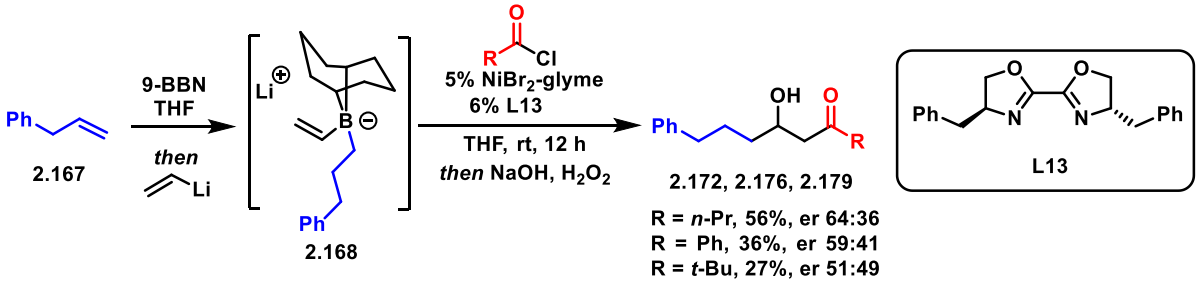

In a glove box, under argon, an oven-dried 2-dram vial equipped with a

magnetic stir bar was charged with a solution of 9-BBN in THF (0.52 mL, 0.5 M, 0.26 mmol, 1.30 equiv.). The vial was cooled to 0 °C, and the olefin (0.26 mmol, 1.30 equiv.) was added via syringe. The reaction mixture was allowed to warm to room temperature and stir for 3 hours before being cooled back to 0°C. A solution of vinyllithium (for the synthesis of halide free vinyllithium see ref[1]) in THF (0.16 mL, 1.38 M, 0.22 mmol, 1.10 equiv.) was added to the reaction mixture which was then warmed to room temperature and stirred for 5 minutes. Meanwhile, a solution of $NiBr_2$-glyme (3.09 mg, 0.010 mmol, 0.050 equiv.) and L6 (0.012 mmol, 0.060 equiv.) in THF (0.4 mL) was allowed to complex for 5 minutes under inert atmosphere. The catalyst solution was added to the boron 'ate' mixture at room temperature followed by addition of acyl chloride (0.20 mmol, 1.00 equiv.) The reaction vial was sealed with a septum cap, taken out of the glovebox and stirred at room temperature for 1h, after which point the reaction mixture was cooled to 0 °C and 30% H_2O_2 (0.5 mL) were added along with 3 M NaOH (0.5 mL). The reaction mixture was allowed to warm up to room temperature and stirred for 3 hours. Aq. saturated $Na_2S_2O_3$ (1 mL) solution was then added to quench the reaction. The aqueous phase was EtOAc (3 x 2 mL). The combined organic layers were dried over $MgSO_4$, filtered, concentrated under reduced pressure,

and subsequently purified via silica gel column chromatography to provide the desired products.

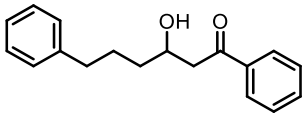

3-hydroxy-1,6-diphenylhexan-1-one (2.179). The reaction was performed according to the general procedure with 9-BBN in THF (0.52 mL, 0.5 M, 0.26 mmol, 1.30 equiv.), allylbenzene (30.7 mg, 0.26 mmol, 1.30 equiv.), halide-free vinyllithium in THF (0.16 mL, 1.38 M, 0.22 mmol, 1.10 equiv.), a solution of $NiBr_2$-glyme (3.09 mg, 0.010 mmol, 0.050 equiv.) and L6 (0.012 mmol, 0.060 equiv.) in THF (0.4 mL), benzoyl chloride (28.1 mg, 0.20 mmol, 1.00 equiv.). The crude mixture was purified by column chromatography (20% EtOAc in hexane, stain in $KMnO_4$) to afford the product as a colorless oil (19.3 mg, 36% yield). Its corresponding spectral data can be found above in section 2.4.3.

Enantioselectivity was determined by chiral SFC. The racemic compound was prepared according to the general procedure with L3 (6 mol%) as the ligand.

Chiral SFC (Chiracel AS-H, 5% IPA, 3 mL/min, 100 bar, 35 °C, 210-289 nm)

Racemic material

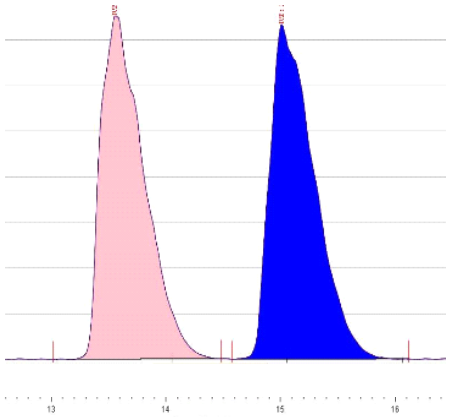

Peak No	% Area	Area	RT (min)
1	49.9903	19738.0387	13.5
2	50.0097	19745.7246	14.95
Total:	100	39483.7633	

Enantioenriched material

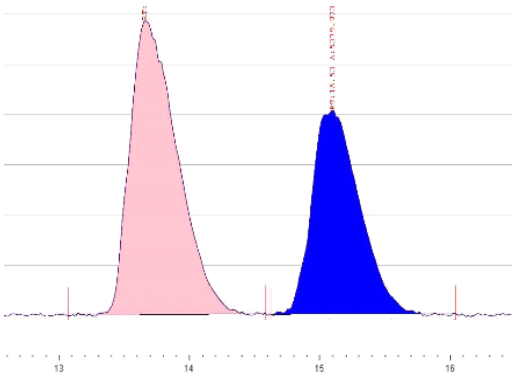

Peak No	% Area	Area	RT (min)
1	59.0118	7745.7033	14.03
2	40.9882	5379.9731	15.53
Total:	100	13125.6764	

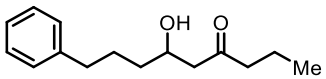

6-hydroxy-9-phenylnonan-4-one (2.172). The reaction was performed according to the general procedure with 9-BBN in THF (0.52 mL, 0.5 M, 0.26 mmol, 1.30 equiv.), allylbenzene (30.7 mg, 0.26 mmol, 1.30 equiv.), halide-free vinyllithium in THF (0.16 mL, 1.38 M, 0.22 mmol, 1.10 equiv.), a solution of $NiBr_2$-glyme (3.09 mg, 0.010 mmol, 0.050 equiv.) and L6 (0.012 mmol, 0.060 equiv.) in THF (0.4 mL), butanoyl chloride (21.3 mg, 0.20 mmol, 1.00 equiv.). The crude mixture was purified by column chromatography (20% EtOAc in hexane, stain in $KMnO_4$) to afford the product as a colorless oil (20.2 mg, 43% yield). Its corresponding spectral data can be found above in section 2.4.3.

Enantioselectivity was determined by chiral SFC. The racemic compound was prepared according to the general procedure with L3 (6 mol%) as the ligand.

Chiral SFC (Chiracel AS-H, 2% IPA, 3 mL/min, 100 bar, 35 °C, 210-289 nm)

Racemic material

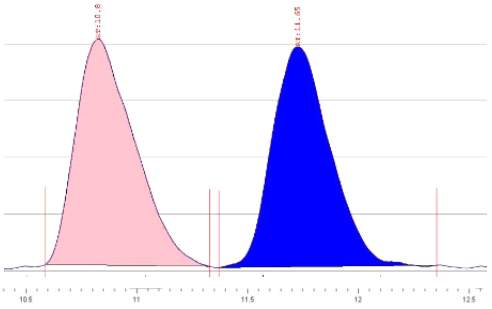

Peak No	% Area	Area	RT (min)
1	51.0302	3457.9941	10.8
2	48.9698	3318.3731	11.65
Total:	100	6776.3672	

Enantioenriched material

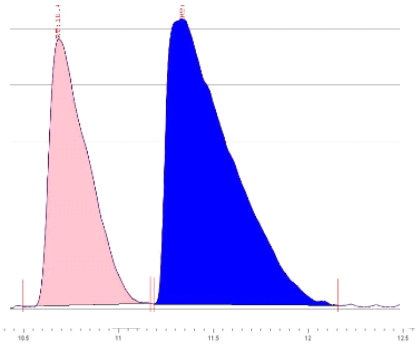

Peak No	% Area	Area	RT (min)
1	36.1664	4258.9027	10.41
2	63.8336	7516.955	11.24
Total:	100	11775.8577	

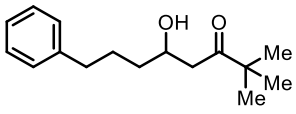

5-hydroxy-2,2-dimethyl-8-phenyloctan-3-one (2.176).

The reaction was performed according to the general procedure with 9-BBN in THF (0.52 mL, 0.5 M, 0.26 mmol, 1.30 equiv.), allylbenzene (30.7 mg, 0.26 mmol, 1.30 equiv.), halide-free vinyllithium in THF (0.16 mL, 1.38 M, 0.22 mmol, 1.10 equiv.), a solution of $NiBr_2$-glyme (2.20 mg, 0.010 mmol,

0.050 equiv.) and L6 (0.012 mmol, 0.060 equiv.) in THF (0.4 mL), pivaloyl chloride (24.1 mg, 0.20 mmol, 1.00 equiv.). The crude mixture was purified by column chromatography (20% EtOAc in hexane, stain in $KMnO_4$) to afford the product as a colorless oil (13.4 mg, 27% yield). Its corresponding spectral data can be found above in section 2.4.3.

Enantioselectivity was determined by chiral SFC. The racemic compound was prepared according to the general procedure with L3 (6 mol%) as the ligand.

Chiral SFC (Chiracel OJ-H, 5% IPA, 3 mL/min, 100 bar, 35 °C, 210-289 nm)

Racemic material

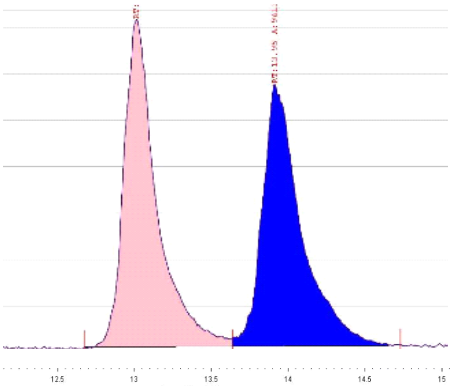

Peak No	% Area	Area	RT (min)
1	51.5896	10244.8632	12.2
2	48.4104	9613.5239	13.95
Total:	100	19858.3871	

Enantioenriched material

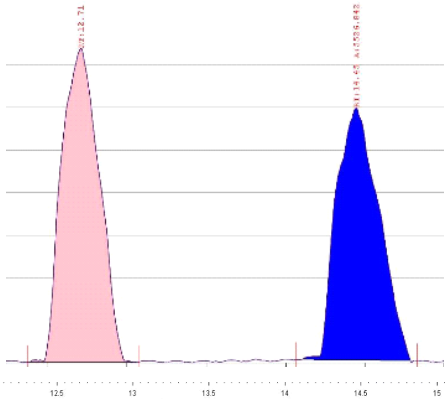

Peak No	% Area	Area	RT (min)
1	52.339	6069.3027	12.71
2	47.661	5526.842	14.45
Total:	100	11596.1447	

2.5.7 Crystallographic Data

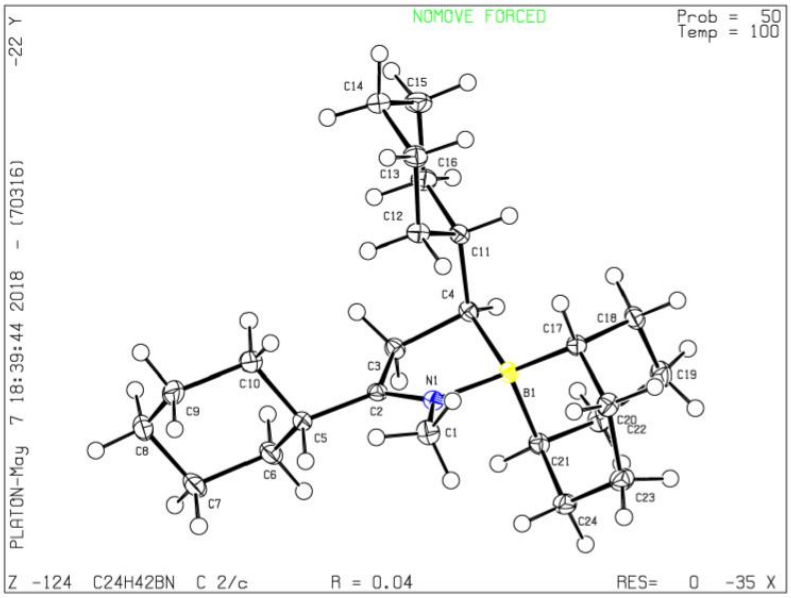

Table 1. Crystal data and structure refinement for C24H42BN.

Identification code	C24H42BN	
Empirical formula	C24 H42 B N	
Formula weight	355.39	
Temperature	100(2) K	
Wavelength	0.71073 Å	
Crystal system	Monoclinic	
Space group	C2/c	
Unit cell dimensions	a = 17.528(3) Å	□= 90°.
	b = 9.8218(11) Å	□= 96.902(3)°.
	c = 24.925(3) Å	□ = 90°.
Volume	4259.8(9) $Å^3$	
Z	8	
Density (calculated)	1.108 Mg/m^3	
Absorption coefficient	0.062 mm^{-1}	
F(000)	1584	
Crystal size	0.500 x 0.360 x 0.220 mm^3	

Theta range for data collection	1.646 to 28.776°.
Index ranges	-23<=h<=23, -13<=k<=13, -33<=l<=33
Reflections collected	46241
Independent reflections	5543 [R(int) = 0.0329]
Completeness to theta = 25.242°	100.0 %
Absorption correction	Semi-empirical from equivalents
Max. and min. transmission	0.7458 and 0.7053
Refinement method	Full-matrix least-squares on F^2
Data / restraints / parameters	5543 / 0 / 236
Goodness-of-fit on F^2	1.032
Final R indices [I>2sigma(I)]	R1 = 0.0416, wR2 = 0.1070
R indices (all data)	R1 = 0.0505, wR2 = 0.1137
Extinction coefficient	n/a
Largest diff. peak and hole	0.387 and -0.225 e.Å^{-3}

Table 2. Atomic coordinates (x 10^4) and equivalent isotropic displacement parameters ($Å^2$x 10^3) for C24H42BN. U(eq) is defined as one third of the trace of the orthogonalized U^{ij} tensor.

	x	y	z	U(eq)
N(1)	5451(1)	5931(1)	3711(1)	13(1)
C(1)	4978(1)	6901(1)	3972(1)	18(1)
C(2)	5929(1)	6309(1)	3385(1)	13(1)
C(3)	6421(1)	5158(1)	3231(1)	14(1)
C(4)	6335(1)	4019(1)	3645(1)	13(1)
C(5)	6011(1)	7718(1)	3162(1)	16(1)
C(6)	6100(1)	7651(1)	2555(1)	21(1)
C(7)	6152(1)	9084(1)	2325(1)	28(1)
C(8)	6828(1)	9858(1)	2623(1)	35(1)
C(9)	6780(1)	9900(1)	3229(1)	32(1)
C(10)	6700(1)	8478(1)	3467(1)	23(1)
C(11)	6957(1)	4094(1)	4141(1)	14(1)
C(12)	6958(1)	5424(1)	4466(1)	16(1)
C(13)	7550(1)	5397(1)	4970(1)	18(1)
C(14)	8356(1)	5150(1)	4819(1)	20(1)
C(15)	8382(1)	3833(1)	4496(1)	22(1)
C(16)	7774(1)	3827(1)	3999(1)	19(1)
C(17)	5191(1)	3569(1)	4313(1)	14(1)
C(18)	5306(1)	2015(1)	4253(1)	18(1)
C(19)	4844(1)	1357(1)	3755(1)	20(1)
C(20)	4858(1)	2161(1)	3226(1)	19(1)
C(21)	4794(1)	3718(1)	3282(1)	15(1)
C(22)	4361(1)	3905(1)	4415(1)	17(1)
C(23)	3737(1)	3736(1)	3928(1)	19(1)
C(24)	3978(1)	4158(1)	3378(1)	18(1)
B(1)	5441(1)	4243(1)	3766(1)	13(1)

Table 3. Bond lengths [Å] and angles [°] for C24H42BN.

N(1)-C(2)	1.2889(12)
N(1)-C(1)	1.4663(12)
N(1)-B(1)	1.6638(13)
C(1)-H(1A)	0.9800
C(1)-H(1B)	0.9800
C(1)-H(1C)	0.9800
C(2)-C(3)	1.5002(13)
C(2)-C(5)	1.5051(13)
C(3)-C(4)	1.5417(13)
C(3)-H(3A)	0.9900
C(3)-H(3B)	0.9900
C(4)-C(11)	1.5491(13)
C(4)-B(1)	1.6463(14)
C(4)-H(4)	1.0000
C(5)-C(10)	1.5402(14)
C(5)-C(6)	1.5406(14)
C(5)-H(5)	1.0000
C(6)-C(7)	1.5267(15)
C(6)-H(6A)	0.9900
C(6)-H(6B)	0.9900
C(7)-C(8)	1.5230(18)
C(7)-H(7A)	0.9900
C(7)-H(7B)	0.9900
C(8)-C(9)	1.523(2)
C(8)-H(8A)	0.9900
C(8)-H(8B)	0.9900
C(9)-C(10)	1.5311(15)
C(9)-H(9A)	0.9900
C(9)-H(9B)	0.9900
C(10)-H(10A)	0.9900
C(10)-H(10B)	0.9900
C(11)-C(12)	1.5375(13)

C(11)-C(16)	1.5388(13)
C(11)-H(11)	1.0000
C(12)-C(13)	1.5290(13)
C(12)-H(12A)	0.9900
C(12)-H(12B)	0.9900
C(13)-C(14)	1.5237(15)
C(13)-H(13A)	0.9900
C(13)-H(13B)	0.9900
C(14)-C(15)	1.5274(15)
C(14)-H(14A)	0.9900
C(14)-H(14B)	0.9900
C(15)-C(16)	1.5341(14)
C(15)-H(15A)	0.9900
C(15)-H(15B)	0.9900
C(16)-H(16A)	0.9900
C(16)-H(16B)	0.9900
C(17)-C(22)	1.5428(13)
C(17)-C(18)	1.5493(14)
C(17)-B(1)	1.6225(14)
C(17)-H(17)	1.0000
C(18)-C(19)	1.5406(14)
C(18)-H(18A)	0.9900
C(18)-H(18B)	0.9900
C(19)-C(20)	1.5382(14)
C(19)-H(19A)	0.9900
C(19)-H(19B)	0.9900
C(20)-C(21)	1.5415(14)
C(20)-H(20A)	0.9900
C(20)-H(20B)	0.9900
C(21)-C(24)	1.5387(14)
C(21)-B(1)	1.6364(14)
C(21)-H(21)	1.0000
C(22)-C(23)	1.5426(14)
C(22)-H(22A)	0.9900

C(22)-H(22B)	0.9900
C(23)-C(24)	1.5392(14)
C(23)-H(23A)	0.9900
C(23)-H(23B)	0.9900
C(24)-H(24A)	0.9900
C(24)-H(24B)	0.9900

C(2)-N(1)-C(1)	122.50(8)
C(2)-N(1)-B(1)	110.70(8)
C(1)-N(1)-B(1)	126.77(8)
N(1)-C(1)-H(1A)	109.5
N(1)-C(1)-H(1B)	109.5
H(1A)-C(1)-H(1B)	109.5
N(1)-C(1)-H(1C)	109.5
H(1A)-C(1)-H(1C)	109.5
H(1B)-C(1)-H(1C)	109.5
N(1)-C(2)-C(3)	112.44(8)
N(1)-C(2)-C(5)	126.55(9)
C(3)-C(2)-C(5)	121.01(8)
C(2)-C(3)-C(4)	105.66(8)
C(2)-C(3)-H(3A)	110.6
C(4)-C(3)-H(3A)	110.6
C(2)-C(3)-H(3B)	110.6
C(4)-C(3)-H(3B)	110.6
H(3A)-C(3)-H(3B)	108.7
C(3)-C(4)-C(11)	112.56(8)
C(3)-C(4)-B(1)	101.41(7)
C(11)-C(4)-B(1)	116.15(7)
C(3)-C(4)-H(4)	108.8
C(11)-C(4)-H(4)	108.8
B(1)-C(4)-H(4)	108.8
C(2)-C(5)-C(10)	111.55(8)
C(2)-C(5)-C(6)	110.37(8)
C(10)-C(5)-C(6)	109.84(9)

C(2)-C(5)-H(5)	108.3
C(10)-C(5)-H(5)	108.3
C(6)-C(5)-H(5)	108.3
C(7)-C(6)-C(5)	110.28(9)
C(7)-C(6)-H(6A)	109.6
C(5)-C(6)-H(6A)	109.6
C(7)-C(6)-H(6B)	109.6
C(5)-C(6)-H(6B)	109.6
H(6A)-C(6)-H(6B)	108.1
C(8)-C(7)-C(6)	110.80(9)
C(8)-C(7)-H(7A)	109.5
C(6)-C(7)-H(7A)	109.5
C(8)-C(7)-H(7B)	109.5
C(6)-C(7)-H(7B)	109.5
H(7A)-C(7)-H(7B)	108.1
C(7)-C(8)-C(9)	111.36(10)
C(7)-C(8)-H(8A)	109.4
C(9)-C(8)-H(8A)	109.4
C(7)-C(8)-H(8B)	109.4
C(9)-C(8)-H(8B)	109.4
H(8A)-C(8)-H(8B)	108.0
C(8)-C(9)-C(10)	112.23(10)
C(8)-C(9)-H(9A)	109.2
C(10)-C(9)-H(9A)	109.2
C(8)-C(9)-H(9B)	109.2
C(10)-C(9)-H(9B)	109.2
H(9A)-C(9)-H(9B)	107.9
C(9)-C(10)-C(5)	110.70(9)
C(9)-C(10)-H(10A)	109.5
C(5)-C(10)-H(10A)	109.5
C(9)-C(10)-H(10B)	109.5
C(5)-C(10)-H(10B)	109.5
H(10A)-C(10)-H(10B)	108.1
C(12)-C(11)-C(16)	108.90(8)

C(12)-C(11)-C(4) 114.71(8)
C(16)-C(11)-C(4) 113.13(8)
C(12)-C(11)-H(11) 106.5
C(16)-C(11)-H(11) 106.5
C(4)-C(11)-H(11) 106.5
C(13)-C(12)-C(11) 112.08(8)
C(13)-C(12)-H(12A) 109.2
C(11)-C(12)-H(12A) 109.2
C(13)-C(12)-H(12B) 109.2
C(11)-C(12)-H(12B) 109.2
H(12A)-C(12)-H(12B)107.9
C(14)-C(13)-C(12) 110.94(8)
C(14)-C(13)-H(13A) 109.5
C(12)-C(13)-H(13A) 109.5
C(14)-C(13)-H(13B) 109.5
C(12)-C(13)-H(13B) 109.5
H(13A)-C(13)-H(13B)108.0
C(13)-C(14)-C(15) 110.61(9)
C(13)-C(14)-H(14A) 109.5
C(15)-C(14)-H(14A) 109.5
C(13)-C(14)-H(14B) 109.5
C(15)-C(14)-H(14B) 109.5
H(14A)-C(14)-H(14B)108.1
C(14)-C(15)-C(16) 111.55(8)
C(14)-C(15)-H(15A) 109.3
C(16)-C(15)-H(15A) 109.3
C(14)-C(15)-H(15B) 109.3
C(16)-C(15)-H(15B) 109.3
H(15A)-C(15)-H(15B)108.0
C(15)-C(16)-C(11) 112.81(8)
C(15)-C(16)-H(16A) 109.0
C(11)-C(16)-H(16A) 109.0
C(15)-C(16)-H(16B) 109.0
C(11)-C(16)-H(16B) 109.0

H(16A)-C(16)-H(16B)107.8
C(22)-C(17)-C(18) 111.30(8)
C(22)-C(17)-B(1) 114.06(8)
C(18)-C(17)-B(1) 105.59(8)
C(22)-C(17)-H(17) 108.6
C(18)-C(17)-H(17) 108.6
B(1)-C(17)-H(17) 108.6
C(19)-C(18)-C(17) 115.43(8)
C(19)-C(18)-H(18A) 108.4
C(17)-C(18)-H(18A) 108.4
C(19)-C(18)-H(18B) 108.4
C(17)-C(18)-H(18B) 108.4
H(18A)-C(18)-H(18B)107.5
C(20)-C(19)-C(18) 114.45(8)
C(20)-C(19)-H(19A) 108.6
C(18)-C(19)-H(19A) 108.6
C(20)-C(19)-H(19B) 108.6
C(18)-C(19)-H(19B) 108.6
H(19A)-C(19)-H(19B)107.6
C(19)-C(20)-C(21) 115.03(8)
C(19)-C(20)-H(20A) 108.5
C(21)-C(20)-H(20A) 108.5
C(19)-C(20)-H(20B) 108.5
C(21)-C(20)-H(20B) 108.5
H(20A)-C(20)-H(20B)107.5
C(24)-C(21)-C(20) 111.84(8)
C(24)-C(21)-B(1) 111.86(8)
C(20)-C(21)-B(1) 109.10(8)
C(24)-C(21)-H(21) 108.0
C(20)-C(21)-H(21) 108.0
B(1)-C(21)-H(21) 108.0
C(23)-C(22)-C(17) 116.10(8)
C(23)-C(22)-H(22A) 108.3
C(17)-C(22)-H(22A) 108.3

C(23)-C(22)-H(22B) 108.3
C(17)-C(22)-H(22B) 108.3
H(22A)-C(22)-H(22B)107.4
C(24)-C(23)-C(22) 115.30(8)
C(24)-C(23)-H(23A) 108.4
C(22)-C(23)-H(23A) 108.4
C(24)-C(23)-H(23B) 108.4
C(22)-C(23)-H(23B) 108.4
H(23A)-C(23)-H(23B)107.5
C(21)-C(24)-C(23) 114.99(8)
C(21)-C(24)-H(24A) 108.5
C(23)-C(24)-H(24A) 108.5
C(21)-C(24)-H(24B) 108.5
C(23)-C(24)-H(24B) 108.5
H(24A)-C(24)-H(24B)107.5
C(17)-B(1)-C(21) 104.89(8)
C(17)-B(1)-C(4) 117.37(8)
C(21)-B(1)-C(4) 114.44(8)
C(17)-B(1)-N(1) 118.85(8)
C(21)-B(1)-N(1) 105.40(7)
C(4)-B(1)-N(1) 95.63(7)

Symmetry transformations used to generate equivalent atoms:

Table 4. Anisotropic displacement parameters ($Å^2 x\ 10^3$) for C24H42BN. The anisotropic displacement factor exponent takes the form: $-2\pi^2[\ h^2 a^{*2} U^{11} + ... + 2\ h\ k\ a^*\ b^*\ U^{12}\ ]$

	U^{11}	U^{22}	U^{33}	U^{23}	U^{13}	U^{12}
N(1)	14(1)	12(1)	13(1)	-1(1)	1(1)	1(1)
C(1)	20(1)	15(1)	20(1)	-2(1)	6(1)	3(1)
C(2)	14(1)	13(1)	12(1)	0(1)	-2(1)	0(1)
C(3)	16(1)	15(1)	13(1)	1(1)	3(1)	1(1)
C(4)	16(1)	11(1)	12(1)	-1(1)	2(1)	1(1)
C(5)	13(1)	14(1)	19(1)	4(1)	1(1)	0(1)
C(6)	20(1)	23(1)	21(1)	8(1)	4(1)	3(1)
C(7)	21(1)	28(1)	34(1)	19(1)	5(1)	4(1)
C(8)	18(1)	28(1)	58(1)	26(1)	4(1)	0(1)
C(9)	21(1)	16(1)	55(1)	10(1)	-6(1)	-4(1)
C(10)	20(1)	15(1)	31(1)	4(1)	-5(1)	-2(1)
C(11)	15(1)	14(1)	14(1)	2(1)	2(1)	2(1)
C(12)	15(1)	17(1)	14(1)	0(1)	1(1)	2(1)
C(13)	20(1)	21(1)	14(1)	0(1)	-1(1)	0(1)
C(14)	16(1)	22(1)	21(1)	3(1)	-2(1)	0(1)
C(15)	17(1)	23(1)	25(1)	2(1)	-1(1)	5(1)
C(16)	17(1)	21(1)	20(1)	-1(1)	3(1)	5(1)
C(17)	16(1)	15(1)	11(1)	0(1)	1(1)	-2(1)
C(18)	21(1)	16(1)	17(1)	4(1)	2(1)	-1(1)
C(19)	25(1)	14(1)	21(1)	-1(1)	2(1)	-3(1)
C(20)	23(1)	17(1)	16(1)	-4(1)	1(1)	-2(1)
C(21)	18(1)	16(1)	11(1)	0(1)	2(1)	-1(1)
C(22)	18(1)	21(1)	14(1)	-1(1)	4(1)	-2(1)
C(23)	16(1)	24(1)	18(1)	1(1)	3(1)	-1(1)
C(24)	16(1)	22(1)	15(1)	2(1)	-1(1)	-1(1)
B(1)	15(1)	11(1)	12(1)	0(1)	1(1)	0(1)

Table 5. Hydrogen coordinates (x 10^4) and isotropic displacement parameters ($Å^2$x 10^3) for C24H42BN.

	x	y	z	U(eq)
H(1A)	5152	7830	3911	27
H(1B)	5026	6717	4361	27
H(1C)	4439	6804	3818	27
H(3A)	6965	5449	3247	17
H(3B)	6245	4840	2859	17
H(4)	6376	3118	3463	16
H(5)	5533	8242	3206	19
H(6A)	6571	7134	2503	25
H(6B)	5654	7170	2360	25
H(7A)	6215	9027	1937	33
H(7B)	5670	9583	2360	33
H(8A)	6833	10799	2482	42
H(8B)	7314	9412	2556	42
H(9A)	6333	10461	3299	38
H(9B)	7249	10339	3413	38
H(10A)	6627	8557	3854	27
H(10B)	7176	7952	3442	27
H(11)	6840	3346	4390	17
H(12A)	7074	6196	4233	19
H(12B)	6441	5574	4576	19
H(13A)	7538	6276	5163	22
H(13B)	7416	4666	5216	22
H(14A)	8724	5092	5152	24
H(14B)	8509	5924	4601	24
H(15A)	8293	3049	4730	26
H(15B)	8898	3728	4379	26
H(16A)	7785	2934	3816	23
H(16B)	7907	4534	3742	23

H(17)	5550	3900	4628	17
H(18A)	5859	1839	4237	21
H(18B)	5163	1560	4581	21
H(19A)	5052	434	3705	24
H(19B)	4304	1254	3826	24
H(20A)	4429	1841	2962	22
H(20B)	5343	1950	3077	22
H(21)	4911	4141	2936	18
H(22A)	4225	3314	4711	21
H(22B)	4348	4859	4543	21
H(23A)	3576	2770	3906	23
H(23B)	3283	4283	3995	23
H(24A)	3608	3765	3088	22
H(24B)	3943	5162	3346	22

Table 6. Torsion angles [°] for C24H42BN.

C(1)-N(1)-C(2)-C(3)	172.08(8)
B(1)-N(1)-C(2)-C(3)	-9.74(10)
C(1)-N(1)-C(2)-C(5)	-8.54(14)
B(1)-N(1)-C(2)-C(5)	169.64(8)
N(1)-C(2)-C(3)-C(4)	-15.66(10)
C(5)-C(2)-C(3)-C(4)	164.92(8)
C(2)-C(3)-C(4)-C(11)	-91.76(9)
C(2)-C(3)-C(4)-B(1)	33.04(9)
N(1)-C(2)-C(5)-C(10)	100.75(11)
C(3)-C(2)-C(5)-C(10)	-79.92(11)
N(1)-C(2)-C(5)-C(6)	-136.85(10)
C(3)-C(2)-C(5)-C(6)	42.48(11)
C(2)-C(5)-C(6)-C(7)	177.81(8)
C(10)-C(5)-C(6)-C(7)	-58.79(11)
C(5)-C(6)-C(7)-C(8)	58.54(12)
C(6)-C(7)-C(8)-C(9)	-55.81(13)
C(7)-C(8)-C(9)-C(10)	54.02(13)
C(8)-C(9)-C(10)-C(5)	-54.47(13)
C(2)-C(5)-C(10)-C(9)	179.14(9)
C(6)-C(5)-C(10)-C(9)	56.43(12)
C(3)-C(4)-C(11)-C(12)	60.10(10)
B(1)-C(4)-C(11)-C(12)	-56.18(11)
C(3)-C(4)-C(11)-C(16)	-65.66(10)
B(1)-C(4)-C(11)-C(16)	178.06(8)
C(16)-C(11)-C(12)-C(13)	-55.74(10)
C(4)-C(11)-C(12)-C(13)	176.33(8)
C(11)-C(12)-C(13)-C(14)	58.13(11)
C(12)-C(13)-C(14)-C(15)	-56.44(11)
C(13)-C(14)-C(15)-C(16)	54.71(11)
C(14)-C(15)-C(16)-C(11)	-54.67(12)
C(12)-C(11)-C(16)-C(15)	54.06(11)
C(4)-C(11)-C(16)-C(15)	-177.12(8)

C(22)-C(17)-C(18)-C(19)	65.62(11)
B(1)-C(17)-C(18)-C(19)	-58.65(11)
C(17)-C(18)-C(19)-C(20)	44.62(12)
C(18)-C(19)-C(20)-C(21)	-40.46(13)
C(19)-C(20)-C(21)-C(24)	-72.25(11)
C(19)-C(20)-C(21)-B(1)	52.03(11)
C(18)-C(17)-C(22)-C(23)	-72.35(11)
B(1)-C(17)-C(22)-C(23)	46.99(12)
C(17)-C(22)-C(23)-C(24)	-37.55(13)
C(20)-C(21)-C(24)-C(23)	68.17(11)
B(1)-C(21)-C(24)-C(23)	-54.56(11)
C(22)-C(23)-C(24)-C(21)	41.70(12)
C(22)-C(17)-B(1)-C(21)	-55.49(10)
C(18)-C(17)-B(1)-C(21)	67.03(9)
C(22)-C(17)-B(1)-C(4)	176.21(8)
C(18)-C(17)-B(1)-C(4)	-61.27(10)
C(22)-C(17)-B(1)-N(1)	61.91(11)
C(18)-C(17)-B(1)-N(1)	-175.57(8)
C(24)-C(21)-B(1)-C(17)	59.02(10)
C(20)-C(21)-B(1)-C(17)	-65.25(9)
C(24)-C(21)-B(1)-C(4)	-170.93(8)
C(20)-C(21)-B(1)-C(4)	64.80(10)
C(24)-C(21)-B(1)-N(1)	-67.22(9)
C(20)-C(21)-B(1)-N(1)	168.51(7)
C(3)-C(4)-B(1)-C(17)	-161.46(8)
C(11)-C(4)-B(1)-C(17)	-39.11(11)
C(3)-C(4)-B(1)-C(21)	74.95(9)
C(11)-C(4)-B(1)-C(21)	-162.69(8)
C(3)-C(4)-B(1)-N(1)	-34.80(8)
C(11)-C(4)-B(1)-N(1)	87.55(8)
C(2)-N(1)-B(1)-C(17)	154.28(8)
C(1)-N(1)-B(1)-C(17)	-27.63(13)
C(2)-N(1)-B(1)-C(21)	-88.59(9)
C(1)-N(1)-B(1)-C(21)	89.50(10)

C(2)-N(1)-B(1)-C(4)	28.70(9)
C(1)-N(1)-B(1)-C(4)	-153.21(8)

Symmetry transformations used to generate equivalent atoms:

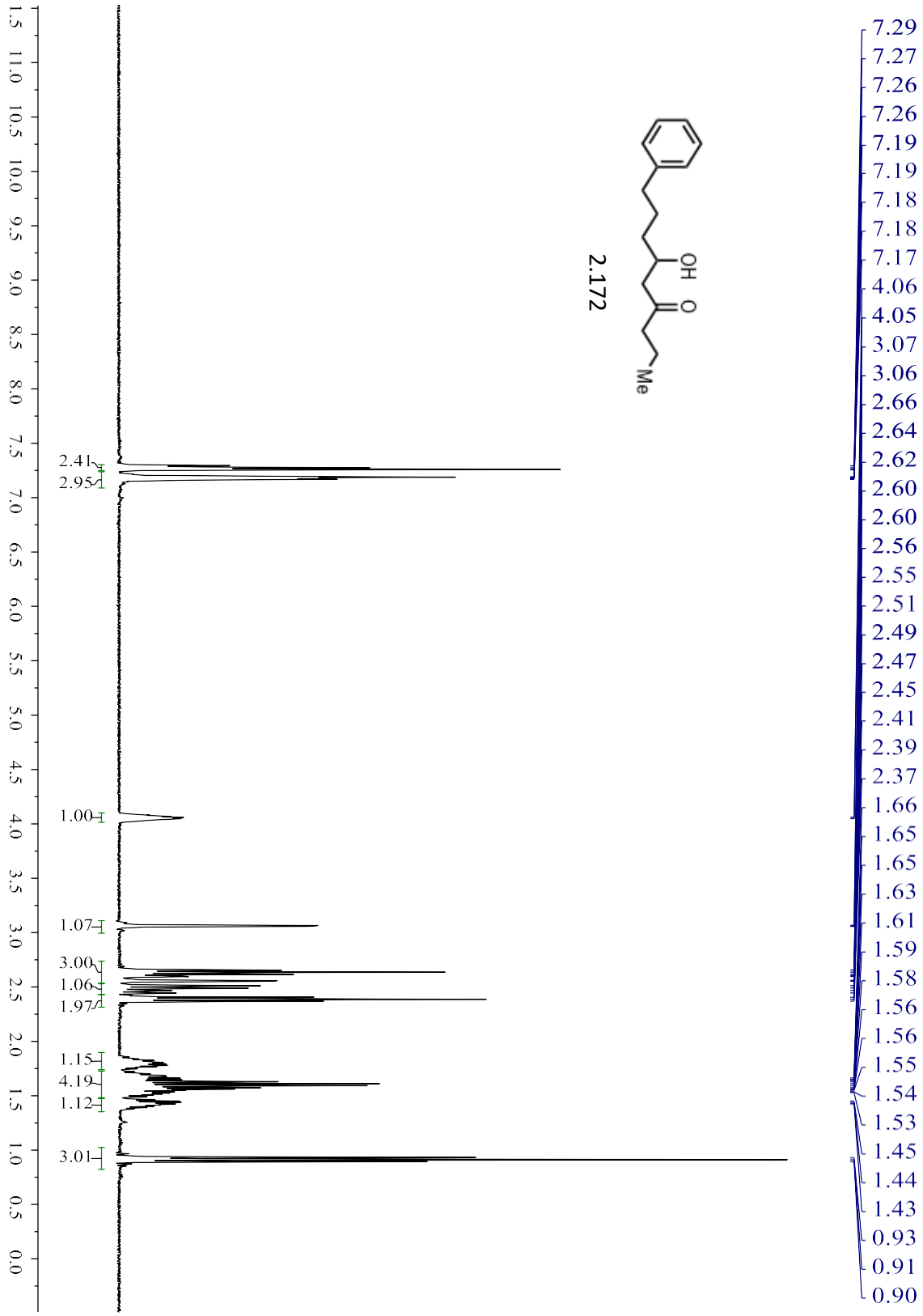
2.172
OH
O
Me
2.41
2.95
1.00
1.07
3.00
1.06
1.97
1.15
4.19
1.12
3.01
7.29
7.27
7.26
7.26
7.19
7.19
7.18
7.18
7.17
4.06
4.05
3.07
3.06
2.66
2.64
2.62
2.60
2.60
2.56
2.55
2.51
2.49
2.47
2.45
2.41
2.39
2.37
1.66
1.65
1.65
1.63
1.61
1.59
1.58
1.56
1.56
1.55
1.54
1.53
1.45
1.44
1.43
0.93
0.91
0.90

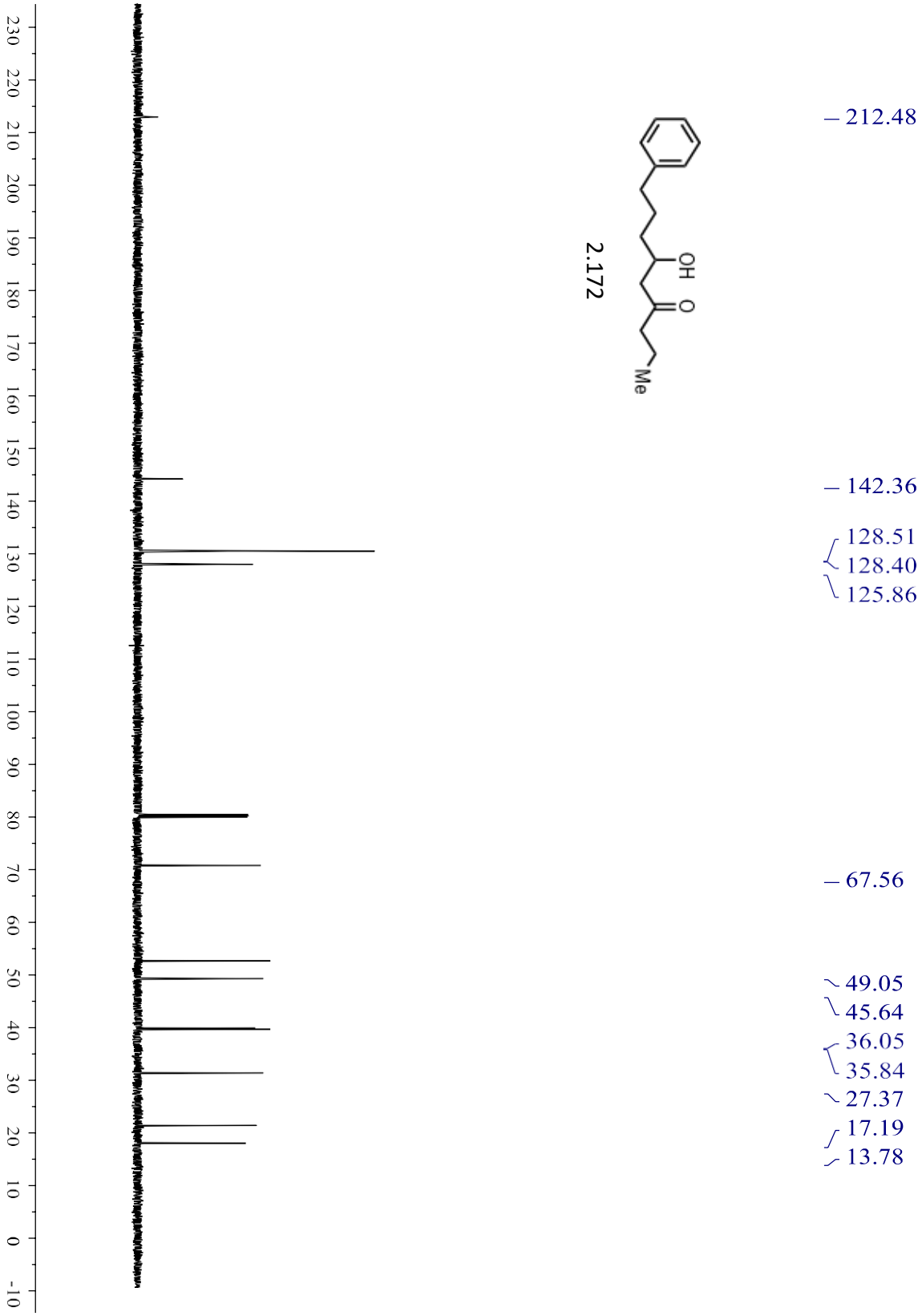
212.48
142.36
128.51
128.40
125.86
67.56
49.05
45.64
36.05
35.84
27.37
17.19
13.78
2.172
OH
O
Me
230
220
210
200
190
180
170
160
150
140
130
120
110
100
90
80
70
60
50
40
30
20
10
0
-10

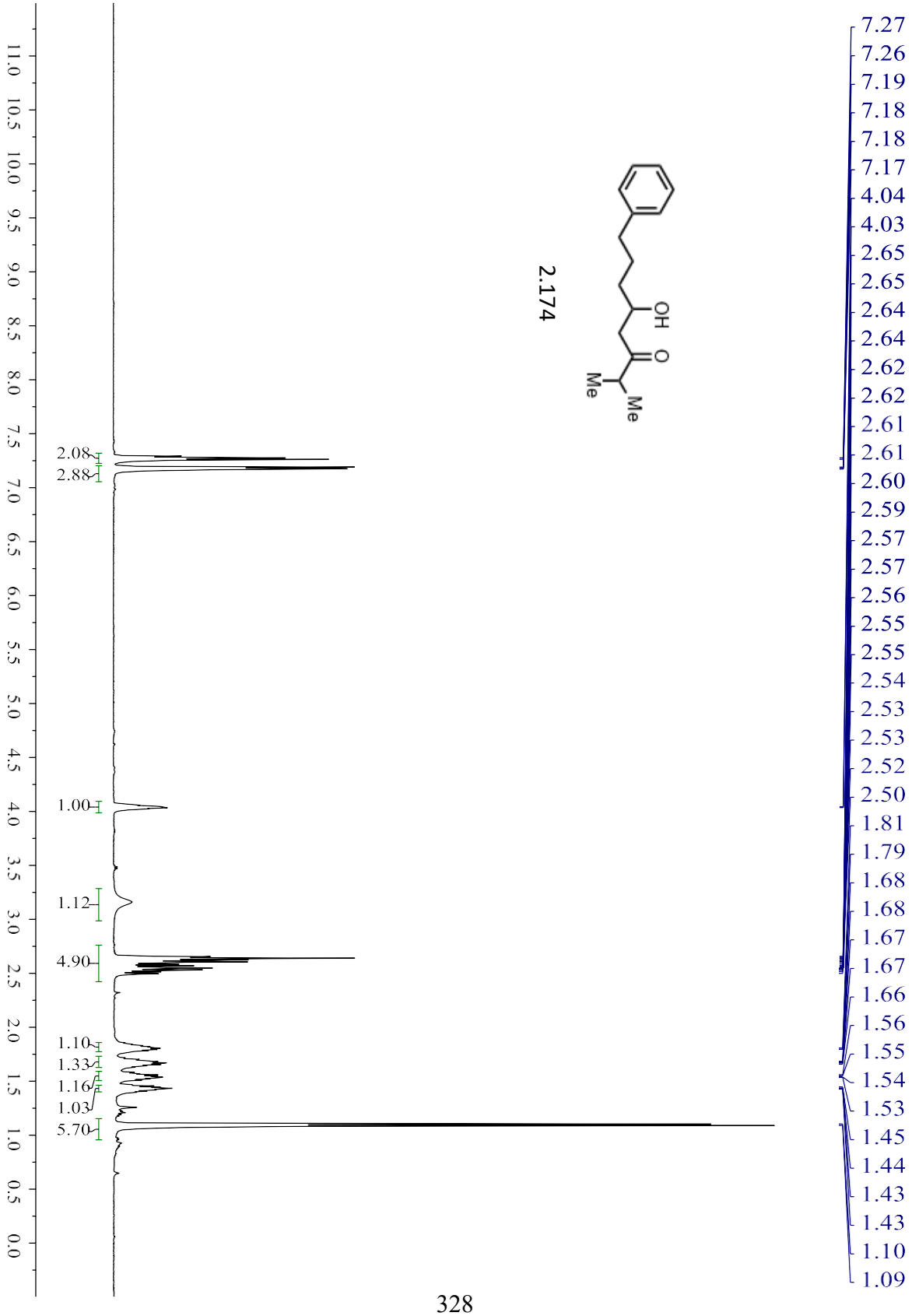
2.174
OH
O
Me
Me
2.08
2.88
1.00
1.12
4.90
1.10
1.33
1.16
1.03
5.70
7.27
7.26
7.19
7.18
7.18
7.17
4.04
4.03
2.65
2.65
2.64
2.64
2.62
2.62
2.61
2.61
2.60
2.59
2.57
2.57
2.56
2.55
2.55
2.54
2.53
2.53
2.52
2.50
1.81
1.79
1.68
1.68
1.67
1.67
1.66
1.56
1.55
1.54
1.53
1.45
1.44
1.43
1.43
1.10
1.09

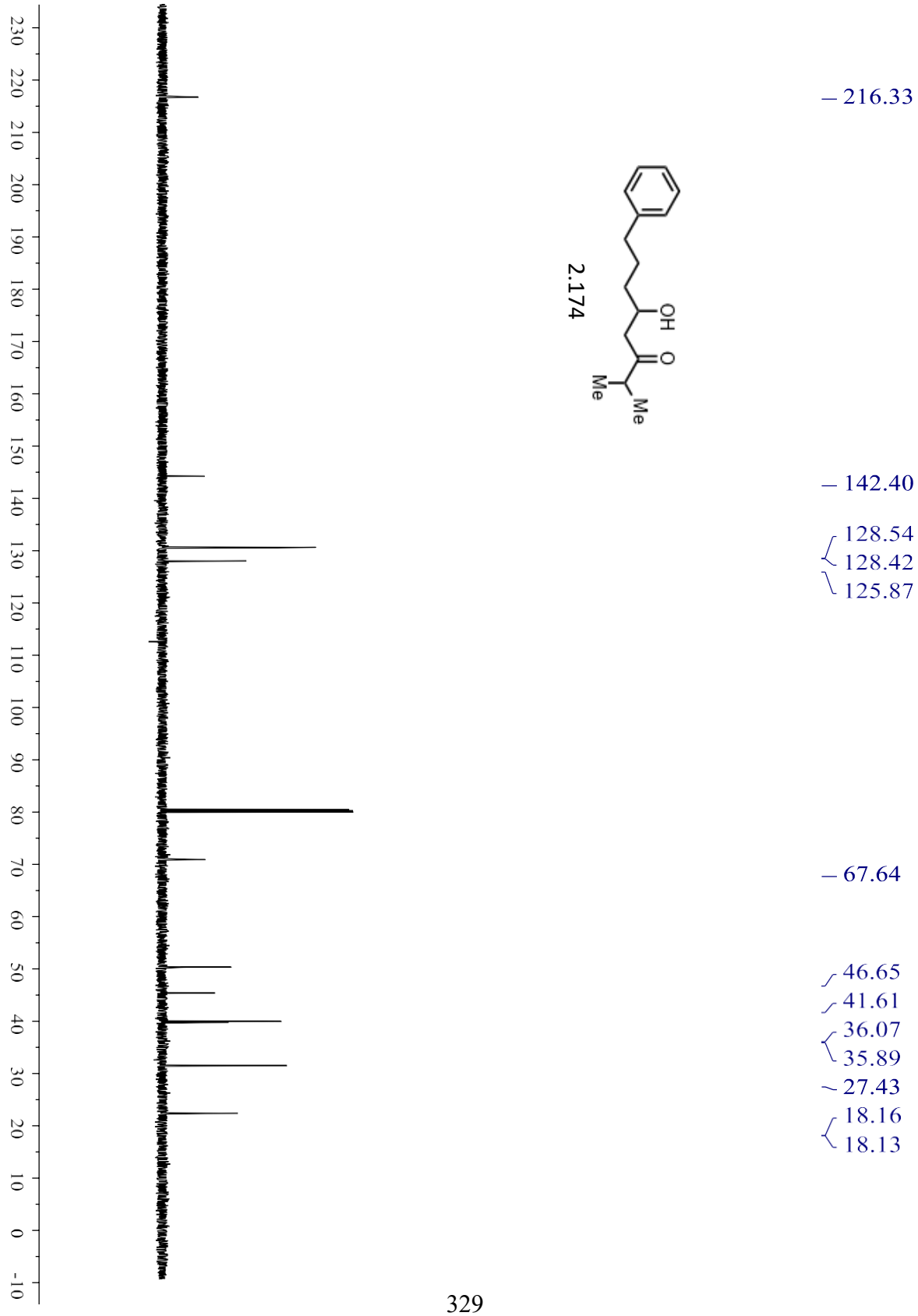
230
220
210
200
190
180
170
160
150
140
130
120
110
100
90
80
70
60
50
40
30
20
10
0
-10
2.174
OH
O
Me
Me
216.33
142.40
128.54
128.42
125.87
67.64
46.65
41.61
36.07
35.89
27.43
18.16
18.13

2.175
OH
O
2.25
3.23
1.00
1.09
3.07
1.14
1.16
4.95
2.63
1.32
1.03
5.53
7.36
7.35
7.35
7.33
7.26
7.26
7.25
7.25
7.24
7.24
3.26
3.26
2.72
2.71
2.70
2.69
2.67
2.67
2.60
2.58
1.91
1.91
1.90
1.90
1.89
1.88
1.88
1.87
1.87
1.86
1.86
1.85
1.85
1.84
1.76
1.75
1.74
1.73
1.72
1.40
1.38
1.38
1.35
1.35
1.32

215.76
142.41
128.54
128.42
125.86
67.61
51.50
46.89
36.06
35.89
28.41
28.40
27.43
25.91
25.69
25.68
2.175
OH
O
230
220
210
200
190
180
170
160
150
140
130
120
110
100
90
80
70
60
50
40
30
20
10
0
-10

2.173
OH
O
Me
11.0 10.5 10.0 9.5 9.0 8.5 8.0 7.5 7.0 6.5 6.0 5.5 5.0 4.5 4.0 3.5 3.0 2.5 2.0 1.5 1.0 0.5 0.0
2.00
2.01
2.84
1.99
1.00
2.93
1.04
1.01
1.02
2.00
1.02
2.02
1.09
7.93
7.92
7.91
7.90
7.29
7.28
7.27
7.26
7.26
7.25
7.20
7.20
7.19
7.18
7.17
6.94
6.93
6.92
6.91
4.22
4.21
4.21
4.20
3.86
3.12
3.12
3.08
3.07
2.99
2.96
2.94
2.92
2.68
2.67
2.65
1.85
1.73
1.71
1.66
1.65
1.64
1.63
1.56
1.55
1.53

210.07

142.34

128.53
128.43
125.89

67.49

50.05

35.97
35.84
27.37

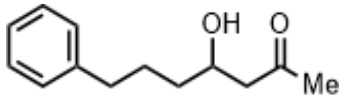

2.173

333

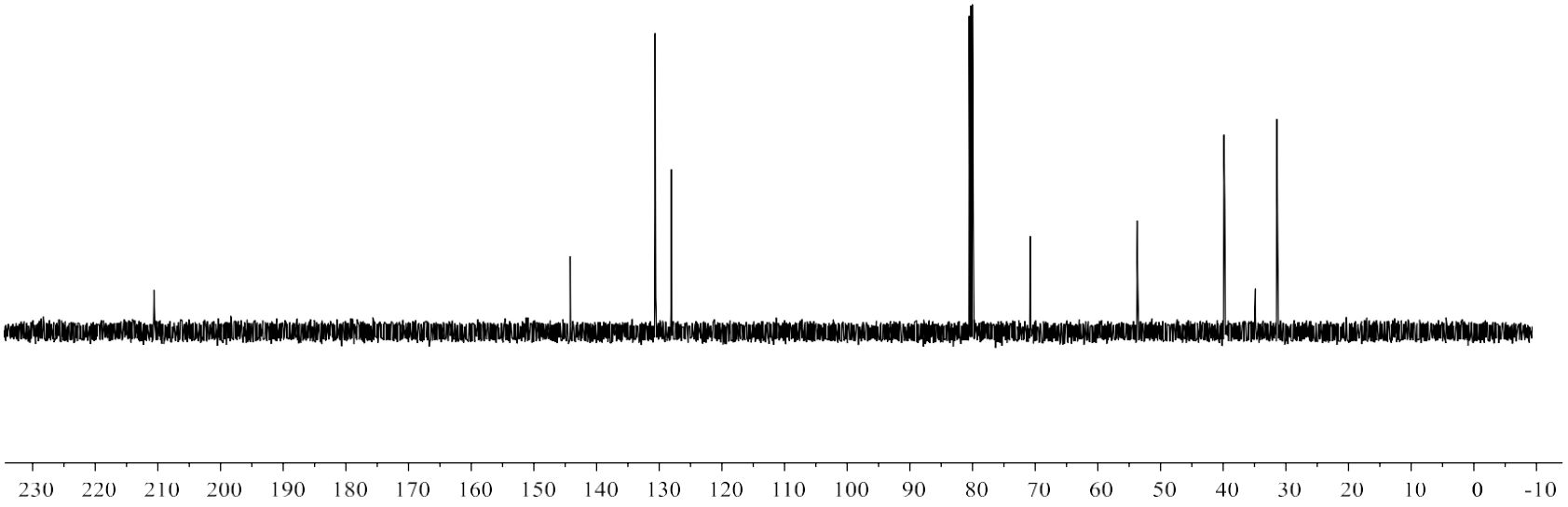

2.176
OH
O
Me
Me
Me
11.0 10.5 10.0 9.5 9.0 8.5 8.0 7.5 7.0 6.5 6.0 5.5 5.0 4.5 4.0 3.5 3.0 2.5 2.0 1.5 1.0 0.5 0.0
2.01
2.82
1.00
0.97
3.19
1.07
1.14
1.23
1.09
1.27
8.46
7.27
7.27
7.25
7.25
7.18
7.17
7.17
7.17
7.17
7.17
4.01
3.26
3.26
2.67
2.67
2.65
2.64
2.64
2.63
2.62
2.54
2.52
2.51
2.49
1.82
1.81
1.80
1.68
1.68
1.67
1.67
1.65
1.61
1.55
1.55
1.54
1.54
1.53
1.45
1.44
1.44
1.43
1.43
1.43
1.12

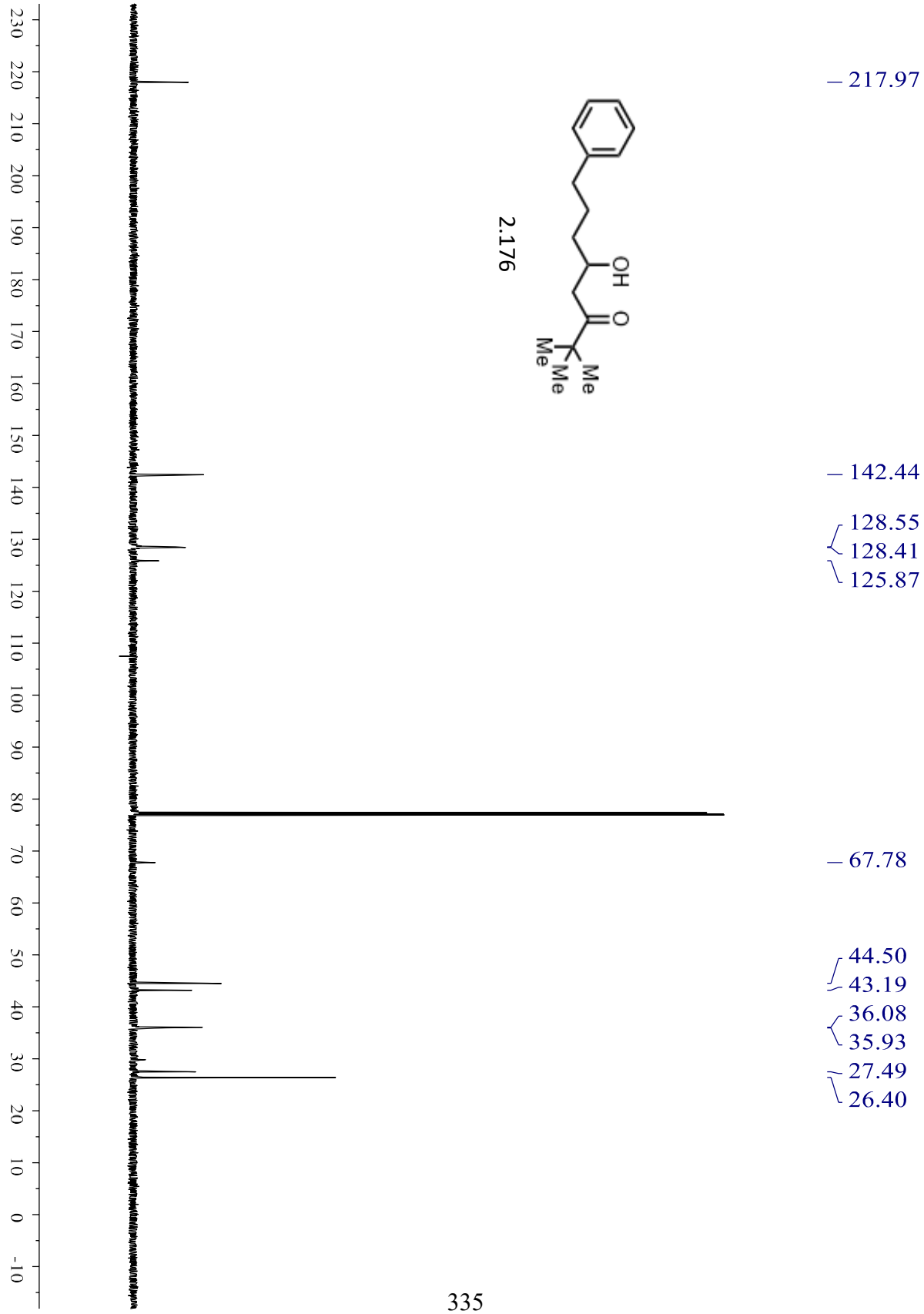
217.97
142.44
128.55
128.41
125.87
67.78
44.50
43.19
36.08
35.93
27.49
26.40
2.176
OH
O
Me
Me
Me
230
220
210
200
190
180
170
160
150
140
130
120
110
100
90
80
70
60
50
40
30
20
10
0
-10

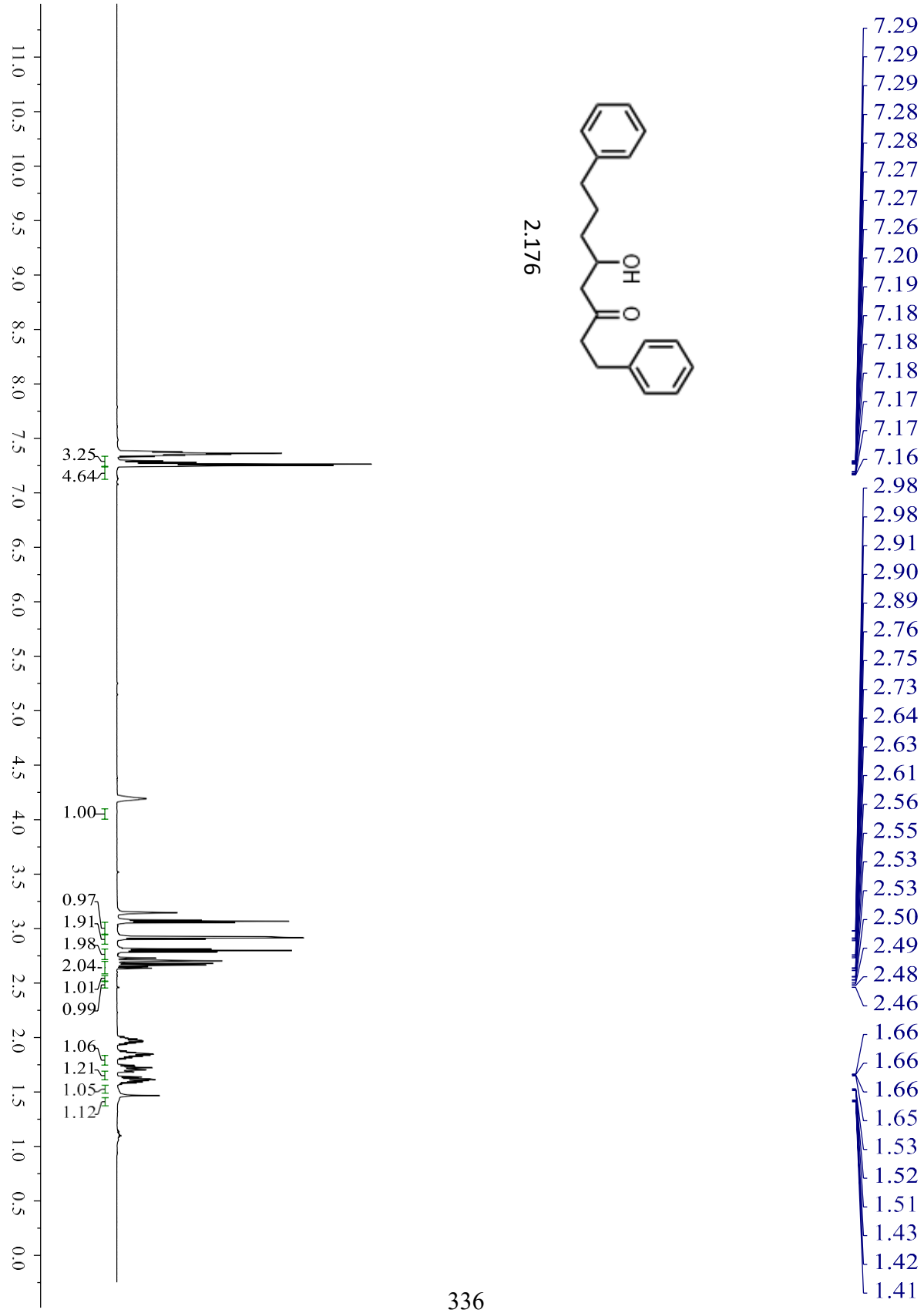
2.176
OH
O
3.25
4.64
1.00
0.97
1.91
1.98
2.04
1.01
0.99
1.06
1.21
1.05
1.12
7.29
7.29
7.29
7.28
7.28
7.27
7.27
7.26
7.20
7.19
7.18
7.18
7.18
7.17
7.17
7.16
2.98
2.98
2.91
2.90
2.89
2.76
2.75
2.73
2.64
2.63
2.61
2.56
2.55
2.53
2.53
2.50
2.49
2.48
2.46
1.66
1.66
1.66
1.65
1.53
1.52
1.51
1.43
1.42
1.41

211.19

142.30
140.79
128.64
128.50
128.41
128.37
126.31
125.86

67.55

49.39
45.11
36.04
35.79
29.61
27.33

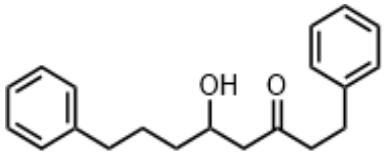

2.176

337

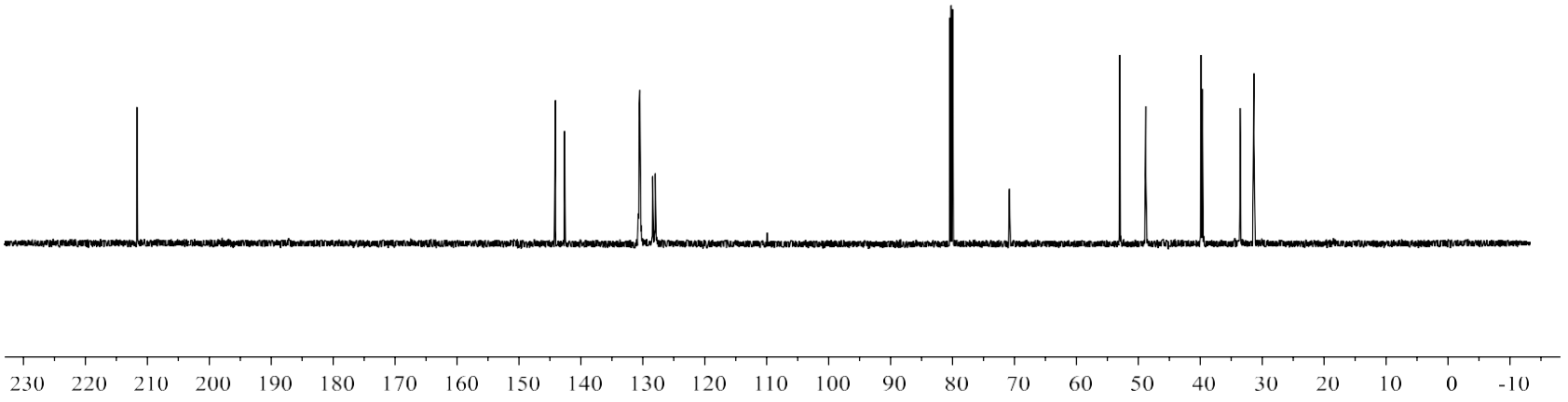


7.28
7.26
7.25
7.18
7.17
7.17
7.16
5.75
5.74
5.02
5.02
4.99
4.99
4.99
4.98
4.98
4.97
4.96
4.05
4.04
4.03
2.64
2.63
2.61
2.57
2.57
2.54
2.54
2.50
2.48
2.45
2.42
2.41
2.39
2.06
2.05
2.04
2.03
1.69
1.68
1.67
1.66
1.64
1.43
1.42

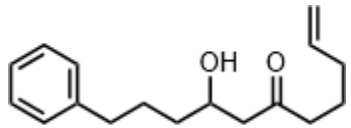
OH
O

2.177

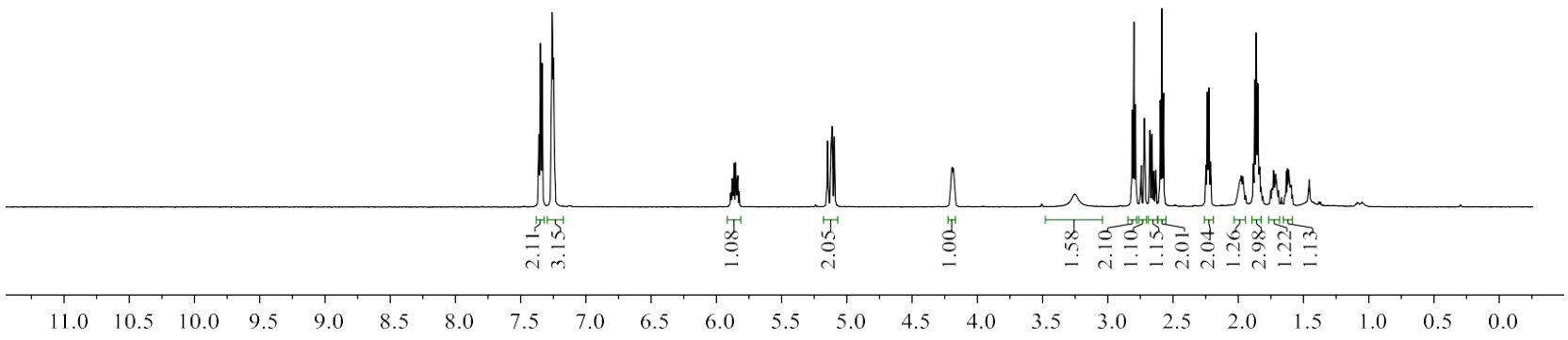
2.11
3.15
1.08
2.05
1.00
1.58
2.10
1.10
1.15
2.01
2.04
1.26
2.98
1.22
1.13
11.0
10.5
10.0
9.5
9.0
8.5
8.0
7.5
7.0
6.5
6.0
5.5
5.0
4.5
4.0
3.5
3.0
2.5
2.0
1.5
1.0
0.5
0.0

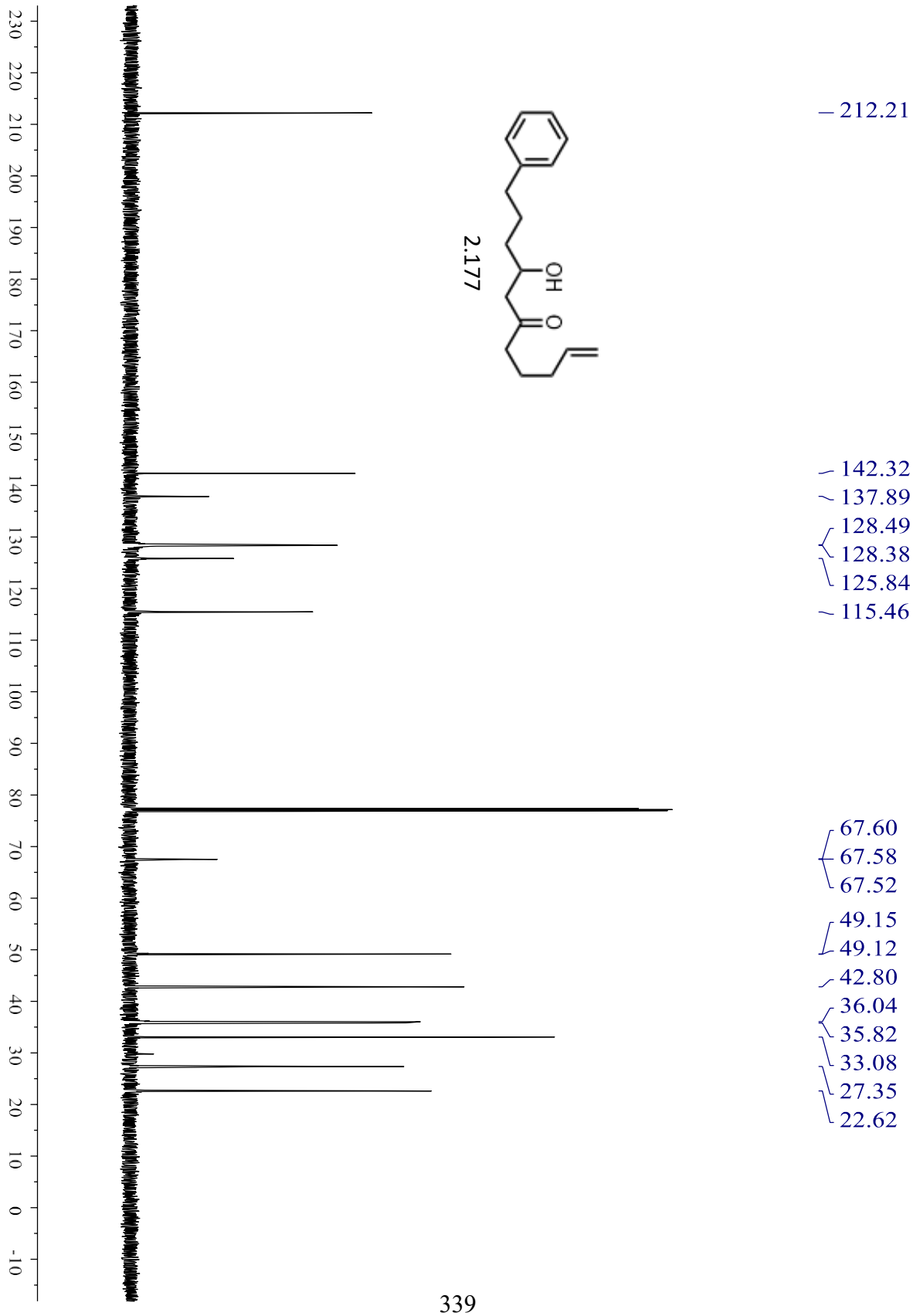
230
220
210
200
190
180
170
160
150
140
130
120
110
100
90
80
70
60
50
40
30
20
10
0
-10
2.177
OH
O
212.21
142.32
137.89
128.49
128.38
125.84
115.46
67.60
67.58
67.52
49.15
49.12
42.80
36.04
35.82
33.08
27.35
22.62

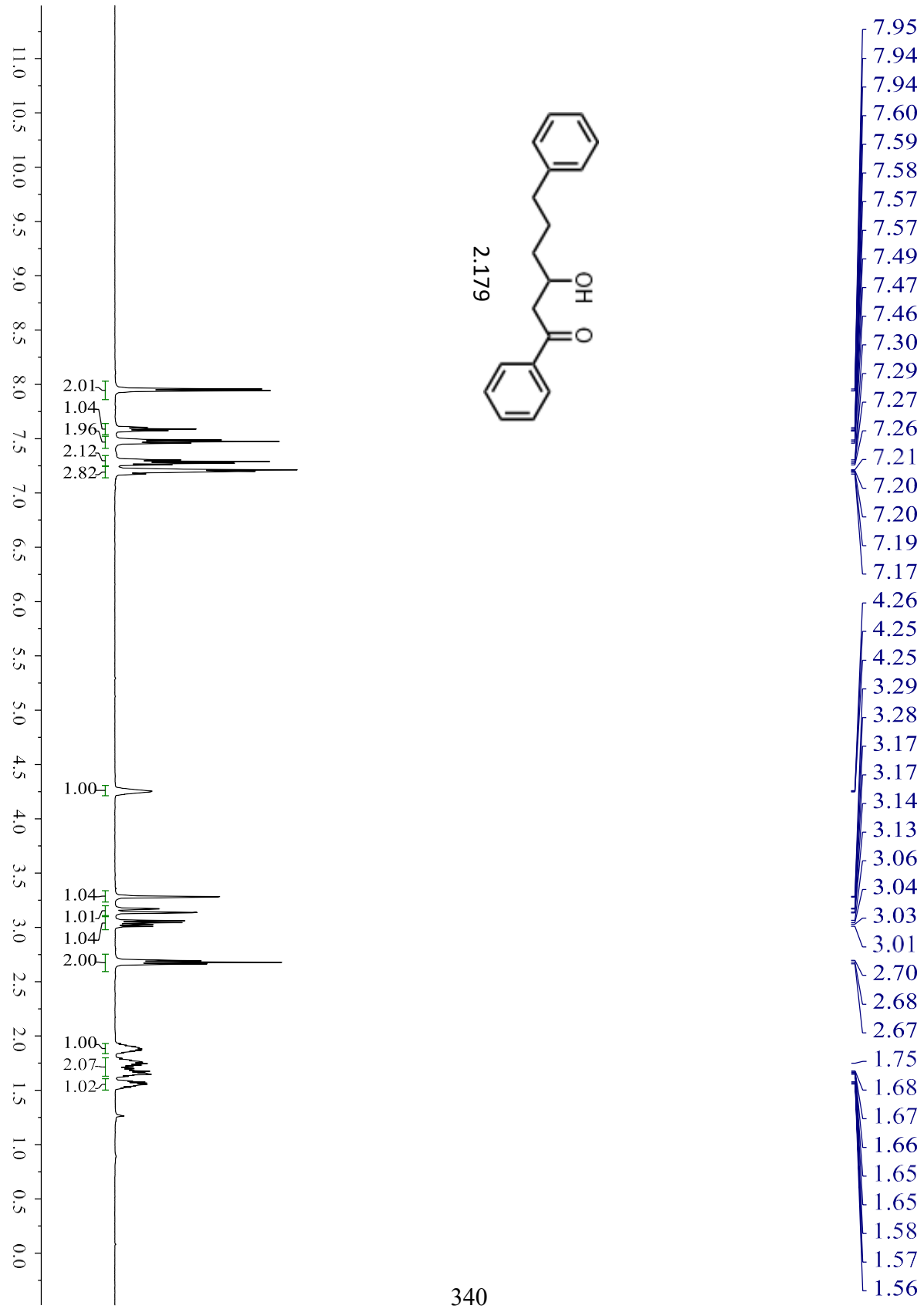
11.0 10.5 10.0 9.5 9.0 8.5 8.0 7.5 7.0 6.5 6.0 5.5 5.0 4.5 4.0 3.5 3.0 2.5 2.0 1.5 1.0 0.5 0.0
2.01
1.04
1.96
2.12
2.82
1.00
1.04
1.01
1.04
2.00
1.00
2.07
1.02
2.179
OH
O
7.95
7.94
7.94
7.60
7.59
7.58
7.57
7.57
7.49
7.47
7.46
7.30
7.29
7.27
7.26
7.21
7.20
7.20
7.19
7.17
4.26
4.25
4.25
3.29
3.28
3.17
3.17
3.14
3.13
3.06
3.04
3.03
3.01
2.70
2.68
2.67
1.75
1.68
1.67
1.66
1.65
1.65
1.58
1.57
1.56

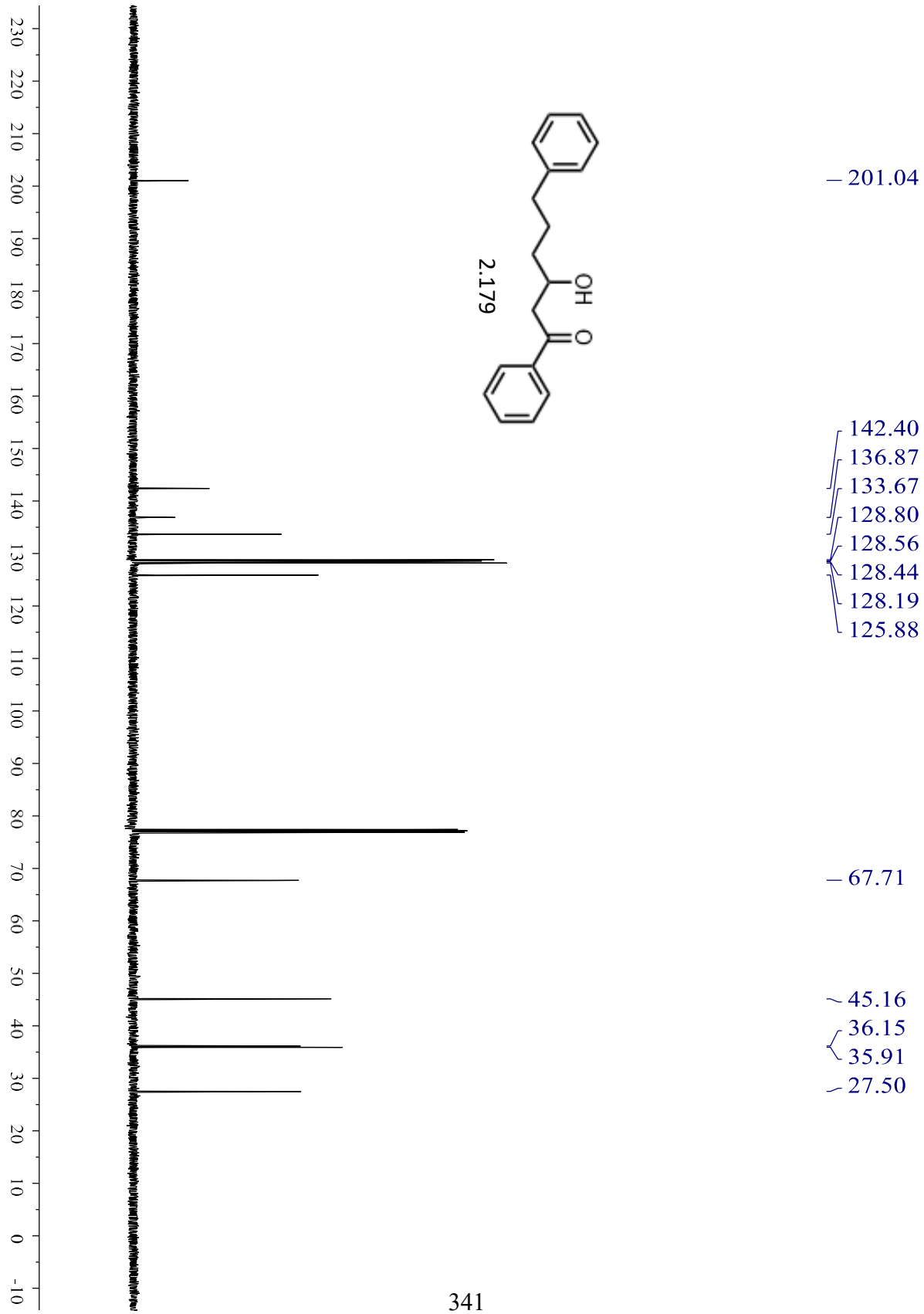
230 220 210 200 190 180 170 160 150 140 130 120 110 100 90 80 70 60 50 40 30 20 10 0 -10
2.179
OH
O
201.04
142.40
136.87
133.67
128.80
128.56
128.44
128.19
125.88
67.71
45.16
36.15
35.91
27.50

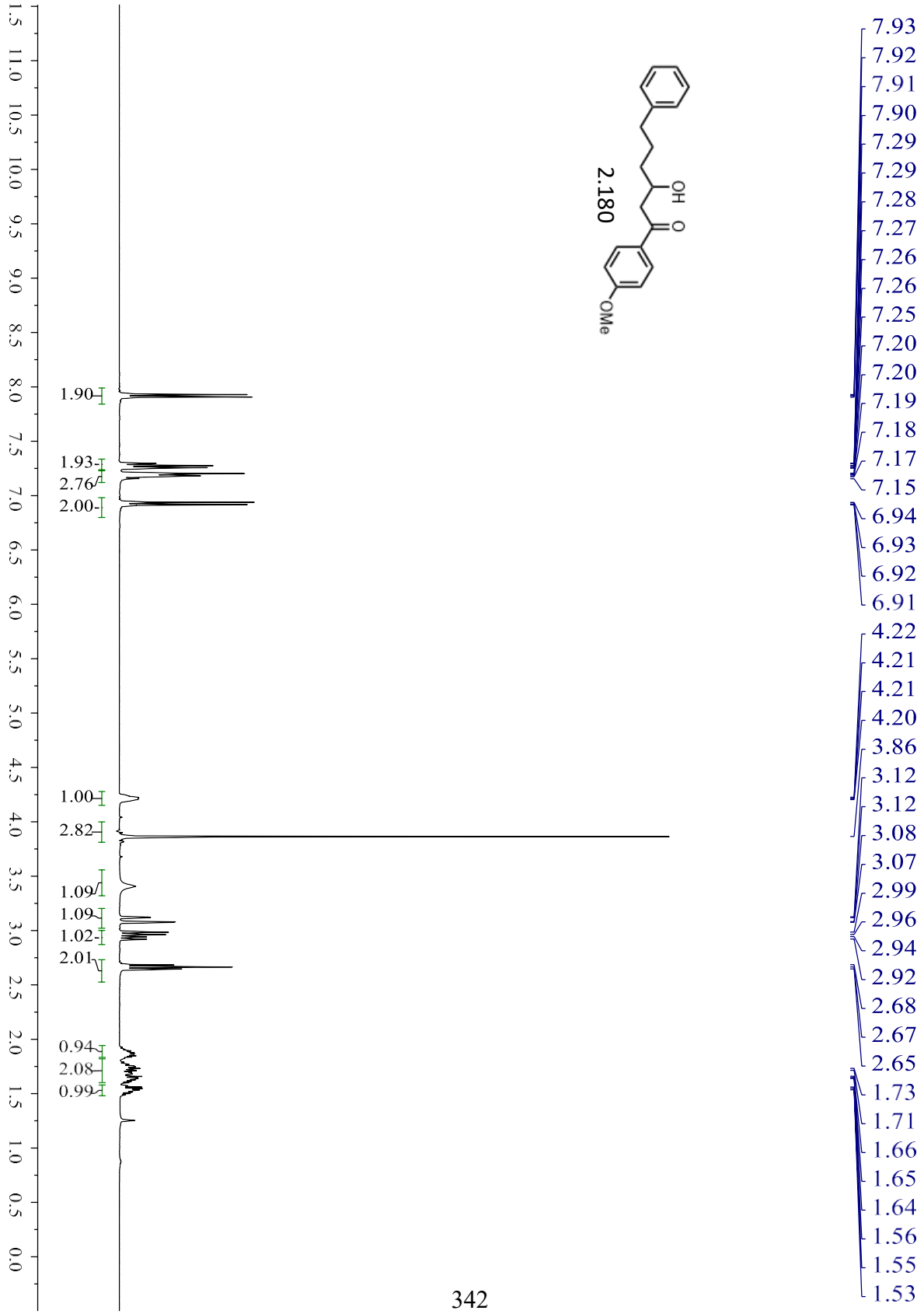
2.180
OH
O
OMe
1.90
1.93
2.76
2.00
1.00
2.82
1.09
1.09
1.02
2.01
0.94
2.08
0.99
7.93
7.92
7.91
7.90
7.29
7.29
7.28
7.27
7.26
7.26
7.25
7.20
7.20
7.19
7.18
7.17
7.15
6.94
6.93
6.92
6.91
4.22
4.21
4.21
4.20
3.86
3.12
3.12
3.08
3.07
2.99
2.96
2.94
2.92
2.68
2.67
2.65
1.73
1.71
1.66
1.65
1.64
1.56
1.55
1.53

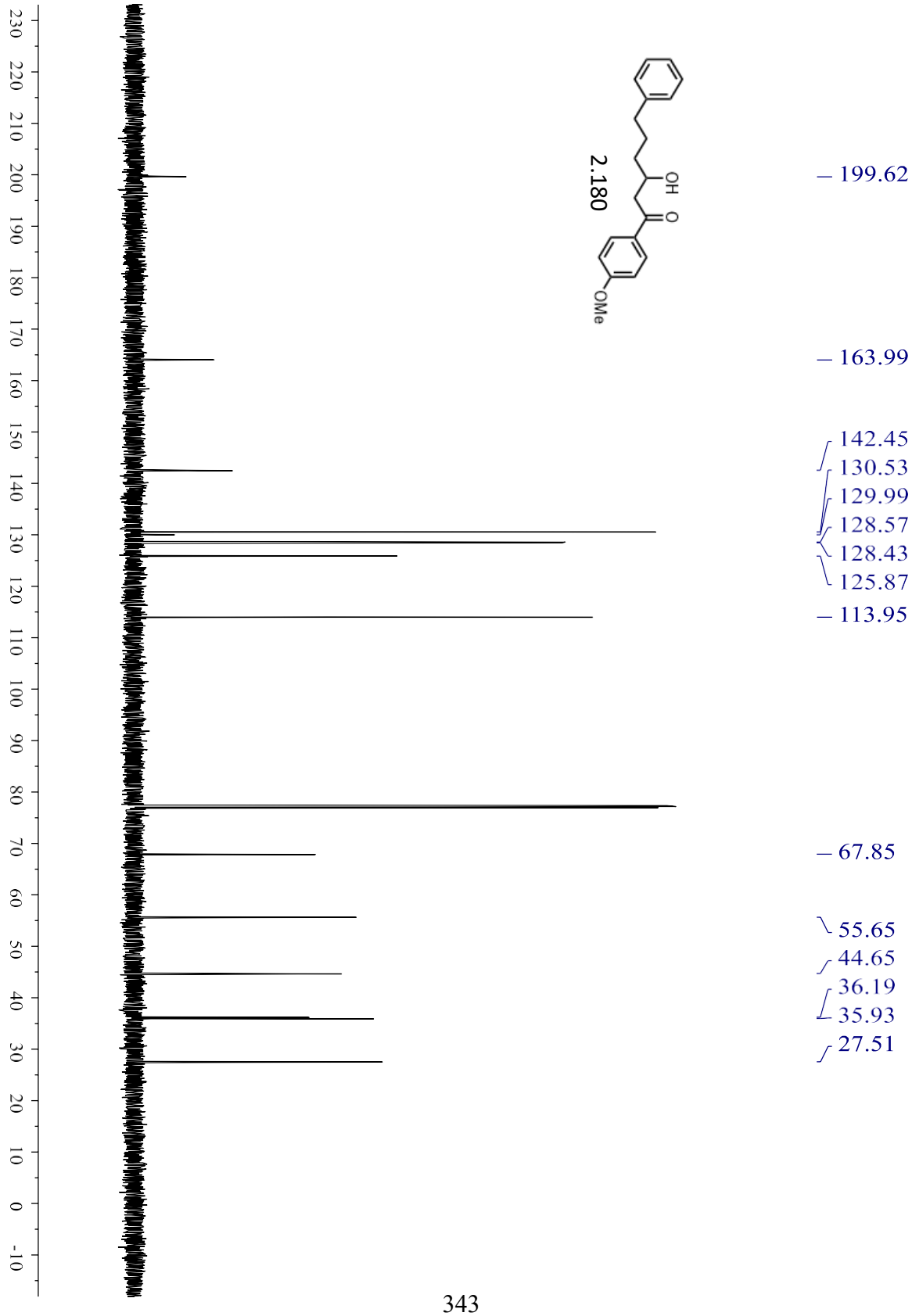
2.180
OH
O
OMe
199.62
163.99
142.45
130.53
129.99
128.57
128.43
125.87
113.95
67.85
55.65
44.65
36.19
35.93
27.51
230
220
210
200
190
180
170
160
150
140
130
120
110
100
90
80
70
60
50
40
30
20
10
0
-10

11.0
10.5
10.0
9.5
9.0
8.5
8.0
7.5
7.0
6.5
6.0
5.5
5.0
4.5
4.0
3.5
3.0
2.5
2.0
1.5
1.0
0.5
0.0
1.94
1.94
2.24
2.98
1.00
1.00
1.01
1.01
1.93
0.99
1.09
1.11
1.05
2.182
OH
O
Cl
7.88
7.87
7.87
7.45
7.45
7.44
7.44
7.43
7.43
7.30
7.29
7.28
7.28
7.27
7.26
7.26
7.20
7.19
7.19
7.19
7.18
4.24
3.17
3.16
3.11
3.11
3.10
3.10
3.08
3.08
3.07
3.07
3.03
3.03
3.02
3.02
3.00
2.99
2.69
2.67
2.66
1.66
1.66
1.65
1.56

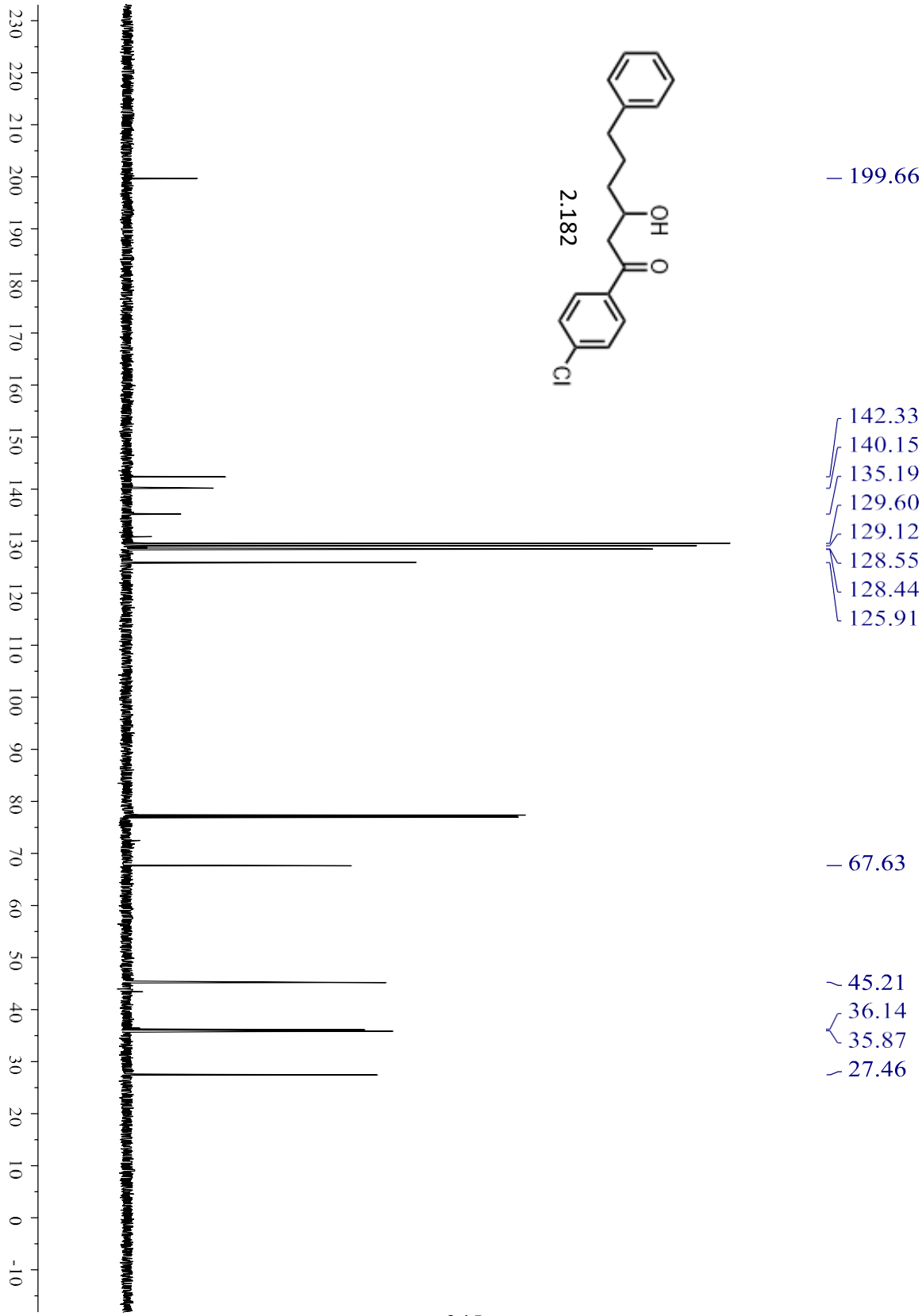
2.182
OH
O
Cl
199.66
142.33
140.15
135.19
129.60
129.12
128.55
128.44
125.91
67.63
45.21
36.14
35.87
27.46
230
220
210
200
190
180
170
160
150
140
130
120
110
100
90
80
70
60
50
40
30
20
10
0
-10

11.0
10.5
10.0
9.5
9.0
8.5
8.0
7.5
7.0
6.5
6.0
5.5
5.0
4.5
4.0
3.5
3.0
2.5
2.0
1.5
1.0
0.5
0.0
1.87
1.94
2.15
2.70
1.00
0.94
0.96
0.94
1.87
0.96
0.92
1.02
1.33
2.183
OH
O
CF3
8.05
8.04
7.74
7.73
7.29
7.28
7.27
7.26
7.20
7.19
4.28
4.27
4.26
4.26
3.15
3.15
3.12
3.12
3.10
3.09
3.07
3.06
3.03
3.03
3.02
2.69
2.68
2.67
1.89
1.88
1.88
1.87
1.75
1.75
1.73
1.67
1.67
1.66
1.66
1.65
1.59
1.58
1.57
1.56
1.56

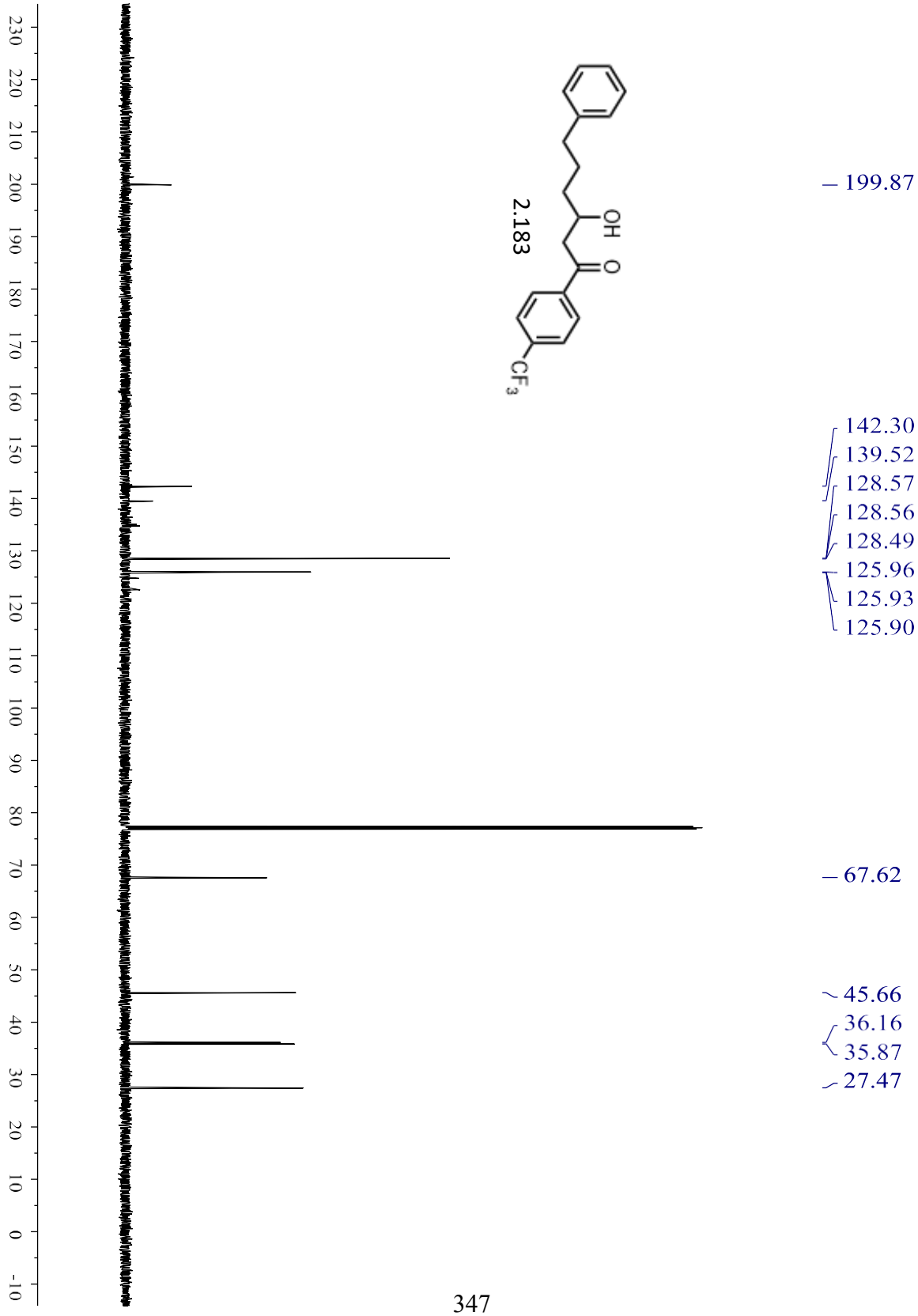
199.87
142.30
139.52
128.57
128.56
128.49
125.96
125.93
125.90
67.62
45.66
36.16
35.87
27.47
2.183
OH
O
CF3

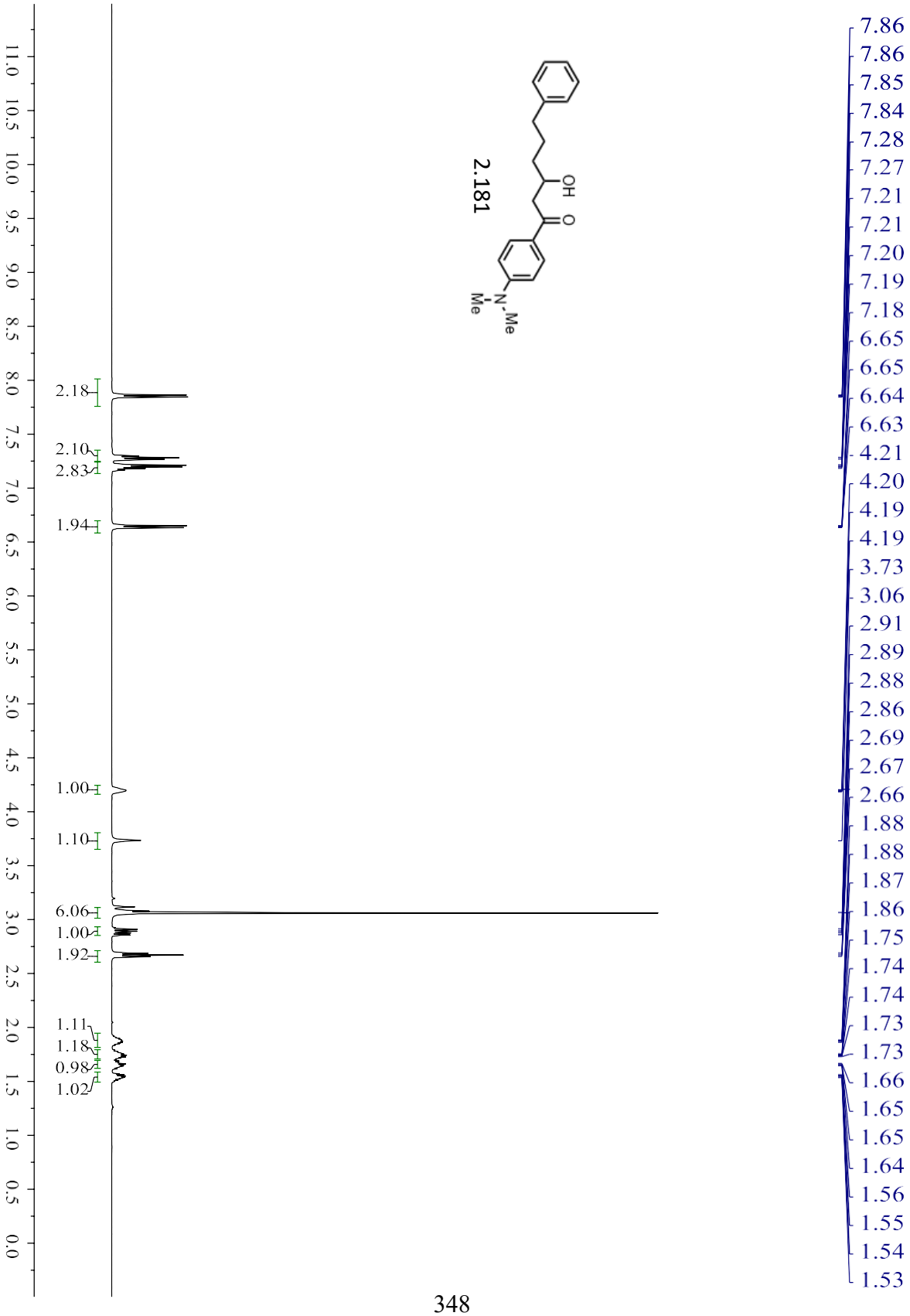
2.181
OH
O
N
Me
Me
2.18
2.10
2.83
1.94
1.00
1.10
6.06
1.00
1.92
1.11
1.18
0.98
1.02
11.0 10.5 10.0 9.5 9.0 8.5 8.0 7.5 7.0 6.5 6.0 5.5 5.0 4.5 4.0 3.5 3.0 2.5 2.0 1.5 1.0 0.5 0.0
7.86
7.86
7.85
7.84
7.28
7.27
7.21
7.21
7.20
7.19
7.18
6.65
6.65
6.64
6.63
4.21
4.20
4.19
4.19
3.73
3.06
2.91
2.89
2.88
2.86
2.69
2.67
2.66
1.88
1.88
1.87
1.86
1.75
1.74
1.74
1.73
1.73
1.66
1.65
1.65
1.64
1.56
1.55
1.54
1.53

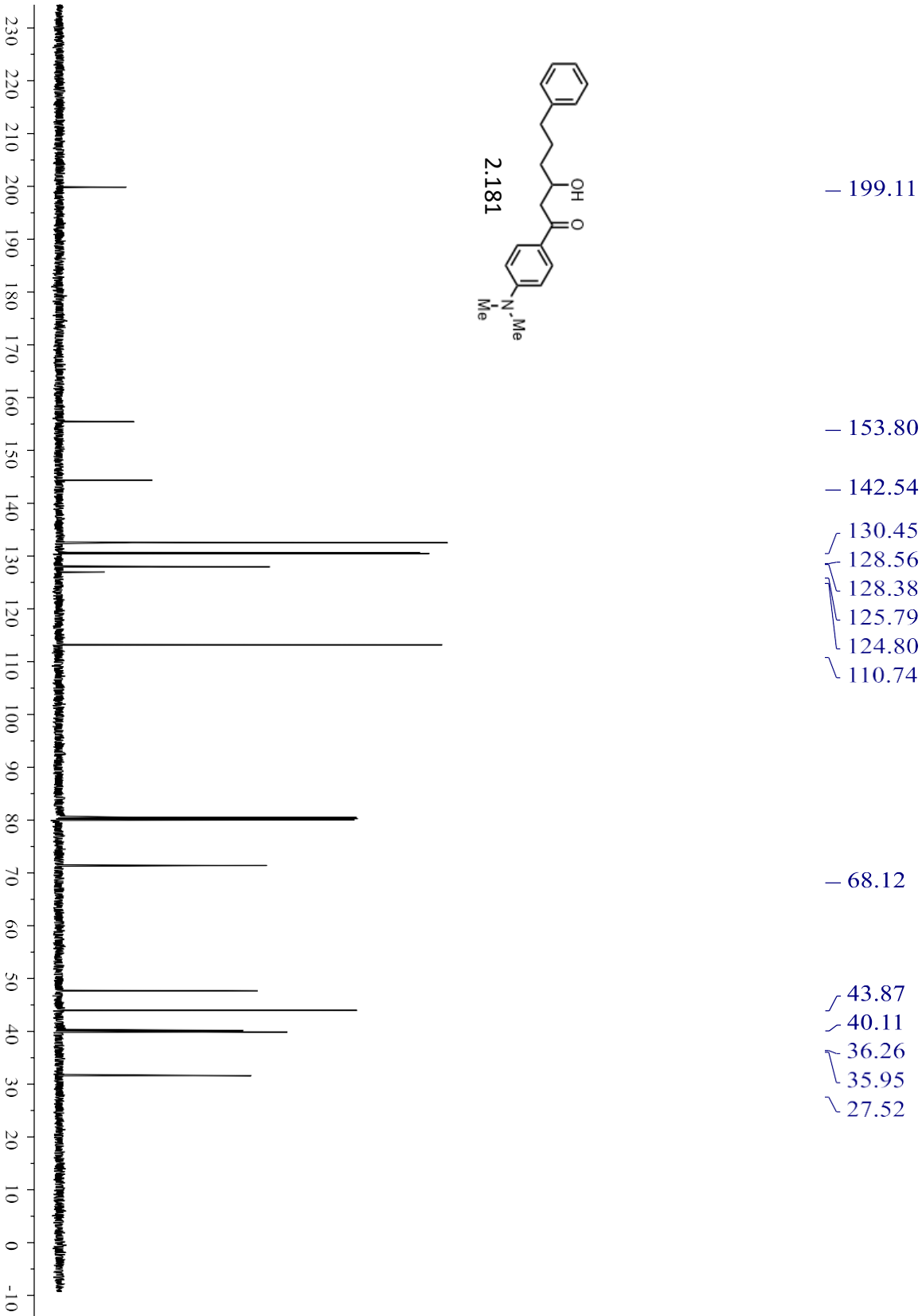
2.181
OH
O
N
Me
Me
199.11
153.80
142.54
130.45
128.56
128.38
125.79
124.80
110.74
68.12
43.87
40.11
36.26
35.95
27.52
230
220
210
200
190
180
170
160
150
140
130
120
110
100
90
80
70
60
50
40
30
20
10
0
-10

2.184
Me
OH
O
Me
11.0
10.5
10.0
9.5
9.0
8.5
8.0
7.5
7.0
6.5
6.0
5.5
5.0
4.5
4.0
3.5
3.0
2.5
2.0
1.5
1.0
0.5
0.0
1.00
1.19
1.01
1.04
1.91
1.96
13.36
2.77
2.80
4.02
4.02
4.01
4.01
4.00
3.06
2.59
2.59
2.56
2.55
2.50
2.48
2.46
2.45
2.41
2.39
2.38
1.62
1.60
1.59
1.57
1.47
1.40
1.39
1.39
1.38
1.37
1.36
1.36
1.31
1.29
1.29
1.28
1.27
1.26
1.25
1.24
1.23
1.22
0.92
0.90
0.89
0.87
0.86
0.85

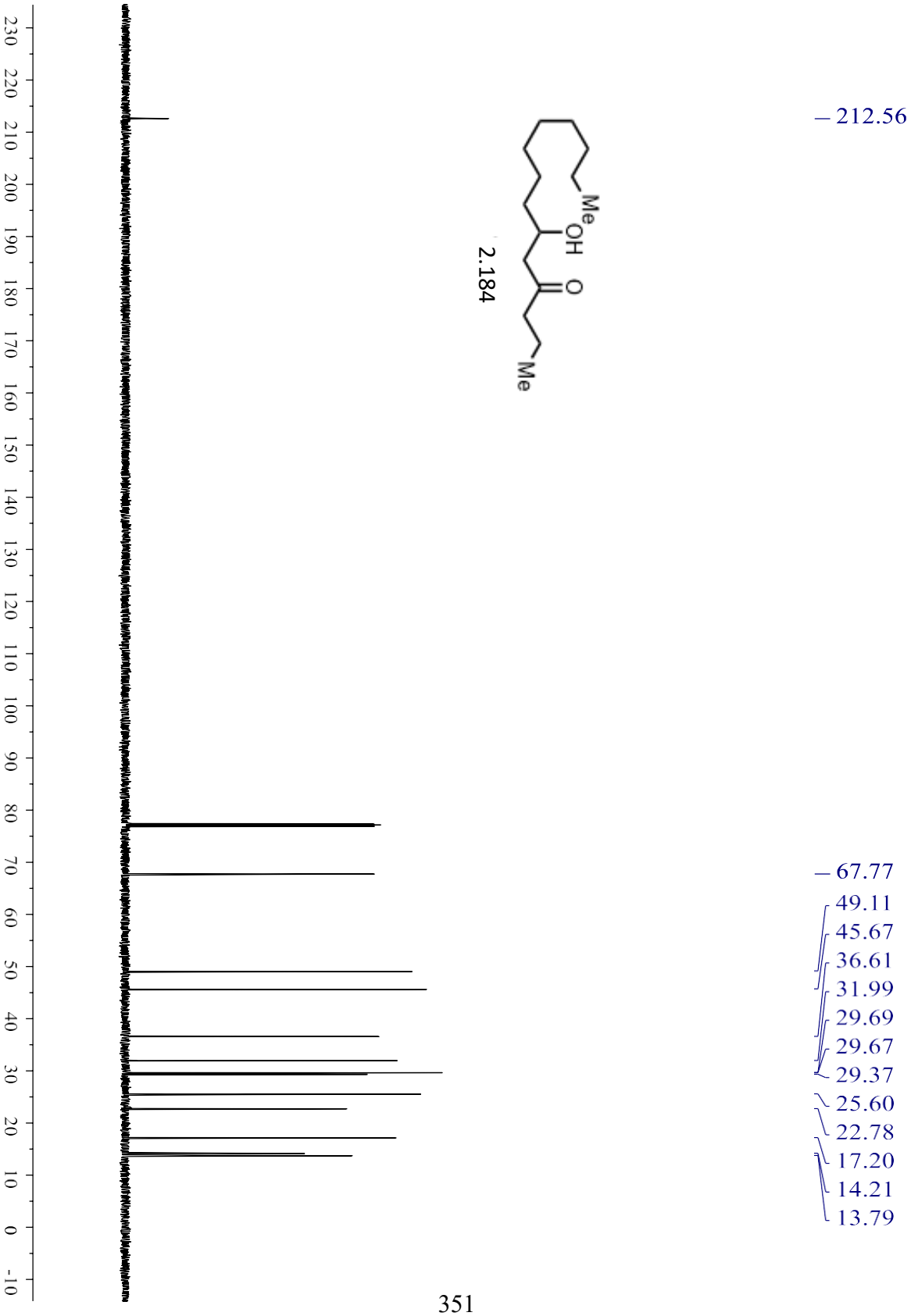
230 220 210 200 190 180 170 160 150 140 130 120 110 100 90 80 70 60 50 40 30 20 10 0 -10
Me
OH
O
Me
2.184
212.56
67.77
49.11
45.67
36.61
31.99
29.69
29.67
29.37
25.60
22.78
17.20
14.21
13.79

11.5 11.0 10.5 10.0 9.5 9.0 8.5 8.0 7.5 7.0 6.5 6.0 5.5 5.0 4.5 4.0 3.5 3.0 2.5 2.0 1.5 1.0 0.5 0.0
1.00
1.00
1.01
1.07
1.90
1.07
2.09
3.89
1.11
3.24
2.04
2.91
OH
O
2.186
Me
2.97
2.97
2.60
2.59
2.57
2.56
2.51
2.50
2.42
2.41
2.40
1.75
1.75
1.75
1.74
1.74
1.74
1.73
1.73
1.65
1.65
1.65
1.64
1.64
1.63
1.63
1.63
1.62
1.62
1.61
1.59
1.58
1.23
1.22
1.22
1.21
1.20
1.20
1.14
1.03
1.01
1.00
0.92
0.91
0.90

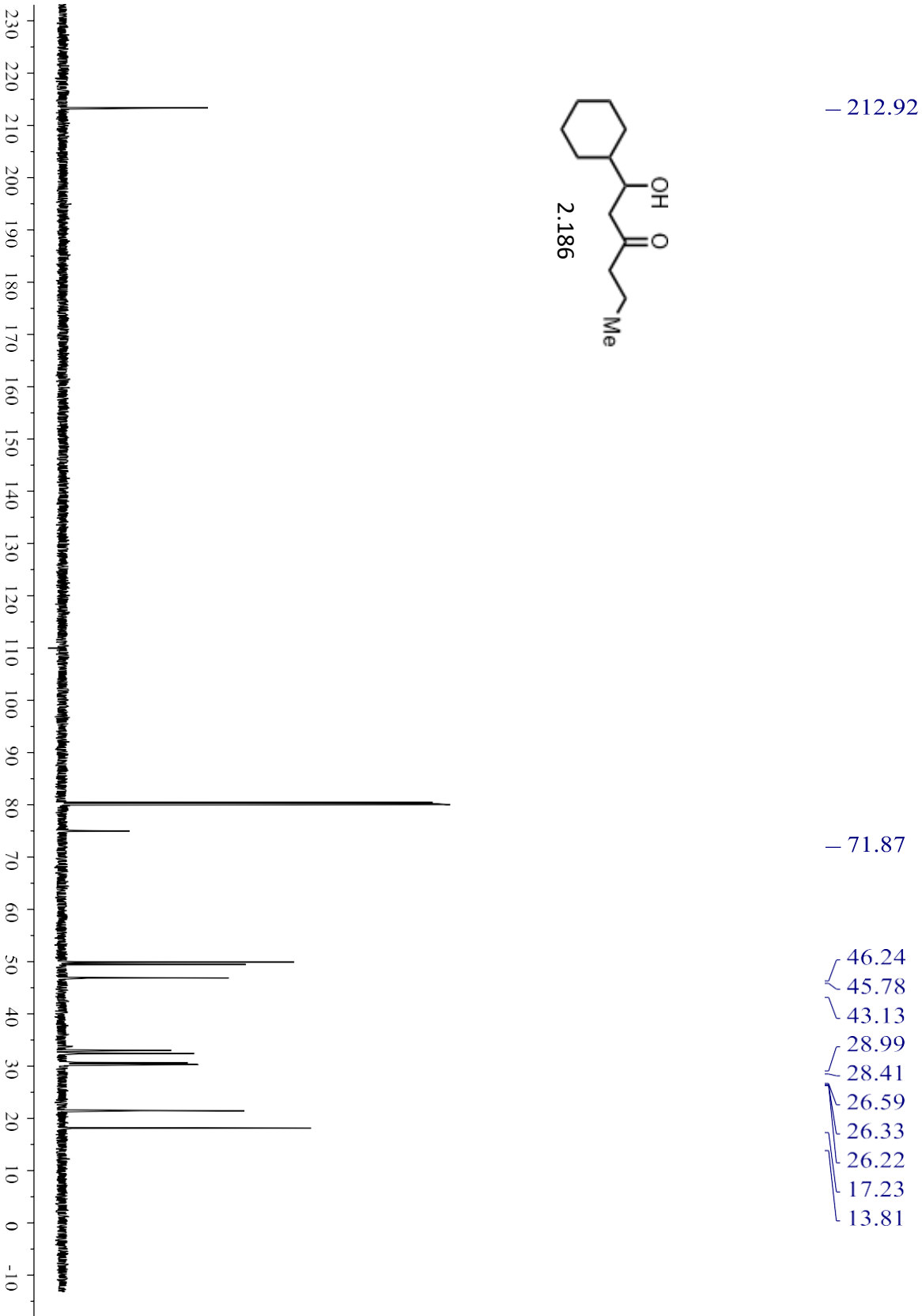
212.92
71.87
46.24
45.78
43.13
28.99
28.41
26.59
26.33
26.22
17.23
13.81
2.186
OH
O
Me
230
220
210
200
190
180
170
160
150
140
130
120
110
100
90
80
70
60
50
40
30
20
10
0
-10

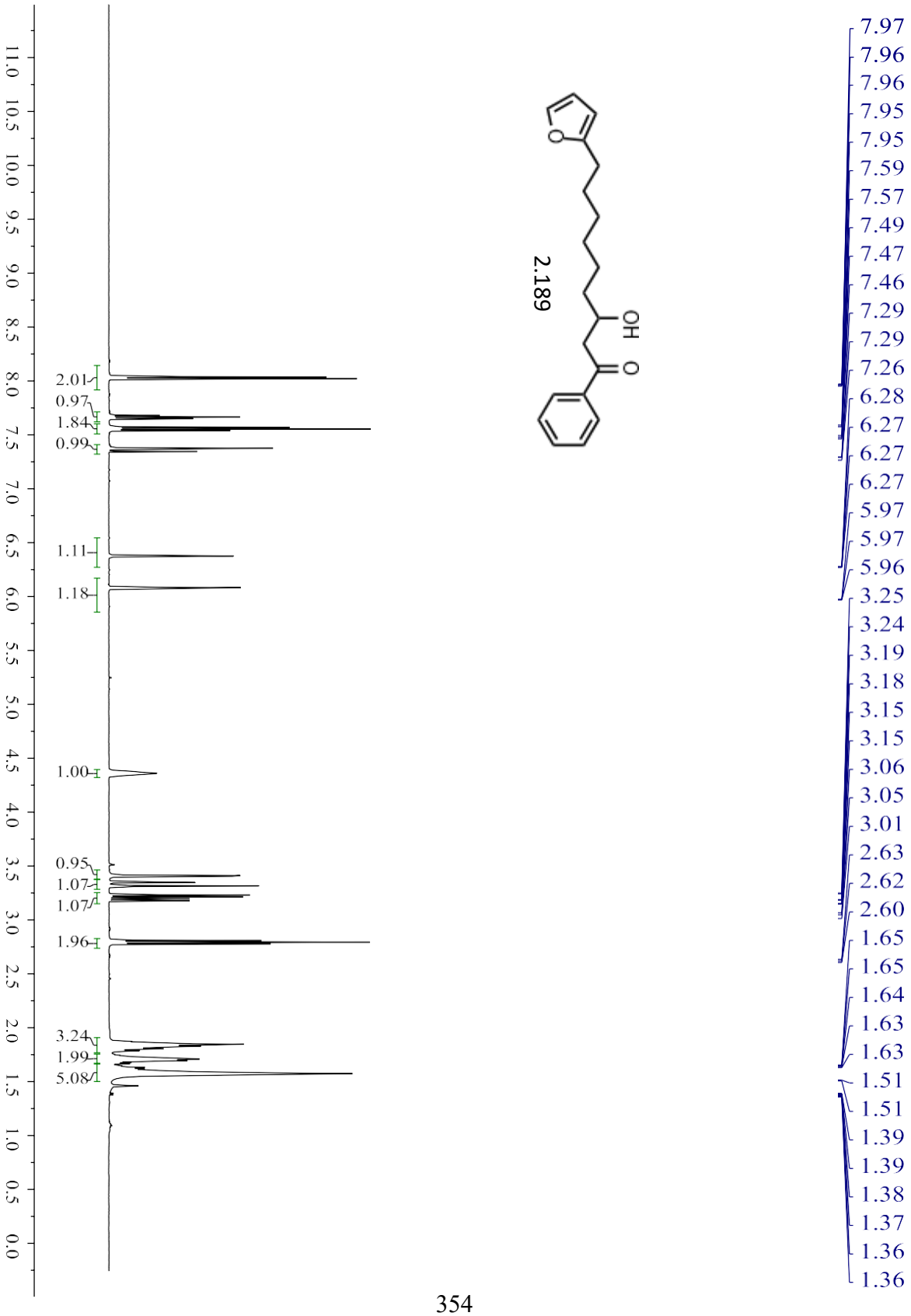
11.0 10.5 10.0 9.5 9.0 8.5 8.0 7.5 7.0 6.5 6.0 5.5 5.0 4.5 4.0 3.5 3.0 2.5 2.0 1.5 1.0 0.5 0.0
2.01
0.97
1.84
0.99
1.11
1.18
1.00
0.95
1.07
1.07
1.96
3.24
1.99
5.08
2.189
OH
O
7.97
7.96
7.96
7.95
7.95
7.59
7.57
7.49
7.47
7.46
7.29
7.29
7.26
6.28
6.27
6.27
6.27
5.97
5.97
5.96
3.25
3.24
3.19
3.18
3.15
3.15
3.06
3.05
3.01
2.63
2.62
2.60
1.65
1.65
1.64
1.63
1.63
1.51
1.51
1.39
1.39
1.38
1.37
1.36
1.36

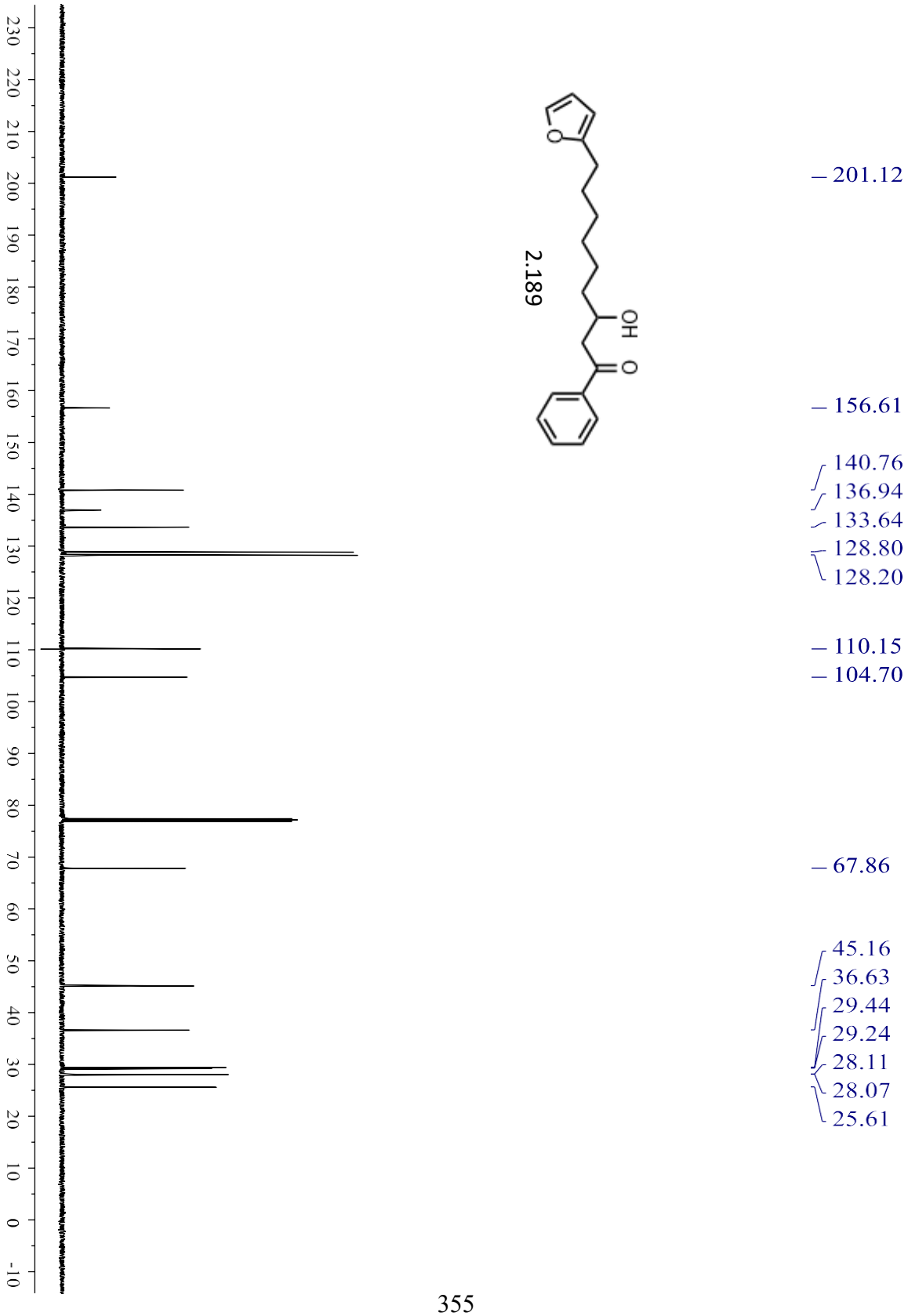
230 220 210 200 190 180 170 160 150 140 130 120 110 100 90 80 70 60 50 40 30 20 10 0 -10
2.189
OH
O
201.12
156.61
140.76
136.94
133.64
128.80
128.20
110.15
104.70
67.86
45.16
36.63
29.44
29.24
28.11
28.07
25.61

TBDPSO
OH
O
Me
2.188
4.35
5.97
1.00
1.98
0.97
2.28
2.10
6.45
8.80
2.96
7.67
7.67
7.65
7.65
7.43
7.41
7.41
7.40
7.38
7.36
4.06
4.04
4.04
4.03
3.70
3.69
3.67
3.24
3.23
2.58
2.55
2.54
2.53
2.51
2.42
2.41
2.39
1.72
1.71
1.69
1.67
1.66
1.64
1.62
1.60
1.59
1.57
1.55
1.53
1.52
1.51
1.05
0.94
0.92
0.91

212.31

135.71
135.70
129.74
127.78

67.62
64.03

49.23
45.70

33.30
28.74
27.00
19.34
17.23
13.84

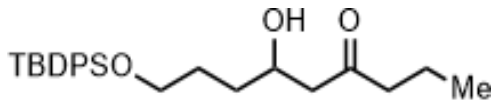

2.188

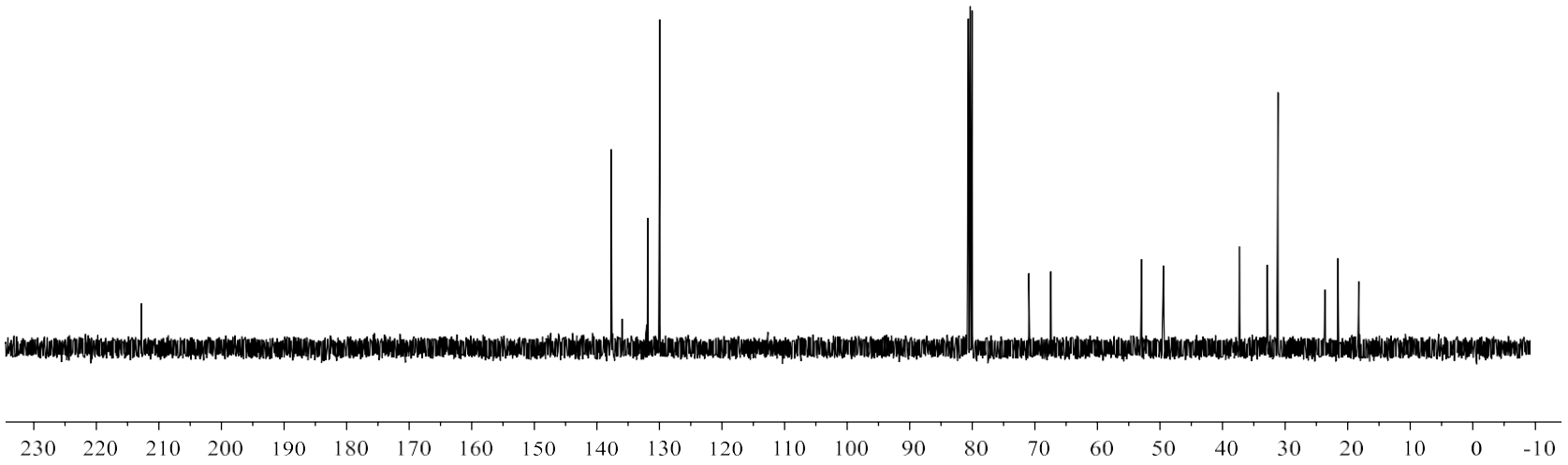

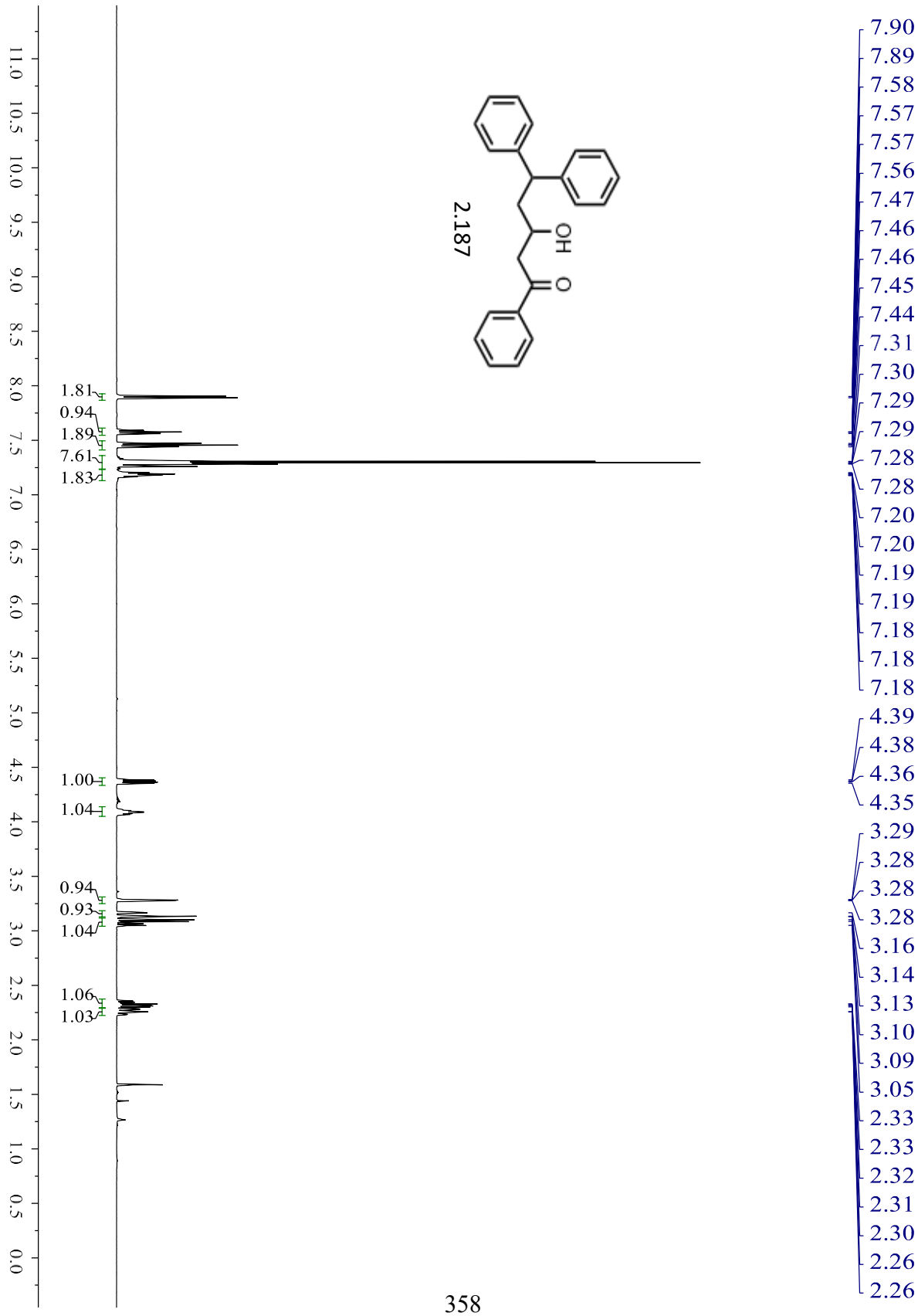
11.0 10.5 10.0 9.5 9.0 8.5 8.0 7.5 7.0 6.5 6.0 5.5 5.0 4.5 4.0 3.5 3.0 2.5 2.0 1.5 1.0 0.5 0.0
1.81
0.94
1.89
7.61
1.83
1.00
1.04
0.94
0.93
1.04
1.06
1.03
2.187
OH
O
7.90
7.89
7.58
7.57
7.57
7.56
7.47
7.46
7.46
7.45
7.44
7.31
7.30
7.29
7.29
7.28
7.28
7.20
7.20
7.19
7.19
7.18
7.18
7.18
4.39
4.38
4.36
4.35
3.29
3.28
3.28
3.28
3.16
3.14
3.13
3.10
3.09
3.05
2.33
2.33
2.32
2.31
2.30
2.26
2.26

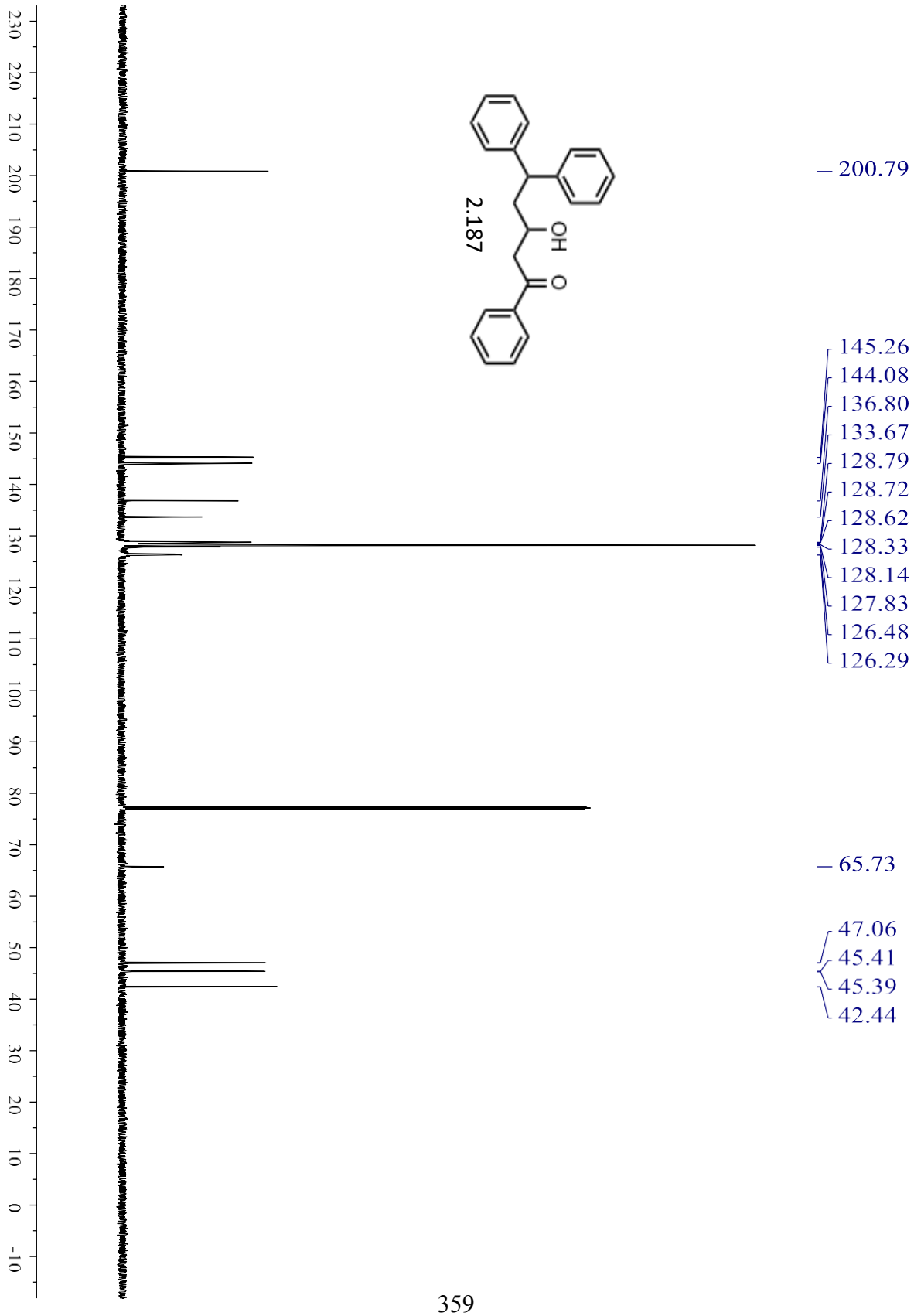
230
220
210
200
190
180
170
160
150
140
130
120
110
100
90
80
70
60
50
40
30
20
10
0
-10
2.187
OH
O
200.79
145.26
144.08
136.80
133.67
128.79
128.72
128.62
128.33
128.14
127.83
126.48
126.29
65.73
47.06
45.41
45.39
42.44

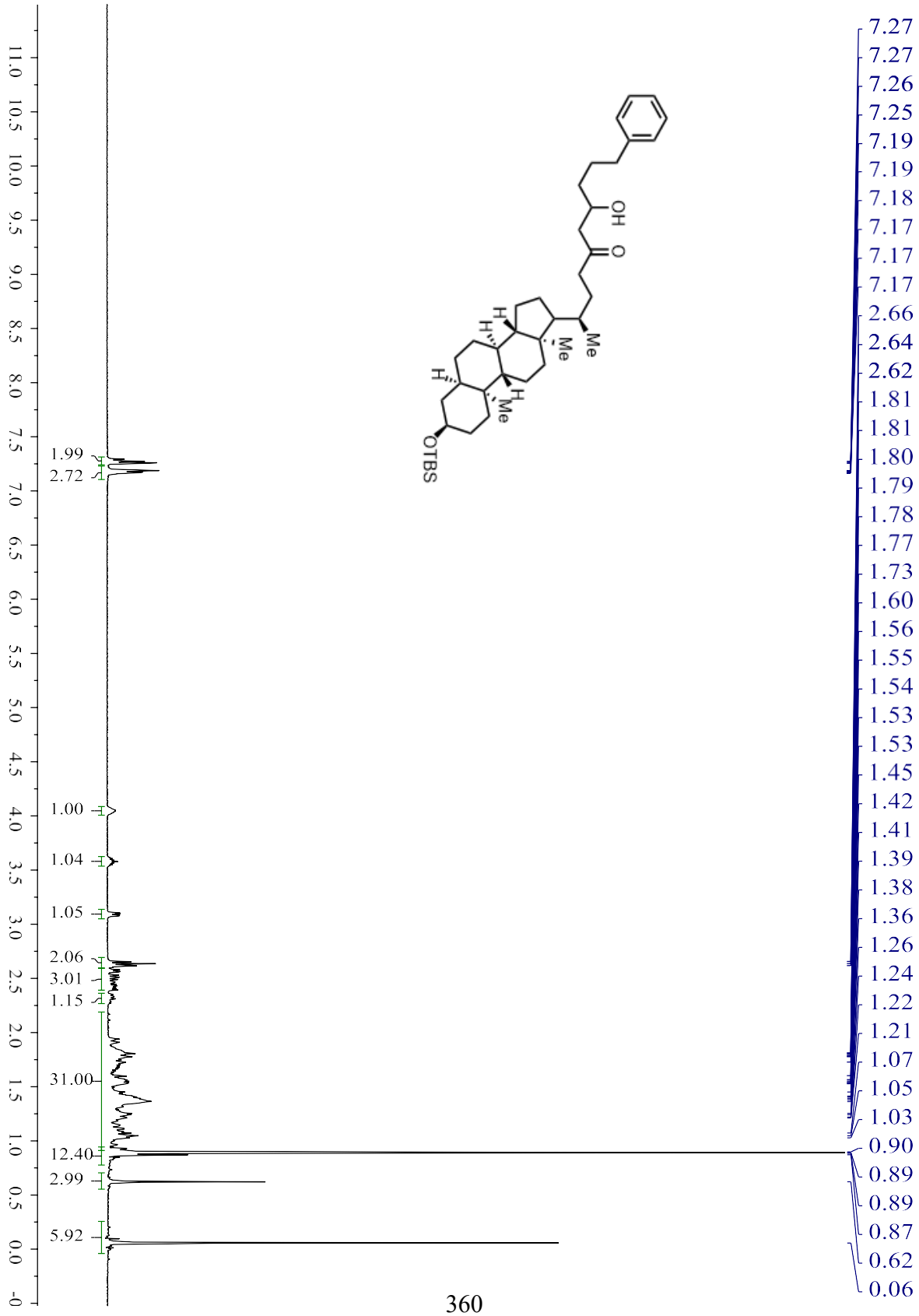
11.0 10.5 10.0 9.5 9.0 8.5 8.0 7.5 7.0 6.5 6.0 5.5 5.0 4.5 4.0 3.5 3.0 2.5 2.0 1.5 1.0 0.5 0.0 -0
1.99
2.72
1.00
1.04
1.05
2.06
3.01
1.15
31.00
12.40
2.99
5.92
OH
O
Me
Me
H
H
H
Me
OTBS
7.27
7.27
7.26
7.25
7.19
7.19
7.18
7.17
7.17
7.17
2.66
2.64
2.62
1.81
1.81
1.80
1.79
1.78
1.77
1.73
1.60
1.56
1.55
1.54
1.53
1.53
1.45
1.42
1.41
1.39
1.38
1.36
1.26
1.24
1.22
1.21
1.07
1.05
1.03
0.90
0.89
0.89
0.87
0.62
0.06

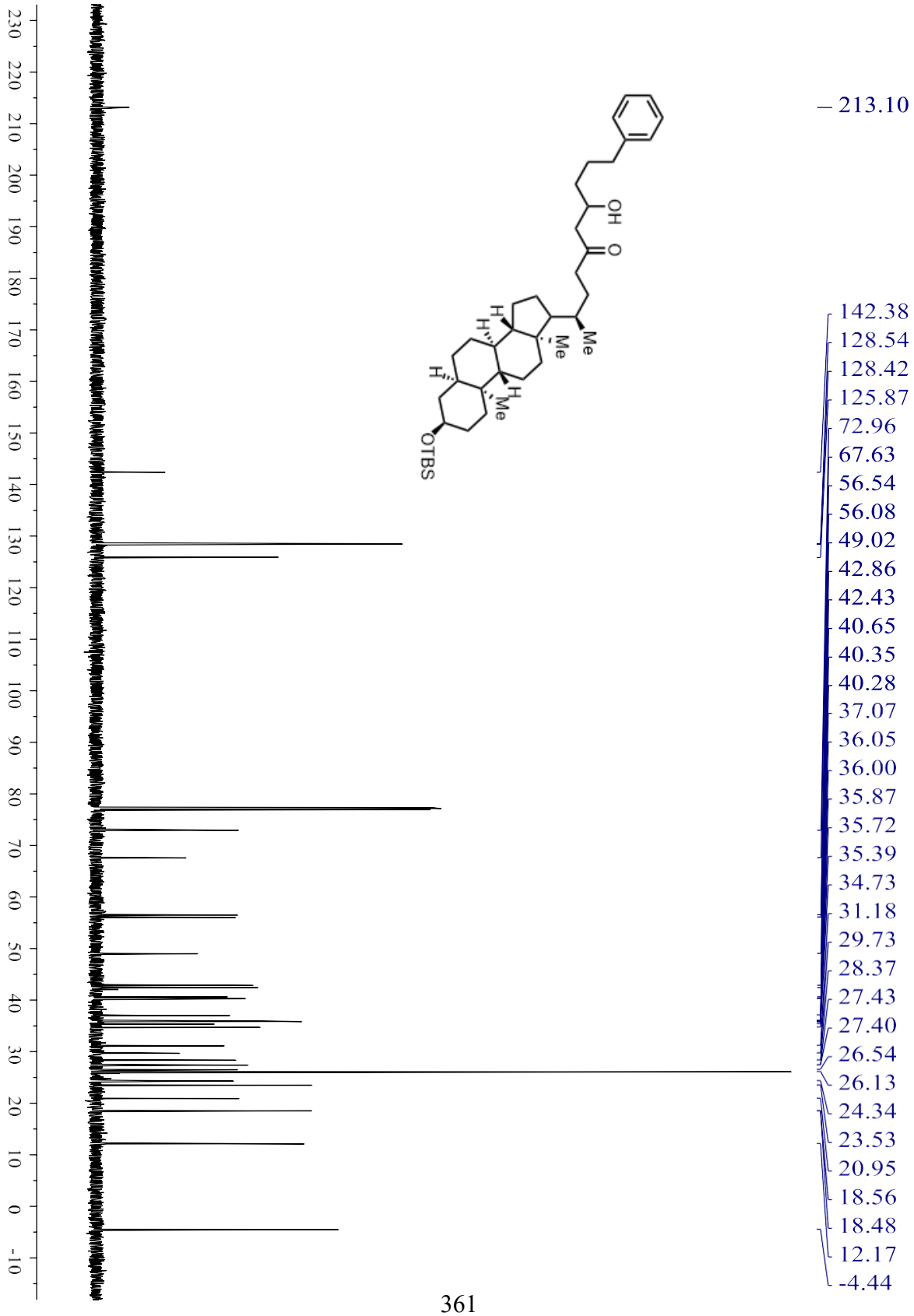
230 220 210 200 190 180 170 160 150 140 130 120 110 100 90 80 70 60 50 40 30 20 10 0 -10
213.10
142.38
128.54
128.42
125.87
72.96
67.63
56.54
56.08
49.02
42.86
42.43
40.65
40.35
40.28
37.07
36.05
36.00
35.87
35.72
35.39
34.73
31.18
29.73
28.37
27.43
27.40
26.54
26.13
24.34
23.53
20.95
18.56
18.48
12.17
-4.44
OH
O
Me
Me
Me
H
H
H
OTBS


5.12
5.12
5.12
5.11
5.08
5.08
5.08
5.08
4.04
4.03
3.02
3.01
2.60
2.60
2.57
2.57
2.52
2.51
2.48
2.42
2.40
2.39
2.12
2.10
2.09
2.08
2.07
2.06
2.04
1.99
1.98
1.97
1.68
1.67
1.62
1.61
1.61
1.60
1.55
1.55
0.93
0.93
0.92
0.92
0.91

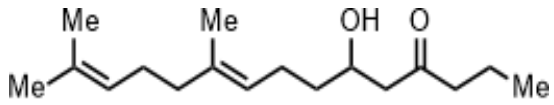
Me
Me
OH
O
Me
Me

2.191

362

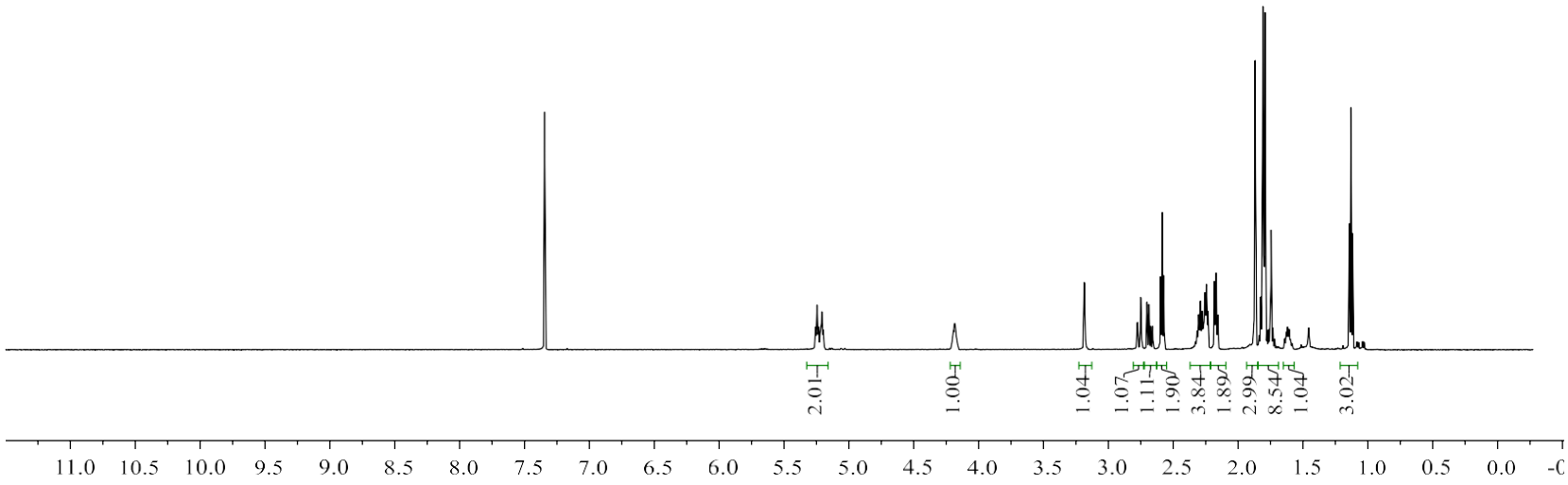
2.01
1.00
1.04
1.07
1.11
1.90
3.84
1.89
2.99
8.54
1.04
3.02
11.0
10.5
10.0
9.5
9.0
8.5
8.0
7.5
7.0
6.5
6.0
5.5
5.0
4.5
4.0
3.5
3.0
2.5
2.0
1.5
1.0
0.5
0.0

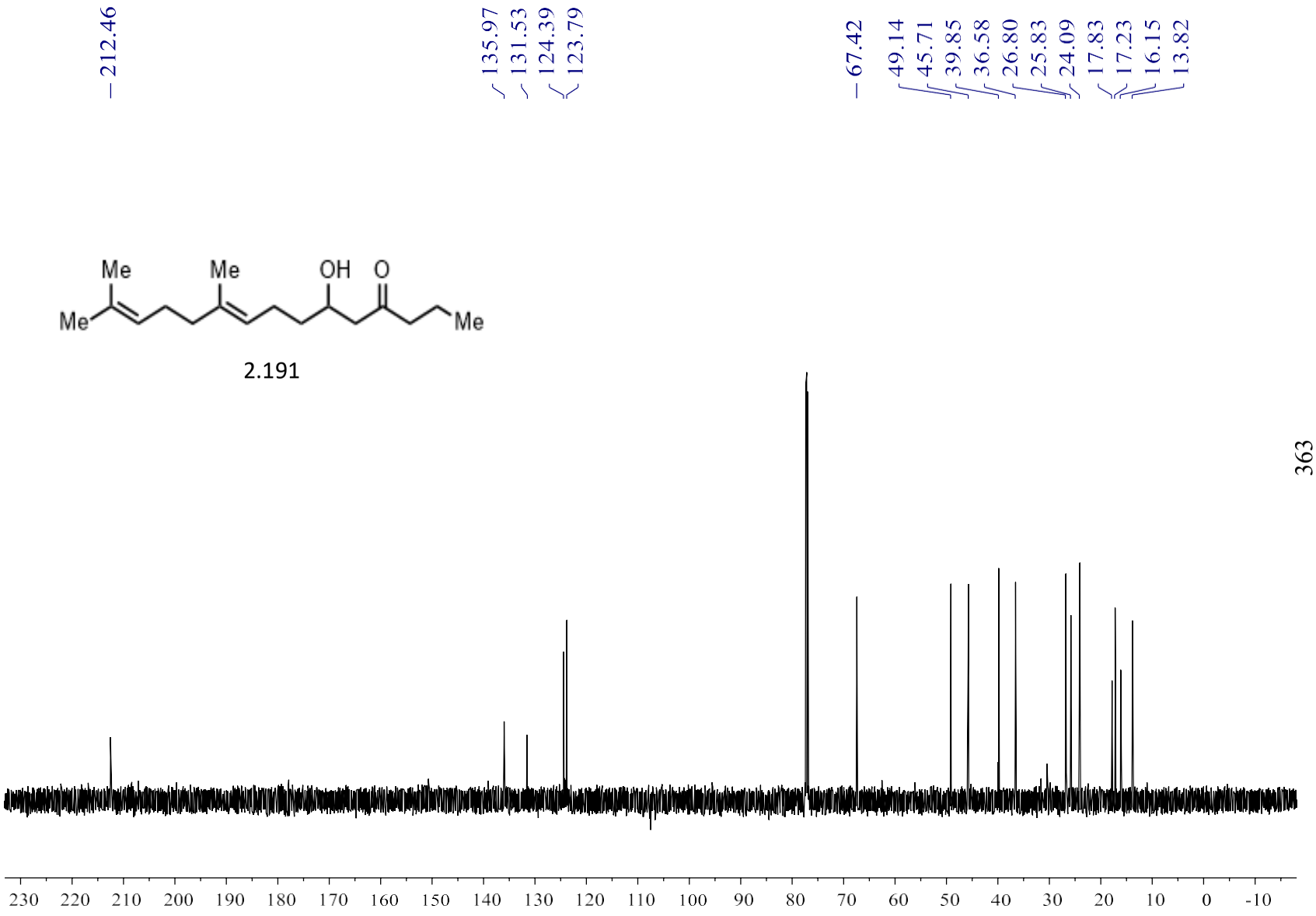
212.46
135.97
131.53
124.39
123.79
67.42
49.14
45.71
39.85
36.58
26.80
25.83
24.09
17.83
17.23
16.15
13.82
Me
Me
OH
O
Me
2.191
363
230 220 210 200 190 180 170 160 150 140 130 120 110 100 90 80 70 60 50 40 30 20 10 0 -10

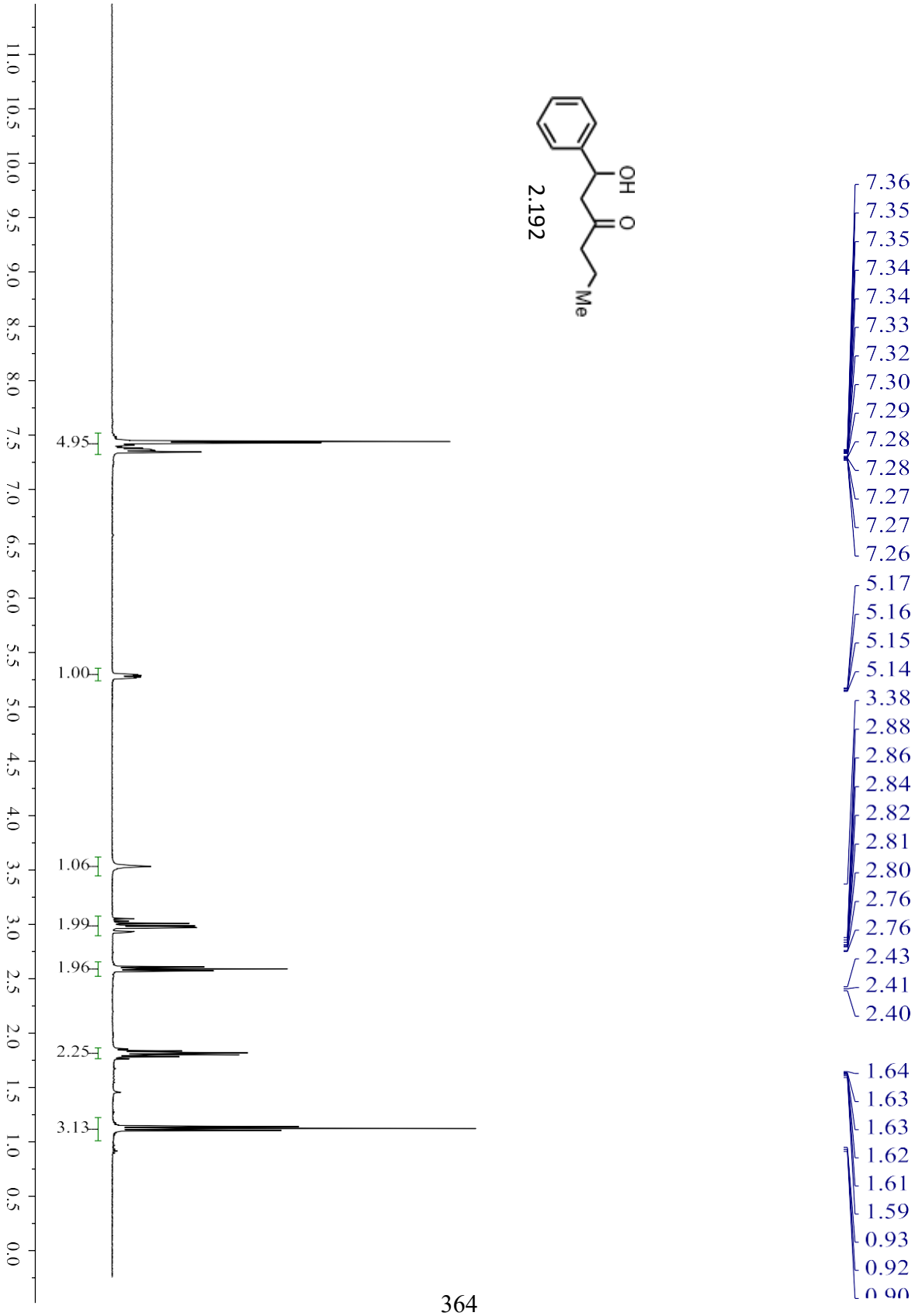
11.0 10.5 10.0 9.5 9.0 8.5 8.0 7.5 7.0 6.5 6.0 5.5 5.0 4.5 4.0 3.5 3.0 2.5 2.0 1.5 1.0 0.5 0.0
4.95
1.00
1.06
1.99
1.96
2.25
3.13
OH
O
Me
2.192
7.36
7.35
7.35
7.34
7.34
7.33
7.32
7.30
7.29
7.28
7.28
7.27
7.27
7.26
5.17
5.16
5.15
5.14
3.38
2.88
2.86
2.84
2.82
2.81
2.80
2.76
2.76
2.43
2.41
2.40
1.64
1.63
1.63
1.62
1.61
1.59
0.93
0.92
0.90

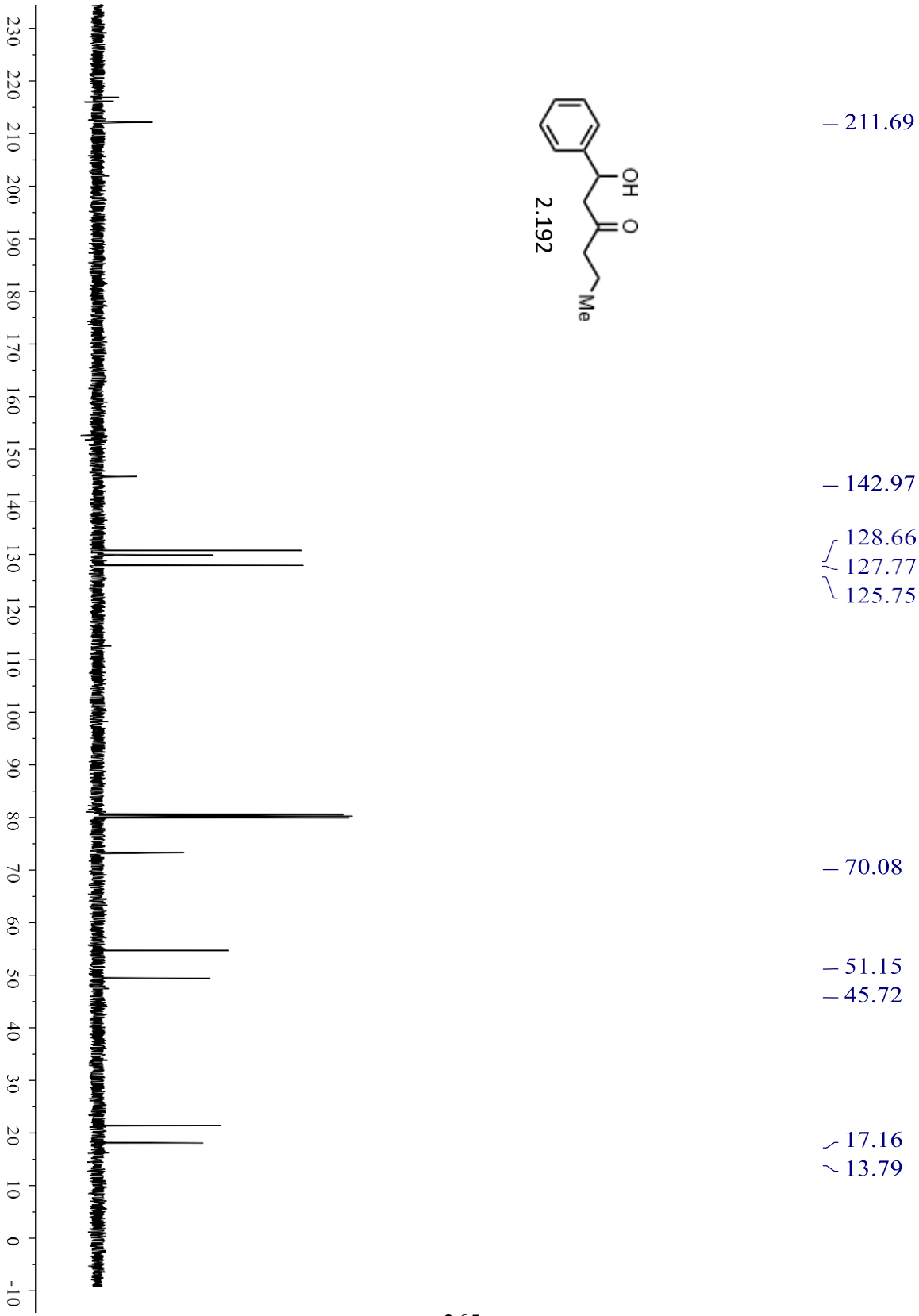
211.69
142.97
128.66
127.77
125.75
70.08
51.15
45.72
17.16
13.79
OH
O
Me
2.192

11.0
10.5
10.0
9.5
9.0
8.5
8.0
7.5
7.0
6.5
6.0
5.5
5.0
4.5
4.0
3.5
3.0
2.5
2.0
1.5
1.0
0.5
0.0
1.86
0.96
1.87
0.99
1.00
1.96
2.15
1.03
1.11
1.08
1.15
3.10
2.13
3.08
1.14

2.190
OH
O

7.95
7.94
7.93
7.93
7.57
7.55
7.47
7.46
7.44
4.52
4.51
4.50
4.10
4.09
4.09
4.08
4.07
4.07
4.06
3.77
3.77
3.76
3.75
3.74
3.72
3.26
3.26
3.13
3.12
3.05
3.03
1.62
1.61
1.61
1.60
1.60
1.59
1.51
1.51
1.51
1.44
1.42
1.42
1.41
1.41

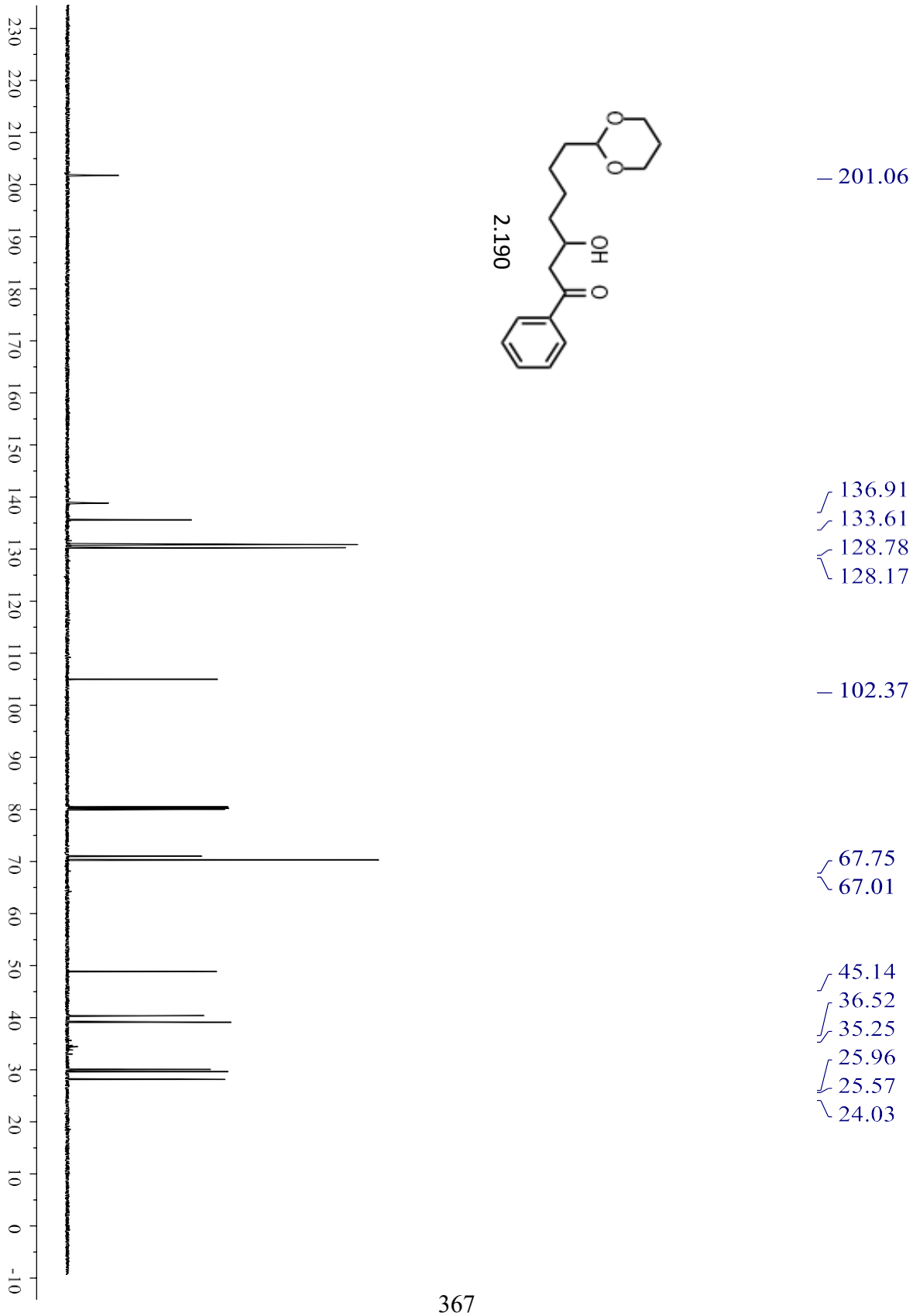
2.190
OH
O
201.06
136.91
133.61
128.78
128.17
102.37
67.75
67.01
45.14
36.52
35.25
25.96
25.57
24.03
230 220 210 200 190 180 170 160 150 140 130 120 110 100 90 80 70 60 50 40 30 20 10 0 -10

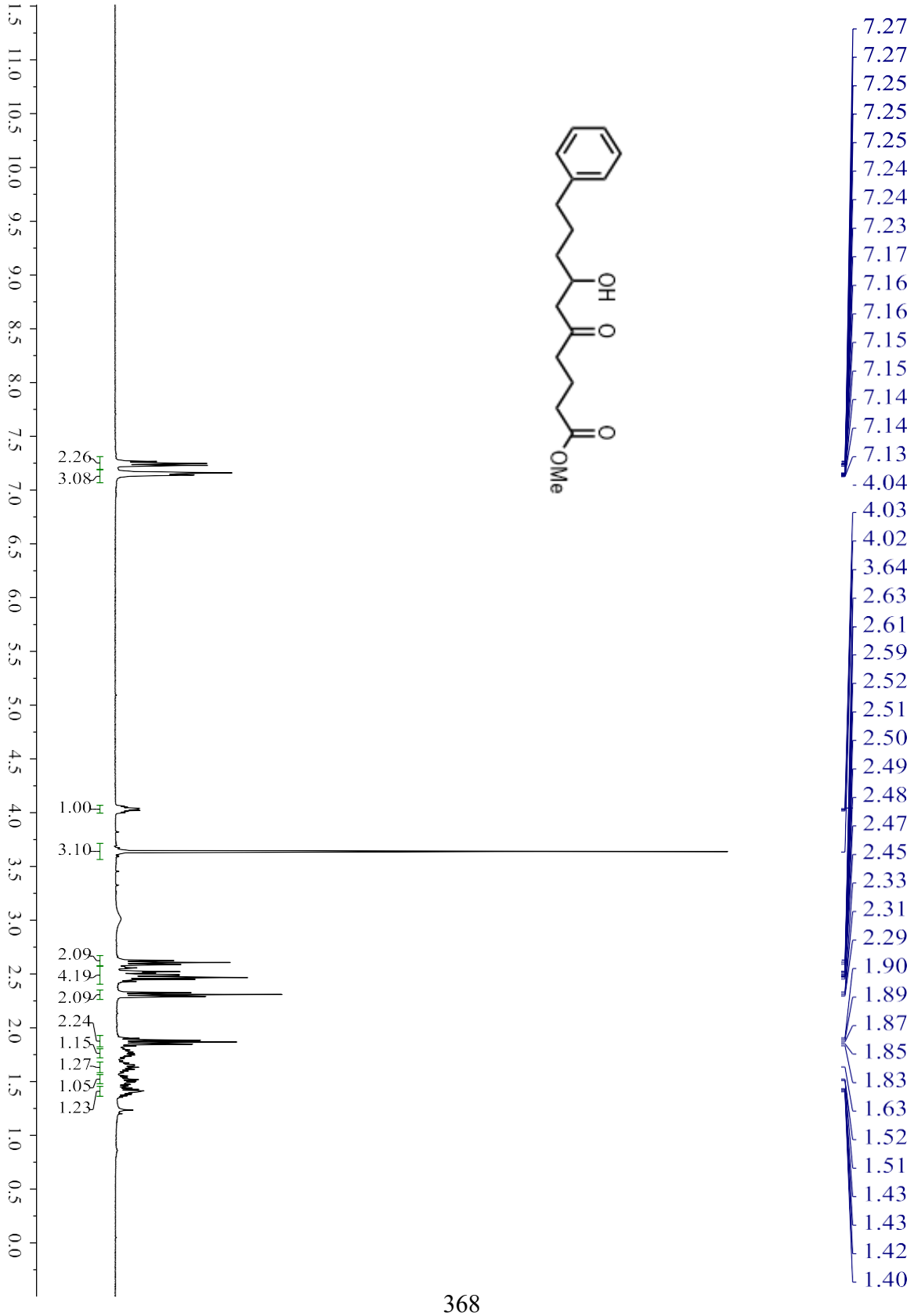
OH
O
O
OMe
7.27
7.27
7.25
7.25
7.25
7.24
7.24
7.23
7.17
7.16
7.16
7.15
7.15
7.14
7.14
7.13
4.04
4.03
4.02
3.64
2.63
2.61
2.59
2.52
2.51
2.50
2.49
2.48
2.47
2.45
2.33
2.31
2.29
1.90
1.89
1.87
1.85
1.83
1.63
1.52
1.51
1.43
1.43
1.42
1.40
2.26
3.08
1.00
3.10
2.09
4.19
2.09
2.24
1.15
1.27
1.05
1.23

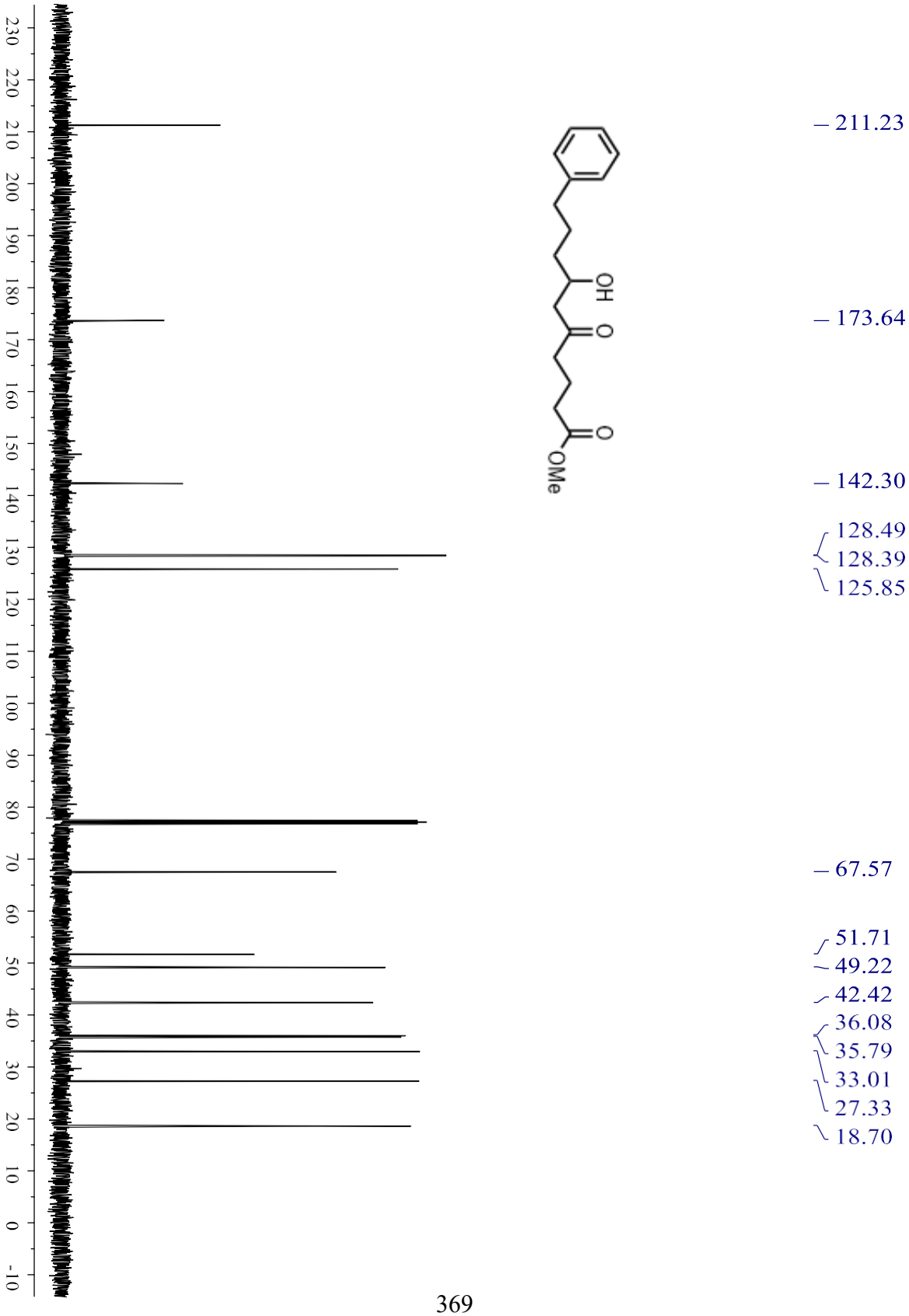
211.23
173.64
142.30
128.49
128.39
125.85
67.57
51.71
49.22
42.42
36.08
35.79
33.01
27.33
18.70
OH
O
O
OMe

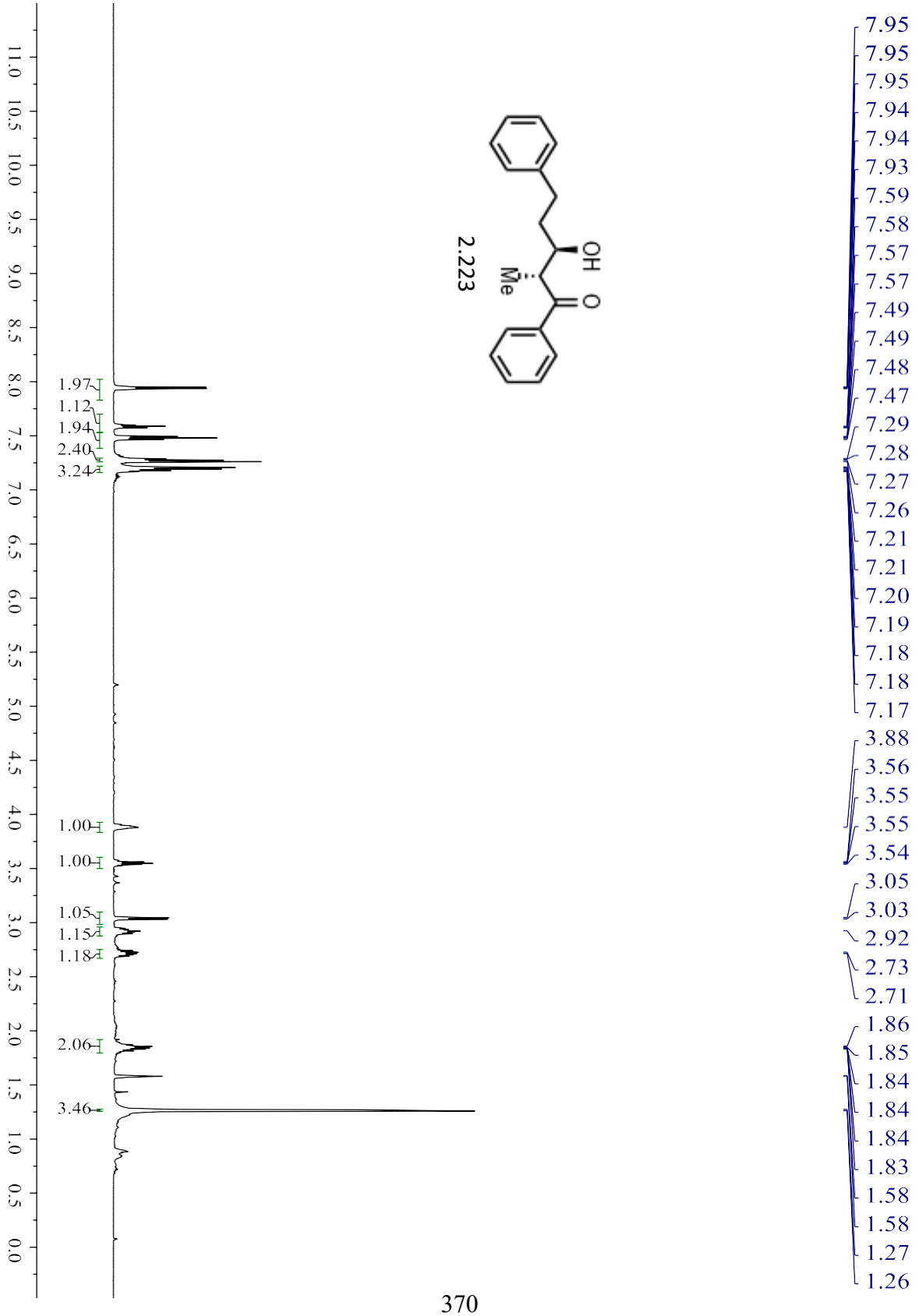
11.0 10.5 10.0 9.5 9.0 8.5 8.0 7.5 7.0 6.5 6.0 5.5 5.0 4.5 4.0 3.5 3.0 2.5 2.0 1.5 1.0 0.5 0.0
1.97
1.12
1.94
2.40
3.24
1.00
1.00
1.05
1.15
1.18
2.06
3.46
OH
O
Me
2.223
7.95
7.95
7.95
7.94
7.94
7.93
7.59
7.58
7.57
7.57
7.49
7.49
7.48
7.47
7.29
7.28
7.27
7.26
7.21
7.21
7.20
7.19
7.18
7.18
7.17
3.88
3.56
3.55
3.55
3.54
3.05
3.03
2.92
2.73
2.71
1.86
1.85
1.84
1.84
1.84
1.83
1.58
1.58
1.27
1.26

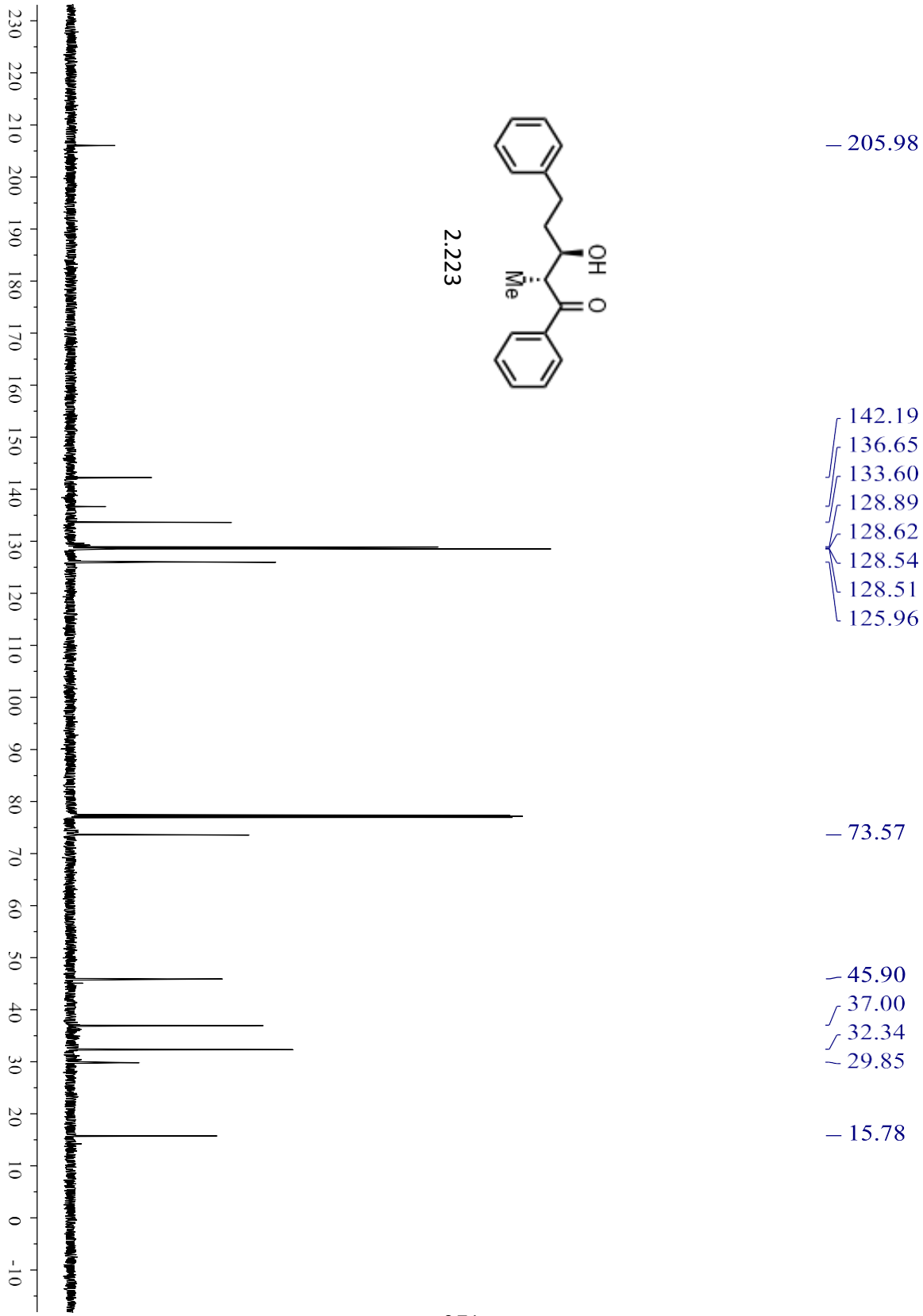
2.223
OH
O
Me
205.98
142.19
136.65
133.60
128.89
128.62
128.54
128.51
125.96
73.57
45.90
37.00
32.34
29.85
15.78
230
220
210
200
190
180
170
160
150
140
130
120
110
100
90
80
70
60
50
40
30
20
10
0
-10

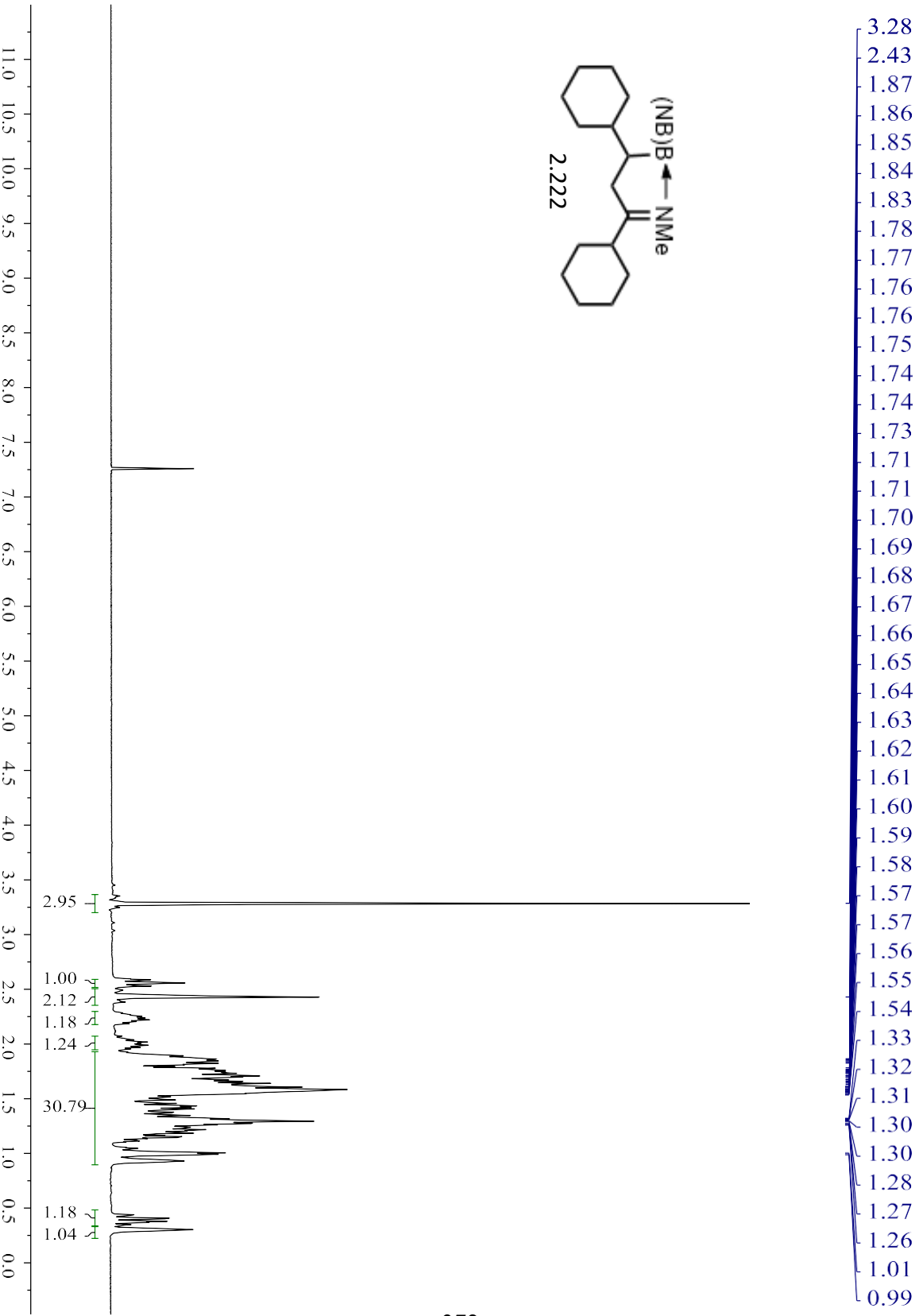
(NB)B← NMe
2.222
11.0 10.5 10.0 9.5 9.0 8.5 8.0 7.5 7.0 6.5 6.0 5.5 5.0 4.5 4.0 3.5 3.0 2.5 2.0 1.5 1.0 0.5 0.0
2.95
1.00
2.12
1.18
1.24
30.79
1.18
1.04
3.28
2.43
1.87
1.86
1.85
1.84
1.83
1.78
1.77
1.76
1.76
1.75
1.74
1.74
1.73
1.71
1.71
1.70
1.69
1.68
1.67
1.66
1.65
1.64
1.63
1.62
1.61
1.60
1.59
1.58
1.57
1.57
1.56
1.55
1.54
1.33
1.32
1.31
1.30
1.30
1.28
1.27
1.26
1.01
0.99

(NB)B
NMe
2.222
189.07
40.42
37.74
36.94
35.78
35.14
34.34
33.24
31.91
30.77
30.65
29.49
29.41
27.39
27.31
27.15
25.95
25.90
25.83
25.24
24.23
230 220 210 200 190 180 170 160 150 140 130 120 110 100 90 80 70 60 50 40 30 20 10 0 -10

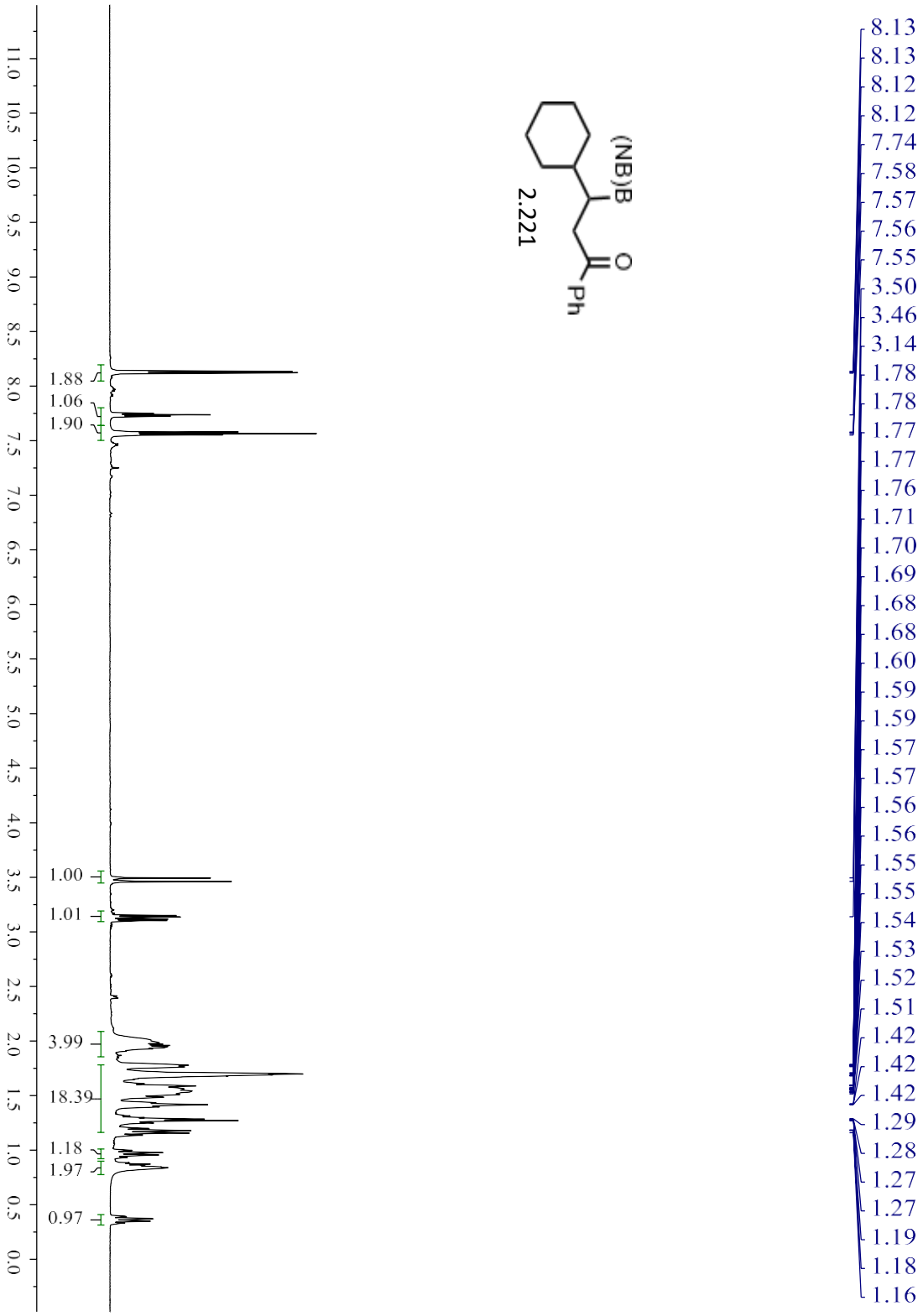
(NB)B
O
Ph
2.221
1.88
1.06
1.90
1.00
1.01
3.99
18.39
1.18
1.97
0.97
8.13
8.13
8.12
8.12
7.74
7.58
7.57
7.56
7.55
3.50
3.46
3.14
1.78
1.78
1.77
1.77
1.76
1.71
1.70
1.69
1.68
1.68
1.60
1.59
1.59
1.57
1.57
1.56
1.56
1.55
1.55
1.54
1.53
1.52
1.51
1.42
1.42
1.42
1.29
1.28
1.27
1.27
1.19
1.18
1.16

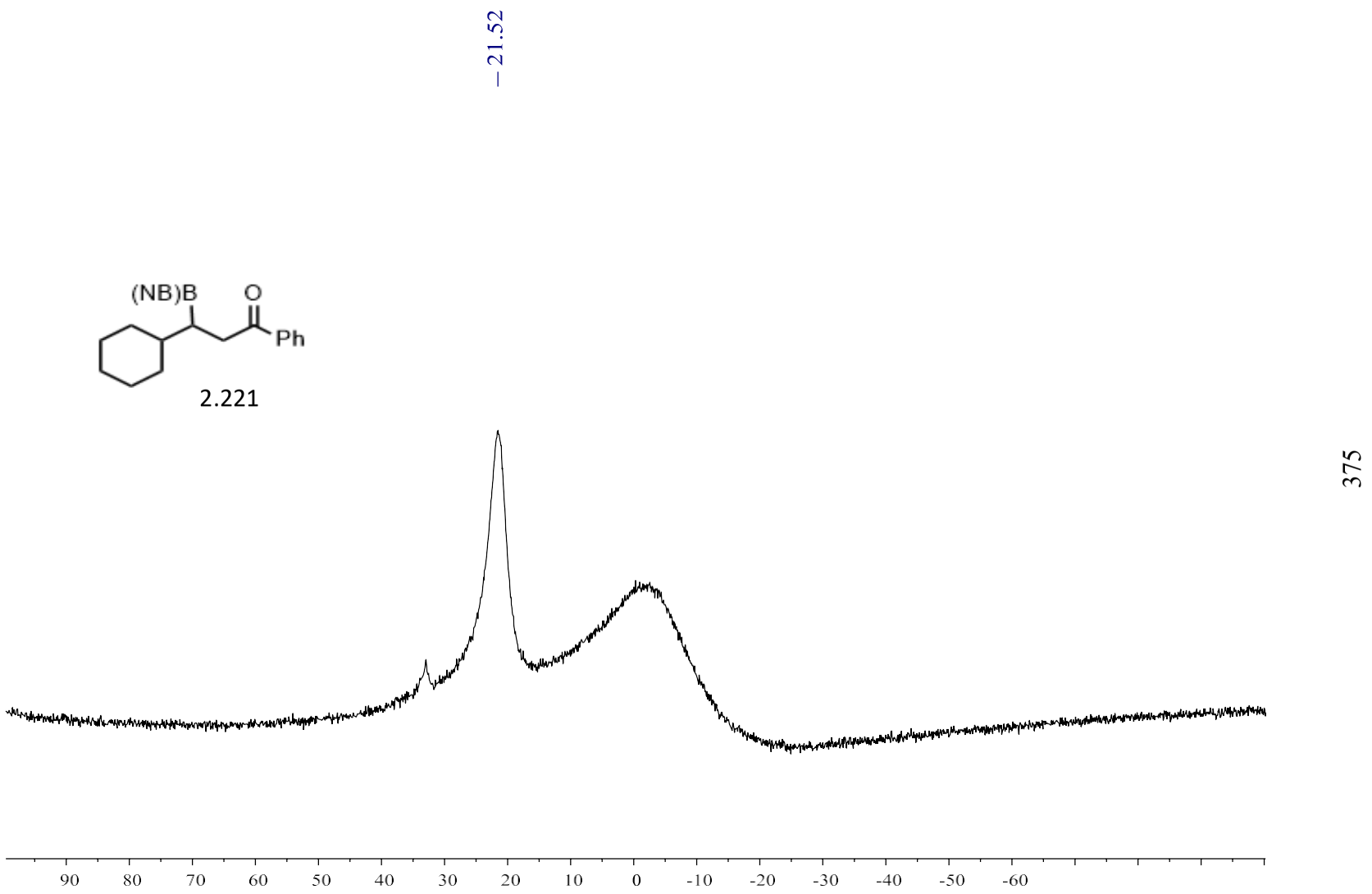
21.52
(NB)B
O
Ph
2.221
375
90
80
70
60
50
40
30
20
10
0
-10
-20
-30
-40
-50
-60

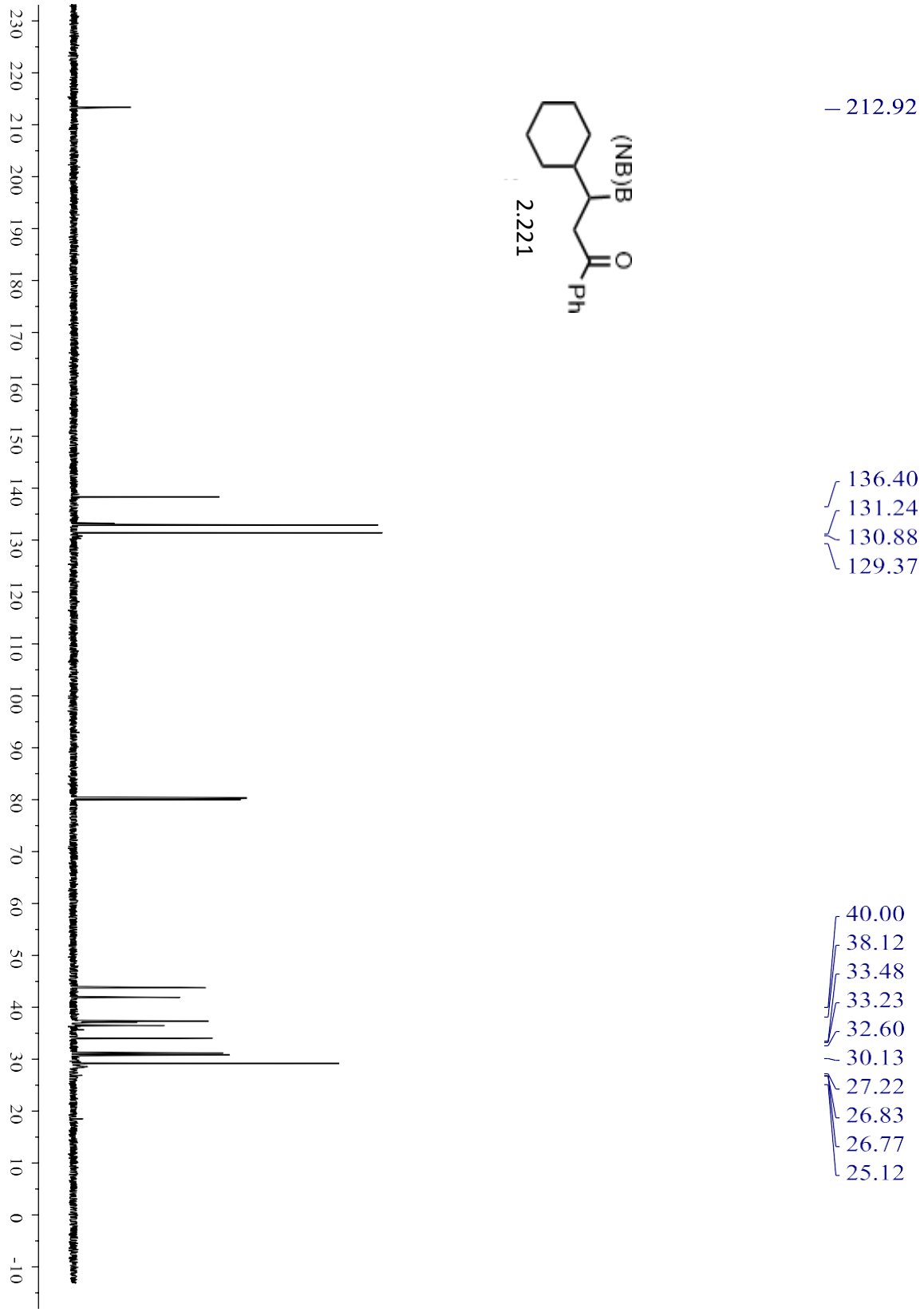
(NB)B
O
Ph
2.221
212.92
136.40
131.24
130.88
129.37
40.00
38.12
33.48
33.23
32.60
30.13
27.22
26.83
26.77
25.12


8.14
8.13
8.13
7.75
7.73
7.59
7.59
7.57
7.56
3.47
2.00
1.99
1.80
1.80
1.79
1.78
1.77
1.72
1.72
1.71
1.70
1.69
1.68
1.61
1.60
1.60
1.58
1.57
1.56
1.55
1.55
1.53
1.53
1.52
1.50
1.44
1.43
1.42
1.28
1.28
1.20
1.19
1.17
0.85
0.85

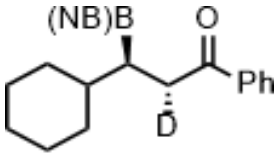
(NB)B
O
Ph
D

2.212

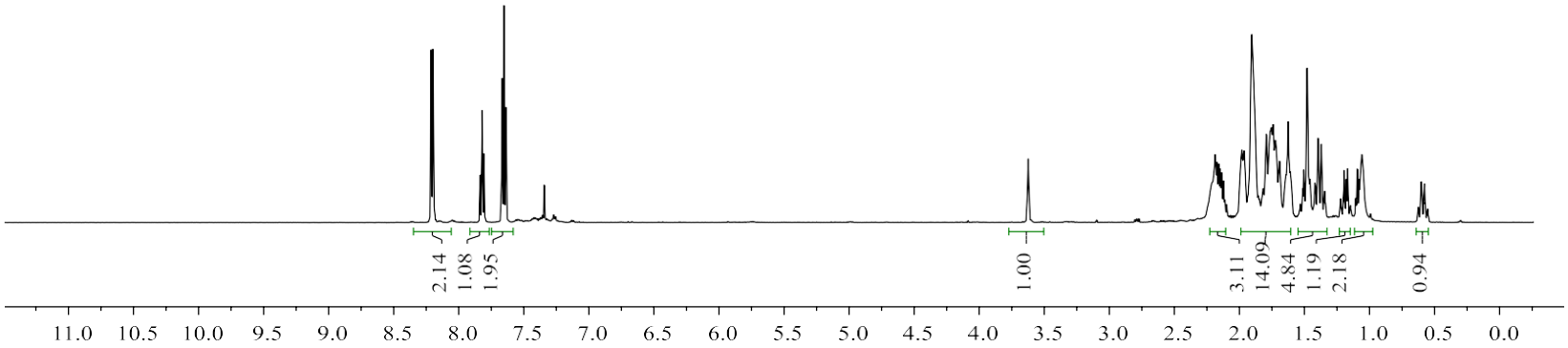
2.14
1.08
1.95
1.00
3.11
14.09
4.84
1.19
2.18
0.94
11.0
10.5
10.0
9.5
9.0
8.5
8.0
7.5
7.0
6.5
6.0
5.5
5.0
4.5
4.0
3.5
3.0
2.5
2.0
1.5
1.0
0.5
0.0

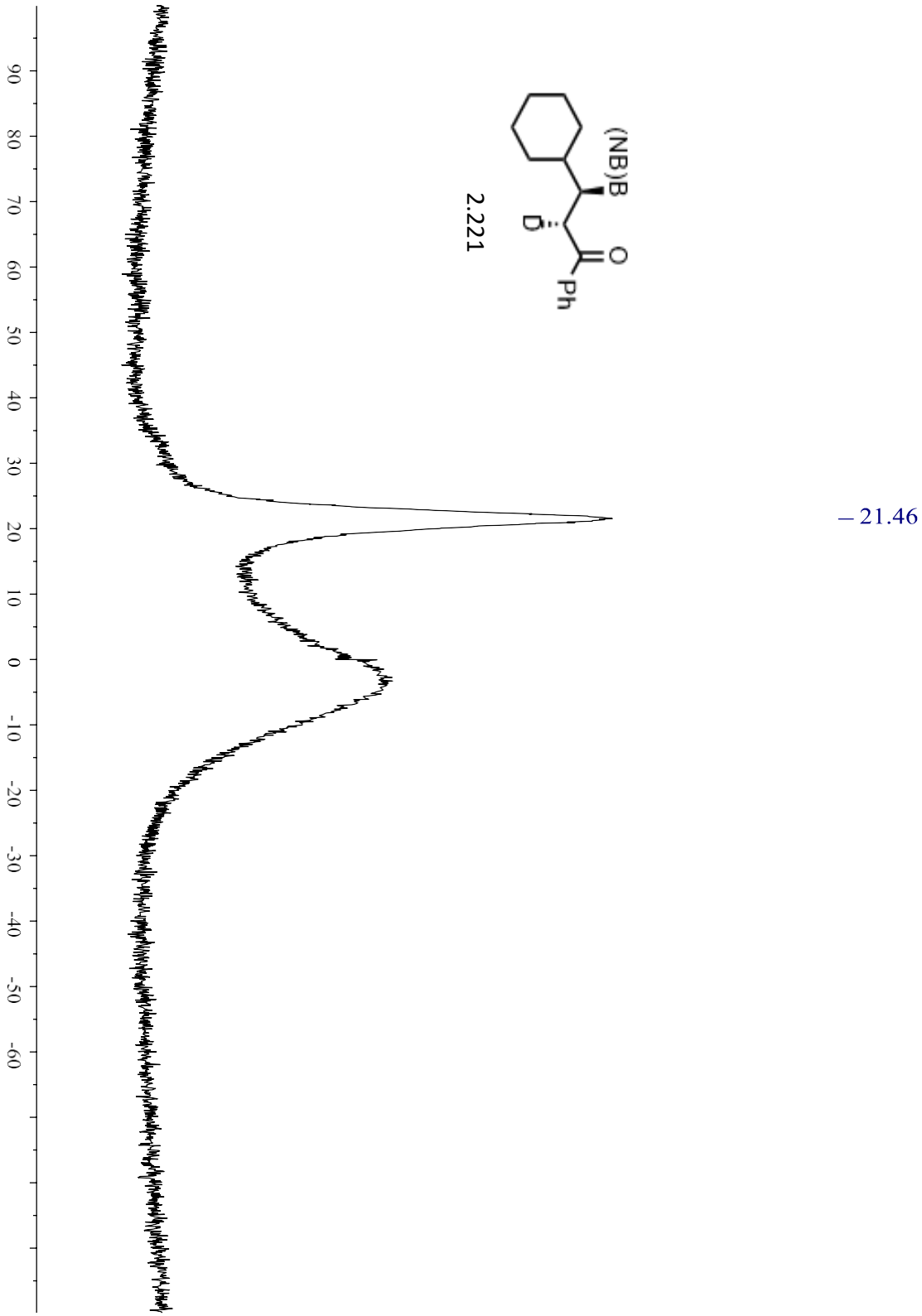
(NB)B
O
Ph
D
2.221
90
80
70
60
50
40
30
20
10
0
-10
-20
-30
-40
-50
-60
– 21.46

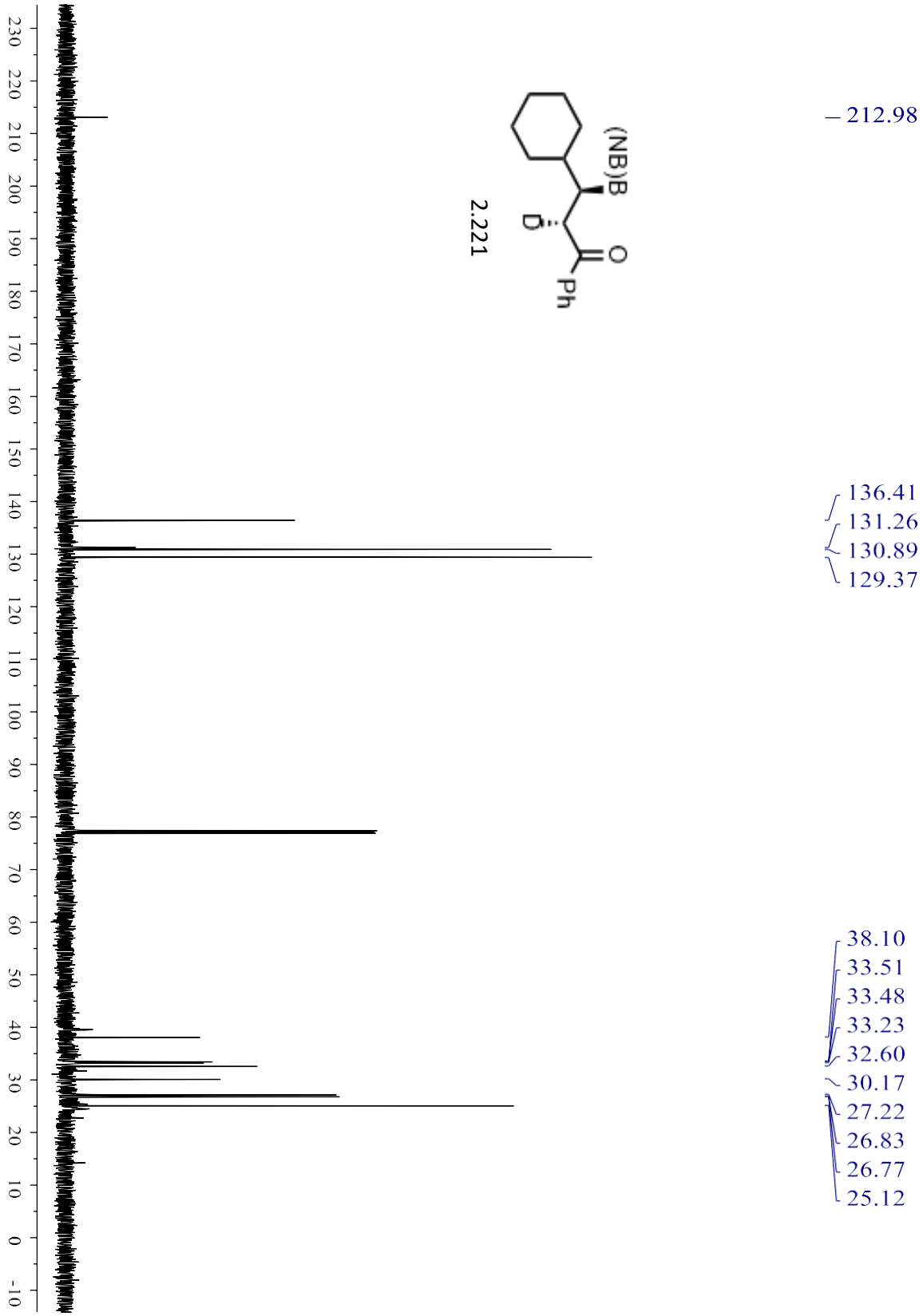
(NB)B
O
Ph
D
2.221
212.98
136.41
131.26
130.89
129.37
38.10
33.51
33.48
33.23
32.60
30.17
27.22
26.83
26.77
25.12
230 220 210 200 190 180 170 160 150 140 130 120 110 100 90 80 70 60 50 40 30 20 10 0 -10

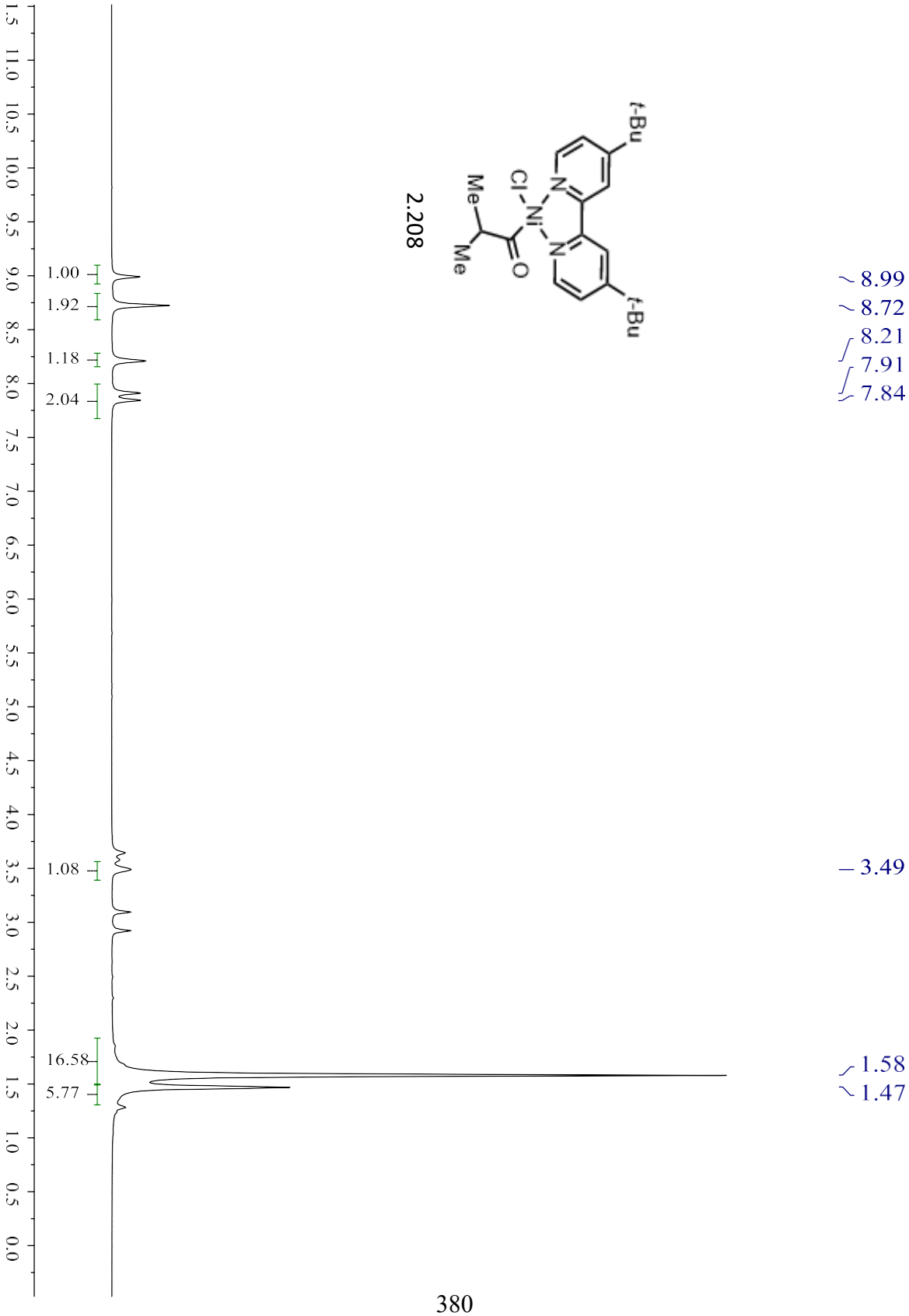
2.208
t-Bu
t-Bu
Cl
Ni
N
N
O
Me
Me
1.00
1.92
1.18
2.04
1.08
16.58
5.77
8.99
8.72
8.21
7.91
7.84
3.49
1.58
1.47

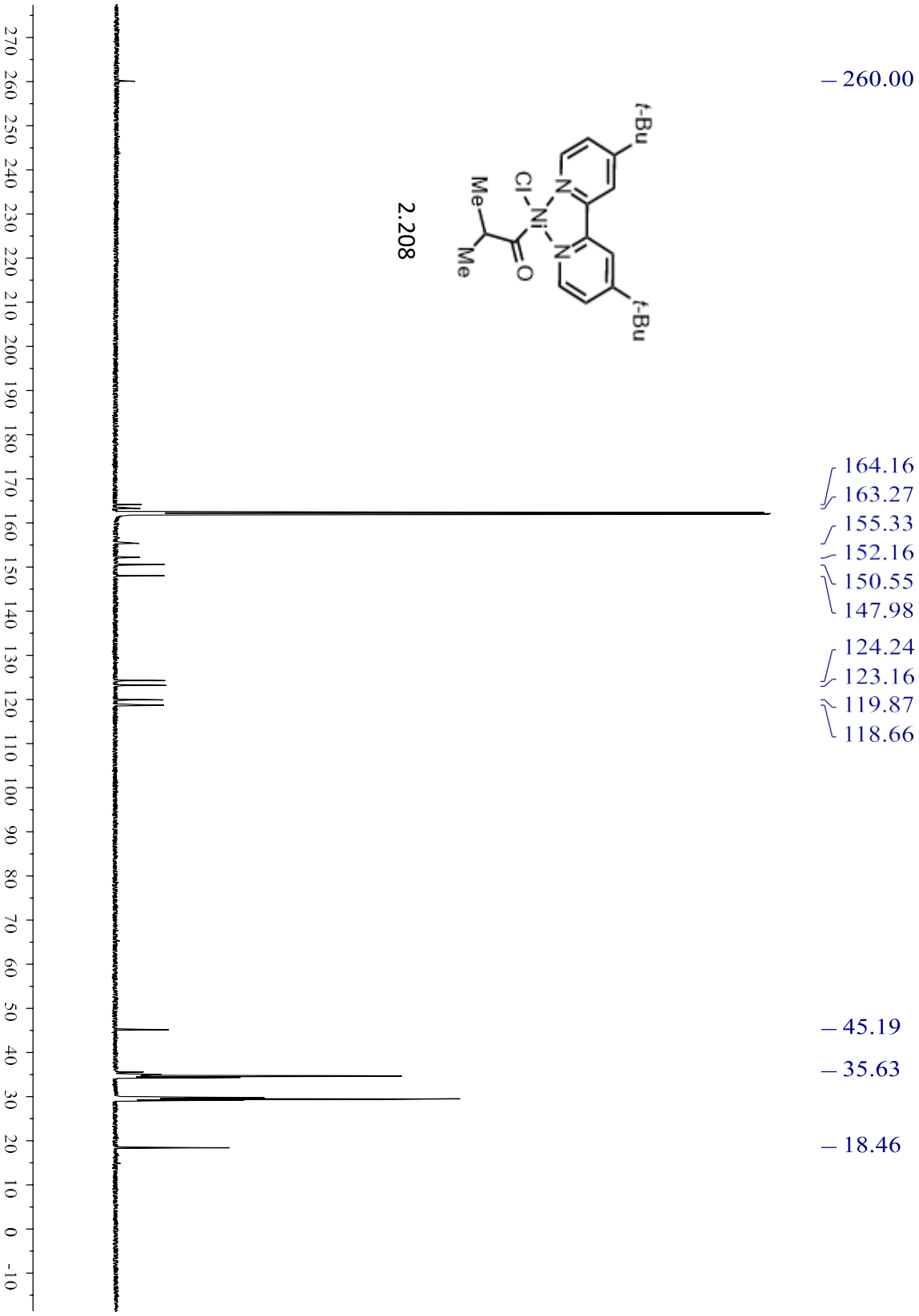
270 260 250 240 230 220 210 200 190 180 170 160 150 140 130 120 110 100 90 80 70 60 50 40 30 20 10 0 -10
2.208
t-Bu
t-Bu
Me
Me
Cl
Ni
O
N
N
260.00
164.16
163.27
155.33
152.16
150.55
147.98
124.24
123.16
119.87
118.66
45.19
35.63
18.46

Chapter 3

Catalytic Enantioselective Synthesis of *anti*-Vicinal Silylboronates by Conjunctive Cross-Coupling

3.1 Introduction

Organometallic compounds have been widely used in organic synthesis since Edward Frankland[1] discovered diethylzinc in 1848 and the subsequent development of Grignard reagents in 1899, for which Victor Grignard won the Nobel Prize in 1912. Many organometallic species have since been identified. Of these, configurationally stable organometallics, such as organoboronates, organosilanes, and organotins, are particularly valuable in modern chemical syntheses.[2] These reagents have found utility in C–C bond-forming processes (e.g., Suzuki-Miyaura cross-couplings), which were the subject of the Nobel Prize in 2010.

Along with the recent development of enantioselective cross-coupling reactions, the needs for synthesizing configurationally stable chiral organometallic compounds surged, especially motifs bearing either germinal

[1] E. Frankland, *Quarterly Journal of the Chemical Society*. **1850**, *2*, 263

[2] a) Organometallics in Synthesis: A Manual, 2nd ed. (Ed: M.Schlosser), Wiley, New York, 2001; b) R. Jana, T. P. Pathak, M. S.Sigman, *Chem. Rev*. **2011**, *111*, 1417; c) A. H. Cherney, N. T.Kadunce, S. E. Reisman, *Chem. Rev*. **2015**, *115*, 9587; d) C.Sandford, V. K. Aggarwal, *Chem. Commun*. **2017**, *53*, 5481.

or vicinal C-M bonds.[3] With these reagents, the complexity of synthetic target can be build up quite quickly as the two functionalizable C-M bonds can be synergistically or orthogonally replaced with valuable functional groups (as an example, see Scheme 1.2). Although tremendous success has been achieved in the synthesis of chiral geminal bimetallics[4], methods that produce enantio-enriched vicinal bimetallics have not been fully explored. Most examples focus on 1,2-diboronate synthesis (see chapter 1, section 1.2.2) along with a few cases of disilanes, silylboronic esters, and stannylboronic esters. The methods mentioned above provide *syn*-1,2-bimetallics as products

Scheme 1. 2 Transformations of 1,2-bisboronates

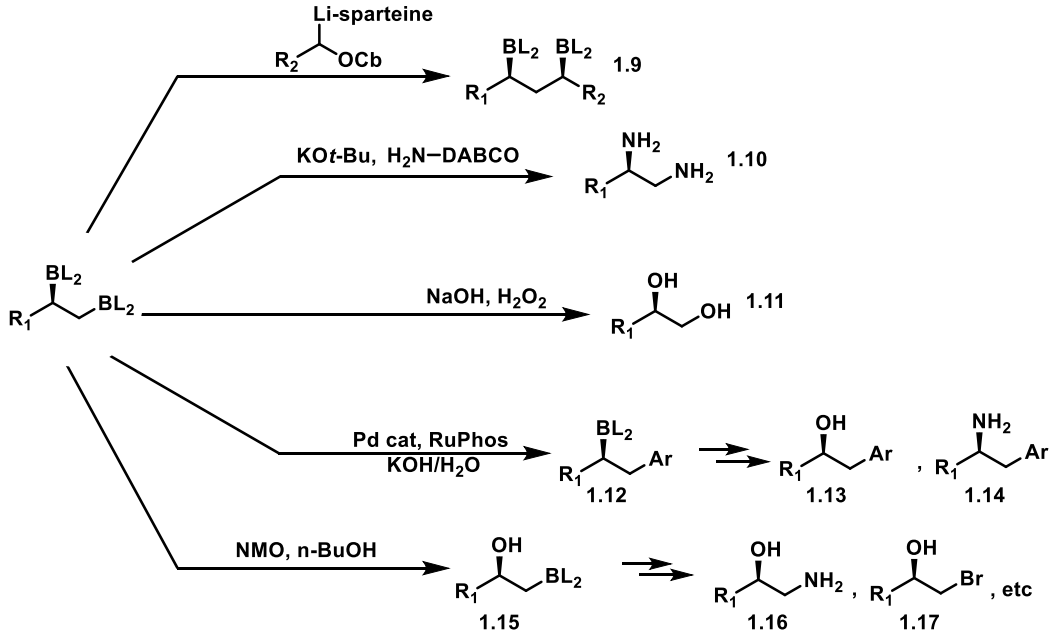

[3] a) M. Suginome, Y. Ito, *Chem. Rev*. **2000**, *100*, 3221; b) I. Beletskaya, C. Moberg, *Chem. Rev.* **2006**, *106*, 2320; c) M. Oestreich, D. Hartmann, M. Mewald, *Chem. Rev*. **2013**, *113*, 402; d) L. Xu, S. Zhang, P. F. Li in Boron Reagents in Synthesis (Ed: A. Coca), American Chemical Society, Washington DC, 2016, pp. 415

[4] a) P. Knochel, J. F. Normant, *Tetrahedron Lett*., **1986**, *27*, 1039; b) P. Knochel, J. F. Normant, *Tetrahedron Lett.,* **1986**, *27*, 1043; c) I. Marek, J. F. Normant, *Chem. Rev*. **1996**, *96*, 3241; d) M. Shimizu, T. Kurahashi, T. Hiyama, *J. Synth. Org. Chem. Jpn.* **2001**, *59*, 1062.

of *syn* addition across the olefin. Thus, significant gaps still exist for the preparation of chiral *anti*-1,2-dimetallics since none of the methods used to produce *syn* products could deliver *anti* products with high efficiency and selectivity.

This chapter will present an alternative strategy to prepare chiral 1,2-dimetallic compounds via palladium-induced stereospecific 1,2-metallate rearrangement. Instead of *syn* addition of two metals across a *Z* alkene, a 1,2-metallate shift allows an *anti* addition of two carbon atoms across an *E* alkene. High selectivity is achieved for the first time by adopting the approach of conjunctive cross-coupling. The corresponding products are further elaborated to showcase chemoselective functionalizations.

3.2 Background

3.2.1 Synthesis of organobimetallic compounds

Two carbon-metalloid (C-M) bonds provide twice the possibilities to forge new C-C bonds and C-Het (heteroatom) bonds sequentially, which makes this organometallics useful in synthesis. Over the past few decades,

dimetallic reagents based on Zn, Mg, Cr, and Cu have been studied, though they were typically either symmetrical or racemic mixed bimetallics.[5]

3.2.1.1 1,1-Geminal dimetallic species

Recently, the interest of researchers has shifted toward configurationally stable, enantioenriched compounds containing one or more metalloid elements such as boron, silicon, or tin. Among these compounds, chiral geminal bis(metallics) have been well-studied in the past decade. Hall[6] and Yun[7] synthesized non-symmetric geminal bis(boronates) through copper-catalyzed protoboration of alkenyl boronates. Hoveyda[8], Aggarwal[9], and Liu[10] constructed chiral geminal silylboronates by either copper catalysis or lithiation-migration reactions. Our group also developed a palladium-catalyzed hydrosilylation reaction to construct similar enantiomerically enriched geminal silylboronates with good yield and selectivity (Scheme 3.1).[11]

[5] I. Marek, J. F. Normant, *Chem. Rev*. **1996**, *96*, 3241
[6] C. H. Lee, R. McDonald, D. G. Hall, *Nat. Chem*. **2011**, *3*, 894
[7] X. Feng, H. Jeon, J. Yun, *Angew. Chem., Int. Ed*. **2013**, *52*, 3989
[8] F. Meng, H. Jang, A. H. Hoveyda, *Chem. Eur. J.* **2013**, *19*, 3204
[9] V. K. Aggarwal, M. Binanzer, M. C. de Ceglie, M. Gallanti, B. W. Glasspoole, S. J. F. Kendrick, R. P. Sonawane, A. Vazquez-Romero, M. P. Webster, *Org. Lett.* **2011**, *13*, 1490
[10] L. Wang, T. Zhang, W. Sun, Z. He, C. Xia, Y. Lan, C. Liu, *J. Am. Chem. Soc*. **2017**, *139*, 5257
[11] A. A. Szymaniak, C. Zhang, J. R. Coombs, J. P. Morken, *ACS Catal.* **2018**, *8*, 2897

Scheme 3.1 Seletive methods in synthesis of geminal bis-metallics

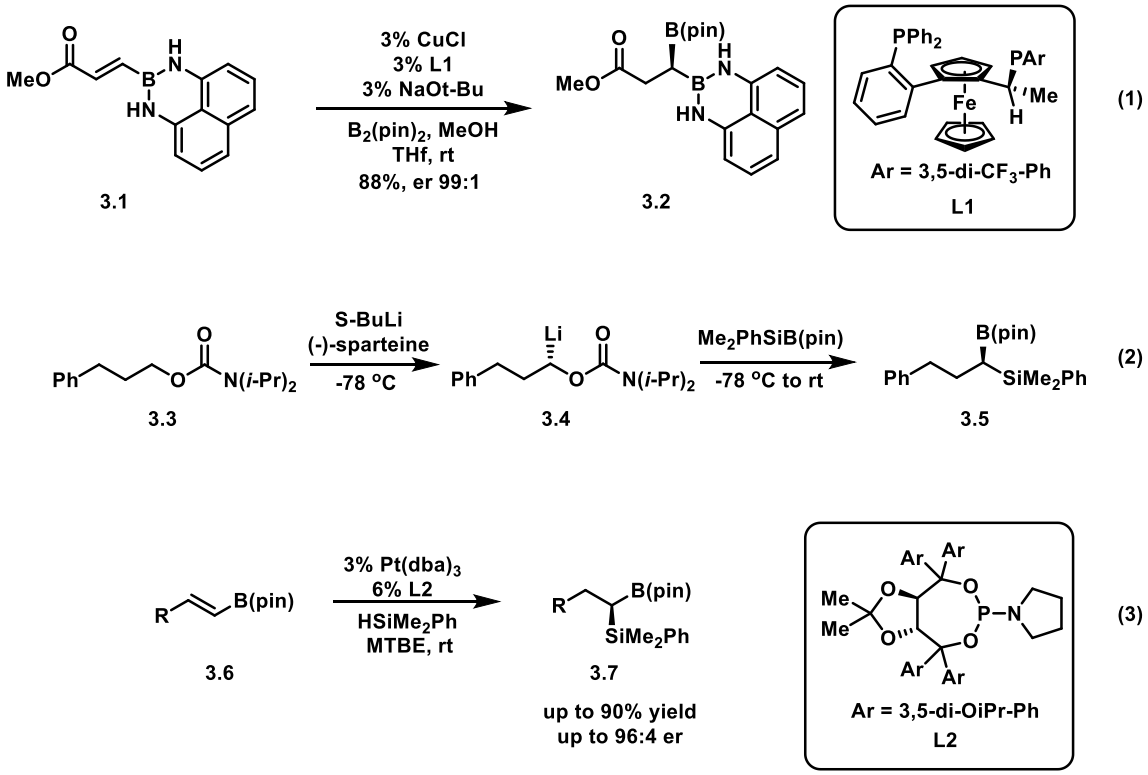

3.2.1.2 1,2-Vicinal dimetalloid species

Configurationally stable 1,2-vicinal dimetalloids [12] are mainly represented by 1,2-bis(boronates) with scattered cases of mixed silylboronates and stannylboronates. Across all the reports, the addition of an M-M reagent across a π bond (i.e., alkene, alkyne, or allene) is the dominant synthesis strategy, as depicted in Scheme 3.2. The products of these reactions fall into

[12] a) M. Suginome, Y. Ito, *Chem. Rev.* **2000**, *100*, 3221; b) I. Beletskaya, C. Moberg, *Chem. Rev*. **2006**, *106*, 2320; c) M. Oestreich, D. Hartmann, M. Mewald, *Chem. Rev*. **2013**, *113*, 402; d) L. Xu, S. Zhang, P. F. Li in *Boron Reagents in Synthesis* (Ed: A. Coca) American Chemical Society, Washington, DC, **2016**, pp. 415

one of three categories: those that possess (1) a single stereogenic center, (2) *syn*-vicinal stereocenters, and (3) *anti*-vincinal stereocenters; these will be discussed in the following sections.

Scheme 3.2 Common disconnection strategies for synthesis of vicinal bimetallics

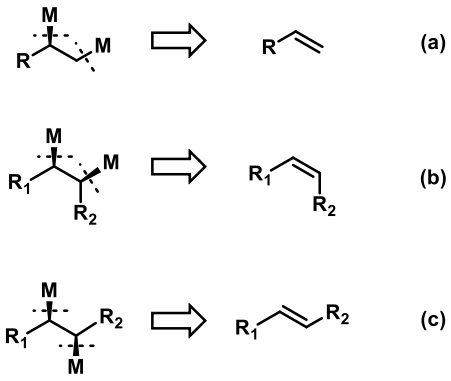

3.2.1.2.1 1,2-Dimetallics with one stereogenic center

1,2-Dimetallic compounds with only one stereogenic center have been extensively studied, with chiral 1,2-bis(boronates) being the most well developed. These compounds are prepared through either transition metal catalysis or small molecule catalysis. As introduced in section 1.2.2, Rh, Pt, Pd, Cu, and carbohydrate-based catalysts have been reported to assist in building non-racemic 1,2-diboronates bearing one stereogenic center.

The synthesis of chiral 1,2-disilanes was pioneered by Hayashi.[13] A tandem dual catalysis involving both platinum and palladium was developed to enable two hydrosilylations on an alkyne substrate. Good yield and selectivity have been accomplished with terminal alkynes as the starting material.

Scheme 3.3 Synthesis of chiral 1,2-disilanes

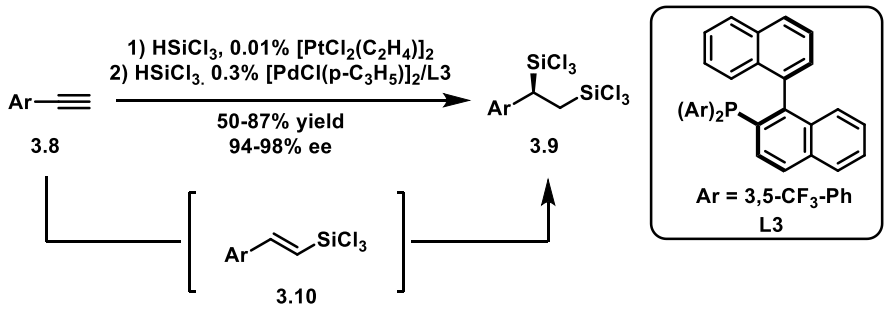

In terms of mixed chiral 1,2-dimetallics, three methods have been reported to prepare 1,2-silylboronates and 1,2-stannylboronates. Chiral 1,2-stannylboronates have been generated from terminal alkenes with the aid of copper catalyst. [14] A chiral copper(I) boronate, generated from transmetallation of a copper alkoxide with B_2pin_2, was added cross alkene (**1.11**) and trapped with tributyltin methoxide to deliver the chiral organostannanes.

[13] T. Shimada, K. Mukaide, A. Shinohara, J. W. Han, T. Hayashi, *J. Am. Chem. Soc.* **2002**,*124*, 1584.
[14] T. Jia, P. Cao, D. Wang, Y. Lou, J. Liao, *Chem. Eur. J.* **2015**, *21*, 4918

Scheme 3.4 Synthesis of chiral stannylboronates

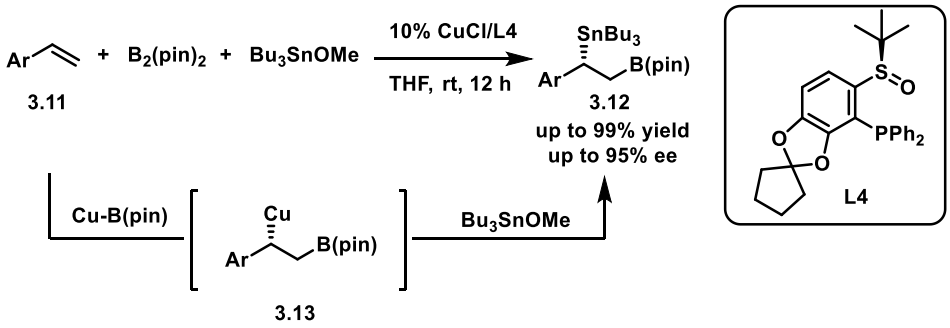

Chiral 1,2-silylboronates have been synthesized by Hoveyda and Suginome. In Hoveyda's report[15], non-racemic silylboronates were generated from *E* alkenyl silanes by catalytic copper-boron addition/protonation reactions. The product bears a boron-containing stereocenter β to the silicon atom (Scheme 3.5).

Scheme 3.5 Copper-catalyzed syntheses of chiral 1,2-silylboronates

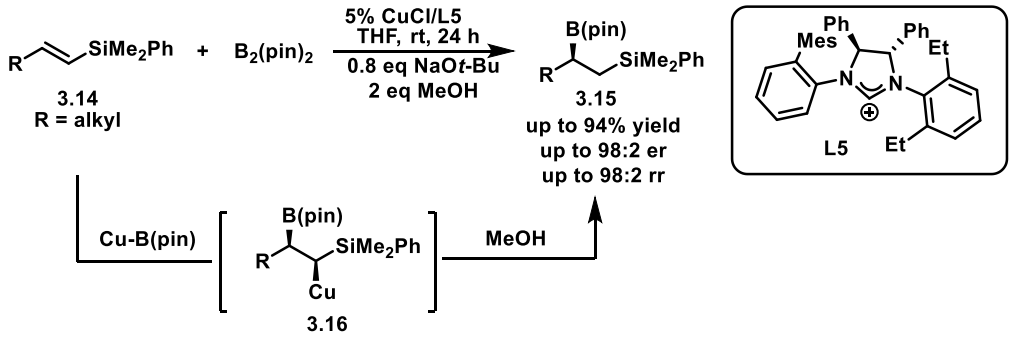

[15] Meng, F.; Jang, H.; Hoveyda, A. H. *Chem. Eur. J.* **2013**, *19*, 3204.

In contrast, Suginome[16] developed a palladium-catalyzed silylboration reaction of mono-substituted allenes (**1.17)** to produce a product with silicon-containing stereocenter (Scheme 3.6).

Scheme 3.6 Palladium-catalyzed syntheses of chiral 1,2-silylboronates

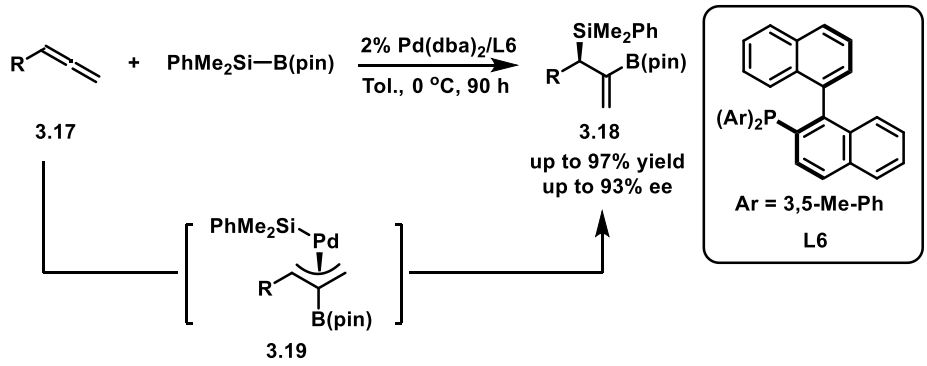

3.2.1.2.2 1,2-Bimetallics with *syn* stereogenic centers

Synthesis of chiral *syn*-1,2-bimetallics is still recognized as a challenging process. Only two examples of constructing enantiomerically enriched *syn*-1,2-diboronates have been published so far. As mentioned in section 1.2.2, Rh and carbohydrate-derivatives catalyze the diboration reaction to deliver *syn*-1,2-diboronates. No mixed chiral *syn*-1,2-dimetallics have been reported due to the difficulty of establishing regio-, diastereo- and enantioselectivity at the same time.

[16] T. Ohmura, H. Taniguchi, M. Suginome, *J. Am. Chem. Soc*. **2006**, *128*, 13682

3.2.1.2.3 1,2-Bimetallics with *anti* stereogenic centers

Unlike synthesis of the corresponding *syn*-1,2-bimetallics, in which there are at least two examples, synthesis of configurationally stable *anti*-1,2-dimetallics has not been achieved with high levels of enantioselectivity, although three attempts have been reported in the literature. Yamamoto[17] reported the first diastereoselective synthesis of *anti*-1,2-silylboronates with up to 92:8 dr (Scheme 3.7). Unfortunately, the products are racemic, and substrates are limited to phenyl-substituted alkenes, in which the phenyl ring is required to stabilize a carbanion intermediate.

Scheme 3.7 Racemic syntheses of anti-1,2-silylboronates

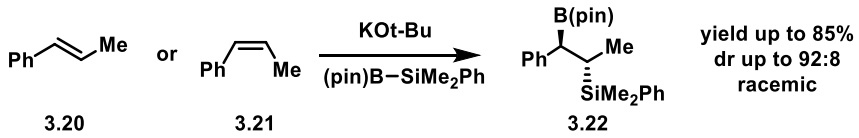

The other two efforts to synthesize *anti* dimetallics targeted diboronates. As described in chapter one, although carbohydrates[18] could catalyze the diboration of *cis* alkenes to deliver 1,2-*anti*-diboronates in good yield, the

[17] H. Ito, Y. Horita, E. Yamamoto, *Chem. Commun*. **2012**, *48*, 8006
[18] L. Yan, Y. Meng, F. Haeffner, R. M. Leon, M. P. Crockett, J. P. Morken, , *J. Am. Chem. Soc.* **2018**, *140*, 3663

enantioselectivity suffered. A similar result was observed when a rhodium-phosphine complex catalyst was used as a catalyst[19].

Scheme 3.8 Asymmetric syntheses of anti-1,2-diboronates

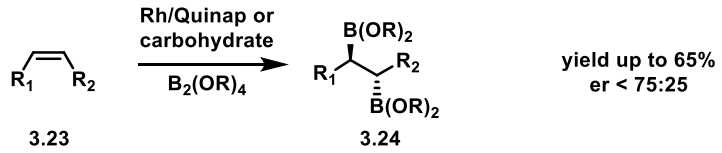

In summary, the synthesis of chiral vicinal dimetalloids has mostly focused on chiral vicinal dimetallics bearing only one stereogenic center. Although several successful methods have been reported for the preparation of vicinal *syn*-bis-(metallics), there is a need to develop protocols for the preparation of *anti*-1,2-dimetallic compounds.

3.2.2 General strategies and challenges for the synthesis of vicinal dimetallics

As discussed in the last section, the most common strategy for the synthesis of vicinal dimetallics with one stereocenter is either *syn* addition of a C-H and a C-M bond across a metal-substituted *E* alkene or *syn* addition of

[19] a) J. B. Morgan, S. P. Miller, J. P. Morken, *J. Am. Chem. Soc.* **2003**, *125*, 8702; b) S. Trudeau, J. B. Morgan, M. Shrestha, J. P. Morken, *J. Org. Chem.* **2005**, *70*, 9538

two C-M bonds across a simple unsaturated site (Scheme 3.9 a). In terms of the synthesis of internal dimetallics, *syn* addition of H-M bonds across a trisubstituted alkene is challenging due to steric effects. Consequently, the *syn* addition of two C-M bonds is a better approach (Scheme 3.9 b). Although the dimetallation strategy is effective for the synthesis of chiral *syn*-dimetallics from *E* alkenes, the method failed to produce chiral *anti*-dimetallics from *Z* alkene in a selective fashion (Scheme 3.9 c). The low enantioselectivity could be attributed to the difficulty of differentiating two prochiral faces of a Z alkene since the two substituents are too sterically similar to be distinguished.

Scheme 3.9 General strategies on the synthesis of 1,2-dimetallic compounds

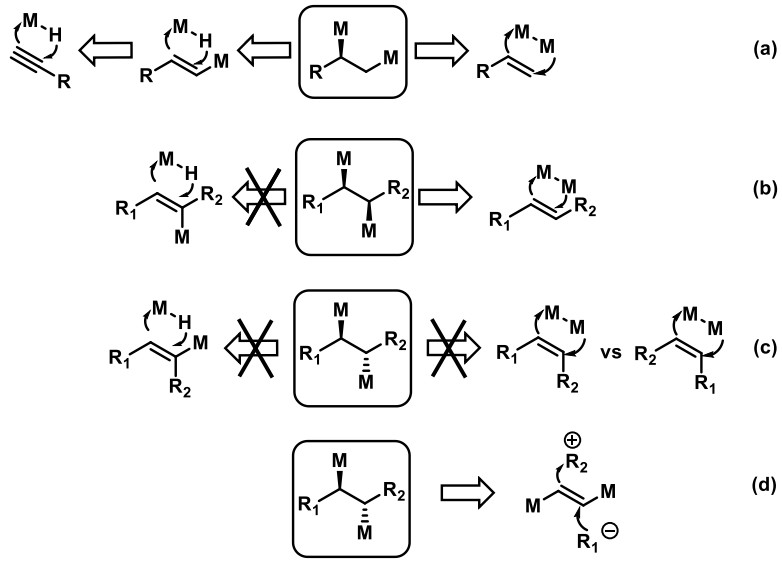

3.2.3 Conjunctive cross-coupling: a new strategy toward the synthesis of *anti*-1,2-dimetallics

To address the synthesis of *anti*-1,2-dimetallics, we proposed an unprecedented synthesis strategy (Scheme 3.9 d). Instead of installing two C-M bonds across a *cis* alkene, *anti*-dimetallics could be produced through *anti* addition of two R groups across *trans* alkenes that bear two metalloid groups.

Scheme 3.10 Reaction design for conjunctive cross-coupling of bimetallics

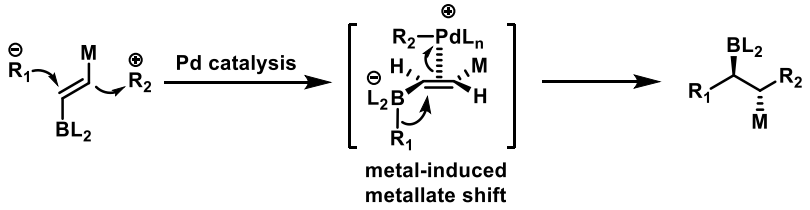

To meet the requirement of this strategy, conjunctive cross-coupling was considered. The essential step of conjunctive cross-coupling, a 1,2-metallate rearrangement, allows *anti* addition of a C-C bond and a C-Pd bond across a *trans* alkene through a stereospecific 1,2-migration of alkenyl boron 'ate' complex. The newly formed C-Pd bond is replaced by a C-C bond in the last step of the cross-coupling. By taking advantage of this stereospecific process, enantioenriched *anti*-dimetallic compounds could be delivered for the first time with the appropriate choice of ligands on palladium and boron.

3.2.4 Crucial advances in conjunctive cross-coupling enabled by novel ligand design

As outlined in chapter 2, conjunctive cross-coupling reactions have been broadly developed and implemented for the synthesis of several valuable building blocks since the first disclosure in 2016. One of the most recent advances in conjunctive cross-coupling paved the path for its potential application to the synthesis of dimetallic compounds. In 2018, our group reported the first example of diastereoselective and enantioselective conjunctive cross-coupling. [20] An unusual boron ligand, methylated acenaphthoquinone (mac), was developed to enhance the reaction chemoselectivity. As shown in Scheme 3.11, compared to the neopentyl glycol boronic ester, the mac-derived substrate reversed the chemoselectivity, favoring the desired product over Suzuki cross-coupling byproducts with a 2.5:1 ratio. Further, the addition of one equivalent of CsF boosted the chemoselectivity to 4.2:1, affording the product in 76% isolated yield with excellent diastereoselectivity and enantioselectivity.

[20] J. A. Myhill, C. A. Wilhelmsen, L. Zhang, J. P. Morken, *J. Am. Chem. Soc*. **2018**, *140,*15181

Scheme 3.11 Adavances in conjunctive cross-coupling

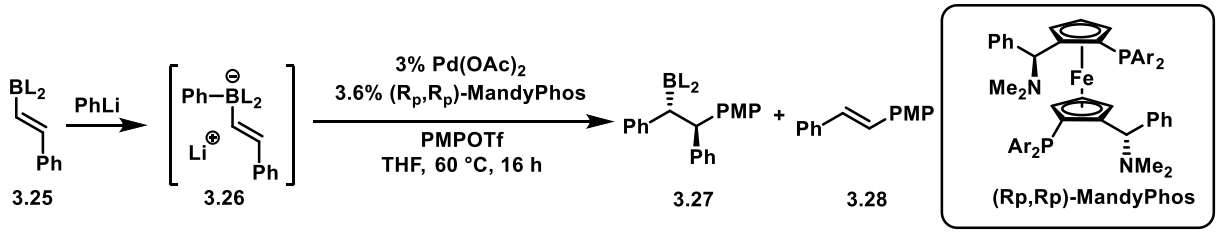

Entry	BL_2	additives	yield	3.27:3.28	dr	er
1	B(neo)	-	10%	1:5.8	>20:1	99:1
2	B(mac)	-	70%	2.5:1	>20:1	99:1
3	B(mac)	1 eq CsF	76%	4.2:1	>20:1	99:1

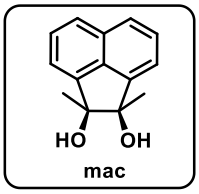

Compared to the original conjunctive cross-coupling with a vinyl boronate 'ate' complex, the β-substituted alkenyl boronate 'ate' complex is bulkier, which impedes association of the alkene to palladium. Consequently, the traditional transmetallation that occurs in the Suzuki reaction, a process that is promoted by coordination between palladium and boronic ester oxygen, is facilitated. The reversed chemoselectivity enabled by the mac diol ligand might arise from the size of the naphthalene ring system. In contrast to pinacol, the mac diol replaced two vicinal methyl groups with a large aromatic ring system, which could better shield the lone pairs of electrons on the boronic ester oxygens, so that palladium has more chance to be associated to the alkene. Therefore, it was hypothesized that the mac diol ligand would also enhance the chemoselectivity in the synthesis of *anti* dimetallic compounds

by conjunctive cross-coupling. The ligand investigation in this project provided solid experimental support for the synthesis of dimetallics via conjunctive cross-coupling.

3.2.5 Organosilanes and their properties

Organosilanes are valuable reagents in organic synthesis, materials science, as well as in pharmaceuticals. Like organoboron reagents, organosilanes can undergo a variety of transformations that forge carbon-heteroatom bonds. These processes include oxidation[21], fluorination[22], and C-C bonds fromations through Sakurai allylation and Hiyama-Denmark cross-coupling. In this section, a brief introduction of organosilane chemistry will be presented.

Scheme 3.12 Common transformations of organosilanes

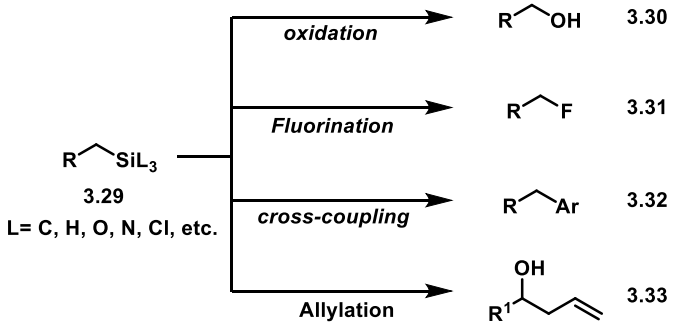

[21] K. Tamao, T. Kahui, M. Akita, T. Iwahara, R. Kanatani, J. Yoshida, M. Kumada, *Tetrahedron*, **1983**, *39*, 983

[22] M. Tredwell, V. Gouverneur, Org. Biomol. Chem., 2006,4, 26

3.2.5.1 Preparation of organosilanes

organosilicon has tetrahedral molecular geometry that can accommodate four different ligands. The first organosilane compound, tetraethylsilane, was prepared by Charles Friedel and James Crafts in 1863 by reacting $SiCl_4$ with Et_2Zn.[23] The general preparation of organosilanes is simple and straightforward, and employs commercially available halogenated silicon precursors. Organosilanes bearing different substituents could be prepared by sequential nucleophilic substitution with various equivalents of nucleophiles (Scheme 3.13 a).[24] Similar to the preparation of organoboronates, organosilanes can also be prepared from hydrosilylation of unsaturated hydrocarbons (Scheme 3.13 b).[25]

Scheme 3.13 Preparation of organosilanes

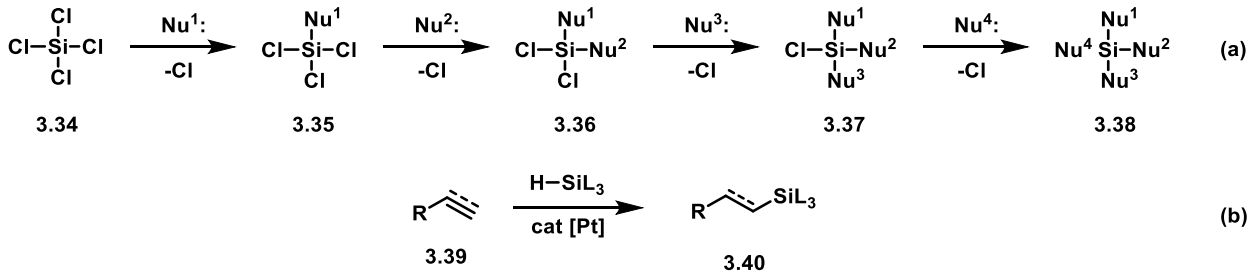

[23] H. Sakurai, Silicon: Organosilicon Chemistry. Encyclopedia of Inorganic Chemistry, Wiley, 2006
[24] Organic Silicon Compounds, Ullmann's Encyclopedia of Industrial Chemistry, Wiley-VCH, 2003
[25] B. Marciniec, Hydrosilylation, Advances in Silicon Science, Springer, 2009

3.2.5.2 Electronic properties of organosilanes

Compared to carbon (Pauling electronegativity 2.55), silicon is less electronegative (Pauling electronegativity 1.9), which leads to different electron density distribution on C-Si bonds as opposed to other carbon-heteroatom bonds. According to molecular orbital theory, the σ(C-Si) bonding orbital has a larger coefficient on carbon, while the σ^*(C-Si) *anti*-bonding orbital has a bigger coefficient on silicon. Two remarkable electronic properties of organosilanes originate from this unusual distribution: the β-silicon effect and the α-silicon effect. Many reactions of organosilanes are driven by these effects, which will be described in the ensuing sections.

Scheme 3.14 Eletronic differences of C-Si bonds

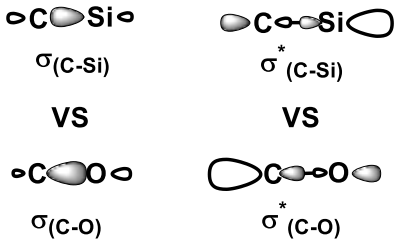

3.2.5.2.1 β-Silicon effect

The β-silicon effect is a special type of hyperconjugation that could be rationalized as a σ(C-Si) bonding orbital donating to an adjacent empty p

orbital, which lowers the energy of the C-Si bonding electrons. Similarly, the $\sigma_{(C\text{-}Si)}$ bonding orbital can overlap with a σ^*(C-X) orbital to promote the cleavage of a β-C-X bond, in which X is a leaving group. As demonstrated by Jorgensen, [26] this stabilization is favored by 38 kcal/mol compared to compounds that do not have a β-silicon present (Scheme 3.15).

Scheme 3.15 β-silicon effect

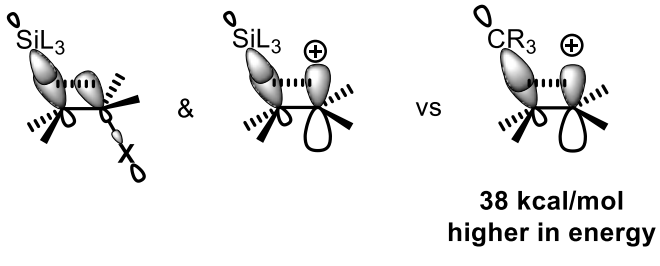

Scheme 3.16 α-silicon effect

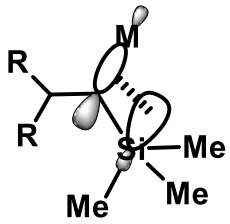

3.2.5.2.2 α-Silicon effect

The α-silicon effect is another hyperconjugation effect that organosilanes possess. As depicted in Scheme 3.16, the overlap between the $\sigma_{(C\text{-}M)}$ orbital and $\sigma^*_{(C\text{-}Si)}$ orbital destabilizes the C-Si bond but significantly stabilizes the C-M bond. The stabilization effect is supported not only by computational studies[27] but also by experimental data. For example, Chen[28]

[26] S.G. Wierschke, J. Chandrasekhar, W. L. Jorgensen, *J. Am. Chem. Soc.* **1985**, 107, 1496
[27] : a) P. V. R. Schleyer, T. Clark, A. J. Kos, G. W. Spitznagel, C. Rohde, D. Arad, K. N. Houk, N. G. Rondan*, J. Am. Chem. Soc.* **1984**, *106*, 6467; b) D. M. Wetzel, J. I. Brauman, *J. Am. Chem. Soc*., **1988**, *110*, 8333
[28] S. Gao, M. Chen, Chem. Sci., **2019**, *10*, 7554

demonstrated that the presence of the α-silicon effect enabled the high regioselectivity of the formation of an allyl copper species (**3.42**) over (**3.44)**, which is trapped by aldehyde selectively (Scheme 3.17). The α-silicon effect thus plays an essential role in transition metal-catalyzed reactions involving organosilanes.

Scheme 3.17 α-silicon effect enabled copper catalysis

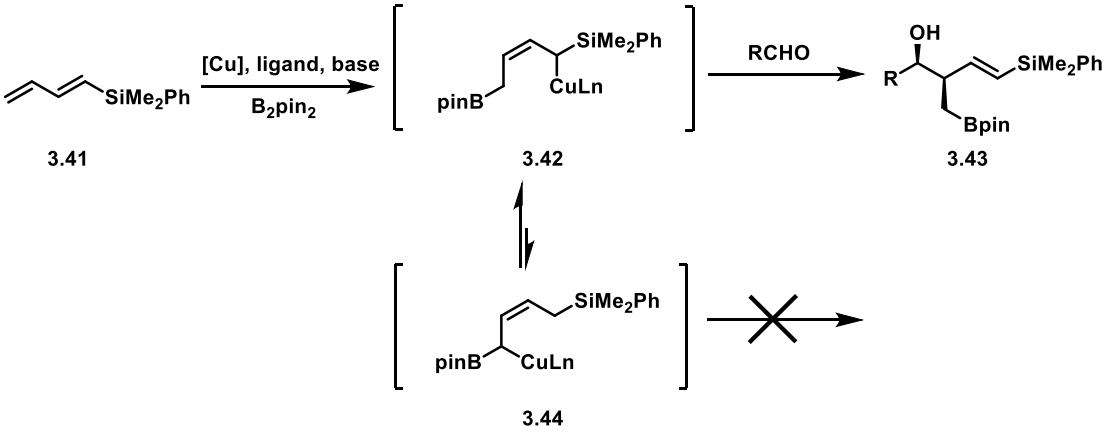

3.2.5.3 Reactivities of organosilanes

3.2.5.3.1 Classification of organosilanes

All organosilanes can be roughly divided into two categories: activated electrophilic organosilanes and unactivated organosilanes. Which category an organosilane belongs to will profoundly affect its reactivity toward certain types of reactions. The classification of organosilanes is defined by the groups attached to it. Any silane bearing a heteroatom (e.g., oxygen, nitrogen,

halogen) is considered activated and electrophilic, whereas an organosilane that only has hydrocarbon groups is considered unactivated and less electrophilic.[23] Because of their strong electrophilicity, the activated organosilanes are not as stable, more reactive and require careful handling, while unactivated organosilanes are generally robust. Nevertheless, the electrophilicity of the organosilane will also enhance its reactivity, which makes the activated compounds easier to transform, as discussed in the next section.

Scheme 3.18 Two common types of organosilanes

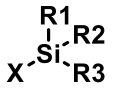

Activated (electrophilic) silane: X= heteroatom or H; R1,R2,R3 = any atoms

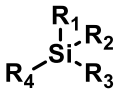

Unactivated (less electrophilic) silane: R_1,R_2,R_3= alkyl, aryl

3.2.5.3.2 Oxidation of organosilanes

Similar to organoboronates, organosilanes are recognized as masked hydroxyl groups since they can be easily oxidized into corresponding alcohols with retention of configuration.[29] Tamao and Fleming are the pioneers in the research of silane oxidation.

[29] K. Tamao, T. Kahui, M. Akita, T. Iwahara, R. Kanatani, J. Yoshida, M. Kumada, *Tetrahedron*, **1983**, *39*, 983

3.2.5.3.2.1 Oxidation of activated organosilanes

Oxidation of activated organosilanes requires peroxides and nucleophilic additives, such as fluoride salts, under acidic, neutral, or basic conditions (Scheme 3.19). [30] Hypervalent silicon intermediates are believed to be involved in this transformation. The activated silane (**3.47)** is attacked by a nucleophile (e.g., fluoride, hydroxide) to form a pentavalent silicon (**3.48**), [23] an even more electrophilic intermediate. The oxidized product is then delivered through peroxide addition, followed by a stereospecific *anti* periplanar migration (Scheme 3.20).[30]

Scheme 3.19 Oxidation conditions for activated organosilanes

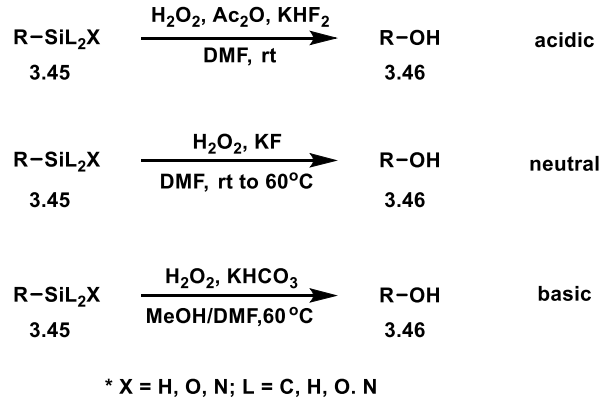

Scheme 3.20 Mechasnim of oxidation reactions of activated silanes

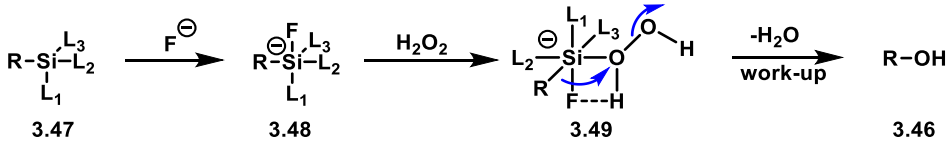

[30] K. Tamao, M. Kumada, K. Maeda, *Tetrahedron Lett*. **1984**, *25*, 321

3.2.5.3.2.2 Oxidation of unactivated organosilanes

Compared to the oxidation of activated silyl groups, oxidation of unactivated organosilanes requires one extra ingredient: an activator that enhances the electrophilicity of the silane. For instance, Fleming discovered that strong Bronsted acids, Lewis acids or electrophiles could activate a commonly used unactivated organosilane, dimethylphenylsilane (**3.50**),[31] through electrophilic substitution. Then, the unactivated organosilanes were transformed into activated compounds (**3.52**) by displacing the phenyl ring with nucleophiles. The rest of the oxidation procedure was similar to that described in the previous section.

Scheme 3.21 Mechasnim of oxidation reactions of unactivated silanes

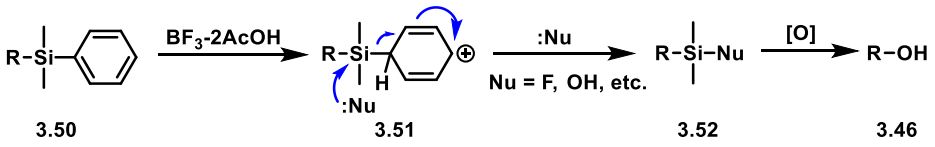

Other unactivated organosilanes could also be oxidized by conversion to activated silanes with various activators, as reviewed by Landais.[32] The trimethylsilyl group, for example, is generally considered inert to oxidation.

[31] a) I. Fleming, R. Henning, H. Plaut, *J. Chem. Soc., Chem. Commun.*, **1984**, 29; b) I. Fleming, P. E.J. Sanderson, *Tetrahedron Lett*., **1987**, *28*, 4229; c) a) I. Fleming, H. Rolf, D. C. Parker, H. E. Plaut, P. E. J. Sanderson, *J. Chem. Soc., Perkin Trans. 1,* **1995**, 317

[32] G. R. Jones, Y. Landais, *Tetrahedron*, **1996**, *52*, 7599

However, an iridium-catalyzed borylation enables oxidation through a sequence of boronic ester oxidation, followed by Brook rearrangement (Scheme 3.22).[33]

Scheme 3. 22 Oxidation of organotrimethylsilanes

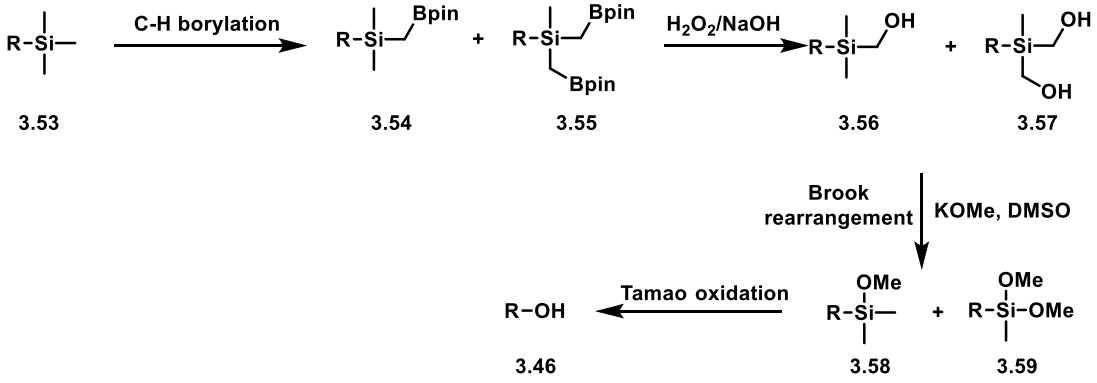

3.2.5.3.3 Allylation of organosilanes

Another useful transformation of organosilanes is the Hosomi-Sakurai reaction,[34] in which allylsilanes act as nucleophiles and add to various aldehydes and acetals. The mechanism of the allylation reaction varies depending on the type of allylsilane used. For instance, when activated organosilanes are employed, the reaction occurs by a closed transition state with the Lewis acidic silicon binding to the carbonyl oxygen.[35] Similar to the

[33] Torigoe, T.; Ohmura, T.; Suginome, M. *J. Org. Chem.* **2017**, *82*, 2943
[34] A. Hosomi, H. Sakurai, *Tetrahedron Lett.,* **1976**, *17*, 1295
[35] a) H. Sakurai, *Synlett*, **1989**, 1, 1; b) S. Kobayashi, K. Nishio, *Tetrahedron Lett.,* **1993**, *34*, 3453

allylboration reaction, the reaction occurs by a chair-like six-membered ring transition state (**3.64**) to forge the C-C bond and cleave the C-Si bond (Scheme 3.23).

Scheme 3. 23 Allylation of organosilanes and aldehydes

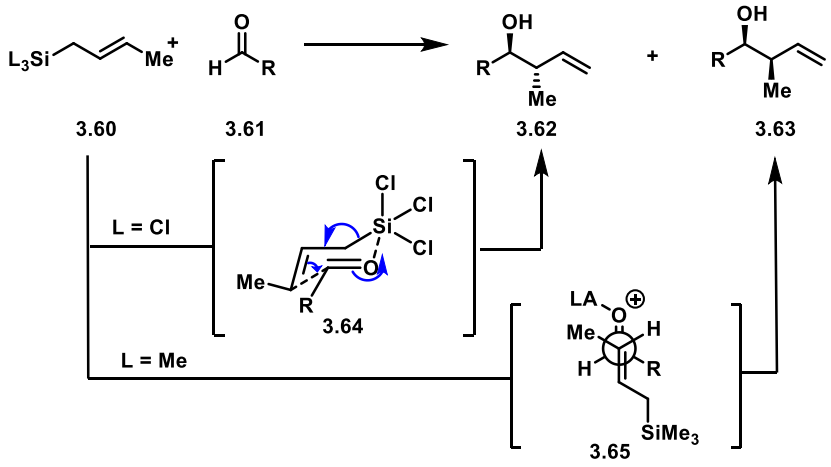

In contrast to electrophilic silanes, unactivated organosilanes react with carbonyls through an open transition state since these organosilanes are not Lewis acidic enough to bind to the carbonyl compounds. Therefore, the allylation reaction using unactivated silanes needs assistance from external Lewis acids to activate carbonyls.[36]

Both enantioselective catalytic allylation reactions[37] and substrate-controlled diastereoselective allylation[38] reactions have been developed as

[36] M. Yus, J. C. Gonzalez-Gomez, F. Foubelo, *Chem. Rev*. **2011**, *111*, 7774
[37] a) D. R. Gauthier, E. M. Carreira. *Angew. Chem., Int. Ed. Engl*. **1996**, 35, 2363; S. E. Denmark, J. Fu, *J. Am. Chem. Soc.* **2000**, *122,* 12021
[38] C.E. Masse, J. S. Panek, *Chem. Rev.* **1995**, *95*, 1293

powerful tools for the formation of C-C bonds with the latter of these being particularly well studied. The Panek group demonstrated that various Lewis acids promoted allylation of enantioenriched secondary dimethylphenyl-silanes with excellent yield and diastereoselectivity.[39] Several aldehydes and masked aldehydes could be employed in the reactions (Scheme 3.24). However, the scope is limited by the difficulty of preparing enantioenriched allylsilanes.[31d] More applications can be expected if new methods were developed to produce allylsilane substrates.

Scheme 3.24 Substrate-controlled diastereoselective allylation of organosilanes

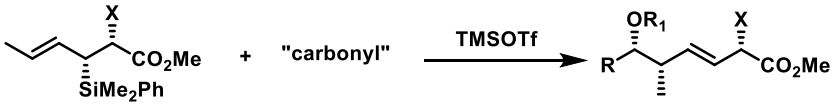

carbonyl	X	yield	dr
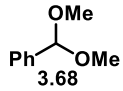 3.68	OMe	90%	13:1
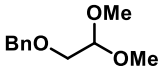 3.69	OMe	90%	30:1
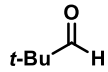 3.70	OAc	87%	30:1

[39] a) J. S. Panek, M. Yang, *J. Am. Chem. Soc.*, **1991**. *113*, 6594; b) J. S. Panek, M. Yang, *J. Am. Chem. Soc.*, **1991**. *113*, 9868; c) J. S. Panek, M. Yang, F. Xu, *J. Org. Chem.*, **1992**. *57*, 4790; d) J. S. Panek, M. Yang, J. S. Solomon, *J. Org. Chem.*, **1993**. *58*, 1003; e) J. S. Panek, M. Yang, I. Muler, *J. Org. Chem.*, **1992**. *57*, 4063;

3.2.5.3.4 Cross-coupling of organosilanes

Another well-known transformation of organosilanes is the cross-coupling reaction with organohalides, also called the Hiyama-Denmark reaction. Tamejiro Hiyama [40] developed this palladium-catalyzed cross-coupling reaction in 1988, where classic oxidative addition, transmetallation, and reductive elimination forge a new C-C bond (Scheme 3.25). The original reaction conditions required fluoride ion or base as an activator to form pentavalent silanes (**3.75**), the active species in transmetallation.

Scheme 3. 25 Classic catalytic cycle of Hiyama cross-coupling reactions

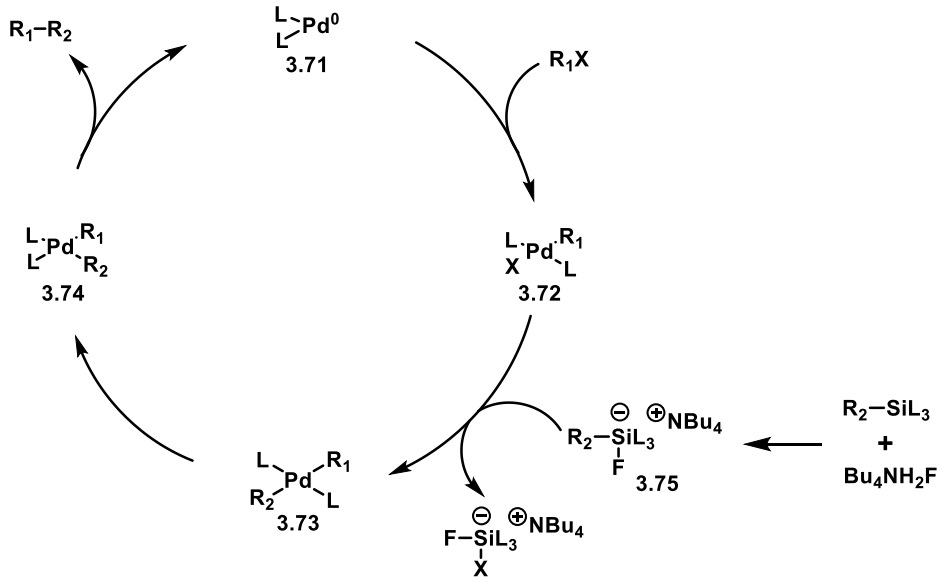

[40] Y. Hatanaka, T. Hiyama, *J. Org. Chem.*, **1988**. *53*, 918

Later, the Denmark group found that the cross-coupling reaction could perform without any additives if deprotonated organosilanols were adopted.[41] A mechanistic study revealed that the transmetallation of deprotonated organosilanols (**3.76**) occurs without formation of the hypervalent silanes (Scheme 3.26). Despite being well-studied in the last two decades, the cross-coupling of organosilanes is still limited to C(sp^2) organosilanes (except the allylic silanes[42]), which impedes its applications in modern organic synthesis.

Scheme 3.26 Denmark's cross-coupling of organosilanols

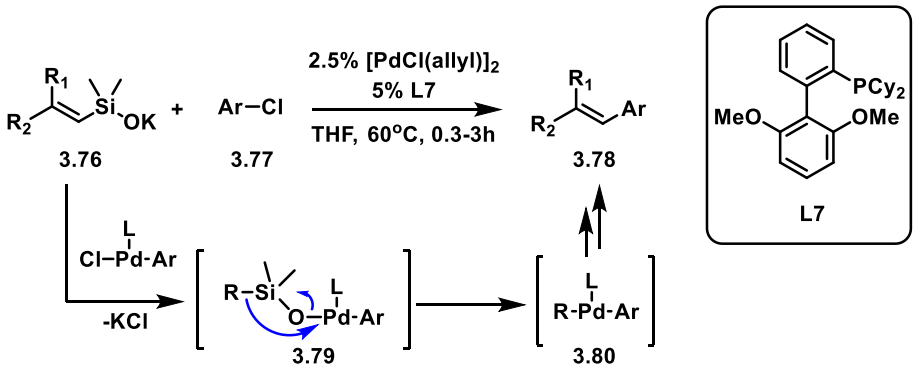

3.3 Development of the reaction

3.3.1 Survey of proper substrate

Our initial discovery originated from the proposal depicted in the Scheme 3.27. By employing a substrate with two carbon-metal bonds in a

[41] S. E. Denmark, C. S. Regens, *Acc. Chem. Res.* **2008**, *41*, 1486
[42] S. E. Denmark, N. S. Werner, *J. Am. Chem. Soc.*, **2008**, *130*, 16382

trans relationship (at least one of the metalloids is boron to ensure the formation of 'ate' complex), conjunctive cross-coupling reaction will deliver the enantioenriched *anti*-dimetallic species as products. Thus, initial investigations focused on how the identity of the second metal affects the reaction.

Scheme 3.27 Experiment design of conjunctive cross-coupling in synthesis of anti-1,2-dimetallics

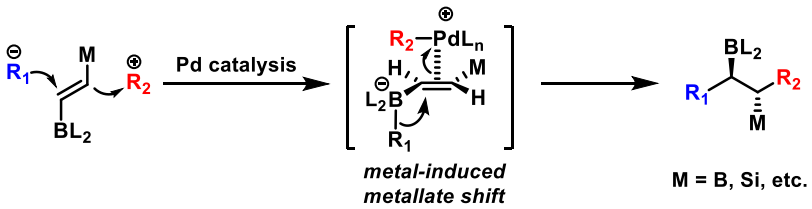

Boron was chosen as the second metalloid to begin the investigation because of its excellent stability and utility. As shown in Scheme 3.28, 1,2-bis(boronates) (**3.81**) and (**3.82)** were synthesized through olefin metathesis. The resulting alkenes were subjected to similar conditions, as previously reported in palladium-catalyzed conjunctive cross-coupling reactions.[43] Unfortunately, both reactions failed to produce any desired product (Scheme 3.29), which was attributed to the formation 'ate' complex are not clean. The intermediate formed after the addition of one equivalent of phenyllithium was

[43] L. Zhang, G. J. Lovinger, E. K. Edelstein, A. A. Szymaniak, M. P. Chierchia, J. P. Morken, *Science*, **2016**, *351*, 70

not consistent with one tetravalent boron and one trivalent boron. More tetravalent boron was formed presumably through oligomerization.

Scheme 3.28 Synthesis of alkenyl 1,2-bisboronates

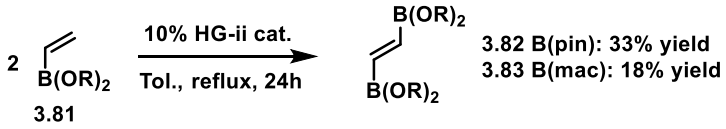

Scheme 3.29 Conjunctive cross-couplings of alkenyl 1,2-bisboronates

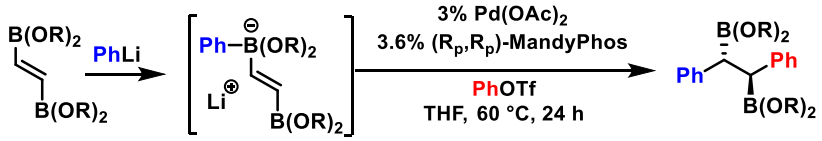

Entry	BL_2	Yield	er
1	B(pin)	<5 %	na
2	B(mac)	<5 %	na

To solve this problem, the mixed boronate (**3.87**) was synthesized through the palladium-catalyzed borylation of (**3.86**), as described by the Burke group (Schme 3.30).[44] The product (**3.87)**, with only one electrophilic boron available for attack, was then subjected to conjunctive cross-coupling. Although the 'ate' complex derived from (**3.87)** was formed cleanly, the

[44] S. J. Lee, K. C. Gray, J. S. Paek and M. D. Burke, *J. Am. Chem. Soc*. **2008**, *130*, 466

resulting complex was not soluble in various organic solvents and this observation prompted us to examine other metals other than boron.

Scheme 3.30 Preparation of mixed-1,2-bisboronates

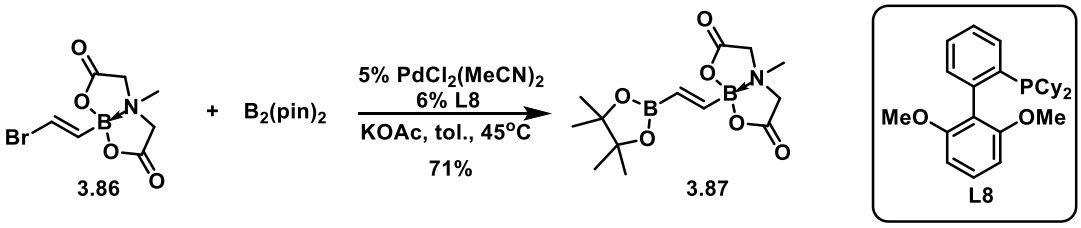

To address the problem described above, a silane was proposed as an alternative second metalloid in lieu of boron. By installing one boron and one silane in the form of a *trans* alkene, there is only one electrophilic boron and this should form a clean 'ate' complex. Moreover, organosilanes possess not only excellent solubility in organic solvents but also interesting electronic properties. In particular, the well-studied α-effect of silanes (Scheme 3.16) could polarize the alkene and stabilize the developing C-Pd bond. Therefore, alkenyl silylboronate (**3.90**) was constructed through hydroboration of trimethylsilyl acetylene (**3.88**), [45] and subsequently subjected to the conjunctive cross-coupling reaction. Although the majority of the mass balance favored the Suzuki cross-coupling byproduct, 19% of the desired product was collected with 73:27 er, which indicated that the *anti* dimetallic

[45] S. Perreira, M. Srebnik, *Organometallics*, **1995**, *14*, 3127

species could be generated through conjunctive cross-coupling (Scheme 3.32, entry 1).

Scheme 3.31 Preparation of alkenyl silaboronates

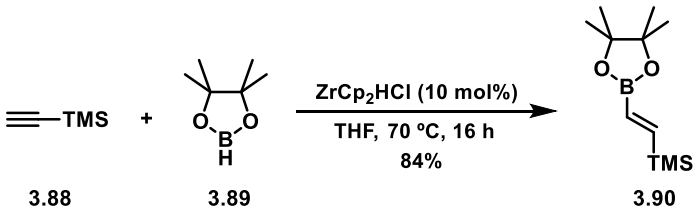

Scheme 3.32 Optimization of ligand on boron, temperature and additive

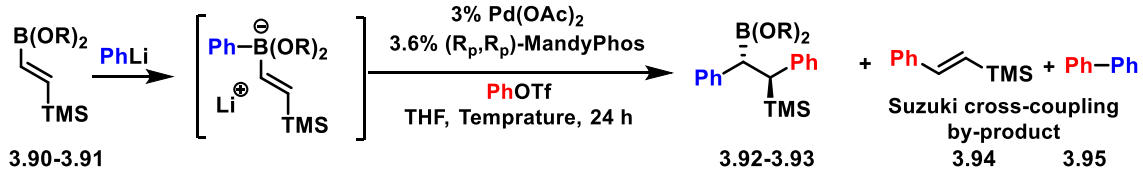

Entry	BL_2	Temp	Additive	Yield	er
1	B(pin)	60°C	-	19%	73:27
2	B(mac)	60°C	-	33%	94:6
3	B(mac)	45°C	-	55%	96:4
4	B(mac)	45°C	CsF	67%	97:3
5	B(mac)	45°C	CsF (pre-mix)	89%	97:3

3.3.2 Reaction optimization

3.3.2.1 Ligands on boron

As shown in the Scheme 3.32, the novel boronate ligand, methylated acenaphthoquinone (mac), designed for diastereoselective conjunctive cross-coupling[18] was adopted to address the chemoselectivity problem. Surprisingly, both the chemoselectivity and enantioselectivity improved when mac was employed as the ligand on boron. This observation can be explained by the bulkiness of the mac ligand, a feature that exacerbates steric penalties with the catalyst such that the alkene preferentially binds through one prochiral face. Of note, conducting the reaction at lower temperature led to higher chemoselectivity (Scheme 3.32, entry 3).

3.3.2.2 Additive effect of CsF

Inspired by previous diastereoselective conjunctive cross-coupling[18], the addition of one equivalent of CsF further boosted the yield to 67% (Scheme 3.32, entry 4). Furthermore, the efficiency of the reaction improved to 89% when the freshly prepared 'ate' complex was pre-mixed with CsF for 30 minutes before the remaining reagents were introduced (Scheme 3.32, entry 5). To better understand the impact CsF had on the reaction outcome, NMR studies were undertaken. As shown in Figure 3.1, a ^{1}H NMR spectrum was acquired after the 'ate' complex was formed from phenyllithium and the

alkenyl boronate in deuterated THF. The NMR spectrum showed two sets of resonances likely representing the pair of diastereomers (**3.96)** and (**3.97)** (as dimethyl substituents *syn* or *anti* to the phenyl ring) even though the assignments of resonances are not available. Then, the 'ate' complex was mixed with CsF for 30 minutes before another ^{1}H NMR spectrum was obtained. In the second spectrum, there were still two sets of resonances but with altered chemical shifts and in an approximate 1:1 ratio (vs. 3:1 in pure

Scheme 3. 33 A pair of diastereomers of 'ate' complex derived from mac-boronates

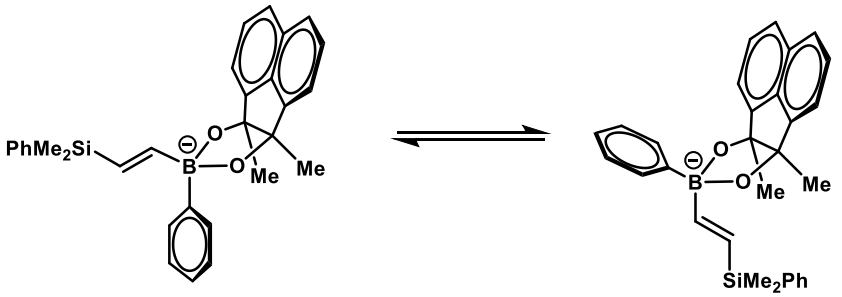

syn-3.96 *anti*-3.97

'ate' complex), which suggested a different pair of diastereomers. This new pair of diastereomers was likely the corresponding cesium counterion 'ate' complexes (**3.100)**, whose formation was driven to completion by precipitation of LiF(solubility: 0.09 mM in THF).[46] (Scheme 3.34).

[46] D. A. Wynn, M. M. Roth, B. D. Polland, *Talanta*, **1984**, *31*, 1036

Figure 3.1 ^{1}H NMR spectrum of 'ate' complex derived from mac-boronates

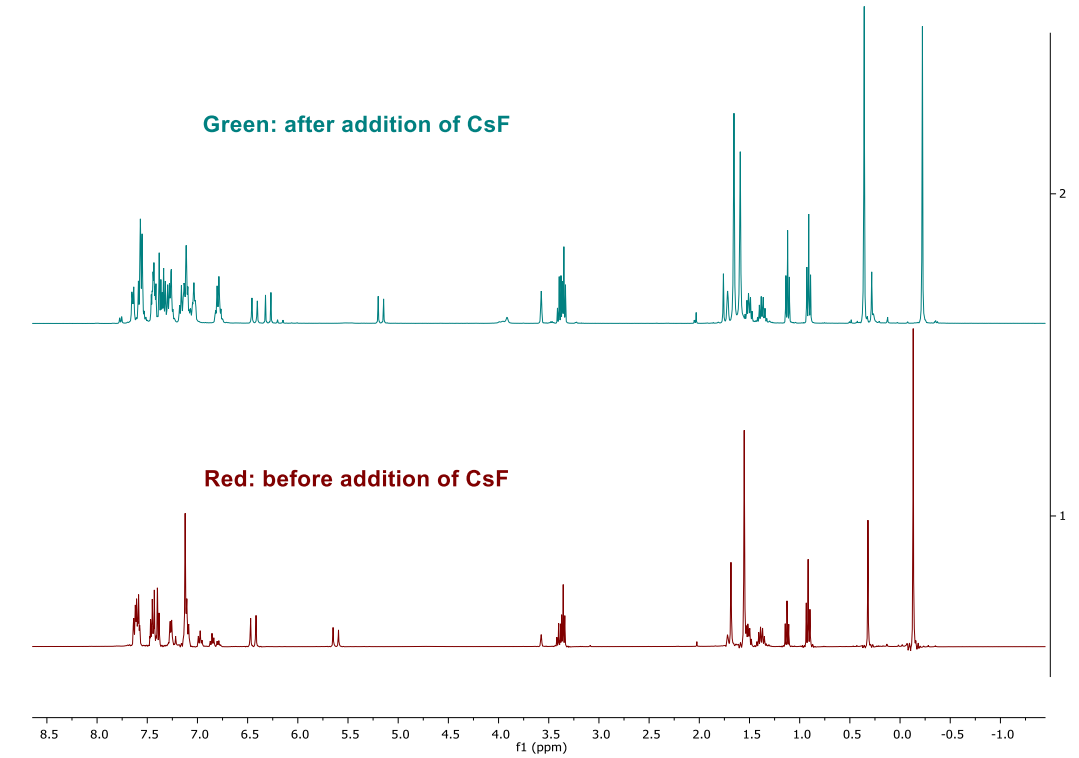

(a) 1H NMR of 'ate' complex before and after the addition of CsF

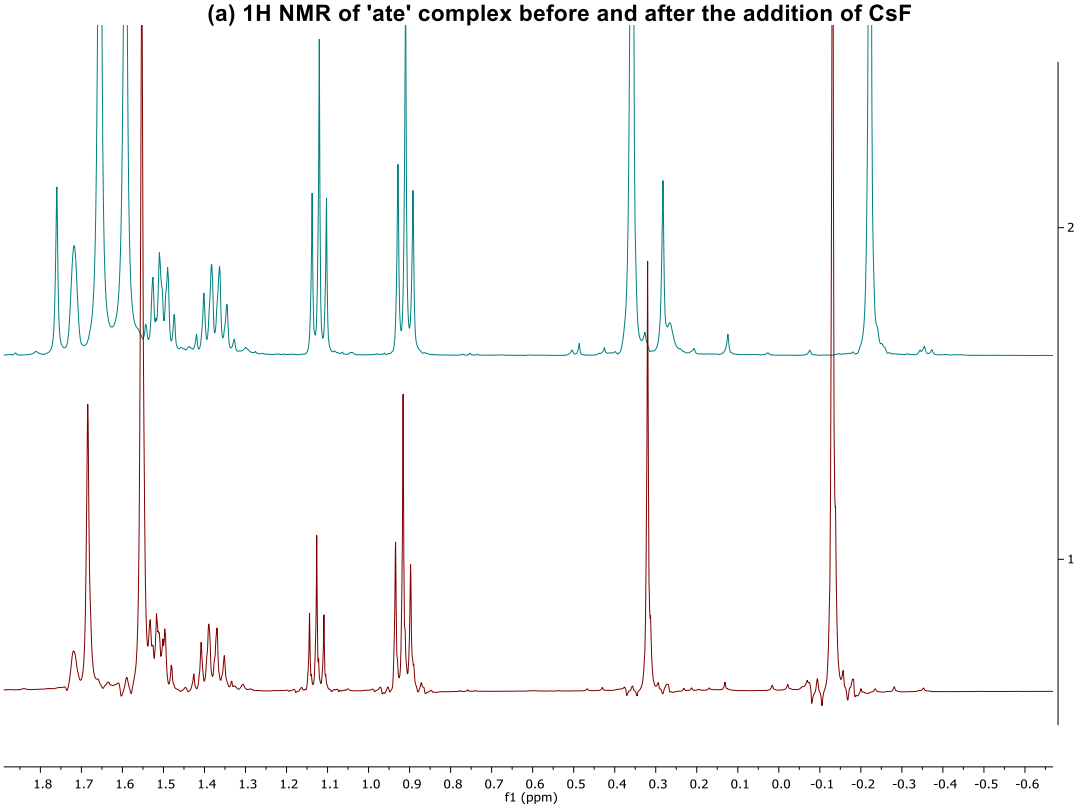

(b) Enlarged 1H NMR between -1 to 1.8 ppm

Scheme 3. 34 Function of CsF: conterion exchange

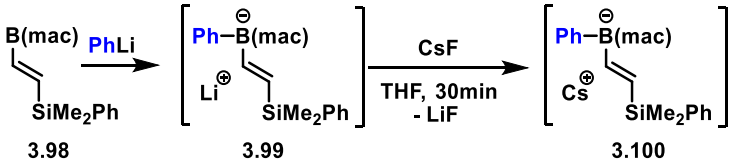

Based on all the observations described above, two hypotheses were proposed regarding the beneficial effect of CsF. First, the counterion exchange produces a 'ate' complex (**3.100)** with Cs as a counterion. Cs could associate with lone pairs of oxygens in boronic esters, which prevent the transmetallation step in the formation of corresponding Suzuki by-product. Alternatively, if one of the diastereomers of the 'ate' complex is more reactive than the other, the addition of CsF could help to equilibrate the less reactive isomer into the reactive one during the reaction time perhaps through a reversible alkoxide dissociation (Scheme 3.33). The possibility of fluoride anion affecting the reactivity was ruled out by the fact that cesium carbonate had a similar effect as cesium fluoride.

3.3.2.3 Ligands on silane

To develop reagents with silicon groups that are useful in synthetic chemistry, other silane groups were investigated, including

dimethylphenylsilane (**3.102**), dimethylbenzyl silane (**3.101**), and *para*-methoxyphenyldimethylsilane (**3.103**). As shown in Scheme 3.35, each of these silanes was well tolerated in conjunctive cross-coupling providing products with excellent enantioselectivity and yield. The Me_2PhSi group showed the best yield and enantiomer ratio. Therefore, substrate (**3.102**) was chosen as the model substrate in subsequent investigations.

Scheme 3.35 Substrate scope of ogranosilanes

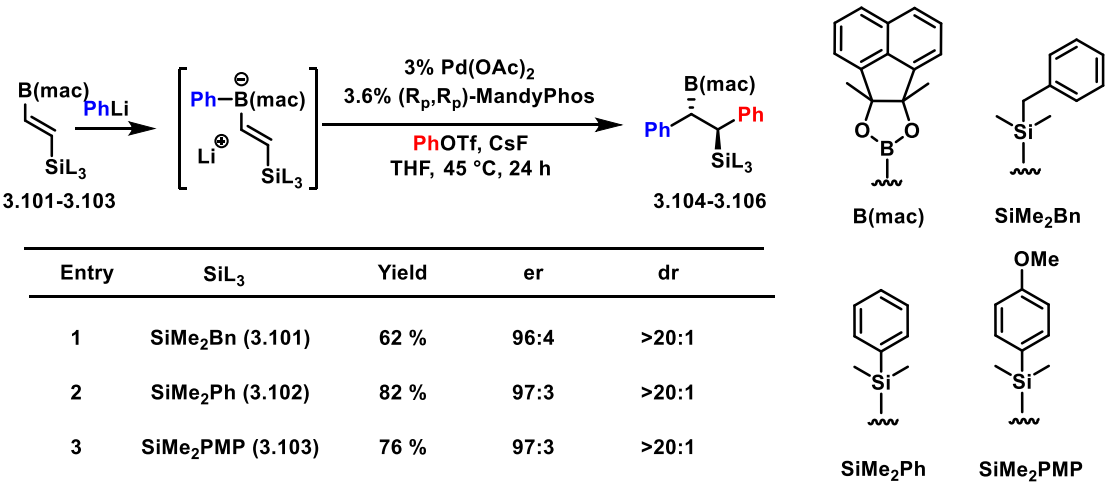

Entry	SiL_3	Yield	er	dr
1	$SiMe_2Bn$ (3.101)	62 %	96:4	>20:1
2	$SiMe_2Ph$ (3.102)	82 %	97:3	>20:1
3	$SiMe_2PMP$ (3.103)	76 %	97:3	>20:1

3.3.2.4 Other optimizations

After surveying the type of precatalyst, catalyst loading, solvent, and other additives, the best conditions were found as shown in Scheme 3.36: 3 mol% palladium acetate with 3.6 mol% MandyPhos ligand, and 1.05 equiv. cesium fluoride in THF ([substrate] = 0.66 M) at 45 °C for 24 hours. Under

these conditions, the product was isolated in 82% yield, and the absolute configuration determined by single-crystal X-ray diffraction (see Sec. 3.5). It is worth noting that the reaction can be carried out with halide electrophiles as well so long as potassium triflate is added (Scheme 3.36, entry 7). A previous report[47] revealed that potassium triflate acts as the halide scavenger to preventing catalyst poisoning.

Scheme 3.36 Optimization of reaction conditions

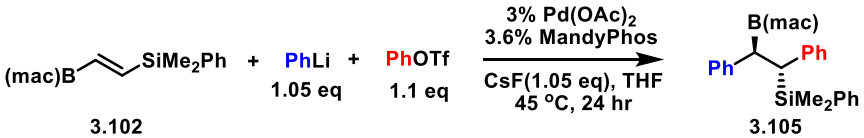

3.102 3.105

Entry	Variation from the conditons above	Yield
1	none	82%
2	$Pd_2(dba)_3$	44%
3	1.5 % catalyst loading	51%
4	THF/Toluene=5:1	59%
5	THF/DMSO=10:1	42%
6	KF instead of CsF	38%
7	1.1 eq PhBr, 2 eq KOTf	77%

3.3.3 Substrate scope

3.3.3.1 Electrophiles scope

[47] G. J. Lovinger, M. D. Aparece, J. P. Morken, *J. Am. Chem. Soc*. **2017**, *139*, 3153

With the optimized reaction conditions in hand, a number of substrates were examined in the conjunctive cross-coupling. As depicted in Scheme 3.37, good reactivity was obtained with both aryl triflates and aryl bromides as electrophiles. Electron-rich aromatic rings (**3.107-3.110**) and heteroaryl rings (**3.114-3.116**) were well tolerated, whereas electron-poor electrophiles (**3.111-3.113**) reacted with diminished enantioselectivity. The reaction tolerated various functional groups, as shown by ketone **(3.112)** and ester (**3.113**).

Scheme 3.37 Substrate scope of electrophiles

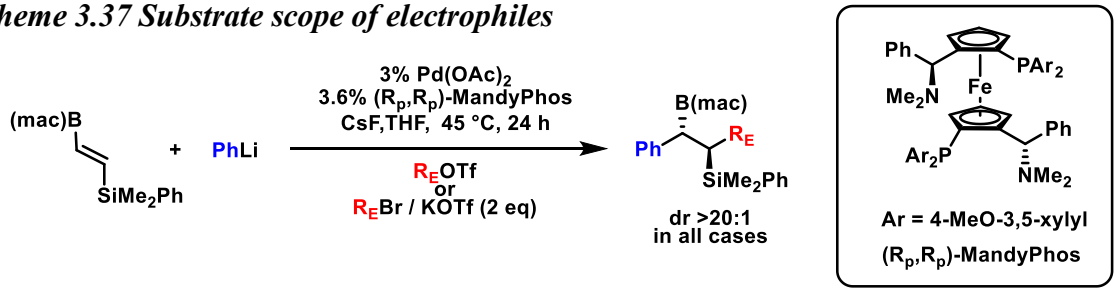

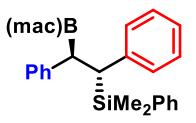

3.105
82%, e.r. 97:3

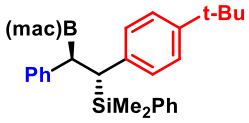

3.107
79%, e.r. 97:3

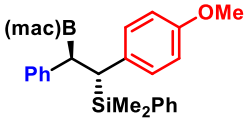

3.108
77%, e.r. 95:5

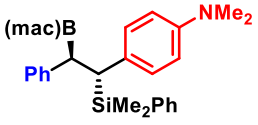

3.109
73%, e.r. 96:4

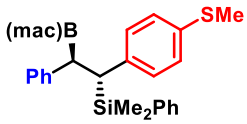

3.110
63%, e.r. 94:6

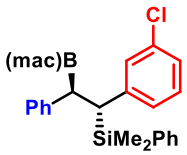

3.111
62%, e.r. 92:8

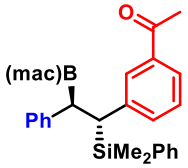

3.112
68%, e.r. 88:12

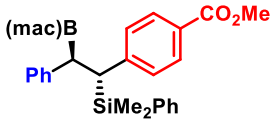

3.113
60%, e.r. 82:18

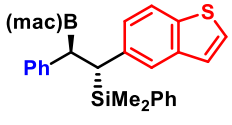

3.114
68%, e.r. 95:5

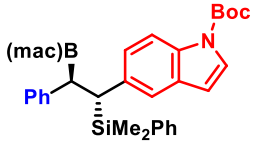

3.115
57%, e.r. 93:7

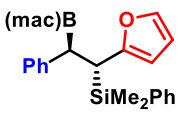

3.116
88 %, e.r. 95:5

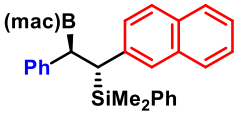

3.117
73%, e.r. 94:6

3.3.3.2 Scope of migrating groups

In terms of the scope of migrating groups, both electron-rich (**3.118**) and electron-poor (**3.119**) aryl groups migrated with good levels of enantioselectivity. In addition, heteroaryl rings (**3.124, 3.125**) also underwent migration to deliver enantioenriched silylboronates. However, the reaction is sensitive to steric effects, demonstrated by the low er obtained for ortho-substituted compound (**3.122**).

Scheme 3.38 Substrate scope of migrating groups

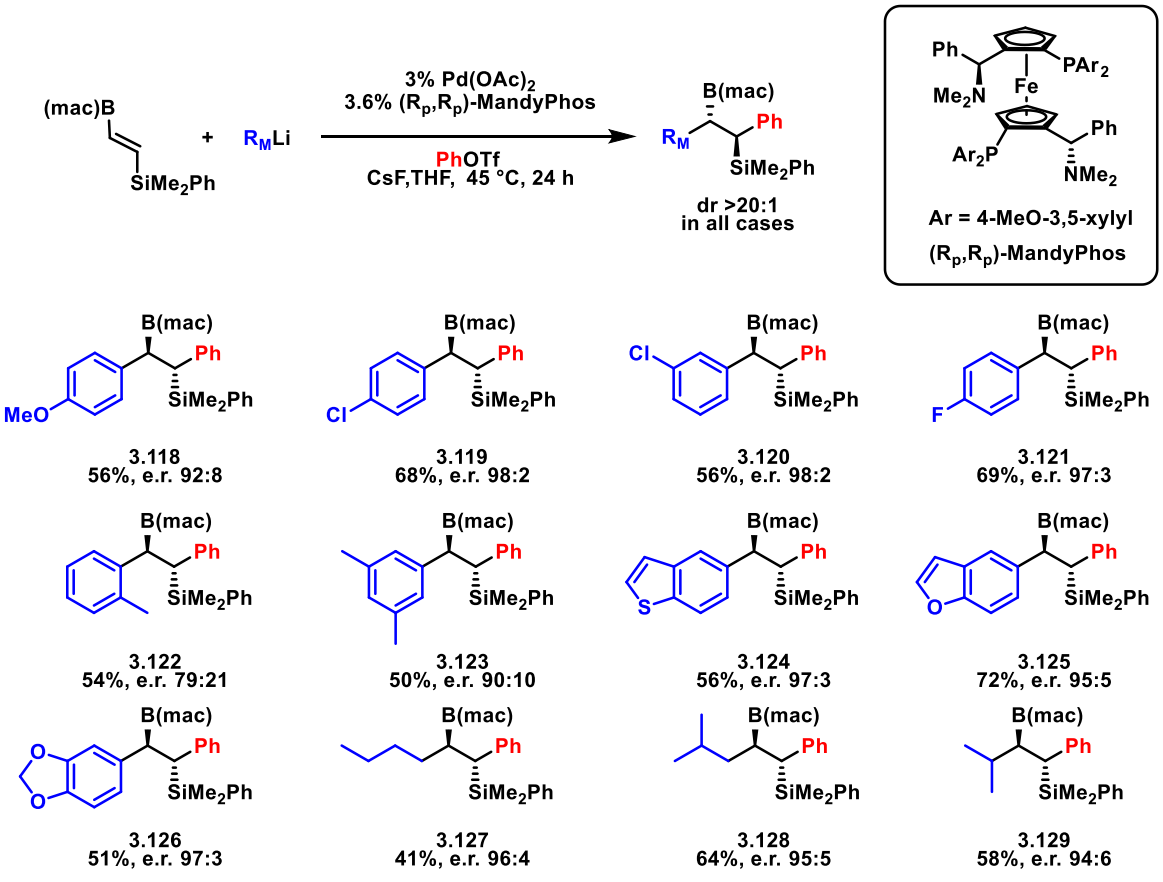

Simple alkyl groups could also be applied as migrating groups, shown by compounds 3.127-3.129. This is an exciting result considering that alkyl substituents did not migrate in the related diastereoselective conjunctive cross-coupling[18] of *E* propenyl boronates. Unlike aromatic rings, alkyl groups are less prone to migrate presumably because the alkyl group can not stabilize the negative charge developed during the 1,2-metallate shift.[48] Alkyl migration may be facile in this particular case due to the strong α-effect which stabilizes the developing carbon-palladium bond in the transition state for the metallate shift(as shown in scheme 3.16).

3.3.3.3 Enantioenriched allylic silane

Another useful product found in the substrate scope exploration was the allyl silane product derived from a simple alkenyl bromide electrophile. As shown in Scheme 3.39, when *E*-propenyl bromide was employed, enantioenriched allyl silane (**3.131**) was produced in good yield and enantioselectivity. The unique reactivity of allyl silanes provides opportunities to further derivatize the conjunctive cross-coupling products

[48] V. K. Aggarwal, G. Fang, X. Ginesta, D. M. Howells, M. Zaja, *Pure. Appl. Chem*., **2006**, *78*, 215

into more complicated but useful structures, which will be discussed in section 3.3.6.

Scheme 3.39 Conjuctive cross-coupling in synthesis of chiral allylic silanes

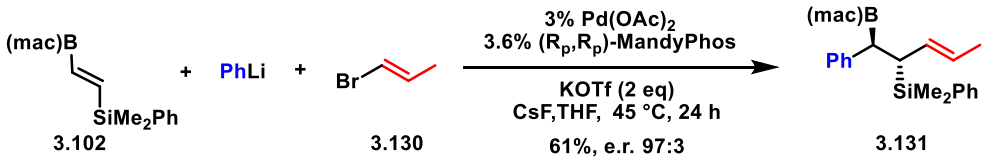

3.3.4 Practical features

3.3.4.1 Substrate synthesis

3.3.4.1.1 Original synthesis route

With an expectation that the method described above could be easily adopted in chemical and pharmaceutical industries, several practical features were investigated and are discussed in this section. Starting material availability is a significant factor determining whether this method will be easily adopted by other scientists.

The model substrate was originally synthesized *via* a three-step sequence, as shown in Scheme 3.40. Commercially available dimethylphenyl-silylacetylene (**3.132**) was mixed with HBpin and a catalytic amount of Schwartz reagent. The crude product (**3.133**) was then treated with KHF_2 to

deliver the corresponding trifluoroborate salt (**3.134**), [49] which was transformed into the mac-derived boronic ester (**3.102**) by a $FeCl_3$ catalyzed condensation reaction (Scheme 3.40). [50] Although the preparation was straightforward and only required one purification step, it required rigorous removal of pinacol after the formation of the trifluoroborate salt, which was laborious and time-consuming even with an improved protocol described by Aggarwal.[38] Therefore, an alternative and refined synthetic route was proposed and optimized.

Scheme 3.40 Orginal synthetic route for substrate 3.102

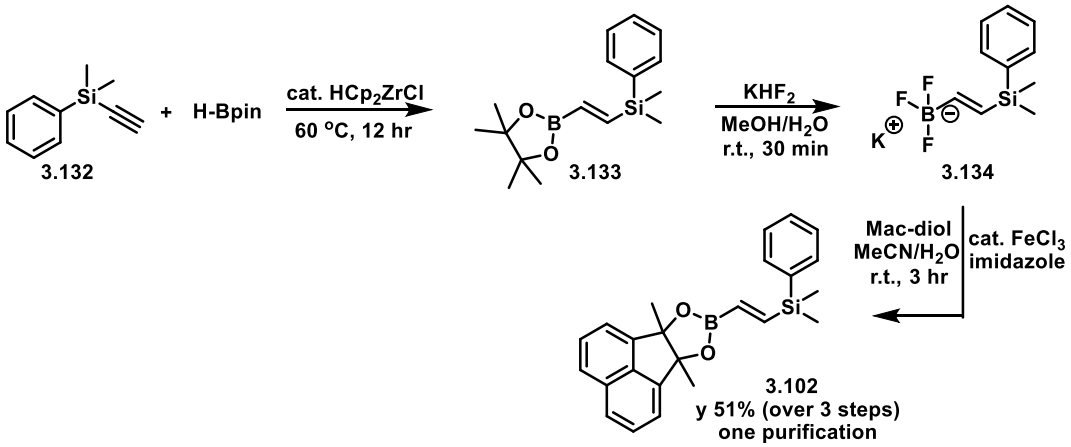

3.3.4.1.2 Improved synthetic route

[49] V. Bagutski, A. Ros, V. K. Aggarwal, *Tetrahedron*, **2009**, *65*, 9956
[50] J. L. Wood, L. D. Marciasini, M. Vaultier, M. Pucheault, *Synlett*, **2014**, *25*, 0551

Hydroboration of silylacetylene 3.132 was still considered as the easiest way to establish stereochemically defined alkenyl boronates if "mac" ligand could be pre-installed into the hydride reagent. Previously, as described by Knochel,[51] pinacol borane was prepared from borane-dimethylsulfide and pinacol. Thus, the corresponding synthesis of HB(mac) (**3.136**) might be plausible from mac diol (**3.135**) and BH_3-SMe_2. A one-pot two-step substrate synthesis was proposed and developed: mac diol was firstly treated with borane-dimethylsulfide in THF at room temperature for 3 hours until the evolution of gas ceased. The borane generated *in situ* was then directly subjected to zirconium-catalyzed hydroboration to deliver the product (**3.102**) as a stable solid; this process was amenable to a gram-scale synthesis of HB(mac).

Scheme 3. 41 New synthetic route for substrate 3.102

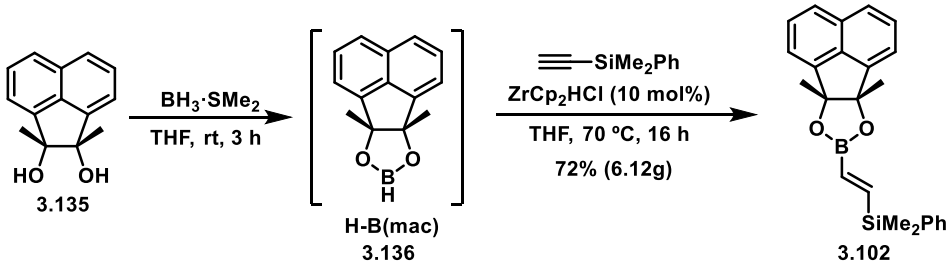

3.3.4.1.3 Alternative method of 'ate' complex formation

[51] C. E. Tucker, J. Davidson, P. Knochel, *J. Org. Chem*, **1992**, *57*, 3482

One of the advantages of conjunctive cross-coupling is that the starting material, the 'ate' complex, can be formed in two ways. As described below (Scheme 3.42), the 'ate' complex, in general, is produced from alkenyl silyl-boronate (**3.102**) and aryl lithium. However, when the organolithium in the previous route is not easily accessible, the same 'ate' complex could also be generated from aryl boronate (**3.139**) and lithiated alkenyl silane (**3.138**). Aryl boronates could be synthesized from its commercially available BF_3K salt and mac-diol under Lewis acid catalysis (vide supra),[39] while the alkenyl lithium could be produced from the corresponding bromide 3.137 *via* a lithium-halogen exchange with *tert*-butyllithium. The alkenyl bromide is readily prepared through hydrozirconation of silylacetylene (**3.132**) followed by trapping with NBS. Although more synthetic steps are needed, the latter route might find its value when migrating groups bearing sensitive functional groups are employed in the reaction.

Scheme 3.42 Two directions of 'ate' complex synthesis

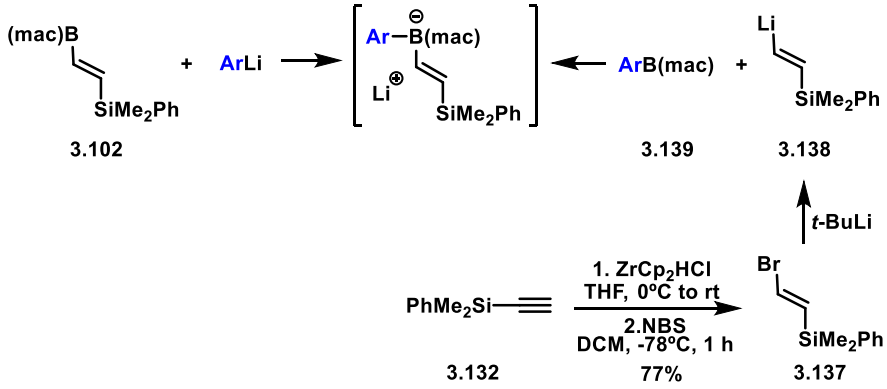

3.3.4.2 Practical scale of the reaction

Besides the accessibility of the starting material, the scale of the reaction is also an important factor when considering if the reaction is suitable for an industrial setting. With an efficient route to access the substrate on a gram scale, the optimization of catalyst loading and reaction time were performed to reduce the cost but maintain high yield and enantioselectivity (Scheme 3.43). The result revealed that only 0.5 mol% catalyst loading was needed to produce grams of chiral silyl boronates (**3.105**).

Scheme 3.43 Gram-scale synthesis of 3.105

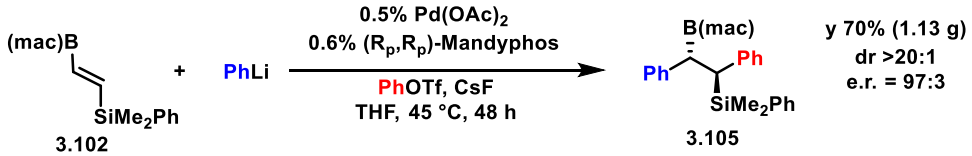

3.3.5 Transformations of dimetalloids

3.3.5.1 Construction of chiral *anti* diols

The most common method to transform boron and silicon groups, other than cross-coupling, is oxidation. In this section, protocols for transforming chiral *anti*-1,2-silylboronates to *anti* diols will be discussed.

3.3.5.1.1 Oxidation of organoboronates

Although oxidation of simple organoboronates is a common reaction, the oxidation of 1,2-silylboronates is not trivial since the corresponding products of oxidation are β-hydroxy silanes, which are extremely sensitive to both strong acid and base. As demonstrated in Peterson olefination reactions (Scheme 3.44),[52] either strong acid or base promotes *anti* or *syn* elimination to produce either *E* or *Z* alkenes, respectively. Therefore, a mild oxidation procedure was needed to oxidize silylboronates.

Scheme 3. 44 Peterson olefination of β-hydroxy silanes

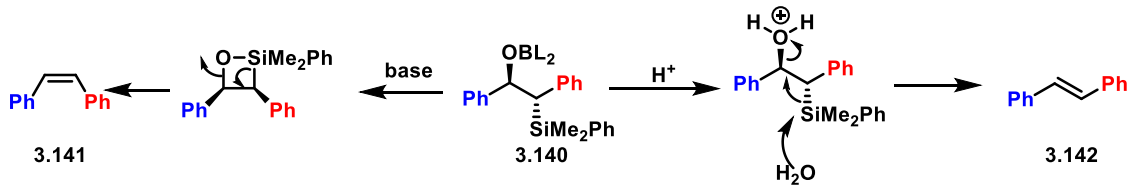

Firstly, neutral oxidation conditions, including sodium perborate and buffered H_2O_2 conditions, were examined (Scheme 3.45, entry 1-2). Unfortunately, the epimerization of one of the stereocenters occurred, which led to low diastereoselectivity. It is believed that the epimerization is promoted by a trace amount of acid introduced during aqueous workup or silica gel purification. As shown in Scheme 3.46, the protonated hydroxyl

[52] D. J. Peterson, *J. Org. Chem*., **1968**, *33*, 780

group is an excellent leaving group such that water may attack in an S_{N2} fashion. Alternatively, the protonated hydroxyl group may leave first to form the carbocation intermediate that is stabilized by the β-silane and phenyl group; the readdition of water from the opposite face may occur and allow epimerization.

Scheme 3.45 Optimizations of oxidation protocol for organobronates

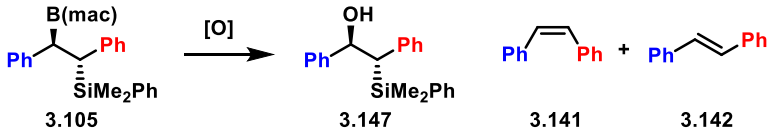

3.105 3.147 3.141 3.142

Entry	Oxidation conditions	Results
1	$NaBO_3$/THF, 12 hr, r.t.	y 81%, d.r.= 15:1
2	H_2O_2/pH=7 Phosphate buffer, 6 hr, r.t.	y 88%,d.r.= 8:1
3	30% H_2O_2/3M NaOH, 3 hr, r.t.	y 77%, 11% alkene d.r.= 5:1
4	30% H_2O_2/3M NaOH, 30 min, r.t.	y 87%, d.r.= 11:1
5	30% H_2O_2(4eq)/3M NaOH (2eq), 5 min, r.t.	y 94%, d.r. > 20:1

Scheme 3.46 Possible mechanism of epimerization

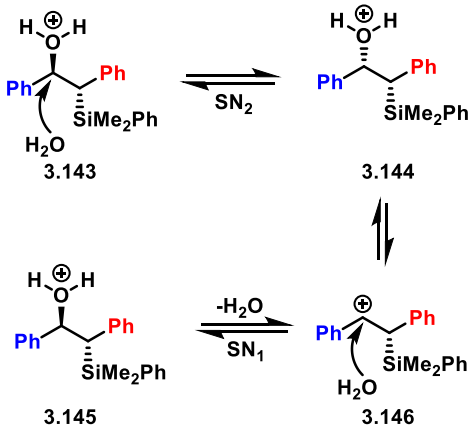

3.143 3.144 3.145 3.146

Unsurprisingly, the most common basic oxidation conditions, produced olefination byproducts in entry 3. Further optimization revealed that the olefination was avoided when the reaction time was shortened to 30 minutes. As shown in Scheme 3.45 entry 5, an efficient oxidation protocol was established by using modest excess of base and oxidant with even shorter reaction time.

3.3.5.1.2 Oxidation of organosilanes

With a clean oxidation protocol for boronates, oxidation of the silyl groups was investigated. The most common oxidation conditions, promoted by a strong acid as reported by Fleming,[25] was not applicable because of the competing olefination side reaction. After an extensive literature search, a buffered oxidation condition developed by Fleming[25c] was adopted. In this protocol, benzoyl protected β-hydroxysilane was oxidized with peracetic acid and bromine (*in situ*-generated). However, the conditions were incompatible with the conjunctive cross-coupling product (Scheme 3.47). Only 11% of the desired product (**3.149**) was delivered with a 44% over-brominated product (**3.150)** representing the mass balance. Compound (**3.150**) arises from the electrophilic substitution of phenyl rings on the backbone. To improve the

selectivity of electrophilic substitution, manipulation of the electron density of the aromatic ring on the silane was taken into consideration. For example, a *para*-methoxy phenyl group would be brominated faster than an unsubstituted phenyl ring. Indeed, the application of this electron-rich *para*-methoxyphenylsilane derived product (**3.153**) led to quick and clean oxidation to deliver enantioenriched *anti* diol (**3.155**) (Scheme 3.48). To the best of our knowledge, this represents the first demonstration of the Me_2PMPSi group in Fleming-Tamao oxidation.

Scheme 3.47 Buffered oxidation of organosilanes

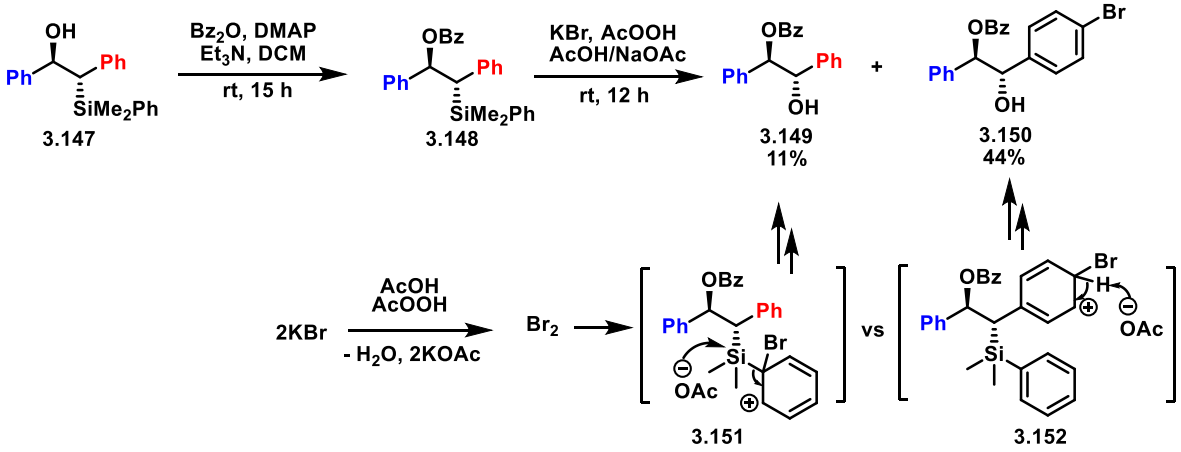

Scheme 3.48 The application of para-methoxyphenylsilane in oxidation reaction

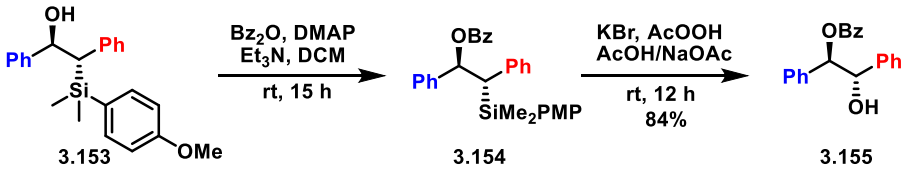

So far, sequential oxidation of conjunctive cross-coupling products to *anti* diols has been demonstrated. This cross-coupling/oxidation sequence is complementary to both traditional osmium-catalyzed enantioselective dihydroxylation reactions [53] and enantioselective diboration/oxidation reactions (chapter 1), which usually perform poorly with *Z* alkenes. Moreover, unlike the two types of reactions mentioned above, the orthogonal reactivity of organoboron and organosilane provides the opportunity to distinguish two secondary hydroxyl groups by step-wise oxidation. The first hydroxyl group derived from organoboron could be functionalized or protected before the second oxidation of organosilane, whereas two hydroxyl groups are established at the same time in the traditional dihydroxylation reactions.

3.3.5.2 Other transformations

Several other selective transformations of organoboron and organosilane could also be accomplished. As depicted in Scheme 3.49, the boronate was selectively converted to an amine with lithiated methoxyamine[54] to deliver the aminosilanes (**3.159)** and (**3.160)**. The buffered silane oxidation

[53] H. C. Kolb, M. S. VanNieuwenhze, K. B. Sharpless, *Chem. Rev.* **1994**, *94*, 2483
[54] S. N. Mlynarski, A. S. Karns, J. P. Morken, *J. Am. Chem. Soc*. **2012**, *134*, 16449.

unveiled the final product, *anti* amino alcohol, as another useful and prevalent motif. The boronates can also be converted into alkenes[55], followed by oxidation of the silane to construct homoallylic alcohols (Scheme 3.50). Furthermore, 1,3-diols could also be produced by Matteson homologation[11] and sequential oxidations.

Scheme 3. 49 Synthesis of chiral anti-1,2-diols and amino alcohols

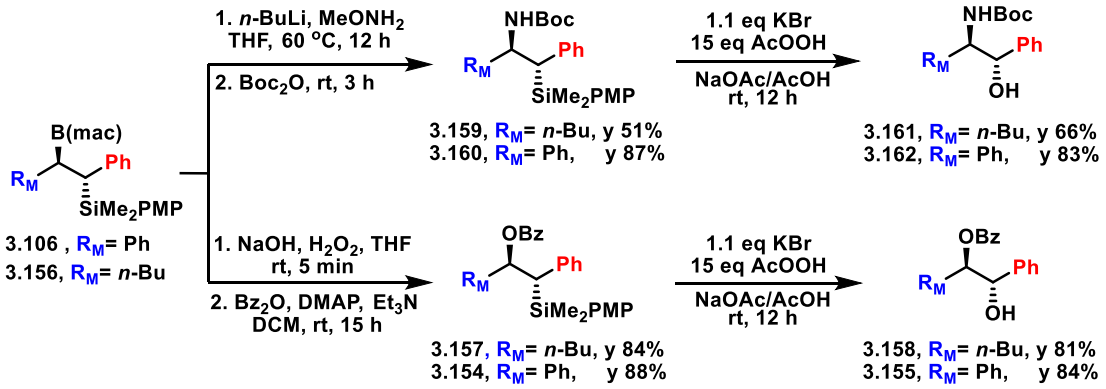

Scheme 3. 50 Other transformations: olefination and homologation

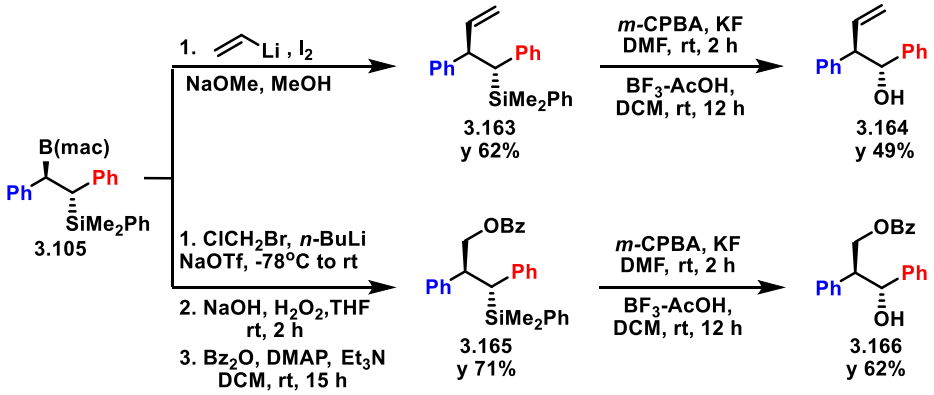

[55] R. J. Armstrong, V. K. Aggarwal, *Synthesis,* **2017**, *49,* 3323

3.3.6 Allylsilylation

3.3.6.1 Development of conjunctive cross-coupling/allylsilylation sequence

As discussed in 3.3.3.3, enantioenriched allylsilanes are another useful class of products because they are poised to undergo diastereoselective allylsilylation reactions to forge a new C-C bond and extend the carbon chain. Inspired by previous reports[30,31], compound (**3.131**) was treated with acetal (**3.167**) and Ti(O*i*-Pr)$_4$ at -78 degrees for 24 hours (Scheme 3.51). After workup and purification, 31% of the desired product (**3.168**) was isolated along with 23% of another byproduct (**3.169**), which formed upon exposure to silica gel. The byproduct was formed through an allylboration reaction of the desired product and benzaldehyde produced by the hydrolysis of acetal (**3.167**) upon purification.

Scheme 3.51 Initial experiment of allylsilylation

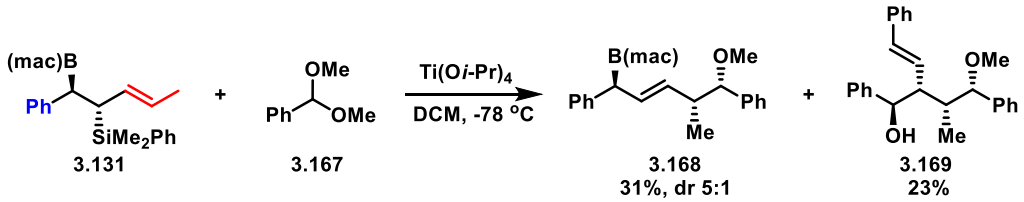

Although the double allylation was undesired, it proved the concept that conjunctive cross-coupling products could be derivatized through allylsilylation reactions. Additionally, the isolation of (**3.169)** suggested that tandem allylations might be possible if a different aldehyde could intercept the allylboron intermediate.

To further improve the reactivity and selectivity, several reaction conditions were investigated, including temperature, reaction time, as well as a variety of Lewis acids (Scheme 3.52). As shown in entry 5, 86% of products were produced with excellent diastereoselectivity when $BF_3{\cdot}Et_2O$ was employed at -30 °C.

Scheme 3.52 Optimization of allylsilylation reaction conditions

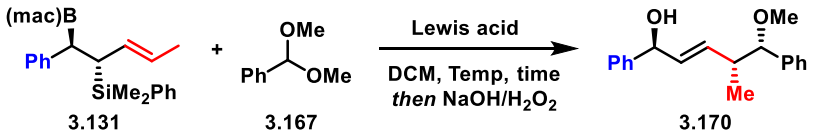

Entry	Lewis acid	temp.	time	yield	dr
1	$Ti(O\textit{i}\text{-}Pr)_4$	-78°C	48h	31%	5:1
2	$Ti(O\textit{i}\text{-}Pr)_4$	-40°C	24h	47%	5:1
3	TMSOTf	-40°C	24h	<5%	N/A
4	$Sc(OTf)_3$	-45°C	24h	<5%	N/A
5	$BF_3\text{-}Et_2O$	-78°C	24h	86%	>20:1

In addition, aliphatic dimethyl acetal was also converted into the desired product in high yield and with a useful level of diastereoselectivity (Scheme 3.53a). Other types of acetals, such as dibenzyl acetal, also reacted with allylsilane (**3.131)** under the optimized condition, but with diminished dr (Scheme 3.53b).

Scheme 3.53 Optimized reaction conditions for allysilylation of various acetals

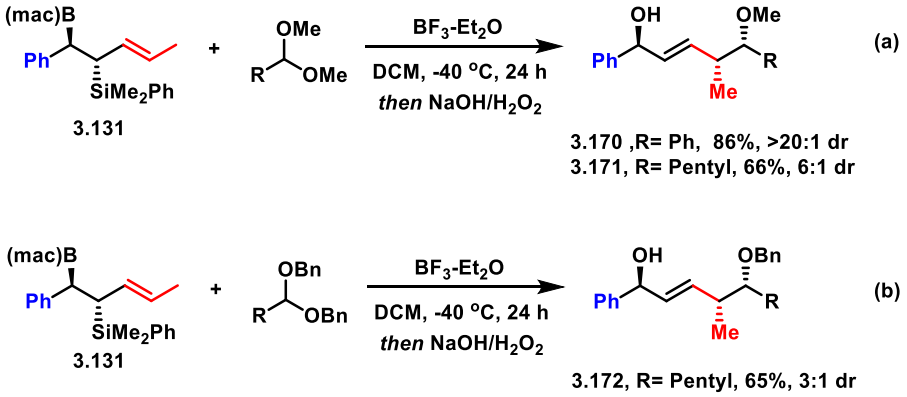

3.3.6.2 Applications in natural products synthesis

The conjunctive cross-coupling/allylsilylation reaction sequence may find its merit in the synthesis of natural products. For instance, the natural product halipeptin A derivative,[56] a potent anti-inflammatory agent, could potentially be constructed featuring the methodology. Previously, the

[56] R. Randazzo, G. Bifulco, C. Giannini, M. Bucci, C. Debitus, G. Cirino, L. Gomez-Paloma, *J. Am. Chem. Soc.* **2001**, *123*, 10870

halipeptin A derivative was assembled by the Nicolaou group[57] from fragment (**3.173)**, which itself was produced in 16 steps (Scheme 3.54). Herein, a five-step sequence was proposed that started with conjunctive cross-coupling of propyllithium and *E* propenyl bromide, followed by allylsilylation and oxidation (Scheme 3.55). This synthesis and the further development of the conjunctive cross-coupling/allylsilylation sequence are an ongoing area of research within the group.

Scheme 3. 54 Nicolaou's retrosynthesis of halipeptin A derivative

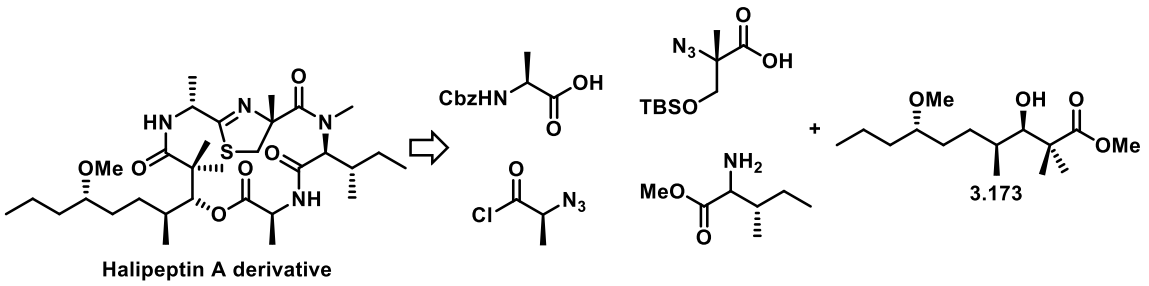

Scheme 3. 55 Proposed retrosynthesis of fragment (3.173) through conjunctive cross-coupling/allylsiylation sequence

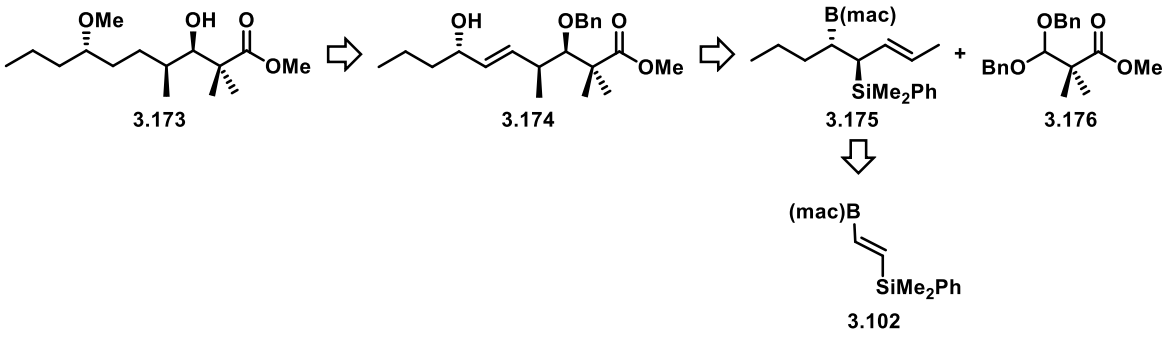

[57] a) K. C. Nicolaou, D. E. Lizos, D. W. Kim, D. Schlawe, R. G. de Noronha, D. A. Longbottom, M. Rodriquez, M. Bucci, G. Cirino, *J. Am. Chem. Soc.* **2006**, *128*, 4460; b) K. C. Nicolaou, D. W. Kim, D. Schlawe, D. E. Lizos, R. G. de Noronha, D. A. Longbottom, *Angew. Chem., Int. Ed*. **2005**, *44*, 4925

3.4 Conclusion

In summary, a new strategy to construct enantioenriched *anti*-1,2-silylboronates through a palladium-catalyzed conjunctive cross-coupling has been developed. The reaction is easy to conduct on a preparative scale, and has the capability to be adopted as a new synthetic method for the synthesis of useful building blocks such as *anti* diols and amino alcohols. The reactivity of the allylsilane should enable further applications of the method in natural product synthesis.

3.5 Experimental data

3.5.1 General Information

^{1}H NMR spectra were recorded on either a Varian Gemini-500 (500 MHz), Varian Gemini-600 (600 MHz), or Varian Inova-500 (500 MHz) spectrometer. Chemical shifts are reported in ppm with the solvent resonance as the internal standard ($CDCl_3$: 7.26 ppm). Data are reported as follows: chemical shift, integration, multiplicity (s = singlet, d = doublet, t = triplet, q = quartet, p = pentet, m = multiplet), and coupling constants (Hz). ^{13}C NMR spectra were recorded on either a Varian Gemini-500 (125 MHz), Varian

Gemini-600 (150 MHz) or a Varian Inova-500 (125 MHz) spectrometer with complete proton decoupling. Chemical shifts are reported in ppm with the solvent resonance as the internal standard ($CDCl_3$: 77.16 ppm). ^{11}B NMR spectra were recorded on a Varian Gemini-500 (128 MHz) spectrometer. Chemical shifts are reported in ppm using trifluroborate etherate as the external standard (BF_3-Et_2O : 0.0 ppm). Infrared (IR) spectra were recorded on a Thermo Fisher ATR1 Spectrometer. Frequencies are reported in wavenumbers (cm^{-1}) as follows: strong (s), broad (br), medium (m), and weak (w). Optical rotations were measured on a Rudolph Analytical Research Autopol IV Polarimeter. High-resolution mass spectrometry was performed at the Mass Spectrometry Facility, Boston College, Chestnut Hill, MA. Liquid chromatography was performed using forced flow (flash chromatography) on silica gel (SiO_2, 230 x 450 Mesh) purchased from Silicycle. Thin layer chromatography (TLC) was performed on 25 μm silica gel Aluminum backed plates from Silicycle. Visualization was performed using ultraviolet light (254 nm), ceric ammonium molybdate (CAM) in ethanol or potassium permanganate (KMnO4). Analytical chiral supercritical fluid chromatography (SFC) was performed on a TharSFC Method Station II equipped with Waters 2998 Photodiode Array Detector with isopropanol as the modifier.

All reactions were conducted in oven- or flame-dried glassware under an inert atmosphere of nitrogen or argon. Tetrahydrofuran (THF), diethyl ether (Et_2O), dichloromethane (DCM) and toluene were purified using Pure Solv MD-4 solvent purification system, from Innovative Technology, Inc., by passing the solvent through two activated alumina columns after purging with argon. Palladium(II) acetate was purchased from Strem, (1*R*,2*R*)-*MandyPhos* (***(R,R)*-L1**) and (1S,2S)-*MandyPhos* (***(S, S)*-L1**) was purchased from Solvias., and dimethylphenylacetylene was purchased from Sigma-Aldrich, Borane-dimethyl sulfide 2M in THF was purchased from Acros, PhLi 1.9M in diethyl ether was purchased from Sigma-Aldrich, Phenyl triflate was purchased from Oakwood. All other reagents were purchased from Sigma Aldrich, Alfa Aesar, Oakwood Chemicals, Combi-Blocks, or Acros Organics and used without further purification.

3.5.2 Experimental Procedures

3.5.2.1 Procedures for preparation of Alkenyl Boronate Substrates

3.5.2.1.1 Procedures for preparation of 1,2-bis-boronate substrates

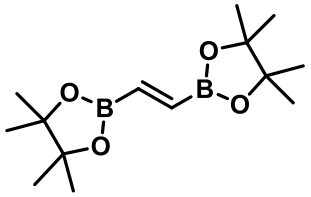

(E)-1,2-bis(4,4,5,5-tetramethyl-1,3,2-dioxaborolan-2-yl)ethane (3.82)

A flame-dried, 20 ml scintillation vial equipped with a magnetic stir bar was purged with N_2. Vinylboronic acid pinacol ester (770mg, 5 mmol) and Hoveyda-Grubbs Catalyst 2nd Generation catalyst (156 mg, 0.05 mmol, 0.1 equiv) and toluene 5 ml were added. The vial was sealed and heated to 110 ^oC for 24 hr before the reaction was quenched by passing through a short silica plug. The filtrate was evaporated and purified by silica gel chromatography (10% EtOAc in Hexane) to give title compound (462.6 mg, 33%). The spectral data was in accordance with the literature.[58]

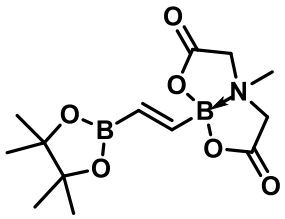

***(E)-6-methyl-2-(2-(4,4,5,5-tetramethyl-1,3,2-dioxaborolan-2-yl)vinyl)-1,3,6,2-dioxazaborocane-4,8-dione* (3.87)**

The title compound was synthesized by palladium catalyzed borylation as reported by Burke *et al.*[59] The spectral data was in accordance with the literature.[2]

[58] N. Selander, B. Willy and K. J. Szabo, *Angew. Chem. Int. Ed.* **2010**,*49*, 4051
[59] S. J. Lee, K. C. Gray, J. S. Paek and M. D. Burke, *J. Am. Chem. Soc*. **2008**, *130*, 466

3.5.2.1.2 Preparation of *trans*-1,2-alkenyl boronsilane substrates

3.5.2.1.2.1 Procedure for preparation of 1,2-dimethyl-1,2-dihydroacenaphthyl-ene-1,2-diol (3.135)

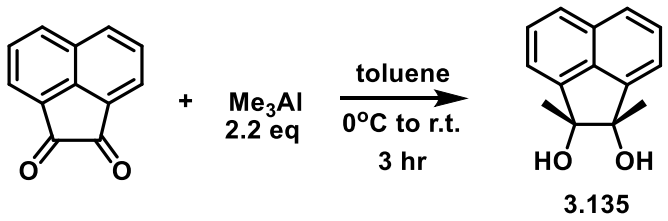

3.135

The title compound was synthesized following a previous report[60] from our group with modifications. A flame-dried 3-neck 1000 mL round bottom flask was equipped with stir bar, a reflux condenser fitted to the middle neck, and the other two necks were sealed with rubber septa. Acenaphthoquinone (11 g, 60.38 mmol) was added, and the flask was evacuated and refilled with nitrogen. 600 ml Dry toluene ([substrate] = 0.1 M) was added via syringe, and the yellow suspension was stirred at 0 ºC. Me_3Al (12.7 mL, 132.8 mmol, 2.2 equiv.) was added dropwise via syringe. Upon completion of addition, the reaction was allowed to stir for 3 hr at r.t., then cooled to 0 ºC and quenched slowly with 20 ml H_2O. The reaction was diluted with 1000 ml EtOAc and stir overnight to facilitate the precipitation of all salts. All salts were filtered

[60] J. A. Myhill, C. A. Wilhelmsen, L. Zhang and J. P. Morken, *J. Am. Chem. Soc*. **2018**, *140*, 15181

through a frit funnel, then the filtrate was poured into separatory funnel containing 200 ml water. The organic layer was washed three times with 300 ml EtOAc then the combined organic layers were washed with brine, then dried over Na_2SO4, filtered, and concentrated. ^1H NMR analysis of the crude material indicates 7.2:1 syn:anti diol. The crude product was recrystallized in hot EtOAc. The resulting precipitate was collected by filtration and rinsed with pentane to yield pure syn-1,2-dimethyl-1,2- dihydroacenaphthylene-1,2-diol as off-white crystals (8.65 g, 40.1 mmol, 66% yield). All spectral data was in accordance with the literature[3].

3.5.2.1.2.2 Procedure for preparation of (6bR,9aS)-6b,9a-dimethyl-6b,9a-dihydroacenaphtho[1,2-d][1,3,2]dioxaborole (3.136)

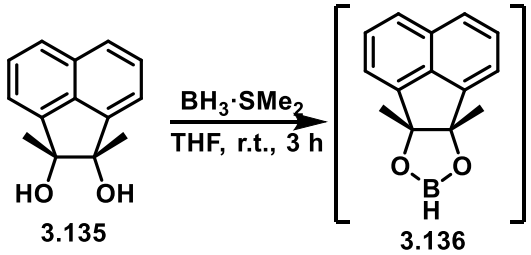

3.135 3.136

1,2-dimethyl-1,2-dihydroacenaphthylene-1,2-diol (mac-diol) 28 (4.93 g, 23 mmol) was dissolved in 10 ml THF in a 100 ml round bottom flask under

N_2. Then, 2M Borane-dimethylsulfide in THF (11.5 ml, 1 equiv) was added dropwise at 0 °C. Upon completion, the reaction was allowed to warm to r.t. and stirred until the bubbles ceased (about 3 hr). Then, the crude solution was used without further purification.

3.5.2.1.2.3 General procedure for preparation of *trans*-1,2-alkenyl boronsilane substrates

A flame-dried, 20 ml scintillation vial equipped with a magnetic stir bar was purged with N_2. The silyl acetylene (20 mmol) was added. The corresponding borane (21 mmol, 1.05 equiv) was introduced as well as Schwartz's reagent (10 mol%) into the solution. The reaction was heated to 70 °C under N_2 for 16 hr before diluting with Et_2O and filtrating through a short pad of silica gel. The filtrate was concentrated under reduced pressure. The crude mixture was purified by silica gel chromatography to give *trans*-1,2-alkenyl boronsilanes.

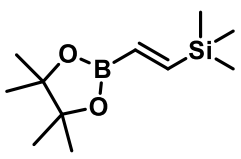

(*E*)-trimethyl(2-(4,4,5,5-tetramethyl-1,3,2-dioxaborolan-2-yl)vinyl)silane (3.133)

The reaction was performed according to the general procedure with trimethylsilylacetylene (1.96 g, 20 mmol), pinacolborane (2.69 g, 21 mmol, 1.05 equiv) and Schwartz's reagent (515.7 mg, 2 mmol, 10 mmol%) in neat. The crude mixture was purified by column chromatography (2% EtOAc in Hexane, stain in $KMnO_4$) to afford the product as white solid (3.55 g, 79% yield). The spectral data was in accordance with the literature.[61]

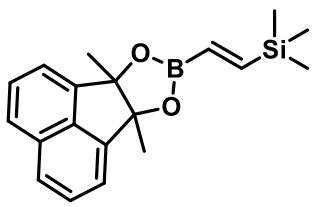

(*E*)-(2-(6b,9a-dimethyl-6b,9a-dihydroacenaphtho[1,2-d][1,3,2]dioxaborol-8-yl)vinyl) (3.91)

The reaction was performed according to the general procedure with trimethylsilylacetylene (1.96 g, 20 mmol), "mac" borane (4.71 g, 21 mmol, 1.05 equiv) and Schwartz's reagent (515.7 mg, 2 mmol, 10 mmol%) in 20.5 ml THF. The crude mixture was purified by column chromatography (3% EtOAc in Hexane, stain in $KMnO_4$) to afford the product as off white solid (4.92 g, 77% yield). ^{1}H NMR (600 MHz, $CDCl_3$) δ 7.78 (dd, J = 7.9, 1.0 Hz, 2H), 7.62 – 7.53 (m, 4H), 7.09 (d, J = 21.8 Hz, 1H), 6.18 (d, J = 21.8 Hz, 1H), 1.81 (s, 6H), 0.01 (s, 9H).; ^{13}C NMR (151 MHz, $CDCl_3$) δ 158.2, 144.7, 134.7,

[61] M. Fleige, J. Mobus, T. Stein, F. Glorius and D. W. Stephan, *Chem. Commun.*, **2016**, *52*, 10830

131.3, 128.5, 125.3, 119.5, 92.0, 22.1, -1.93, -1.94.; ^{11}B NMR (160 MHz, CDCl3) δ 29.44.; **IR** (neat) ν_{max} 2973.3 (w), 2954.4 (w), 1594.1 (w), 1365.2 (m), 1321.3 (s), 1277.4 (s), 1261.0 (s), 1246.9 (m), 1115.7 (s), 1077.9 (m), 837.7 (s), 805.3 (s), 777.6 (s) cm^{-1}.; **HRMS** (DART) for $C_{27}H_{41}OSi$ $[M+H]^+$: Calc'd: 409.2927, found: 409.2926.

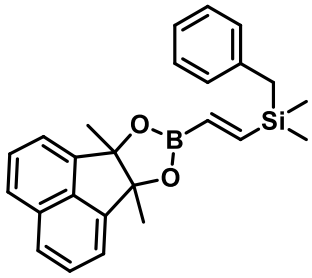

(*E*)-benzyl(2-(6b,9a-dimethyl-6b,9a-dihydroacenaphtho[1,2-d][1,3,2]dioxaborol-8-yl)vinyl)dimethylsilane (3.101)

The reaction was performed according to the general procedure with dimethylbenzylsilylacetylene (prepared according to previous literature[62]) (174 mg, 1 mmol), "mac" borane (235 mg, 1.05 mmol, 1.05 equiv) and Schwartz's reagent (25.8 mg, 0.1 mmol, 10 mmol%) in 2 ml THF. The crude mixture was purified by column chromatography (4% EtOAc in Hexane, stain in $KMnO_4$) to afford the product as off white solid (262.3 mg, 66% yield).^{1}H NMR (500 MHz, $CDCl_3$) δ 7.81 (dt, *J* = 8.0, 0.9 Hz, 2H), 7.62 (ddt, *J* = 8.4, 7.3, 1.1 Hz, 2H), 7.59 (dt, *J* = 7.0, 0.9 Hz, 2H), 7.18 (td, *J* = 7.8, 2.0 Hz, 2H), 7.09 (d, J= 21.9 Hz, 1H), 7.07 – 6.99 (m, 1H), 7.01 – 6.93 (m,

[62] S. E. Denmark and S. A. Tymonko, *J. Am. Chem. Soc*. **2005**, *127*, 8004

2H), 6.23 (d, J= 21.9 Hz, 1H), 2.11 (s, 2H), 1.85 – 1.78 (s, 6H), -0.01(s, 6H).; ^{13}C NMR (126 MHz, $CDCl_3$) δ 156.1, 144.7, 139.7, 134.7, 131.4, 128.5, 128.2, 128.1, 125.3, 124.0, 119.5, 92.0, 25.2, 22.1, -4.0; ^{11}B NMR (160 MHz, $CDCl_3$) δ 29.57.; **IR** (neat) ν_{max} 2973.6 (w), 1598.0 (w), 1324.3 (s), 2923.30 (s), 1277.8 (m), 1262.3 (w), 1116.2 (m), 1078.4 (w), 825.4 (s), 778.9 (s), 699.0 (w) cm^{-1}.; **HRMS** (DART) for $C_{25}H_{28}SiBO_2$ $[M+H]^+$: Calc'd: 399.1946, found: 399.1954.

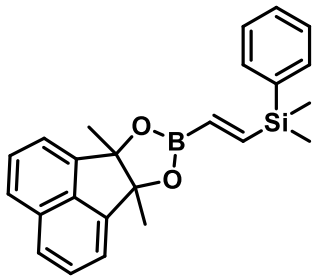

(*E*)-(2-(6b,9a-dimethyl-6b,9a-dihydroacenaphtho[1,2-d][1,3,2]dioxaborol-8-yl)vinyl)dimethyl(phenyl)silane (3.102)

The reaction was performed according to the general procedure with dimethylphenylsilylacetylene (3.56 g, 22.2 mmol), "mac" borane (5.15 g, 23 mmol, 1.05 equiv) and Schwartz's reagent (572.5 mg, 2.22 mmol, 10 mmol%) in 21.5 ml THF. The crude mixture was purified by column chromatography (3% EtOAc in Hexane, stain in $KMnO_4$) to afford the product as off white solid after recrystallization from methanol (6.12 g, 72% yield).^{1}H NMR (600 MHz, $CDCl_3$) δ 7.80 (dd, *J* = 8.0, 1.0 Hz, 2H), 7.61 (dd, *J* = 8.0,

6.9 Hz, 2H), 7.57 (dd, *J* = 6.9, 0.9 Hz, 2H), 7.50 – 7.45 (m, 2H), 7.32 (td, *J* = 5.7, 2.5 Hz, 3H), 7.21 (d, *J* = 21.8 Hz, 1H), 6.27 (d, *J* = 21.7 Hz, 1H), 1.82 (s, 6H), 0.32 (s, 6H).; ^{13}C NMR (151 MHz, $CDCl_3$) δ 158.31, 147.33, 140.32, 137.38, 136.54, 134.03, 131.70, 131.15, 130.41, 127.97, 122.15, 94.69, 24.76, -0.59.; ^{11}B NMR (160 MHz, $CDCl_3$) δ 29.45.; **IR** (neat) ν_{max} 3045.4 (w), 2974.3 (w), 1593.2 (w), 1427.2 (w), 1320.2 (s), 1277.0 (s), 1261.4 (m), 1211.4 (w), 1114.0 (s), 1076.8 (s), 1015.9 (m), 823.5 (s), 776.6 (s), 730.3 (m), 698.3 (m) cm^{-1}.; **HRMS** (DART) for $C_{24}H_{26}O_2BSi$ $[M+H]^+$: Calc'd: 385.1790, found: 385.1793.

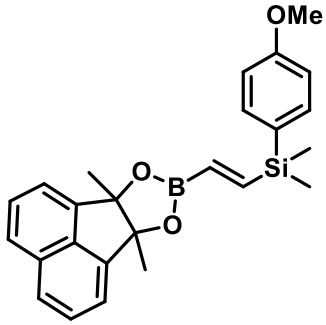

(*E*)-(2-(6b,9a-dimethyl-6b,9a-dihydroacenaphtho[1,2-d][1,3,2]dioxaborol-8-yl)vinyl)(4-methoxyphenyl)-dimethylsilane (3.103)

The reaction was performed according to the general procedure with dimethyl-*para*-methoxyphenylsilylacetylene (1.45g, 7.6 mmol) (prepared according to previous literature[63]), "mac" borane (1.79 g, 7.98 mmol, 1.05 equiv) and Schwartz's reagent (196.0 mg, 0.76 mmol, 0.1 equiv) in 8 ml THF. The crude mixture was purified by column

[63] M. Hasegawa, M. Murakami, J. Org. Chem. 2007, *72*, 3764

chromatography (5% EtOAc in Hexane, stain in $KMnO_4$) to afford the product as white solid after recrystallization from methanol (2.33 g, 73% yield). ^{1}H NMR (600 MHz, $CDCl_3$) δ 7.78 (dd, J = 8.1, 0.9 Hz, 2H), 7.63 – 7.52 (m, 4H), 7.40 – 7.31 (m, 2H), 7.16 (d, J = 21.7 Hz, 1H), 6.88 – 6.81 (m, 2H), 6.21 (d, J = 21.7 Hz, 1H), 3.77 (s, 3H), 1.80 (s, 6H), 0.27 (s, 6H).; ^{13}C NMR (126 MHz, $CDCl_3$) δ 160.5, 156.2, 144.7, 135.4, 134.7, 131.4, 128.5, 128.5, 125.3, 119.5, 113.6, 92.0, 55.0, 22.1, -3.1.; ^{11}B NMR (160 MHz, $CDCl_3$) δ 29.55.; **IR** (neat) ν_{max} 2971.9 (w), 2359.1 (w), 1592.7 (m), 1501.6 (m), 1322.4 (s), 1276.5 (s), 1246.2 (s), 1181.9 (m), 1111.8 (s), 1077.9 (m), 1016.9 (m), 824.6 (s), 777.9 (s) cm^{-1}. **HRMS** (DART) for $C_{25}H_{28}O_3BSi$ $[M+H]^+$: Calc'd: 415.1895, found: 415.1888.

3.5.2.2 Representative Procedures for Conjunctive Cross-Coupling

3.5.2.2.1 Procedure A

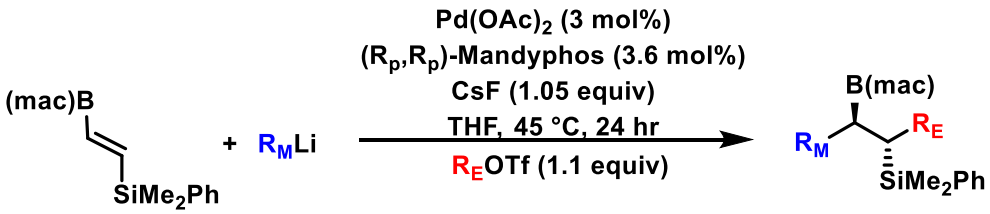

In a glovebox, under argon, an oven-dried 2-dram vial equipped with a magnetic stir bar was charged with Alkenyl boron substrate (0.2 mmol, 1

uiv.) in 0.4 ml Et_2O. The vial was sealed and brought out of the glovebox. Then the vial was cooled to 0 ℃, and organolithium (0.21 mmol, 1.05 equiv.) was added dropwise. The reaction mixture was allowed to warm to room temperature and stir for 30 minutes. Then the reaction mixture was connected to High Vacumn for 30 minutes to evaporate solvents. Then the vial was refilled with N_2 and brought back to glovebox. And cesium fluoride (0.21 mmol, 1.05 eq) was added in the reaction mixture. 0.4 ml THF was added to re-dissolve the mixture and stired for 30 min before the stock solution of catalyst [$Pd(OAc)_2$ (0.006 mmol, 0.03 equiv.) and *(R,R)*-Mandyphos (0.0072 mmol, 0.036 equiv.) in THF (0.4 mL) was stirred for 30 min before use]was added. Finally, aryl triflate (0.22 mmol, 1.1 equiv.) was introduced. The vial was sealed and brought out of glovebox. The reaction was heated at 45 ^{o}C for 24 hours. Upon completion, the reaction was quenched with 2 ml water and 2 ml Et_2O. The aqueous phase was extracted with Et_2O (3 x 2 mL). The combined organic layers were dried over $MgSO_4$, filtered, concentrated under reduced pressure, and subsequently oxidized and purified via silica gel column chromatography to provide the desired products.

3.5.2.2.2 Procedure B:

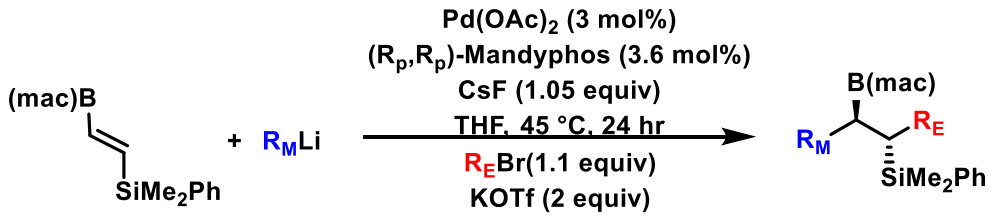

The reaction can be carried out using aryl bromides instead of aryl triflates by following the same method described in **procedure A** with a slight modification. The reaction requires anhydrous KOTf (0.4 mmol, 2 equiv.) which can be added as solid to the reaction mixture before catalyst stock solution was added.

3.5.2.2.3 Procedure C:

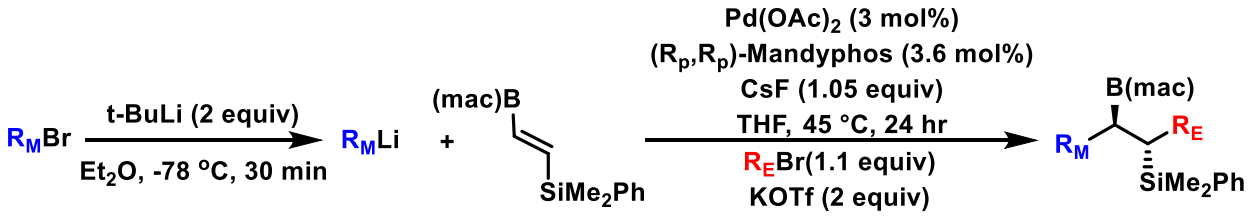

In a glovebox, under argon, an oven-dried 2-dram vial equipped with a magnetic stir bar was charged with aryl bromide (0.21 mmol, 1.05 equiv.) in 0.4 ml Et_2O. Alkenyl boron substrate (0.2 mmol, 1 equiv.) was dissolved in

0.5 ml Et_2O and transferred into a syringe. The vial was sealed and brought out of the glovebox. Then the vial was cooled to -78 ℃, and *tert*-butyllithium (0.4 mmol, 2 equiv.) was added dropwise. The reaction mixture was allowed to stir for 30 minutes at -78 ℃. Then the solution of alkenyl boronate was added dropwise and allowed to warm up to r.t. for 30 min. The reaction mixture was connected to high vacumn (around 0.5 mmHg) for another 30 minutes to evaporate solvents. Then the vial was refilled with N_2 and brought back to glovebox. And cesium fluoride (0.21 mmol, 1.05 eq) was added in the reaction mixture. 0.4 ml THF was added to re-dissolve the mixture and stired for 30 min before the stock solution of catalyst [$Pd(OAc)_2$ (0.006 mmol, 0.03 equiv.) and *(R,R)*-Mandyphos (0.0072 mmol, 0.036 equiv.) in THF (0.4 mL) was stirred for 30 min before use] and KOTf (0.4 mmol, 2 equiv.) were added. Finally, aryl triflate (0.22 mmol, 1.1 equiv.) was introduced. The vial was sealed and brought out of glovebox. The reaction was heated at 45 ^{o}C for 24 hours. Upon completion, the reaction was quenched with 2 ml water and 2 ml Et_2O. The aqueous phase was extracted with Et_2O (3 x 2 mL). The combined organic layers were dried over $MgSO_4$, filtered, concentrated under reduced pressure, and subsequently oxidized and purified via silica gel column chromatography to provide the desired products.

3.5.2.3 Procedure for Oxidation of Boron

In a 20 ml scintillation vial equipped with a magnetic stir bar was charged with conjunctive cross-coupling product (0.2 mmol) and 4 ml THF. 3M NaOH (0.2 ml, 0.6 mmol, 3 equiv) and 30% H_2O_2 (0.15 ml, 1.47 mmol, 7 equiv) were added in one portion at 0 °C. The reaction was quenched with 2 ml saturated $Na_2S_2O_3$ after 5-15 min (To avoid any elimination or epimerization, the reaction was quenched after 15 min if it is alkyl group migration or the reaction was quenched after 5 min if it is aryl group migration). The organic layer was extracted with 3ml Et_2O for three times. The combined organics were dried with $MgSO_4$ and concentrated under reduced pressure, and purified via silica gel column chromatography to provide the corresponding alcohols.

3.5.3 Characterization of Conjunctive Cross Coupling Products and Analysis of Stereochemistry

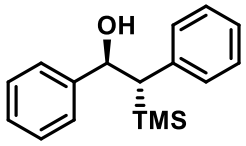

(1R,2S)-1,2-diphenyl-2-(trimethylsilyl)ethan-1-ol (3.92)

The reaction was performed according to the general **procedure A** with trimethylsilyl vinyl B(pin) (45.2mg, 0.2 mmol, 1 equiv) or trimethylsily vinyl B(mac) (64.4 mg, 0.2 mmol, 1 equiv), Phenyl lithium (1.78

M in dibutyl ether, 0.11 ml, 0.21 mmol, 1.05 equiv.), phenyl triflate (49.8 mg, 0.22 mmol, 1.1 equiv.), palladium (II) acetate (1.35mg, 6.0 μmol, 0.030 equiv.), (R_p, R_p)-L (7.6 mg, 7.2 μmol), 0.036 equiv.) and cesium fluoride (30.4 mg, 0.2 mmol, 1.0 equiv) in THF (0.80 mL, 0.25 M). The crude mixture was oxidized by $NaOH/H_2O_2$ and purified as corresponding alcohols by silica gel chromatography (10% EtOAc in hexane, stain in $KMnO_4$ stain) to afford a white solid (22.3 mg, 41% yield for alkenyl Bpin) or (48.0 mg, 89% yield for alkenyl Bmac). ^{1}H NMR (600 MHz, $CDCl_3$) δ 7.45 – 7.40 (m, 2H), 7.38 – 7.26 (m, 5H), 7.27 – 7.23 (m, 2H), 7.23 – 7.15 (m, 1H), 5.18 (dd, *J* = 10.2, 1.8 Hz, 1H), 2.59 (d, *J* = 10.2 Hz, 1H), 2.01 (d, *J* = 2.0 Hz, 1H), -0.33 (s, 9H).; ^{13}C NMR (126 MHz, $CDCl_3$) δ 143.3, 140.9, 128.7, 128.7, 128.5, 128.1, 127.2, 125.6, 76.1, 48.0, -2.0.; **IR** (neat) ν_{max} 3420.9 (br, w), 3027.6 (w), 2951.4 (w), 1599.3 (w), 1493.9 (w), 1450.9 (w), 1247.4 (m), 1027.7 (m), 874.9 (m), 835.3 (s), 760.9 (m), 698.9 (s) cm^{-1}.; **HRMS** (DART) for $C_{17}H_{21}SiO$ $[M\text{-}H^-]^+$: Calc'd: 269.1356, found: 269.1355. $\mathbf{[\alpha]_D^{20}}$ = + 17.52 (*c* =1.0, $CHCl_3$, *l* = 50 mm).

Analysis of Stereochemistry:

Diastereomer ratio was determined by ^{1}H NMR analysis of the crude reaction mixture. Racemic compound was prepared according to the procedure described above with $Pd(OAc)_2$ (3 mol%) and a mixture of (R_p, R_p)-L and (S_p, S_p)-L (3.6 mol%) as the catalyst. Absolute stereochemistry was assigned by analogy (see compound 8a).

Chiral SFC (Chiracel OD-H, 6% IPA, 3 mL/min, 100 bar, 35 °C, 210-289 nm) – analysis of (1R,2S)-1,2-diphenyl-2-(trimethylsilyl)ethan-1-ol.

Racemic Material

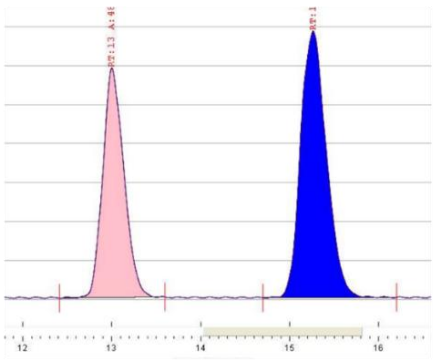

Peak No	% Area	Area	RT (min)
1	41.4048	4869.9048	13
2	58.5952	6891.7973	15.26
Total:	100	11761.7021	

Enantioenriched Material(alkenyl B(pin))

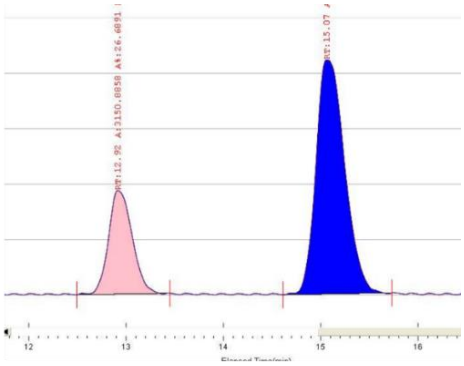

Peak No	% Area	Area	RT (min)
1	26.6891	3150.8858	12.92
2	73.3109	8655.0184	15.07
Total:	100	11805.9042	

Racemic Material

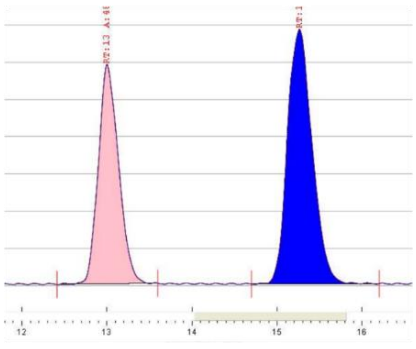

Peak No	% Area	Area	RT (min)
1	41.4048	4869.9048	13
2	58.5952	6891.7973	15.26
Total:	100	11761.7021	

Enantioenriched Material(alkenyl B(mac))

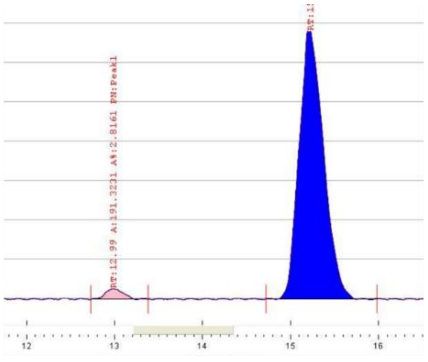

Peak No	% Area	Area	RT (min)
1	2.8161	191.3231	12.99
2	97.1839	6602.5871	15.23
Total:	100	6793.9102	

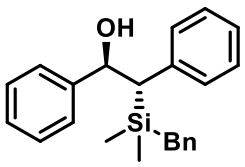

(1R,2S)-2-(benzyldimethylsilyl)-1,2-diphenylethan-1-ol (3.104)

The reaction was performed according to the general **procedure A** with dimethylbenzylsilyl vinyl B(mac) (79.7 mg, 0.2 mmol, 1 equiv.), Phenyl lithium (1.78 M in dibutyl ether, 0.11 ml, 0.21 mmol, 1.05 equiv.), phenyl triflate (49.8 mg, 0.22 mmol, 1.1 equiv.), palladium (II) acetate (1.35mg, 6.0 μmol, 0.030 equiv.), (R_p, R_p)-L (7.6 mg, 7.2 μmol), 0.036 equiv.) and cesium fluoride (30.4 mg, 0.2 mmol, 1.0 equiv) in THF (0.80 mL, 0.25 M). The crude mixture was oxidized by $NaOH/H_2O_2$ and purified by silica gel chromatography (7% EtOAc in hexanes, stain in $KMnO_4$ stain) to afford a colorless oil (43.3 mg, 62% yield). ^{1}H NMR (500 MHz, $CDCl_3$) δ 7.47 – 7.41 (m, 2H), 7.41 – 7.28 (m, 5H), 7.30 – 7.18 (m, 3H), 7.14 (t, J = 7.7 Hz, 2H), 7.07 – 6.98 (m, 1H), 6.81 – 6.76 (m, 2H), 5.24 (d, J = 9.7 Hz, 1H), 2.68 (d, J = 9.7 Hz, 1H), 2.04 (s, 1H), 1.74 (d, J = 13.7 Hz, 1H), 1.62 (d, J = 13.7 Hz, 1H), -0.29 (s, 3H), -0.34 (s, 3H).; ^{13}C NMR (126 MHz, $CDCl_3$) δ 143.3, 140.3, 139.6, 129.0, 128.8, 128.5, 128.3, 128.2, 128.0, 127.1, 125.8, 124.0, 76.0, 47.2, 24.2, -3.9, -4.2.; **IR** (neat) ν_{max} 3563.5 (br, w), 3432.1 (w), 3023.7 (w), 2894.4 (w), 1598.9 (w), 1492.4 (m), 1248.3 (m), 1027.9 (w), 828.5 (s), 761.6 (s), 698.7 (s).; **HRMS** (DART) for $C_{23}H_{25}Si$ $[M+H-H_2O]^+$:

Calc'd: 329.1720, found: 329.1724. $[\alpha]_D^{20}$ = + 1.96 (*c* = 1.00, $CHCl_3$, *l* = 50 mm).

Analysis of Stereochemistry:

Diastereomer ratio was determined by ^1H NMR analysis of the crude reaction mixture. Racemic

compound was prepared according to the procedure described above with $Pd(OAc)_2$ (3 mol%) and a mixture of (R_p, R_p)-L and (S_p, S_p)-L (3.6 mol%) as the catalyst. Absolute stereochemistry was assigned by analogy (see compound 8a).

Chiral SFC (Chiracel OD-H, 10% IPA, 3 mL/min, 100 bar, 35 °C, 210-289 nm) – analysis of (1R,2S)-2-(benzyldimethylsilyl)-1,2-diphenylethan-1-ol.

Racemic Material

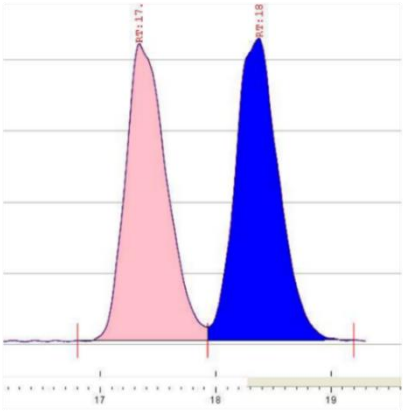

Peak No	% Area	Area	RT (min)
1	48.3303	10423.0253	17.34
2	51.6697	11143.2037	18.38
Total:	100	21566.229	

Enantioenriched Material

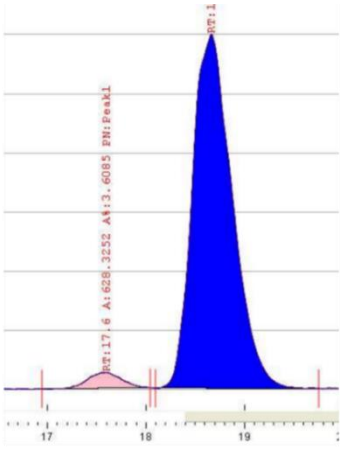

Peak No	% Area	Area	RT (min)
1	3.6085	628.3252	17.6
2	96.3915	16784.2147	18.67
Total:	100	17412.5399	

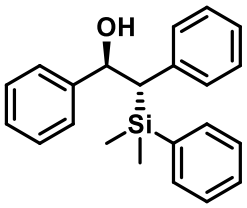

(1R,2S)-2-(dimethyl(phenyl)silyl)-1,2-diphenylethan-1-ol (3.105)

The reaction was performed according to the general **procedure A** with dimethylphenylsilyl vinyl B(mac) (76.9 mg, 0.2 mmol, 1 equiv.), phenyl lithium (1.78 M in dibutyl ether, 0.11 ml, 0.21 mmol, 1.05 equiv.), phenyl triflate (49.8mg, 0.22 mmol, 1.1 equiv.), palladium (II) acetate (1.35mg, 6.0 μmol, 0.030 equiv.), (R_p, R_p)-L (7.6 mg, 7.2 μmol), 0.036 equiv.) and cesium fluoride (30.4 mg, 0.2 mmol, 1.0 equiv) in THF (0.80 mL, 0.25 M). The crude mixture was oxidized by $NaOH/H_2O_2$ and purified by silica gel chromatography (7% EtOAc in hexanes, stain in $KMnO_4$ stain) to afford a white solid (54.8 mg, 82% yield). ^{1}H NMR (500 MHz, $CDCl_3$) δ 7.34 – 7.27 (m, 3H), 7.29 – 7.20 (m, 9H), 7.18 – 7.08 (m, 3H), 5.14 (dd, J = 9.1, 2.3 Hz, 1H), 2.80 (d, J = 9.1 Hz, 1H), 1.96 (d, J = 2.4 Hz, 1H), 0.06 (s, 3H), -0.02 (s, 3H).; ^{13}C NMR (126 MHz, $CDCl_3$) δ 143.1, 139.9, 137.2, 134.1, 129.3, 128.9, 128.4, 128.3, 127.9, 127.4, 127.1, 125.6, 75.6, 47.4, -3.4, -3.5.; **IR** (neat) ν_{max} 3558.0 (br, w), 3431.2 (br, w), 3066.7 (w), 3024.9 (w), 2955.6 (w), 1599.3 (w), 1492.6 (w), 1427.0 (w), 1248.1 (m), 1112.3 (m), 832.8 (m), 764.7 (m), 699.2 (s) cm^{-1}.; **HRMS** (DART) for $C_{22}H_{23}Si$ $[M+H-H_2O]^+$: Calc'd: 315.1564, found: 315.1540. $\mathbf{[\alpha]_D^{20}}$ = + 5.92 (c = 1.00, $CHCl_3$, l = 50 mm).

Analysis of Stereochemistry:

Diastereomer ratio was determined by ^{1}H NMR analysis of the crude reaction mixture. Racemic compound was prepared according to the procedure described above with $Pd(OAc)_2$ (3 mol%) and a mixture of (R_p, R_p)-L and (S_p, S_p)-L (3.6 mol%) as the catalyst. Absolute stereochemistry was assigned by analogy (see compound 8a).

Chiral SFC (Chiracel OD-H, 10% IPA, 3 mL/min, 100 bar, 35 °C, 210-289 nm) – analysis of (1R,2S)-2-(dimethyl(phenyl)silyl)-1,2-diphenylethan-1-ol.

Racemic Material

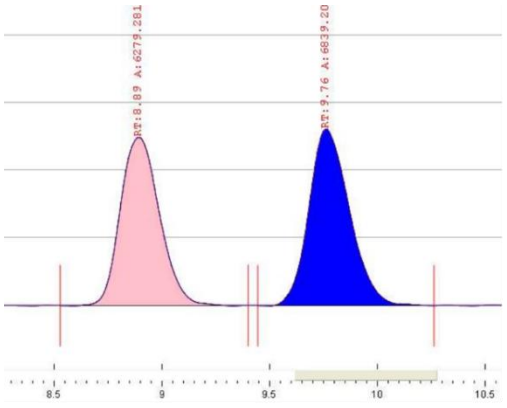

Peak No	% Area	Area	RT (min)
1	47.8659	6279.2812	8.89
2	52.1341	6839.2046	9.76
Total:	100	13118.4858	

Enantioenriched Materia

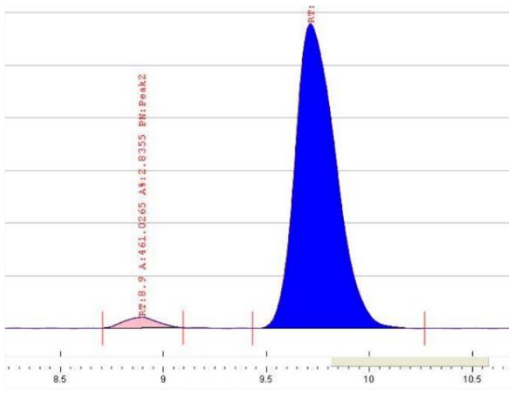

Peak No	% Area	Area	RT (min)
1	2.8355	461.0265	8.9
2	97.1645	15797.8379	9.72
Total:	100	16258.8644	

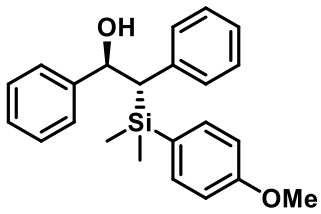

(1R,2S)-2-((4-methoxyphenyl)dimethylsilyl)-1,2-diphenylethan-1-ol (3.106)

The reaction was performed according to the general **procedure A** with dimethyl-*para*-methoxyphenylsilyl vinyl B(mac) (82.9 mg, 0.2 mmol, 1 equiv.), phenyl lithium (1.78 M in dibutyl ether, 0.11 ml, 0.21 mmol, 1.05 equiv.), phenyl triflate (49.8mg, 0.22 mmol, 1.1 equiv.), palladium (II) acetate (1.35mg, 6.0 μmol, 0.030 equiv.), (R_p, R_p)-L (7.6 mg, 7.2 μmol), 0.036 equiv.) and cesium fluoride (30.4 mg, 0.2 mmol, 1.0 equiv) in THF (0.80 mL, 0.25 M). The crude mixture was oxidized by $NaOH/H_2O_2$ and purified by silica gel chromatography (7% EtOAc in hexanes, stain in $KMnO_4$ stain) to afford a white solid (55.0 mg, 76% yield). ^1H NMR (500 MHz, $CDCl_3$) δ 7.33 – 7.21 (m, 7H), 7.20 – 7.09 (m, 5H), 6.85 – 6.79 (m, 2H), 5.13 (dt, J = 9.2, 1.9 Hz, 1H), 3.82 (s, 3H), 2.78 (dd, J = 9.2, 1.4 Hz, 1H), 1.99 (bs, 1H), 0.03 (s, 3H), -0.05 (s, 2H).; ^{13}C NMR (126 MHz, $CDCl_3$) δ 160.3, 143.2, 140.0, 135.7, 129.3, 128.3, 128.3, 127.9, 127.9, 127.1, 125.5, 113.2, 75.6, 55.0, 47.6, -3.2, -3.3.; **IR** (neat) ν_{max} 3550.7 (br, w), 3440.6 (br, w), 3024.4 (w), 2955.4 (w), 1594.4 (s), 1502.2 (s), 1277.2 (s), 1246.8 (s), 1182.9 (m), 1110.3 (s), 1029.5 (m), 822.3 (s), 764.7 (m), 701.2 (s) cm^{-1}. **HRMS**

(DART) for $C_{23}H_{27}O_2Si$ $[M+H]^+$: Calc'd: 363.1775, found: 363.1774. **$[\alpha]_D^{20}$** = + 4.00 (*c* =1.4, $CHCl_3$, *l* = 50 mm).

Analysis of Stereochemistry:

Diastereomer ratio was determined by ^1H NMR analysis of the crude reaction mixture. Racemic compound was prepared according to the procedure described above with $Pd(OAc)_2$ (3 mol%) and a mixture of (R_p, R_p)-L and (S_p, S_p)-L (3.6 mol%) as the catalyst. Absolute stereochemistry was assigned by analogy (see compound 8a).

Chiral SFC (Chiracel OJ-H, 10% IPA, 3 mL/min, 100 bar, 35 °C, 210-289 nm) analysis of (1R,2S)-2-((4-methoxyphenyl)dimethylsilyl)-1,2-diphenylethan-1-ol.

Racemic Material

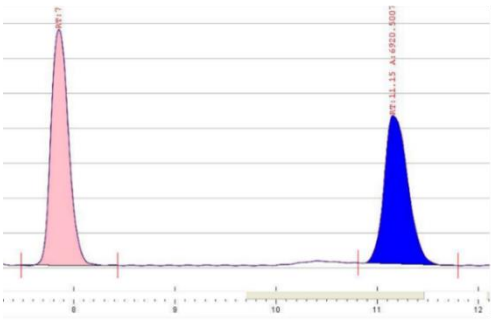

Peak No	% Area	Area	RT (min)
1	54.0734	8148.118	7.85
2	45.9266	6920.5007	11.15
Total:	100	15068.6187	

Enantioenriched Material

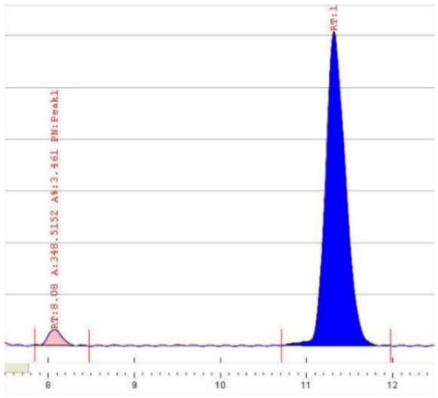

Peak No	% Area	Area	RT (min)
1	3.461	348.5152	8.08
2	96.539	9721.2149	11.32
Total:	100	10069.7301	

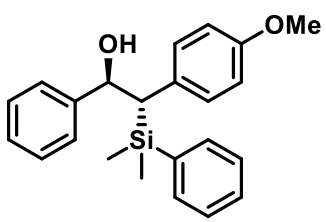

(1R,2S)-2-(dimethyl(phenyl)silyl)-2-(4-methoxyphenyl)-1-phenylethan-1-ol (3.108)

The reaction was performed according to the general **procedure A** with dimethylphenylsilyl vinyl B(mac) (76.9 mg, 0.2 mmol, 1 equiv.), Phenyl lithium (1.78 M in dibutyl ether, 0.11 ml, 0.21 mmol, 1.05 equiv.), *para*-methoxyphenyl triflate (56.4 mg, 0.22 mmol, 1.1 equiv.), palladium (II) acetate (1.35 mg, 6.0 μmol, 0.030 equiv.), (R_p, R_p)-L (7.6 mg, 7.2 μmol), 0.036 equiv.) and cesium fluoride (30.4 mg, 0.2 mmol, 1.0 equiv) in THF (0.80 mL, 0.25 M). The crude mixture was oxidized by $NaOH/H_2O_2$ and purified by silica gel chromatography (9% EtOAc in hexanes, stain in KMnO4 stain) to afford a white solid (55.8 mg, 77% yield). ^{1}H NMR (500 MHz, $CDCl_3$) δ 7.36-7.19 (m, 10H), 7.03 (d, J = 8.6 Hz, 2H), 6.8 (d, J = 8.7 Hz, 2H), 5.07 (dd, J = 8.9, 2.4 Hz, 1H), 3.80 (s, 3H), 2.73 (d, J = 8.8 Hz, 1H), 1.99 (d, J = 2.4 Hz, 1H), 0.08 (s, 3H), -0.02 (s, 3H).; ^{13}C NMR (126 MHz, $CDCl_3$) δ 157.6, 143.2, 137.4, 134.1, 131.5, 130.3, 128.8, 128.2, 127.8, 127.4, 127.0, 113.8, 75.6, 55.2, 46.2, -3.3, -3.5.; **IR** (neat) ν_{max} 3565.1 (br, w), 3026.7 (w), 2953.8 (w), 1607.9 (w), 1508.6 (s), 1247.2 (s), 1178.7 (w), 1111.1 (w), 1035.9 (m), 835.5 (m), 699.7 (m) cm^{-1}. **HRMS** (DART) for $C_{23}H_{25}SiO$ [M+H-

$H_2O]^+$: Calc'd: 345.1669, found: 345.1663. $\mathbf{[\alpha]_D^{20}}$ = + 3.04 (c = 1.00, $CHCl_3$, l = 50 mm).

Analysis of Stereochemistry:

Diastereomer ratio was determined by ^{1}H NMR analysis of the crude reaction mixture. Racemic compound was prepared according to the procedure described above with $Pd(OAc)_2$ (3 mol%) and a mixture of (R_p, R_p)-L and (S_p, S_p)-L (3.6 mol%) as the catalyst. Absolute stereochemistry was assigned by analogy (see compound 8a).

Chiral SFC (Chiracel OJ-H, 10% IPA, 3 mL/min, 100 bar, 35 °C, 210-289 nm) – analysis of (1R,2S)-2-(dimethyl(phenyl)silyl)-2-(4-methoxyphenyl)-1-phenylethan-1-ol.

Racemic Material

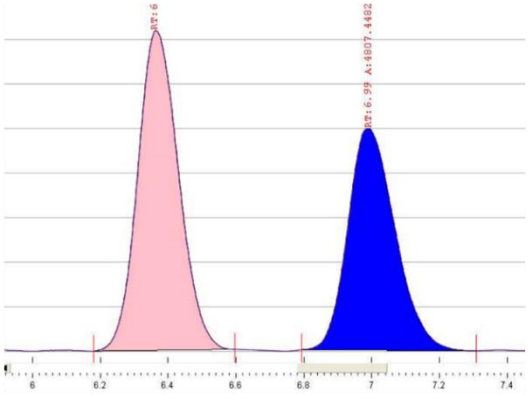

Peak No	% Area	Area	RT (min)
1	55.4822	5991.4825	6.36
2	44.5178	4807.4482	6.99
Total:	100	10798.9307	

Enantioenriched Material

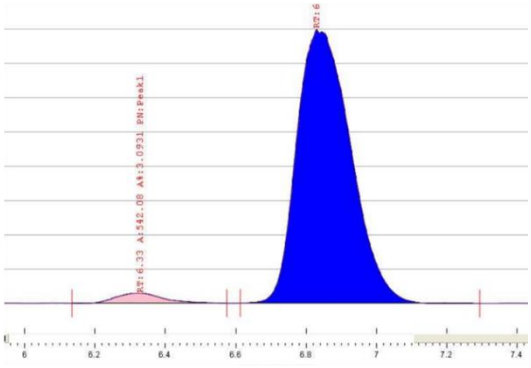

Peak No	% Area	Area	RT (min)
1	3.0931	542.08	6.33
2	96.9069	16983.571	6.83
Total:	100	17525.651	

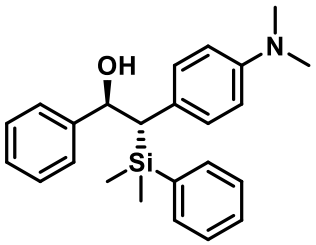

(1R,2S)-2-(dimethyl(phenyl)silyl)-2-(4-(dimethylamino)phenyl)-1-phenylethan-1-ol (3.109)

The reaction was performed according to the general **procedure B** with dimethylphenylsilyl vinyl B(mac) (76.9 mg, 0.2 mmol, 1 equiv.), phenyl lithium (1.78 M in dibutyl ether, 0.11 ml, 0.21 mmol, 1.05 equiv.), 4-dimethylamino phenyl bromide (44.0 mg, 0.22 mmol, 1.1 equiv.), potassium triflate (75.3 mg, 0.4 mmol, 2 equiv), palladium (II) acetate (1.35 mg, 6.0 μmol, 0.030 equiv.), (R_p, R_p)-L (7.6 mg, 7.2 μmol), 0.036 equiv.) and cesium fluoride (30.4 mg, 0.2 mmol, 1.0 equiv) in THF (0.80 mL, 0.25 M). The crude mixture was oxidized by $NaOH/H_2O_2$ and purified by silica gel chromatography (10% EtOAc in hexanes, stain in $KMnO_4$ stain) to afford a white solid (54.9 mg, 73% yield). ^{1}H NMR (600 MHz, $CDCl_3$) δ 7.33 – 7.26 (m, 3H), 7.29 – 7.18 (m, 7H), 7.00 – 6.95 (m, 2H), 6.69 – 6.63 (m, 2H), 5.02 (dd, J = 9.4, 2.2 Hz, 1H), 2.92 (s, 6H), 2.68 (d, J = 9.5 Hz, 1H), 2.05 (d, J = 2.3 Hz, 1H), 0.04 (s, 3H), -0.10 (s, 3H).; ^{13}C NMR (126 MHz, $CDCl_3$) δ 148.9, 143.1, 137.6, 134.2, 130.0, 128.7, 128.2, 127.9, 127.33, 127.27, 127.16, 113.1, 75.7, 46.1, 40.8, -3.1, -3.4.; **IR** (neat) ν_{max} 3549.5 (br, w), 3441.4 (br, w), 2953.2 (w), 2886.1 (w), 1612.1 (m), 1516.3 (s), 1345.0 (m), 1246.3 (m),

1110.8 (m), 1046.9 (w), 810.6 (s), 735.2 (m), 699.0 (s) cm^{-1}. **HRMS** (DART) for $C_{24}H_{28}SiN$ $[M+H-H_2O]^+$: Calc'd: 358.1986, found: 358.1990. $\mathbf{[\alpha]_D^{20}}$ = -17.96 (*c* = 1.00, $CHCl_3$, *l* = 50 mm).

Analysis of Stereochemistry:

Diastereomer ratio was determined by ^1H NMR analysis of the crude reaction mixture. Racemic compound was prepared according to the procedure described above with $Pd(OAc)_2$ (3 mol%) and a mixture of (R_p, R_p)-L and (S_p, S_p)-L (3.6 mol%) as the catalyst. Absolute stereochemistry was assigned by analogy (see compound 8a).

Chiral SFC (Chiracel OJ-H, 10% IPA, 3 mL/min, 100 bar, 35 °C, 210-289 nm) – analysis of (1R,2S)-2-(dimethyl(phenyl)silyl)-2-(4-(dimethylamino)phenyl)-1-phenylethan-1-ol.

Racemic Material

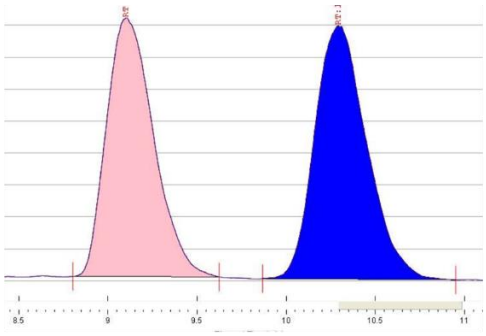

Peak No	% Area	Area	RT (min)
1	48.1097	14916.547	9.1
2	51.8903	16088.7153	10.29
Total:	100	31005.2623	

Enantioenriched Material

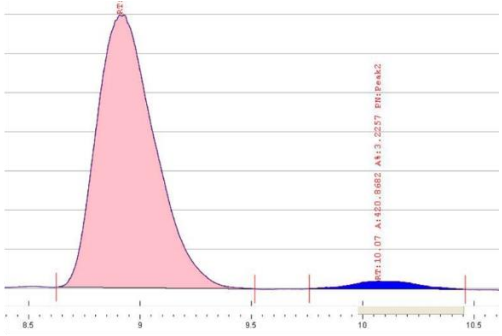

Peak No	% Area	Area	RT (min)
1	96.7743	12626.557	8.91
2	3.2257	420.8682	10.07
Total:	100	13047.4252	

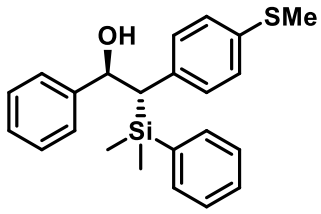

(1R,2S)-2-(dimethyl(phenyl)silyl)-2-(4-(methylthio)phenyl)-1-phenylethan-1-ol (3.110)

The reaction was performed according to the general **procedure B** with dimethylphenylsilyl vinyl B(mac) (76.9 mg, 0.2 mmol, 1 equiv.), phenyl lithium (1.78 M in dibutyl ether, 0.11 ml, 0.21 mmol, 1.05 equiv.), (4-bromophenyl)thioanisole (44.7 mg, 0.22 mmol, 1.1 equiv.), potassium triflate (75.3 mg, 0.4 mmol, 2 equiv), palladium (II) acetate (1.35 mg, 6.0 μmol, 0.030 equiv.), (R_p, R_p)-L (7.6 mg, 7.2 μmol), 0.036 equiv.) and cesium fluoride (30.4 mg, 0.2 mmol, 1.0 equiv) in THF (0.80 mL, 0.25 M). The crude mixture was oxidized by $NaOH/H_2O_2$ and purified by silica gel chromatography (10% EtOAc in hexanes, stain in $KMnO_4$ stain) to afford a white solid (47.6 mg, 63% yield). ^{1}H NMR (500 MHz, $CDCl_3$) δ 7.35 – 7.29 (m, 1H), 7.32 – 7.18 (m, 9H), 7.14 (d, J = 8.2 Hz, 2H), 7.04 (d, J = 8.1 Hz, 2H), 5.09 (d, J = 8.7 Hz, 1H), 2.75 (d, J = 8.6 Hz, 1H), 2.47 (s, 3H), 0.10 (s, 3H), -0.01 (s, 3H).; ^{13}C NMR (126 MHz, $CDCl_3$) δ 143.2, 137.2, 136.9, 134.9, 134.1, 129.8, 129.0, 128.3, 127.9, 127.5, 127.0, 126.9, 75.5, 46.8, 16.2, -3.3, -3.5.; **IR** (neat) ν_{max} 3553.3 (br, w), 3440.6 (br, w), 3067.1 (w), 2954.8 (w), 2358.7 (w), 1492.1 (m), 1427.0 (w), 1248.2 (m), 1111.6 (m), 1028.5 (m), 835.8 (s), 764.5 (s), 700.1 (s) cm^{-1}. **HRMS** (DART) for $C_{23}H_{27}SiOS$ $[M+H]^+$:

Calc'd: 379.1546, found: 379.1538. $[\alpha]_D^{20}$ = - 18.73 (*c* = 1.00, $CHCl_3$, *l* = 50 mm).

Analysis of Stereochemistry:

Diastereomer ratio was determined by ^1H NMR analysis of the crude reaction mixture. Racemic compound was prepared according to the procedure described above with $Pd(OAc)_2$ (3 mol%) and a mixture of (R_p, R_p)-L and (S_p, S_p)-L (3.6 mol%) as the catalyst. Absolute stereochemistry was assigned by analogy (see compound 8a).

Chiral SFC (Chiracel ODR-H, 9% IPA, 3 mL/min, 100 bar, 35 °C, 210-289 nm) – analysis of (1R,2S)-2-(dimethyl(phenyl)silyl)-2-(4-(methylthio)phenyl)-1-phenylethan-1-ol.

Racemic Material

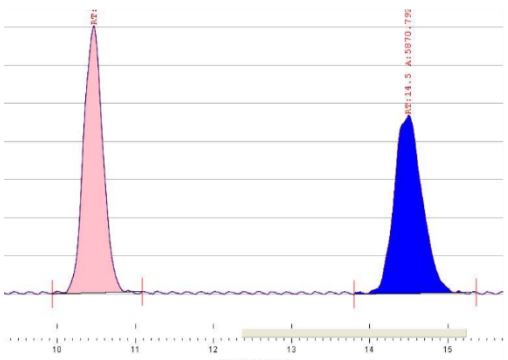

Peak No	% Area	Area	RT (min)
1	50.5611	6004.0603	10.47
2	49.4389	5870.7921	14.5
Total:	100	11874.8524	

Enantioenriched Material

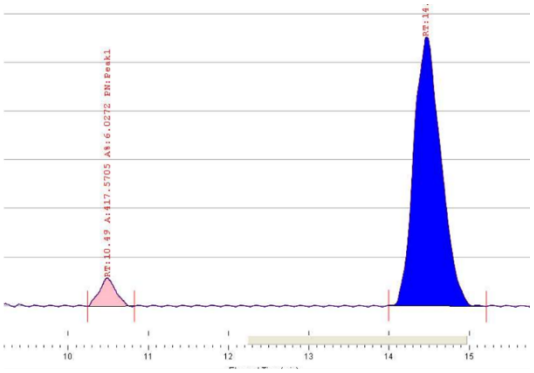

Peak No	% Area	Area	RT (min)
1	6.0272	417.5705	10.49
2	93.9728	6510.4841	14.46
Total:	100	6928.0546	

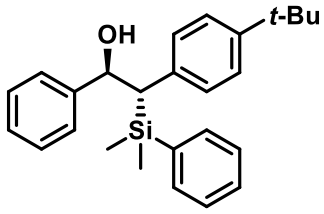

(1R,2S)-2-(4-(tert-butyl)phenyl)-2-(dimethyl(phenyl)silyl)-1-phenylethan-1-ol (3.107)

The reaction was performed according to the general **procedure B** with dimethylphenylsilyl vinyl B(mac) (76.9 mg, 0.2 mmol, 1 equiv.), phenyl lithium (1.78 M in dibutyl ether, 0.11 ml, 0.21 mmol, 1.05 equiv.), 1-bromo-4-tert-butylbenzene (46.9 mg, 0.22 mmol, 1.1 equiv.), potassium triflate (75.3 mg, 0.4 mmol, 2 equiv), palladium (II) acetate (1.35 mg, 6.0 μmol, 0.030 equiv.), (R_p, R_p)-L (7.6 mg, 7.2 μmol), 0.036 equiv.) and cesium fluoride (30.4 mg, 0.2 mmol, 1.0 equiv) in THF (0.80 mL, 0.25 M). The crude mixture was oxidized by $NaOH/H_2O_2$ and purified by silica gel chromatography (5% EtOAc in hexanes, stain in $KMnO_4$ stain) to afford a white solid (61.2 mg, 79% yield). ^{1}H NMR (500 MHz, $CDCl_3$) δ 7.34 – 7.30 (m, 2H), 7.30 - 7.23 (m, 6H), 7.23 – 7.17 (m, 2H), 7.17 – 7.12 (m, 2H), 7.04 (dd, J = 8.4, 2.5 Hz, 2H), 5.12 (d, J = 9.8, 1H), 2.79 (dd, J = 9.9, 2.6 Hz, 1H), 2.03 (bs, 1H), 1.56 (s, 1H), 1.32 (m, 9H), 0.00 (s, 3H), -0.05 (s, 3H).; ^{13}C NMR (126 MHz, $CDCl_3$) δ 148.5, 142.9, 137.4, 136.5, 134.1, 128.7, 128.7, 128.3, 128.0, 127.3, 127.3, 125.3, 75.6, 46.9, 34.3, 31.4, -3.4, -3.6.; **IR** (neat) ν_{max} 3565.1 (br, w), 3441.4 (br, w), 2960.8 (s), 2902.3 (w), 1427.0 (w), 1247.9 (m), 1111.9 (m), 1028.6 (m), 835.4 (s), 812.3 (s), 735.8 (m), 699.1 (s) cm^{-1}. **HRMS**

(DART) for $C_{26}H_{31}Si$ $[M+H-H_2O]^+$: Calc'd: 371.2190, found: 371.2189. $[\alpha]_D^{20}$ = + 3.60 (*c* = 1.00, $CHCl_3$, *l* = 50 mm).

Analysis of Stereochemistry:

Diastereomer ratio was determined by ^1H NMR analysis of the crude reaction mixture. Racemic compound was prepared according to the procedure described above with $Pd(OAc)_2$ (3 mol%) and a mixture of (R_p, R_p)-L and (S_p, S_p)-L (3.6 mol%) as the catalyst. Absolute stereochemistry was assigned by analogy (see compound 8a).

Chiral SFC (Chiracel OD-H, 6% IPA, 3 mL/min, 100 bar, 35 °C, 210-289 nm) – analysis of (1R,2S)-2-(4-(tert-butyl)phenyl)-2-(dimethyl(phenyl)silyl)-1-phenylethan-1-ol.

Racemic Material

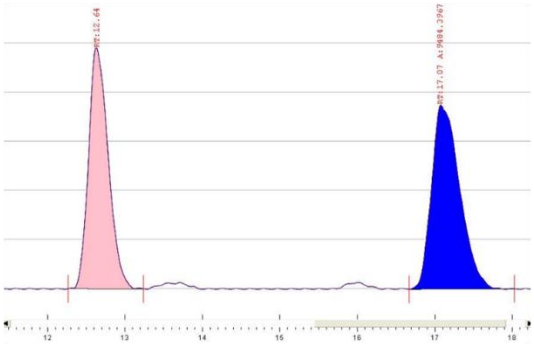

Peak No	% Area	Area	RT (min)
1	47.7437	8665.3828	12.64
2	52.2563	9484.3967	17.07
Total:	100	18149.7795	

Enantioenriched Material

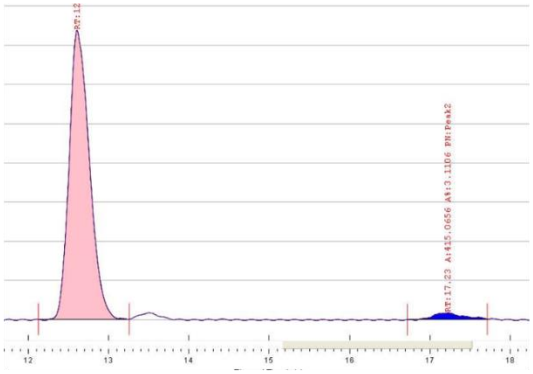

Peak No	% Area	Area	RT (min)
1	96.8894	12928.4479	12.61
2	3.1106	415.0656	17.23
Total:	100	13343.5135	

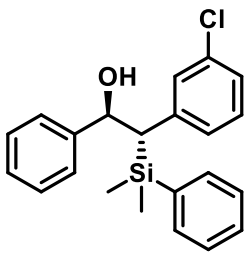

(1R,2S)-2-(3-chlorophenyl)-2-(dimethyl(phenyl)silyl)-1-phenylethan-1-ol (3.111)

The reaction was performed according to the general **procedure B** with dimethylphenylsilyl vinyl B(mac) (76.9 mg, 0.2 mmol, 1 equiv.), phenyl lithium (1.78 M in dibutyl ether, 0.11 ml, 0.21 mmol, 1.05 equiv.), 1-bromo-3-chlorobenzene (42.1 mg, 0.22 mmol, 1.1 equiv.), potassium triflate (75.3 mg, 0.4 mmol, 2 equiv), palladium (II) acetate (1.35 mg, 6.0 μmol, 0.030 equiv.), (R_p, R_p)-L (7.6 mg, 7.2 μmol), 0.036 equiv.) and cesium fluoride (30.4 mg, 0.2 mmol, 1.0 equiv) in THF (0.80 mL, 0.25 M). The crude mixture was oxidized by $NaOH/H_2O_2$ and purified by silica gel chromatography (6% EtOAc in hexanes, stain in $KMnO_4$ stain) to afford a colorless oil (45.7 mg, 62% yield). ^{1}H NMR (500 MHz, $CDCl_3$) δ 7.38 – 7.29 (m, 1H), 7.32 – 7.19 (m, 9H), 7.17 – 7.08 (m, 3H), 6.98 (dt, J = 6.9, 1.8 Hz, 1H), 5.11 (dd, J = 8.3, 2.4 Hz, 1H), 2.76 (d, J = 8.3 Hz, 1H), 1.91 (d, J = 2.6 Hz, 1H), 0.12 (s, 3H), 0.04 (s, 3H).; ^{13}C NMR (126 MHz, $CDCl_3$) δ 143.1, 142.2, 136.8, 134.1, 134.0, 129.29, 129.28, 129.1, 128.3, 127.9, 127.6, 127.5, 126.7, 125.5, 75.3, 47.1, -3.5, -3.6.; **IR** (neat) ν_{max} 3552.8 (br, w), 3413.9 (br, w), 3067.5 (w), 2955.8 (w), 1592.7 (m), 1474.7 (w), 1427.1 (m), 1249.5 (m), 1112.5 (w), 832.2 (m), 767.0 (m), 699.4 (s) cm^{-1}. **HRMS** (DART) for

$C_{22}H_{22}OSiCl$ $[M\text{-}H^-]^+$: Calc'd: 365.1123, found: 365.1126. $[\alpha]_D^{20}$ = - 6.11 (*c* = 1.00, $CHCl_3$, *l* = 50 mm).

Analysis of Stereochemistry:

Diastereomer ratio was determined by ^1H NMR analysis of the crude reaction mixture. Racemic compound was prepared according to the procedure described above with $Pd(OAc)_2$ (3 mol%) and a mixture of (R_p, R_p)-L and (S_p, S_p)-L (3.6 mol%) as the catalyst. Absolute stereochemistry was assigned by analogy (see compound 8a).

Chiral SFC (Chiracel OD-H, 10% IPA, 3 mL/min, 100 bar, 35 °C, 210-289 nm) – analysis of (1R,2S)-2-(3-chlorophenyl)-2-(dimethyl(phenyl)silyl)-1-phenylethan-1-ol.

Racemic Material

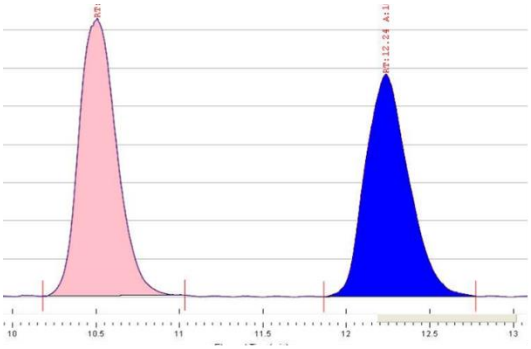

Peak No	% Area	Area	RT (min)
1	52.0407	11363.8911	10.51
2	47.9593	10472.656	12.24
Total:	100	21836.5471	

Enantioenriched Material

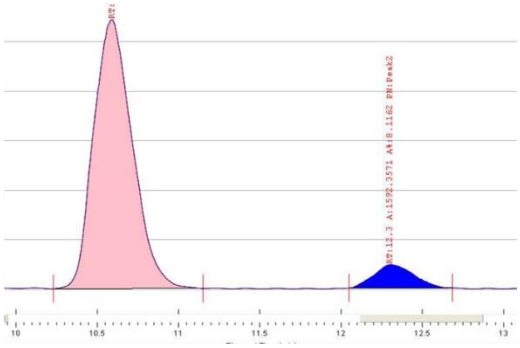

Peak No	% Area	Area	RT (min)
1	91.8838	18027.0231	10.59
2	8.1162	1592.3571	12.3
Total:	100	19619.3802	

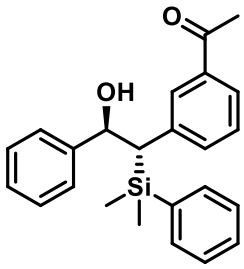

1-(3-((1S,2R)-1-(dimethyl(phenyl)silyl)-2-hydroxy-2-phenylethyl)phenyl)ethan-1-one (3.112)

The reaction was performed according to the general **procedure B** with dimethylphenylsilyl vinyl B(mac) (76.9 mg, 0.2 mmol, 1 equiv.), phenyl lithium (1.78 M in dibutyl ether, 0.11 ml, 0.21 mmol, 1.05 equiv.), 1-(3-Bromophenyl)ethanone (43.8 mg, 0.22 mmol, 1.1 equiv.), potassium triflate (75.3 mg, 0.4 mmol, 2 equiv), palladium (II) acetate (1.35 mg, 6.0 µmol, 0.030 equiv.), (R_p, R_p)-L (7.6 mg, 7.2 µmol), 0.036 equiv.) and cesium fluoride (30.4 mg, 0.2 mmol, 1.0 equiv) in THF (0.80 mL, 0.25 M). The crude mixture was oxidized by $NaOH/H_2O_2$ and purified by silica gel chromatography (10% EtOAc in hexanes, stain in $KMnO_4$ stain) to afford a colorless oil (51.0 mg, 68% yield). ^{1}H NMR (500 MHz, $CDCl_3$) δ 7.74 – 7.69 (m, 1H), 7.64 – 7.60 (m, 1H), 7.37 – 7.19 (m, 12H), 5.21 (d, J = 8.3, 1H), 2.86 (d, J = 8.2, 1H), 2.48 (s, 3H), 2.00 (bs, 1H), 1.66 (d, J = 1.8 Hz, 0H), 0.11 (s, 3H), 0.07 (s, 3H).; ^{13}C NMR (126 MHz, $CDCl_3$) δ 198.35, 143.30, 140.60, 136.94, 136.81, 134.08, 133.99, 129.39, 129.10, 128.3, 128.3, 127.9, 127.6, 126.7, 125.3, 75.3, 47.1, 26.6, -3.6, -3.7.; **IR** (neat) ν_{max} 3445.0 (br, m), 3067.5 (w), 2955.4 (w), 1680.1 (s), 1579.1 (w), 1427.3 (w), 1358.0 (w), 1269.5 (m), 1112.4 (m), 833.5 (m), 734.4 (m), 698.8 (s) cm^{-1}. **HRMS** (DART)

for $C_{24}H_{25}OSi$ $[M+H-H_2O]^+$: Calc'd: 357.1669, found: 357.1665. $[\alpha]_D^{20}$ = + 2.20 (*c* = 1.00, $CHCl_3$, *l* = 50 mm).

Analysis of Stereochemistry:

Diastereomer ratio was determined by ^1H NMR analysis of the crude reaction mixture. Racemic compound was prepared according to the procedure described above with $Pd(OAc)_2$ (3 mol%) and a mixture of (R_p, R_p)-L and (S_p, S_p)-L (3.6 mol%) as the catalyst. Absolute stereochemistry was assigned by analogy (see compound 8a).

Chiral SFC (Chiracel OD-H, 10% IPA, 3 mL/min, 100 bar, 35 °C, 210-289 nm) – analysis of 1-(3-((1S,2R)-1-(dimethyl(phenyl)silyl)-2-hydroxy-2-phenylethyl)phenyl)ethan-1-one.

Racemic Material

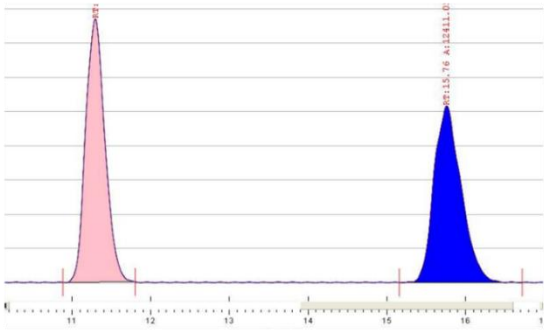

Peak No	% Area	Area	RT (min)
1	51.4683	13162.0234	11.3
2	48.5317	12411.0597	15.76
Total:	100	25573.0831	

Enantioenriched Material

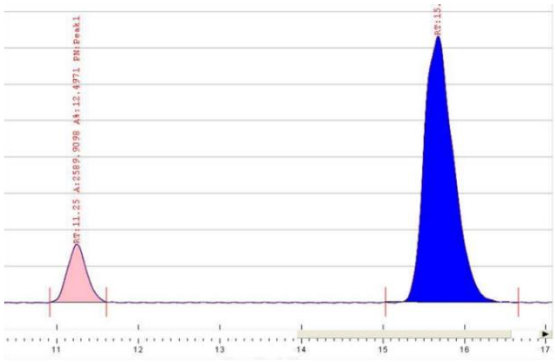

Peak No	% Area	Area	RT (min)
1	12.4971	2589.9098	11.25
2	87.5029	18134.1636	15.67
Total:	100	20724.0734	

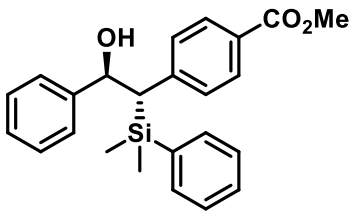

methyl 3-((1S,2R)-1-(dimethyl(phenyl)silyl)-2-hydroxy-2-phenylethyl)benzoate (3.113)

The reaction was performed according to the general **procedure B** with dimethylphenylsilyl vinyl B(mac) (76.9 mg, 0.2 mmol, 1 equiv.), phenyl lithium (1.78 M in dibutyl ether, 0.11 ml, 0.21 mmol, 1.05 equiv.), 4-methoxycarbonylphenyl bromide (47.3 mg, 0.22 mmol, 1.1 equiv.), potassium triflate (75.3 mg, 0.4 mmol, 2 equiv), palladium (II) acetate (1.35 mg, 6.0 μmol, 0.030 equiv.), (R_p, R_p)-L (7.6 mg, 7.2 μmol), 0.036 equiv.) and cesium fluoride (30.4 mg, 0.2 mmol, 1.0 equiv) in THF (0.80 mL, 0.25 M). The crude mixture was oxidized by $NaOH/H_2O_2$ and purified by silica gel chromatography (10% EtOAc in hexanes, stain in $KMnO_4$ stain) to afford a white solid. (46.7 mg, 60% yield). ^{1}H NMR (500 MHz, $CDCl_3$) δ 7.88 (d, J = 7.9 Hz, 2H), 7.34 (dtd, J = 8.7, 4.4, 1.4 Hz, 1H), 7.34 – 7.18 (m, 9H), 7.18 (d, J = 8.0 Hz, 2H), 5.18 (d, J = 8.0 Hz, 1H), 3.90 (s, 3H), 2.87 (d, J = 8.1 Hz, 1H), 1.92 (d, J = 2.5 Hz, 1H), 0.13 (s, 3H), 0.05 (s, 3H).; ^{13}C NMR (126 MHz, $CDCl_3$) δ 167.2, 146.1, 143.2, 136.8, 134.1, 129.4, 129.3, 129.1, 128.3, 127.9, 127.6, 127.2, 126.6, 77.3, 77.0, 76.8, 75.2, 51.9, 47.7, -3.5, -3.6.; **IR** (neat) ν_{max} 3487.4 (br, m), 2952.2 (w), 1717.6 (s), 1606.6 (m), 1435.4 (m), 1281.0 (s), 1180.7 (m), 1112.8 (s), 856.0 (m), 701.3 (m) cm^{-1}. **HRMS** (DART) for

$C_{24}H_{25}O_2Si$ $[M+H-H_2O]^+$: Calc'd: 373.1618, found: 373.1621. $[\alpha]_D^{20}$ = - 17.38 (c = 1.00, $CHCl_3$, l = 50 mm).

Analysis of Stereochemistry:

Diastereomer ratio was determined by ^1H NMR analysis of the crude reaction mixture. Racemic compound was prepared according to the procedure described above with $Pd(OAc)_2$ (3 mol%) and a mixture of (R_p, R_p)-L and (S_p, S_p)-L (3.6 mol%) as the catalyst. Absolute stereochemistry was assigned by analogy (see compound 8a).

Chiral SFC (Chiracel OJ-H, 10% IPA, 3 mL/min, 100 bar, 35 °C, 210-289 nm) – analysis of methyl 3-((1S,2R)-1-(dimethyl(phenyl)silyl)-2-hydroxy-2-phenylethyl)benzoate.

Racemic Material

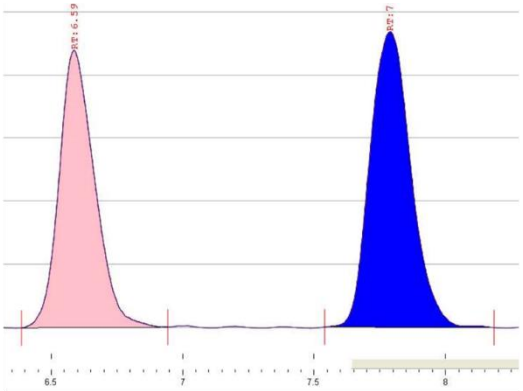

Peak No	% Area	Area	RT (min)
1	44.9071	4107.2281	6.59
2	55.0929	5038.818	7.79
Total:	100	9146.0461	

Enantioenriched Material

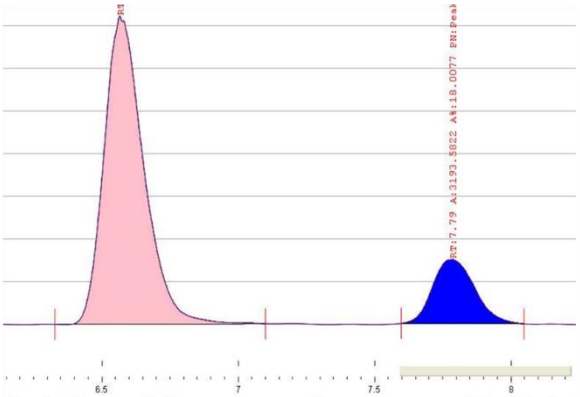

Peak No	% Area	Area	RT (min)
1	81.9923	14540.9412	6.57
2	18.0077	3193.5822	7.79
Total:	100	17734.5234	

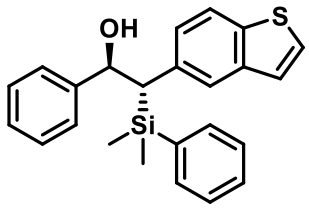

(1R,2S)-2-(benzo[b]thiophen-5-yl)-2-(dimethyl(phenyl)silyl)-1-phenylethan-1-ol (3.114)

The reaction was performed according to the general **procedure B** with dimethylphenylsilyl vinyl B(mac) (76.9 mg, 0.2 mmol, 1 equiv.), phenyl lithium (1.78 M in dibutyl ether, 0.11 ml, 0.21 mmol, 1.05 equiv.), 5-bromobenzothiophene (46.9 mg, 0.22 mmol, 1.1 equiv.), potassium triflate (75.3 mg, 0.4 mmol, 2 equiv), palladium (II) acetate (1.35 mg, 6.0 μmol, 0.030 equiv.), (R_p, R_p)-L (7.6 mg, 7.2 μmol), 0.036 equiv.) and cesium fluoride (30.4 mg, 0.2 mmol, 1.0 equiv) in THF (0.80 mL, 0.25 M). The crude mixture was oxidized by $NaOH/H_2O_2$ and purified by silica gel chromatography (8% EtOAc in hexanes, stain in KMnO4 stain) to afford a colorless oil (52.9 mg, 68% yield). ^{1}H NMR (500 MHz, $CDCl_3$) δ 7.75 (d, J = 8.3 Hz, 1H), 7.59 (d, J = 1.7 Hz, 1H), 7.42 (d, J = 5.4 Hz, 1H), 7.38 – 7.29 (m, 3H), 7.31 – 7.20 (m, 8H), 7.13 (dd, J = 8.3, 1.8 Hz, 1H), 5.19 (d, J = 8.9, 1H), 2.93 (d, J = 8.9 Hz, 1H), 2.02 (s, 1H), 0.12 (s, 3H), -0.01 (s, 3H).; ^{13}C NMR (101 MHz, $CDCl_3$) δ 143.1, 140.0, 137.2, 137.1, 135.9, 134.2, 128.9, 128.3, 127.9, 127.4, 127.1, 126.4, 126.2, 123.9, 123.7, 122.2, 75.7, 47.1, -3.2, -3.5.; **IR** (neat) ν_{max} 3555.5 (br, w), 3421.9 (br, w), 3067.2 (w), 3024.9 (w), 2954.7 (w), 1599.5 (w), 1426.8 (w), 1247.8 (m), 1111.9 (m), 1028.8 (m),

833.3 (m), 758.5 (m), 698.6 (s) cm^{-1}. **HRMS** (DART) for $C_{24}H_{24}SiOS$ $[M\text{-}e]^+$: Calc'd: 388.1312, found: 388.1299. $\mathbf{[\alpha]_D^{20}}$ = - 18.88 (*c* = 1.00, $CHCl_3$, *l* = 50 mm).

Analysis of Stereochemistry:

Diastereomer ratio was determined by ^1H NMR analysis of the crude reaction mixture. Racemic compound was prepared according to the procedure described above with $Pd(OAc)_2$ (3 mol%) and a mixture of (R_p, R_p)-L and (S_p, S_p)-L (3.6 mol%) as the catalyst. Absolute stereochemistry was assigned by analogy (see compound 8a).

Chiral SFC (Chiracel ODR-H, 10% IPA, 3 mL/min, 100 bar, 35 °C, 210-289 nm) analysis of (1R,2S)-2-(benzo[b]thiophen-5-yl)-2-(dimethyl(phenyl)silyl)-1-phenylethan-1-ol.

Racemic Material

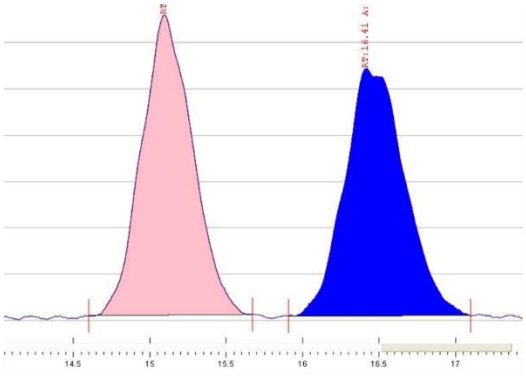

Peak No	% Area	Area	RT (min)
1	50.5164	7523.4216	15.09
2	49.4836	7369.6187	16.41
Total:	100	14893.0403	

Enantioenriched Material

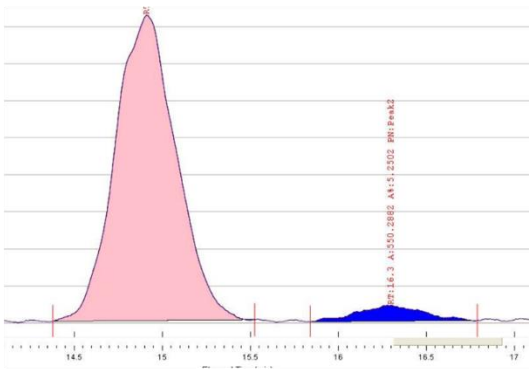

Peak No	% Area	Area	RT (min)
1	94.7498	9931.0031	14.91
2	5.2502	550.2882	16.3
Total:	100	10481.2913	

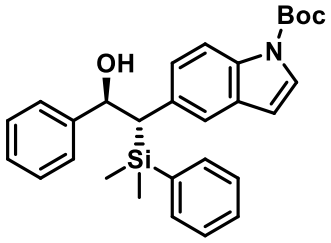

tert-butyl 5-((1S,2R)-1-(dimethyl(phenyl)silyl)-2-hydroxy-2-phenylethyl)-1H-indole-1-carboxylate (3.115)

The reaction was performed according to the general **procedure B** with dimethylphenylsilyl vinyl B(mac) (76.9 mg, 0.2 mmol, 1 equiv.), phenyl lithium (1.78 M in dibutyl ether, 0.11 ml, 0.21 mmol, 1.05 equiv.), 5-bromo-indole-1-carboxylic acid tert-butyl ester (65.2 mg, 0.22 mmol, 1.1 equiv.), potassium triflate (75.3 mg, 0.4 mmol, 2 equiv), palladium (II) acetate (1.35 mg, 6.0 μmol, 0.030 equiv.), (R_p, R_p)-L (7.6 mg, 7.2 μmol), 0.036 equiv.) and cesium fluoride (30.4 mg, 0.2 mmol, 1.0 equiv) in THF (0.80 mL, 0.25 M). The crude mixture was oxidized by $NaOH/H_2O_2$ and purified by silica gel chromatography (12% EtOAc in hexanes, stain in $KMnO_4$ stain) to afford a white solid (53.4 mg, 57% yield). ^{1}H NMR (600 MHz, $CDCl_3$) δ 8.01 (bs, 1H), 7.56 (bs, 1H), 7.34 – 7.27 (m, 4H), 7.27 – 7.17 (m, 7H), 7.10 (dd, J = 8.5, 1.8 Hz, 1H), 6.48 (d, J = 3.6 Hz, 1H), 5.14 (d, J = 9.0 Hz, 1H), 2.87 (d, J = 9.0 Hz, 1H), 1.68 (s, 9H), 0.10 (s, 3H), -0.06 (s, 3H).; ^{13}C NMR (126 MHz, $CDCl_3$) δ 149.8, 143.1, 137.4, 134.2, 133.9, 133.6, 130.9, 128.9, 128.2, 127.9, 127.4, 127.1, 126.0, 125.8, 121.4, 115.0, 107.2, 83.5, 75.8, 47.0, 28.2, -3.1, -3.4.; **IR** (neat) ν_{max} 3540.8 (br, m), 2976.0 (m), 1731.5 (s), 1465.5 (m), 1372.8 (s),

1348.5 (s), 1328.8 (s), 1254.9 (s), 1164.1 (m), 1128.4 (s), 1024.1 (m), 833.6 (m), 699.9 (s) cm^{-1}. **HRMS** (DART) for $C_{29}H_{32}NO_2Si$ $[M+H-H_2O]^+$: Calc'd: 454.2197, found: 454.2190. $\mathbf{[\alpha]_D^{20}}$ = - 12.62 (*c* = 1.00, $CHCl_3$, *l* = 50 mm).

Analysis of Stereochemistry:

Diastereomer ratio was determined by ^1H NMR analysis of the crude reaction mixture. Racemic compound was prepared according to the procedure described above with $Pd(OAc)_2$ (3 mol%) and a mixture of (R_p, R_p)-L and (S_p, S_p)-L (3.6 mol%) as the catalyst. Absolute stereochemistry was assigned by analogy (see compound 8a).

Chiral SFC (Chiracel OD-H, 10% IPA, 3 mL/min, 100 bar, 35 °C, 210-289 nm) – analysis of tert-butyl 5-((1S,2R)-1-(dimethyl(phenyl)silyl)-2-hydroxy-2-phenylethyl)-1H-indole-1-carboxylate.

Racemic Material

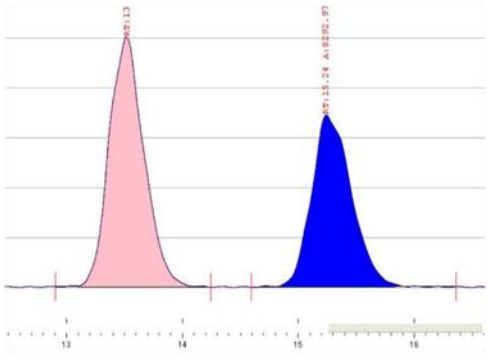

Peak No	% Area	Area	RT (min)
1	55.9154	10518.5328	13.52
2	44.0846	8292.9775	15.24
Total:	100	18811.5103	

Enantioenriched Material

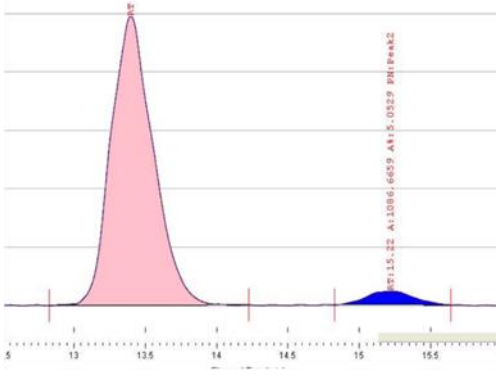

Peak No	% Area	Area	RT (min)
1	94.9471	20419.1843	13.4
2	5.0529	1086.6659	15.22
Total:	100	21505.8502	

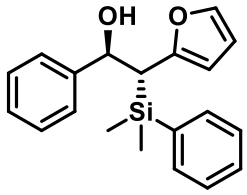

(1R,2R)-2-(dimethyl(phenyl)silyl)-2-(furan-2-yl)-1-phenylethan-1-ol (3.116)

The reaction was performed according to the general **procedure B** with dimethylphenylsilyl vinyl B(mac) (76.9 mg, 0.2 mmol, 1 equiv.), phenyl lithium (1.78 M in dibutyl ether, 0.11 ml, 0.21 mmol, 1.05 equiv.), 2-bromofuran (32.3 mg, 0.22 mmol, 1.1 equiv.), potassium triflate (75.3 mg, 0.4 mmol, 2 equiv), palladium (II) acetate (1.35 mg, 6.0 μmol, 0.030 equiv.), (R_p, R_p)-L (7.6 mg, 7.2 μmol), 0.036 equiv.) and cesium fluoride (30.4 mg, 0.2 mmol, 1.0 equiv) in THF (0.80 mL, 0.25 M). The crude mixture was oxidized by $NaOH/H_2O_2$ and purified by silica gel chromatography (8% EtOAc in hexanes, stain in $KMnO_4$ stain) to afford a light yellow oil (56.4 mg, 88% yield). ^1H NMR (600 MHz, $CDCl_3$) δ 7.43-7.39 (m, 2H), 7.39 – 7.29 (m, 4H), 7.27 – 7.19 (m, 3H), 7.17 – 7.13 (m, 2H), 6.28 (dt, J = 3.0, 1.4 Hz, 1H), 5.93 (d, J = 3.1 Hz, 1H), 5.01 (dd, J = 6.9, 4.6 Hz, 1H), 2.92 (d, J = 6.9 Hz, 1H), 2.42 (d, J = 4.7 Hz, 1H), 0.26 (s, 3H), 0.18 (s, 3H).; ^{13}C NMR (151 MHz, $CDCl_3$) δ 154.0, 143.2, 141.1, 137.1, 134.0, 129.1, 128.1, 127.6, 127.6, 126.4, 110.5, 107.3, 74.2, 40.0, -3.3, -3.4.; **IR** (neat) ν_{max} 3067.5 (br, w), 2956.8 (w), 2586.7 (br, w), 2215.5 (w), 1749.6 (br, m), 1608.4 (w), 1427.7 (w), 1254.3 (m), 1118.7 (s), 1060.9 (m), 831.4 (s), 791.1 (s), 699.1 (s) cm^{-1}. **HRMS**

(DART) for $C_{20}H_{21}SiO_2$ $[M\text{-}H^-]^+$: Calc'd: 321.1305, found: 321.1305. **$[\alpha]_D^{20}$** = + 1.65 (*c* = 1.00, $CHCl_3$, *l* = 50 mm).

Analysis of Stereochemistry:

Diastereomer ratio was determined by ^1H NMR analysis of the crude reaction mixture. Racemic compound was prepared according to the procedure described above with $Pd(OAc)_2$ (3 mol%) and a mixture of (R_p, R_p)-L and (S_p, S_p)-L (3.6 mol%) as the catalyst. Absolute stereochemistry was assigned by analogy (see compound 8a).

Chiral SFC (Chiracel OJ-H, 10% IPA, 3 mL/min, 100 bar, 35 °C, 210-289 nm) analysis of (1R,2R)-2-(dimethyl(phenyl)silyl)-2-(furan-2-yl)-1-phenylethan-1-ol

Racemic Material

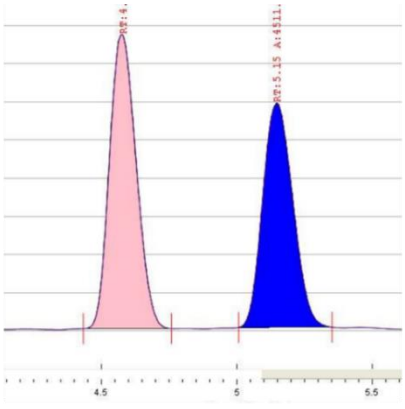

Peak No	% Area	Area	RT (min)
1	53.7681	5246.4328	4.58
2	46.2319	4511.0785	5.15
Total:	100	9757.5113	

Enantioenriched Material

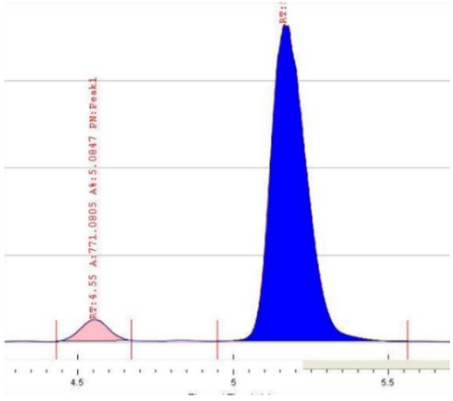

Peak No	% Area	Area	RT (min)
1	5.0847	771.0805	4.55
2	94.9153	14393.5634	5.16
Total:	100	15164.6439	

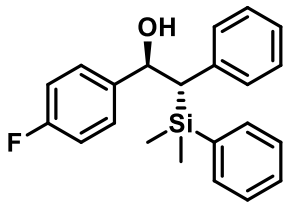

(1R,2S)-2-(dimethyl(phenyl)silyl)-1-(4-fluorophenyl)-2-phenylethan-1-ol (3.121)

The reaction was performed according to the general **procedure C** with dimethylphenylsilyl vinyl B(mac) (76.9 mg, 0.2 mmol, 1 equiv.), *tert*-butyl lithium (1.63 M in pentane, 0.25 ml, 0.4 mmol, 2 equiv.), 1-bromo-4-fluorobenzene (36.8 mg, 0.21 mmol, 1.05 equiv.), potassium triflate (75.3 mg, 0.4 mmol, 2 equiv), palladium (II) acetate (1.35 mg, 6.0 μmol, 0.030 equiv.), (R_p, R_p)-L (7.6 mg, 7.2 μmol), 0.036 equiv.) and cesium fluoride (30.4 mg, 0.2 mmol, 1.0 equiv) in THF (0.80 mL, 0.25 M). The crude mixture was oxidized by $NaOH/H_2O_2$ and purified by silica gel chromatography (10% EtOAc in hexanes, stain in $KMnO_4$ stain) to afford a white solid (48.3 mg, 69% yield). ^{1}H NMR (500 MHz, $CDCl_3$) δ 7.36 – 7.29 (m, 1H), 7.29 – 7.20 (m, 8H), 7.20 - 7.12 (m, 3H), 7.14 (d, J = 7.2 Hz, 2H), 6.94 – 6.86 (m, 2H), 5.13 (dd, J = 9.1, 2.3 Hz, 1H), 2.77 (d, J = 9.1 Hz, 1H), 2.00 (d, J = 2.3 Hz, 1H), 0.14 (s, 2H), -0.01 (s, 3H).; ^{13}C NMR (126 MHz, $CDCl_3$) δ 163.3, 161.4, 139.7, 138.8, 138.7, 137.1, 134.0, 129.2, 128.9, 128.7, 128.6, 128.5, 127.5, 125.7, 115.1, 114.9, 74.9, 47.6, -3.1, -3.8.; **IR** (neat) ν_{max} 3556.0 (br, w), 3420.0 (br, w), 3067.8 (w), 2955.4 (w), 2219.7 (w), 1603.4 (m), 1508.4 (s), 1427.0 (w), 1248.7 (m), 1223.5 (s), 1156.3 (m), 834.3 (s),

700.6 (s) cm^{-1}. **HRMS** (DART) for $C_{22}H_{22}SiF$ $[M+H-H_2O]^+$: Calc'd: 333.1469, found: 333.1469. $[\alpha]_D^{20}$ = + 14.43 (*c* = 1.00, $CHCl_3$, *l* = 50 mm).

Analysis of Stereochemistry:

Diastereomer ratio was determined by ^1H NMR analysis of the crude reaction mixture. Racemic compound was prepared according to the procedure described above with $Pd(OAc)_2$ (3 mol%) and a mixture of (R_p, R_p)-L and (S_p, S_p)-L (3.6 mol%) as the catalyst. Absolute stereochemistry was assigned by analogy (see compound 8a).

Chiral SFC (Chiracel OJ-H, 10% IPA, 3 mL/min, 100 bar, 35 °C, 210-289 nm) – analysis of (1R,2S)-2-(dimethyl(phenyl)silyl)-1-(4-fluorophenyl)-2-phenylethan-1-ol.

Racemic Material

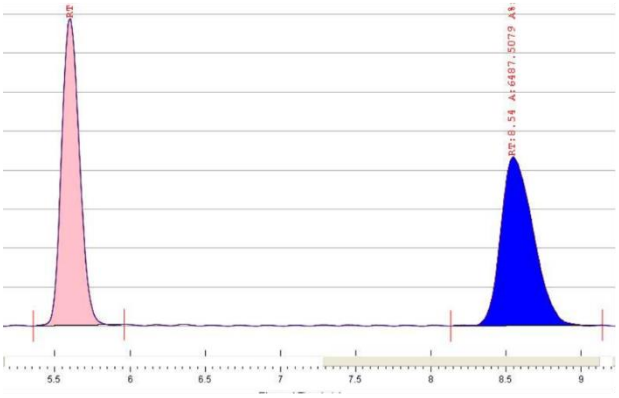

Peak No	% Area	Area	RT (min)
1	50.0877	6510.3139	5.6
2	49.9123	6487.5079	8.54
Total:	100	12997.8218	

Enantioenriched Material

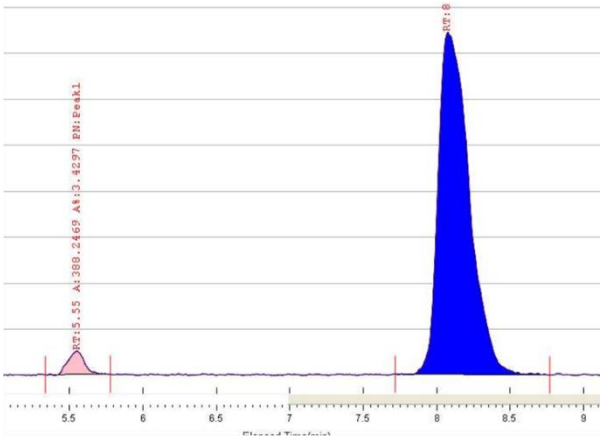

Peak No	% Area	Area	RT (min)
1	3.4297	388.2469	5.55
2	96.5703	10931.9067	8.07
Total:	100	11320.1536	

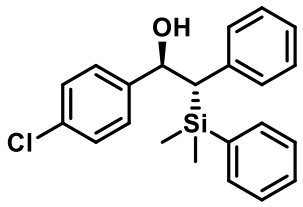

(1R,2S)-1-(4-chlorophenyl)-2-(dimethyl(phenyl)silyl)-2-phenylethan-1-ol (3.119)

The reaction was performed according to the general **procedure C** with dimethylphenylsilyl vinyl B(mac) (76.9 mg, 0.2 mmol, 1 equiv.), *tert*-butyl lithium (1.63 M in pentane, 0.25 ml, 0.4 mmol, 2 equiv.), 1-bromo-4-chlorobenzene (42.1 mg, 0.21 mmol, 1.05 equiv.), potassium triflate (75.3 mg, 0.4 mmol, 2 equiv), palladium (II) acetate (1.35 mg, 6.0 μmol, 0.030 equiv.), (R_p, R_p)-L (7.6 mg, 7.2 μmol), 0.036 equiv.) and cesium fluoride (30.4 mg, 0.2 mmol, 1.0 equiv) in THF (0.80 mL, 0.25 M). The crude mixture was oxidized by $NaOH/H_2O_2$ and purified by silica gel chromatography (10 % EtOAc in hexanes, stain in $KMnO_4$ stain) to afford a white solid (49.6 mg, 68% yield). ^{1}H NMR (500 MHz, $CDCl_3$) δ 7.37 – 7.29 (m, 1H), 7.29 – 7.19 (m, 6H), 7.21 – 7.10 (m, 7H), 5.11 (dd, J = 8.8, 2.6 Hz, 1H), 2.74 (d, J = 8.7 Hz, 1H), 1.98 (d, J = 2.5 Hz, 1H), 0.18 (s, 3H), -0.00 (s, 3H).; ^{13}C NMR (126 MHz, $CDCl_3$) δ 141.5, 139.5, 137.1, 133.9, 133.4, 129.3, 128.9, 128.5, 128.3, 128.3, 127.5, 125.7, 74.9, 47.4, -2.9, -3.9.; **IR** (neat) ν_{max} 3525.6 (br, w), 3424.0 (br, w), 3067.7 (w), 2956.0 (w), 2358.7 (w), 1599.0 (m), 1491.3 (m), 1249.2 (m), 1112.4 (m), 1028.6 (m), 832.6 (s), 764.6 (m),

700.8 (s) cm^{-1}. **HRMS** (DART) for $C_{22}H_{22}SiCl$ $[M+H-H_2O]^+$: Calc'd: 349.1174, found: 349.1183. $[\alpha]_D^{20}$ = + 12.96 (*c* = 1.00, $CHCl_3$, *l* = 50 mm).

Analysis of Stereochemistry:

Diastereomer ratio was determined by ^1H NMR analysis of the crude reaction mixture. Racemic compound was prepared according to the procedure described above with $Pd(OAc)_2$ (3 mol%) and a mixture of (R_p, R_p)-L and (S_p, S_p)-L (3.6 mol%) as the catalyst. Absolute stereochemistry was assigned by analogy (see compound 8a).

Chiral SFC (Chiracel OD-H, 9% IPA, 3 mL/min, 100 bar, 35 °C, 210-289 nm) – analysis of (1R,2S)-1-(4-chlorophenyl)-2-(dimethyl(phenyl)silyl)-2-phenylethan-1-ol.

Racemic Material

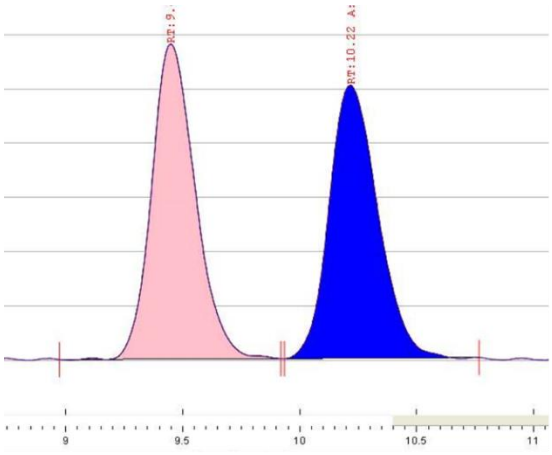

Peak No	% Area	Area	RT (min)
1	51.0181	7546.2062	9.45
2	48.9819	7245.0333	10.22
Total:	100	14791.2395	

Enantioenriched Material

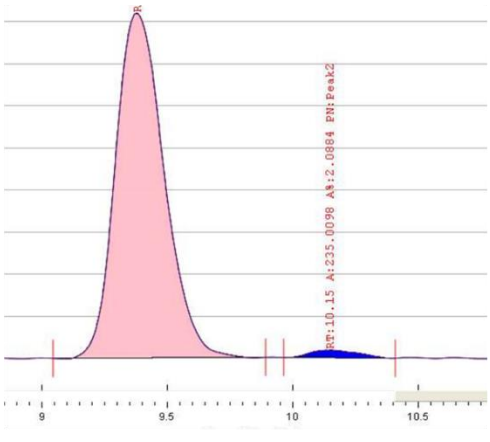

Peak No	% Area	Area	RT (min)
1	97.9116	11017.9216	9.38
2	2.0884	235.0098	10.15
Total:	100	11252.9314	

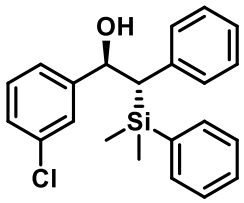

(1R,2S)-1-(3-chlorophenyl)-2-(dimethyl(phenyl)silyl)-2-phenylethan-1-ol (3.120)

The reaction was performed according to the general **procedure C** with dimethylphenylsilyl vinyl B(mac) (76.9 mg, 0.2 mmol, 1 equiv.), *tert*-butyl lithium (1.63 M in pentane, 0.25 ml, 0.4 mmol, 2 equiv.), 1-bromo-3-chlorobenzene (42.1 mg, 0.21 mmol, 1.05 equiv.), potassium triflate (75.3 mg, 0.4 mmol, 2 equiv), palladium (II) acetate (1.35 mg, 6.0 μmol, 0.030 equiv.), (R_p, R_p)-L (7.6 mg, 7.2 μmol), 0.036 equiv.) and cesium fluoride (30.4 mg, 0.2 mmol, 1.0 equiv) in THF (0.80 mL, 0.25 M). The crude mixture was oxidized by $NaOH/H_2O_2$ and purified by silica gel chromatography (9% EtOAc in hexanes, stain in $KMnO_4$ stain) to afford a colorless oil (28.0 mg, 40% yield). ^{1}H NMR (500 MHz, $CDCl_3$) δ 7.36 – 7.21 (m, 8H), 7.20 – 7.10 (m, 6H), 5.09 (d, J = 8.7 Hz, 1H), 2.75 (d, J = 8.6 Hz, 1H), 2.01 (bs, 1H), 0.17 (s, 3H), 0.01 (s, 3H).; ^{13}C NMR (126 MHz, $CDCl_3$) δ 145.1, 139.3, 137.0, 134.0, 134.0, 129.4, 129.3, 129.0, 128.5, 127.9, 127.5, 127.2, 125.8, 125.1, 75.0, 47.3, -3.1, -3.8.; **IR** (neat) ν_{max} 3555.3 (br, w), 3421.4 (br, w), 3067.6 (w), 2954.9 (w), 2356.6 (w), 1597.3 (w), 1490.7 (w), 1427.2 (w), 1249.3 (m), 1112.5 (m), 834.2 (m), 786.1 (m), 701.0 (s) cm^{-1}.

HRMS (DART) for $C_{22}H_{22}SiCl$ $[M+H-H_2O]^+$: Calc'd: 349.1174, found: 349.1188. $[\alpha]_D^{20}$ = + 7.64 (*c* = 1.00, $CHCl_3$, *l* = 50 mm).

Analysis of Stereochemistry:

Diastereomer ratio was determined by ^1H NMR analysis of the crude reaction mixture. Racemic compound was prepared according to the procedure described above with $Pd(OAc)_2$ (3 mol%) and a mixture of (R_p, R_p)-L and (S_p, S_p)-L (3.6 mol%) as the catalyst. Absolute stereochemistry was assigned by analogy (see compound 8a).

Chiral SFC (Chiracel OD-H, 10% IPA, 3 mL/min, 100 bar, 35 °C, 210-289 nm) – analysis of (1R,2S)-1-(3-chlorophenyl)-2-(dimethyl(phenyl)silyl)-2-phenylethan-1-ol.

Racemic Material

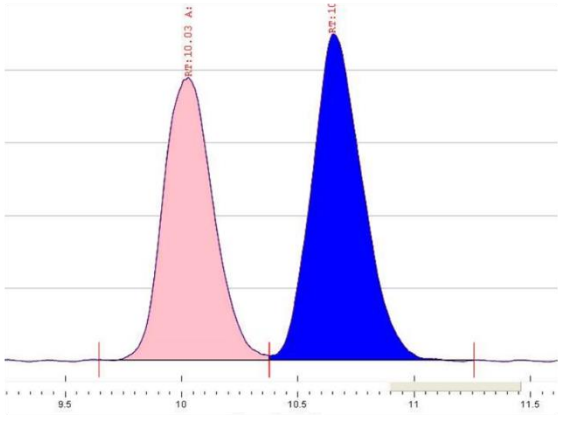

Peak No	% Area	Area	RT (min)
1	46.1419	5797.2608	10.03
2	53.8581	6766.7162	10.65
Total:	100	12563.977	

Enantioenriched Material

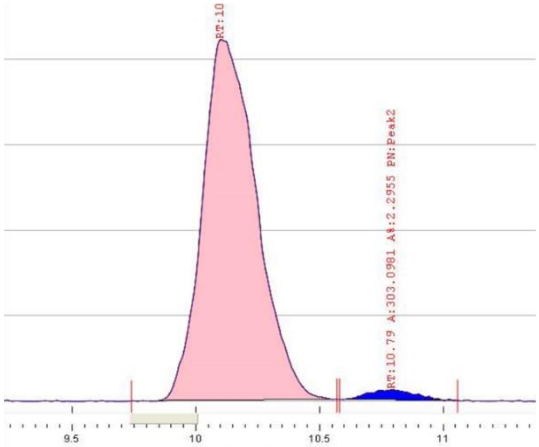

Peak No	% Area	Area	RT (min)
1	97.7045	12901.1323	10.1
2	2.2955	303.0981	10.79
Total:	100	13204.2304	

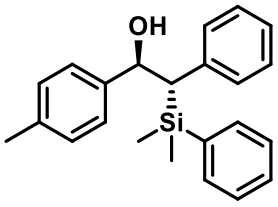

(1R,2S)-2-(dimethyl(phenyl)silyl)-2-phenyl-1-(p-tolyl)ethan-1-ol (22)

The reaction was performed according to the general **procedure C** with dimethylphenylsilyl vinyl B(mac) (76.9 mg, 0.2 mmol, 1 equiv.), *tert*-butyl lithium (1.63 M in pentane, 0.25 ml, 0.4 mmol, 2 equiv.), *para*-bromotoluene (37.6 mg, 0.21 mmol, 1.05 equiv.), potassium triflate (75.3 mg, 0.4 mmol, 2 equiv), palladium (II) acetate (1.35 mg, 6.0 μmol, 0.030 equiv.), (R_p, R_p)-L (7.6 mg, 7.2 μmol), 0.036 equiv.) and cesium fluoride (30.4 mg, 0.2 mmol, 1.0 equiv) in THF (0.80 mL, 0.25 M). The crude mixture was oxidized by $NaOH/H_2O_2$ and purified by silica gel chromatography (4% EtOAc in hexanes, stain in $KMnO_4$ stain) to afford a colorless oil (38.0 mg, 55% yield). ^{1}H NMR (600 MHz, $CDCl_3$) δ 7.30 (td, J = 7.4, 1.6 Hz, 1H), 7.30 – 7.19 (m, 6H), 7.19 – 7.11 (m, 5H), 7.04 (d, J = 7.7 Hz, 2H), 5.10 (dd, J = 9.4, 2.3 Hz, 1H), 2.81 (d, J = 9.3 Hz, 1H), 2.31 (s, 3H), 1.93 (d, J = 2.0 Hz, 1H), 0.07 (s, 3H), -0.03 (s, 3H).; ^{13}C NMR (126 MHz, $CDCl_3$) δ 140.1, 140.0, 137.6, 137.3, 134.1, 129.2, 128.9, 128.7, 128.4, 127.3, 127.0, 125.5, 75.4, 47.4, 21.2, -3.2, -3.6.; **IR** (neat) ν_{max} 3553.5 (br, w), 3423.0 (w), 3023.0 (w), 2954.6 (w), 1597.5 (w), 1489.1 (w), 1427.0 (m), 1247.7 (m), 1111.0 (m), 1028.7 (w), 831.2 (s), 817.0 (s), 700.4 (s) cm^{-1}. **HRMS** (DART) for $C_{23}H_{25}Si$ $[M+H-H_2O]^+$:

Calc'd: 329.1720, found: 329.1698. $[\alpha]_D^{20}$ = +13.40 (*c* = 1.00, $CHCl_3$, *l* = 50 mm).

Analysis of Stereochemistry:

Diastereomer ratio was determined by ^1H NMR analysis of the crude reaction mixture. Racemic compound was prepared according to the procedure described above with $Pd(OAc)_2$ (3 mol%) and a mixture of (R_p, R_p)-L and (S_p, S_p)-L (3.6 mol%) as the catalyst. Absolute stereochemistry was assigned by analogy (see compound 8a).

Chiral SFC (Chiracel OJ-H, 3% IPA, 3 mL/min, 100 bar, 35 °C, 210-289 nm) – analysis of (1R,2S)-2-(dimethyl(phenyl)silyl)-2-phenyl-1-(p-tolyl)ethan-1-ol.

Racemic Material

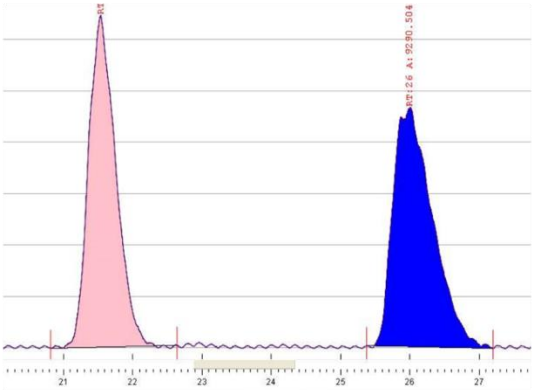

Peak No	% Area	Area	RT (min)
1	48.7186	8826.2118	21.54
2	51.2814	9290.5042	26
Total:	100	18116.716	

Enantioenriched Material

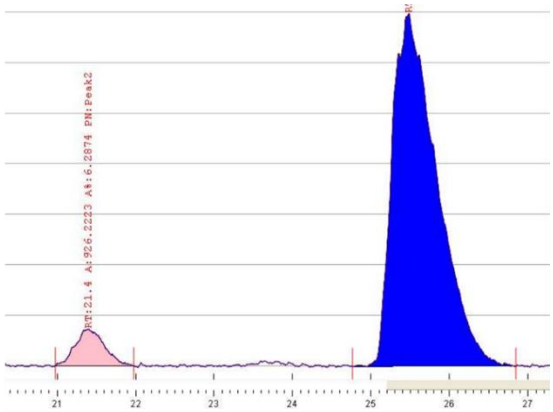

Peak No	% Area	Area	RT (min)
1	6.2874	926.2223	21.4
2	93.7126	13805.2578	25.48
Total:	100	14731.4801	

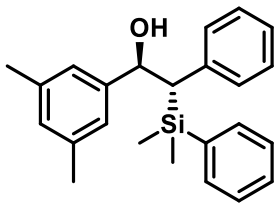

(1R,2S)-2-(dimethyl(phenyl)silyl)-1-(3,5-dimethylphenyl)-2-phenylethan-1-ol (3.123)

The reaction was performed according to the general **procedure C** with dimethylphenylsilyl vinyl B(mac) (76.9 mg, 0.2 mmol, 1 equiv.), *tert*-butyl lithium (1.63 M in pentane, 0.25 ml, 0.4 mmol, 2 equiv.), 5-bromo-1,3-xylene (38.9 mg, 0.21 mmol, 1.05 equiv.), potassium triflate (75.3 mg, 0.4 mmol, 2 equiv), palladium (II) acetate (1.35 mg, 6.0 μmol, 0.030 equiv.), (R_p, R_p)-L (7.6 mg, 7.2 μmol), 0.036 equiv.) and cesium fluoride (30.4 mg, 0.2 mmol, 1.0 equiv) in THF (0.80 mL, 0.25 M). The crude mixture was oxidized by $NaOH/H_2O_2$ and purified by silica gel chromatography (3% EtOAc in hexanes, stain in $KMnO_4$ stain) to afford a colorless oil (36.2 mg, 50% yield). 1H NMR (400 MHz, $CDCl_3$) δ 7.32 – 7.18 (m, 5H), 7.28 – 7.11 (m, 5H), 6.87 (s, 2H), 6.82 (s, 1H), 5.04 (d, J = 9.7 Hz, 1H), 2.81 (d, J = 9.7 Hz, 1H), 2.24 (s, 6H), 1.91 (d, J = 2.2 Hz, 1H), 0.05 (s, 3H), -0.09 (s, 3H).; 13C NMR (101 MHz, $CDCl_3$) δ 142.4, 140.3, 137.7, 137.3, 134.0, 129.6, 129.1, 128.7, 128.4, 127.2, 125.5, 125.1, 75.8, 47.3, 21.2, -3.2, -3.8.; **IR** (neat) ν_{max} 3553.7 (br, w), 3435.3 (w), 3022.4 (w), 2955.2 (w), 2919.1 (w), 1599.9 (m), 1426.9 (m), 1247.8 (m), 1111.9 (m), 1023.2 (m), 845.8 (m), 831.5(m),

700.0 (s) cm^{-1}. **HRMS** (DART) for $C_{24}H_{27}Si$ $[M+H-H_2O]^+$: Calc'd: 343.1877, found: 343.1861. $\mathbf{[\alpha]_D^{20}}$ = + 19.96 (*c* = 1.00, $CHCl_3$, *l* = 50 mm).

Analysis of Stereochemistry:

Diastereomer ratio was determined by ^1H NMR analysis of the crude reaction mixture. Racemic compound was prepared according to the procedure described above with $Pd(OAc)_2$ (3 mol%) and a mixture of (R_p, R_p)-L and (S_p, S_p)-L (3.6 mol%) as the catalyst. Absolute stereochemistry was assigned by analogy (see compound 8a).

Chiral SFC (Chiracel OJ-H, 4% IPA, 3 mL/min, 100 bar, 35 °C, 210-289 nm) – analysis of (1R,2S)-2-(dimethyl(phenyl)silyl)-1-(3,5-dimethylphenyl)-2-phenylethan-1-ol.

Racemic Material

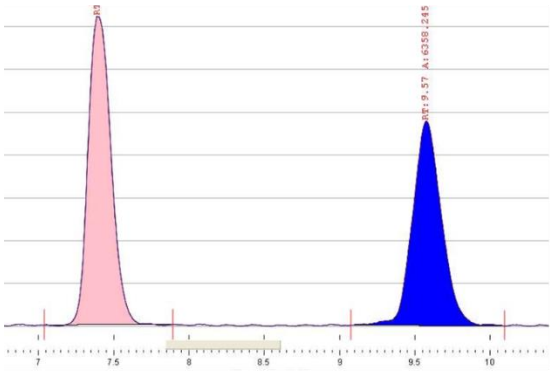

Peak No	% Area	Area	RT (min)
1	54.4996	7615.8047	7.39
2	45.5004	6358.2459	9.57
Total:	100	13974.0506	

Enantioenriched Material

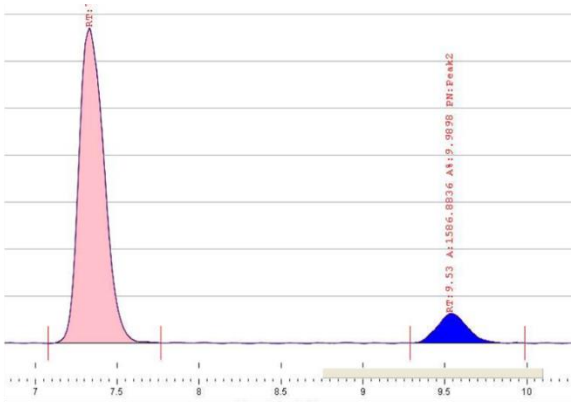

Peak No	% Area	Area	RT (min)
1	90.0102	14298.1691	7.33
2	9.9898	1586.8836	9.53
Total:	100	15885.0527	

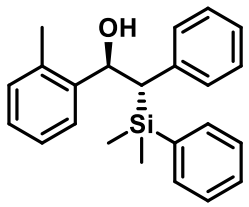

(1R,2S)-2-(dimethyl(phenyl)silyl)-2-phenyl-1-(o-tolyl)ethan-1-ol (3.122)

The reaction was performed according to the general **procedure C** with dimethylphenylsilyl vinyl B(mac) (76.9 mg, 0.2 mmol, 1 equiv.), *tert*-butyl lithium (1.63 M in pentane, 0.25 ml, 0.4 mmol, 2 equiv.), *meta*-bromotoluene (37.6 mg, 0.21 mmol, 1.05 equiv.), potassium triflate (75.3 mg, 0.4 mmol, 2 equiv), palladium (II) acetate (1.35 mg, 6.0 μmol, 0.030 equiv.), (R_p, R_p)-L (7.6 mg, 7.2 μmol), 0.036 equiv.) and cesium fluoride (30.4 mg, 0.2 mmol, 1.0 equiv) in THF (0.80 mL, 0.25 M). The crude mixture was oxidized by $NaOH/H_2O_2$ and purified by silica gel chromatography (3% EtOAc in hexanes, stain in $KMnO_4$ stain) to afford a white solid (37.8 mg, 54% yield). ^1H NMR (600 MHz, $CDCl_3$) δ 7.37 – 7.29 (m, 3H), 7.29 – 7.25 (m, 2H), 7.24 – 7.19 (m, 2H), 7.18 – 7.10 (m, 4H), 7.10 – 7.02 (m, 2H), 7.01 (m, 1H), 5.36 (dd, J = 7.5, 2.8 Hz, 1H), 2.80 (d, J = 7.4 Hz, 1H), 2.25 (s, 3H), 1.82 (d, J = 2.8 Hz, 1H), 0.21 (s 3H), 0.11 (s, 3H).; ^{13}C NMR (151 MHz, $CDCl_3$) δ 141.1, 139.6, 137.6, 134.5, 134.1, 130.5, 129.8, 129.0, 128.2, 127.5, 127.3, 126.9, 125.7, 125.5, 71.6, 45.0, 19.3, -3.0, -3.4.; **IR** (neat) ν_{max} 3554.0 (br, w), 3067.5 (w), 3022.8 (w), 2954.8 (w), 1599.6 (w), 1490.7 (m), 1427.0 (w), 1247.7 (m), 1112.2 (m), 1039.5 (m), 833.5 (m), 734.9 (m), 700.9 (s) cm^-

[1]. **HRMS** (DART) for $C_{23}H_{25}Si$ $[M+H-H_2O]^+$: Calc'd: 329.1720, found: 329.1699. $[\alpha]_D^{20}$ = - 13.79 (*c* = 1.00, $CHCl_3$, *l* = 50 mm).

Analysis of Stereochemistry:

Diastereomer ratio was determined by ^1H NMR analysis of the crude reaction mixture. Racemic compound was prepared according to the procedure described above with $Pd(OAc)_2$ (3 mol%) and a mixture of (R_p, R_p)-L and (S_p, S_p)-L (3.6 mol%) as the catalyst. Absolute stereochemistry was assigned by analogy (see compound 8a).

Chiral SFC (Chiracel ODR-H, 4% IPA, 3 mL/min, 100 bar, 35 °C, 210-289 nm) – analysis of (1R,2S)-2-(dimethyl(phenyl)silyl)-2-phenyl-1-(o-tolyl)ethan-1-ol.

Racemic Material

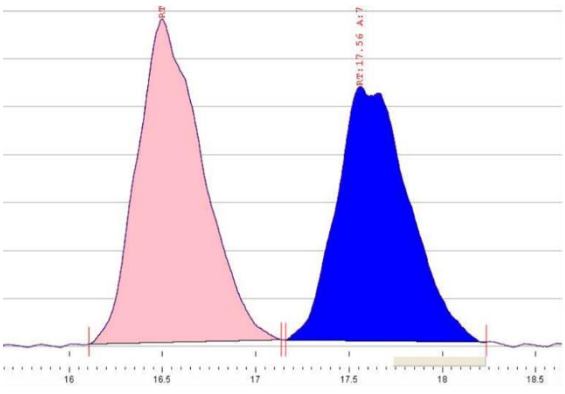

Peak No	% Area	Area	RT (min)
1	53.3468	8217.9205	16.5
2	46.6532	7186.7876	17.56
Total:	100	15404.7081	

Enantioenriched Material

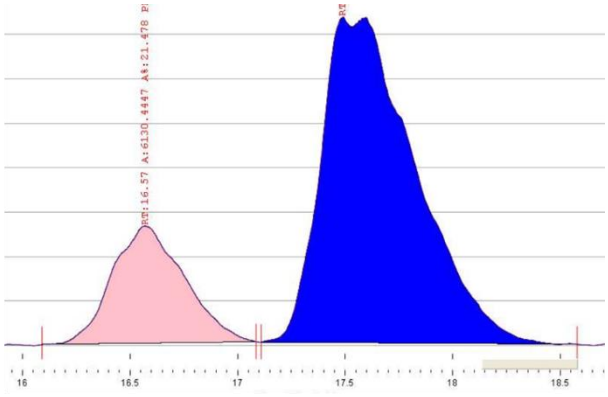

Peak No	% Area	Area	RT (min)
1	21.478	6130.4447	16.57
2	78.522	22412.3918	17.49
Total:	100	28542.8365	

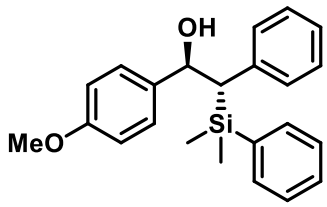

(1R,2S)-2-(dimethyl(phenyl)silyl)-1-(4-methoxyphenyl)-2-phenylethan-1-ol (3.118)

The reaction was performed according to the general **procedure C** with dimethylphenylsilyl vinyl B(mac) (76.9 mg, 0.2 mmol, 1 equiv.), *tert*-butyl lithium (1.63 M in pentane, 0.25 ml, 0.4 mmol, 2 equiv.), *1*-bromo-4-methoxy-benzene (39.3 mg, 0.21 mmol, 1.05 equiv.), potassium triflate (75.3 mg, 0.4 mmol, 2 equiv), palladium (II) acetate (1.35 mg, 6.0 μmol, 0.030 equiv.), (R_p, R_p)-L (7.6 mg, 7.2 μmol), 0.036 equiv.) and cesium fluoride (30.4 mg, 0.2 mmol, 1.0 equiv) in THF (0.80 mL, 0.25 M). The crude mixture was oxidized by $NaOH/H_2O_2$ and purified by silica gel chromatography (9% EtOAc in hexanes, stain in $KMnO_4$ stain) to afford a white solid (40.8 mg, 56% yield). ^{1}H NMR (600 MHz, $CDCl_3$) δ 7.32 – 7.10 (m, 12H), 6.76 (d, J = 8.5 Hz, 2H), 5.09 (dd, J = 9.7, 2.2 Hz, 1H), 3.78 (s, 3H), 2.80 (d, J = 9.7 Hz, 1H), 1.92 (d, J = 2.3 Hz, 1H), 0.06 (s, 3H), -0.05 (s, 3H).; ^{13}C NMR (151 MHz, $CDCl_3$) δ 159.3, 140.2, 137.2, 135.1, 134.1, 129.1, 128.7, 128.4, 128.3, 127.3, 125.6, 113.6, 77.2, 77.0, 76.8, 75.1, 55.2, 47.5, -3.2, -3.7.; **IR** (neat) ν_{max} 3552.1 (br, w), 3423.0 (br, w), 3067.3 (w), 2955.2 (w), 2358.2 (w), 1611.2 (m), 1511.8 (s), 1248.0 (s), 1174.6 (m), 1033.5 (m), 833.0 (s), 758.1 (m), 701.0 (s) cm^{-1}. **HRMS** (DART) for $C_{23}H_{25}SiO$ $[M+H-H_2O]^+$:

Calc'd: 345.1669, found: 345.1663. $[\alpha]_D^{20}$ = + 10.60 (*c* = 1.00, $CHCl_3$, *l* = 50 mm).

Analysis of Stereochemistry:

Diastereomer ratio was determined by ^1H NMR analysis of the crude reaction mixture. Racemic compound was prepared according to the procedure described above with $Pd(OAc)_2$ (3 mol%) and a mixture of (R_p, R_p)-L and (S_p, S_p)-L (3.6 mol%) as the catalyst. Absolute stereochemistry was assigned by analogy (see compound 8a).

Chiral SFC (Chiracel OJ-H, 10% IPA, 3 mL/min, 100 bar, 35 °C, 210-289 nm) – analysis of (1R,2S)-2-(dimethyl(phenyl)silyl)-1-(4-methoxyphenyl)-2-phenylethan-1-ol.

Racemic Material

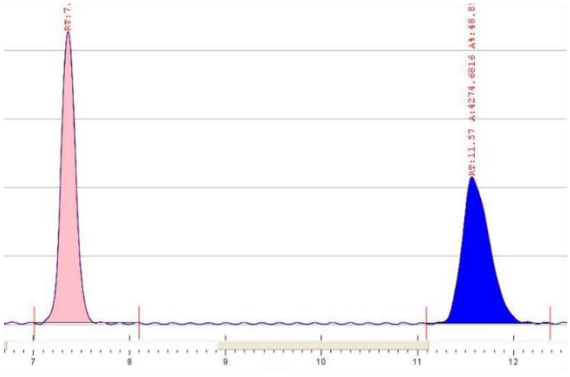

Peak No	% Area	Area	RT (min)
1	51.1062	4468.1051	7.36
2	48.8938	4274.6816	11.57
Total:	100	8742.7867	

Enantioenriched Material

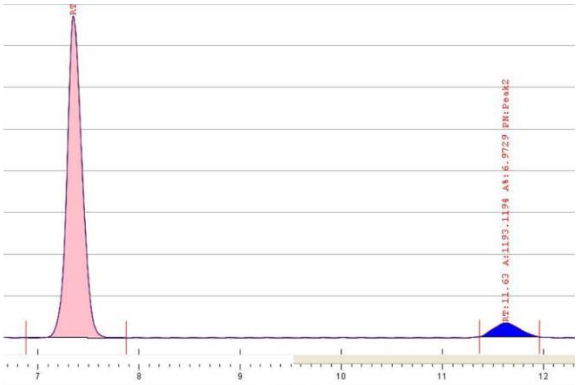

Peak No	% Area	Area	RT (min)
1	93.0271	15917.693	7.35
2	6.9729	1193.1194	11.63
Total:	100	17110.8124	

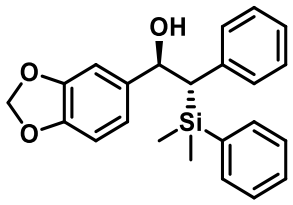

(1R,2S)-1-(benzo[d][1,3]dioxol-5-yl)-2-(dimethyl(phenyl)silyl)-2-phenylethan-1-ol (3.126)

The reaction was performed according to the general **procedure C** with dimethylphenylsilyl vinyl B(mac) (76.9 mg, 0.2 mmol, 1 equiv.), *tert*-butyl lithium (1.63 M in pentane, 0.25 ml, 0.4 mmol, 2 equiv.), 1,2-(methylenedioxy)-4-bromobenzene (42.2 mg, 0.21 mmol, 1.05 equiv.), potassium triflate (75.3 mg, 0.4 mmol, 2 equiv), palladium (II) acetate (1.35 mg, 6.0 μmol, 0.030 equiv.), (R_p, R_p)-L (7.6 mg, 7.2 μmol), 0.036 equiv.) and cesium fluoride (30.4 mg, 0.2 mmol, 1.0 equiv) in THF (0.80 mL, 0.25 M). The crude mixture was oxidized by $NaOH/H_2O_2$ and purified by silica gel chromatography (10% EtOAc in hexanes, stain in $KMnO_4$ stain) to afford a white solid (44.9 mg, 60% yield). ^{1}H NMR (600 MHz, $CDCl_3$) δ 7.30 – 7.24 (m, 3H), 7.24 – 7.20 (m, 2H), 7.20 – 7.11 (m, 5H), 6.76 – 6.72 (m, 2H), 6.64 (d, J = 7.3 Hz, 1H), 5.88 (d, J = 14.8 Hz, 2H), 5.05 (dd, J = 9.8, 1.9 Hz, 1H), 2.76 (d, J = 9.7 Hz, 1H), 1.92 (d, J = 2.0 Hz, 1H), 0.14 (s, 3H), -0.04 (s, 3H).; ^{13}C NMR (126 MHz, $CDCl_3$) δ 147.6, 147.2, 140.0, 137.3, 136.8, 133.9, 129.1, 128.7, 128.5, 127.3, 125.7, 120.6, 107.7, 107.4, 100.9, 75.4, 47.6, -3.0, -4.1.; **IR** (neat) ν_{max} 3552.2 (br, w), 3439.7 (br, w), 3023.3 (w), 2895.6 (w), 2358.0 (w), 1598.9 (w), 1487.9 (s), 1443.3 (m), 1246.6 (s), 1039.5 (m), 815.7 (m),

737.1 (m), 701.3 (s) cm^{-1}. **HRMS** (DART) for $C_{23}H_{23}SiO_2$ $[M+H-H_2O]^+$: Calc'd: 359.1462, found: 359.1457. $[\alpha]_D^{20}$ = + 19.91 (*c* = 1.00, $CHCl_3$, *l* = 50 mm).

Analysis of Stereochemistry:

Diastereomer ratio was determined by ^1H NMR analysis of the crude reaction mixture. Racemic compound was prepared according to the procedure described above with $Pd(OAc)_2$ (3 mol%) and a mixture of (R_p, R_p)-L and (S_p, S_p)-L (3.6 mol%) as the catalyst. Absolute stereochemistry was assigned by analogy (see compound 8a).

Chiral SFC (Chiracel OJ-H, 12% IPA, 3 mL/min, 100 bar, 35 °C, 210-289 nm) – analysis of (1R,2S)-2-(dimethyl(phenyl)silyl)-1-(4-methoxyphenyl)-2-phenylethan-1-ol.

Racemic Material

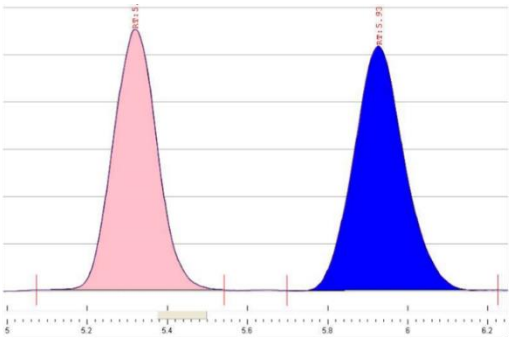

Peak No	% Area	Area	RT (min)
1	48.1967	4208.0634	5.32
2	51.8033	4522.9586	5.93
Total:	100	8731.022	

Enantioenriched Material

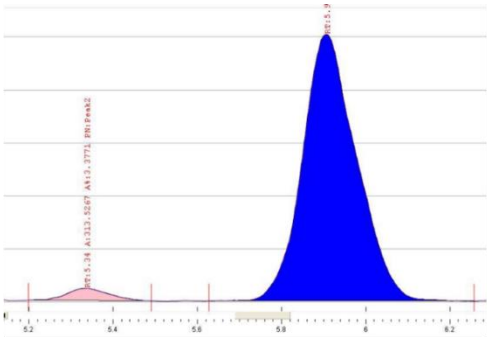

Peak No	% Area	Area	RT (min)
1	3.3771	313.5267	5.34
2	96.6229	8970.2727	5.91
Total:	100	9283.7994	

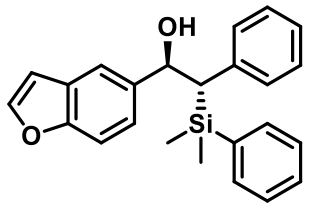

(1R,2S)-1-(benzofuran-5-yl)-2-(dimethyl(phenyl)silyl)-2-phenylethan-1-ol (3.125)

The reaction was performed according to the general **procedure C** with dimethylphenylsilyl vinyl B(mac) (76.9 mg, 0.2 mmol, 1 equiv.), *tert*-butyl lithium (1.63 M in pentane, 0.25 ml, 0.4 mmol, 2 equiv.), 5-bromobenzofuran (41.4 mg, 0.21 mmol, 1.05 equiv.), potassium triflate (75.3 mg, 0.4 mmol, 2 equiv), palladium (II) acetate (1.35 mg, 6.0 μmol, 0.030 equiv.), (R_p, R_p)-L (7.6 mg, 7.2 μmol), 0.036 equiv.) and cesium fluoride (30.4 mg, 0.2 mmol, 1.0 equiv) in THF (0.80 mL, 0.25 M). The crude mixture was oxidized by $NaOH/H_2O_2$ and purified by silica gel chromatography (10% EtOAc in hexanes, stain in $KMnO_4$ stain) to afford a white solid (48.3 mg, 65% yield). ^{1}H NMR (500 MHz, $CDCl_3$) δ 7.61 (d, J = 2.1 Hz, 1H), 7.50 (d, J = 1.7 Hz, 1H), 7.35 (d, J = 8.5 Hz, 1H), 7.32 – 7.21 (m, 4H), 7.24 – 7.13 (m, 7H), 6.71 (dd, J = 2.1, 1.0 Hz, 1H), 5.26 (dd, J = 9.6, 2.2 Hz, 1H), 2.89 (d, J = 9.6 Hz, 1H), 2.06 (d, J = 2.2 Hz, 1H), 0.09 (s, 3H), -0.06 (s, 3H).; ^{13}C NMR (126 MHz, $CDCl_3$) δ 154.7, 145.2, 140.1, 137.5, 137.2, 133.9, 129.2, 128.7, 128.5, 127.2, 127.2, 125.6, 123.5, 119.9, 111.1, 106.6, 75.8, 48.0, -3.1, -3.8.; **IR** (neat) ν_{max} 3556.0 (br, w), 3421.9 (br, w), 3022.9 (w), 2985.0 (w), 2356.3 (w), 1599.2 (w), 1468.1 (w), 1427.1 (w), 1260.8 (m), 1109.5 (m), 1030.7 (m),

816.8 (m), 736.6 (s), 700.8 (s) cm^{-1}. **HRMS** (DART) for $C_{24}H_{24}SiO_2$ $[M\text{-}e]^+$: Calc'd: 372.1540, found: 372.1533. $\mathbf{[\alpha]_D^{20}}$ = + 8.76 (*c* = 1.00, $CHCl_3$, *l* = 50 mm).

Analysis of Stereochemistry:

Diastereomer ratio was determined by ^1H NMR analysis of the crude reaction mixture. Racemic compound was prepared according to the procedure described above with $Pd(OAc)_2$ (3 mol%) and a mixture of (R_p, R_p)-L and (S_p, S_p)-L (3.6 mol%) as the catalyst. Absolute stereochemistry was assigned by analogy (see compound 8a).

Chiral SFC (Chiracel ODR-H, 8% IPA, 3 mL/min, 100 bar, 35 °C, 210-289 nm) – analysis of (1R,2S)-1-(benzofuran-5-yl)-2-(dimethyl(phenyl)silyl)-2-phenylethan-1-ol.

Racemic Material

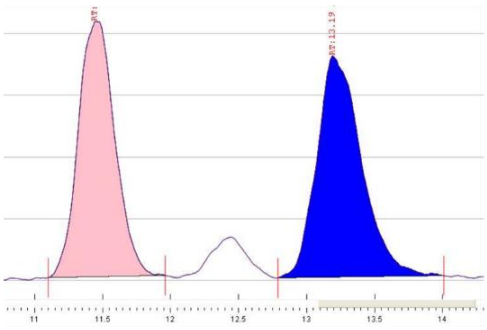

Peak No	% Area	Area	RT (min)
1	48.617	7768.3941	11.44
2	51.383	8210.3758	13.19
Total:	100	15978.7699	

Enantioenriched Material

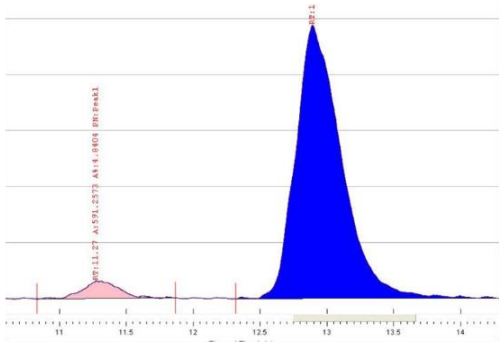

Peak No	% Area	Area	RT (min)
1	4.8404	591.2573	11.27
2	95.1596	11623.7829	12.89
Total:	100	12215.0402	

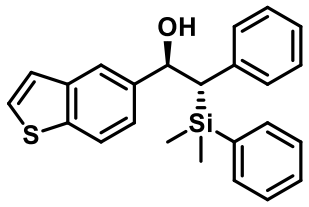

(1R,2S)-1-(benzo[b]thiophen-5-yl)-2-(dimethyl(phenyl)silyl)-2-phenylethan-1-ol (3.124)

The reaction was performed according to the general **procedure C** with dimethylphenylsilyl vinyl B(mac) (76.9 mg, 0.2 mmol, 1 equiv.), *tert*-butyl lithium (1.63 M in pentane, 0.25 ml, 0.4 mmol, 2 equiv.), 5-bromobenzothiophene (44.8 mg, 0.21 mmol, 1.05 equiv.), potassium triflate (75.3 mg, 0.4 mmol, 2 equiv), palladium (II) acetate (1.35 mg, 6.0 μmol, 0.030 equiv.), (R_p, R_p)-L (7.6 mg, 7.2 μmol), 0.036 equiv.) and cesium fluoride (30.4 mg, 0.2 mmol, 1.0 equiv) in THF (0.80 mL, 0.25 M). The crude mixture was oxidized by $NaOH/H_2O_2$ and purified by silica gel chromatography (8% EtOAc in hexanes, stain in $KMnO_4$ stain) to afford a white solid (49.6 mg, 64% yield). ^1H NMR (600 MHz, $CDCl_3$) δ 7.73 – 7.66 (m, 2H), 7.43 (d, J = 5.4 Hz, 1H), 7.29 – 7.12 (m, 12H), 5.27 (dd, J = 9.3, 2.2 Hz, 1H), 2.91 (d, J = 9.3 Hz, 1H), 2.07 (d, J = 2.3 Hz, 1H), 0.13 (s, 3H), -0.05 (s, 3H).; ^{13}C NMR (101 MHz, $CDCl_3$) δ 143.1, 140.0, 137.2, 137.1, 135.9, 134.2, 128.9, 128.3, 127.9, 127.4, 127.1, 126.4, 126.2, 123.9, 123.7, 122.2, 75.7, 47.1, -3.2, -3.5.; **IR** (neat) ν_{max} 3565.6 (br, w), 3429.3 (br, w), 3067.4 (w), 2954.4 (w), 2358.7 (w), 2215.3 (w), 1599.0 (w), 1426.7 (w), 1248.0 (m), 1111.9 (w), 1089.2 (w), 829.5 (s), 814.4 (s), 698.9 (s) cm^{-1}. **HRMS** (DART) for $C_{26}H_{31}SiOS$ $[M\text{-}e]^+$:

Calc'd: 388.1312, found: 388.1300. $[\alpha]_D^{20}$ = + 6.16 (*c* = 1.00, $CHCl_3$, *l* = 50 mm).

Analysis of Stereochemistry:

Diastereomer ratio was determined by ^1H NMR analysis of the crude reaction mixture. Racemic compound was prepared according to the procedure described above with $Pd(OAc)_2$ (3 mol%) and a mixture of (R_p, R_p)-L and (S_p, S_p)-L (3.6 mol%) as the catalyst. Absolute stereochemistry was assigned by analogy (see compound 8a).

Chiral SFC (Chiracel AS-H, 10% IPA, 3 mL/min, 100 bar, 35 °C, 210-289 nm) – analysis of (1R,2S)-1-(benzo[b]thiophen-5-yl)-2-(dimethyl(phenyl)silyl)-2-phenylethan-1-ol.

Racemic Material

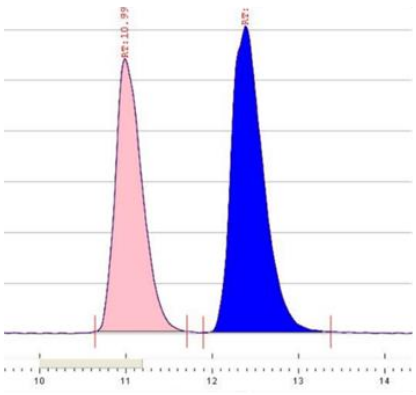

Peak No	% Area	Area	RT (min)
1	43.0698	23261.4598	10.99
2	56.9302	30747.3405	12.39
Total:	100	54008.8003	

Enantioenriched Material

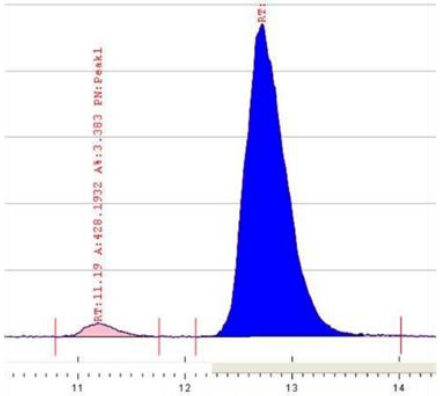

Peak No	% Area	Area	RT (min)
1	3.383	428.1932	11.19
2	96.617	12229.1576	12.72
Total:	100	12657.3508	

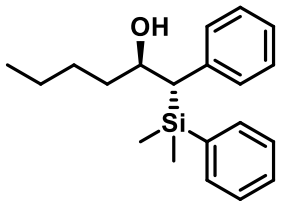

(1S,2R)-1-(dimethyl(phenyl)silyl)-1-phenylhexan-2-ol (3.127)

The reaction was performed according to the general **procedure A** with dimethylphenylsilyl vinyl B(mac) (76.9 mg, 0.2 mmol, 1 equiv.), butyl lithium (2.26 M in Hexane, 0.09 ml, 0.21 mmol, 1.05 equiv.), phenyl triflate (49.8mg, 0.22 mmol, 1.1 equiv.), palladium (II) acetate (1.35mg, 6.0 μmol, 0.030 equiv.), (R_p, R_p)-L (7.6 mg, 7.2 μmol), 0.036 equiv.) and cesium fluoride (30.4 mg, 0.2 mmol, 1.0 equiv) in THF (0.80 mL, 0.25 M). The crude mixture was oxidized by $NaOH/H_2O_2$ and purified by silica gel chromatography (3% EtOAc in hexanes, stain in KMnO4 stain) to afford a colorless oil (25.7 mg, 41% yield). ^{1}H NMR (500 MHz, $CDCl_3$) δ 7.52 – 7.46 (m, 2H), 7.40 – 7.32 (m, 3H), 7.29 – 7.22 (m, 2H), 7.19 – 7.12 (m, 3H), 4.10 – 4.02 (m, 1H), 2.42 (d, J = 6.5, 1H), 1.50 – 1.11 (m, 6H), 0.81 (t, J = 7.2, 3H), 0.37 (s, 3H), 0.20 (s, 3H).; ^{13}C NMR (126 MHz, $CDCl_3$) δ 140.3, 138.2, 134.0, 129.5, 129.0, 128.2, 127.7, 125.3, 72.6, 44.5, 36.5, 28.1, 22.5, 14.0, -2.4, -3.9.; **IR** (neat) ν_{max} 3569.7 (br, w), 3454.4 (br, w), 2955.4 (m), 2929.0 (m), 2858.2 (w), 1598.5 (w), 1427.2 (w), 1248.9 (m), 1112.3 (m), 829.4 (m), 701.8 (s) cm^{-1}.; **HRMS** (DART) for $C_{20}H_{27}Si$ $[M+H-H_2O]^+$: Calc'd: 295.1877, found: 295.1884. $[\alpha]_D^{20}$ = + 44.55 (c = 1.00, $CHCl_3$, l = 50 mm).

Analysis of Stereochemistry:

Diastereomer ratio was determined by ^{1}H NMR analysis of the crude reaction mixture. Racemic compound was prepared according to the procedure described above with $Pd(OAc)_2$ (3 mol%) and a mixture of (R_p, R_p)-L and (S_p, S_p)-L (3.6 mol%) as the catalyst. Absolute stereochemistry was assigned by analogy (see compound 8a).

Chiral SFC (Chiracel OJ-H, 3% IPA, 3 mL/min, 100 bar, 35 °C, 210-289 nm) – analysis of (1S,2R)-1-(dimethyl(phenyl)silyl)-1-phenylhexan-2-ol.

Racemic Material

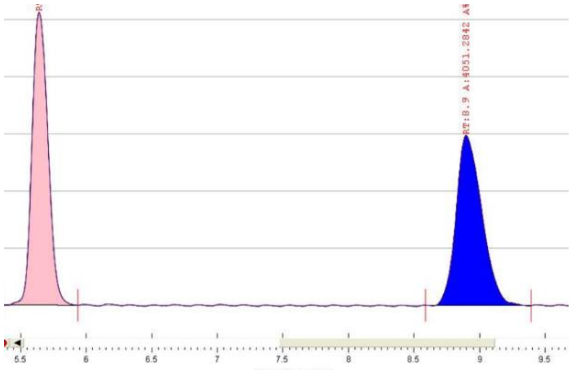

Peak No	% Area	Area	RT (min)
1	51.5773	4315.2096	5.64
2	48.4227	4051.2842	8.9
Total:	100	8366.4938	

Enantioenriched Material

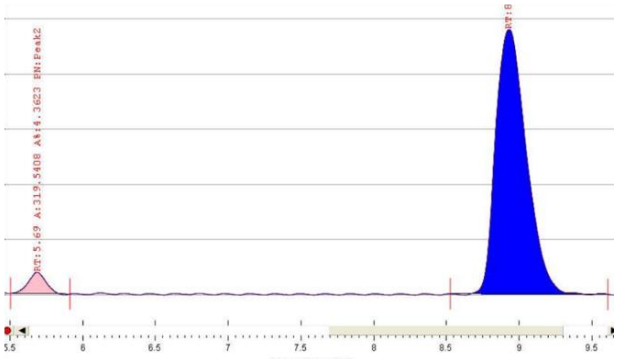

Peak No	% Area	Area	RT (min)
1	4.3623	319.5408	5.69
2	95.6377	7005.5453	8.93
Total:	100	7325.0861	

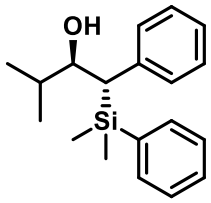

(1S,2R)-1-(dimethyl(phenyl)silyl)-3-methyl-1-phenylbutan-2-ol (30)

The reaction was performed according to the general **procedure A** with dimethylphenylsilyl vinyl B(mac) (76.9 mg, 0.2 mmol, 1 equiv.), isopropyl lithium (0.7 M in petane, 0.3 ml, 0.21 mmol, 1.05 equiv.), phenyl triflate (49.8mg, 0.22 mmol, 1.1 equiv.), palladium (II) acetate (1.35mg, 6.0 μmol, 0.030 equiv.), (R_p, R_p)-L (7.6 mg, 7.2 μmol), 0.036 equiv.) and cesium fluoride (30.4 mg, 0.2 mmol, 1.0 equiv) in THF (0.80 mL, 0.25 M). The crude mixture was oxidized by $NaOH/H_2O_2$ and purified by silica gel chromatography (2% EtOAc in hexanes, stain in $KMnO_4$ stain) to afford a colorless oil (32.9 mg, 55% yield).; ^{1}H NMR (500 MHz, $CDCl_3$) δ 7.50-7.44 (m, 2H), 7.39-7.30 (m, 3H), 7.29 – 7.17 (m, 2H), 7.19 – 7.11 (m, 3H), 3.69 – 3.62 (m, 1H), 2.55 (dt, J = 5.2, 2.4 Hz, 1H), 1.63 (hd, J = 6.7, 2.9 Hz, 1H), 0.86 – 0.76 (m, 6H), 0.37 (d, J = 2.9 Hz, 3H), 0.22 (d, J = 2.9 Hz, 3H).; ^{13}C NMR (126 MHz, $CDCl_3$) δ 140.2, 138.2, 134.1, 129.8, 129.0, 128.0, 127.6, 125.1, 78.3, 41.8, 32.0, 19.7, 17.8, -2.7, -3.8.; **IR** (neat) ν_{max} 3593.6 (br, w), 2957.0 (m), 2871.7 (w), 1599.7 (w), 1427.2 (w), 1247.6 (m), 1112.2 (m), 1072.2 (m), 834.3 (m), 814.3 (m), 735.8 (m), 702.2 (s) cm^{-1}.; **HRMS** (DART)

for $C_{19}H_{25}Si$ $[M+H-H_2O]^+$: Calc'd: 281.1720, found: 281.1709. $[\alpha]_D^{20}$ = + 51.23 (*c* = 1.00, $CHCl_3$, *l* = 50 mm).

Analysis of Stereochemistry:

Diastereomer ratio was determined by ^1H NMR analysis of the crude reaction mixture. Racemic compound was prepared according to the procedure described above with $Pd(OAc)_2$ (3 mol%) and a mixture of (R_p, R_p)-L and (S_p, S_p)-L (3.6 mol%) as the catalyst. Absolute stereochemistry was assigned by analogy (see compound 8a).

Chiral SFC (Chiracel OJ-H, 4% IPA, 3 mL/min, 100 bar, 35 °C, 210-289 nm) – analysis of (1S,2R)-1-(dimethyl(phenyl)silyl)-3-methyl-1-phenylbutan-2-ol

Racemic Material

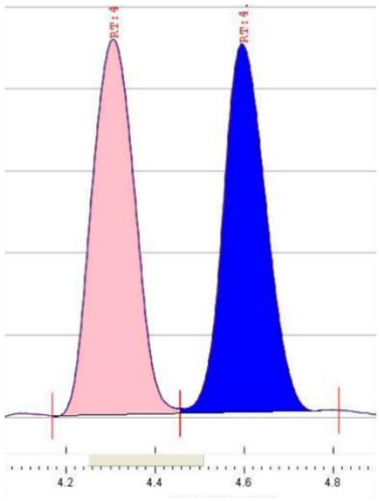

Peak No	% Area	Area	RT (min)
1	50.6105	1513.0636	4.31
2	49.3895	1476.5575	4.6
Total:	100	2989.6211	

Enantioenriched Material

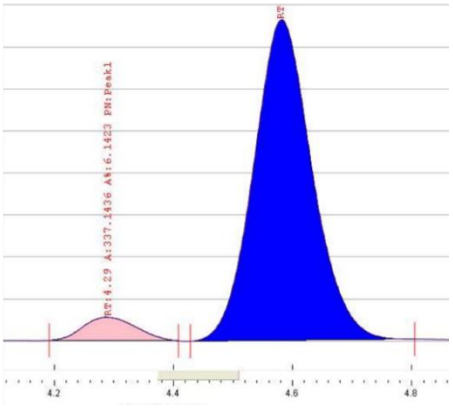

Peak No	% Area	Area	RT (min)
1	6.1423	337.1436	4.29
2	93.8577	5151.7337	4.58
Total:	100	5488.8773	

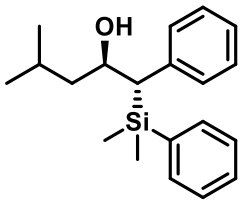

(1S,2R)-1-(dimethyl(phenyl)silyl)-4-methyl-1-phenylpentan-2-ol (3.128)

The reaction was performed according to the general **procedure A** with dimethylphenylsilyl vinyl B(mac) (76.9 mg, 0.2 mmol, 1 equiv.), *iso*-butyl lithium (1.7 M in Heptane, 0.13 ml, 0.21 mmol, 1.05 equiv.), phenyl triflate (49.8mg, 0.22 mmol, 1.1 equiv.), palladium (II) acetate (1.35mg, 6.0 μmol, 0.030 equiv.), (R_p, R_p)-L (7.6 mg, 7.2 μmol), 0.036 equiv.) and cesium fluoride (30.4 mg, 0.2 mmol, 1.0 equiv) in THF (0.80 mL, 0.25 M). The crude mixture was oxidized by $NaOH/H_2O_2$ and purified by silica gel chromatography (4% EtOAc in hexanes, stain in $KMnO_4$ stain) to afford a colorless oil (40.1 mg, 64% yield).; ^1H NMR (500 MHz, $CDCl_3$) δ 7.53 – 7.43 (m, 2H), 7.42 – 7.30 (m, 3H), 7.29 – 7.20 (m, 2H), 7.20 – 7.09 (m, 3H), 4.19 - 4.11 (m, 1H), 2.37 (d, J = 6.4 Hz, 1H), 1.76 – 1.64 (m, 1H), 1.43 (d, J = 4.0 Hz, 1H), 1.30 – 1.16 (m, 2H), 0.81 (d, J = 6.6 Hz, 6H), 0.35 (s, 3H), 0.21 (s, 3H).; ^{13}C NMR (126 MHz, $CDCl_3$) δ 140.3, 138.1, 134.0, 129.5, 129.0, 128.3, 127.7, 125.3, 70.5, 46.1, 45.2, 24.8, 23.3, 21.9, -2.3, -3.7.; **IR** (neat) ν_{max} 3576.8 (br, w), 3468.9 (br, w), 2954.7 (s), 2867.8 (w), 2359.0 (w), 1598.7 (w), 1427.2 (w), 1249.5 (m), 1112.4 (m), 832.4 (s), 816.5 (m), 701.8 (s) cm^{-1}.

HRMS (DART) for $C_{20}H_{27}Si$ $[M+H-H_2O]^+$: Calc'd: 295.1877, found: 295.1875. $[\alpha]_D^{20}$ = + 48.19 (*c* = 1.00, $CHCl_3$, *l* = 50 mm).

Analysis of Stereochemistry:

Diastereomer ratio was determined by ^1H NMR analysis of the crude reaction mixture. Racemic compound was prepared according to the procedure described above with $Pd(OAc)_2$ (3 mol%) and a mixture of (R_p, R_p)-L and (S_p, S_p)-L (3.6 mol%) as the catalyst. Absolute stereochemistry was assigned by analogy (see compound 8a).

Chiral SFC (Chiracel OJ-H, 2% IPA, 3 mL/min, 100 bar, 35 °C, 210-289 nm) – analysis of (1S,2R)-1-(dimethyl(phenyl)silyl)-4-methyl-1-phenylpentan-2-ol.

Racemic Material

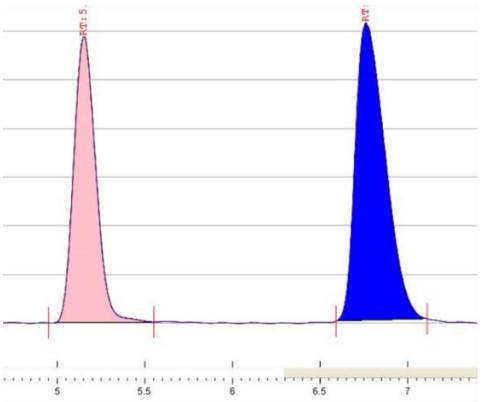

Peak No	% Area	Area	RT (min)
1	41.5909	10278.9389	5.15
2	58.4091	14435.4258	6.76
Total:	100	24714.3647	

Enantioenriched Material

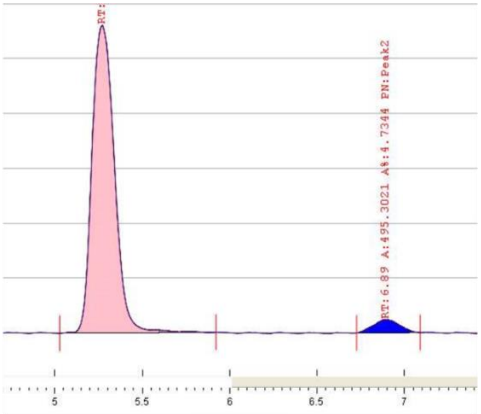

Peak No	% Area	Area	RT (min)
1	95.2656	9966.5299	5.27
2	4.7344	495.3021	6.89
Total:	100	10461.832	

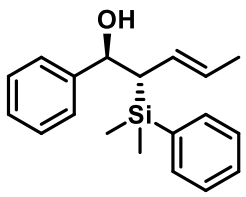

(1R,2S, *E*)-2-(dimethyl(phenyl)silyl)-1-phenylpent-3-en-1-ol (3.131)

The reaction was performed according to the general **procedure B** with dimethylphenylsilyl vinyl B(mac) (76.9 mg, 0.2 mmol, 1 equiv.), Phenyl lithium (1.78 M in dibutyl ether, 0.11 ml, 0.21 mmol, 1.05 equiv.), *trans*-2-propenyl bromide (26.6 mg, 0.22 mmol, 1.1 equiv.), potassium triflate (75.3 mg, 0.4 mmol, 2 equiv), palladium (II) acetate (1.35 mg, 6.0 μmol, 0.030 equiv.), (R_p, R_p)-L (7.6 mg, 7.2 μmol), 0.036 equiv.) and cesium fluoride (30.4 mg, 0.2 mmol, 1.0 equiv) in THF (0.80 mL, 0.25 M). The crude mixture was oxidized by $NaOH/H_2O_2$ and purified by silica gel chromatography (8% EtOAc in hexanes, stain in $KMnO_4$ stain) to afford a colorless oil (36.3 mg, 61% yield). ^{1}H NMR (400 MHz, $CDCl_3$) δ 7.39 (m, 2H), 7.34 – 7.29 (m, 3H), 7.27-7.23 (m, 5H), 5.46 (dd, J = 15.3, 10.2 Hz, 1H), 5.34 (m, 1H), 4.64 (d, J = 7.9 Hz, 1H), 2.20 – 2.10 (m, 2H), 1.67 (dd, J = 6.2, 3H), 0.11 (s, 3H), 0.00 (s, 3H).; ^{13}C NMR (101 MHz, $CDCl_3$) δ 143.6, 137.6, 134.1, 128.9, 128.1, 127.8, 127.8, 127.6, 127.5, 126.9, 74.5, 43.5, 18.2, -3.4, -4.0.; **IR** (neat) ν_{max} 3562.4 (br, w), 3428.7 (br, w), 3023.6 (w), 2956.7 (w), 1452.0 (w), 1427.5 (m), 1247.4 (m), 1112.1 (m), 1026.5 (w), 972.9 (w), 832.0 (m), 812.4 (s), 734.9 (s), 699.3 (s) cm^{-1}.; **HRMS** (DART) for $C_{19}H_{23}Si$ [M+H-

$H_2O]^+$: Calc'd: 279.1564, found: 279.1576. $[\alpha]_D^{20}$ = + 21.96 (*c* = 1.00, $CHCl_3$, *l* = 50 mm).

Analysis of Stereochemistry:

Diastereomer ratio was determined by ^1H NMR analysis of the crude reaction mixture. Racemic compound was prepared according to the procedure described above with $Pd(OAc)_2$ (3 mol%) and a mixture of (R_p, R_p)-L and (S_p, S_p)-L (3.6 mol%) as the catalyst. Absolute stereochemistry was assigned by analogy (see compound 8a).

Chiral SFC (Chiracel OD-H, 5% IPA, 3 mL/min, 100 bar, 35 °C, 210-289 nm) – analysis of (1R,2S, E)-2-(dimethyl(phenyl)silyl)-1-phenylpent-3-en-1-ol

Racemic Material

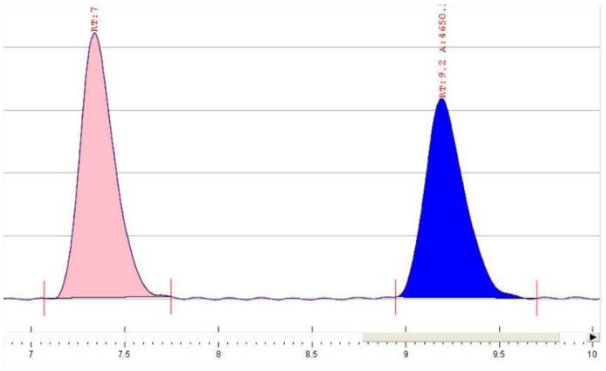

Peak No	% Area	Area	RT (min)
1	53.4776	5345.3652	7.34
2	46.5224	4650.1564	9.2
Total:	100	9995.5216	

Enantioenriched Material

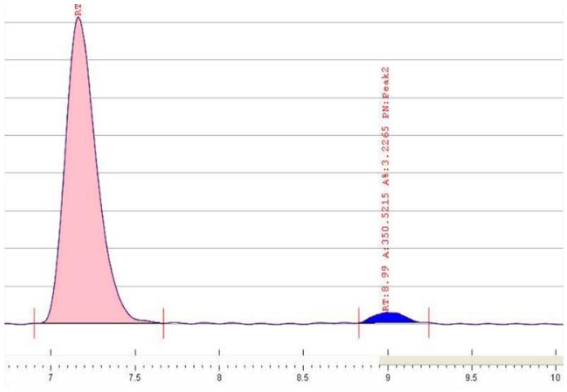

Peak No	% Area	Area	RT (min)
1	96.7735	10513.259	7.16
2	3.2265	350.5215	8.99
Total:	100	10863.7805	

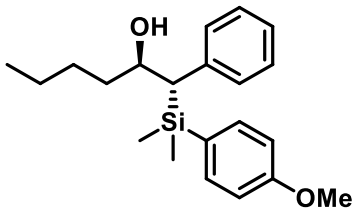

(1S,2R)-1-((4-methoxyphenyl)dimethylsilyl)-1-phenylhexan-2-ol (3.156)

The reaction was performed according to the general **procedure A** with dimethyl-*para*-methoxyphenylsilyl vinyl B(mac) (82.9 mg, 0.2 mmol, 1 equiv.), butyl lithium (2.26 M in Hexane, 0.09 ml, 0.21 mmol, 1.05 equiv), phenyl triflate (49.8mg, 0.22 mmol, 1.1 equiv.), palladium (II) acetate (1.35mg, 6.0 μmol, 0.030 equiv.), (R_p, R_p)-L (7.6 mg, 7.2 μmol), 0.036 equiv.) and cesium fluoride (30.4 mg, 0.2 mmol, 1.0 equiv) in THF (0.80 mL, 0.25 M). The crude mixture was oxidized by $NaOH/H_2O_2$ and purified by silica gel chromatography (5% EtOAc in hexanes, stain in $KMnO_4$ stain) to afford a white solid (27.1 mg, 40% yield). ^{1}H NMR (400 MHz, $CDCl_3$) δ 7.38 (d, J = 8.2 Hz, 2H), 7.28 – 7.18 (m, 2H), 7.17 – 7.09 (m, 3H), 6.88 (d, J = 8.1 Hz, 2H), 4.09 – 3.96 (m, 1H), 3.81 (s, 3H), 2.36 (d, J = 6.4 Hz, 1H), 1.49 – 1.37 (m, 2H), 1.36 – 1.08 (m, 5H), 0.80 (t, J = 7.0 Hz, 3H), 0.30 (s, 3H), 0.16 (s, 3H).; ^{13}C NMR (101 MHz, $CDCl_3$) δ 160.4, 140.4, 135.5, 129.5, 128.8, 128.2, 125.2, 113.5, 72.6, 55.0, 44.7, 36.5, 28.1, 22.5, 14.0, -2.2, -3.7.; **IR** (neat) ν_{max} 2954.8 (m), 2930.6 (m), 2858.1 (w), 1594.6 (s), 1502.4 (m), 1464.4 (w), 1277.3 (s), 1246.8 (s), 1182.6 (m), 1110.2 (s), 1032.0 (m), 828.2 (s), 807.1 (m), 703.4 (m) cm^{-1}.; **HRMS** (DART) for $C_{21}H_{31}SiO_2$ $[M+H]^+$:

Calc'd: 343.2088, found: 343.2093 $[\alpha]_D^{20}$ = + 42.97 (*c* = 1.00, $CHCl_3$, *l* = 50 mm).

Analysis of Stereochemistry:

Diastereomer ratio was determined by ^1H NMR analysis of the crude reaction mixture. Racemic compound was prepared according to the procedure described above with $Pd(OAc)_2$ (3 mol%) and a mixture of (R_p, R_p)-L and (S_p, S_p)-L (3.6 mol%) as the catalyst. Absolute stereochemistry was assigned by analogy (see compound 8a).

Chiral SFC (Chiracel OJ-H, 5% IPA, 3 mL/min, 100 bar, 35 °C, 210-289 nm) – analysis of (1S,2R)-1-((4-methoxyphenyl)dimethylsilyl)-1-phenylhexan-2-ol

Racemic Material

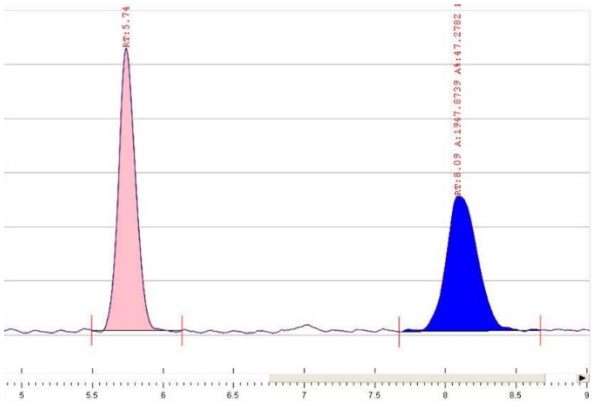

Peak No	% Area	Area	RT (min)
1	52.7218	2172.149	5.74
2	47.2782	1947.8739	8.09
Total:	100	4120.0229	

Enantioenriched Material

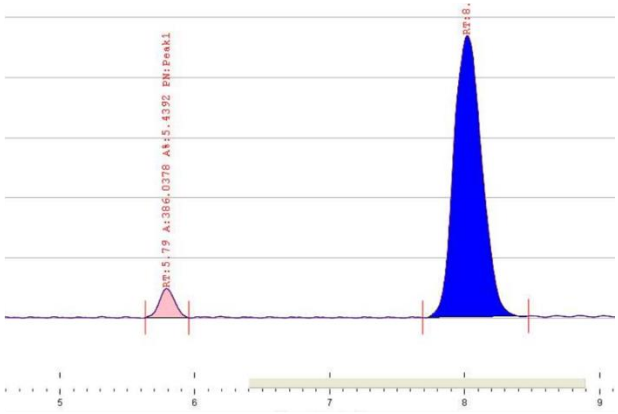

Peak No	% Area	Area	RT (min)
1	5.4392	386.0378	5.79
2	94.5608	6711.3024	8.02
Total:	100	7097.3402	

3.5.4 Procedures and Characterization for Gram-Scale Reaction

In a glovebox, under argon, an oven-dried 20 ml scintillation vial equipped with a magnetic stir bar was charged with Alkenyl boron substrate (1.15g, 3 mmol, 1 equiv.) in 4 ml Et_2O. The vial was sealed and brought out of the glovebox. Then the vial was cooled to 0 °C, and 1.9M phenyl lithium solution (1.61 ml, 3.06 mmol, 1.02 equiv.) was added dropwise. The reaction mixture was allowed to warm to room temperature and stir for 45 minutes. Then the reaction mixture was connected to High Vacumn for 1 hr to evaporate solvents. Then the vial was refilled with nitrogen and brought back to glovebox. And cesium fluoride (478.5 mg, 3.15 mmol, 1.05 equiv) was added in the reaction mixture. 4 ml THF was added to re-dissolve the mixture and stired for 45 min before the stock solution of catalyst [$Pd(OAc)_2$ (3.4 mg, 0.015 mmol, 0.005 equiv.) and ***(R,R)*-L1** (19.0 mg, 0.018 mmol, 0.006 equiv.) in THF (1 mL) was stirred for 45 min before use]was added. Finally, aryl triflate (746.4 mg, 3.3 mmol, 1.1 equiv.) was introduced. And then the vial was sealed and brought out of glovebox. The reaction was heated at 45 ^{o}C for 48 hours. Upon completion, the reaction was quenched with 4 ml water and 5 ml Et_2O. The aqueous phase was extracted with Et_2O (5 x 3 mL). The combined organic layers were dried over $MgSO_4$, filtered, concentrated under

reduced pressure, and subsequently passed through a short silica gel pad to remove metal particles. The collected filtrate was concentrated and purified via recrystallization out of methanol to provide the desired products.

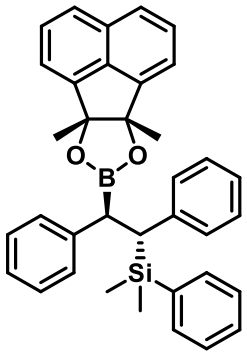

((1R,2R)-2-((6bR,9aS)-6b,9a-dimethyl-6b,9a-dihydroacenaphtho[1,2-d][1,3,2]dioxaborol-8-yl)-1,2-diphenylethyl)dimethyl(phenyl)silane (3.105)

^{1}H NMR (500 MHz, $CDCl_3$) δ 7.67 (d, *J* = 8.2 Hz, 2H), 7.48 (dddd, *J* = 12.6, 8.0, 6.9, 1.0 Hz, 2H), 7.36 (dd, *J* = 7.0, 0.9 Hz, 1H), 7.33 – 7.28 (m, 3H), 7.27 – 7.19 (m, 1H), 7.20 – 7.12 (m, 4H), 7.13 – 7.03 (m, 3H), 6.81 – 6.76 (m, 2H), 6.73-6.70 (m, 2H), 6.69 – 6.61 (m, 1H), 2.92 (d, *J* = 12.7 Hz, 1H), 2.81 (d, *J* = 12.7 Hz, 1H), 1.37 (s, 3H), 1.35 (s, 3H), -0.15 (s, 3H), -0.18 (s, 3H).; ^{13}C NMR (126 MHz, $CDCl_3$) δ 144.5, 144.2, 143.0, 141.5, 137.6, 134.5, 134.3, 131.3, 129.4, 128.5, 128.3, 128.11, 128.07, 127.1, 127.0, 125.6, 124.9, 124.5, 119.0, 118.9, 91.6, 91.5, 40.3, 21.7, 21.6, -3.4, -3.6.; **IR** (neat) ν_{max} 3023.7 (br, w), 2970.4 (br, w), 1738.8 (w), 1493.3 (w), 1341.5 (m), 1312.2 (m), 1115.5 (s), 1077.0 (m), 824.7 (s), 778.3

(s), 699.0 (s) cm^{-1}.; **HRMS** (DART) for $C_{36}H_{39}SiBNO_2$ $[M+NH_4]^+$: Calc'd: 556.2838, found: 556.2845. $\mathbf{[\alpha]_D^{20}}$ = + 76.94 (*c* = 1.00, $CHCl_3$, *l* = 50 mm).

Analysis of Stereochemistry:

Diastereomer ratio was determined by ^1H NMR analysis of the crude reaction mixture. Enantiomeric ratio was determined by chiral SFC analysis of the corresponding alcohols (see Compound 8). Absolute stereochemistry was determined by single crystal X-ray diffraction.

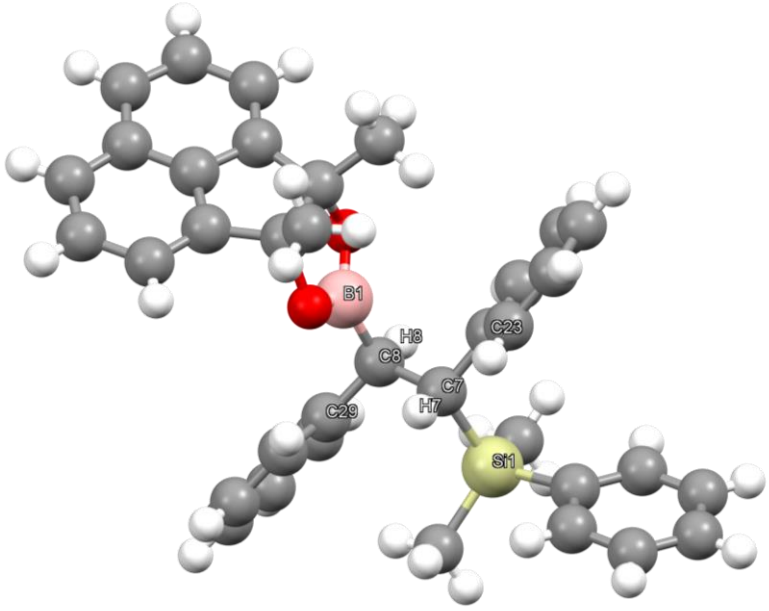

3.5.5 Procedures and Characterization for Transformations of Chiral *anti*-1,2-Boronsilane

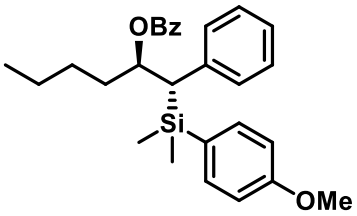

((1S,2R)-1-((4-methoxyphenyl)dimethylsilyl)-1-phenylhexan-2-yl benzoate (3.157)

A 2-dram vial equipped with a magnetic stir bar was charged with oxidation crude mixture of hydroxylsilane S10 (0.2 mmol scale), benzoic anhydride (113.1 mg, 0.5 mmol, 2.5 equiv), DMAP (73.3 mg, 0.6 mmol, 3 equiv). The reaction vial was sealed and 2 ml DCM was added followed by Et_3N (0.08 ml, 0.6 mmol, 3 equiv). Then, the reaction was stirred at r.t for 15 hr before quenched by passing through a short silica gel plug. The filtrate was concentrated in vacuo to give the crude reaction mixture, which was subjected to column chromatography (3% EtOAc in Hexane) to give title compound (31.2 mg, 84% yield). ^{1}H NMR (500 MHz, $CDCl_3$) δ 7.88 (ddd, *J* = 8.4, 2.6, 1.3 Hz, 2H), 7.57 – 7.50 (m, 1H), 7.48 – 7.37 (m, 2H), 7.36 – 7.11 (m, 7H), 6.80 – 6.73 (m, 2H), 5.63 – 5.55 (m, 1H), 3.77 (s, 3H), 2.65 (d, *J* = 5.4 Hz, 1H), 1.60 – 1.51 (m, 2H), 1.23 – 1.09 (m, 4H), 0.76 (t, *J* = 7.1 Hz, 3H), 0.28 (s, 3H), 0.21 (s, 3H).; ^{13}C NMR (126 MHz, $CDCl_3$) δ 166.0, 160.4, 139.6, 135.5, 132.6, 130.8, 129.7, 129.5, 128.2, 127.98, 127.95, 125.2, 113.4, 76.0,

54.9, 42.0, 33.6, 27.6, 22.4, 13.9, -3.0, -3.8.; **IR** (neat) ν_{max} 2955.8 (w), 2929.8 (w), 1714.5 (s), 1595.0 (s), 1503.2 (m), 1274.7(s), 1248.6 (m), 1183.0 (w), 1110.5 (s), 1026.4 (w), 826.4 (w), 710.8 (m) cm^{-1}. **$[\alpha]_D^{20}$** = + 61.39 (*c* = 1.00, $CHCl_3$, *l* = 50 mm).

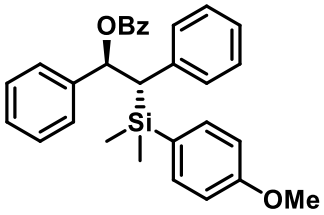

(1R,2S)-2-((4-methoxyphenyl)dimethylsilyl)-1,2-diphenylethyl benzoate (3.154)

A 2-dram vial equipped with a magnetic stir bar was charged with oxidation crude mixture of hydroxylsilane S9 (0.2 mmol scale), benzoic anhydride (113.1 mg, 0.5 mmol, 2.5 equiv), DMAP (73.3 mg, 0.6 mmol, 3 equiv). The reaction vial was sealed and 2 ml DCM was added followed by Et_3N (0.08 ml, 0.6 mmol, 3 equiv). Then, the reaction was stirred at r.t for 15 hr before quenched by passing through a short silica gel plug. The filtrate was concentrated in vacuo to give the crude reaction mixture, which was subjected to column chromatography (4% EtOAc in Hexane) to give title compound (62.0mg, 88% yield). ^1H NMR (500 MHz, $CDCl_3$) δ 7.79 – 7.73 (m, 2H), 7.50 – 7.42 (m, 1H), 7.38 – 7.29 (m, 4H), 7.28 – 7.05 (m, 10H), 6.83 – 6.76 (m, 2H), 6.45 (d, *J* = 9.3 Hz, 1H), 3.81 (s, 3H), 3.07 (d, *J* = 9.3 Hz, 1H), 0.10 (s, 3H), 0.03 (s, 3H).; ^{13}C NMR (126 MHz, $CDCl_3$) δ 165.8, 160.5, 140.1,

139.8, 135.7, 132.6, 130.5, 129.4, 129.0, 128.2, 128.11, 128.09, 128.0, 127.5, 127.3, 125.2, 113.3, 77.9, 55.0, 45.1, -3.2, -3.3. **IR** (neat) ν_{max} 3027.0 (w), 2954.3 (w), 1713.5 (s), 1594.3 (s), 1502.5 (m), 1450.8 (m), 1268.1 (s), 1248.4 (s), 1182.8 (m), 1110.0 (s), 1026.5 (w), 822.6 (m), 700.5 (s) cm^{-1}. $\mathbf{[\alpha]_D^{20}}$ = + 67.51 (*c* = 1.00, $CHCl_3$, *l* = 50 mm)

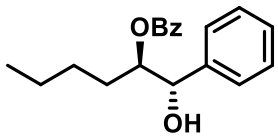

(1S,2R)-1-hydroxy-1-phenylhexan-2-yl benzoate (3.158)

The title compound was synthesized following previous reports[64,65] with modifications. A 2-dram vial equipped with a magnetic stir bar was charged with compound 31 (31.2 mg, 0.07 mmol), KBr (9.6 mg, 0.08 mmol, 1.15 eq), NaOAc (86.1 mg, 1.05 mmol, 15 equiv). The reaction vial was sealed and cooled to 0 ° C. A solution of 15% AcOOH in AcOH (1.12 ml, 2.1 mmol, 30 equiv) was added and the reaction was allowed to warm to r.t for 12 hr. Then, the reaction was quenched with NaS_2O_3 (4 mL). The organic layer was washed with aqueous $NaHCO_3$ until no gas evolves. The combined organics were dried over Na_2SO_4, filtered, and concentrated in vacuo to give the crude

[64] I. Fleming, H. Rolf, D. C. Parker, H. E. Plaut and P. E. J. Sanderson, *J. Chem. Soc., Perkin Trans. 1,* **1995**, 317
[65] G. R. Jones, Y. Landais, *Tetrahedron*, **1996**, *52*, 7599

reaction mixture, which was subjected to column chromatography (10% EtOAc in Hexane) to afford white solid (17.0 mg, 81% yield). ^{1}H NMR (500 MHz, $CDCl_3$) δ 8.07 – 8.01 (m, 2H), 7.58 (ddt, *J* = 8.0, 7.0, 1.3 Hz, 1H), 7.50 – 7.41 (m, 4H), 7.41 – 7.32 (m, 2H), 7.33 – 7.26 (m, 1H), 5.39 (dt, *J* = 9.7, 3.6 Hz, 1H), 5.02 (t, *J* = 3.3 Hz, 1H), 2.41 (d, *J* = 3.3 Hz, 1H), 1.82 – 1.70 (m, 1H), 1.68 – 1.57 (m, 1H), 1.44 - 1.19 (m, 4H), 0.84 (t, *J* = 7.1 Hz, 2H).; ^{13}C NMR (126 MHz, $CDCl_3$) δ 166.6, 139.9, 133.0, 130.2, 129.7, 128.4, 128.3, 127.8, 126.7, 78.3, 75.5, 28.4, 27.8, 22.5, 13.9.; **IR** (neat) ν_{max} 3473.2 (br, m), 2956.9 (w), 2929.4 (w), 2860.3 (w), 1715.0 (s), 1451.1 (m), 1274.5 (s), 1114.6 (m), 1026.7 (w), 711.2 (s) cm^{-1}.; **HRMS** (DART) for $C_{19}H_{21}O_2$ $[M+H-H_2O]^+$: Calc'd: 281.1536, found: 281.1534. **$[\alpha]_D^{20}$** = + 19.72 (*c* = 1.00, $CHCl_3$, *l* = 50 mm).

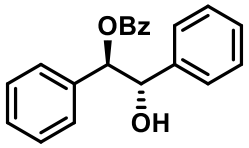

(1R,2S)-2-hydroxy-1,2-diphenylethyl benzoate (3.155)

The title compound was synthesized following the same procedure described in compound 33. A 2-dram vial equipped with a magnetic stir bar was charged with compound 32 (46.7 mg, 0.1 mmol), KBr (13.7 mg, 0.115 mmol, 1.15 eq), NaOAc (123.0 mg, 1.5 mmol, 15 equiv). The reaction vial was sealed and

cooled to 0 ° C. A solution of 15% AcOOH in AcOH (1.6 ml, 3 mmol, 30 equiv) was added and the reaction was allowed to warm to r.t for 12 hr. Then, the reaction was quenched with NaS_2O_3 (5 mL). The organic layer was washed with aqueous $NaHCO_3$ until no gas evolves. The combined organics were dried over Na_2SO_4, filtered, and concentrated in vacuo to give the crude reaction mixture, which was subjected to column chromatography (13% EtOAc in Hexane) to afford white solid (26.6 mg, 84% yield). The spectral data was in accordance with the literature.[66]

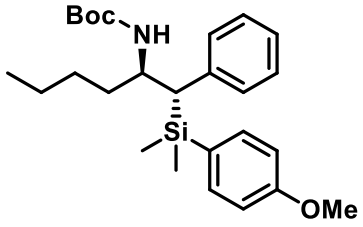

***tert*-butyl ((1S,2R)-1-((4-methoxyphenyl)dimethylsilyl)-1-phenylhexan-2-yl)carbamate (3.159)**

The title compound was synthesized following a previous report[67] from our group with modifications. A flame-dried, 2-dram vial equipped with a magnetic stir bar was purged with N_2. O-methylhydroxylamine solution (0.42 mL, 0.9 mmol, 2.16 M in THF, 3 equiv) was added and diluted with THF (2 mL). The reaction vial was cooled to -78° C in a dry ice/acetone bath. A

[66] S. J. Canipa, A. Stute and P. O'Brien, *Tetrahedron*, **2014**, *70*, 7395
[67] S. N. Mlynarski, A. S. Karns and J. P. Morken*, J. Am. Chem. Soc*. **2012**, *134,* 16449

solution of n-butyl lithium in hexanes (0.4 mL, 0.9 mmol, 2.26 M in Hexane, 3 equiv) was added dropwise and the reaction was allowed to stir at -78° C for 30 min. A solution of un-oxidized crude mixture of pinacol ester S10 (0.3 mmol scale reaction) and sodium triflate (103.2 mg, 0.6 mmol, 2 equiv) in 1 ml THF was then added dropwise via syringe. The reaction flask was warmed to room temperature and then heated to 70° C. After stirring at 70° C for 18 h, the reaction flask was cooled to room temperature and Boc anhydride (0.23 mL, 1 mmol, 3.3 equiv.) was added. After stirring at room temperature for 2 h the reaction was quenched with water (5 mL). The layers were separated and the aqueous layer was extracted with EtOAc (3 x 10 mL). The combined organics were dried over Na_2SO_4, filtered, and concentrated in vacuo to give the crude reaction mixture, which was subjected to column chromatography (8% EtOAc in Hexane) to give title compound (27.0 mg, 51% yield). ^{1}H NMR (600 MHz, $CDCl_3$) δ 7.34 (d, *J* = 8.5 Hz 2H), 7.21 (t, *J* = 7.5 Hz, 2H), 7.12 (t, *J* = 7.3 Hz, 1H), 7.00 (d, *J* = 7.0 Hz, 2H), 6.86 (d, *J* = 8.1 Hz, 2H), 4.19 (d, *J* = 10.1 Hz, 1H), 4.10 (s, 1H), 3.80 (s, 3H), 2.34 (d, *J* = 6.9 Hz, 1H), 1.46 – 1.40 (m, 2H), 1.35 (s, 9H), 1.24 – 1.07 (m, 4H), 0.78 (t, *J* = 6.6 Hz, 3H), 0.33 (s, 3H), 0.16 (s, 3H).; ^{13}C NMR (101 MHz, $CDCl_3$) δ 160.3, 155.4, 140.6, 135.5, 129.5, 128.8, 128.1, 125.2, 113.4, 78.7, 55.0, 50.9, 42.7, 36.2, 28.4,

28.0, 22.4, 14.0, -2.4, -3.9.; **IR** (neat) ν_{max} 3443.9 (br, w), 2956.0 (m), 2930.8 (m), 1712.2 (s), 1594.9 (s), 1502.2 (s), 1365.0 (m), 1277.3 (s), 1246.9 (s), 1181.5 (s), 1171.2 (s), 1110.1 (s), 1032.7 (m), 831.2 (m) cm^{-1}.; **HRMS** (AccuTOF) for $C_{19}H_{32}NO_2Si$ $[M\text{-}C_7H_7O]^+$: Calc'd: 334.2197, found: 334.2232 $\mathbf{[\alpha]_D^{20}}$ = + 68.71 (*c* = 1.00, $CHCl_3$, *l* = 50 mm).

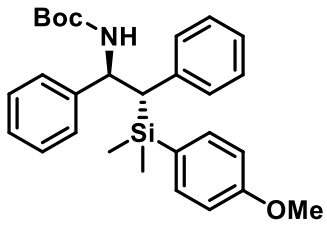

tert-butyl ((1R,2S)-2-((4-methoxyphenyl)dimethylsilyl)-1,2-diphenylethyl)carbamate (3.160)

The title compound was synthesized following a previous report[9] from our group. A flame-dried, 2-dram vial equipped with a magnetic stir bar was purged with N2. O-methylhydroxylamine solution (0.42 mL, 0.9 mmol, 2.16 M in THF, 3 equiv) was added and diluted with THF (2 mL). The reaction vial was cooled to -78° C in a dry ice/acetone bath. A solution of n-butyl lithium in hexanes (0.4 mL, 0.9 mmol, 2.26 M, 3 equiv) was added dropwise and the reaction was allowed to stir at -78° C for 30 min. A solution of un-oxidized crude mixture of pinacol ester S9 (0.3 mmol scale reaction) in 1 ml THF was then added dropwise via syringe. The reaction flask was warmed to room temperature and then heated to 60° C. After stirring at 60° C for 12 h,

the reaction flask was cooled to room temperature and Boc anhydride (0.23 mL, 1 mmol, 3.3 equiv) was added. After stirring at room temperature for 2 h the reaction was quenched with water (5 mL). The layers were separated and the aqueous layer was extracted with EtOAc (3 x 10 mL). The combined organics were dried over Na2SO4, filtered, and concentrated in vacuo to give the crude reaction mixture, which was subjected to column chromatography (10% EtOAc in Hexane) to give title compound (91.7 mg, 87% yield). ^{1}H NMR (500 MHz, $CDCl_3$) δ 7.30 – 7.17 (m, 7H), 7.17 – 7.06 (m, 3H), 7.00 – 6.94 (m, 2H), 6.82 – 6.75 (m, 2H), 5.09 (bs, 1H), 4.67 (bs, 1H), 3.81 (s, 3H), 2.66 (d, J = 10.3 Hz, 1H), 1.25 (s, 9H), -0.02 (s, 3H), -0.06 (s, 3H).; ^{13}C NMR (126 MHz, $CDCl_3$) δ 160.3, 154.9, 143.1, 139.8, 135.7, 129.2, 128.3, 128.1, 127.7, 127.33, 127.30, 125.4, 113.2, 79.1, 55.0, 44.8, 28.2, -3.2, -3.4.; **IR** (neat) ν_{max} 3443.6 (br, w), 2973.6 (br, w), 1698.4 (s), 1594.3 (m), 1501.6 (s), 1365.0 (m), 1277.3 (m), 1245.9 (s), 1166.8 (m), 1110.0 (s), 1031.0 (w), 823.2 (s), 699.6 (s) cm^{-1}.; **HRMS** (DART) for $C_{21}H_{28}NO_2Si$ $[M\text{-}C_7H_7O^-]^+$: Calc'd: 354.1884, found: 354.1880. $\mathbf{[\alpha]_D^{20}}$ = + 38.79 (c = 1.00, $CHCl_3$, l = 50 mm).

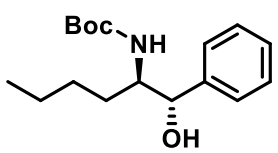

tert-butyl ((1S,2R)-1-hydroxy-1-phenylhexan-2-yl) carbamate (3.161)

The title compound was synthesized following the same procedure described in compound 33. A 2-dram vial equipped with a magnetic stir bar was charged with aminosilane 35 (44.2 mg, 0.1 mmol), KBr (13.7 mg, 0.115 mmol, 1.15 eq), NaOAc (123.0 mg, 1.5 mmol, 15 equiv). The reaction vial was sealed and cooled to 0 ° C. A solution of 15% AcOOH in AcOH (1.6 ml, 3 mmol, 30 equiv) was added and the reaction was allowed to warm to r.t for 12 hr. Then, the reaction was quenched with $Na_2S_2O_3$ (5 mL). The organic layer was washed with aqueous $NaHCO_3$ until no gas evolves. The combined organics were dried over Na_2SO_4, filtered, and concentrated in vacuo to give the crude reaction mixture, which was subjected to column chromatography (20% EtOAc in Hexane) to afford white solid (19.3 mg, 66% yield). ^{1}H NMR (500 MHz, $CDCl_3$) δ 7.39 – 7.24 (m, 5H), 4.85 (bs, 1H), 4.48 (d, J = 8.6 Hz, 1H), 3.90 (m, 1H), 3.50 (bs, 1H), 1.47 (s, 9H), 1.38 – 1.15 (m, 6H), 0.85 (t, J = 6.7 Hz, 3H).; ^{13}C NMR (101 MHz, $CDCl_3$) δ 157.1, 140.7, 128.1, 127.4, 126.5, 79.8, 77.0, 56.5, 29.3, 28.4, 22.4, 13.9.; **IR** (neat) ν_{max} 3364.3 (br, s), 2957.3 (w), 2927.0 (w), 1683.0 (s), 1528.8 (s), 1458.2 (w), 1367.2 (w), 1247.3 (w), 1173.6 (m), 997.1 (m), 700.8 (m) cm^{-1}.; **HRMS** (DART) for $C_{17}H_{28}NO_3$

[M+H]$^+$: Calc'd: 294.2064, found: 294.2066. $[\alpha]_D^{20}$ = + 133.17 (*c* = 1.00, $CHCl_3$, *l* = 50 mm).

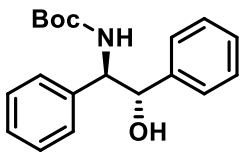

tert-butyl((1R,2S)-2-hydroxy-1,2 diphenylethyl)carbamate (3.162)

The title compound was synthesized following the same procedure described in compound 33. A 2-dram vial equipped with a magnetic stir bar was charged with aminosilane 36 (46.2 mg, 0.1 mmol), KBr (13.7 mg, 0.115 mmol, 1.15 eq), NaOAc (123.0 mg, 1.5 mmol, 15 equiv). The reaction vial was sealed and cooled to 0 ° C. A solution of 15% AcOOH in AcOH (1.6 ml, 3 mmol, 30 equiv) was added and the reaction was allowed to warm to r.t for 12 hr. Then, the reaction was quenched with $Na_2S_2O_3$ (5 mL). The organic layer was washed with aqueous $NaHCO_3$ until no gas evolves. The combined organics were dried over Na_2SO_4, filtered, and concentrated in vacuo to give the crude reaction mixture, which was subjected to column chromatography (20% EtOAc in Hexane) to give title compound. The spectral data was in accordance with the literature[68].

[68] R. Kaur and S. K. Pandey, *Tetrahedron: Asymmetry*, **2016**, *27*, 338

3.5.6 Crystallographic Data

Table 1. Crystal data and structure refinement for C36H35BO2Si.

Identification code	C36H35BO2Si	
Empirical formula	C36 H35 B O2 Si	
Formula weight	538.54	
Temperature	100(2) K	
Wavelength	1.54178 Å	
Crystal system	Monoclinic	
Space group	$P2_1$	
Unit cell dimensions	a = 13.6994(4) Å	a= 90°.
	b = 6.5420(2) Å	b= 101.3630(10)°.
	c = 16.7228(4) Å	g = 90°.
Volume	1469.34(7) $Å^3$	
Z	2	
Density (calculated)	1.217 Mg/m^3	
Absorption coefficient	0.936 mm^{-1}	
F(000)	572	
Crystal size	0.480 x 0.260 x 0.140 mm^3	

Theta range for data collection	2.695 to 65.493°.
Index ranges	-16<=h<=14, -7<=k<=7, -19<=l<=19
Reflections collected	10734
Independent reflections	4703 [R(int) = 0.0199]
Completeness to theta = 65.493°	98.0 %
Absorption correction	Semi-empirical from equivalents
Max. and min. transmission	0.7528 and 0.6454
Refinement method	Full-matrix least-squares on F^2
Data / restraints / parameters	4703 / 1 / 361
Goodness-of-fit on F^2	1.049
Final R indices [I>2sigma(I)]	R1 = 0.0268, wR2 = 0.0699
R indices (all data)	R1 = 0.0276, wR2 = 0.0710
Absolute structure parameter	-0.011(10)
Extinction coefficient	n/a
Largest diff. peak and hole	0.118 and -0.170 e.$Å^{-3}$

Table 2. Atomic coordinates (x 10^4) and equivalent isotropic displacement parameters ($Å^2$x 10^3) for C36H35BO2Si. U(eq) is defined as one third of the trace of the orthogonalized U^{ij} tensor.

	x	y	z	U(eq)
Si(1)	7014(1)	6812(1)	774(1)	23(1)
O(1)	7547(1)	6415(2)	3974(1)	22(1)
O(2)	7172(1)	3232(2)	3431(1)	24(1)
B(1)	7146(2)	5296(4)	3304(1)	22(1)
C(1)	8599(2)	7855(4)	-55(1)	38(1)
C(2)	9228(2)	7527(4)	-597(2)	46(1)
C(3)	9248(2)	5654(5)	-967(2)	47(1)
C(4)	8655(2)	4096(5)	-784(2)	47(1)
C(5)	8032(2)	4421(4)	-235(2)	37(1)
C(6)	7976(2)	6318(3)	135(1)	28(1)
C(7)	7405(2)	5630(3)	1835(1)	23(1)
C(8)	6728(1)	6309(3)	2450(1)	22(1)
C(9)	8008(2)	5030(3)	4619(1)	22(1)

C(10)	7563(2)	5320(3)	5368(1)	24(1)
C(11)	7687(2)	6822(4)	5948(1)	34(1)
C(12)	7127(2)	6694(4)	6574(1)	43(1)
C(13)	6488(2)	5115(4)	6621(1)	41(1)
C(14)	6358(2)	3511(4)	6038(1)	30(1)
C(15)	5742(2)	1770(4)	6002(1)	36(1)
C(16)	5696(2)	375(4)	5382(2)	34(1)
C(17)	6265(2)	583(3)	4765(1)	28(1)
C(18)	6874(2)	2248(3)	4789(1)	22(1)
C(19)	6911(2)	3691(3)	5419(1)	24(1)
C(20)	7631(2)	2848(3)	4279(1)	21(1)
C(21)	6867(2)	9643(4)	861(2)	34(1)
C(22)	5832(2)	5630(4)	219(1)	32(1)
C(23)	8500(2)	6007(3)	2187(1)	26(1)
C(24)	8845(2)	7896(4)	2505(1)	33(1)
C(25)	9849(2)	8228(5)	2822(2)	42(1)
C(26)	10529(2)	6659(6)	2823(2)	49(1)
C(27)	10203(2)	4783(5)	2518(2)	51(1)
C(28)	9194(2)	4453(4)	2197(2)	38(1)

C(29)	5634(2)	5855(3)	2154(1)	23(1)
C(30)	5274(2)	3849(3)	2061(1)	28(1)
C(31)	4268(2)	3476(4)	1786(1)	33(1)
C(32)	3598(2)	5062(4)	1601(1)	36(1)
C(33)	3942(2)	7057(4)	1696(1)	36(1)
C(34)	4946(2)	7439(3)	1971(1)	29(1)
C(35)	9120(2)	5392(4)	4766(1)	31(1)
C(36)	8422(2)	1232(3)	4299(1)	29(1)

Table 3. Bond lengths [Å] and angles [°] for C36H35BO2Si.

Si(1)-C(22)	1.868(2)
Si(1)-C(21)	1.871(2)
Si(1)-C(6)	1.882(2)
Si(1)-C(7)	1.913(2)
O(1)-B(1)	1.360(3)
O(1)-C(9)	1.454(2)
O(2)-B(1)	1.366(3)
O(2)-C(20)	1.455(2)
B(1)-C(8)	1.577(3)
C(1)-C(2)	1.385(3)
C(1)-C(6)	1.396(3)
C(1)-H(1)	0.9500
C(2)-C(3)	1.375(4)
C(2)-H(2)	0.9500
C(3)-C(4)	1.375(4)
C(3)-H(3)	0.9500
C(4)-C(5)	1.387(3)

C(4)-H(4)	0.9500
C(5)-C(6)	1.395(3)
C(5)-H(5)	0.9500
C(7)-C(23)	1.519(3)
C(7)-C(8)	1.578(3)
C(7)-H(7)	1.0000
C(8)-C(29)	1.512(3)
C(8)-H(8)	1.0000
C(9)-C(10)	1.509(3)
C(9)-C(35)	1.513(3)
C(9)-C(20)	1.585(3)
C(10)-C(11)	1.368(3)
C(10)-C(19)	1.403(3)
C(11)-C(12)	1.417(3)
C(11)-H(11)	0.9500
C(12)-C(13)	1.366(4)
C(12)-H(12)	0.9500
C(13)-C(14)	1.420(3)
C(13)-H(13)	0.9500

C(14)-C(19)	1.402(3)
C(14)-C(15)	1.412(4)
C(15)-C(16)	1.374(4)
C(15)-H(15)	0.9500
C(16)-C(17)	1.416(3)
C(16)-H(16)	0.9500
C(17)-C(18)	1.368(3)
C(17)-H(17)	0.9500
C(18)-C(19)	1.408(3)
C(18)-C(20)	1.519(3)
C(20)-C(36)	1.509(3)
C(21)-H(21A)	0.9800
C(21)-H(21B)	0.9800
C(21)-H(21C)	0.9800
C(22)-H(22A)	0.9800
C(22)-H(22B)	0.9800
C(22)-H(22C)	0.9800
C(23)-C(28)	1.390(3)
C(23)-C(24)	1.391(3)

C(24)-C(25)	1.390(3)
C(24)-H(24)	0.9500
C(25)-C(26)	1.386(4)
C(25)-H(25)	0.9500
C(26)-C(27)	1.370(5)
C(26)-H(26)	0.9500
C(27)-C(28)	1.397(4)
C(27)-H(27)	0.9500
C(28)-H(28)	0.9500
C(29)-C(34)	1.394(3)
C(29)-C(30)	1.400(3)
C(30)-C(31)	1.386(3)
C(30)-H(30)	0.9500
C(31)-C(32)	1.380(4)
C(31)-H(31)	0.9500
C(32)-C(33)	1.386(4)
C(32)-H(32)	0.9500
C(33)-C(34)	1.384(3)
C(33)-H(33)	0.9500

C(34)-H(34)	0.9500
C(35)-H(35A)	0.9800
C(35)-H(35B)	0.9800
C(35)-H(35C)	0.9800
C(36)-H(36A)	0.9800
C(36)-H(36B)	0.9800
C(36)-H(36C)	0.9800
C(22)-Si(1)-C(21)	110.63(11)
C(22)-Si(1)-C(6)	106.41(10)
C(21)-Si(1)-C(6)	108.19(10)
C(22)-Si(1)-C(7)	110.53(10)
C(21)-Si(1)-C(7)	110.06(10)
C(6)-Si(1)-C(7)	110.94(9)
B(1)-O(1)-C(9)	108.74(15)
B(1)-O(2)-C(20)	108.36(15)
O(1)-B(1)-O(2)	114.21(18)
O(1)-B(1)-C(8)	122.38(19)
O(2)-B(1)-C(8)	123.37(18)
C(2)-C(1)-C(6)	121.6(2)

C(2)-C(1)-H(1)	119.2
C(6)-C(1)-H(1)	119.2
C(3)-C(2)-C(1)	120.2(2)
C(3)-C(2)-H(2)	119.9
C(1)-C(2)-H(2)	119.9
C(4)-C(3)-C(2)	119.8(2)
C(4)-C(3)-H(3)	120.1
C(2)-C(3)-H(3)	120.1
C(3)-C(4)-C(5)	120.0(3)
C(3)-C(4)-H(4)	120.0
C(5)-C(4)-H(4)	120.0
C(4)-C(5)-C(6)	121.6(2)
C(4)-C(5)-H(5)	119.2
C(6)-C(5)-H(5)	119.2
C(5)-C(6)-C(1)	116.8(2)
C(5)-C(6)-Si(1)	120.69(17)
C(1)-C(6)-Si(1)	122.25(17)
C(23)-C(7)-C(8)	111.37(16)
C(23)-C(7)-Si(1)	111.63(13)

C(8)-C(7)-Si(1)	113.38(13)
C(23)-C(7)-H(7)	106.7
C(8)-C(7)-H(7)	106.7
Si(1)-C(7)-H(7)	106.7
C(29)-C(8)-B(1)	111.91(16)
C(29)-C(8)-C(7)	113.82(15)
B(1)-C(8)-C(7)	108.44(15)
C(29)-C(8)-H(8)	107.5
B(1)-C(8)-H(8)	107.5
C(7)-C(8)-H(8)	107.5
O(1)-C(9)-C(10)	110.45(15)
O(1)-C(9)-C(35)	107.42(15)
C(10)-C(9)-C(35)	113.83(17)
O(1)-C(9)-C(20)	103.39(14)
C(10)-C(9)-C(20)	104.76(15)
C(35)-C(9)-C(20)	116.48(17)
C(11)-C(10)-C(19)	119.60(19)
C(11)-C(10)-C(9)	131.7(2)
C(19)-C(10)-C(9)	108.75(17)

C(10)-C(11)-C(12) 118.1(2)

C(10)-C(11)-H(11) 120.9

C(12)-C(11)-H(11) 120.9

C(13)-C(12)-C(11) 122.3(2)

C(13)-C(12)-H(12) 118.9

C(11)-C(12)-H(12) 118.9

C(12)-C(13)-C(14) 120.9(2)

C(12)-C(13)-H(13) 119.5

C(14)-C(13)-H(13) 119.5

C(19)-C(14)-C(15) 116.3(2)

C(19)-C(14)-C(13) 115.6(2)

C(15)-C(14)-C(13) 128.1(2)

C(16)-C(15)-C(14) 120.30(19)

C(16)-C(15)-H(15) 119.8

C(14)-C(15)-H(15) 119.8

C(15)-C(16)-C(17) 122.5(2)

C(15)-C(16)-H(16) 118.8

C(17)-C(16)-H(16) 118.8

C(18)-C(17)-C(16) 118.4(2)

C(18)-C(17)-H(17) 120.8

C(16)-C(17)-H(17) 120.8

C(17)-C(18)-C(19) 119.18(18)

C(17)-C(18)-C(20) 132.02(18)

C(19)-C(18)-C(20) 108.62(17)

C(14)-C(19)-C(10) 123.47(19)

C(14)-C(19)-C(18) 123.40(19)

C(10)-C(19)-C(18) 113.13(18)

O(2)-C(20)-C(36) 108.25(16)

O(2)-C(20)-C(18) 112.33(15)

C(36)-C(20)-C(18) 111.90(16)

O(2)-C(20)-C(9) 104.02(14)

C(36)-C(20)-C(9) 116.19(16)

C(18)-C(20)-C(9) 103.95(15)

Si(1)-C(21)-H(21A) 109.5

Si(1)-C(21)-H(21B) 109.5

H(21A)-C(21)-H(21B)109.5

Si(1)-C(21)-H(21C) 109.5

H(21A)-C(21)-H(21C)109.5

H(21B)-C(21)-H(21C)109.5

Si(1)-C(22)-H(22A) 109.5

Si(1)-C(22)-H(22B) 109.5

H(22A)-C(22)-H(22B)109.5

Si(1)-C(22)-H(22C) 109.5

H(22A)-C(22)-H(22C)109.5

H(22B)-C(22)-H(22C)109.5

C(28)-C(23)-C(24) 117.7(2)

C(28)-C(23)-C(7) 120.5(2)

C(24)-C(23)-C(7) 121.82(19)

C(25)-C(24)-C(23) 121.4(2)

C(25)-C(24)-H(24) 119.3

C(23)-C(24)-H(24) 119.3

C(26)-C(25)-C(24) 119.9(3)

C(26)-C(25)-H(25) 120.0

C(24)-C(25)-H(25) 120.0

C(27)-C(26)-C(25) 119.6(2)

C(27)-C(26)-H(26) 120.2

C(25)-C(26)-H(26) 120.2

C(26)-C(27)-C(28) 120.5(3)

C(26)-C(27)-H(27) 119.8

C(28)-C(27)-H(27) 119.8

C(23)-C(28)-C(27) 121.0(3)

C(23)-C(28)-H(28) 119.5

C(27)-C(28)-H(28) 119.5

C(34)-C(29)-C(30) 117.65(19)

C(34)-C(29)-C(8) 120.64(19)

C(30)-C(29)-C(8) 121.71(19)

C(31)-C(30)-C(29) 120.5(2)

C(31)-C(30)-H(30) 119.7

C(29)-C(30)-H(30) 119.7

C(32)-C(31)-C(30) 121.1(2)

C(32)-C(31)-H(31) 119.5

C(30)-C(31)-H(31) 119.5

C(31)-C(32)-C(33) 119.1(2)

C(31)-C(32)-H(32) 120.5

C(33)-C(32)-H(32) 120.5

C(34)-C(33)-C(32) 120.1(2)

C(34)-C(33)-H(33) 120.0

C(32)-C(33)-H(33) 120.0

C(33)-C(34)-C(29) 121.6(2)

C(33)-C(34)-H(34) 119.2

C(29)-C(34)-H(34) 119.2

C(9)-C(35)-H(35A) 109.5

C(9)-C(35)-H(35B) 109.5

H(35A)-C(35)-H(35B)109.5

C(9)-C(35)-H(35C) 109.5

H(35A)-C(35)-H(35C)109.5

H(35B)-C(35)-H(35C)109.5

C(20)-C(36)-H(36A) 109.5

C(20)-C(36)-H(36B) 109.5

H(36A)-C(36)-H(36B)109.5

C(20)-C(36)-H(36C) 109.5

H(36A)-C(36)-H(36C)109.5

H(36B)-C(36)-H(36C)109.5

Symmetry transformations used to generate equivalent atoms:

Table 4. Anisotropic displacement parameters ($Å^2 x\ 10^3$) for C36H35BO2Si. The anisotropic displacement factor exponent takes the form: $-2p^2[\ h^2\ a^{*2}U^{11} + ...\ + 2\ h\ k\ a^*\ b^*\ U^{12}]$

	U^{11}	U^{22}	U^{33}	U^{23}	U^{13}	U^{12}
Si(1)	25(1)	27(1)	19(1)	1(1)	6(1)	-1(1)
O(1)	28(1)	19(1)	20(1)	1(1)	4(1)	0(1)
O(2)	31(1)	22(1)	19(1)	-1(1)	3(1)	-2(1)
B(1)	21(1)	25(1)	22(1)	-2(1)	8(1)	-1(1)
C(1)	36(1)	43(1)	36(1)	0(1)	12(1)	-6(1)
C(2)	38(1)	60(2)	46(2)	7(1)	19(1)	-8(1)
C(3)	36(1)	74(2)	37(1)	-1(1)	18(1)	5(1)
C(4)	46(2)	54(2)	44(2)	-14(1)	17(1)	3(1)
C(5)	34(1)	41(1)	38(1)	-4(1)	12(1)	-2(1)
C(6)	24(1)	38(1)	20(1)	3(1)	3(1)	0(1)
C(7)	26(1)	24(1)	20(1)	1(1)	7(1)	1(1)
C(8)	26(1)	21(1)	20(1)	0(1)	7(1)	1(1)

C(9)	23(1)	20(1)	21(1)	2(1)	2(1)	0(1)
C(10)	27(1)	22(1)	21(1)	0(1)	1(1)	1(1)
C(11)	46(1)	28(1)	25(1)	-2(1)	4(1)	-7(1)
C(12)	71(2)	36(1)	24(1)	-8(1)	14(1)	-3(1)
C(13)	62(2)	40(1)	27(1)	-2(1)	21(1)	-1(1)
C(14)	36(1)	32(1)	25(1)	4(1)	10(1)	2(1)
C(15)	39(1)	42(1)	33(1)	6(1)	18(1)	-2(1)
C(16)	32(1)	32(1)	39(1)	5(1)	10(1)	-8(1)
C(17)	29(1)	25(1)	31(1)	-1(1)	5(1)	-3(1)
C(18)	20(1)	22(1)	23(1)	2(1)	2(1)	2(1)
C(19)	26(1)	25(1)	20(1)	2(1)	2(1)	2(1)
C(20)	22(1)	21(1)	19(1)	0(1)	2(1)	0(1)
C(21)	42(1)	29(1)	33(1)	4(1)	10(1)	2(1)
C(22)	29(1)	43(1)	23(1)	-1(1)	6(1)	-1(1)
C(23)	26(1)	35(1)	17(1)	2(1)	6(1)	2(1)
C(24)	33(1)	38(1)	28(1)	1(1)	6(1)	-2(1)
C(25)	36(1)	57(2)	33(1)	-2(1)	6(1)	-15(1)
C(26)	24(1)	84(2)	38(1)	-1(2)	4(1)	-6(2)
C(27)	29(1)	75(2)	48(2)	-5(2)	4(1)	14(1)

C(28)	31(1)	47(1)	36(1)	-5(1)	5(1)	8(1)
C(29)	27(1)	29(1)	16(1)	0(1)	7(1)	2(1)
C(30)	30(1)	29(1)	24(1)	3(1)	6(1)	-1(1)
C(31)	34(1)	38(1)	26(1)	-1(1)	6(1)	-10(1)
C(32)	23(1)	58(2)	27(1)	-3(1)	3(1)	-3(1)
C(33)	28(1)	49(1)	29(1)	-1(1)	3(1)	10(1)
C(34)	32(1)	31(1)	25(1)	-2(1)	8(1)	3(1)
C(35)	23(1)	29(1)	39(1)	-1(1)	2(1)	-4(1)
C(36)	26(1)	24(1)	37(1)	-1(1)	8(1)	2(1)

Table 5. Hydrogen coordinates (x 10^4) and isotropic displacement parameters ($Å^2$x 10^3) for C36H35BO2Si.

	x	y	z	U(eq)
H(1)	8592	9159	194	45
H(2)	9646	8598	-715	55
H(3)	9669	5437	-1347	57
H(4)	8671	2796	-1034	56
H(5)	7634	3325	-107	44
H(7)	7322	4118	1765	28
H(8)	6799	7823	2520	26
H(11)	8136	7921	5931	40
H(12)	7198	7742	6975	51
H(13)	6126	5089	7051	50
H(15)	5356	1562	6410	43
H(16)	5268	-772	5366	41
H(17)	6224	-409	4345	34

H(21A)	7494	10235	1153	51
H(21B)	6695	10242	314	51
H(21C)	6336	9933	1161	51
H(22A)	5923	4151	180	47
H(22B)	5297	5906	517	47
H(22C)	5656	6215	-330	47
H(24)	8385	8982	2505	39
H(25)	10069	9530	3038	50
H(26)	11217	6883	3034	59
H(27)	10666	3699	2524	62
H(28)	8980	3148	1982	46
H(30)	5722	2735	2188	33
H(31)	4036	2106	1723	39
H(32)	2910	4791	1411	44
H(33)	3488	8164	1573	43
H(34)	5171	8813	2036	35
H(35A)	9454	4479	5199	46
H(35B)	9364	5117	4264	46
H(35C)	9263	6816	4931	46

H(36A)	8740	952	4866	43
H(36B)	8116	-23	4045	43
H(36C)	8923	1718	3998	43

Table 6. Torsion angles [°] for C36H35BO2Si.

C(9)-O(1)-B(1)-O(2)	7.1(2)
C(9)-O(1)-B(1)-C(8)	-170.63(17)
C(20)-O(2)-B(1)-O(1)	0.5(2)
C(20)-O(2)-B(1)-C(8)	178.19(17)
C(6)-C(1)-C(2)-C(3)	0.2(4)
C(1)-C(2)-C(3)-C(4)	-1.2(4)
C(2)-C(3)-C(4)-C(5)	0.6(4)
C(3)-C(4)-C(5)-C(6)	1.0(4)
C(4)-C(5)-C(6)-C(1)	-1.9(4)
C(4)-C(5)-C(6)-Si(1)	172.3(2)
C(2)-C(1)-C(6)-C(5)	1.3(4)
C(2)-C(1)-C(6)-Si(1)	-172.8(2)
C(22)-Si(1)-C(6)-C(5)	-41.8(2)
C(21)-Si(1)-C(6)-C(5)	-160.73(18)
C(7)-Si(1)-C(6)-C(5)	78.5(2)
C(22)-Si(1)-C(6)-C(1)	132.08(19)
C(21)-Si(1)-C(6)-C(1)	13.2(2)

C(7)-Si(1)-C(6)-C(1)	-107.64(19)
O(1)-B(1)-C(8)-C(29)	-119.7(2)
O(2)-B(1)-C(8)-C(29)	62.7(3)
O(1)-B(1)-C(8)-C(7)	113.9(2)
O(2)-B(1)-C(8)-C(7)	-63.6(2)
C(23)-C(7)-C(8)-C(29)	-176.54(17)
Si(1)-C(7)-C(8)-C(29)	56.57(19)
C(23)-C(7)-C(8)-B(1)	-51.3(2)
Si(1)-C(7)-C(8)-B(1)	-178.17(14)
B(1)-O(1)-C(9)-C(10)	-122.37(17)
B(1)-O(1)-C(9)-C(35)	112.95(18)
B(1)-O(1)-C(9)-C(20)	-10.76(19)
O(1)-C(9)-C(10)-C(11)	-75.2(3)
C(35)-C(9)-C(10)-C(11)	45.7(3)
C(20)-C(9)-C(10)-C(11)	174.1(2)
O(1)-C(9)-C(10)-C(19)	104.21(18)
C(35)-C(9)-C(10)-C(19)	-134.86(18)
C(20)-C(9)-C(10)-C(19)	-6.5(2)
C(19)-C(10)-C(11)-C(12)	-1.5(3)

C(9)-C(10)-C(11)-C(12)	177.9(2)
C(10)-C(11)-C(12)-C(13)	1.1(4)
C(11)-C(12)-C(13)-C(14)	0.1(4)
C(12)-C(13)-C(14)-C(19)	-0.9(4)
C(12)-C(13)-C(14)-C(15)	179.3(2)
C(19)-C(14)-C(15)-C(16)	-0.8(3)
C(13)-C(14)-C(15)-C(16)	179.0(2)
C(14)-C(15)-C(16)-C(17)	1.1(4)
C(15)-C(16)-C(17)-C(18)	-0.5(3)
C(16)-C(17)-C(18)-C(19)	-0.3(3)
C(16)-C(17)-C(18)-C(20)	174.3(2)
C(15)-C(14)-C(19)-C(10)	-179.6(2)
C(13)-C(14)-C(19)-C(10)	0.5(3)
C(15)-C(14)-C(19)-C(18)	-0.1(3)
C(13)-C(14)-C(19)-C(18)	-179.9(2)
C(11)-C(10)-C(19)-C(14)	0.7(3)
C(9)-C(10)-C(19)-C(14)	-178.80(19)
C(11)-C(10)-C(19)-C(18)	-178.9(2)
C(9)-C(10)-C(19)-C(18)	1.6(2)

C(17)-C(18)-C(19)-C(14)	0.6(3)
C(20)-C(18)-C(19)-C(14)	-175.21(19)
C(17)-C(18)-C(19)-C(10)	-179.81(18)
C(20)-C(18)-C(19)-C(10)	4.4(2)
B(1)-O(2)-C(20)-C(36)	-131.21(18)
B(1)-O(2)-C(20)-C(18)	104.74(19)
B(1)-O(2)-C(20)-C(9)	-7.1(2)
C(17)-C(18)-C(20)-O(2)	65.1(3)
C(19)-C(18)-C(20)-O(2)	-119.90(17)
C(17)-C(18)-C(20)-C(36)	-56.9(3)
C(19)-C(18)-C(20)-C(36)	118.09(19)
C(17)-C(18)-C(20)-C(9)	176.9(2)
C(19)-C(18)-C(20)-C(9)	-8.1(2)
O(1)-C(9)-C(20)-O(2)	10.69(18)
C(10)-C(9)-C(20)-O(2)	126.41(16)
C(35)-C(9)-C(20)-O(2)	-106.86(18)
O(1)-C(9)-C(20)-C(36)	129.54(17)
C(10)-C(9)-C(20)-C(36)	-114.73(19)
C(35)-C(9)-C(20)-C(36)	12.0(2)

O(1)-C(9)-C(20)-C(18)	-107.06(16)
C(10)-C(9)-C(20)-C(18)	8.66(19)
C(35)-C(9)-C(20)-C(18)	135.39(18)
C(8)-C(7)-C(23)-C(28)	128.8(2)
Si(1)-C(7)-C(23)-C(28)	-103.4(2)
C(8)-C(7)-C(23)-C(24)	-51.5(2)
Si(1)-C(7)-C(23)-C(24)	76.3(2)
C(28)-C(23)-C(24)-C(25)	0.0(3)
C(7)-C(23)-C(24)-C(25)	-179.7(2)
C(23)-C(24)-C(25)-C(26)	0.2(4)
C(24)-C(25)-C(26)-C(27)	-0.6(4)
C(25)-C(26)-C(27)-C(28)	0.8(4)
C(24)-C(23)-C(28)-C(27)	0.2(3)
C(7)-C(23)-C(28)-C(27)	179.9(2)
C(26)-C(27)-C(28)-C(23)	-0.6(4)
B(1)-C(8)-C(29)-C(34)	122.7(2)
C(7)-C(8)-C(29)-C(34)	-113.9(2)
B(1)-C(8)-C(29)-C(30)	-56.8(2)
C(7)-C(8)-C(29)-C(30)	66.6(2)

C(34)-C(29)-C(30)-C(31)	0.9(3)
C(8)-C(29)-C(30)-C(31)	-179.70(18)
C(29)-C(30)-C(31)-C(32)	-0.4(3)
C(30)-C(31)-C(32)-C(33)	-0.1(3)
C(31)-C(32)-C(33)-C(34)	0.2(3)
C(32)-C(33)-C(34)-C(29)	0.3(3)
C(30)-C(29)-C(34)-C(33)	-0.8(3)
C(8)-C(29)-C(34)-C(33)	179.73(18)

Symmetry transformations used to generate equivalent atoms:

1 (1H NMR, 600 MHz)

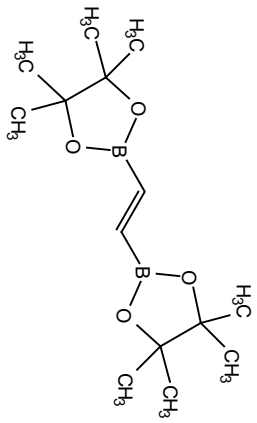

7.27 cdcl3

6.65
6.64

2.00

28.29

1.26
1.26
1.26

f1 (ppm)

1 (13C NMR, 126 MHz)

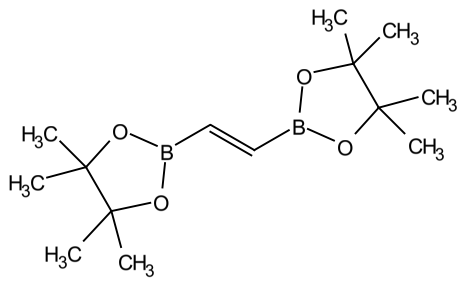

83.40
77.25 cdcl3
77.00 cdcl3
76.74 cdcl3
24.72
555

180 170 160 150 140 130 120 110 100 90 80 70 60 50 40 30 20 10 0 -10
f1 (ppm)

2 (1H NMR, 500 MHz)

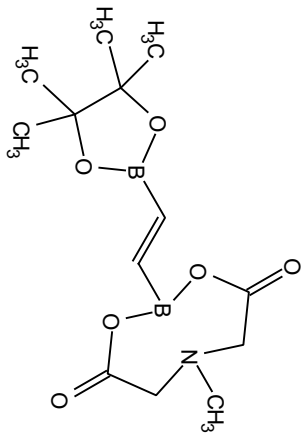

1.02
1.00
2.01
2.26
3.12
12.03

6.80
6.76
6.19
6.14
4.26
4.22
4.10
4.06
3.00
2.99
2.85 HDO
2.07 acetone
2.07 acetone
2.06 acetone
2.06 acetone
2.05 acetone
1.98
1.25

f1 (ppm)

2 (13C NMR, 126 MHz)

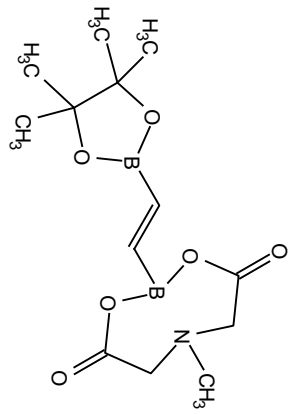

205.35
168.13
82.92
61.56
46.46
29.44 acetone
29.29 acetone
29.14 acetone
28.98 acetone
28.83 acetone
28.67 acetone
28.52 acetone
24.26

f1 (ppm)

3 (1H NMR, 500 MHz)

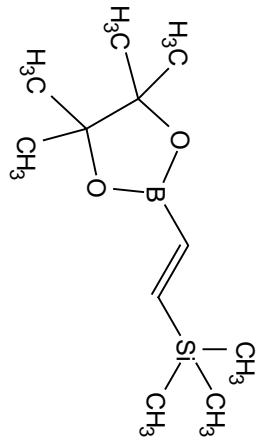

3 (13C NMR, 126 MHz)

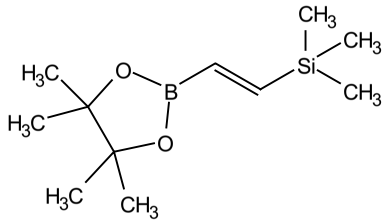

157.85
83.34
77.24 cdcl3
76.99 cdcl3
76.74 cdcl3
24.80
-1.87

559

180 170 160 150 140 130 120 110 100 90 80 70 60 50 40 30 20 10 0 -10
f1 (ppm)

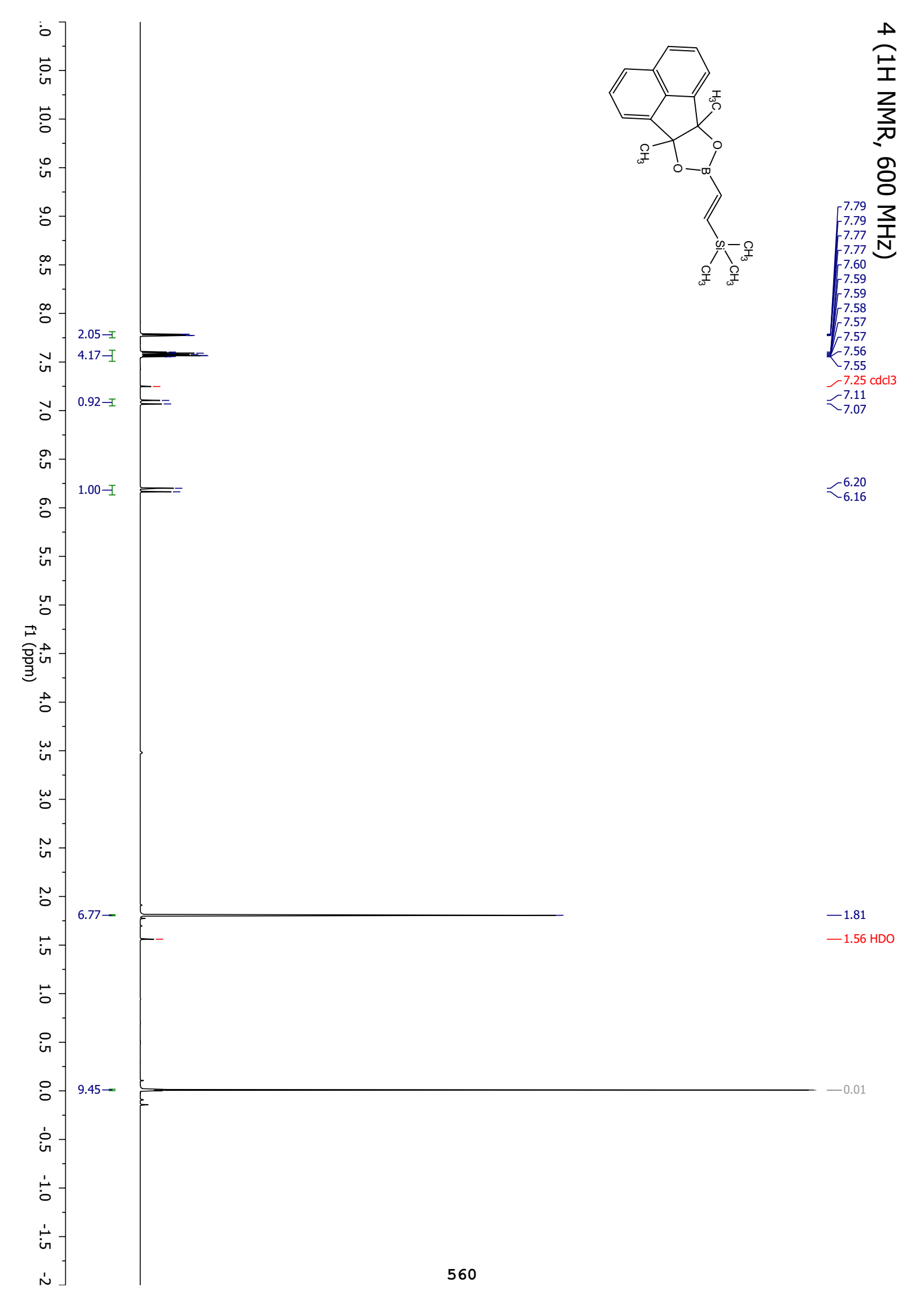
4 (1H NMR, 600 MHz)
f1 (ppm)
2.05
4.17
0.92
1.00
6.77
9.45
7.79
7.79
7.77
7.77
7.60
7.59
7.59
7.58
7.57
7.57
7.56
7.55
7.25 cdcl3
7.11
7.07
6.20
6.16
1.81
1.56 HDO
0.01

4 (13C NMR, 151 MHz)

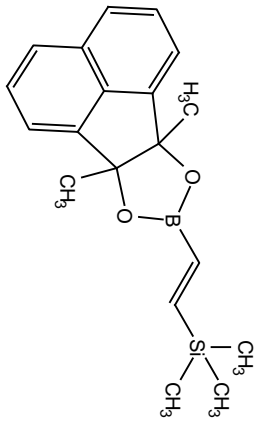

158.18
144.66
134.67
131.32
128.45
125.25
119.44
91.94
77.20 cdcl3
76.99 cdcl3
76.78 cdcl3
22.07
-1.91
-1.92
-1.94
-1.96

f1 (ppm)

5 (1H NMR, 500 MHz)

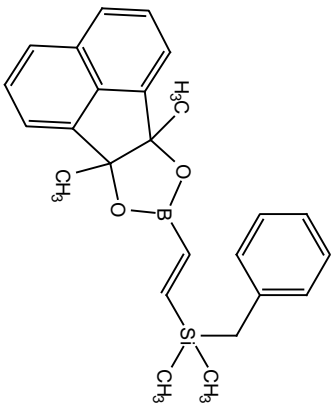

f1 (ppm)

5 (13C NMR, 126 MHz)

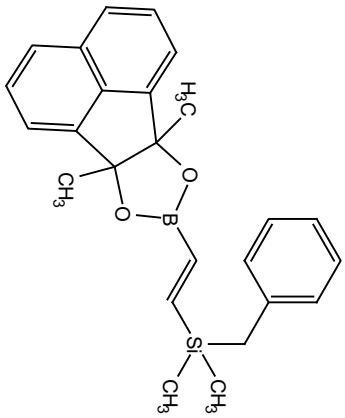

156.14
144.71
139.66
134.75
131.39
128.52
128.23
128.16
125.33
124.04
119.52
92.05
77.32 cdcl3
77.07 cdcl3
76.81 cdcl3
25.24
22.14
-3.92

f1 (ppm)

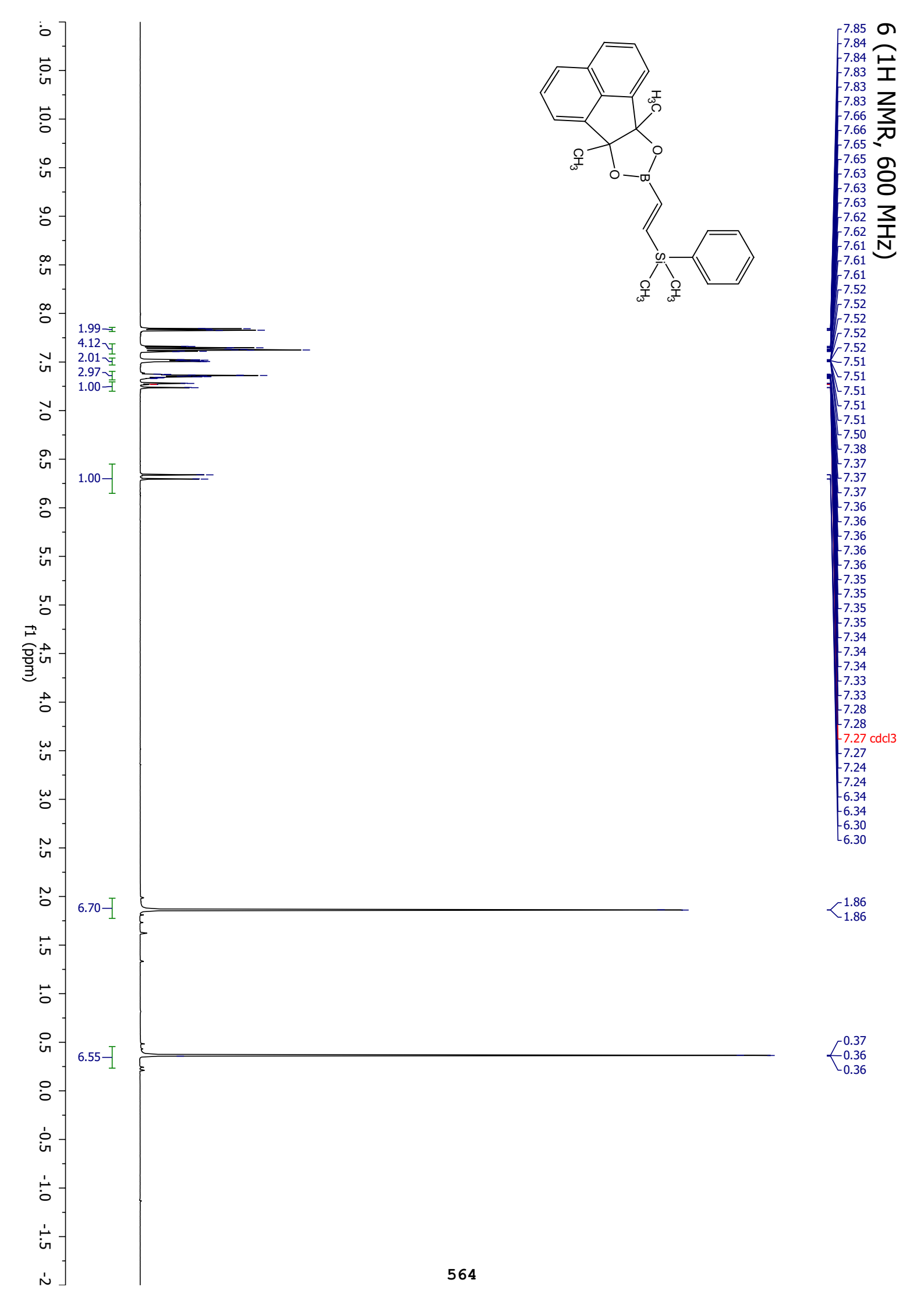
6 (1H NMR, 600 MHz)
f1 (ppm)
1.99
4.12
2.01
2.97
1.00
1.00
6.70
6.55
7.27 cdcl3
1.86
0.37

6 (13C NMR, 151 MHz)

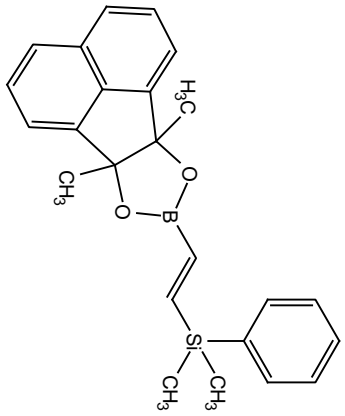

158.29
147.31
140.31
137.36
136.53
134.01
131.68
131.14
130.40
127.95
122.13
94.68
79.91 cdcl3
79.69 cdcl3
79.48 cdcl3
24.76
-0.59

f1 (ppm)

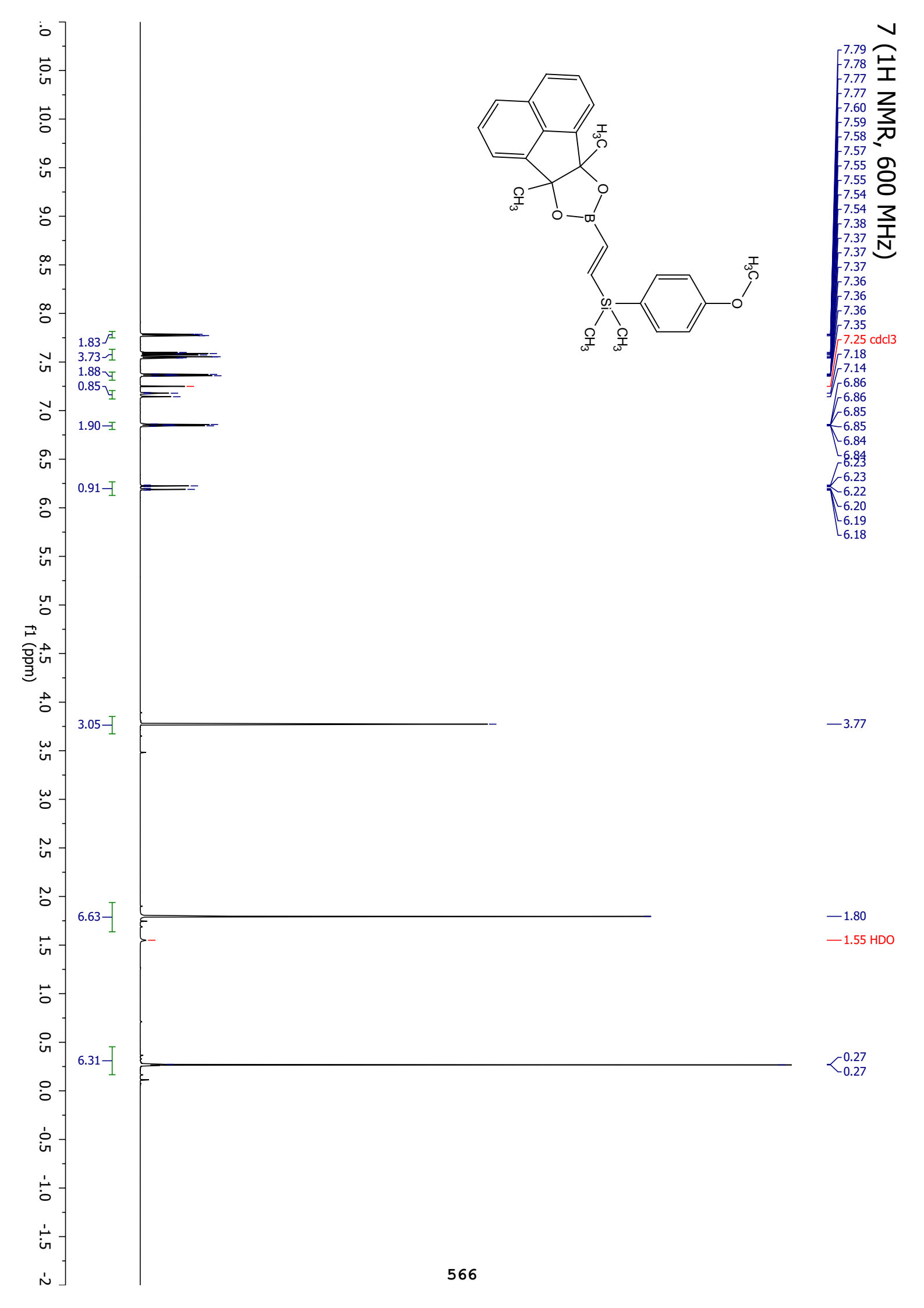
7 (1H NMR, 600 MHz)
f1 (ppm)
1.83
3.73
1.88
0.85
1.90
0.91
3.05
6.63
6.31
7.79
7.78
7.77
7.77
7.60
7.59
7.58
7.57
7.55
7.55
7.54
7.54
7.38
7.37
7.37
7.37
7.36
7.36
7.36
7.35
7.25 cdcl3
7.18
7.14
6.86
6.86
6.85
6.85
6.84
6.84
6.23
6.23
6.22
6.20
6.19
6.18
3.77
1.80
1.55 HDO
0.27
0.27

7 (13C NMR, 126 MHz)

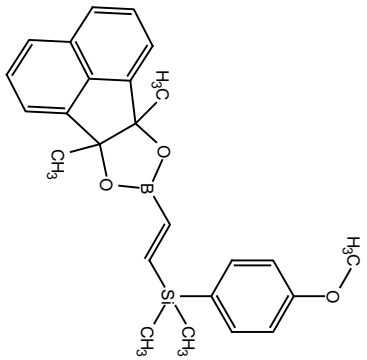

160.46
156.13
144.68
135.33
134.71
131.36
128.48
128.44
125.29
119.48
113.57
92.01
77.30 cdcl3
77.05 cdcl3
76.79 cdcl3
55.01
22.10
-3.05

f1 (ppm)

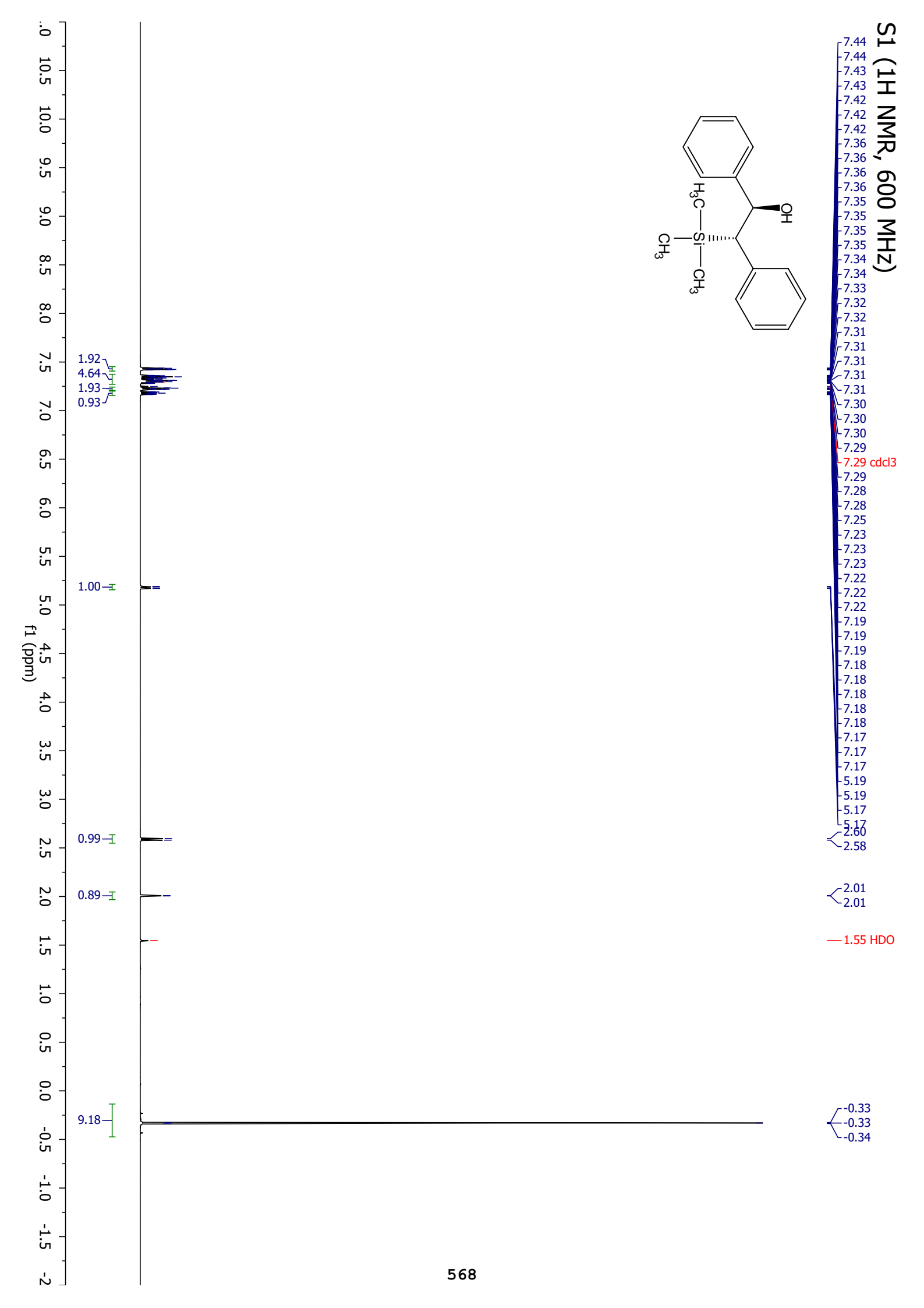
S1 (1H NMR, 600 MHz)
f1 (ppm)
1.92
4.64
1.93
0.93
1.00
0.99
0.89
9.18
7.44
7.43
7.42
7.36
7.35
7.34
7.33
7.32
7.31
7.30
7.29
7.29 cdcl3
7.28
7.25
7.23
7.22
7.19
7.18
7.17
5.19
5.17
2.60
2.58
2.01
1.55 HDO
-0.33
-0.34
OH
H3C
Si
CH3

S1 (13C NMR, 126 MHz)

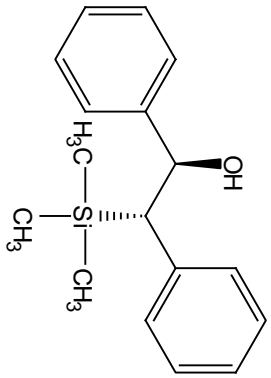

143.29
140.86
128.72
128.68
128.48
128.12
127.17
125.59
77.28 cdcl3
77.03 cdcl3
76.77 cdcl3
76.10
47.99
-2.03

f1 (ppm)

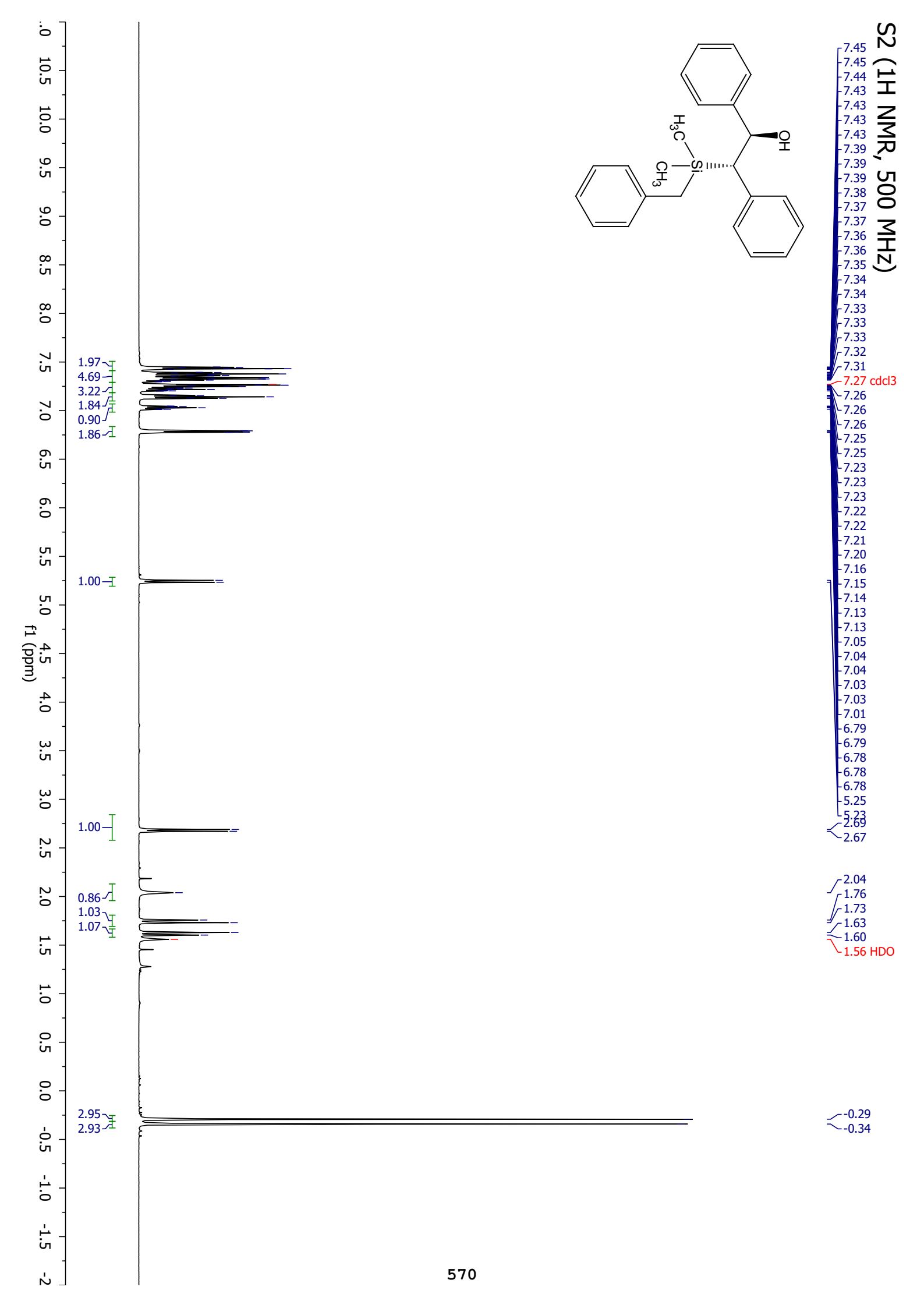
S2 (1H NMR, 500 MHz)
f1 (ppm)
1.97
4.69
3.22
1.84
0.90
1.86
1.00
1.00
0.86
1.03
1.07
2.95
2.93
7.27 cdcl3
1.56 HDO
-0.29
-0.34

S2 (13C NMR, 126 MHz)

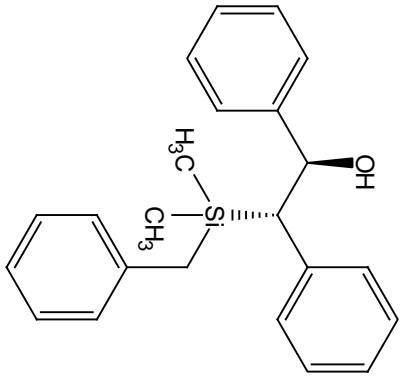

143.25
140.34
139.58
129.01
128.75
128.51
128.25
128.22
128.03
127.11
125.78
123.99
77.26 cdcl3
77.01 cdcl3
76.76 cdcl3
75.95
47.15
24.23
-3.94
-4.16

f1 (ppm)

8, (1H NMR, 500 MHz)

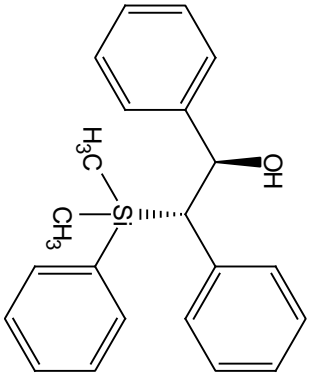

f1 (ppm)

2.89
9.55
2.86
1.00
0.99
0.83
2.93
2.95

7.32 7.32 7.31 7.31 7.31 7.30 7.30 7.30 7.30 7.29 7.29 7.29 7.29 7.28 7.27 7.27 7.27 cdcl3 7.26 7.26 7.25 7.25 7.25 7.25 7.25 7.24 7.24 7.24 7.23 7.23 7.22 7.22 7.21 7.21 7.21 7.16 7.16 7.16 7.15 7.14 7.13 7.13 7.13 7.12 7.12 7.12 7.11 7.11 7.11 7.11 5.15 5.14 5.13 5.12 2.81 2.79 1.96 1.96 1.55 HDO 1.55 HDO 0.06 0.06 -0.02 -0.02

8 (13C NMR, 126 MHz)

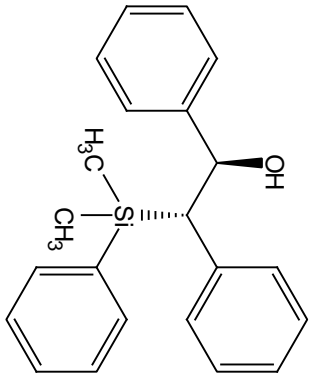

143.07
139.84
137.22
134.11
129.29
128.86
128.35
128.25
127.92
127.41
127.05
125.55

77.27 cdcl3
77.02 cdcl3
76.76 cdcl3
75.57

47.39

-3.36
-3.53

f1 (ppm)

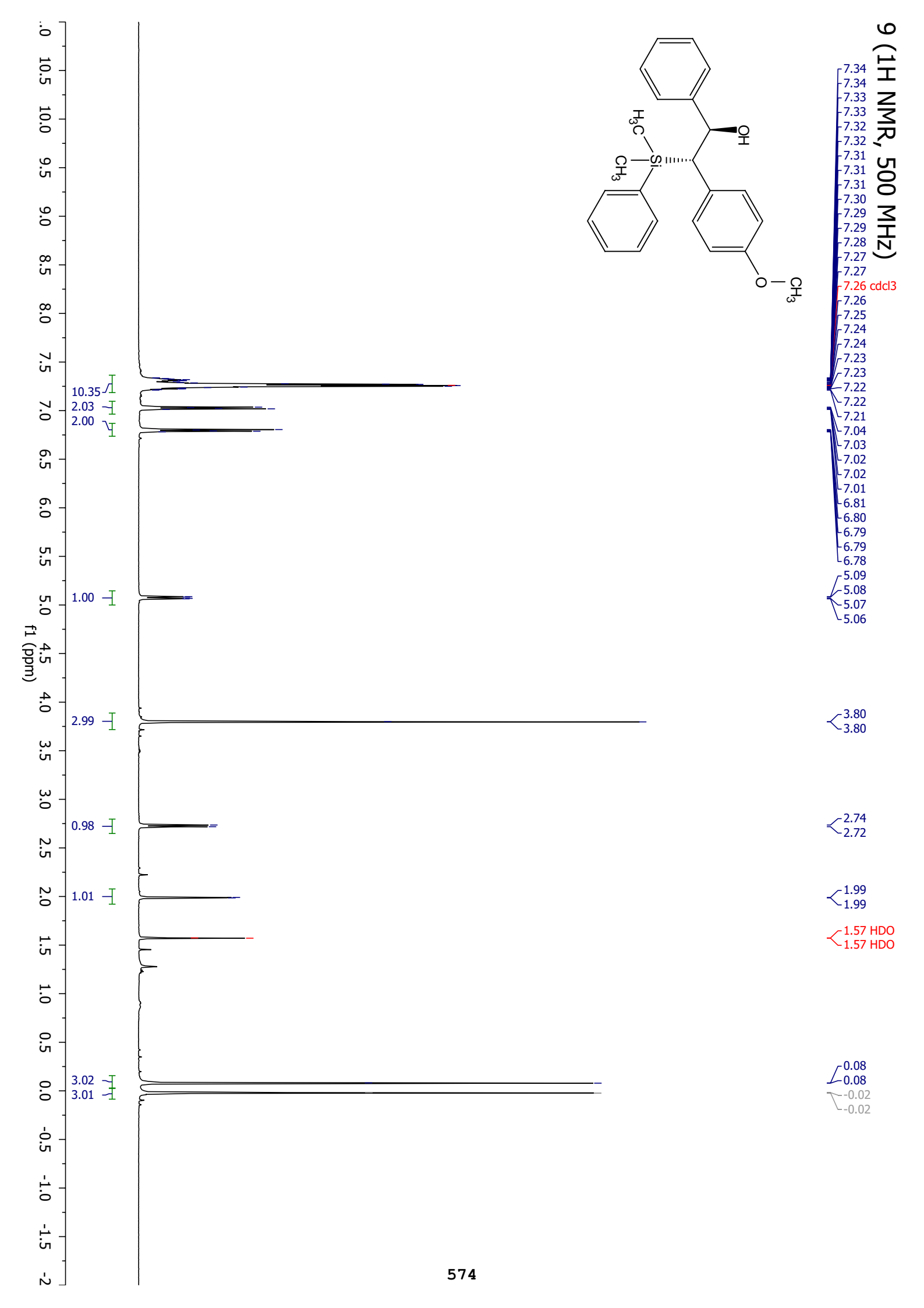
9 (1H NMR, 500 MHz)
f1 (ppm)
10.35
2.03
2.00
1.00
2.99
0.98
1.01
3.02
3.01
7.34
7.34
7.33
7.33
7.32
7.32
7.31
7.31
7.31
7.30
7.29
7.29
7.28
7.27
7.27
7.26 cdcl3
7.26
7.25
7.24
7.24
7.23
7.23
7.22
7.22
7.21
7.04
7.03
7.02
7.02
7.01
6.81
6.80
6.79
6.79
6.78
5.09
5.08
5.07
5.06
3.80
3.80
2.74
2.72
1.99
1.99
1.57 HDO
1.57 HDO
0.08
0.08
-0.02
-0.02
OH
Si
H3C
CH3
O
CH3

9 (13C NMR, 126 MHz)

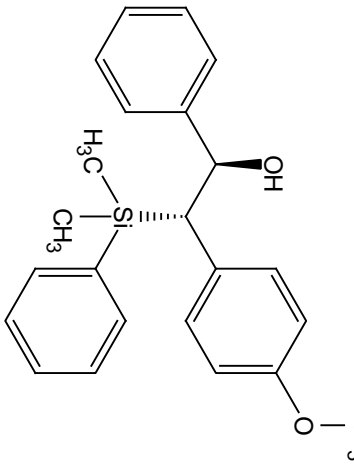

157.62
143.19
137.38
134.14
131.50
130.25
128.83
128.21
127.84
127.41
127.02
113.83
77.27 cdcl3
77.01 cdcl3
76.76 cdcl3
75.61
55.19
46.22
-3.30
-3.47

f1 (ppm)

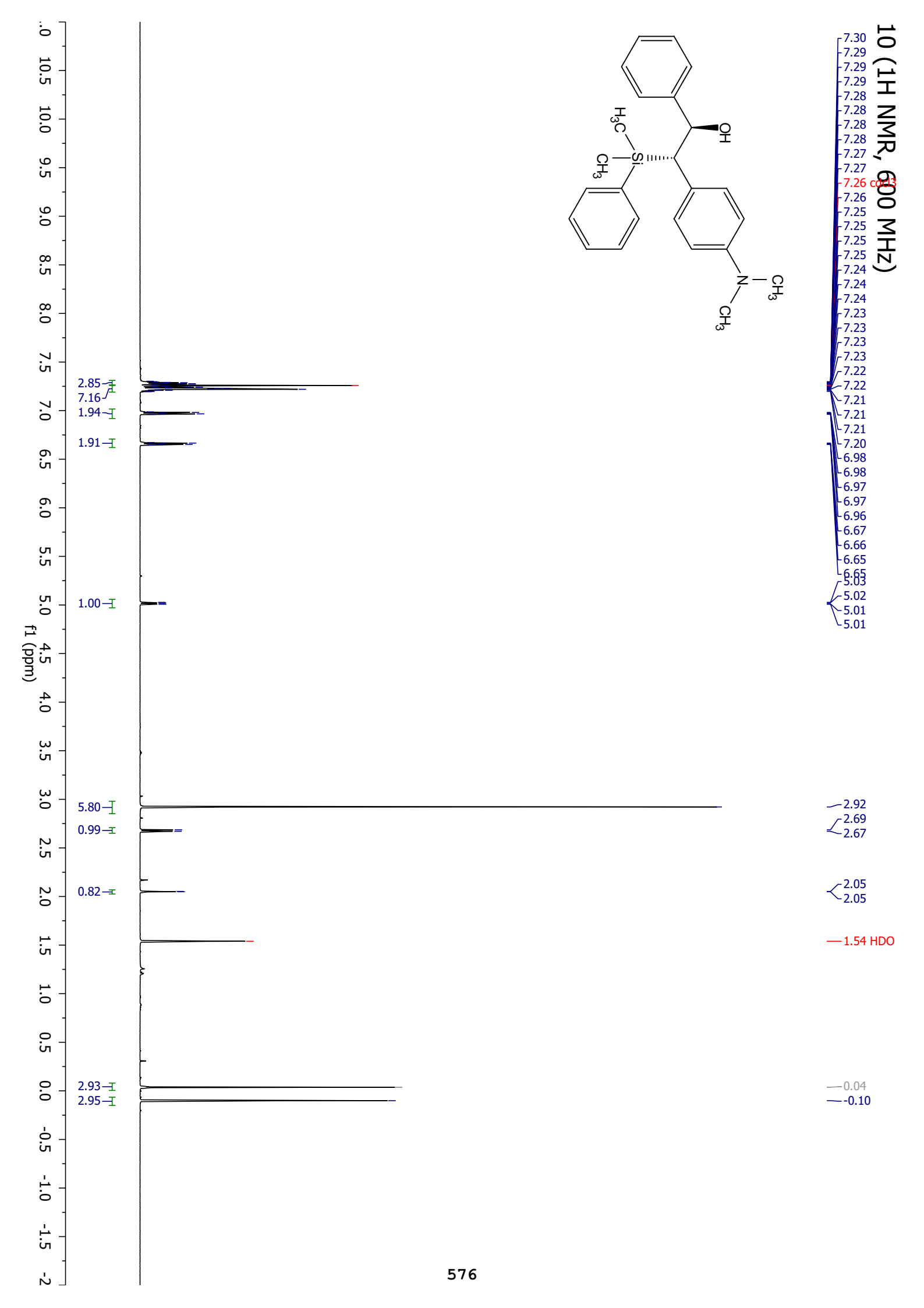
10 (1H NMR, 600 MHz)
f1 (ppm)
2.85
7.16
1.94
1.91
1.00
5.80
0.99
0.82
2.93
2.95
7.30
7.29
7.29
7.29
7.28
7.28
7.28
7.28
7.27
7.27
7.26 cdl3
7.26
7.25
7.25
7.25
7.25
7.24
7.24
7.24
7.23
7.23
7.23
7.23
7.22
7.22
7.21
7.21
7.21
7.20
6.98
6.98
6.97
6.97
6.96
6.67
6.66
6.65
6.65
5.03
5.02
5.01
5.01
2.92
2.69
2.67
2.05
2.05
1.54 HDO
0.04
-0.10
OH
Si
H3C
CH3
N
CH3
CH3

10 (13C NMR, 126 MHz)

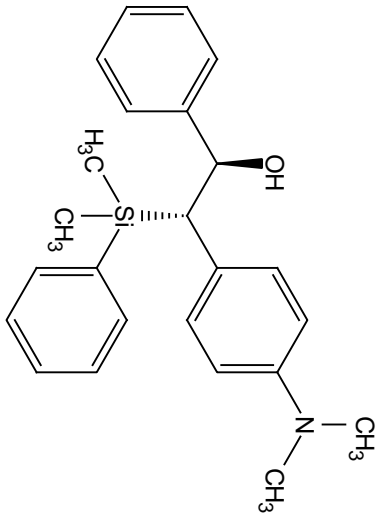

148.89
143.13
137.63
134.22
129.98
128.69
128.19
127.85
127.33
127.27
127.16
113.10
77.28 cdcl3
77.02 cdcl3
76.77 cdcl3
75.67
46.08
40.78
-3.11
-3.40

f1 (ppm)

11 (1H NMR, 500 MHz)

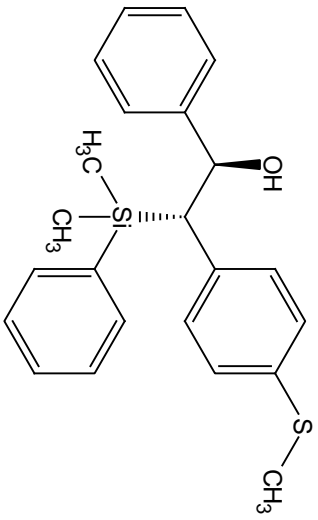

11 (13C NMR, 126 MHz)

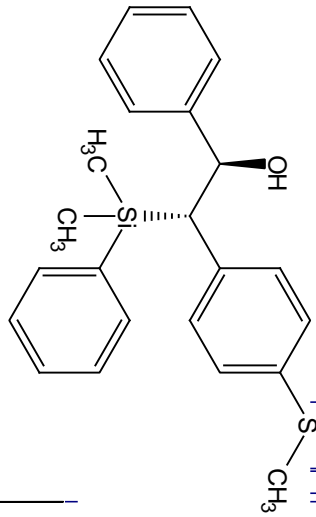

143.18
137.15
136.91
134.91
134.14
129.83
128.95
128.25
127.87
127.48
126.98
126.92

77.30 cdcl3
77.05 cdcl3
76.79 cdcl3
75.45

46.75

16.22

-3.33
-3.48

f1 (ppm)

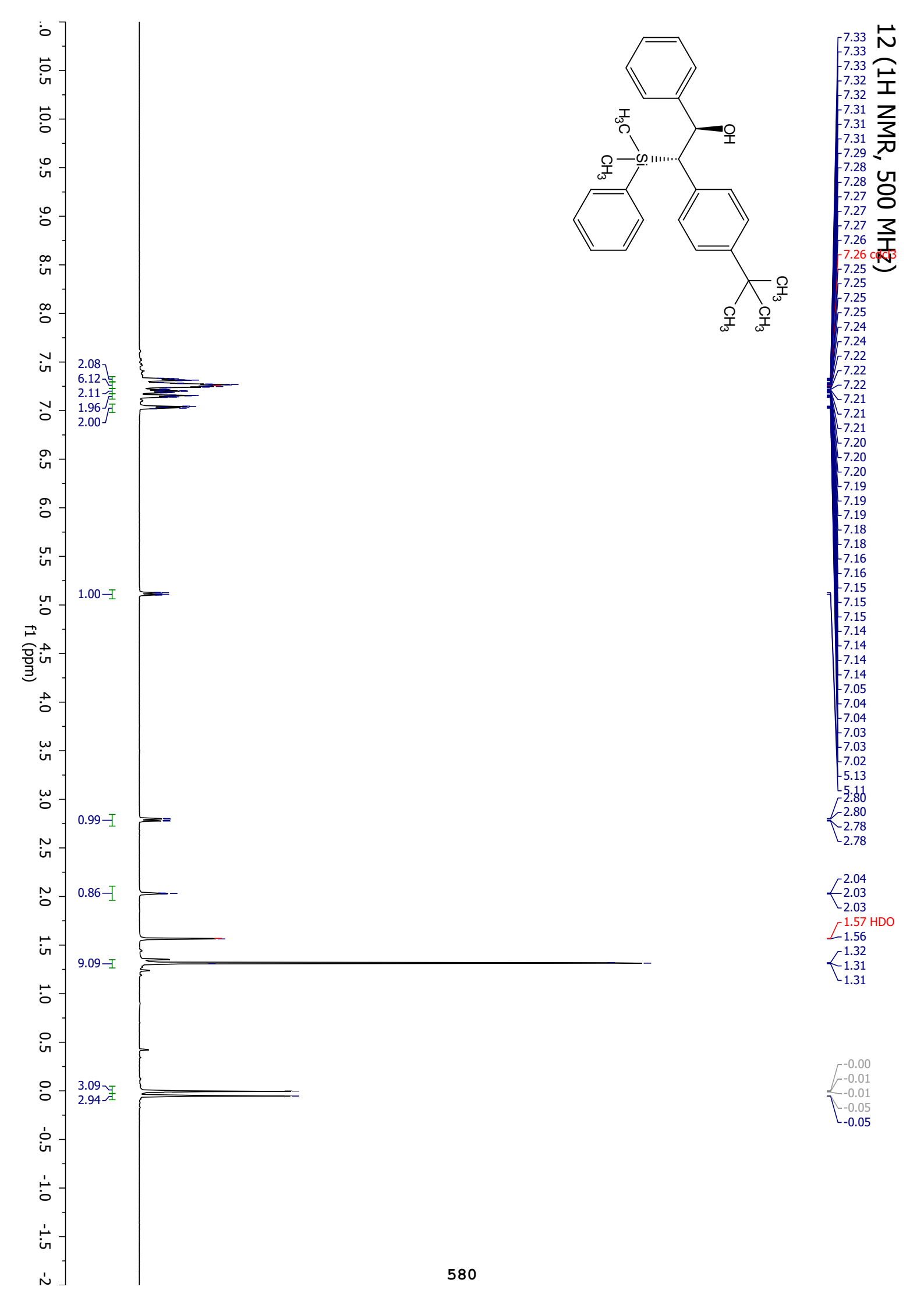
12 (1H NMR, 500 MHz)
f1 (ppm)
2.08
6.12
2.11
1.96
2.00
1.00
0.99
0.86
9.09
3.09
2.94
7.33
7.26 CDCl3
1.57 HDO
-0.00
-0.01
-0.05
OH
Si
H3C
CH3
CH3
CH3
CH3

12 (13C NMR, 126 MHz)

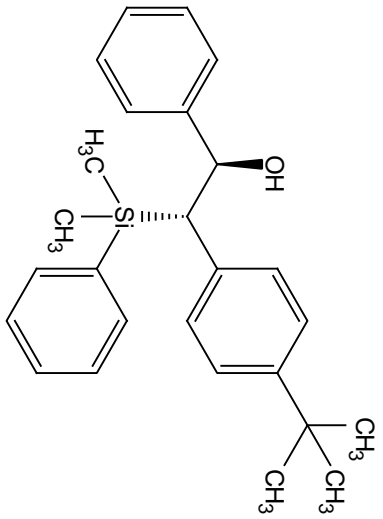

148.45
142.94
137.36
136.49
134.08
128.72
128.71
128.27
128.02
127.30
127.28
125.32
77.28 cdcl3
77.02 cdcl3
76.77 cdcl3
75.64
46.94
34.32
31.42
-3.37
-3.60

f1 (ppm)

13 (1H NMR, 500 MHz)

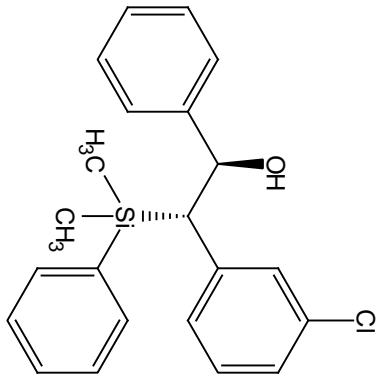

7.36
7.35
7.35
7.35
7.34
7.34
7.34
7.33
7.33
7.33
7.30
7.30
7.30
7.29
7.29
7.28
7.27 cdcl3
7.27
7.27
7.27
7.26
7.26
7.26
7.25
7.24
7.24
7.23
7.23
7.23
7.23
7.23
7.22
7.21
7.15
7.14
7.13
7.12
7.12
7.12
7.12
7.11
7.11
7.11
7.10
6.99
6.98
6.98
6.97
6.97
6.96
5.12
5.12
5.11
5.10
2.76
2.76
2.75
1.91
1.91
1.55 HDO
0.13
0.12
0.04

1.08
9.37
3.10
1.03
1.00
1.00
1.01
3.10
3.05

f1 (ppm)

13 (13C NMR, 126 MHz)

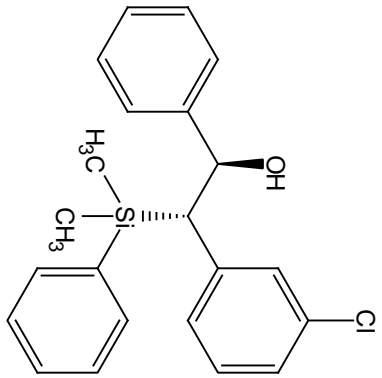

143.08
142.23
136.79
134.06
133.95
129.29
129.28
129.11
128.30
127.93
127.55
127.48
126.74
125.54
77.27 cdcl3
77.02 cdcl3
76.76 cdcl3
75.32
47.07
-3.52
-3.61

f1 (ppm)

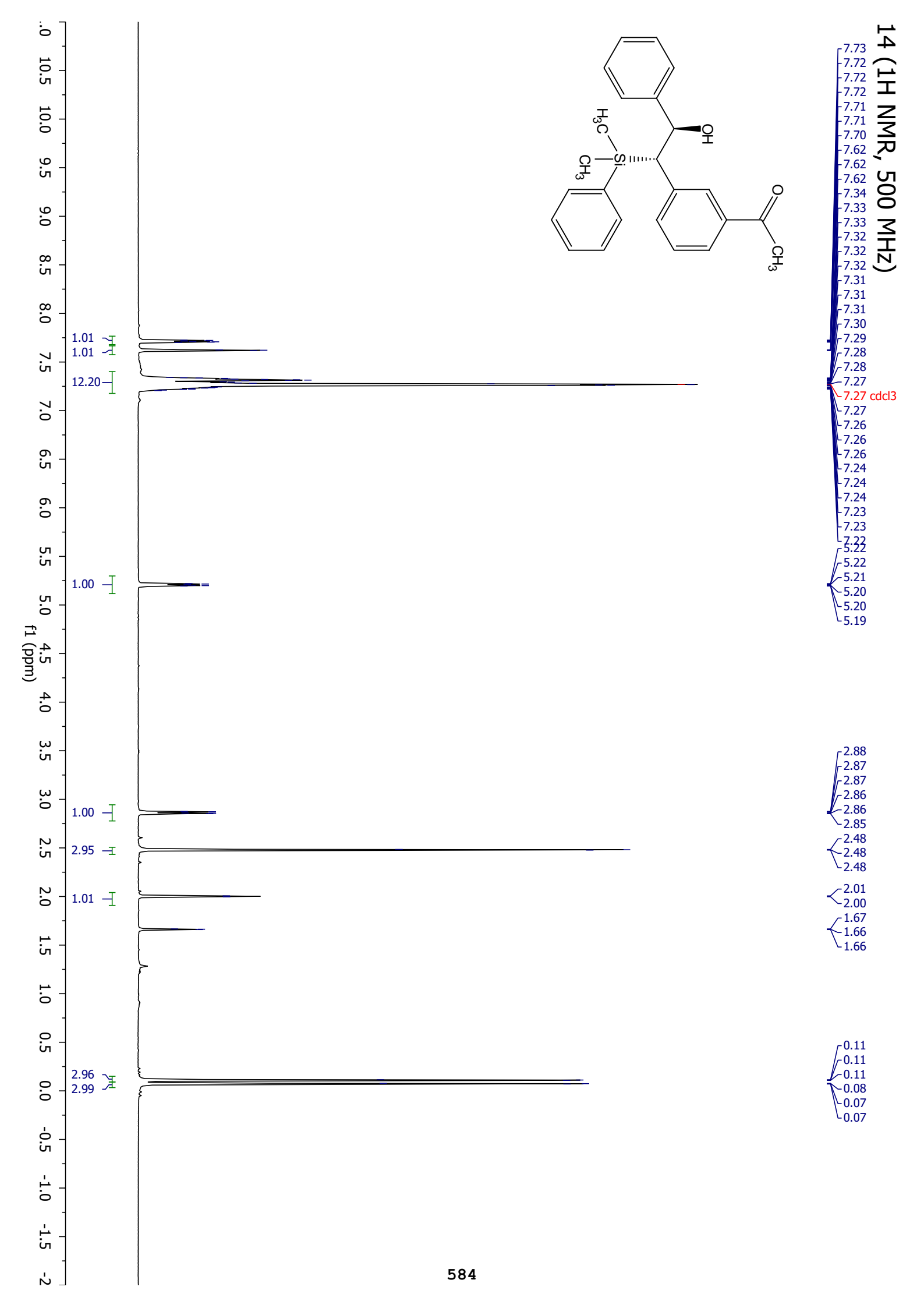
14 (1H NMR, 500 MHz)
f1 (ppm)
1.01
1.01
12.20
1.00
1.00
2.95
1.01
2.96
2.99
7.27 cdcl3
OH
Si
CH3
H3C
O
CH3

14 (13C NMR, 126 MHz)

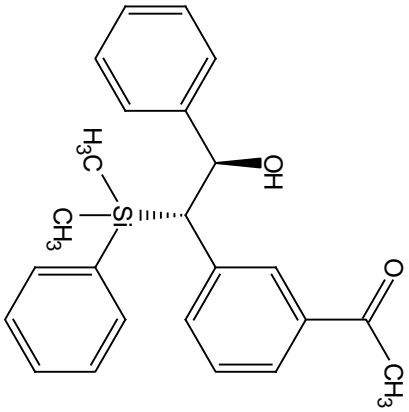

198.35

143.30
140.60
136.94
136.81
134.08
133.99
129.39
129.10
128.31
128.29
127.89
127.56
126.68
125.34

77.29 cdcl3
77.04 cdcl3
76.79 cdcl3
75.25

47.12

26.56

-3.57
-3.69

f1 (ppm)

585

15 (1H NMR, 500 MHz)

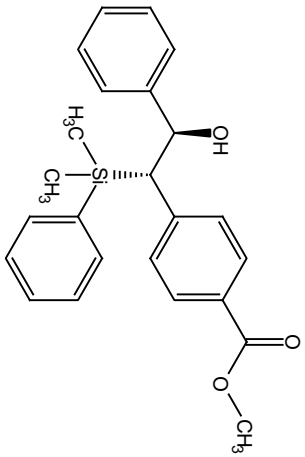

f1 (ppm)

1.99
1.13
9.05
2.03
1.00
2.98
0.99
1.00
2.89
2.97

7.89 7.88 7.88 7.87 7.87 7.86 7.36 7.35 7.35 7.35 7.34 7.34 7.33 7.33 7.32 7.32 7.31 7.29 7.29 7.28 7.28 7.27 cdcl3 7.27 7.27 7.27 7.26 7.25 7.25 7.24 7.24 7.24 7.22 7.22 7.22 7.22 7.22 7.21 7.21 7.20 7.20 7.19 7.19 7.18 7.17 7.17 7.17 5.19 5.19 5.18 5.17 5.17 5.17 3.90 3.90 2.88 2.88 2.86 2.86 1.92 1.92 1.58 1.58 HDO 0.14 0.13 0.13 0.05 0.05 0.04

15 (13C NMR, 126 MHz)

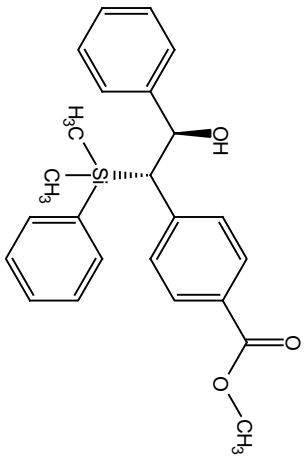

167.23
146.10
143.20
136.75
134.07
129.41
129.28
129.14
128.27
127.86
127.58
127.16
126.63
77.29 cdcl3
77.03 cdcl3
76.78 cdcl3
75.24
51.92
47.67
-3.49
-3.57

f1 (ppm)

587

16 (1H NMR, 500 MHz)

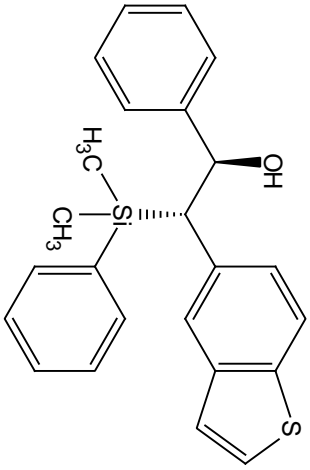

7.76
7.74
7.60
7.59
7.43
7.42
7.35
7.34
7.34
7.34
7.33
7.33
7.33
7.32
7.32
7.31
7.31
7.29
7.28
7.28
7.27
7.26 cdcl3
7.26
7.25
7.25
7.25
7.24
7.24
7.23
7.23
7.22
7.22
7.14
7.14
7.13
7.12

5.20
5.20
5.19
5.18

2.94
2.93
2.92

2.03
2.02

1.56 HDO

0.12
-0.01

0.99
1.04
1.11
3.17
8.85
1.09

1.00

1.02

1.02

3.18
3.02

f1 (ppm)

16 (13C NMR, 101 MHz)

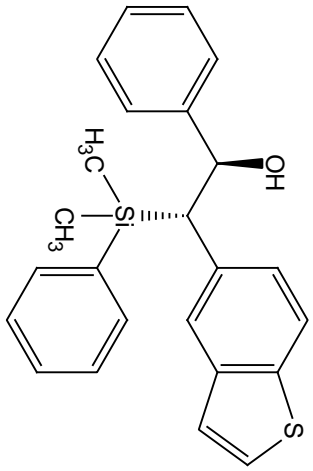

143.10
139.97
137.16
137.11
135.95
134.20
128.94
128.27
127.92
127.44
127.05
126.39
126.23
123.90
123.73
122.24

77.37 cdcl3
77.05 cdcl3
76.73 cdcl3
75.71

47.11

-3.23
-3.45

f1 (ppm)

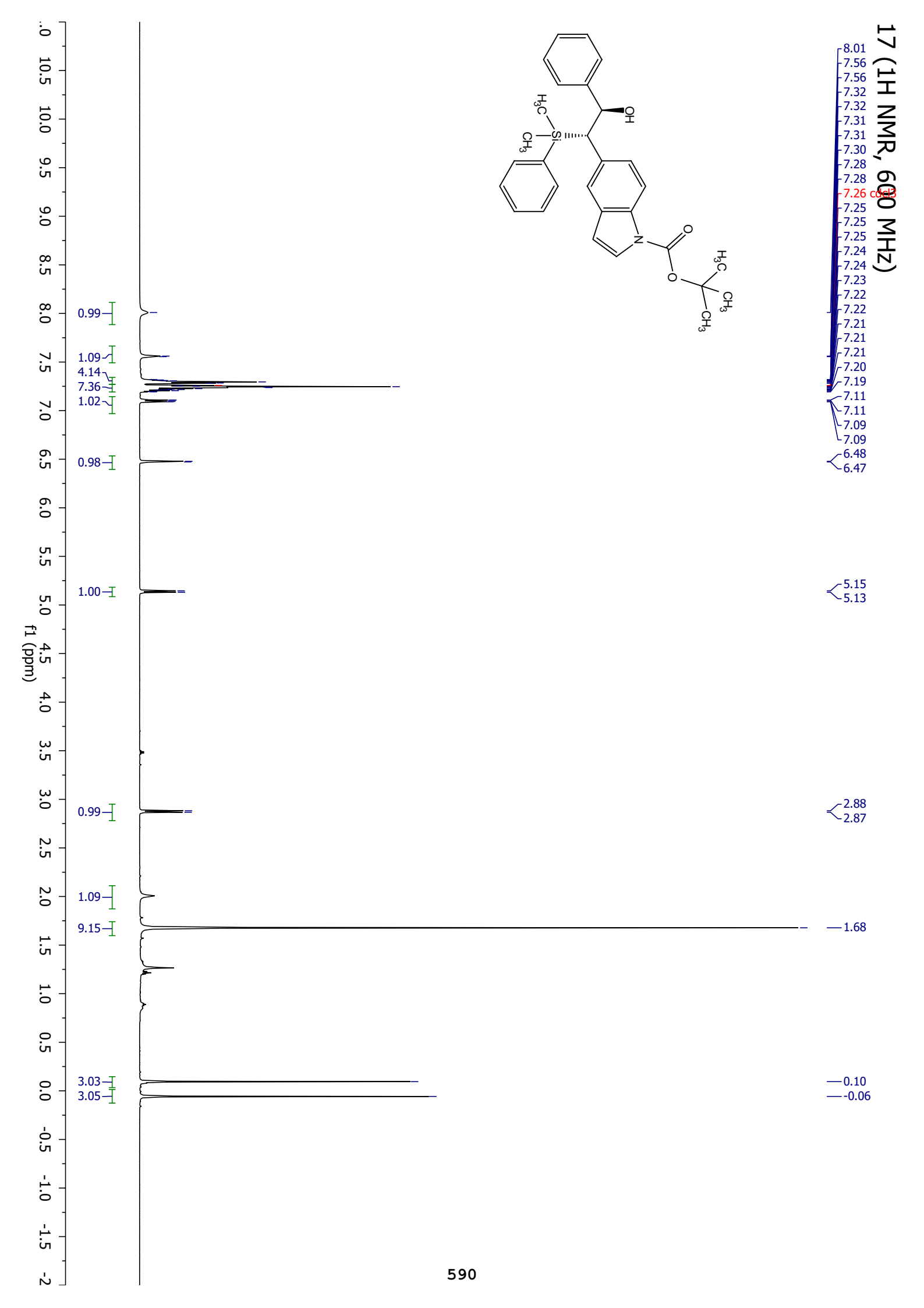
17 (1H NMR, 600 MHz)
f1 (ppm)
0.99
1.09
4.14
7.36
1.02
0.98
1.00
0.99
1.09
9.15
3.03
3.05
8.01
7.56
7.56
7.32
7.32
7.31
7.31
7.30
7.28
7.28
7.26 cdcl3
7.25
7.25
7.25
7.24
7.24
7.23
7.22
7.22
7.21
7.21
7.21
7.20
7.19
7.11
7.11
7.09
7.09
6.48
6.47
5.15
5.13
2.88
2.87
1.68
0.10
-0.06
OH
Si
N
O
O
CH3
CH3
CH3
H3C

17 (13C NMR, 126 MHz)

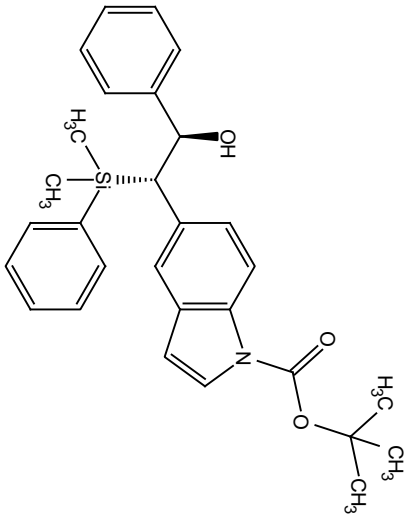

f1 (ppm)

149.78
143.11
137.35
134.21
133.93
133.58
130.87
128.84
128.22
127.86
127.41
127.11
125.95
125.80
121.41
114.99
107.18
83.51
77.27 cdcl3
77.01 cdcl3
76.76 cdcl3
75.81
47.01
28.22
-3.11
-3.44

18 (1H NMR, 600 MHz)

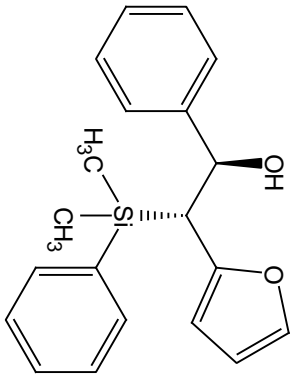

f1 (ppm)

18 (13C NMR, 151 MHz)

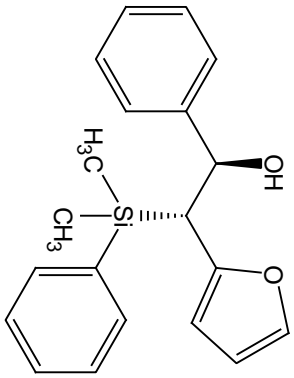

154.03
143.21
141.11
137.06
133.96
129.09
128.14
127.62
127.61
126.36
110.45
107.25
77.28 cdcl3
77.07 cdcl3
76.85 cdcl3
74.21
40.02
-3.29
-3.40

f1 (ppm)

19 (1H NMR, 500 MHz)

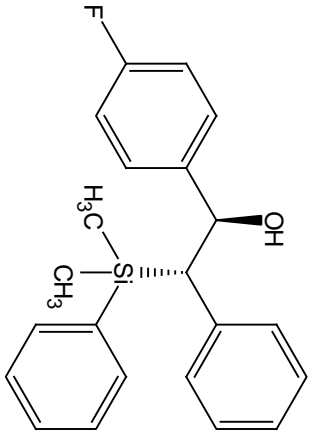

f1 (ppm)

1.05
9.06
1.95
1.97
1.00
0.99
1.01
3.00
3.00

7.34 7.34 7.33 7.32 7.32 7.31 7.31 7.28 7.27 7.27 7.27 cdcl3 7.25 7.25 7.24 7.23 7.23 7.22 7.21 7.21 7.21 7.20 7.19 7.19 7.18 7.17 7.17 7.16 7.16 7.15 7.15 7.13 6.92 6.91 6.90 6.90 6.89 6.88

5.14 5.13 5.12 5.12

2.78 2.76

2.01 2.00

1.56 HDO

0.14 0.13 -0.01 -0.02

19 (13C NMR, 126 MHz)

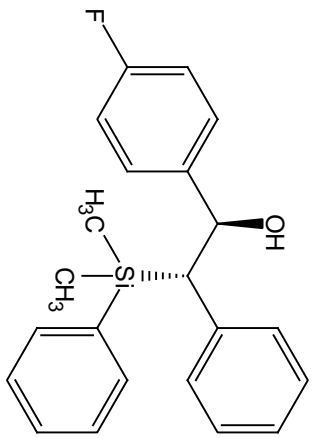

163.33
161.37
139.66
138.75
138.72
137.09
133.96
129.23
128.90
128.66
128.60
128.48
127.47
125.72
115.07
114.90
77.28 cdcl3
77.02 cdcl3
76.77 cdcl3
74.90
47.61
-3.08
-3.82

f1 (ppm)

595

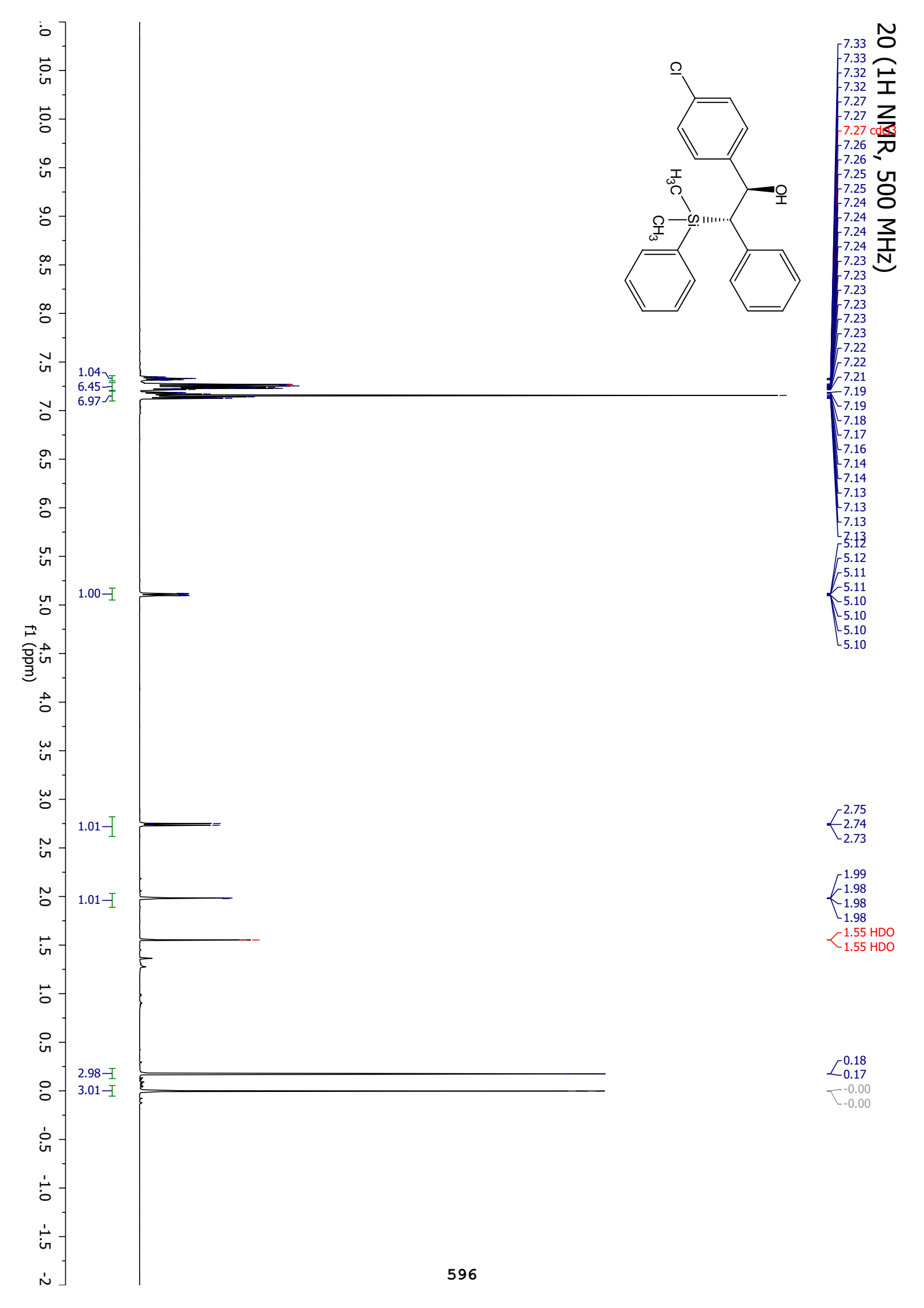
20 (1H NMR, 500 MHz)
f1 (ppm)
Cl
H3C
Si
CH3
OH
7.33
7.33
7.32
7.32
7.27
7.27
7.27 CDCl3
7.26
7.26
7.25
7.25
7.24
7.24
7.24
7.24
7.23
7.23
7.23
7.23
7.23
7.23
7.22
7.22
7.21
7.19
7.19
7.18
7.17
7.16
7.14
7.14
7.13
7.13
7.13
7.13
5.12
5.12
5.11
5.11
5.10
5.10
5.10
5.10
2.75
2.74
2.73
1.99
1.98
1.98
1.98
1.55 HDO
1.55 HDO
0.18
0.17
-0.00
-0.00
1.04
6.45
6.97
1.00
1.01
1.01
2.98
3.01

20 (13C NMR, 126 MHz)

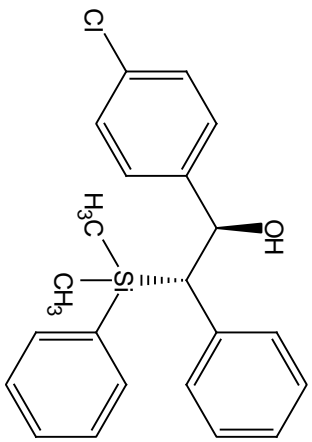

141.51
139.49
137.08
133.93
133.40
129.29
128.91
128.48
128.30
128.26
127.54
125.74

77.31 cdcl3
77.06 cdcl3
76.80 cdcl3
74.92

47.43

-2.94
-3.88

f1 (ppm)

21 (1H NMR, 500 MHz)

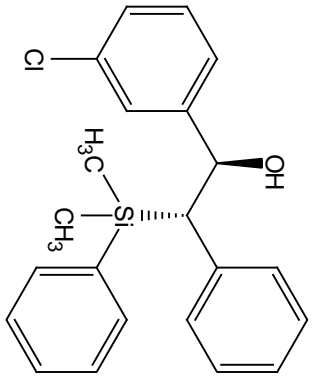

f1 (ppm)

8.36
5.92
1.00
0.98
1.02
2.93
3.01

7.34 7.34 7.33 7.33 7.33 7.32 7.32 7.32 7.31 7.31 7.30 7.29 7.29 7.27 7.27 cdcl3 7.26 7.26 7.25 7.24 7.23 7.22 7.19 7.19 7.17 7.17 7.16 7.15 7.14 7.14 7.13

5.10 5.10 5.10 5.09 5.08 5.08

2.76 2.75 2.74 2.74

2.01 2.01 2.00

1.55 HDO

0.18 0.17 0.01 0.00

21 (13C NMR, 126 MHz)

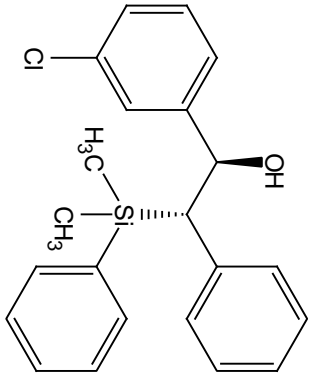

145.08
139.33
136.99
134.04
133.97
129.42
129.28
129.02
128.46
127.88
127.51
127.23
125.76
125.07
77.27 cdcl3
77.01 cdcl3
76.76 cdcl3
75.01
47.29
-3.04
-3.79

f1 (ppm)

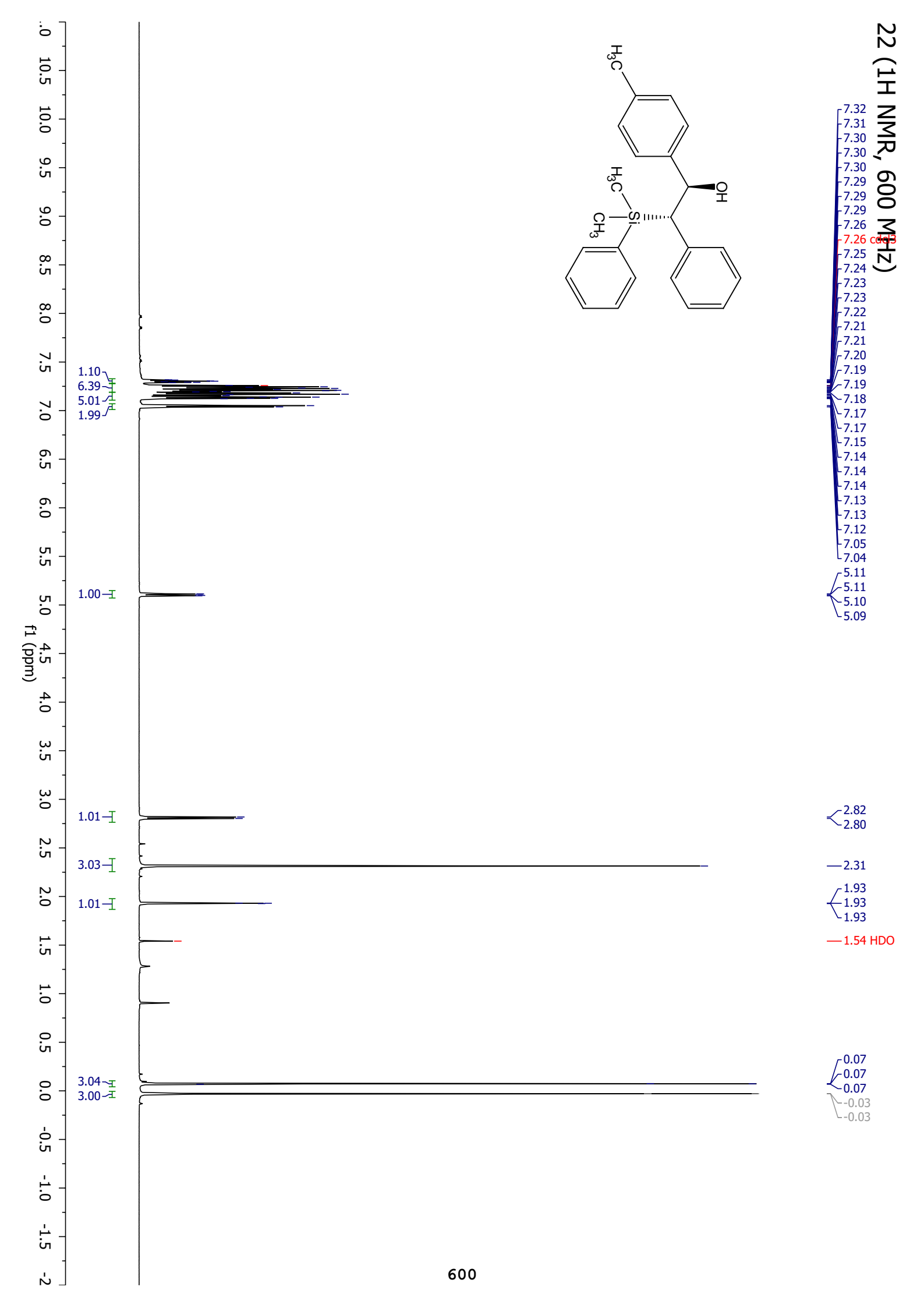
22 (1H NMR, 600 MHz)
f1 (ppm)
600
H3C
H3C
Si
CH3
OH
1.10
6.39
5.01
1.99
1.00
1.01
3.03
1.01
3.04
3.00
7.32
7.31
7.30
7.30
7.30
7.29
7.29
7.29
7.26
7.26 cdcl3
7.25
7.24
7.23
7.23
7.22
7.21
7.21
7.20
7.19
7.19
7.18
7.17
7.17
7.15
7.14
7.14
7.14
7.13
7.13
7.12
7.05
7.04
5.11
5.11
5.10
5.09
2.82
2.80
2.31
1.93
1.93
1.93
1.54 HDO
0.07
0.07
0.07
-0.03
-0.03

22 (13C NMR, 126 MHz)

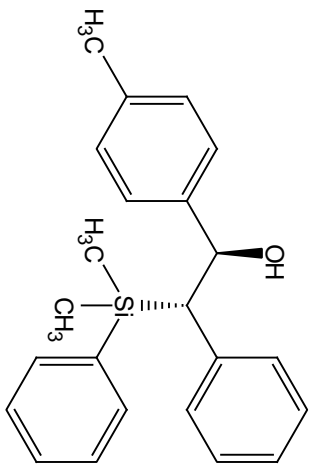

140.11
139.99
137.56
137.26
134.10
129.21
128.90
128.70
128.37
127.33
127.01
125.51

77.29 cdcl3
77.03 cdcl3
76.78 cdcl3
75.41

47.41

21.16

-3.24
-3.64

f1 (ppm)

601

23 (1H NMR, 400 MHz)

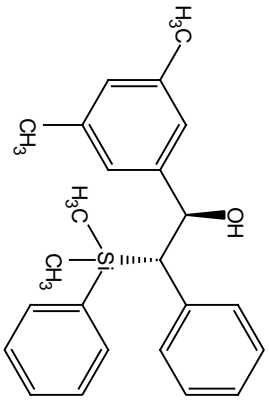

f1 (ppm)

5.35
4.85
1.93
0.99
1.00
0.98
6.08
1.01
3.00
3.00

7.29
7.27
7.26
7.25
7.25 cdcl3
7.25
7.24
7.23
7.21
7.19
7.17
7.17
7.15
7.13
6.87
6.82
5.05
5.02
2.82
2.80
2.24
1.91
1.91
1.53 HDO
0.05
0.05
-0.08
-0.09

23 (13C NMR, 101 MHz)

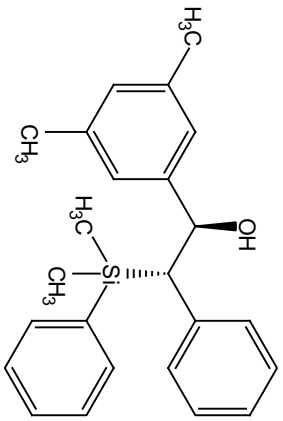

142.43
140.30
137.66
137.31
134.01
129.58
129.07
128.72
128.44
127.17
125.53
125.08

77.32 cdcl3
77.00 cdcl3
76.68 cdcl3
75.76

47.26

21.22

-3.16
-3.75

f1 (ppm)

603

24 (1H NMR, 600 MHz)

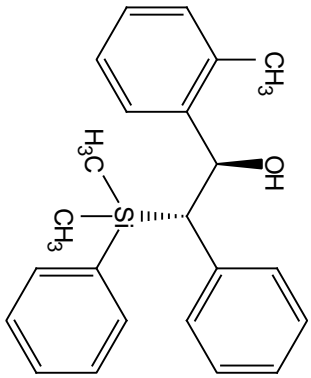

f1 (ppm)

3.09
1.88
2.01
3.96
2.03
0.98
1.00
1.02
2.98
1.00
3.01
3.05

7.26 cdcl3
1.53 HDO

24 (13C NMR, 151 MHz)

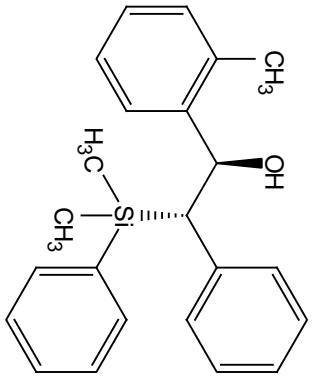

141.05
139.57
137.55
134.52
134.06
130.46
129.78
128.97
128.15
127.52
127.29
126.93
125.67
125.49

77.25 cdcl3
77.04 cdcl3
76.82 cdcl3

71.60

45.01

19.27

-3.00
-3.43

f1 (ppm)

605

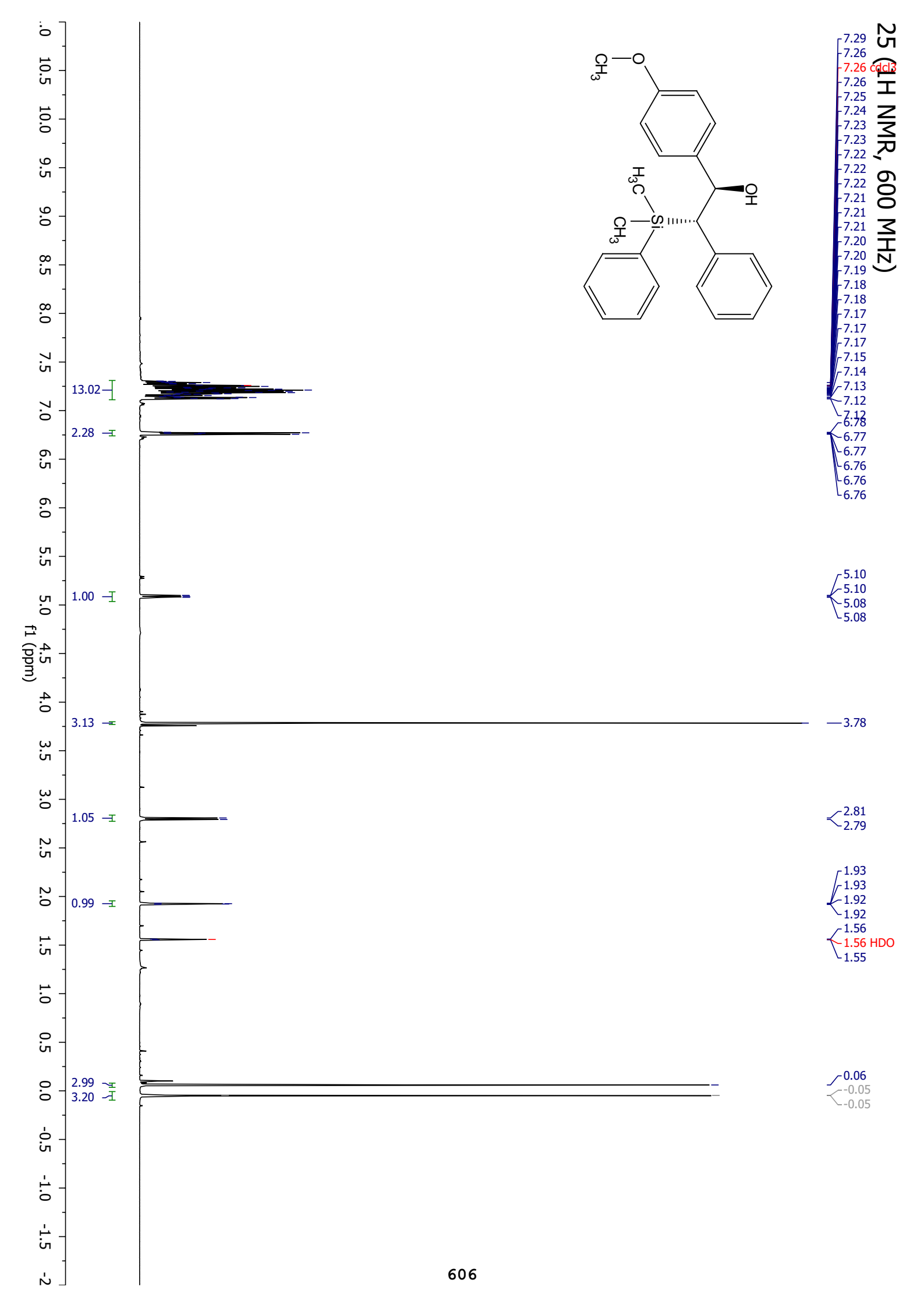
25 (1H NMR, 600 MHz)
f1 (ppm)
13.02
2.28
1.00
3.13
1.05
0.99
2.99
3.20
7.29
7.26
7.26 cdcl3
7.25
7.24
7.23
7.22
7.21
7.20
7.19
7.18
7.17
7.15
7.14
7.13
7.12
6.78
6.77
6.76
5.10
5.08
3.78
2.81
2.79
1.93
1.92
1.56
1.56 HDO
1.55
0.06
-0.05
CH3
O
H3C
Si
OH

25 (13C NMR, 151 MHz)

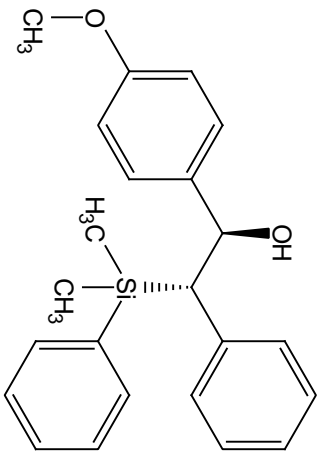

159.33
140.15
137.24
135.05
134.05
129.11
128.74
128.43
128.32
127.33
125.55
113.61
77.23 cdcl3
77.02 cdcl3
76.81 cdcl3
75.13
55.23
47.52
-3.20
-3.71

f1 (ppm)

26 (1H NMR, 600 MHz)

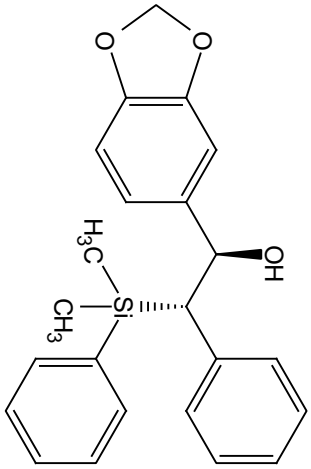

f1 (ppm)

3.63
2.03
4.98
1.98
1.03
1.98
1.00
0.98
0.99
2.95
3.00

7.29
7.29
7.28
7.27
7.27
7.27
7.26 CDCl3
7.26
7.25
7.23
7.22
7.21
7.19
7.19
7.19
7.18
7.18
7.18
7.17
7.17
7.16
7.15
7.14
7.14
7.13
6.75
6.75
6.74
6.65
6.65
6.65
6.64
6.64
5.90
5.90
5.89
5.87
5.87
5.87
5.06
5.06
5.05
5.04
2.77
2.75
1.92
1.92
1.54 HDO
0.14
-0.04

26 (13C NMR, 126 MHz)

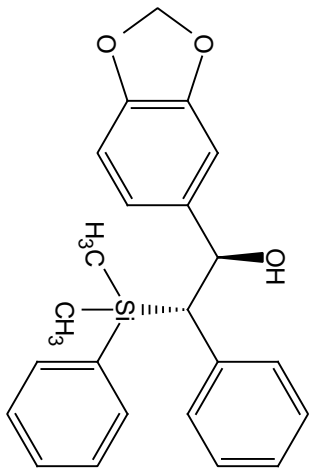

147.56
147.24
139.96
137.26
136.81
133.93
129.09
128.68
128.52
127.31
125.67
120.64
107.72
107.42
100.90
77.28 cdcl3
77.02 cdcl3
76.77 cdcl3
75.41
47.64
-2.99
-4.12

f1 (ppm)

609

27 (1H NMR, 500 MHz)

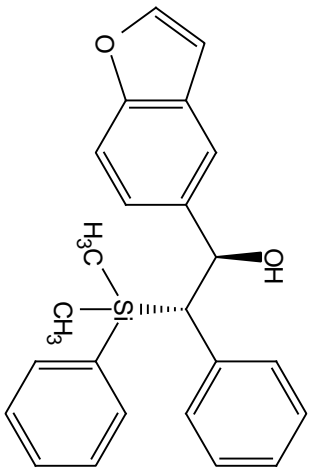

f1 (ppm)

0.99
1.00
1.02
4.16
6.93
1.01
1.00
0.99
1.02
2.97
3.01

7.62
7.61
7.50
7.50
7.36
7.34
7.29
7.29
7.28
7.27
7.27
7.26
7.26
7.25
7.24
7.24
7.20
7.20
7.19
7.18
7.18
7.17
7.17
7.16
7.16
7.16
7.15
6.71
6.71
6.71
6.71
6.71
5.27
5.26
5.25
5.24
2.90
2.88
2.07
2.07
2.06
1.57 HDO
0.09
0.09
0.09
-0.06
-0.06
-0.07

27 (13C NMR, 126 MHz)

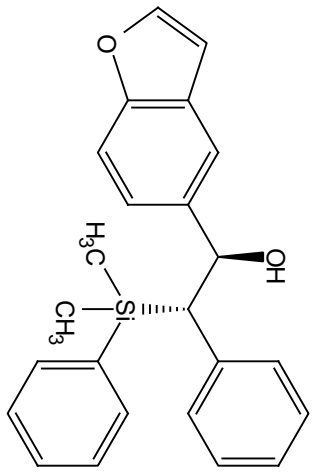

154.70
145.19
140.14
137.54
137.15
133.94
129.17
128.72
128.49
127.21
127.18
125.63
123.51
119.91
111.09
106.64
77.29 cdcl3
77.04 cdcl3
76.78 cdcl3
75.76
48.00
-3.10
-3.87

f1 (ppm)

28 (1H NMR, 600 MHz)

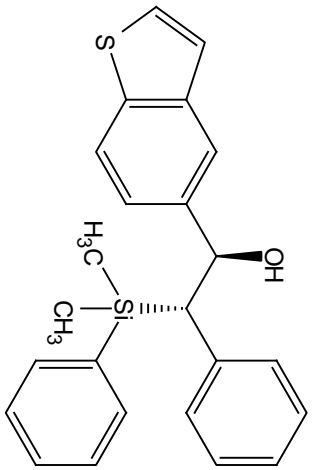

f1 (ppm)

2.00
1.03
12.30
1.00
0.98
1.01
3.00
3.01

7.71
7.69
7.67
7.67
7.42
7.41
7.29
7.28 CHCl3
7.27
7.26
7.26
7.25
7.24
7.23
7.23
7.22
7.21
7.21
7.20
7.19
7.18
7.17
7.16
7.16
7.15
7.14
7.13
7.12
5.27
5.27
5.25
5.25
2.90
2.89
2.06
2.06
1.55 HDO
0.12
-0.06

28 (13C NMR, 101 MHz)

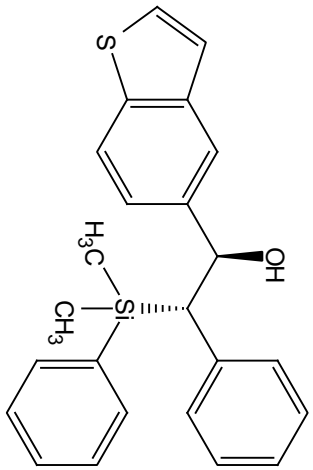

140.04
139.43
139.28
139.14
137.09
133.88
129.21
128.68
128.49
127.20
126.55
125.65
123.85
123.44
122.30
122.22

77.30 cdcl3
77.04 cdcl3
76.79 cdcl3
75.76

47.76

-2.97
-3.89

f1 (ppm)

29 (1H NMR, 500 MHz)

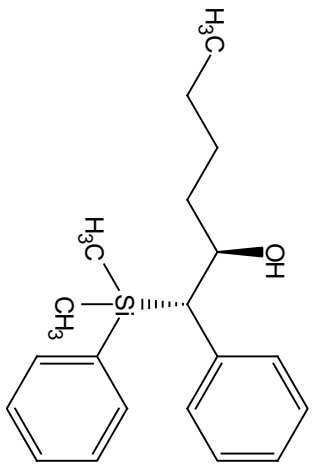

f1 (ppm)

1.97
2.87
2.07
2.83
1.00
0.99
6.34
3.05
3.11
2.96

7.25 cdcl3
1.51 HDO

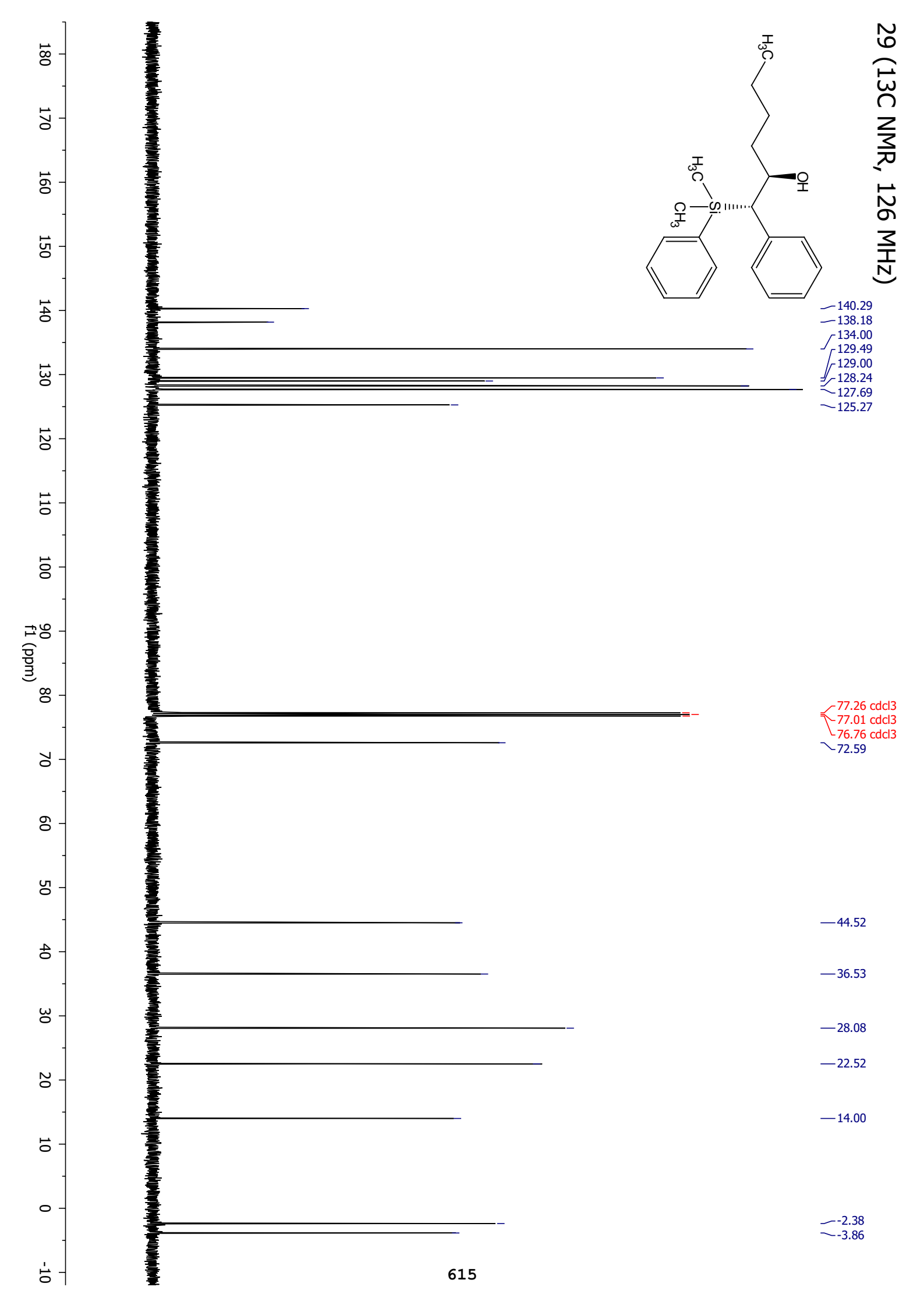
29 (13C NMR, 126 MHz)
f1 (ppm)
180
170
160
150
140
130
120
110
100
90
80
70
60
50
40
30
20
10
0
-10
H3C
OH
H3C
Si
CH3
140.29
138.18
134.00
129.49
129.00
128.24
127.69
125.27
77.26 cdcl3
77.01 cdcl3
76.76 cdcl3
72.59
44.52
36.53
28.08
22.52
14.00
-2.38
-3.86
615

30 (1H NMR, 500 MHz)

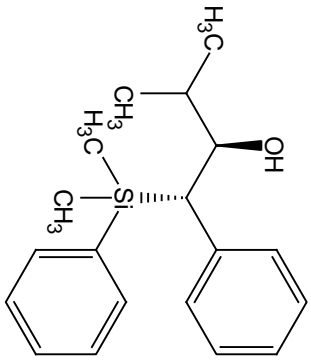

f1 (ppm)

2.03
3.25
2.14
3.18
1.00
1.02
1.10
6.26
3.08
3.05

7.49 7.48 7.48 7.48 7.47 7.47 7.46 7.46 7.46 7.38 7.37 7.37 7.36 7.36 7.35 7.35 7.34 7.34 7.34 7.33 7.33 7.32 7.32 7.28 7.27 7.27 7.26 7.25 cdcl3 7.24 7.23 7.23 7.22 7.21 7.21 7.19 7.18 7.18 7.18 7.17 7.17 7.16 7.16 7.16 7.15 7.15 7.14 7.14 7.14 7.13 7.13 3.67 3.66 3.65 3.65 3.65 3.64 2.56 2.55 2.55 2.54 2.54 1.64 1.64 1.63 1.62 1.62 1.61 1.56 HDO 1.56 HDO 0.84 0.84 0.83 0.82 0.82 0.80 0.80 0.79 0.79 0.78 0.37 0.36 0.36 0.36 0.22 0.22 0.21 0.21

30 (13C NMR, 126 MHz)

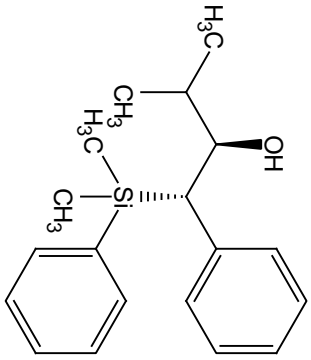

140.18
138.20
134.05
129.76
128.93
127.99
127.63
125.05

78.32
77.25 cdcl3
77.00 cdcl3
76.74 cdcl3

41.78
31.95
19.75
17.77
-2.69
-3.77

f1 (ppm)

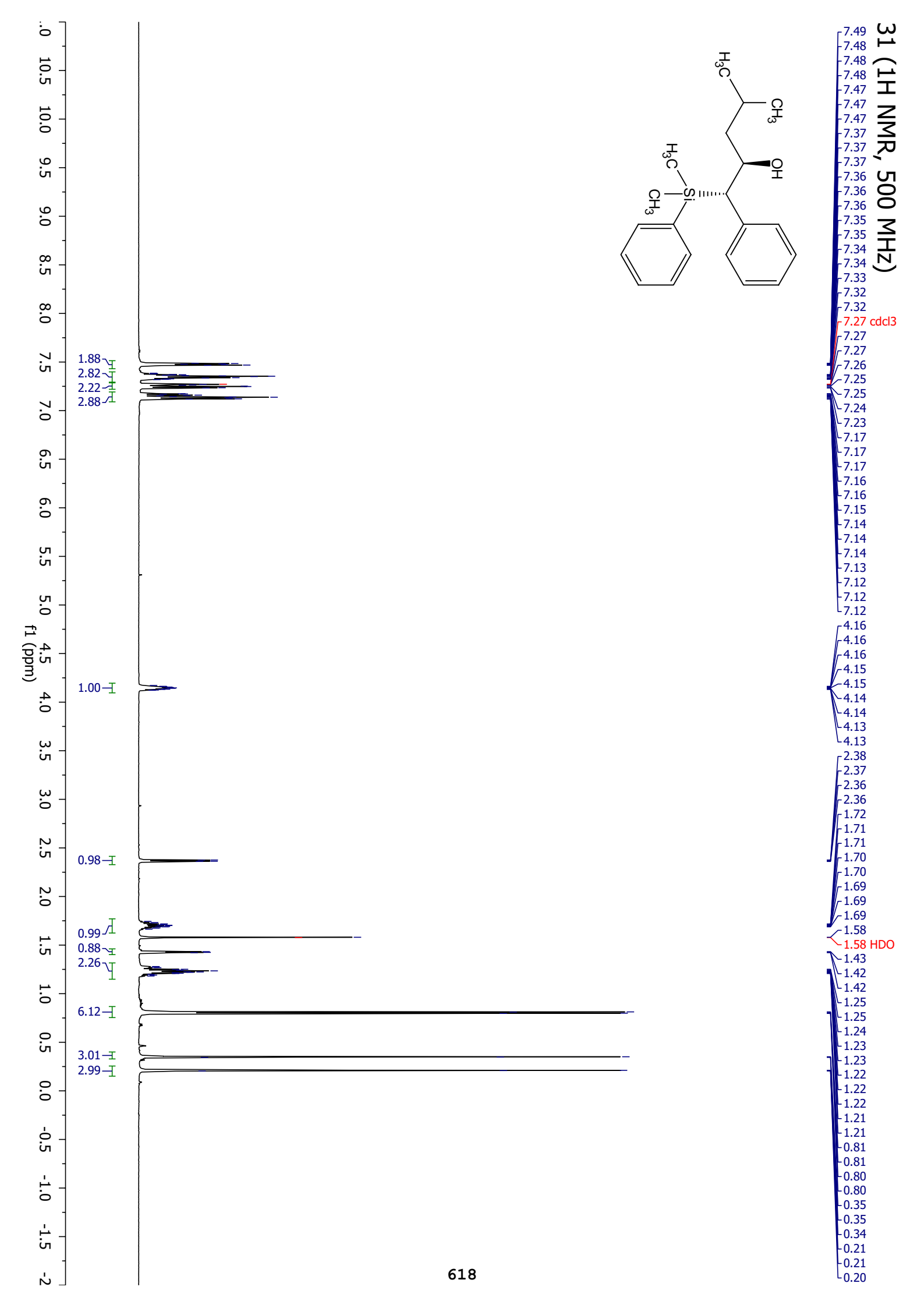
31 (1H NMR, 500 MHz)
f1 (ppm)
1.88
2.82
2.22
2.88
1.00
0.98
0.99
0.88
2.26
6.12
3.01
2.99
7.27 cdcl3
1.58 HDO

31 (13C NMR, 126 MHz)

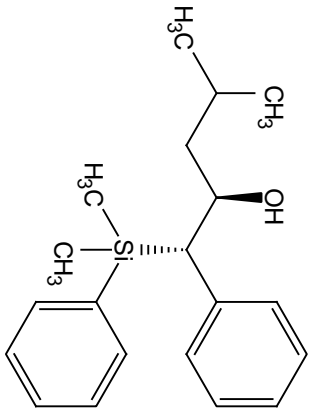

32 (1H NMR, 500 MHz)

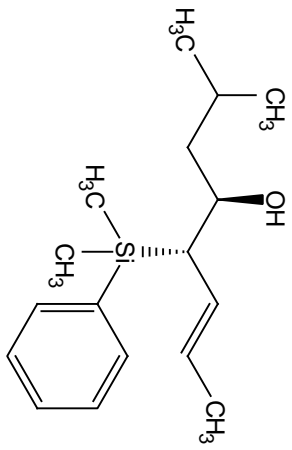

f1 (ppm)

2.06
3.02
1.00
1.00
0.99
1.03
2.98
1.02
2.51
1.08
6.06
2.94
3.02

7.54
7.54
7.53
7.52
7.36
7.36
7.35
7.27
7.27 cdcl3

5.45
5.43
5.42
5.40
5.38
5.36
5.35
5.34
5.33
5.32
5.31

3.80
3.79
3.78
3.77
3.76
3.75

1.80
1.79
1.78
1.77
1.72
1.70
1.68
1.67
1.65
1.64
1.57 HDO
1.36
1.35
1.33
1.32
1.31
1.30
1.29
1.28
1.27
1.20
1.19
1.18
1.17
1.16
1.16
1.15
0.83
0.81
0.80
0.35
0.32

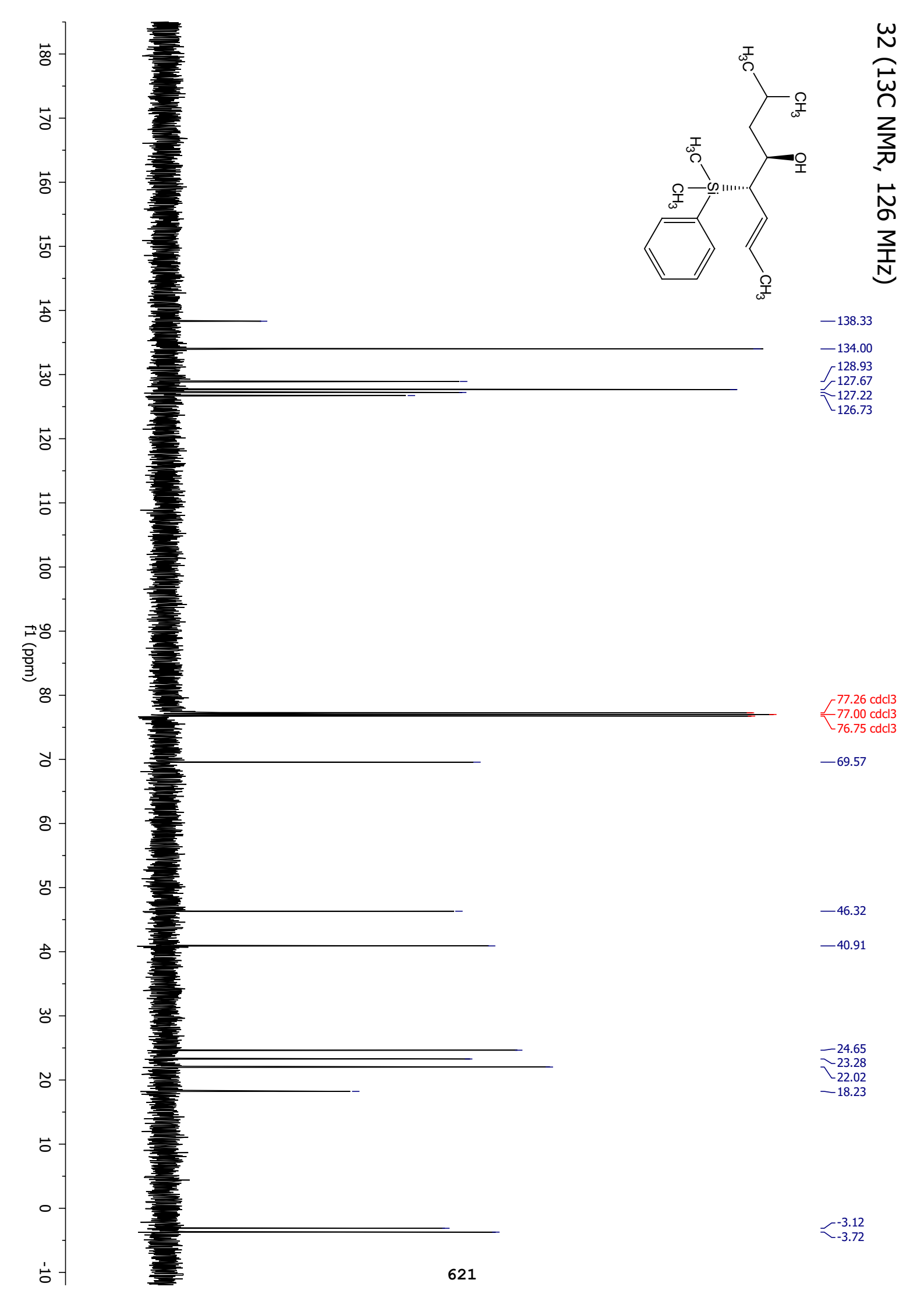
32 (13C NMR, 126 MHz)
f1 (ppm)
180
170
160
150
140
130
120
110
100
90
80
70
60
50
40
30
20
10
0
-10
H3C
CH3
OH
H3C
Si
CH3
CH3
138.33
134.00
128.93
127.67
127.22
126.73
77.26 cdcl3
77.00 cdcl3
76.75 cdcl3
69.57
46.32
40.91
24.65
23.28
22.02
18.23
-3.12
-3.72

33 (1H NMR, 400 MHz)

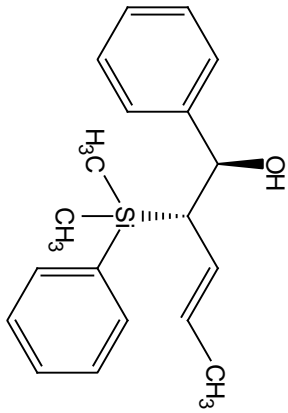

7.41
7.40
7.40
7.39
7.39
7.38
7.35
7.34
7.32
7.32
7.30
7.30
7.29
7.27
7.25
7.25
7.24 cdcl3
7.23
7.22
7.21
7.20
7.19

5.49
5.47
5.46
5.45
5.43
5.38
5.37
5.37
5.35
5.35
5.34
5.33
5.33
5.31
5.30
4.65
4.63

2.18
2.16
2.16
2.13
2.13
1.68
1.66
1.66
1.54 HDO
1.54 HDO

0.12
0.11
-0.00
-0.00

2.12
3.03
5.28
0.99
0.96
1.00
1.91
3.14
3.18
3.05

f1 (ppm)

33 (13C NMR, 101 MHz)

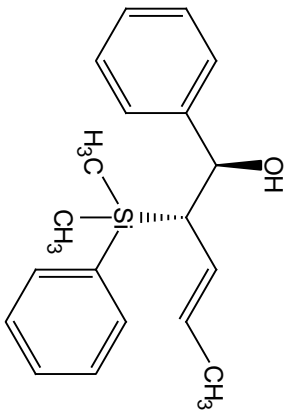

34 (1H NMR, 400 MHz)

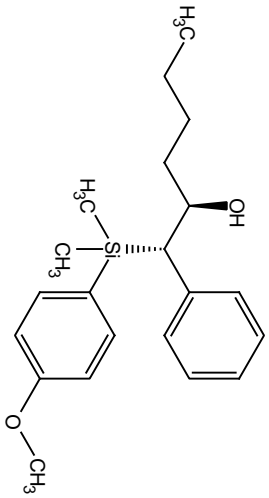

f1 (ppm)

1.92
2.19
2.85
1.89
1.00
2.90
0.97
1.97
5.17
2.95
3.00
2.94

7.39
7.37
7.25
7.23
7.21
7.15
7.15
7.14
7.12
7.10
6.89
6.87

4.06
4.05
4.04
4.03
4.02
4.01
4.00
3.81

2.37
2.35
1.55 HDO
1.45
1.44
1.42
1.41
1.40
1.33
1.32
1.30
1.29
1.28
1.27
1.26
1.25
1.23
1.22
1.20
1.19
1.17
1.15
1.13
0.81
0.80
0.78
0.30
0.16

34 (13C NMR, 101 MHz)

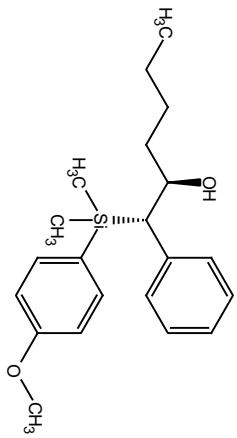

160.39
140.41
135.45
129.46
128.80
128.19
125.19
113.47
77.31 cdcl3
76.99 cdcl3
76.67 cdcl3
72.60
55.00
44.72
36.50
28.11
22.54
14.02
-2.22
-3.65

f1 (ppm)

35 (1H NMR, 500 MHz)

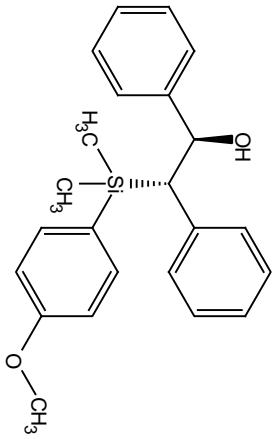

f1 (ppm)

7.02
4.92
1.90
1.00
3.04
1.01
0.95
3.00
2.98

7.32 7.31 7.31 7.30 7.30 7.30 7.29 7.28 7.28 7.27 7.27 7.26 7.26 7.26 cdcl3 7.25 7.25 7.25 7.23 7.23 7.18 7.17 7.17 7.17 7.16 7.16 7.15 7.15 7.13 7.13 7.12 7.11 7.11 7.11 6.83 6.83 6.82 6.81 6.81

5.14 5.12

3.82

2.79 2.77

1.99 1.99 1.98

1.57 1.57 HDO

0.03 0.03 -0.05 -0.05

35 (13C NMR, 126 MHz)

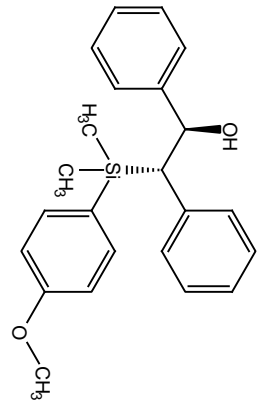

160.33
143.17
140.00
135.65
129.30
128.33
128.25
127.92
127.90
127.10
125.51
113.23
77.27 cdcl3
77.02 cdcl3
76.77 cdcl3
75.60
55.00
47.60
-3.22
-3.25

f1 (ppm)

8a (1H NMR, 500 MHz)

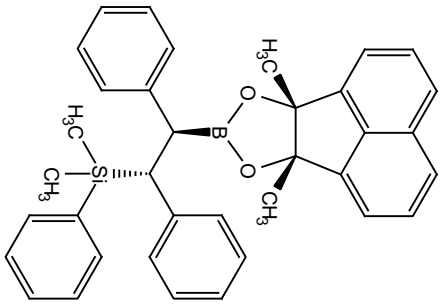

f1 (ppm)

1.88
1.98
0.96
2.93
1.20
3.80
2.85
1.97
1.93
0.95
1.00
1.00
2.99
2.95
2.95
2.95

7.68 7.68 7.66 7.66 7.50 7.50 7.49 7.49 7.49 7.48 7.48 7.47 7.47 7.47 7.46 7.46 7.45 7.45 7.37 7.37 7.37 7.36 7.35 7.35 7.31 7.31 7.30 cdcl3 7.27 7.27 7.26 7.24 7.24 7.23 7.23 7.18 7.18 7.17 7.17 7.17 7.16 7.16 7.16 7.15 7.15 7.14 7.14 7.09 7.09 7.09 7.08 7.08 7.08 7.08 7.07 7.07 7.07 7.05 7.05 6.79 6.78 6.78 6.77 6.77 6.77 6.73 6.73 6.72 6.72 6.71 6.71 6.70 6.66 6.66 6.65 2.93 2.91 2.82 2.79 1.55 HDO 1.37 1.37 1.35 1.35 -0.15 -0.15 -0.18 -0.18

8a (13C NMR, 126 MHz)

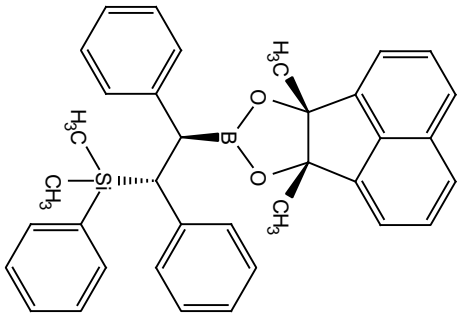

144.49
144.22
142.99
141.51
137.55
134.48
134.28
131.29
129.42
128.47
128.31
128.11
128.07
127.07
126.95
125.56
124.85
124.47
119.00
118.92
91.63
91.54
77.27 cdcl3
77.02 cdcl3
76.76 cdcl3
40.33
21.70
21.57
-3.35
-3.56

f1 (ppm)

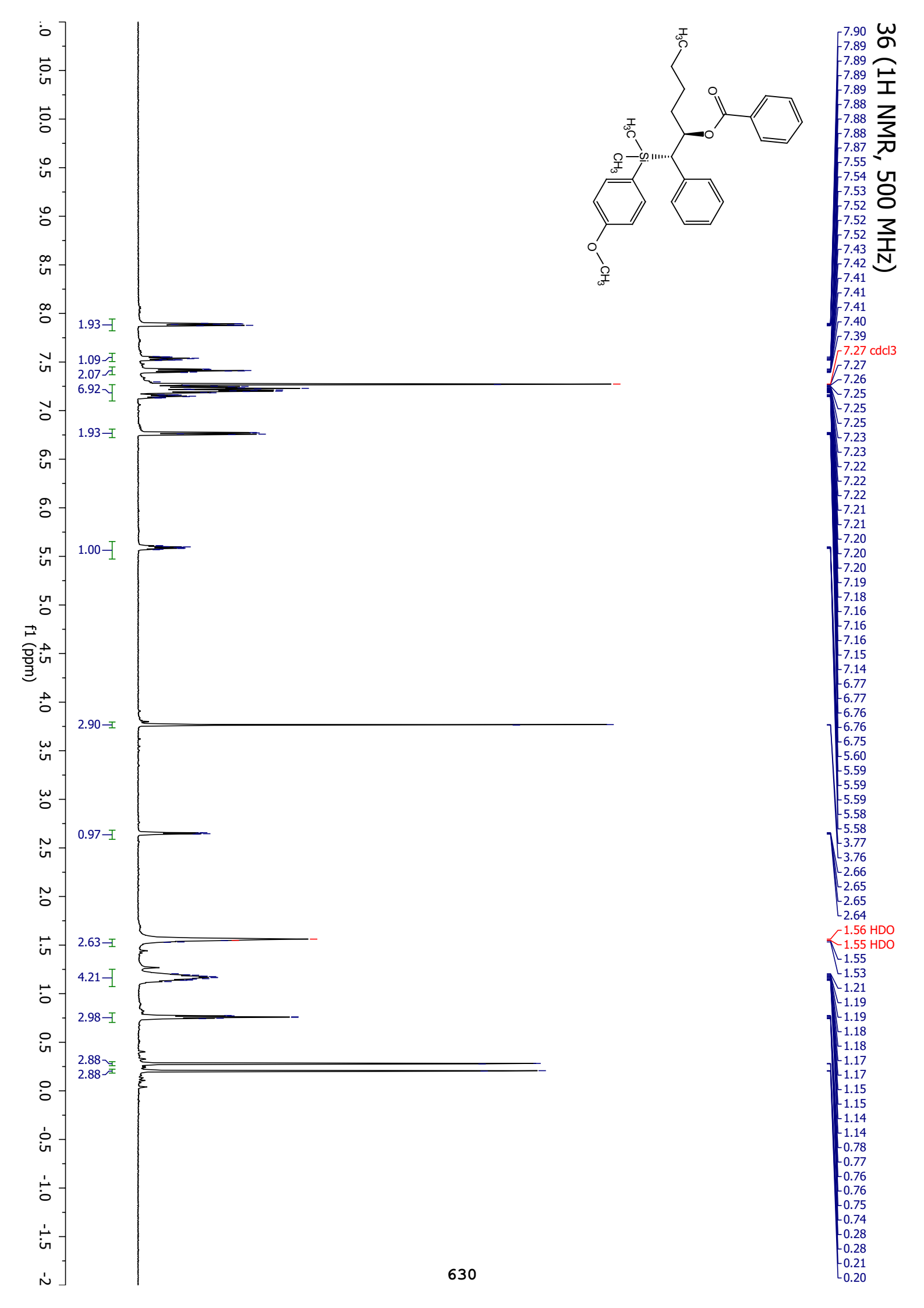
36 (1H NMR, 500 MHz)
f1 (ppm)
1.93
1.09
2.07
6.92
1.93
1.00
2.90
0.97
2.63
4.21
2.98
2.88
2.88
7.27 cdcl3
1.56 HDO
1.55 HDO

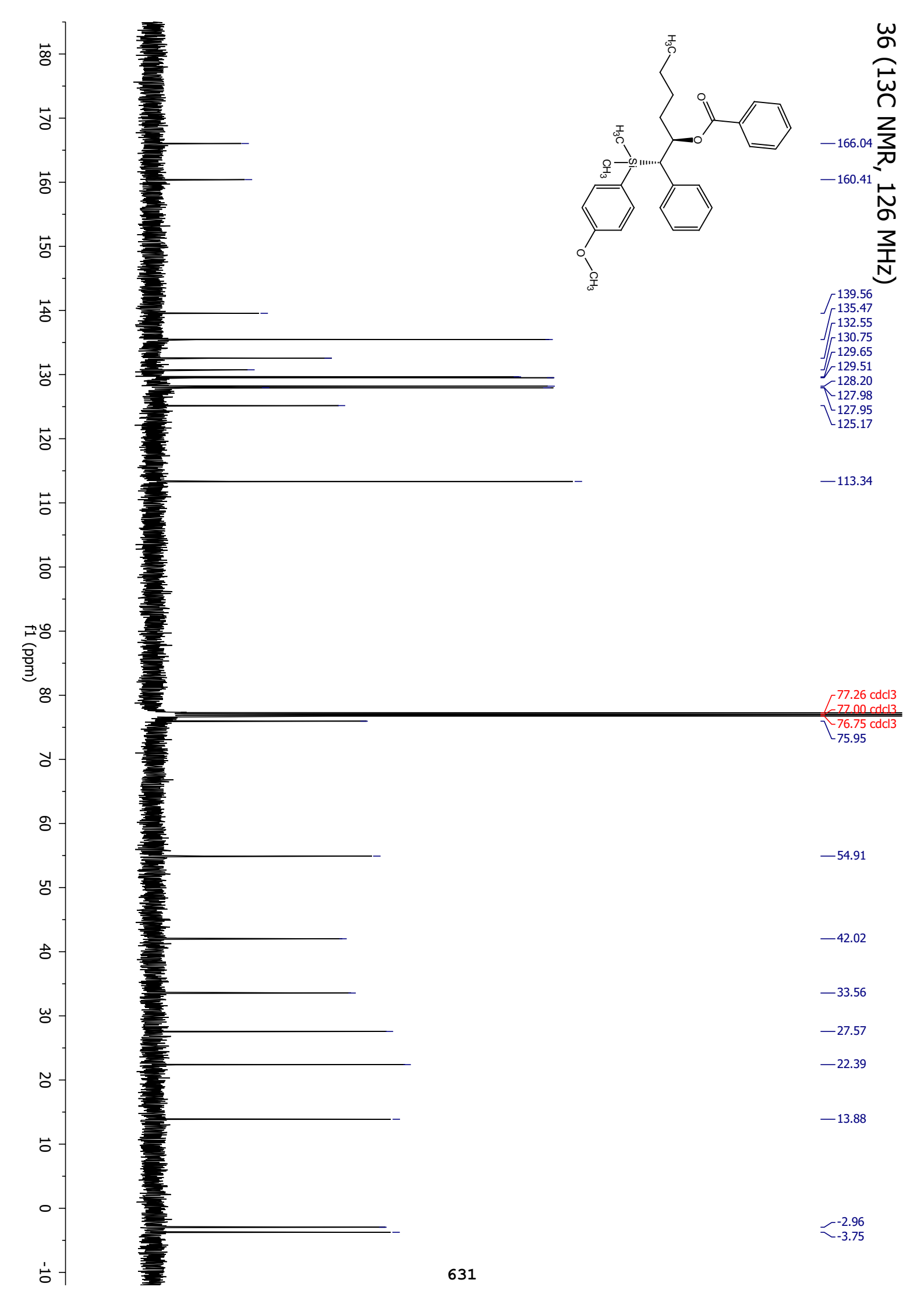
36 (13C NMR, 126 MHz)
166.04
160.41
139.56
135.47
132.55
130.75
129.65
129.51
128.20
127.98
127.95
125.17
113.34
77.26 cdcl3
77.00 cdcl3
76.75 cdcl3
75.95
54.91
42.02
33.56
27.57
22.39
13.88
-2.96
-3.75
f1 (ppm)
180
170
160
150
140
130
120
110
100
90
80
70
60
50
40
30
20
10
0
-10

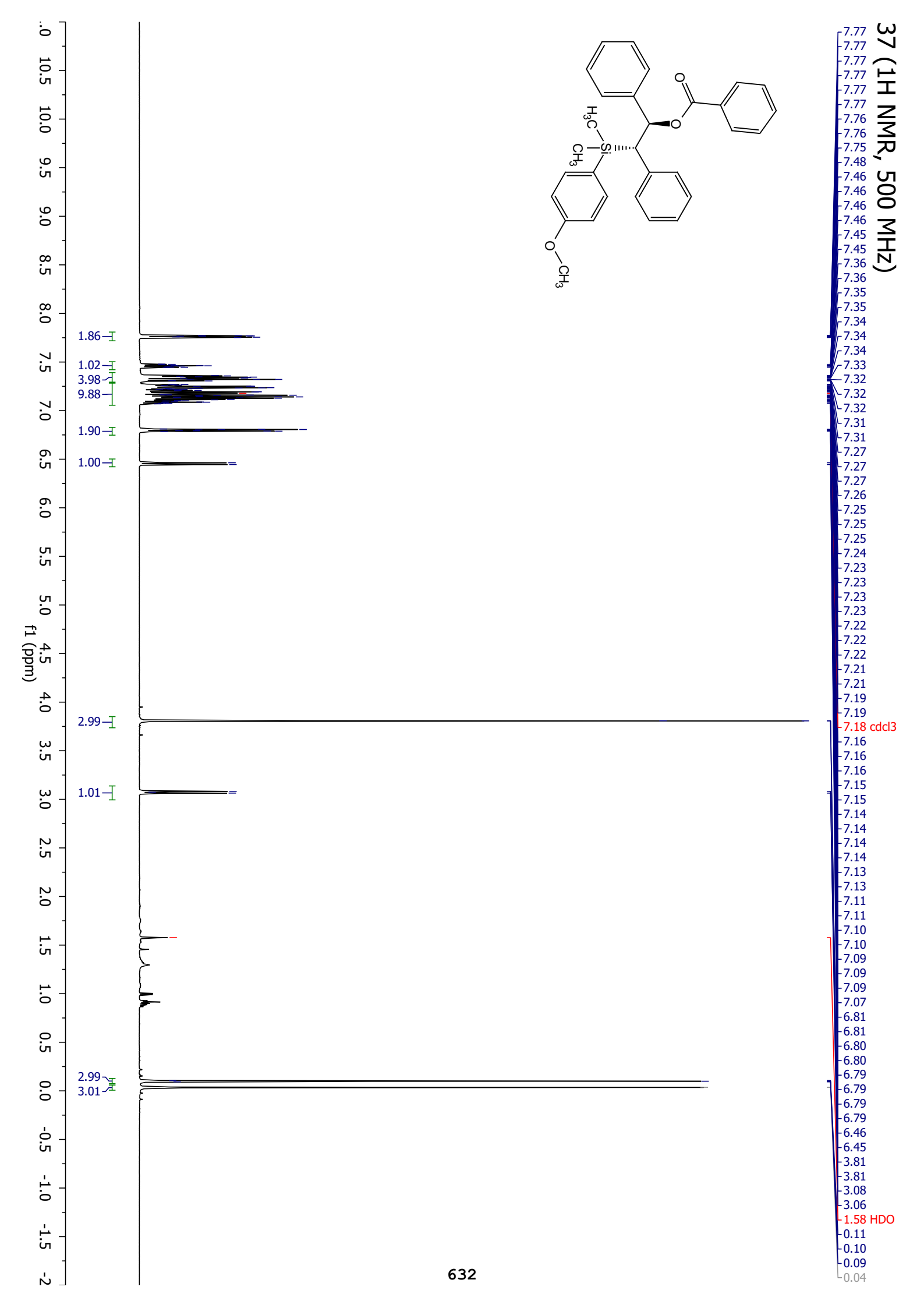
37 (1H NMR, 500 MHz)
f1 (ppm)
1.86
1.02
3.98
9.88
1.90
1.00
2.99
1.01
2.99
3.01
7.18 cdcl3
1.58 HDO

37 (13C NMR, 126 MHz)

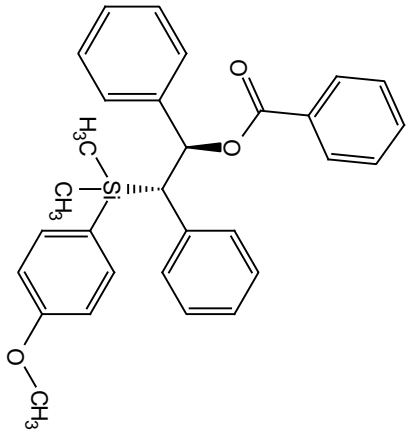

165.79
160.45
140.13
139.81
135.68
132.55
130.53
129.41
128.98
128.17
128.11
128.09
127.98
127.45
127.30
125.22
113.32
77.89
77.29 cdcl3
77.03 cdcl3
76.78 cdcl3
54.99
45.09
-3.21
-3.31

f1 (ppm)

633

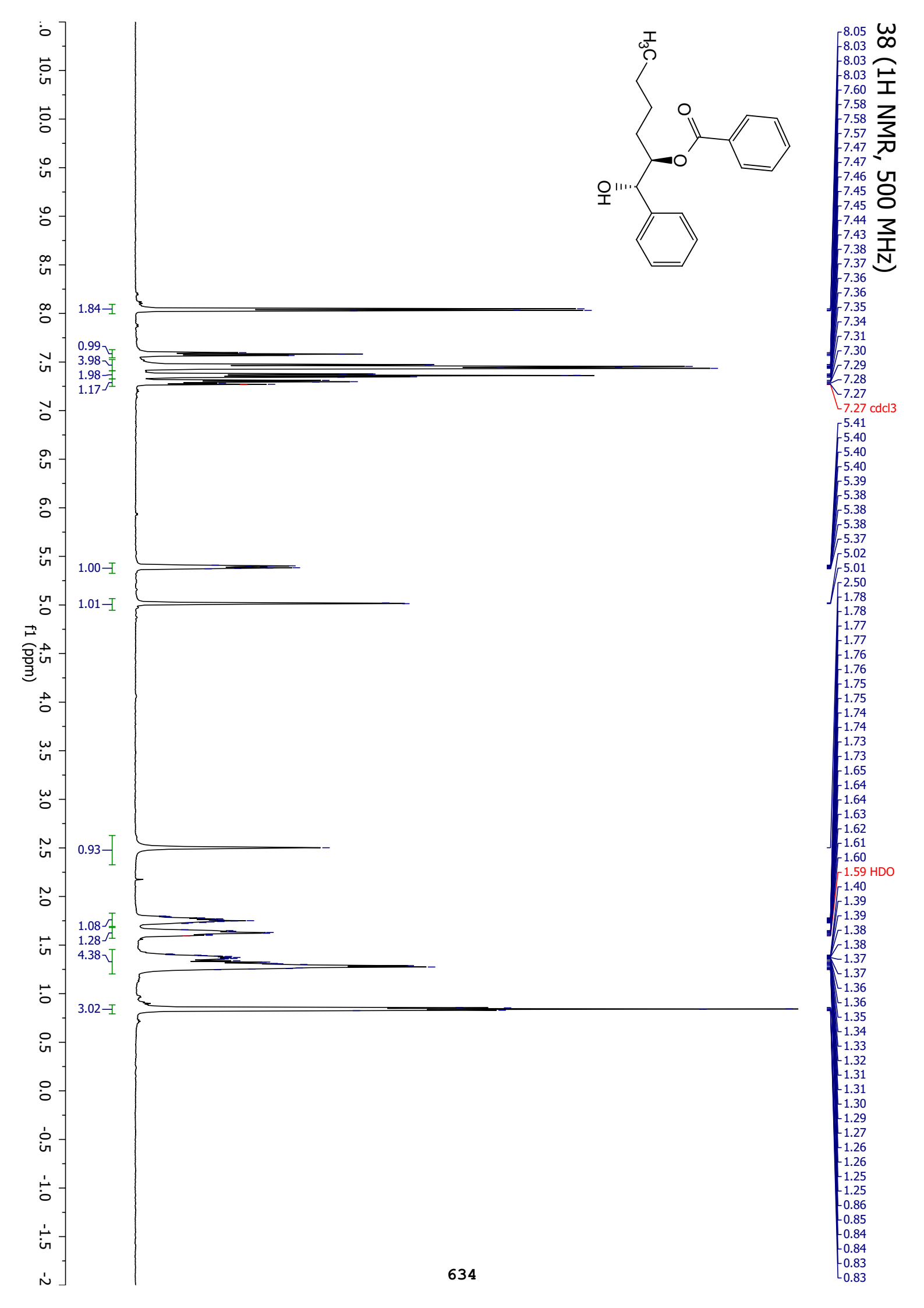
38 (1H NMR, 500 MHz)
f1 (ppm)
1.84
0.99
3.98
1.98
1.17
1.00
1.01
0.93
1.08
1.28
4.38
3.02
7.27 cdcl3
1.59 HDO

38 (13C NMR, 126 MHz)

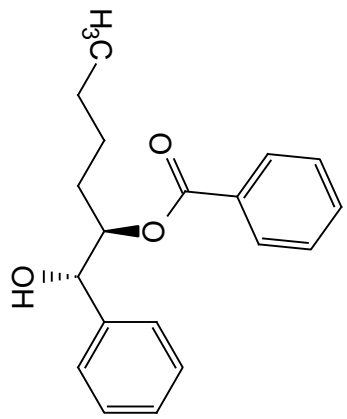

166.62
139.91
133.04
130.16
129.67
128.38
128.25
127.81
126.66
78.30
77.27 cdcl3
77.01 cdcl3
76.76 cdcl3
75.52
28.40
27.77
22.47
13.90

f1 (ppm)

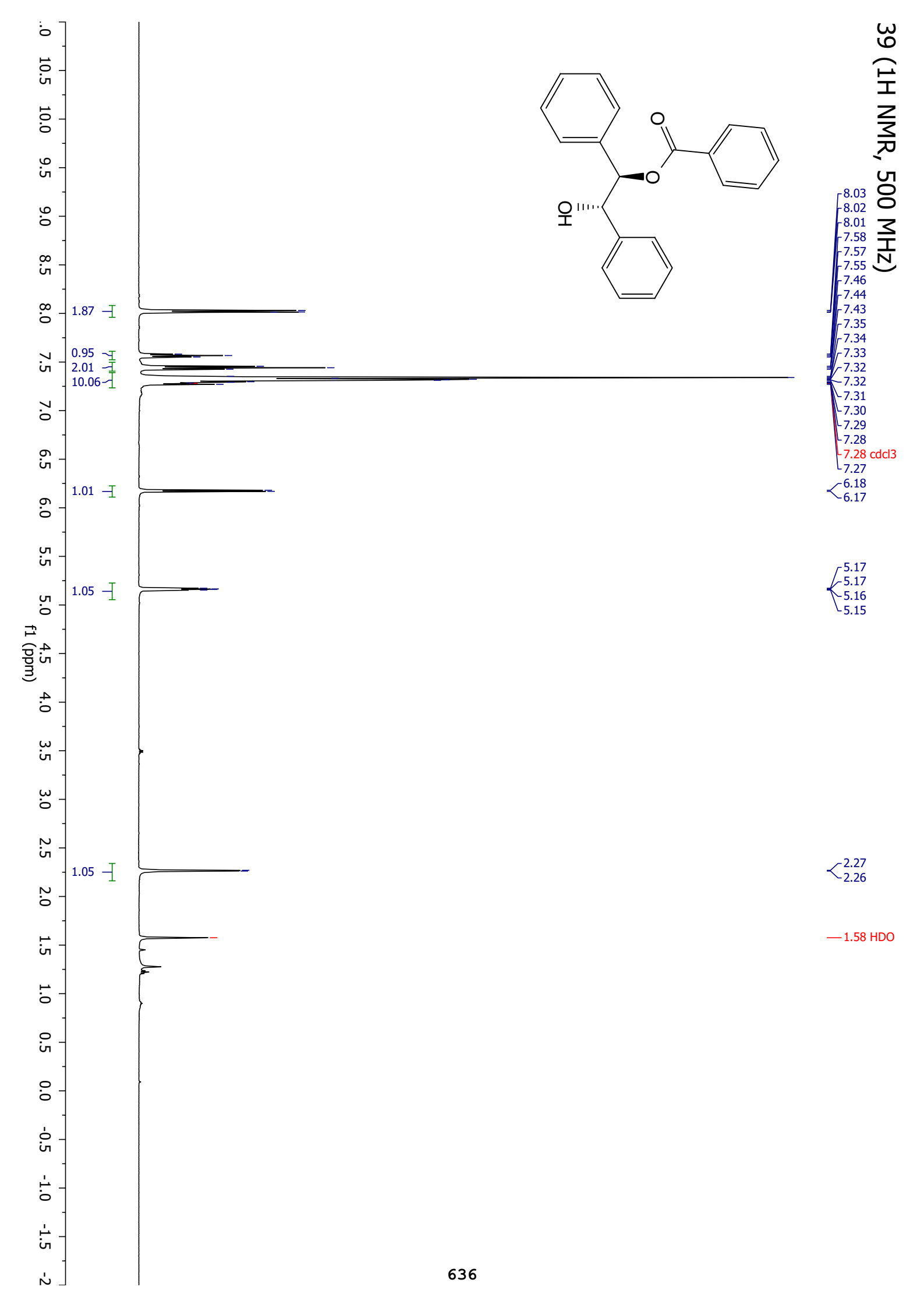
39 (1H NMR, 500 MHz)
f1 (ppm)
1.87
0.95
2.01
10.06
1.01
1.05
1.05
8.03
8.02
8.01
7.58
7.57
7.55
7.46
7.44
7.43
7.35
7.34
7.33
7.32
7.32
7.31
7.30
7.29
7.28
7.28 cdcl3
7.27
6.18
6.17
5.17
5.17
5.16
5.15
2.27
2.26
1.58 HDO
OH
O
O

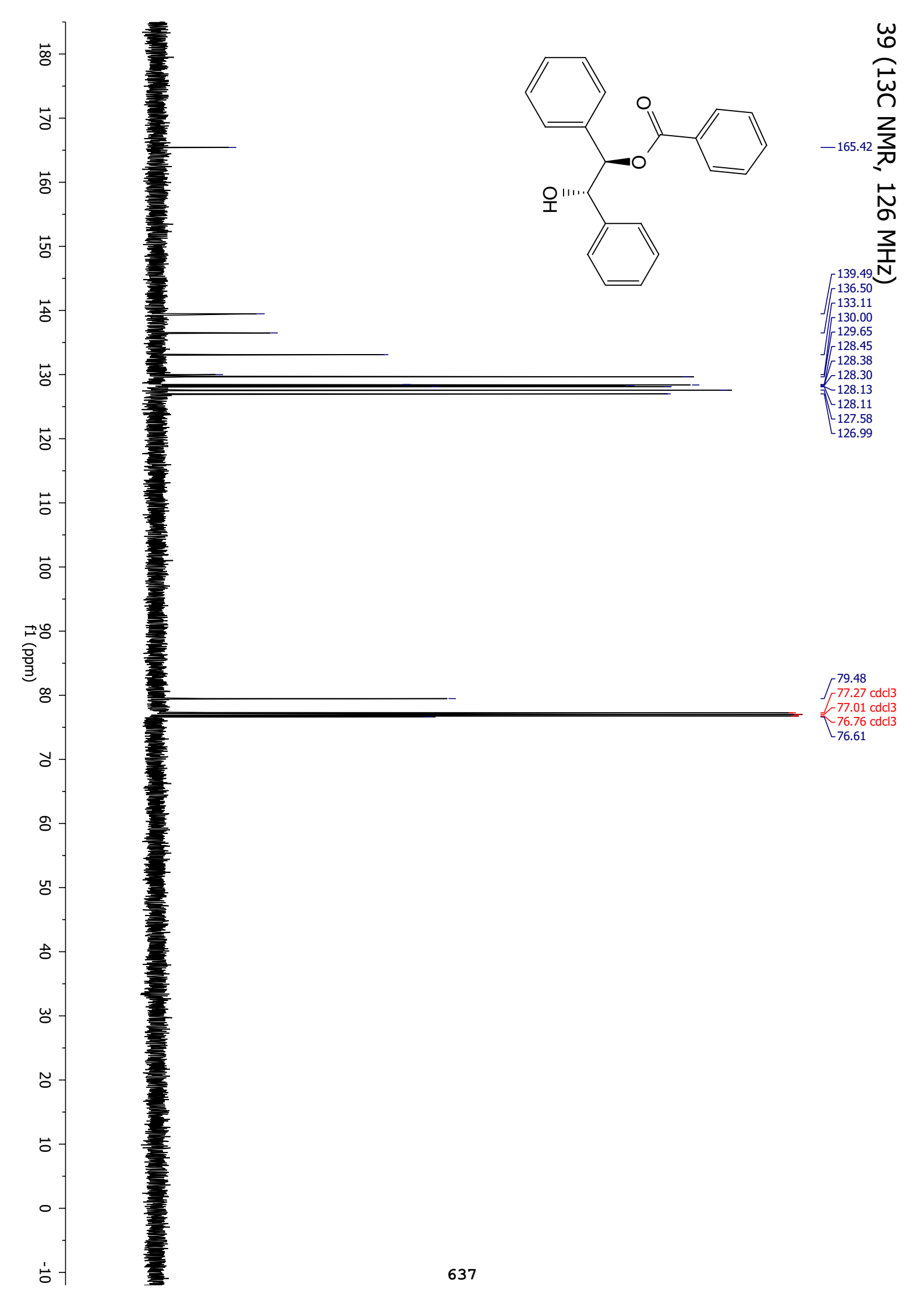
39 (13C NMR, 126 MHz)
165.42
139.49
136.50
133.11
130.00
129.65
128.45
128.38
128.30
128.13
128.11
127.58
126.99
79.48
77.27 cdcl3
77.01 cdcl3
76.76 cdcl3
76.61
OH
O
O
f1 (ppm)
180
170
160
150
140
130
120
110
100
90
80
70
60
50
40
30
20
10
0
-10

40 (1H NMR, 600 MHz)

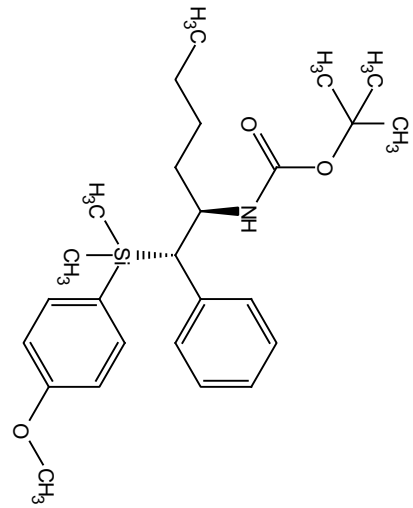

f1 (ppm)

2.01
1.94
1.03
1.95
1.88
0.83
0.89
2.88
1.00
2.83
8.19
5.39
2.98
3.08
2.96

7.35
7.35
7.34
7.34
7.33
7.26 cdcl3
7.22
7.22
7.21
7.20
7.13
7.12
7.11
7.01
7.00
6.99
6.87
6.85
4.20
4.18
4.13
4.12
4.10
3.80
2.34
2.33
1.58 HDO
1.44
1.43
1.42
1.41
1.35
1.22
1.21
1.20
1.20
1.19
1.18
1.18
1.17
1.16
1.15
1.14
1.13
1.11
1.11
1.10
1.10
0.79
0.78
0.77
0.33
0.16
0.03

40 (13 NMR, 101 MHz)

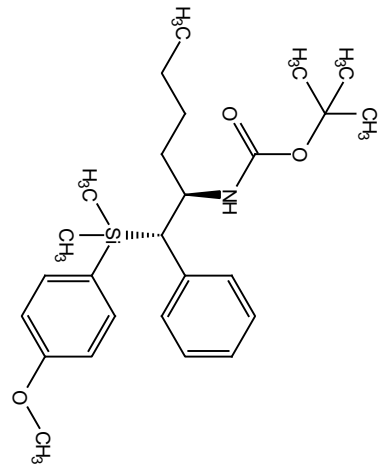

160.33
155.39
140.56
135.47
129.49
128.82
128.10
125.16
113.39
78.65
77.31 cdcl3
76.99 cdcl3
76.67 cdcl3
54.96
50.86
42.67
36.23
28.37
28.01
22.40
14.01
-2.37
-3.85

f1 (ppm)

41 (1H NMR, 500 MHz)

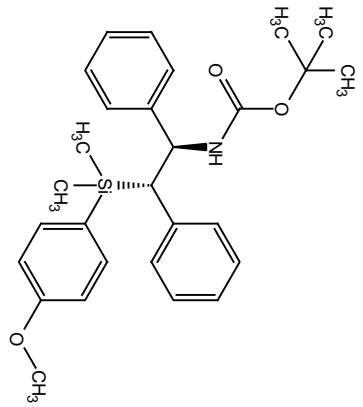

f1 (ppm)

7.41
3.10
2.02
1.93
0.97
0.98
3.11
1.00
9.18
3.05
3.02

7.27
7.27
7.27 cdcl3
7.26
7.26
7.25
7.25
7.25
7.23
7.23
7.23
7.23
7.22
7.22
7.21
7.21
7.20
7.19
7.19
7.15
7.14
7.13
7.10
7.10
7.09
7.09
7.09
7.08
6.98
6.98
6.98
6.97
6.96
6.96
6.80
6.80
6.79
6.78
6.78
5.09
4.67
3.81
3.81
2.67
2.65
1.60 HDO
1.25
1.24
-0.01
-0.02
-0.06
-0.06

41 (13C NMR, 126 MHz)

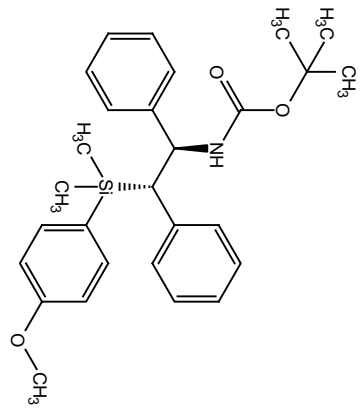

160.32
154.92
143.13
139.81
135.67
129.17
128.27
128.12
127.66
127.33
127.30
125.41
113.21
79.11
77.26 cdcl3
77.01 cdcl3
76.76 cdcl3
54.99
44.80
28.24
-3.16
-3.37

f1 (ppm)

42 (1H NMR, 500 MHz)

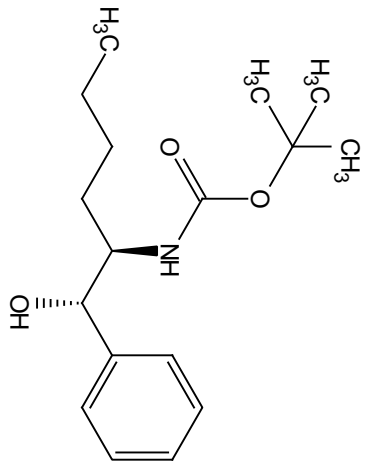

7.37
7.35
7.34
7.32
7.29
7.29
7.28
7.28
7.27 cdcl3
7.26
7.26

4.85
4.49
4.47
3.92
3.90
3.89
3.50

1.47
1.41
1.36
1.34
1.32
1.31
1.29
1.28
1.27
1.24
1.22
1.22
1.20
1.18
0.86
0.85
0.83

5.54
1.11
1.03
1.00
0.94
10.47
6.81
3.44

f1 (ppm)

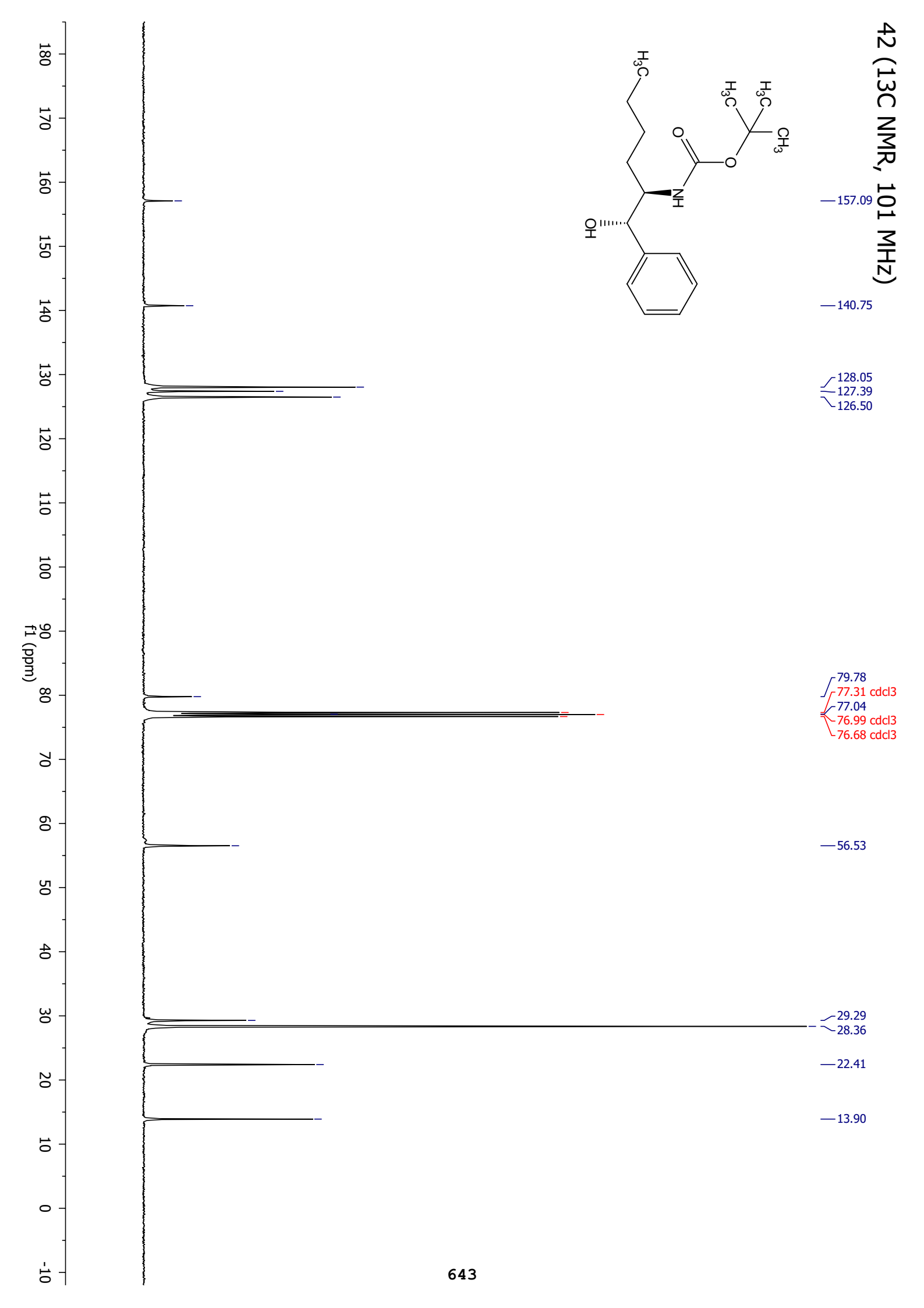
42 (13C NMR, 101 MHz)
157.09
140.75
128.05
127.39
126.50
79.78
77.31 cdcl3
77.04
76.99 cdcl3
76.68 cdcl3
56.53
29.29
28.36
22.41
13.90
f1 (ppm)
180
170
160
150
140
130
120
110
100
90
80
70
60
50
40
30
20
10
0
-10

43 (1H NMR, 600 MHz)

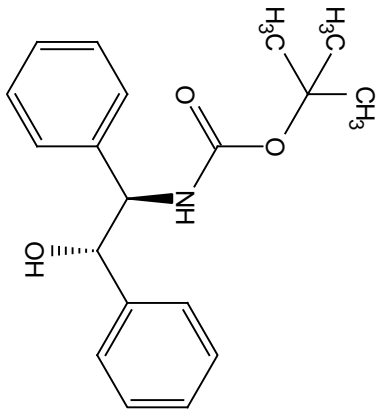

43 (13C NMR, 151 MHz)